

2 Modify S'_e to determine S_e .

p. 287 $S_e = k_a k_b k_c k_d k_e k_f S'_e \quad (6-18)$

$$k_a = a S_{ut}^b \quad (6-19)$$

Table 6-2

Parameters for Marin Surface Modification Factor, Eq. (6-19)

Surface Finish	Factor a S_{ut} , ksi	Exponent b S_{ut} , MPa
Ground	1.34	1.58
Machined or cold-drawn	2.70	4.51
Hot-rolled	14.4	57.7
As-forged	39.9	272.

Rotating shaft. For bending or torsion,

p. 288 $k_b = \begin{cases} (d/0.3)^{-0.107} = 0.879d^{-0.107} & 0.11 \leq d \leq 2 \text{ in} \\ 0.91d^{-0.157} & 2 < d \leq 10 \text{ in} \\ (d/7.62)^{-0.107} = 1.24d^{-0.107} & 2.79 \leq d \leq 51 \text{ mm} \\ 1.51d^{-0.157} & 51 < 254 \text{ mm} \end{cases} \quad (6-20)$

For axial,

$$k_b = 1 \quad (6-21)$$

Nonrotating member. Use Table 6-3, p. 290, for d_e and substitute into Eq. (6-20) for d .

p. 290 $k_c = \begin{cases} 1 & \text{bending} \\ 0.85 & \text{axial} \\ 0.59 & \text{torsion} \end{cases} \quad (6-26)$

p. 291 Use Table 6-4 for k_d , or

$$\begin{aligned} k_d = 0.975 + 0.432(10^{-3})T_F - 0.115(10^{-5})T_F^2 \\ + 0.104(10^{-8})T_F^3 - 0.595(10^{-12})T_F^4 \end{aligned} \quad (6-27)$$

pp. 292–293, k_e

Table 6-5

	Reliability, %	Transformation Variate z_a	Reliability Factor k_e
Reliability Factor k_e	50	0	1.000
Corresponding to 8 Percent Standard Deviation of the Endurance Limit	90	1.288	0.897
	95	1.645	0.868
	99	2.326	0.814
	99.9	3.091	0.753
	99.99	3.719	0.702
	99.999	4.265	0.659
	99.9999	4.753	0.620

pp. 293–294, k_f

- 3** Determine fatigue stress-concentration factor, K_f or K_{fs} . First, find K_t or K_{ts} from Table A-15.

p. 295
$$K_f = 1 + q(K_t - 1) \quad \text{or} \quad K_{fs} = 1 + q(K_{ts} - 1) \quad (6-32)$$

Obtain q from either Fig. 6-20 or 6-21, pp. 295–296.

Alternatively,

p. 296
$$K_f = 1 + \frac{K_t - 1}{1 + \sqrt{a/r}} \quad (6-33)$$

For \sqrt{a} in units of $\sqrt{\text{in}}$, and S_{ut} in kpsi

Bending or axial: $\sqrt{a} = 0.246 - 3.08(10^{-3})S_{ut} + 1.51(10^{-5})S_{ut}^2 - 2.67(10^{-8})S_{ut}^3$ (6-35a)

Torsion: $\sqrt{a} = 0.190 - 2.51(10^{-3})S_{ut} + 1.35(10^{-5})S_{ut}^2 - 2.67(10^{-8})S_{ut}^3$ (6-35b)

- 4** Apply K_f or K_{fs} by either dividing S_e by it or multiplying it with the purely reversing stress, *not* both.

- 5** Determine fatigue life constants a and b . If $S_{ut} \geq 70$ kpsi, determine f from Fig. 6-18, p. 285. If $S_{ut} < 70$ kpsi, let $f = 0.9$.

p. 285
$$a = (f S_{ut})^2 / S_e \quad (6-14)$$

$$b = -[\log(f S_{ut}/S_e)]/3 \quad (6-15)$$

- 6** Determine fatigue strength S_f at N cycles, or, N cycles to failure at a reversing stress σ_{rev}

(Note: this only applies to purely reversing stresses where $\sigma_m = 0$).

p. 285
$$S_f = aN^b \quad (6-13)$$

$$N = (\sigma_{rev}/a)^{1/b} \quad (6-16)$$

Fluctuating Simple Loading

For S_e , K_f or K_{fs} , see previous subsection.

- 1** Calculate σ_m and σ_a . Apply K_f to both stresses.

p. 301
$$\sigma_m = (\sigma_{max} + \sigma_{min})/2 \quad \sigma_a = |\sigma_{max} - \sigma_{min}|/2 \quad (6-36)$$

- 2** Apply to a fatigue failure criterion, p. 306

$$\sigma_m \geq 0$$

Soderburg
$$\sigma_a/S_e + \sigma_m/S_y = 1/n \quad (6-45)$$

mod-Goodman
$$\sigma_a/S_e + \sigma_m/S_{ut} = 1/n \quad (6-46)$$

Gerber
$$n\sigma_a/S_e + (n\sigma_m/S_{ut})^2 = 1 \quad (6-47)$$

ASME-elliptic
$$(\sigma_a/S_e)^2 + (\sigma_m/S_y)^2 = 1/n^2 \quad (6-48)$$

$$\sigma_m < 0$$

p. 305
$$\sigma_a = S_e/n$$

Torsion. Use the same equations as apply for $\sigma_m \geq 0$, except replace σ_m and σ_a with τ_m and τ_a , use $k_c = 0.59$ for S_e , replace S_{ut} with $S_{su} = 0.67S_{ut}$ [Eq. (6-54), p. 317], and replace S_y with $S_{sy} = 0.577S_y$ [Eq. (5-21), p. 297]

- 3 Check for localized yielding.

$$\text{p. 306} \quad \sigma_a + \sigma_m = S_y/n \quad (6-49)$$

$$\text{or, for torsion,} \quad \tau_a + \tau_m = 0.577S_y/n$$

- 4 For finite-life fatigue strength, equivalent completely reversed stress (see Ex. 6-12, pp. 313-314),

$$\text{mod-Goodman} \quad \sigma_{\text{rev}} = \frac{\sigma_a}{1 - (\sigma_m/S_{ut})}$$

$$\text{Gerber} \quad \sigma_{\text{rev}} = \frac{\sigma_a}{1 - (\sigma_m/S_{ut})^2}$$

If determining the finite life N with a factor of safety n , substitute σ_{rev}/n for σ_{rev} in Eq. (6-16). That is,

$$N = \left(\frac{\sigma_{\text{rev}}/n}{a} \right)^{1/b}$$

Combination of Loading Modes

See previous subsections for earlier definitions.

- 1 Calculate von Mises stresses for alternating and midrange stress states, σ'_a and σ'_m . When determining S_e , do not use k_c nor divide by K_f or K_{fs} . Apply K_f and/or K_{fs} directly to each specific alternating and midrange stress. If axial stress is present divide the alternating axial stress by $k_c = 0.85$. For the special case of combined bending, torsional shear, and axial stresses

p. 318

$$\sigma'_a = \left\{ \left[(K_f)_{\text{bending}}(\sigma_a)_{\text{bending}} + (K_f)_{\text{axial}} \frac{(\sigma_a)_{\text{axial}}}{0.85} \right]^2 + 3 [(K_{fs})_{\text{torsion}}(\tau_a)_{\text{torsion}}]^2 \right\}^{1/2} \quad (6-55)$$

$$\sigma'_m = \left\{ \left[(K_f)_{\text{bending}}(\sigma_m)_{\text{bending}} + (K_f)_{\text{axial}}(\sigma_m)_{\text{axial}} \right]^2 + 3 [(K_{fs})_{\text{torsion}}(\tau_m)_{\text{torsion}}]^2 \right\}^{1/2} \quad (6-56)$$

- 2 Apply stresses to fatigue criterion [see Eqs. (6-45) to (6-48), p. 346 in previous subsection].
- 3 Conservative check for localized yielding using von Mises stresses.

$$\text{p. 306} \quad \sigma'_a + \sigma'_m = S_y/n \quad (6-49)$$

PROBLEMS

Problems marked with an asterisk (*) are linked to problems in other chapters, as summarized in Table 1–1 of Sec. 1–16, p. 24.

Problems 6–1 to 6–63 are to be solved by deterministic methods. Problems 6–64 to 6–78 are to be solved by stochastic methods. Problems 6–71 to 6–78 are computer problems.

Deterministic Problems

- 6–1** A 10-mm drill rod was heat-treated and ground. The measured hardness was found to be 300 Brinell. Estimate the endurance strength in MPa if the rod is used in rotating bending.
- 6–2** Estimate S'_e in kpsi for the following materials:
(a) AISI 1035 CD steel.
(b) AISI 1050 HR steel.
(c) 2024 T4 aluminum.
(d) AISI 4130 steel heat-treated to a tensile strength of 235 kpsi.
- 6–3** A steel rotating-beam test specimen has an ultimate strength of 120 kpsi. Estimate the life of the specimen if it is tested at a completely reversed stress amplitude of 70 kpsi.
- 6–4** A steel rotating-beam test specimen has an ultimate strength of 1600 MPa. Estimate the life of the specimen if it is tested at a completely reversed stress amplitude of 900 MPa.
- 6–5** A steel rotating-beam test specimen has an ultimate strength of 230 kpsi. Estimate the fatigue strength corresponding to a life of 150 kcycles of stress reversal.
- 6–6** Repeat Prob. 6–5 with the specimen having an ultimate strength of 1100 MPa.
- 6–7** A steel rotating-beam test specimen has an ultimate strength of 150 kpsi and a yield strength of 135 kpsi. It is desired to test low-cycle fatigue at approximately 500 cycles. Check if this is possible without yielding by determining the necessary reversed stress amplitude.
- 6–8** Derive Eq. (6–17). Rearrange the equation to solve for N .
- 6–9** For the interval $10^3 \leq N \leq 10^6$ cycles, develop an expression for the axial fatigue strength $(S'_f)_{ax}$ for the polished specimens of 4130 used to obtain Fig. 6–10. The ultimate strength is $S_{ut} = 125$ kpsi and the endurance limit is $(S'_e)_{ax} = 50$ kpsi.
- 6–10** Estimate the endurance strength of a 1.5-in-diameter rod of AISI 1040 steel having a machined finish and heat-treated to a tensile strength of 110 kpsi.
- 6–11** Two steels are being considered for manufacture of as-forged connecting rods. One is AISI 4340 Cr-Mo-Ni steel capable of being heat-treated to a tensile strength of 260 kpsi. The other is a plain carbon steel AISI 1040 with an attainable S_{ut} of 113 kpsi. If each rod is to have a size giving an equivalent diameter d_e of 0.75 in, is there any advantage to using the alloy steel for this fatigue application?
- 6–12** A 1-in-diameter solid round bar has a groove 0.1-in deep with a 0.1-in radius machined into it. The bar is made of AISI 1020 CD steel and is subjected to a purely reversing torque of 1800 lbf · in. For the S - N curve of this material, let $f = 0.9$.
(a) Estimate the number of cycles to failure.
(b) If the bar is also placed in an environment with a temperature of 750°F, estimate the number of cycles to failure.
- 6–13** A solid square rod is cantilevered at one end. The rod is 0.6 m long and supports a completely reversing transverse load at the other end of ± 2 kN. The material is AISI 1080 hot-rolled steel. If the rod must support this load for 10^4 cycles with a factor of safety of 1.5, what dimension should the square cross section have? Neglect any stress concentrations at the support end.

6-14

A rectangular bar is cut from an AISI 1020 cold-drawn steel flat. The bar is 2.5 in wide by $\frac{3}{8}$ in thick and has a 0.5-in-dia. hole drilled through the center as depicted in Table A-15-1. The bar is concentrically loaded in push-pull fatigue by axial forces F_a , uniformly distributed across the width. Using a design factor of $n_d = 2$, estimate the largest force F_a that can be applied ignoring column action.

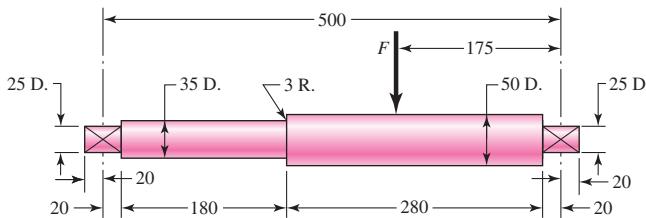
6-15

A solid round bar with diameter of 2 in has a groove cut to a diameter of 1.8 in, with a radius of 0.1 in. The bar is not rotating. The bar is loaded with a repeated bending load that causes the bending moment at the groove to fluctuate between 0 and 25 000 lbf · in. The bar is hot-rolled AISI 1095, but the groove has been machined. Determine the factor of safety for fatigue based on infinite life and the factor of safety for yielding.

6-16

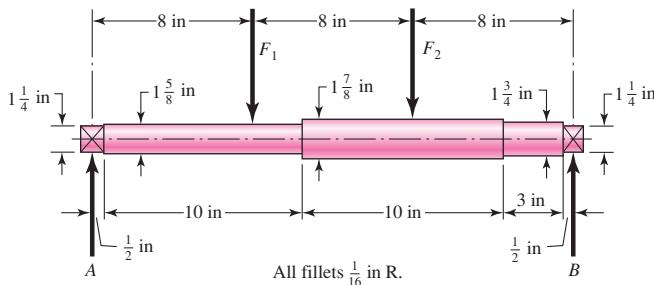
The rotating shaft shown in the figure is machined from AISI 1020 CD steel. It is subjected to a force of $F = 6$ kN. Find the minimum factor of safety for fatigue based on infinite life. If the life is not infinite, estimate the number of cycles. Be sure to check for yielding.

Problem 6-16
Dimensions in millimeters

**6-17**

The shaft shown in the figure is machined from AISI 1040 CD steel. The shaft rotates at 1600 rpm and is supported in rolling bearings at A and B . The applied forces are $F_1 = 2500$ lbf and $F_2 = 1000$ lbf. Determine the minimum fatigue factor of safety based on achieving infinite life. If infinite life is not predicted, estimate the number of cycles to failure. Also check for yielding.

Problem 6-17

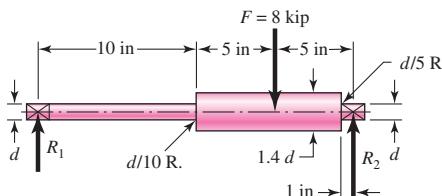
**6-18**

Solve Prob. 6-17 except with forces $F_1 = 1200$ lbf and $F_2 = 2400$ lbf.

6-19

Bearing reactions R_1 and R_2 are exerted on the shaft shown in the figure, which rotates at 950 rev/min and supports an 8-kip bending force. Use a 1095 HR steel. Specify a diameter d using a design factor of $n_d = 1.6$ for a life of 10 hr. The surfaces are machined.

Problem 6-19



6-20

A bar of steel has the minimum properties $S_e = 40$ kpsi, $S_y = 60$ kpsi, and $S_{ut} = 80$ kpsi. The bar is subjected to a steady torsional stress of 15 kpsi and an alternating bending stress of 25 kpsi. Find the factor of safety guarding against a static failure, and either the factor of safety guarding against a fatigue failure or the expected life of the part. For the fatigue analysis use:

- Modified Goodman criterion.
- Gerber criterion.
- ASME-elliptic criterion.

6-21

Repeat Prob. 6-20 but with a steady torsional stress of 20 kpsi and an alternating bending stress of 10 kpsi.

6-22

Repeat Prob. 6-20 but with a steady torsional stress of 15 kpsi, an alternating torsional stress of 10 kpsi, and an alternating bending stress of 12 kpsi.

6-23

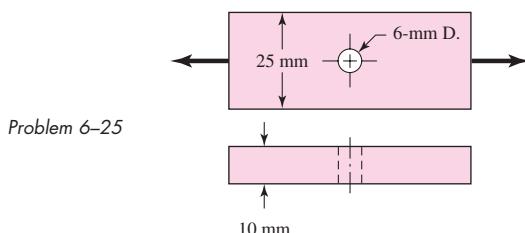
Repeat Prob. 6-20 but with an alternating torsional stress of 30 kpsi.

6-24

Repeat Prob. 6-20 but with an alternating torsional stress of 15 kpsi and a steady bending stress of 15 kpsi.

6-25

The cold-drawn AISI 1040 steel bar shown in the figure is subjected to a completely reversed axial load fluctuating between 28 kN in compression to 28 kN in tension. Estimate the fatigue factor of safety based on achieving infinite life, and the yielding factor of safety. If infinite life is not predicted, estimate the number of cycles to failure.

**6-26**

Repeat Prob. 6-25 for a load that fluctuates from 12 kN to 28 kN. Use the Modified Goodman, Gerber, and ASME-elliptic criteria and compare their predictions.

6-27

Repeat Prob. 6-25 for each of the following loading conditions:

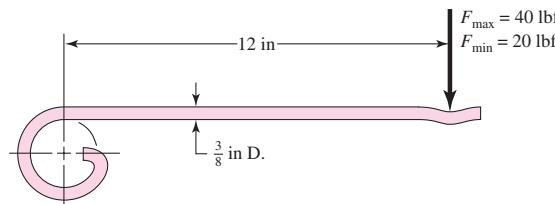
- 0 kN to 28 kN
- 12 kN to 28 kN
- 28 kN to 12 kN

6-28

The figure shows a formed round-wire cantilever spring subjected to a varying force. The hardness tests made on 50 springs gave a minimum hardness of 400 Brinell. It is apparent from the mounting details that there is no stress concentration. A visual inspection of the springs indicates that the surface finish corresponds closely to a hot-rolled finish. What number of applications is likely to cause failure? Solve using:

- Modified Goodman criterion.
- Gerber criterion.

Problem 6-28

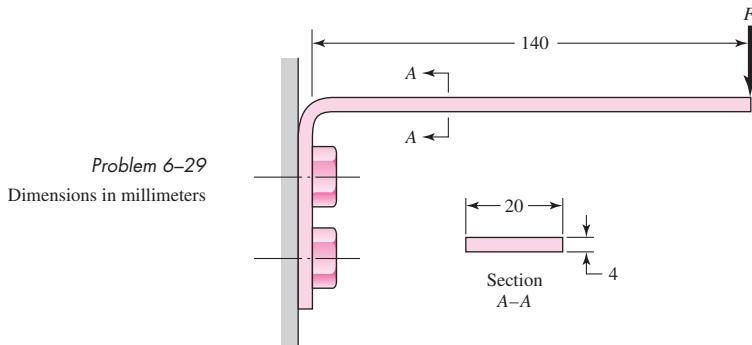


6-29

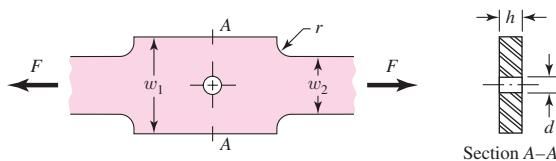
The figure is a drawing of a 4- by 20-mm latching spring. A preload is obtained during assembly by shimming under the bolts to obtain an estimated initial deflection of 2 mm. The latching operation itself requires an additional deflection of exactly 4 mm. The material is ground high-carbon steel, bent then hardened and tempered to a minimum hardness of 490 Bhn. The radius of the bend is 4 mm. Estimate the yield strength to be 90 percent of the ultimate strength.

(a) Find the maximum and minimum latching forces.

(b) Is it likely the spring will achieve infinite life?

**6-30**

The figure shows the free-body diagram of a connecting-link portion having stress concentration at three sections. The dimensions are $r = 0.25$ in, $d = 0.40$ in, $h = 0.50$ in, $w_1 = 3.50$ in, and $w_2 = 3.0$ in. The forces F fluctuate between a tension of 5 kip and a compression of 16 kip. Neglect column action and find the least factor of safety if the material is cold-drawn AISI 1018 steel.

Problem 6-30**6-31**

Solve Prob. 6-30 except let $w_1 = 2.5$ in, $w_2 = 1.5$ in, and the force fluctuates between a tension of 16 kips and a compression of 4 kips.

6-32

For the part in Prob. 6-30, recommend a fillet radius r that will cause the fatigue factor of safety to be the same at the hole and at the fillet.

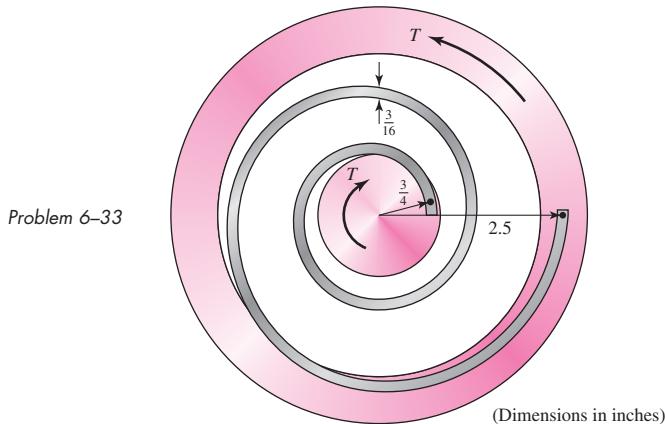
6-33

The torsional coupling in the figure is composed of a curved beam of square cross section that is welded to an input shaft and output plate. A torque is applied to the shaft and cycles from zero to T . The cross section of the beam has dimensions of $\frac{3}{16} \times \frac{3}{16}$ in, and the centroidal axis of the beam describes a curve of the form $r = 0.75 + 0.4375 \theta/\pi$, where r and θ are in inches and radians, respectively ($0 \leq \theta \leq 4\pi$). The curved beam has a machined surface with yield and ultimate strength values of 60 and 110 ksi, respectively.

(a) Determine the maximum allowable value of T such that the coupling will have an infinite life with a factor of safety, $n = 3$, using the modified Goodman criterion.

(b) Repeat part (a) using the Gerber criterion.

(c) Using T found in part (b), determine the factor of safety guarding against yield.



6-34 Repeat Prob. 6-33 ignoring curvature effects on the bending stress.

6-35 A part is loaded with a combination of bending, axial, and torsion such that the following stresses are created at a particular location:

- Bending: Completely reversed, with a maximum stress of 60 MPa
- Axial: Constant stress of 20 MPa
- Torsion: Repeated load, varying from 0 MPa to 50 MPa

Assume the varying stresses are in phase with each other. The part contains a notch such that $K_{f,bending} = 1.4$, $K_{f,axial} = 1.1$, and $K_{f,torsion} = 2.0$. The material properties are $S_y = 300$ MPa and $S_u = 400$ MPa. The completely adjusted endurance limit is found to be $S_e = 200$ MPa. Find the factor of safety for fatigue based on infinite life. If the life is not infinite, estimate the number of cycles. Be sure to check for yielding.

6-36 Repeat the requirements of Prob. 6-35 with the following loading conditions:

- Bending: Fluctuating stress from -40 MPa to 150 MPa
- Axial: None
- Torsion: Mean stress of 90 MPa, with an alternating stress of 10 percent of the mean stress

**6-37* to
6-46***

For the problem specified in the table, build upon the results of the original problem to determine the minimum factor of safety for fatigue based on infinite life. The shaft rotates at a constant speed, has a constant diameter, and is made from cold-drawn AISI 1018 steel.

Problem Number	Original Problem, Page Number
6-37*	3-68, 137
6-38*	3-69, 137
6-39*	3-70, 137
6-40*	3-71, 137
6-41*	3-72, 138
6-42*	3-73, 138
6-43*	3-74, 138
6-44*	3-76, 139
6-45*	3-77, 139
6-46*	3-79, 139

**6-47* to
6-50***

For the problem specified in the table, build upon the results of the original problem to determine the minimum factor of safety for fatigue based on infinite life. If the life is not infinite, estimate the number of cycles. The force F is applied as a repeated load. The material is AISI 1018 CD steel. The fillet radius at the wall is 0.1 in, with theoretical stress concentrations of 1.5 for bending, 1.2 for axial, and 2.1 for torsion.

Problem Number	Original Problem, Page Number
6-47*	3-80, 139
6-48*	3-81, 140
6-49*	3-82, 140
6-50*	3-83, 140

**6-51* to
6-53***

For the problem specified in the table, build upon the results of the original problem to determine the minimum factor of safety for fatigue at point A, based on infinite life. If the life is not infinite, estimate the number of cycles. The force F is applied as a repeated load. The material is AISI 1018 CD steel.

Problem Number	Original Problem, Page Number
6-51*	3-84, 140
6-52*	3-85, 141
6-53*	3-86, 141

6-54

Solve Prob. 6-17 except include a steady torque of 2500 lbf · in being transmitted through the shaft between the points of application of the forces.

6-55

Solve Prob. 6-18 except include a steady torque of 2200 lbf · in being transmitted through the shaft between the points of application of the forces.

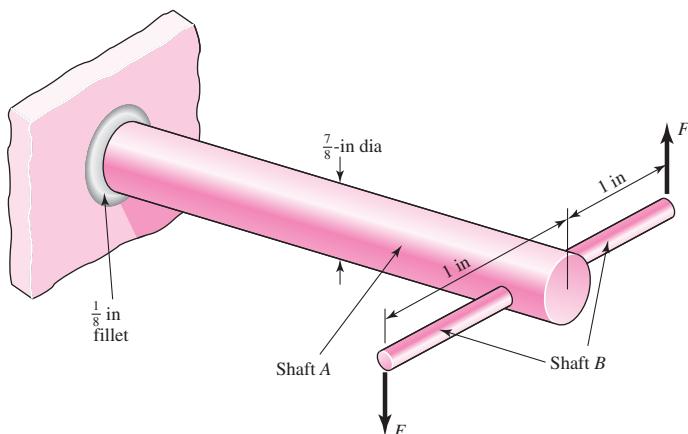
6-56

In the figure shown, shaft A, made of AISI 1020 hot-rolled steel, is welded to a fixed support and is subjected to loading by equal and opposite forces F via shaft B. A theoretical stress-concentration factor K_{ts} of 1.6 is induced by the $\frac{1}{8}$ -in fillet. The length of shaft A from the fixed support to the connection at shaft B is 2 ft. The load F cycles from 150 to 500 lbf.

(a) For shaft A, find the factor of safety for infinite life using the modified Goodman fatigue failure criterion.

(b) Repeat part (a) using the Gerber fatigue failure criterion.

Problem 6-56



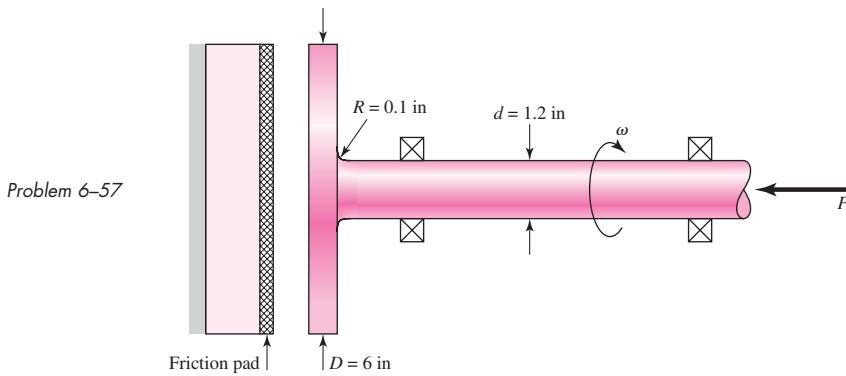
6-57

A schematic of a clutch-testing machine is shown. The steel shaft rotates at a constant speed ω . An axial load is applied to the shaft and is cycled from zero to P . The torque T induced by the clutch face onto the shaft is given by

$$T = \frac{f P(D + d)}{4}$$

where D and d are defined in the figure and f is the coefficient of friction of the clutch face. The shaft is machined with $S_y = 120$ kpsi and $S_{ut} = 145$ kpsi. The theoretical stress-concentration factors for the fillet are 3.0 and 1.8 for the axial and torsional loading, respectively.

Assume the load variation P is synchronous with shaft rotation. With $f = 0.3$, find the maximum allowable load P such that the shaft will survive a minimum of 10^6 cycles with a factor of safety of 3. Use the modified Goodman criterion. Determine the corresponding factor of safety guarding against yielding.

**6-58**

For the clutch of Prob. 6-57, the external load P is cycled between 4.5 kips and 18 kips. Assuming that the shaft is rotating synchronous with the external load cycle, estimate the number of cycles to failure. Use the modified Goodman fatigue failure criteria.

6-59

A flat leaf spring has fluctuating stress of $\sigma_{\max} = 360$ MPa and $\sigma_{\min} = 160$ MPa applied for $8(10^4)$ cycles. If the load changes to $\sigma_{\max} = 320$ MPa and $\sigma_{\min} = -200$ MPa, how many cycles should the spring survive? The material is AISI 1020 CD and has a fully corrected endurance strength of $S_e = 175$ MPa. Assume that $f = 0.9$.

(a) Use Miner's method.

(b) Use Manson's method.

6-60

A rotating-beam specimen with an endurance limit of 50 kpsi and an ultimate strength of 140 kpsi is cycled 20 percent of the time at 95 kpsi, 50 percent at 80 kpsi, and 30 percent at 65 kpsi. Let $f = 0.8$ and estimate the number of cycles to failure.

6-61

A machine part will be cycled at ± 350 MPa for $5(10^3)$ cycles. Then the loading will be changed to ± 260 MPa for $5(10^4)$ cycles. Finally, the load will be changed to ± 225 MPa. How many cycles of operation can be expected at this stress level? For the part, $S_{ut} = 530$ MPa, $f = 0.9$, and has a fully corrected endurance strength of $S_e = 210$ MPa.

(a) Use Miner's method.

(b) Use Manson's method.

6-62

The material properties of a machine part are $S_{ut} = 85$ kpsi, $f = 0.86$, and a fully corrected endurance limit of $S_e = 45$ kpsi. The part is to be cycled at $\sigma_a = 35$ kpsi and $\sigma_m = 30$ kpsi

for 12 (10^3) cycles. Using the Gerber criterion, estimate the new endurance limit after cycling.

- (a) Use Miner's method.
- (b) Use Manson's method.

6-63 Repeat Prob. 6-62 using the Goodman criterion.

Stochastic Problems

6-64 Solve Prob. 6-1 if the ultimate strength of production pieces is found to be $S_{ut} = 1030LN(1, 0.0508)$ MPa.

6-65 The situation is similar to that of Prob. 6-14 wherein the imposed completely reversed axial load $F_a = 3.8LN(1, 0.20)$ kip is to be carried by the link with a thickness to be specified by you, the designer. Use the 1020 cold-drawn steel of Prob. 6-14 with $S_{ut} = 68LN(1, 0.28)$ and $S_y = 57LN(1, 0.058)$ kpsi. The reliability goal must exceed 0.99. Using the correlation method, specify the thickness t .

6-66 A solid round steel bar is machined to a diameter of 32 mm. A groove 3 mm deep with a radius of 3 mm is cut into the bar. The material has a mean tensile strength of 780 MPa. A completely reversed bending moment $M = 160$ N · m is applied. Estimate the reliability. The size factor should be based on the gross diameter. The bar rotates.

6-67 Repeat Prob. 6-66, with a completely reversed torsional moment of $T = 160$ N · m applied.

6-68 A $1\frac{1}{2}$ -in-diameter hot-rolled steel bar has a $\frac{3}{16}$ -in diameter hole drilled transversely through it. The bar is nonrotating and is subject to a completely reversed bending moment of $M = 1500$ lbf · in in the same plane as the axis of the transverse hole. The material has a mean tensile strength of 76 kpsi. Estimate the reliability. The size factor should be based on the gross size. Use Table A-16 for K_t .

6-69 Repeat Prob. 6-68, with the bar subject to a completely reversed torsional moment of 2000 lbf · in.

6-70 The plan view of a link is the same as in Prob. 6-30; however, the forces F are completely reversed, the reliability goal is 0.998, and the material properties are $S_{ut} = 64LN(1, 0.045)$ kpsi and $S_y = 54LN(1, 0.077)$ kpsi. Treat F_a as deterministic, and specify the thickness h .

Computer Problems

6-71 A $\frac{1}{4}$ by $1\frac{1}{2}$ -in steel bar has a $\frac{3}{4}$ -in drilled hole located in the center, much as is shown in Table A-15-1. The bar is subjected to a completely reversed axial load with a deterministic load of 1200 lbf. The material has a mean ultimate tensile strength of $\bar{S}_{ut} = 80$ kpsi.

- (a) Estimate the reliability.
- (b) Conduct a computer simulation to confirm your answer to part a.

6-72 From your experience with Prob. 6-71 and Ex. 6-19, you observed that for completely reversed axial and bending fatigue, it is possible to

- Observe the COVs associated with a priori design considerations.
- Note the reliability goal.
- Find the mean design factor \bar{n}_d that will permit making a geometric design decision that will attain the goal using deterministic methods in conjunction with \bar{n}_d .

Formulate an interactive computer program that will enable the user to find \bar{n}_d . While the material properties S_{ut} , S_y , and the load COV must be input by the user, all of the COVs associated with

$\phi_{0.30}$, \mathbf{k}_a , \mathbf{k}_c , \mathbf{k}_d , and \mathbf{K}_f can be internal, and answers to questions will allow C_σ and C_S , as well as C_n and \bar{n}_d , to be calculated. Later you can add improvements. Test your program with problems you have already solved.

- 6-73** When using the Gerber fatigue failure criterion in a stochastic problem, Eqs. (6-80) and (6-81) are useful. They are also computationally complicated. It is helpful to have a computer subroutine or procedure that performs these calculations. When writing an executive program, and it is appropriate to find S_a and C_{Sa} , a simple call to the subroutine does this with a minimum of effort. Also, once the subroutine is tested, it is always ready to perform. Write and test such a program.
- 6-74** Repeat Problem 6-73 for the ASME-elliptic fatigue failure locus, implementing Eqs. (6-82) and (6-83).
- 6-75** Repeat Prob. 6-73 for the Smith-Dolan fatigue failure locus, implementing Eqs. (6-86) and (6-87).
- 6-76** Write and test computer subroutines or procedures that will implement
(a) Table 6-2, returning a , b , C , and \bar{k}_a .
(b) Equation (6-20) using Table 6-4, returning k_b .
(c) Table 6-11, returning α , β , C , and \bar{k}_c .
(d) Equations (6-27) and (6-75), returning \bar{k}_d and C_{kd} .
- 6-77** Write and test a computer subroutine or procedure that implements Eqs. (6-76) and (6-77), returning \bar{q} , $\hat{\sigma}_q$, and C_q .
- 6-78** Write and test a computer subroutine or procedure that implements Eq. (6-78) and Table 6-15, returning \sqrt{a} , C_{Kf} , and \bar{K}_f .

This page intentionally left blank

PART

3

Design of Mechanical Elements



7

Shafts and Shaft Components

Chapter Outline

- 7-1** Introduction **360**
- 7-2** Shaft Materials **360**
- 7-3** Shaft Layout **361**
- 7-4** Shaft Design for Stress **366**
- 7-5** Deflection Considerations **379**
- 7-6** Critical Speeds for Shafts **383**
- 7-7** Miscellaneous Shaft Components **388**
- 7-8** Limits and Fits **395**

7-1 Introduction

A *shaft* is a rotating member, usually of circular cross section, used to transmit power or motion. It provides the axis of rotation, or oscillation, of elements such as gears, pulleys, flywheels, cranks, sprockets, and the like and controls the geometry of their motion. An *axle* is a nonrotating member that carries no torque and is used to support rotating wheels, pulleys, and the like. The automotive axle is not a true axle; the term is a carryover from the horse-and-buggy era, when the wheels rotated on nonrotating members. A nonrotating axle can readily be designed and analyzed as a static beam, and will not warrant the special attention given in this chapter to the rotating shafts which are subject to fatigue loading.

There is really nothing unique about a shaft that requires any special treatment beyond the basic methods already developed in previous chapters. However, because of the ubiquity of the shaft in so many machine design applications, there is some advantage in giving the shaft and its design a closer inspection. A complete shaft design has much interdependence on the design of the components. The design of the machine itself will dictate that certain gears, pulleys, bearings, and other elements will have at least been partially analyzed and their size and spacing tentatively determined. Chapter 18 provides a complete case study of a power transmission, focusing on the overall design process. In this chapter, details of the shaft itself will be examined, including the following:

- Material selection
- Geometric layout
- Stress and strength
 - Static strength
 - Fatigue strength
- Deflection and rigidity
 - Bending deflection
 - Torsional deflection
 - Slope at bearings and shaft-supported elements
 - Shear deflection due to transverse loading of short shafts
- Vibration due to natural frequency

In deciding on an approach to shaft sizing, it is necessary to realize that a stress analysis at a specific point on a shaft can be made using only the shaft geometry in the vicinity of that point. Thus the geometry of the entire shaft is not needed. In design it is usually possible to locate the critical areas, size these to meet the strength requirements, and then size the rest of the shaft to meet the requirements of the shaft-supported elements.

The deflection and slope analyses cannot be made until the geometry of the entire shaft has been defined. Thus deflection is a function of the geometry *everywhere*, whereas the stress at a section of interest is a function of *local geometry*. For this reason, shaft design allows a consideration of stress first. Then, after tentative values for the shaft dimensions have been established, the determination of the deflections and slopes can be made.

7-2 Shaft Materials

Deflection is not affected by strength, but rather by stiffness as represented by the modulus of elasticity, which is essentially constant for all steels. For that reason, rigidity cannot be controlled by material decisions, but only by geometric decisions.

Necessary strength to resist loading stresses affects the choice of materials and their treatments. Many shafts are made from low carbon, cold-drawn or hot-rolled steel, such as ANSI 1020-1050 steels.

Significant strengthening from heat treatment and high alloy content are often not warranted. Fatigue failure is reduced moderately by increase in strength, and then only to a certain level before adverse effects in endurance limit and notch sensitivity begin to counteract the benefits of higher strength. A good practice is to start with an inexpensive, low or medium carbon steel for the first time through the design calculations. If strength considerations turn out to dominate over deflection, then a higher strength material should be tried, allowing the shaft sizes to be reduced until excess deflection becomes an issue. The cost of the material and its processing must be weighed against the need for smaller shaft diameters. When warranted, typical alloy steels for heat treatment include ANSI 1340-50, 3140-50, 4140, 4340, 5140, and 8650.

Shafts usually don't need to be surface hardened unless they serve as the actual journal of a bearing surface. Typical material choices for surface hardening include carburizing grades of ANSI 1020, 4320, 4820, and 8620.

Cold drawn steel is usually used for diameters under about 3 inches. The nominal diameter of the bar can be left unmachined in areas that do not require fitting of components. Hot rolled steel should be machined all over. For large shafts requiring much material removal, the residual stresses may tend to cause warping. If concentricity is important, it may be necessary to rough machine, then heat treat to remove residual stresses and increase the strength, then finish machine to the final dimensions.

In approaching material selection, the amount to be produced is a salient factor. For low production, turning is the usual primary shaping process. An economic viewpoint may require removing the least material. High production may permit a volume-conservative shaping method (hot or cold forming, casting), and minimum material in the shaft can become a design goal. Cast iron may be specified if the production quantity is high, and the gears are to be integrally cast with the shaft.

Properties of the shaft locally depend on its history—cold work, cold forming, rolling of fillet features, heat treatment, including quenching medium, agitation, and tempering regimen.¹

Stainless steel may be appropriate for some environments.

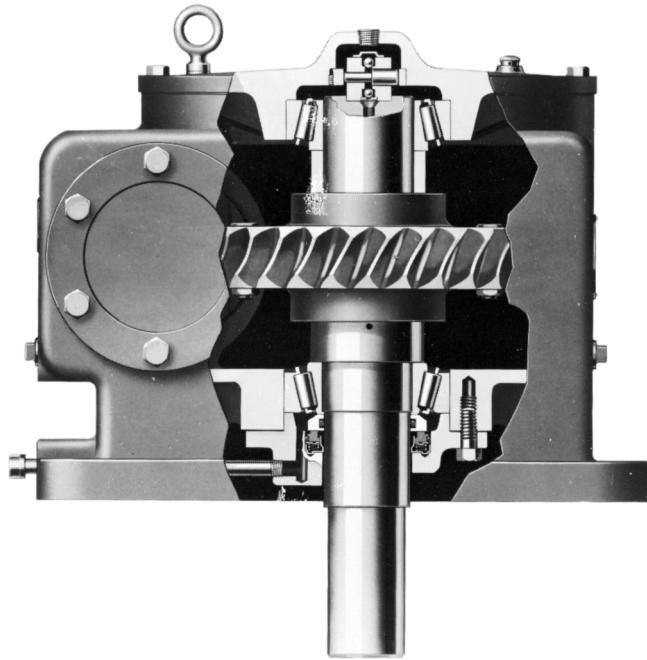
7-3 Shaft Layout

The general layout of a shaft to accommodate shaft elements, e.g., gears, bearings, and pulleys, must be specified early in the design process in order to perform a free body force analysis and to obtain shear-moment diagrams. The geometry of a shaft is generally that of a stepped cylinder. The use of shaft shoulders is an excellent means of axially locating the shaft elements and to carry any thrust loads. Figure 7-1 shows an example of a stepped shaft supporting the gear of a worm-gear speed reducer. Each shoulder in the shaft serves a specific purpose, which you should attempt to determine by observation.

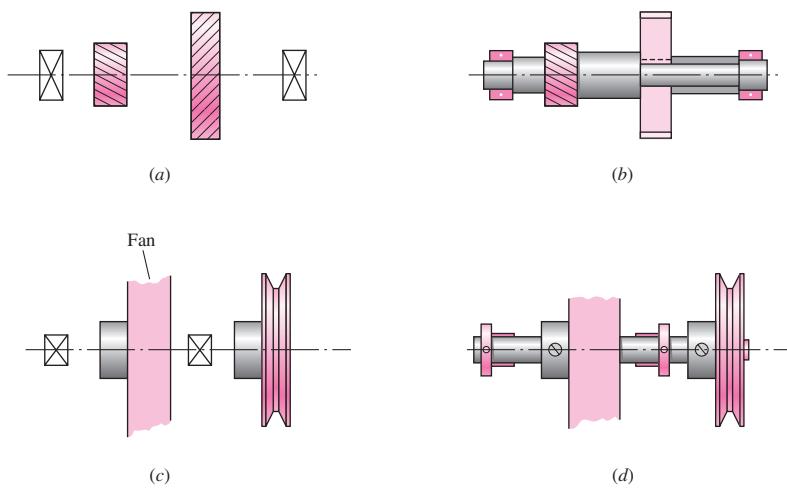
¹See Joseph E. Shigley, Charles R. Mischke, and Thomas H. Brown, Jr. (eds-in-chief), *Standard Handbook of Machine Design*, 3rd ed., McGraw-Hill, New York, 2004. For cold-worked property prediction see Chap. 29, and for heat-treated property prediction see Chaps. 29 and 33.

Figure 7-1

A vertical worm-gear speed reducer. (Courtesy of the Cleveland Gear Company.)

**Figure 7-2**

- (a) Choose a shaft configuration to support and locate the two gears and two bearings. (b) Solution uses an integral pinion, three shaft shoulders, key and keyway, and sleeve. The housing locates the bearings on their outer rings and receives the thrust loads. (c) Choose fan-shaft configuration. (d) Solution uses sleeve bearings, a straight-through shaft, locating collars, and setscrews for collars, fan pulley, and fan itself. The fan housing supports the sleeve bearings.



The geometric configuration of a shaft to be designed is often simply a revision of existing models in which a limited number of changes must be made. If there is no existing design to use as a starter, then the determination of the shaft layout may have many solutions. This problem is illustrated by the two examples of Fig. 7-2. In Fig. 7-2a a geared countershaft is to be supported by two bearings. In Fig. 7-2c a fanshaft is to be configured. The solutions shown in Fig. 7-2b and 7-2d are not necessarily the best ones, but they do illustrate how the shaft-mounted devices are fixed and located in the axial direction, and how provision is made for torque transfer from one element to another. There are no absolute rules for specifying the general layout, but the following guidelines may be helpful.

Axial Layout of Components

The axial positioning of components is often dictated by the layout of the housing and other meshing components. In general, it is best to support load-carrying components between bearings, such as in Fig. 7–2a, rather than cantilevered outboard of the bearings, such as in Fig. 7–2c. Pulleys and sprockets often need to be mounted outboard for ease of installation of the belt or chain. The length of the cantilever should be kept short to minimize the deflection.

Only two bearings should be used in most cases. For extremely long shafts carrying several load-bearing components, it may be necessary to provide more than two bearing supports. In this case, particular care must be given to the alignment of the bearings.

Shafts should be kept short to minimize bending moments and deflections. Some axial space between components is desirable to allow for lubricant flow and to provide access space for disassembly of components with a puller. Load bearing components should be placed near the bearings, again to minimize the bending moment at the locations that will likely have stress concentrations, and to minimize the deflection at the load-carrying components.

The components must be accurately located on the shaft to line up with other mating components, and provision must be made to securely hold the components in position. The primary means of locating the components is to position them against a shoulder of the shaft. A shoulder also provides a solid support to minimize deflection and vibration of the component. Sometimes when the magnitudes of the forces are reasonably low, shoulders can be constructed with retaining rings in grooves, sleeves between components, or clamp-on collars. In cases where axial loads are very small, it may be feasible to do without the shoulders entirely, and rely on press fits, pins, or collars with setscrews to maintain an axial location. See Fig. 7–2b and 7–2d for examples of some of these means of axial location.

Supporting Axial Loads

In cases where axial loads are not trivial, it is necessary to provide a means to transfer the axial loads into the shaft, then through a bearing to the ground. This will be particularly necessary with helical or bevel gears, or tapered roller bearings, as each of these produces axial force components. Often, the same means of providing axial location, e.g., shoulders, retaining rings, and pins, will be used to also transmit the axial load into the shaft.

It is generally best to have only one bearing carry the axial load, to allow greater tolerances on shaft length dimensions, and to prevent binding if the shaft expands due to temperature changes. This is particularly important for long shafts. Figures 7–3 and 7–4 show examples of shafts with only one bearing carrying the axial load against a shoulder, while the other bearing is simply press-fit onto the shaft with no shoulder.

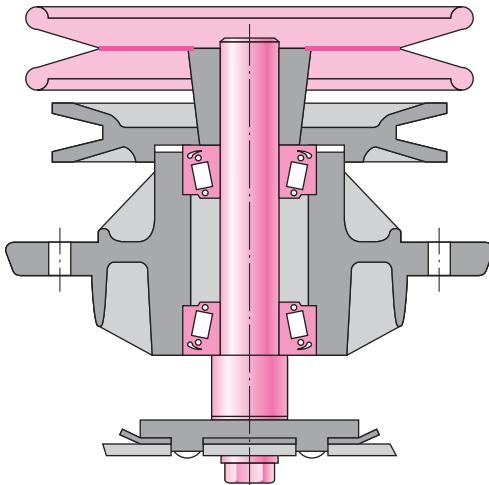
Providing for Torque Transmission

Most shafts serve to transmit torque from an input gear or pulley, through the shaft, to an output gear or pulley. Of course, the shaft itself must be sized to support the torsional stress and torsional deflection. It is also necessary to provide a means of transmitting the torque between the shaft and the gears. Common torque-transfer elements are:

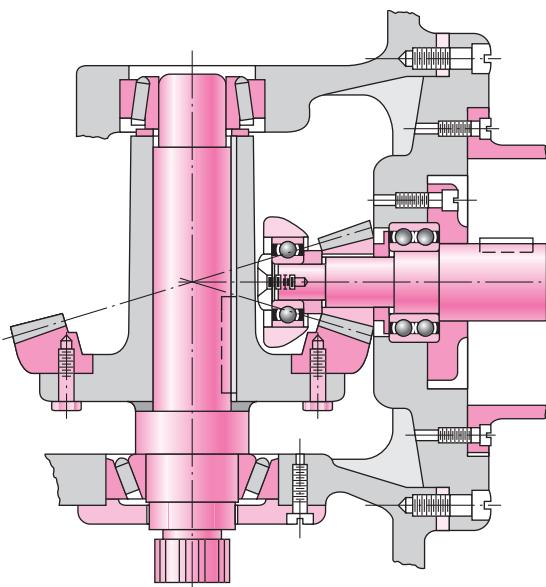
- Keys
- Splines
- Setscrews

Figure 7-3

Tapered roller bearings used in a mowing machine spindle. This design represents good practice for the situation in which one or more torque-transfer elements must be mounted outboard. (Source: Redrawn from material furnished by The Timken Company.)

**Figure 7-4**

A bevel-gear drive in which both pinion and gear are straddle-mounted. (Source: Redrawn from material furnished by Gleason Machine Division.)



- Pins
- Press or shrink fits
- Tapered fits

In addition to transmitting the torque, many of these devices are designed to fail if the torque exceeds acceptable operating limits, protecting more expensive components.

Details regarding hardware components such as *keys*, *pins*, and *setscrews* are addressed in detail in Sec. 7-7. One of the most effective and economical means of transmitting moderate to high levels of torque is through a key that fits in a groove in the shaft and gear. Keyed components generally have a slip fit onto the shaft, so assembly and disassembly is easy. The key provides for positive angular orientation of the component, which is useful in cases where phase angle timing is important.

Splines are essentially stubby gear teeth formed on the outside of the shaft and on the inside of the hub of the load-transmitting component. Splines are generally much more expensive to manufacture than keys, and are usually not necessary for simple torque transmission. They are typically used to transfer high torques. One feature of a spline is that it can be made with a reasonably loose slip fit to allow for large axial motion between the shaft and component while still transmitting torque. This is useful for connecting two shafts where relative motion between them is common, such as in connecting a power takeoff (PTO) shaft of a tractor to an implement. SAE and ANSI publish standards for splines. Stress-concentration factors are greatest where the spline ends and blends into the shaft, but are generally quite moderate.

For cases of low torque transmission, various means of transmitting torque are available. These include pins, setscrews in hubs, tapered fits, and press fits.

Press and shrink fits for securing hubs to shafts are used both for torque transfer and for preserving axial location. The resulting stress-concentration factor is usually quite small. See Sec. 7–8 for guidelines regarding appropriate sizing and tolerancing to transmit torque with press and shrink fits. A similar method is to use a split hub with screws to clamp the hub to the shaft. This method allows for disassembly and lateral adjustments. Another similar method uses a two-part hub consisting of a split inner member that fits into a tapered hole. The assembly is then tightened to the shaft with screws, which forces the inner part into the wheel and clamps the whole assembly against the shaft.

Tapered fits between the shaft and the shaft-mounted device, such as a wheel, are often used on the overhanging end of a shaft. Screw threads at the shaft end then permit the use of a nut to lock the wheel tightly to the shaft. This approach is useful because it can be disassembled, but it does not provide good axial location of the wheel on the shaft.

At the early stages of the shaft layout, the important thing is to select an appropriate means of transmitting torque, and to determine how it affects the overall shaft layout. It is necessary to know where the shaft discontinuities, such as keyways, holes, and splines, will be in order to determine critical locations for analysis.

Assembly and Disassembly

Consideration should be given to the method of assembling the components onto the shaft, and the shaft assembly into the frame. This generally requires the largest diameter in the center of the shaft, with progressively smaller diameters towards the ends to allow components to be slid on from the ends. If a shoulder is needed on both sides of a component, one of them must be created by such means as a retaining ring or by a sleeve between two components. The gearbox itself will need means to physically position the shaft into its bearings, and the bearings into the frame. This is typically accomplished by providing access through the housing to the bearing at one end of the shaft. See Figs. 7–5 through 7–8 for examples.

Figure 7–5

Arrangement showing bearing inner rings press-fitted to shaft while outer rings float in the housing. The axial clearance should be sufficient only to allow for machinery vibrations. Note the labyrinth seal on the right.

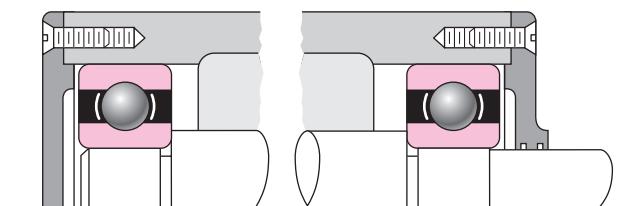
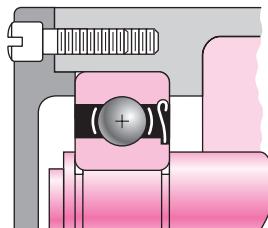
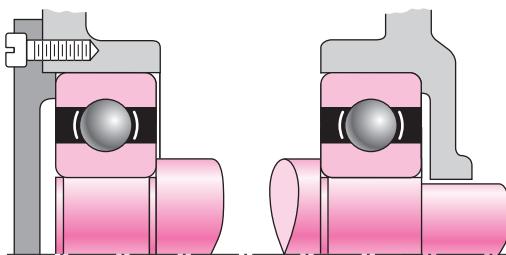
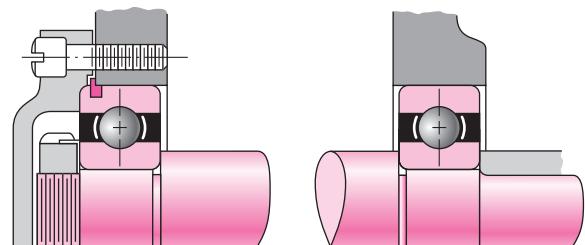


Figure 7-6

Similar to the arrangement of Fig. 7-5 except that the outer bearing rings are preloaded.

**Figure 7-8**

This arrangement is similar to Fig. 7-7 in that the left-hand bearing positions the entire shaft assembly. In this case the inner ring is secured to the shaft using a snap ring. Note the use of a shield to prevent dirt generated from within the machine from entering the bearing.

**Figure 7-7**

In this arrangement the inner ring of the left-hand bearing is locked to the shaft between a nut and a shaft shoulder. The locknut and washer are AFBMA standard. The snap ring in the outer race is used to positively locate the shaft assembly in the axial direction. Note the floating right-hand bearing and the grinding runout grooves in the shaft.

When components are to be press-fit to the shaft, the shaft should be designed so that it is not necessary to press the component down a long length of shaft. This may require an extra change in diameter, but it will reduce manufacturing and assembly cost by only requiring the close tolerance for a short length.

Consideration should also be given to the necessity of disassembling the components from the shaft. This requires consideration of issues such as accessibility of retaining rings, space for pullers to access bearings, openings in the housing to allow pressing the shaft or bearings out, etc.

7-4

Shaft Design for Stress

Critical Locations

It is not necessary to evaluate the stresses in a shaft at every point; a few potentially critical locations will suffice. Critical locations will usually be on the outer surface, at axial locations where the bending moment is large, where the torque is present, and where stress concentrations exist. By direct comparison of various points along the shaft, a few critical locations can be identified upon which to base the design. An assessment of typical stress situations will help.

Most shafts will transmit torque through a portion of the shaft. Typically the torque comes into the shaft at one gear and leaves the shaft at another gear. A free body diagram of the shaft will allow the torque at any section to be determined. The torque is often relatively constant at steady state operation. The shear stress due to the torsion will be greatest on outer surfaces.

The bending moments on a shaft can be determined by shear and bending moment diagrams. Since most shaft problems incorporate gears or pulleys that introduce forces in two planes, the shear and bending moment diagrams will generally be needed in two planes. Resultant moments are obtained by summing moments as vectors at points of interest along the shaft. The phase angle of the moments is not important since the shaft rotates. A steady bending moment will produce a completely reversed moment on a rotating shaft, as a specific stress element will alternate from compression to tension in every revolution of the shaft. The normal stress due to bending moments will be greatest on the outer surfaces. In situations where a bearing is located at the end of the shaft, stresses near the bearing are often not critical since the bending moment is small.

Axial stresses on shafts due to the axial components transmitted through helical gears or tapered roller bearings will almost always be negligibly small compared to the bending moment stress. They are often also constant, so they contribute little to fatigue. Consequently, it is usually acceptable to neglect the axial stresses induced by the gears and bearings when bending is present in a shaft. If an axial load is applied to the shaft in some other way, it is not safe to assume it is negligible without checking magnitudes.

Shaft Stresses

Bending, torsion, and axial stresses may be present in both midrange and alternating components. For analysis, it is simple enough to combine the different types of stresses into alternating and midrange von Mises stresses, as shown in Sec. 6–14, p. 317. It is sometimes convenient to customize the equations specifically for shaft applications. Axial loads are usually comparatively very small at critical locations where bending and torsion dominate, so they will be left out of the following equations. The fluctuating stresses due to bending and torsion are given by

$$\sigma_a = K_f \frac{M_a c}{I} \quad \sigma_m = K_f \frac{M_m c}{I} \quad (7-1)$$

$$\tau_a = K_{fs} \frac{T_a c}{J} \quad \tau_m = K_{fs} \frac{T_m c}{J} \quad (7-2)$$

where M_m and M_a are the midrange and alternating bending moments, T_m and T_a are the midrange and alternating torques, and K_f and K_{fs} are the fatigue stress-concentration factors for bending and torsion, respectively.

Assuming a solid shaft with round cross section, appropriate geometry terms can be introduced for c , I , and J resulting in

$$\sigma_a = K_f \frac{32M_a}{\pi d^3} \quad \sigma_m = K_f \frac{32M_m}{\pi d^3} \quad (7-3)$$

$$\tau_a = K_{fs} \frac{16T_a}{\pi d^3} \quad \tau_m = K_{fs} \frac{16T_m}{\pi d^3} \quad (7-4)$$

Combining these stresses in accordance with the distortion energy failure theory, the von Mises stresses for rotating round, solid shafts, neglecting axial loads, are given by

$$\sigma'_a = (\sigma_a^2 + 3\tau_a^2)^{1/2} = \left[\left(\frac{32K_f M_a}{\pi d^3} \right)^2 + 3 \left(\frac{16K_{fs} T_a}{\pi d^3} \right)^2 \right]^{1/2} \quad (7-5)$$

$$\sigma'_m = (\sigma_m^2 + 3\tau_m^2)^{1/2} = \left[\left(\frac{32K_f M_m}{\pi d^3} \right)^2 + 3 \left(\frac{16K_{fs} T_m}{\pi d^3} \right)^2 \right]^{1/2} \quad (7-6)$$

Note that the stress-concentration factors are sometimes considered optional for the midrange components with ductile materials, because of the capacity of the ductile material to yield locally at the discontinuity.

These equivalent alternating and midrange stresses can be evaluated using an appropriate failure curve on the modified Goodman diagram (See Sec. 6–12, p. 303, and Fig. 6–27). For example, the fatigue failure criteria for the modified Goodman line as expressed previously in Eq. (6–46) is

$$\frac{1}{n} = \frac{\sigma'_a}{S_e} + \frac{\sigma'_m}{S_{ut}}$$

Substitution of σ'_a and σ'_m from Eqs. (7–5) and (7–6) results in

$$\frac{1}{n} = \frac{16}{\pi d^3} \left\{ \frac{1}{S_e} [4(K_f M_a)^2 + 3(K_{fs} T_a)^2]^{1/2} + \frac{1}{S_{ut}} [4(K_f M_m)^2 + 3(K_{fs} T_m)^2]^{1/2} \right\}$$

For design purposes, it is also desirable to solve the equation for the diameter. This results in

$$d = \left(\frac{16n}{\pi} \left\{ \frac{1}{S_e} [4(K_f M_a)^2 + 3(K_{fs} T_a)^2]^{1/2} + \frac{1}{S_{ut}} [4(K_f M_m)^2 + 3(K_{fs} T_m)^2]^{1/2} \right\} \right)^{1/3}$$

Similar expressions can be obtained for any of the common failure criteria by substituting the von Mises stresses from Eqs. (7–5) and (7–6) into any of the failure criteria expressed by Eqs. (6–45) through (6–48), p. 306. The resulting equations for several of the commonly used failure curves are summarized below. The names given to each set of equations identifies the significant failure theory, followed by a fatigue failure locus name. For example, DE-Gerber indicates the stresses are combined using the distortion energy (DE) theory, and the Gerber criteria is used for the fatigue failure.

DE-Goodman

$$\frac{1}{n} = \frac{16}{\pi d^3} \left\{ \frac{1}{S_e} [4(K_f M_a)^2 + 3(K_{fs} T_a)^2]^{1/2} + \frac{1}{S_{ut}} [4(K_f M_m)^2 + 3(K_{fs} T_m)^2]^{1/2} \right\} \quad (7-7)$$

$$d = \left(\frac{16n}{\pi} \left\{ \frac{1}{S_e} [4(K_f M_a)^2 + 3(K_{fs} T_a)^2]^{1/2} + \frac{1}{S_{ut}} [4(K_f M_m)^2 + 3(K_{fs} T_m)^2]^{1/2} \right\} \right)^{1/3} \quad (7-8)$$

DE-Gerber

$$\frac{1}{n} = \frac{8A}{\pi d^3 S_e} \left\{ 1 + \left[1 + \left(\frac{2BS_e}{AS_{ut}} \right)^2 \right]^{1/2} \right\} \quad (7-9)$$

$$d = \left(\frac{8nA}{\pi S_e} \left\{ 1 + \left[1 + \left(\frac{2BS_e}{AS_{ut}} \right)^2 \right]^{1/2} \right\} \right)^{1/3} \quad (7-10)$$

where

$$A = \sqrt{4(K_f M_a)^2 + 3(K_{fs} T_a)^2}$$

$$B = \sqrt{4(K_f M_m)^2 + 3(K_{fs} T_m)^2}$$

DE-ASME Elliptic

$$\frac{1}{n} = \frac{16}{\pi d^3} \left[4 \left(\frac{K_f M_a}{S_e} \right)^2 + 3 \left(\frac{K_{fs} T_a}{S_e} \right)^2 + 4 \left(\frac{K_f M_m}{S_y} \right)^2 + 3 \left(\frac{K_{fs} T_m}{S_y} \right)^2 \right]^{1/2} \quad (7-11)$$

$$d = \left\{ \frac{16n}{\pi} \left[4 \left(\frac{K_f M_a}{S_e} \right)^2 + 3 \left(\frac{K_{fs} T_a}{S_e} \right)^2 + 4 \left(\frac{K_f M_m}{S_y} \right)^2 + 3 \left(\frac{K_{fs} T_m}{S_y} \right)^2 \right]^{1/2} \right\}^{1/3} \quad (7-12)$$

DE-Soderberg

$$\frac{1}{n} = \frac{16}{\pi d^3} \left\{ \frac{1}{S_e} [4(K_f M_a)^2 + 3(K_{fs} T_a)^2]^{1/2} + \frac{1}{S_{yt}} [4(K_f M_m)^2 + 3(K_{fs} T_m)^2]^{1/2} \right\} \quad (7-13)$$

$$d = \left(\frac{16n}{\pi} \left\{ \frac{1}{S_e} [4(K_f M_a)^2 + 3(K_{fs} T_a)^2]^{1/2} + \frac{1}{S_{yt}} [4(K_f M_m)^2 + 3(K_{fs} T_m)^2]^{1/2} \right\} \right)^{1/3} \quad (7-14)$$

For a rotating shaft with constant bending and torsion, the bending stress is completely reversed and the torsion is steady. Equations (7-7) through (7-14) can be simplified by setting M_m and T_a equal to 0, which simply drops out some of the terms.

Note that in an analysis situation in which the diameter is known and the factor of safety is desired, as an alternative to using the specialized equations above, it is always still valid to calculate the alternating and mid-range stresses using Eqs. (7-5) and (7-6), and substitute them into one of the equations for the failure criteria, Eqs. (6-45) through (6-48), and solve directly for n . In a design situation, however, having the equations pre-solved for diameter is quite helpful.

It is always necessary to consider the possibility of static failure in the first load cycle. The Soderberg criteria inherently guards against yielding, as can be seen by noting that its failure curve is conservatively within the yield (Langer) line on Fig. 6-27, p. 305. The ASME Elliptic also takes yielding into account, but is not entirely conservative

throughout its entire range. This is evident by noting that it crosses the yield line in Fig. 6–27. The Gerber and modified Goodman criteria do not guard against yielding, requiring a separate check for yielding. A von Mises maximum stress is calculated for this purpose.

$$\begin{aligned}\sigma'_{\max} &= [(\sigma_m + \sigma_a)^2 + 3(\tau_m + \tau_a)^2]^{1/2} \\ &= \left[\left(\frac{32K_f(M_m + M_a)}{\pi d^3} \right)^2 + 3 \left(\frac{16K_{fs}(T_m + T_a)}{\pi d^3} \right)^2 \right]^{1/2}\end{aligned}\quad (7-15)$$

To check for yielding, this von Mises maximum stress is compared to the yield strength, as usual.

$$n_y = \frac{S_y}{\sigma'_{\max}} \quad (7-16)$$

For a quick, conservative check, an estimate for σ'_{\max} can be obtained by simply adding σ'_a and σ'_m . $(\sigma'_a + \sigma'_m)$ will always be greater than or equal to σ'_{\max} , and will therefore be conservative.

EXAMPLE 7-1

At a machined shaft shoulder the small diameter d is 1.100 in, the large diameter D is 1.65 in, and the fillet radius is 0.11 in. The bending moment is 1260 lbf · in and the steady torsion moment is 1100 lbf · in. The heat-treated steel shaft has an ultimate strength of $S_{ut} = 105$ kpsi and a yield strength of $S_y = 82$ kpsi. The reliability goal is 0.99.

- (a) Determine the fatigue factor of safety of the design using each of the fatigue failure criteria described in this section.
- (b) Determine the yielding factor of safety.

Solution

- (a) $D/d = 1.65/1.100 = 1.50$, $r/d = 0.11/1.100 = 0.10$, $K_t = 1.68$ (Fig. A-15-9), $K_{ts} = 1.42$ (Fig. A-15-8), $q = 0.85$ (Fig. 6-20), $q_{\text{shear}} = 0.88$ (Fig. 6-21).

From Eq. (6-32),

$$K_f = 1 + 0.85(1.68 - 1) = 1.58$$

$$K_{fs} = 1 + 0.88(1.42 - 1) = 1.37$$

$$\text{Eq. (6-8):} \quad S'_e = 0.5(105) = 52.5 \text{ kpsi}$$

$$\text{Eq. (6-19):} \quad k_a = 2.70(105)^{-0.265} = 0.787$$

$$\text{Eq. (6-20):} \quad k_b = \left(\frac{1.100}{0.30} \right)^{-0.107} = 0.870$$

$$k_c = k_d = k_f = 1$$

Table 6–6:

$$k_e = 0.814$$

$$S_e = 0.787(0.870)0.814(52.5) = 29.3 \text{ kpsi}$$

For a rotating shaft, the constant bending moment will create a completely reversed bending stress.

$$M_a = 1260 \text{ lbf} \cdot \text{in} \quad T_m = 1100 \text{ lbf} \cdot \text{in} \quad M_m = T_a = 0$$

Applying Eq. (7–7) for the DE-Goodman criteria gives

$$\frac{1}{n} = \frac{16}{\pi(1.1)^3} \left\{ \frac{[4(1.58 \cdot 1260)^2]^{1/2}}{29300} + \frac{[3(1.37 \cdot 1100)^2]^{1/2}}{105000} \right\} = 0.615$$

Answer

$$n = 1.63 \quad \text{DE-Goodman}$$

Similarly, applying Eqs. (7–9), (7–11), and (7–13) for the other failure criteria,

Answer

$$n = 1.87 \quad \text{DE-Gerber}$$

Answer

$$n = 1.88 \quad \text{DE-ASME Elliptic}$$

Answer

$$n = 1.56 \quad \text{DE-Soderberg}$$

For comparison, consider an equivalent approach of calculating the stresses and applying the fatigue failure criteria directly. From Eqs. (7–5) and (7–6),

$$\sigma'_a = \left[\left(\frac{32 \cdot 1.58 \cdot 1260}{\pi(1.1)^3} \right)^2 \right]^{1/2} = 15235 \text{ psi}$$

$$\sigma'_m = \left[3 \left(\frac{16 \cdot 1.37 \cdot 1100}{\pi(1.1)^3} \right)^2 \right]^{1/2} = 9988 \text{ psi}$$

Taking, for example, the Goodman failure criteria, application of Eq. (6–46) gives

$$\frac{1}{n} = \frac{\sigma'_a}{S_e} + \frac{\sigma'_m}{S_{ut}} = \frac{15235}{29300} + \frac{9988}{105000} = 0.615$$

$$n = 1.63$$

which is identical with the previous result. The same process could be used for the other failure criteria.

(b) For the yielding factor of safety, determine an equivalent von Mises maximum stress using Eq. (7–15).

$$\sigma'_{\max} = \left[\left(\frac{32(1.58)(1260)}{\pi(1.1)^3} \right)^2 + 3 \left(\frac{16(1.37)(1100)}{\pi(1.1)^3} \right)^2 \right]^{1/2} = 18220 \text{ psi}$$

Answer

$$n_y = \frac{S_y}{\sigma'_{\max}} = \frac{82000}{18220} = 4.50$$

For comparison, a quick and very conservative check on yielding can be obtained by replacing σ'_{\max} with $\sigma'_a + \sigma'_m$. This just saves the extra time of calculating σ'_{\max} if σ'_a and σ'_m have already been determined. For this example,

$$n_y = \frac{S_y}{\sigma'_a + \sigma'_m} = \frac{82\,000}{15\,235 + 9\,988} = 3.25$$

which is quite conservative compared with $n_y = 4.50$.

Estimating Stress Concentrations

The stress analysis process for fatigue is highly dependent on stress concentrations. Stress concentrations for shoulders and keyways are dependent on size specifications that are not known the first time through the process. Fortunately, since these elements are usually of standard proportions, it is possible to estimate the stress-concentration factors for initial design of the shaft. These stress concentrations will be fine-tuned in successive iterations, once the details are known.

Shoulders for bearing and gear support should match the catalog recommendation for the specific bearing or gear. A look through bearing catalogs shows that a typical bearing calls for the ratio of D/d to be between 1.2 and 1.5. For a first approximation, the worst case of 1.5 can be assumed. Similarly, the fillet radius at the shoulder needs to be sized to avoid interference with the fillet radius of the mating component. There is a significant variation in typical bearings in the ratio of fillet radius versus bore diameter, with r/d typically ranging from around 0.02 to 0.06. A quick look at the stress concentration charts (Figures A-15-8 and A-15-9) shows that the stress concentrations for bending and torsion increase significantly in this range. For example, with $D/d = 1.5$ for bending, $K_t = 2.7$ at $r/d = 0.02$, and reduces to $K_t = 2.1$ at $r/d = 0.05$, and further down to $K_t = 1.7$ at $r/d = 0.1$. This indicates that this is an area where some attention to detail could make a significant difference. Fortunately, in most cases the shear and bending moment diagrams show that bending moments are quite low near the bearings, since the bending moments from the ground reaction forces are small.

In cases where the shoulder at the bearing is found to be critical, the designer should plan to select a bearing with generous fillet radius, or consider providing for a larger fillet radius on the shaft by relieving it into the base of the shoulder as shown in Fig. 7-9a. This effectively creates a dead zone in the shoulder area that does not

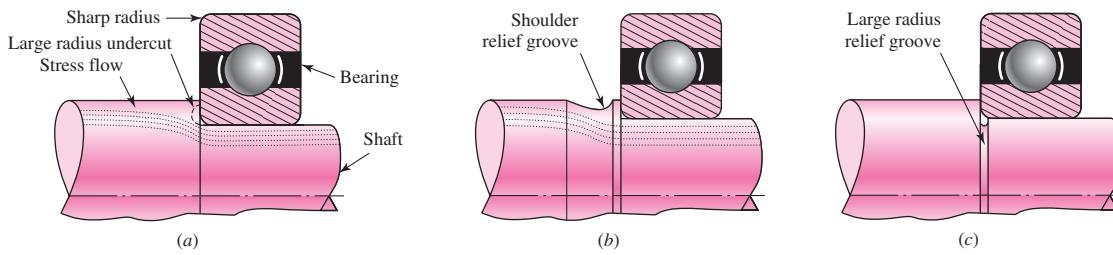


Figure 7-9

Techniques for reducing stress concentration at a shoulder supporting a bearing with a sharp radius. (a) Large radius undercut into the shoulder. (b) Large radius relief groove into the back of the shoulder. (c) Large radius relief groove into the small diameter.

carry the bending stresses, as shown by the stress flow lines. A shoulder relief groove as shown in Fig. 7–9b can accomplish a similar purpose. Another option is to cut a large-radius relief groove into the small diameter of the shaft, as shown in Fig. 7–9c. This has the disadvantage of reducing the cross-sectional area, but is often used in cases where it is useful to provide a relief groove before the shoulder to prevent the grinding or turning operation from having to go all the way to the shoulder.

For the standard shoulder fillet, for estimating K_t values for the first iteration, an r/d ratio should be selected so K_t values can be obtained. For the worst end of the spectrum, with $r/d = 0.02$ and $D/d = 1.5$, K_t values from the stress concentration charts for shoulders indicate 2.7 for bending, 2.2 for torsion, and 3.0 for axial.

A keyway will produce a stress concentration near a critical point where the load-transmitting component is located. The stress concentration in an end-milled keyseat is a function of the ratio of the radius r at the bottom of the groove and the shaft diameter d . For early stages of the design process, it is possible to estimate the stress concentration for keyways regardless of the actual shaft dimensions by assuming a typical ratio of $r/d = 0.02$. This gives $K_t = 2.14$ for bending and $K_{ts} = 3.0$ for torsion, assuming the key is in place.

Figures A–15–16 and A–15–17 give values for stress concentrations for flat-bottomed grooves such as used for retaining rings. By examining typical retaining ring specifications in vendor catalogs, it can be seen that the groove width is typically slightly greater than the groove depth, and the radius at the bottom of the groove is around 1/10 of the groove width. From Figs. A–15–16 and A–15–17, stress-concentration factors for typical retaining ring dimensions are around 5 for bending and axial, and 3 for torsion. Fortunately, the small radius will often lead to a smaller notch sensitivity, reducing K_f .

Table 7–1 summarizes some typical stress-concentration factors for the first iteration in the design of a shaft. Similar estimates can be made for other features. The point is to notice that stress concentrations are essentially normalized so that they are dependent on ratios of geometry features, not on the specific dimensions. Consequently, by estimating the appropriate ratios, the first iteration values for stress concentrations can be obtained. These values can be used for initial design, then actual values inserted once diameters have been determined.

Table 7–1

First Iteration Estimates for Stress-Concentration Factors K_t and K_{ts} .

Warning: These factors are only estimates for use when actual dimensions are not yet determined. Do *not* use these once actual dimensions are available.

	Bending	Torsional	Axial
Shoulder fillet—sharp ($r/d = 0.02$)	2.7	2.2	3.0
Shoulder fillet—well rounded ($r/d = 0.1$)	1.7	1.5	1.9
End-mill keyseat ($r/d = 0.02$)	2.14	3.0	—
Sled runner keyseat	1.7	—	—
Retaining ring groove	5.0	3.0	5.0

Missing values in the table are not readily available.

EXAMPLE 7-2

This example problem is part of a larger case study. See Chap. 18 for the full context.

A double reduction gearbox design has developed to the point that the general layout and axial dimensions of the countershaft carrying two spur gears has been proposed, as shown in Fig. 7-10. The gears and bearings are located and supported by shoulders, and held in place by retaining rings. The gears transmit torque through keys. Gears have been specified as shown, allowing the tangential and radial forces transmitted through the gears to be determined as follows.

$$W_{23}^t = 540 \text{ lbf}$$

$$W_{54}^t = 2431 \text{ lbf}$$

$$W_{23}^r = 197 \text{ lbf}$$

$$W_{54}^r = 885 \text{ lbf}$$

where the superscripts *t* and *r* represent tangential and radial directions, respectively; and, the subscripts 23 and 54 represent the forces exerted by gears 2 and 5 (not shown) on gears 3 and 4, respectively.

Proceed with the next phase of the design, in which a suitable material is selected, and appropriate diameters for each section of the shaft are estimated, based on providing sufficient fatigue and static stress capacity for infinite life of the shaft, with minimum safety factors of 1.5.

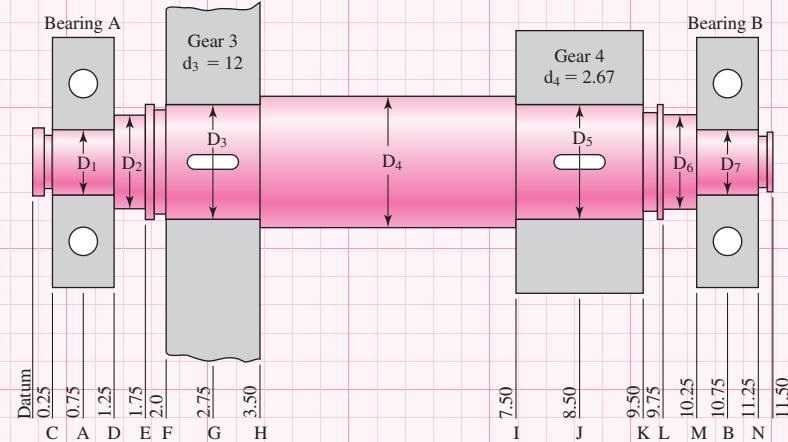


Figure 7-10

Shaft layout for Ex. 7-2. Dimensions in inches.

Solution

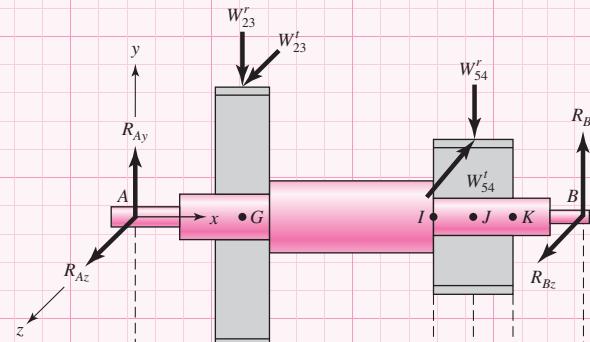
Perform free body diagram analysis to get reaction forces at the bearings.

$$R_{Az} = 115.0 \text{ lbf}$$

$$R_{Ay} = 356.7 \text{ lbf}$$

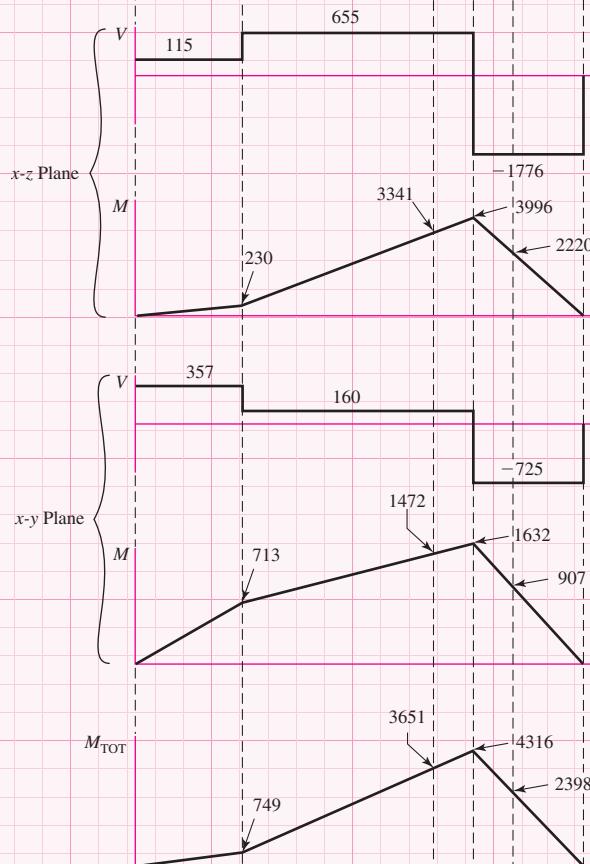
$$R_{Bz} = 1776.0 \text{ lbf}$$

$$R_{By} = 725.3 \text{ lbf}$$



From $\sum M_x$, find the torque in the shaft between the gears,
 $T = W_{23}^t(d_3/2) = 540(12/2) = 3240 \text{ lbf} \cdot \text{in.}$

Generate shear-moment diagrams for two planes.



Combine orthogonal planes as vectors to get total moments, e.g., at J, $\sqrt{3996^2 + 1632^2} = 4316 \text{ lbf} \cdot \text{in.}$

Start with Point I, where the bending moment is high, there is a stress concentration at the shoulder, and the torque is present.

At I, $M_a = 3651 \text{ lbf} \cdot \text{in}$, $T_m = 3240 \text{ lbf} \cdot \text{in}$, $M_m = T_a = 0$

Assume generous fillet radius for gear at I.

From Table 7-1, estimate $K_t = 1.7$, $K_{ts} = 1.5$. For quick, conservative first pass, assume $K_f = K_t$, $K_{fs} = K_{ts}$.

Choose inexpensive steel, 1020 CD, with $S_{ut} = 68$ kpsi. For S_e ,

$$\text{Eq. (6-19)} \quad k_a = aS_{ut}^b = 2.7(68)^{-0.265} = 0.883$$

Guess $k_b = 0.9$. Check later when d is known.

$$k_c = k_d = k_e = 1$$

$$\text{Eq. (6-18)} \quad S_e = (0.883)(0.9)(0.5)(68) = 27.0 \text{ kpsi}$$

For first estimate of the small diameter at the shoulder at point I, use the DE-Goodman criterion of Eq. (7-8). This criterion is good for the initial design, since it is simple and conservative. With $M_m = T_a = 0$, Eq. (7-8) reduces to

$$d = \left\{ \frac{16n}{\pi} \left(\frac{2(K_f M_a)}{S_e} + \frac{\left[3(K_{fs} T_m) \right]^{1/2}}{S_{ut}} \right) \right\}^{1/3}$$

$$d = \left\{ \frac{16(1.5)}{\pi} \left(\frac{2(1.7)(3651)}{27000} + \frac{\{3[(1.5)(3240)]^2\}^{1/2}}{68000} \right) \right\}^{1/3}$$

$$d = 1.65 \text{ in}$$

All estimates have probably been conservative, so select the next standard size below 1.65 in. and check, $d = 1.625$ in.

A typical D/d ratio for support at a shoulder is $D/d = 1.2$, thus, $D = 1.2(1.625) = 1.95$ in. Increase to $D = 2.0$ in. A nominal 2 in. cold-drawn shaft diameter can be used. Check if estimates were acceptable.

$$D/d = 2/1.625 = 1.23$$

Assume fillet radius $r = d/10 \cong 0.16$ in. $r/d = 0.1$

$$K_t = 1.6 \text{ (Fig. A-15-9)}, q = 0.82 \text{ (Fig. 6-20)}$$

$$\text{Eq. (6-32)} \quad K_f = 1 + 0.82(1.6 - 1) = 1.49$$

$$K_{ts} = 1.35 \text{ (Fig. A-15-8)}, q_s = 0.85 \text{ (Fig. 6-21)}$$

$$K_{fs} = 1 + 0.85(1.35 - 1) = 1.30$$

$$k_a = 0.883 \text{ (no change)}$$

$$\text{Eq. (6-20)} \quad k_b = \left(\frac{1.625}{0.3} \right)^{-0.107} = 0.835$$

$$S_e = (0.883)(0.835)(0.5)(68) = 25.1 \text{ kpsi}$$

$$\text{Eq. (7-5)} \quad \sigma'_a = \frac{32K_f M_a}{\pi d^3} = \frac{32(1.49)(3651)}{\pi(1.625)^3} = 12910 \text{ psi}$$

$$\text{Eq. (7-6)} \quad \sigma'_m = \left[3 \left(\frac{16K_{fs} T_m}{\pi d^3} \right)^2 \right]^{1/2} = \frac{\sqrt{3}(16)(1.30)(3240)}{\pi(1.625)^3} = 8659 \text{ psi}$$

Using Goodman criterion

$$\frac{1}{n_f} = \frac{\sigma'_a}{S_e} + \frac{\sigma'_m}{S_{ut}} = \frac{12910}{25100} + \frac{8659}{68000} = 0.642$$

$$n_f = 1.56$$

Note that we could have used Eq. (7-7) directly.

Check yielding.

$$n_y = \frac{S_y}{\sigma'_{\max}} > \frac{S_y}{\sigma'_a + \sigma'_m} = \frac{57\,000}{12\,910 + 8659} = 2.64$$

Also check this diameter at the end of the keyway, just to the right of point *I*, and at the groove at point *K*. From moment diagram, estimate M at end of keyway to be $M = 3750$ lbf-in.

Assume the radius at the bottom of the keyway will be the standard $r/d = 0.02$, $r = 0.02$ $d = 0.02$ (1.625) = 0.0325 in.

$$K_t = 2.14 \text{ (Table 7-1), } q = 0.65 \text{ (Fig. 6-20)}$$

$$K_f = 1 + 0.65(2.14 - 1) = 1.74$$

$$K_{ts} = 3.0 \text{ (Table 7-1), } q_s = 0.71 \text{ (Fig. 6-21)}$$

$$K_{fs} = 1 + 0.71(3 - 1) = 2.42$$

$$\sigma'_a = \frac{32K_f M_a}{\pi d^3} = \frac{32(1.74)(3750)}{\pi(1.625)^3} = 15\,490 \text{ psi}$$

$$\sigma'_m = \sqrt{3}(16) \frac{K_{fs} T_m}{\pi d^3} = \frac{\sqrt{3}(16)(2.42)(3240)}{\pi(1.625)^3} = 16\,120 \text{ psi}$$

$$\frac{1}{n_f} = \frac{\sigma'_a}{S_e} + \frac{\sigma'_m}{S_{ut}} = \frac{15\,490}{25\,100} + \frac{16\,120}{68\,000} = 0.854$$

$$n_f = 1.17$$

The keyway turns out to be more critical than the shoulder. We can either increase the diameter or use a higher strength material. Unless the deflection analysis shows a need for larger diameters, let us choose to increase the strength. We started with a very low strength and can afford to increase it some to avoid larger sizes. Try 1050 CD with $S_{ut} = 100$ ksi.

Recalculate factors affected by S_{ut} , i.e., $k_a \rightarrow S_e$; $q \rightarrow K_f \rightarrow \sigma'_a$

$$k_a = 2.7(100)^{-0.265} = 0.797, \quad S_e = 0.797(0.835)(0.5)(100) = 33.3 \text{ kpsi}$$

$$q = 0.72, \quad K_f = 1 + 0.72(2.14 - 1) = 1.82$$

$$\sigma'_a = \frac{32(1.82)(3750)}{\pi(1.625)^3} = 16\,200 \text{ psi}$$

$$\frac{1}{n_f} = \frac{16\,200}{33\,300} + \frac{16\,120}{100\,000} = 0.648$$

$$n_f = 1.54$$

Since the Goodman criterion is conservative, we will accept this as close enough to the requested 1.5.

Check at the groove at *K*, since K_t for flat-bottomed grooves are often very high. From the torque diagram, note that no torque is present at the groove. From the moment diagram, $M_a = 2398$ lbf · in, $M_m = T_a = T_m = 0$. To quickly check if this location is potentially critical, just use $K_f = K_t = 5.0$ as an estimate, from Table 7-1.

$$\sigma_a = \frac{32K_f M_a}{\pi d^3} = \frac{32(5)(2398)}{\pi(1.625)^3} = 28\,460 \text{ psi}$$

$$n_f = \frac{S_e}{\sigma_a} = \frac{33\,300}{28\,460} = 1.17$$

This is low. We will look up data for a specific retaining ring to obtain K_f more accurately. With a quick online search of a retaining ring specification using the website www.globalspec.com, appropriate groove specifications for a retaining ring for a shaft diameter of 1.625 in are obtained as follows: width, $a = 0.068$ in; depth, $t = 0.048$ in; and corner radius at bottom of groove, $r = 0.01$ in. From Fig. A-15-16, with $r/t = 0.01/0.048 = 0.208$, and $a/t = 0.068/0.048 = 1.42$

$$K_t = 4.3, q = 0.65 \text{ (Fig. 6-20)}$$

$$K_f = 1 + 0.65(4.3 - 1) = 3.15$$

$$\sigma_a = \frac{32K_f M_a}{\pi d^3} = \frac{32(3.15)(2398)}{\pi(1.625)^3} = 17930 \text{ psi}$$

$$n_f = \frac{S_e}{\sigma_a} = \frac{33300}{17930} = 1.86$$

Quickly check if point M might be critical. Only bending is present, and the moment is small, but the diameter is small and the stress concentration is high for a sharp fillet required for a bearing. From the moment diagram,

$M_a = 959 \text{ lbf} \cdot \text{in}$, and $M_m = T_m = T_a = 0$.

Estimate $K_t = 2.7$ from Table 7-1, $d = 1.0$ in, and fillet radius r to fit a typical bearing.

$$r/d = 0.02, r = 0.02(1) = 0.02$$

$$q = 0.7 \text{ (Fig. 6-20)}$$

$$K_f = 1 + (0.7)(2.7 - 1) = 2.19$$

$$\sigma_a = \frac{32K_f M_a}{\pi d^3} = \frac{32(2.19)(959)}{\pi(1)^3} = 21390 \text{ psi}$$

$$n_f = \frac{S_e}{\sigma_a} = \frac{33300}{21390} = 1.56$$

Should be OK. Close enough to recheck after bearing is selected.

With the diameters specified for the critical locations, fill in trial values for the rest of the diameters, taking into account typical shoulder heights for bearing and gear support.

$$D_1 = D_7 = 1.0 \text{ in}$$

$$D_2 = D_6 = 1.4 \text{ in}$$

$$D_3 = D_5 = 1.625 \text{ in}$$

$$D_4 = 2.0 \text{ in}$$

The bending moments are much less on the left end of shaft, so D_1 , D_2 , and D_3 could be smaller. However, unless weight is an issue, there is little advantage to requiring more material removal. Also, the extra rigidity may be needed to keep deflections small.

Table 7-2

Typical Maximum
Ranges for Slopes and
Transverse Deflections

Slopes	
Tapered roller	0.0005–0.0012 rad
Cylindrical roller	0.0008–0.0012 rad
Deep-groove ball	0.001–0.003 rad
Spherical ball	0.026–0.052 rad
Self-align ball	0.026–0.052 rad
Uncrowned spur gear	< 0.0005 rad
Transverse Deflections	
Spur gears with $P < 10$ teeth/in	0.010 in
Spur gears with $11 < P < 19$	0.005 in
Spur gears with $20 < P < 50$	0.003 in

7-5 Deflection Considerations

Deflection analysis at even a single point of interest requires complete geometry information for the entire shaft. For this reason, it is desirable to design the dimensions at critical locations to handle the stresses, and fill in reasonable estimates for all other dimensions, before performing a deflection analysis. Deflection of the shaft, both linear and angular, should be checked at gears and bearings. Allowable deflections will depend on many factors, and bearing and gear catalogs should be used for guidance on allowable misalignment for specific bearings and gears. As a rough guideline, typical ranges for maximum slopes and transverse deflections of the shaft centerline are given in Table 7-2. The allowable transverse deflections for spur gears are dependent on the size of the teeth, as represented by the diametral pitch $P = \text{number of teeth/pitch diameter}$.

In Sec. 4-4 several beam deflection methods are described. For shafts, where the deflections may be sought at a number of different points, integration using either singularity functions or numerical integration is practical. In a stepped shaft, the cross-sectional properties change along the shaft at each step, increasing the complexity of integration, since both M and I vary. Fortunately, only the gross geometric dimensions need to be included, as the local factors such as fillets, grooves, and keyways do not have much impact on deflection. Example 4-7 demonstrates the use of singularity functions for a stepped shaft. Many shafts will include forces in multiple planes, requiring either a three-dimensional analysis, or the use of superposition to obtain deflections in two planes which can then be summed as vectors.

A deflection analysis is straightforward, but it is lengthy and tedious to carry out manually, particularly for multiple points of interest. Consequently, practically all shaft deflection analysis will be evaluated with the assistance of software. Any general-purpose finite-element software can readily handle a shaft problem (see Chap. 19). This is practical if the designer is already familiar with using the software and with how to properly model the shaft. Special-purpose software solutions for 3-D shaft analysis are available, but somewhat expensive if only used occasionally. Software requiring very little training is readily available for planar beam analysis, and can be downloaded from the internet. Example 7-3 demonstrates how to incorporate such a program for a shaft with forces in multiple planes.

EXAMPLE 7-3

This example problem is part of a larger case study. See Chap. 18 for the full context.

In Ex. 7-2, a preliminary shaft geometry was obtained on the basis of design for stress. The resulting shaft is shown in Fig. 7-10, with proposed diameters of

$$D_1 = D_7 = 1 \text{ in}$$

$$D_2 = D_6 = 1.4 \text{ in}$$

$$D_3 = D_5 = 1.625 \text{ in}$$

$$D_4 = 2.0 \text{ in}$$

Check that the deflections and slopes at the gears and bearings are acceptable. If necessary, propose changes in the geometry to resolve any problems.

Solution

A simple planar beam analysis program will be used. By modeling the shaft twice, with loads in two orthogonal planes, and combining the results, the shaft deflections can readily be obtained. For both planes, the material is selected (steel with $E = 30 \text{ Mpsi}$), the shaft lengths and diameters are entered, and the bearing locations are specified. Local details like grooves and keyways are ignored, as they will have insignificant effect on the deflections. Then the tangential gear forces are entered in the horizontal xz plane model, and the radial gear forces are entered in the vertical xy plane model. The software can calculate the bearing reaction forces, and numerically integrate to generate plots for shear, moment, slope, and deflection, as shown in Fig. 7-11.

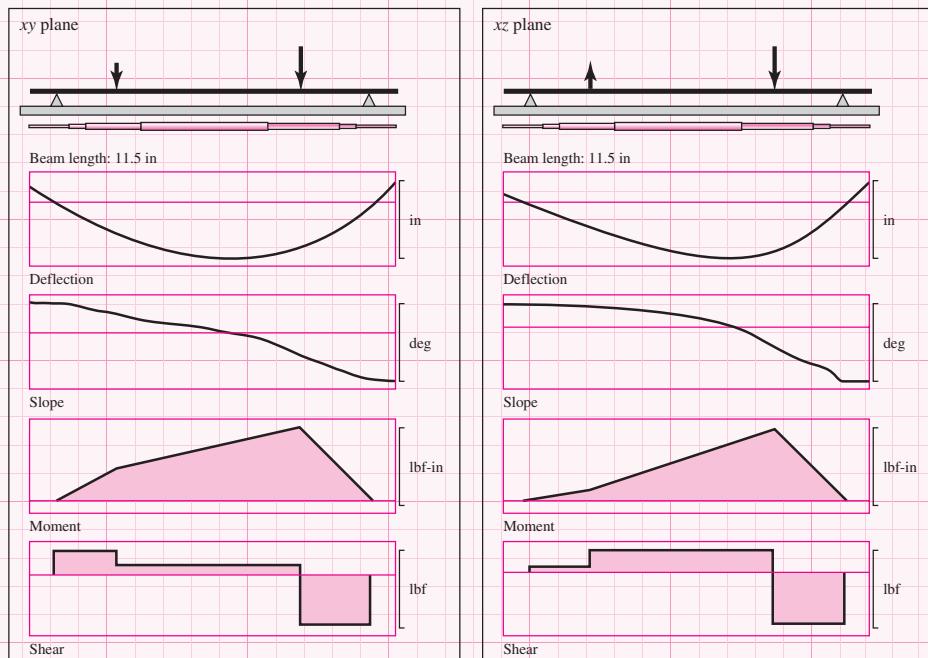


Figure 7-11

Shear, moment, slope, and deflection plots from two planes. (Source: Beam 2D Stress Analysis, Orand Systems, Inc.)

Point of Interest	xz Plane	xy Plane	Total
Left bearing slope	0.02263 deg	0.01770 deg	0.02872 deg 0.000501 rad
Right bearing slope	0.05711 deg	0.02599 deg	0.06274 deg 0.001095 rad
Left gear slope	0.02067 deg	0.01162 deg	0.02371 deg 0.000414 rad
Right gear slope	0.02155 deg	0.01149 deg	0.02442 deg 0.000426 rad
Left gear deflection	0.0007568 in	0.0005153 in	0.0009155 in
Right gear deflection	0.0015870 in	0.0007535 in	0.0017567 in

Table 7-3

Slope and Deflection Values at Key Locations

The deflections and slopes at points of interest are obtained from the plots, and combined with orthogonal vector addition, that is, $\delta = \sqrt{\delta_{xz}^2 + \delta_{xy}^2}$. Results are shown in Table 7-3.

Whether these values are acceptable will depend on the specific bearings and gears selected, as well as the level of performance expected. According to the guidelines in Table 7-2, all of the bearing slopes are well below typical limits for ball bearings. The right bearing slope is within the typical range for cylindrical bearings. Since the load on the right bearing is relatively high, a cylindrical bearing might be used. This constraint should be checked against the specific bearing specifications once the bearing is selected.

The gear slopes and deflections more than satisfy the limits recommended in Table 7-2. It is recommended to proceed with the design, with an awareness that changes that reduce rigidity should warrant another deflection check.

Once deflections at various points have been determined, if any value is larger than the allowable deflection at that point, since I is proportional to d^4 , a new diameter can be found from

$$d_{\text{new}} = d_{\text{old}} \left| \frac{n_d y_{\text{old}}}{y_{\text{all}}} \right|^{1/4} \quad (7-17)$$

where y_{all} is the allowable deflection at that station and n_d is the design factor. Similarly, if any slope is larger than the allowable slope θ_{all} , a new diameter can be found from

$$d_{\text{new}} = d_{\text{old}} \left| \frac{n_d (dy/dx)_{\text{old}}}{(\text{slope})_{\text{all}}} \right|^{1/4} \quad (7-18)$$

where $(\text{slope})_{\text{all}}$ is the allowable slope. As a result of these calculations, determine the largest $d_{\text{new}}/d_{\text{old}}$ ratio, then multiply *all* diameters by this ratio. The tight constraint will be just tight, and all others will be loose. Don't be too concerned about end journal sizes, as their influence is usually negligible. The beauty of the method is that the deflections need to be completed just once and constraints can be rendered loose but for one, with diameters all identified without reworking every deflection.

EXAMPLE 7-4

For the shaft in Ex. 7-3, it was noted that the slope at the right bearing is near the limit for a cylindrical roller bearing. Determine an appropriate increase in diameters to bring this slope down to 0.0005 rad.

Solution

Applying Eq. (7-17) to the deflection at the right bearing gives

$$d_{\text{new}} = d_{\text{old}} \left| \frac{n_d \text{slope}_{\text{old}}}{\text{slope}_{\text{all}}} \right|^{1/4} = 1.0 \left| \frac{(1)(0.001095)}{(0.0005)} \right|^{1/4} = 1.216 \text{ in}$$

Multiplying all diameters by the ratio

$$\frac{d_{\text{new}}}{d_{\text{old}}} = \frac{1.216}{1.0} = 1.216$$

gives a new set of diameters,

$$D_1 = D_7 = 1.216 \text{ in}$$

$$D_2 = D_6 = 1.702 \text{ in}$$

$$D_3 = D_5 = 1.976 \text{ in}$$

$$D_4 = 2.432 \text{ in}$$

Repeating the beam deflection analysis of Ex. 7-3 with these new diameters produces a slope at the right bearing of 0.0005 in, with all other deflections less than their previous values.

The transverse shear V at a section of a beam in flexure imposes a shearing deflection, which is superposed on the bending deflection. Usually such shearing deflection is less than 1 percent of the transverse bending deflection, and it is seldom evaluated. However, when the shaft length-to-diameter ratio is less than 10, the shear component of transverse deflection merits attention. There are many short shafts. A tabular method is explained in detail elsewhere², including examples.

For right-circular cylindrical shafts in torsion the angular deflection θ is given in Eq. (4-5). For a stepped shaft with individual cylinder length l_i and torque T_i , the angular deflection can be estimated from

$$\theta = \sum \theta_i = \sum \frac{T_i l_i}{G_i J_i} \quad (7-19)$$

or, for a constant torque throughout homogeneous material, from

$$\theta = \frac{T}{G} \sum \frac{l_i}{J_i} \quad (7-20)$$

This should be treated only as an estimate, since experimental evidence shows that the actual θ is larger than given by Eqs. (7-19) and (7-20).³

²C.R. Mischke, "Tabular Method for Transverse Shear Deflection," Sec. 17.3 in Joseph E. Shigley, Charles R. Mischke, and Thomas H. Brown, Jr. (eds.), *Standard Handbook of Machine Design*, 3rd ed., McGraw-Hill, New York, 2004.

³R. Bruce Hopkins, *Design Analysis of Shafts and Beams*, McGraw-Hill, New York, 1970, pp. 93–99.

If torsional stiffness is defined as $k_i = T_i/\theta_i$ and, since $\theta_i = T_i/k_i$ and $\theta = \sum \theta_i = \sum(T_i/k_i)$, for constant torque $\theta = T \sum(1/k_i)$, it follows that the torsional stiffness of the shaft k in terms of segment stiffnesses is

$$\frac{1}{k} = \sum \frac{1}{k_i} \quad (7-21)$$

7-6 Critical Speeds for Shafts

When a shaft is turning, eccentricity causes a centrifugal force deflection, which is resisted by the shaft's flexural rigidity EI . As long as deflections are small, no harm is done. Another potential problem, however, is called *critical speeds*: at certain speeds the shaft is unstable, with deflections increasing without upper bound. It is fortunate that although the dynamic deflection shape is unknown, using a static deflection curve gives an excellent estimate of the lowest critical speed. Such a curve meets the boundary condition of the differential equation (zero moment and deflection at both bearings) and the shaft energy is not particularly sensitive to the exact shape of the deflection curve. Designers seek first critical speeds at least twice the operating speed.

The shaft, because of its own mass, has a critical speed. The ensemble of attachments to a shaft likewise has a critical speed that is much lower than the shaft's intrinsic critical speed. Estimating these critical speeds (and harmonics) is a task of the designer. When geometry is simple, as in a shaft of uniform diameter, simply supported, the task is easy. It can be expressed⁴ as

$$\omega_1 = \left(\frac{\pi}{l}\right)^2 \sqrt{\frac{EI}{m}} = \left(\frac{\pi}{l}\right)^2 \sqrt{\frac{gEI}{A\gamma}} \quad (7-22)$$

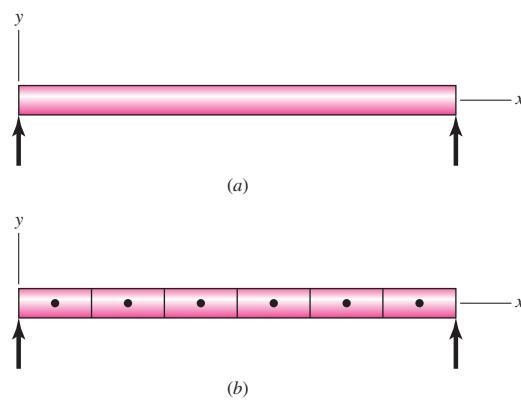
where m is the mass per unit length, A the cross-sectional area, and γ the specific weight. For an ensemble of attachments, Rayleigh's method for lumped masses gives⁵

$$\omega_1 = \sqrt{\frac{g \sum w_i y_i}{\sum w_i y_i^2}} \quad (7-23)$$

where w_i is the weight of the i th location and y_i is the deflection at the i th body location. It is possible to use Eq. (7-23) for the case of Eq. (7-22) by partitioning the shaft into segments and placing its weight force at the segment centroid as seen in Fig. 7-12.

Figure 7-12

(a) A uniform-diameter shaft for Eq. (7-22). (b) A segmented uniform-diameter shaft for Eq. (7-23).

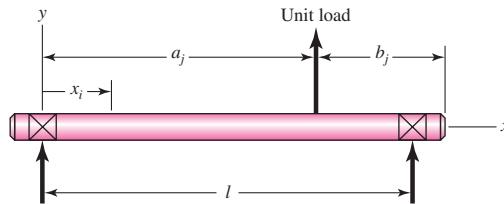


⁴William T. Thomson and Marie Dillon Dahleh, *Theory of Vibration with Applications*, Prentice Hall, 5th ed., 1998, p. 273.

⁵Thomson, op. cit., p. 357.

Figure 7-13

The influence coefficient δ_{ij} is the deflection at i due to a unit load at j .



Computer assistance is often used to lessen the difficulty in finding transverse deflections of a stepped shaft. Rayleigh's equation overestimates the critical speed.

To counter the increasing complexity of detail, we adopt a useful viewpoint. Inasmuch as the shaft is an elastic body, we can use *influence coefficients*. An influence coefficient is the transverse deflection at location i on a shaft due to a unit load at location j on the shaft. From Table A-9-6 we obtain, for a simply supported beam with a single unit load as shown in Fig. 7-13,

$$\delta_{ij} = \begin{cases} \frac{b_j x_i}{6EIl} (l^2 - b_j^2 - x_i^2) & x_i \leq a_i \\ \frac{a_j (l - x_i)}{6EIl} (2lx_i - a_j^2 - x_i^2) & x_i > a_i \end{cases} \quad (7-24)$$

For three loads the influence coefficients may be displayed as

i	j		
	1	2	3
1	δ_{11}	δ_{12}	δ_{13}
2	δ_{21}	δ_{22}	δ_{23}
3	δ_{31}	δ_{32}	δ_{33}

Maxwell's reciprocity theorem⁶ states that there is a symmetry about the main diagonal, composed of δ_{11} , δ_{22} , and δ_{33} , of the form $\delta_{ij} = \delta_{ji}$. This relation reduces the work of finding the influence coefficients. From the influence coefficients above, one can find the deflections y_1 , y_2 , and y_3 of Eq. (7-23) as follows:

$$\begin{aligned} y_1 &= F_1 \delta_{11} + F_2 \delta_{12} + F_3 \delta_{13} \\ y_2 &= F_1 \delta_{21} + F_2 \delta_{22} + F_3 \delta_{23} \\ y_3 &= F_1 \delta_{31} + F_2 \delta_{32} + F_3 \delta_{33} \end{aligned} \quad (7-25)$$

The forces F_i can arise from weight attached w_i or centrifugal forces $m_i \omega^2 y_i$. The equation set (7-25) written with inertial forces can be displayed as

$$\begin{aligned} y_1 &= m_1 \omega^2 y_1 \delta_{11} + m_2 \omega^2 y_2 \delta_{12} + m_3 \omega^2 y_3 \delta_{13} \\ y_2 &= m_1 \omega^2 y_1 \delta_{21} + m_2 \omega^2 y_2 \delta_{22} + m_3 \omega^2 y_3 \delta_{23} \\ y_3 &= m_1 \omega^2 y_1 \delta_{31} + m_2 \omega^2 y_2 \delta_{32} + m_3 \omega^2 y_3 \delta_{33} \end{aligned}$$

⁶Thomson, op. cit., p. 167.

which can be rewritten as

$$\begin{aligned}(m_1\delta_{11} - 1/\omega^2)y_1 + (m_2\delta_{12})y_2 + (m_3\delta_{13})y_3 &= 0 \\ (m_1\delta_{21})y_1 + (m_2\delta_{22} - 1/\omega^2)y_2 + (m_3\delta_{23})y_3 &= 0 \\ (m_1\delta_{31})y_1 + (m_2\delta_{32})y_2 + (m_3\delta_{33} - 1/\omega^2)y_3 &= 0\end{aligned}\quad (a)$$

Equation set (a) is three simultaneous equations in terms of y_1 , y_2 , and y_3 . To avoid the trivial solution $y_1 = y_2 = y_3 = 0$, the determinant of the coefficients of y_1 , y_2 , and y_3 must be zero (eigenvalue problem). Thus,

$$\begin{vmatrix} (m_1\delta_{11} - 1/\omega^2) & m_2\delta_{12} & m_3\delta_{13} \\ m_1\delta_{21} & (m_2\delta_{22} - 1/\omega^2) & m_3\delta_{23} \\ m_1\delta_{31} & m_2\delta_{32} & (m_3\delta_{33} - 1/\omega^2) \end{vmatrix} = 0 \quad (7-26)$$

which says that a deflection other than zero exists only at three distinct values of ω , the critical speeds. Expanding the determinant, we obtain

$$\left(\frac{1}{\omega^2}\right)^3 - (m_1\delta_{11} + m_2\delta_{22} + m_3\delta_{33})\left(\frac{1}{\omega^2}\right)^2 + \dots = 0 \quad (7-27)$$

The three roots of Eq. (7-27) can be expressed as $1/\omega_1^2$, $1/\omega_2^2$, and $1/\omega_3^2$. Thus Eq. (7-27) can be written in the form

$$\left(\frac{1}{\omega^2} - \frac{1}{\omega_1^2}\right)\left(\frac{1}{\omega^2} - \frac{1}{\omega_2^2}\right)\left(\frac{1}{\omega^2} - \frac{1}{\omega_3^2}\right) = 0$$

or

$$\left(\frac{1}{\omega^2}\right)^3 - \left(\frac{1}{\omega_1^2} + \frac{1}{\omega_2^2} + \frac{1}{\omega_3^2}\right)\left(\frac{1}{\omega^2}\right)^2 + \dots = 0 \quad (7-28)$$

Comparing Eqs. (7-27) and (7-28) we see that

$$\frac{1}{\omega_1^2} + \frac{1}{\omega_2^2} + \frac{1}{\omega_3^2} = m_1\delta_{11} + m_2\delta_{22} + m_3\delta_{33} \quad (7-29)$$

If we had only a single mass m_1 alone, the critical speed would be given by $1/\omega^2 = m_1\delta_{11}$. Denote this critical speed as ω_{11} (which considers only m_1 acting alone). Likewise for m_2 or m_3 acting alone, we similarly define the terms $1/\omega_{22}^2 = m_2\delta_{22}$ or $1/\omega_{33}^2 = m_3\delta_{33}$, respectively. Thus, Eq. (7-29) can be rewritten as

$$\frac{1}{\omega_1^2} + \frac{1}{\omega_2^2} + \frac{1}{\omega_3^2} = \frac{1}{\omega_{11}^2} + \frac{1}{\omega_{22}^2} + \frac{1}{\omega_{33}^2} \quad (7-30)$$

If we order the critical speeds such that $\omega_1 < \omega_2 < \omega_3$, then $1/\omega_1^2 \gg 1/\omega_2^2$, and $1/\omega_3^2$. So the first, or fundamental, critical speed ω_1 can be approximated by

$$\frac{1}{\omega_1^2} \doteq \frac{1}{\omega_{11}^2} + \frac{1}{\omega_{22}^2} + \frac{1}{\omega_{33}^2} \quad (7-31)$$

This idea can be extended to an n -body shaft:

$$\frac{1}{\omega_1^2} \doteq \sum_{i=1}^n \frac{1}{\omega_{ii}^2} \quad (7-32)$$

This is called *Dunkerley's equation*. By ignoring the higher mode term(s), the first critical speed estimate is *lower* than actually is the case.

Since Eq. (7-32) has no loads appearing in the equation, it follows that if each load could be placed at some convenient location transformed into an equivalent load, then the critical speed of an array of loads could be found by summing the equivalent loads, all placed at a single convenient location. For the load at station 1, placed at the center of span, denoted with the subscript c , the equivalent load is found from

$$\omega_{11}^2 = \frac{1}{m_1 \delta_{11}} = \frac{g}{w_1 \delta_{11}} = \frac{g}{w_{1c} \delta_{cc}}$$

or

$$w_{1c} = w_1 \frac{\delta_{11}}{\delta_{cc}} \quad (7-33)$$

EXAMPLE 7-5

Consider a simply supported steel shaft as depicted in Fig. 7-14, with 1 in diameter and a 31-in span between bearings, carrying two gears weighing 35 and 55 lbf.

- (a) Find the influence coefficients.
- (b) Find $\sum wy$ and $\sum wy^2$ and the first critical speed using Rayleigh's equation, Eq. (7-23).
- (c) From the influence coefficients, find ω_{11} and ω_{22} .
- (d) Using Dunkerley's equation, Eq. (7-32), estimate the first critical speed.
- (e) Use superposition to estimate the first critical speed.
- (f) Estimate the shaft's intrinsic critical speed. Suggest a modification to Dunkerley's equation to include the effect of the shaft's mass on the first critical speed of the attachments.

Solution

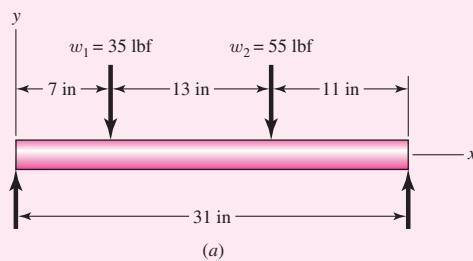
(a)

$$I = \frac{\pi d^4}{64} = \frac{\pi (1)^4}{64} = 0.049\ 09 \text{ in}^4$$

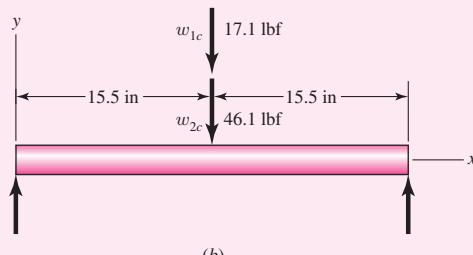
$$6EI = 6(30)10^6(0.049\ 09)31 = 0.2739(10^9) \text{ lbf} \cdot \text{in}^3$$

Figure 7-14

- (a) A 1-in uniform-diameter shaft for Ex. 7-5.
- (b) Superposing of equivalent loads at the center of the shaft for the purpose of finding the first critical speed.



(a)



(b)

From Eq. set (7-24),

$$\delta_{11} = \frac{24(7)(31^2 - 24^2 - 7^2)}{0.2739(10^9)} = 2.061(10^{-4}) \text{ in/lbf}$$

$$\delta_{22} = \frac{11(20)(31^2 - 11^2 - 20^2)}{0.2739(10^9)} = 3.534(10^{-4}) \text{ in/lbf}$$

$$\delta_{12} = \delta_{21} = \frac{11(7)(31^2 - 11^2 - 7^2)}{0.2739(10^9)} = 2.224(10^{-4}) \text{ in/lbf}$$

Answer

	<i>i</i>	<i>j</i>
	1	2
1	2.061(10 ⁻⁴)	2.224(10 ⁻⁴)
2	2.224(10 ⁻⁴)	3.534(10 ⁻⁴)

$$y_1 = w_1 \delta_{11} + w_2 \delta_{12} = 35(2.061)10^{-4} + 55(2.224)10^{-4} = 0.01945 \text{ in}$$

$$y_2 = w_1 \delta_{21} + w_2 \delta_{22} = 35(2.224)10^{-4} + 55(3.534)10^{-4} = 0.02722 \text{ in}$$

$$(b) \quad \sum w_i y_i = 35(0.01945) + 55(0.02722) = 2.178 \text{ lbf} \cdot \text{in}$$

Answer

$$\sum w_i y_i^2 = 35(0.01945)^2 + 55(0.02722)^2 = 0.05399 \text{ lbf} \cdot \text{in}^2$$

Answer

$$\omega = \sqrt{\frac{386.1(2.178)}{0.05399}} = 124.8 \text{ rad/s, or } 1192 \text{ rev/min}$$

(c)

Answer

$$\frac{1}{\omega_{11}^2} = \frac{w_1}{g} \delta_{11}$$

$$\omega_{11} = \sqrt{\frac{g}{w_1 \delta_{11}}} = \sqrt{\frac{386.1}{35(2.061)10^{-4}}} = 231.4 \text{ rad/s, or } 2210 \text{ rev/min}$$

Answer

$$\omega_{22} = \sqrt{\frac{g}{w_2 \delta_{22}}} = \sqrt{\frac{386.1}{55(3.534)10^{-4}}} = 140.9 \text{ rad/s, or } 1346 \text{ rev/min}$$

(d)

$$\frac{1}{\omega_1^2} \doteq \sum \frac{1}{\omega_{ii}^2} = \frac{1}{231.4^2} + \frac{1}{140.9^2} = 6.905(10^{-5}) \quad (1)$$

Answer

$$\omega_1 \doteq \sqrt{\frac{1}{6.905(10^{-5})}} = 120.3 \text{ rad/s, or } 1149 \text{ rev/min}$$

which is less than part *b*, as expected.

(e) From Eq. (7-24),

$$\begin{aligned} \delta_{cc} &= \frac{b_{cc}x_{cc}(l^2 - b_{cc}^2 - x_{cc}^2)}{6EI} = \frac{15.5(15.5)(31^2 - 15.5^2 - 15.5^2)}{0.2739(10^9)} \\ &= 4.215(10^{-4}) \text{ in/lbf} \end{aligned}$$

From Eq. (7-33),

$$w_{1c} = w_1 \frac{\delta_{11}}{\delta_{cc}} = 35 \frac{2.061(10^{-4})}{4.215(10^{-4})} = 17.11 \text{ lbf}$$

$$w_{2c} = w_2 \frac{\delta_{22}}{\delta_{cc}} = 55 \frac{3.534(10^{-4})}{4.215(10^{-4})} = 46.11 \text{ lbf}$$

Answer $\omega = \sqrt{\frac{g}{\delta_{cc} \sum w_{ic}}} = \sqrt{\frac{386.1}{4.215(10^{-4})(17.11 + 46.11)}} = 120.4 \text{ rad/s, or } 1150 \text{ rev/min}$

which, except for rounding, agrees with part *d*, as expected.

(f) For the shaft, $E = 30(10^6)$ psi, $\gamma = 0.282$ lbf/in³, and $A = \pi(1^2)/4 = 0.7854$ in². Considering the shaft alone, the critical speed, from Eq. (7-22), is

Answer
$$\omega_s = \left(\frac{\pi}{l}\right)^2 \sqrt{\frac{gEI}{A\gamma}} = \left(\frac{\pi}{31}\right)^2 \sqrt{\frac{386.1(30)10^6(0.049\ 09)}{0.7854(0.282)}} \\ = 520.4 \text{ rad/s, or } 4970 \text{ rev/min}$$

We can simply add $1/\omega_s^2$ to the right side of Dunkerley's equation, Eq. (1), to include the shaft's contribution,

Answer
$$\frac{1}{\omega_1^2} \doteq \frac{1}{520.4^2} + 6.905(10^{-5}) = 7.274(10^{-5}) \\ \omega_1 \doteq 117.3 \text{ rad/s, or } 1120 \text{ rev/min}$$

which is slightly less than part *d*, as expected.

The shaft's first critical speed ω_s is just one more single effect to add to Dunkerley's equation. Since it does not fit into the summation, it is usually written up front.

Answer
$$\frac{1}{\omega_1^2} \doteq \frac{1}{\omega_s^2} + \sum_{i=1}^n \frac{1}{\omega_{ii}^2} \quad (7-34)$$

Common shafts are complicated by the stepped-cylinder geometry, which makes the influence-coefficient determination part of a numerical solution.

7-7 Miscellaneous Shaft Components

Setscrews

Unlike bolts and cap screws, which depend on tension to develop a clamping force, the setscrew depends on compression to develop the clamping force. The resistance to axial motion of the collar or hub relative to the shaft is called *holding power*. This holding power, which is really a force resistance, is due to frictional resistance of the contacting portions of the collar and shaft as well as any slight penetration of the setscrew into the shaft.

Figure 7–15 shows the point types available with socket setscrews. These are also manufactured with screwdriver slots and with square heads.

Table 7–4 lists values of the seating torque and the corresponding holding power for inch-series setscrews. The values listed apply to both axial holding power, for resisting

Figure 7–15

Socket setscrews: (a) flat point; (b) cup point; (c) oval point; (d) cone point; (e) half-dog point.

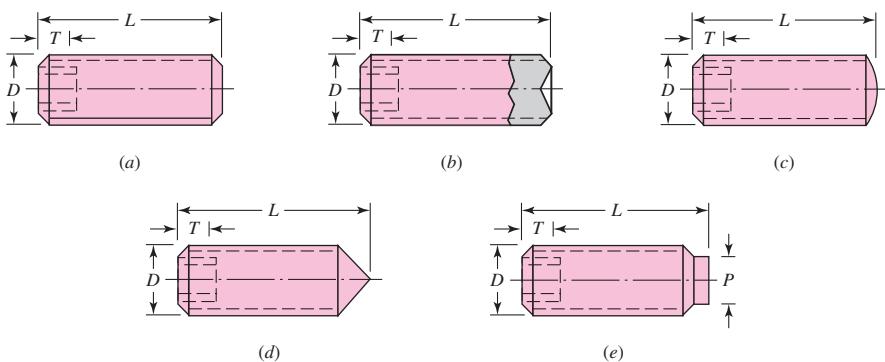


Table 7–4

Typical Holding Power (Force) for Socket Setscrews*

Source: Unbrako Division, SPS Technologies, Jenkintown, Pa.

Size, in	Seating Torque, lbf · in	Holding Power, lbf
#0	1.0	50
#1	1.8	65
#2	1.8	85
#3	5	120
#4	5	160
#5	10	200
#6	10	250
#8	20	385
#10	36	540
$\frac{1}{4}$	87	1000
$\frac{5}{16}$	165	1500
$\frac{3}{8}$	290	2000
$\frac{7}{16}$	430	2500
$\frac{1}{2}$	620	3000
$\frac{9}{16}$	620	3500
$\frac{5}{8}$	1325	4000
$\frac{3}{4}$	2400	5000
$\frac{7}{8}$	5200	6000
1	7200	7000

*Based on alloy-steel screw against steel shaft, class 3A coarse or fine threads in class 2B holes, and cup-point socket setscrews.

thrust, and the tangential holding power, for resisting torsion. Typical factors of safety are 1.5 to 2.0 for static loads and 4 to 8 for various dynamic loads.

Setscrews should have a length of about half of the shaft diameter. Note that this practice also provides a rough rule for the radial thickness of a hub or collar.

Keys and Pins

Keys and pins are used on shafts to secure rotating elements, such as gears, pulleys, or other wheels. Keys are used to enable the transmission of torque from the shaft to the shaft-supported element. Pins are used for axial positioning and for the transfer of torque or thrust or both.

Figure 7–16 shows a variety of keys and pins. Pins are useful when the principal loading is shear and when both torsion and thrust are present. Taper pins are sized according to the diameter at the large end. Some of the most useful sizes of these are listed in Table 7–5. The diameter at the small end is

$$d = D - 0.0208L \quad (7-35)$$

where d = diameter at small end, in

D = diameter at large end, in

L = length, in

Figure 7–16

(a) Square key; (b) round key; (c and d) round pins; (e) taper pin; (f) split tubular spring pin. The pins in parts (e) and (f) are shown longer than necessary, to illustrate the chamfer on the ends, but their lengths should be kept smaller than the hub diameters to prevent injuries due to projections on rotating parts.

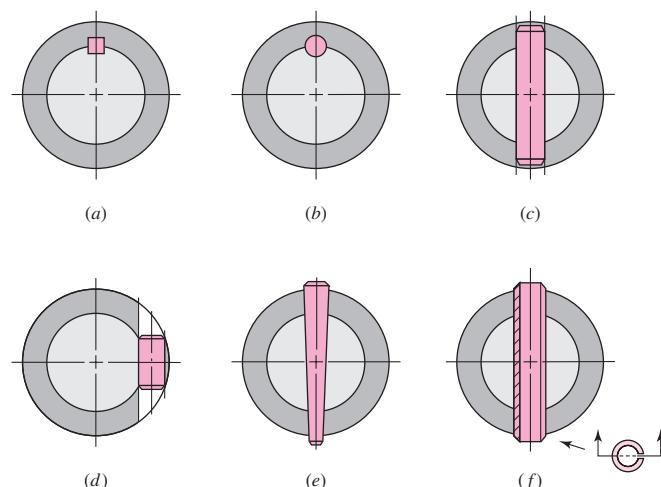


Table 7–5

Dimensions at Large End
of Some Standard Taper
Pins—Inch Series

Size	Commercial		Precision	
	Maximum	Minimum	Maximum	Minimum
4/0	0.1103	0.1083	0.1100	0.1090
2/0	0.1423	0.1403	0.1420	0.1410
0	0.1573	0.1553	0.1570	0.1560
2	0.1943	0.1923	0.1940	0.1930
4	0.2513	0.2493	0.2510	0.2500
6	0.3423	0.3403	0.3420	0.3410
8	0.4933	0.4913	0.4930	0.4920

Table 7–6

Inch Dimensions for Some Standard Square- and Rectangular-Key Applications
*Source: Joseph E. Shigley, "Unthreaded Fasteners," Chap. 24 in Joseph E. Shigley, Charles R. Mischke, and Thomas H. Brown, Jr. (eds.), *Standard Handbook of Machine Design*, 3rd ed., McGraw-Hill, New York, 2004.*

Shaft Diameter Over	To (Incl.)	Key Size		
		w	h	Keyway Depth
$\frac{5}{16}$	$\frac{7}{16}$	$\frac{3}{32}$	$\frac{3}{32}$	$\frac{3}{64}$
$\frac{7}{16}$	$\frac{9}{16}$	$\frac{1}{8}$	$\frac{3}{32}$	$\frac{3}{64}$
		$\frac{1}{8}$	$\frac{1}{8}$	$\frac{1}{16}$
$\frac{9}{16}$	$\frac{7}{8}$	$\frac{3}{16}$	$\frac{1}{8}$	$\frac{1}{16}$
		$\frac{3}{16}$	$\frac{3}{16}$	$\frac{3}{32}$
$\frac{7}{8}$	$1\frac{1}{4}$	$\frac{1}{4}$	$\frac{3}{16}$	$\frac{3}{32}$
		$\frac{1}{4}$	$\frac{1}{4}$	$\frac{1}{8}$
$1\frac{1}{4}$	$1\frac{3}{8}$	$\frac{5}{16}$	$\frac{1}{4}$	$\frac{1}{8}$
		$\frac{5}{16}$	$\frac{5}{16}$	$\frac{5}{32}$
$1\frac{3}{8}$	$1\frac{3}{4}$	$\frac{3}{8}$	$\frac{1}{4}$	$\frac{1}{8}$
		$\frac{3}{8}$	$\frac{3}{8}$	$\frac{3}{16}$
$1\frac{3}{4}$	$2\frac{1}{4}$	$\frac{1}{2}$	$\frac{3}{8}$	$\frac{3}{16}$
		$\frac{1}{2}$	$\frac{1}{2}$	$\frac{1}{4}$
$2\frac{1}{4}$	$2\frac{3}{4}$	$\frac{5}{8}$	$\frac{7}{16}$	$\frac{7}{32}$
		$\frac{5}{8}$	$\frac{5}{8}$	$\frac{5}{16}$
$2\frac{3}{4}$	$3\frac{1}{4}$	$\frac{3}{4}$	$\frac{1}{2}$	$\frac{1}{4}$
		$\frac{3}{4}$	$\frac{3}{4}$	$\frac{3}{8}$

For less important applications, a dowel pin or a drive pin can be used. A large variety of these are listed in manufacturers' catalogs.⁷

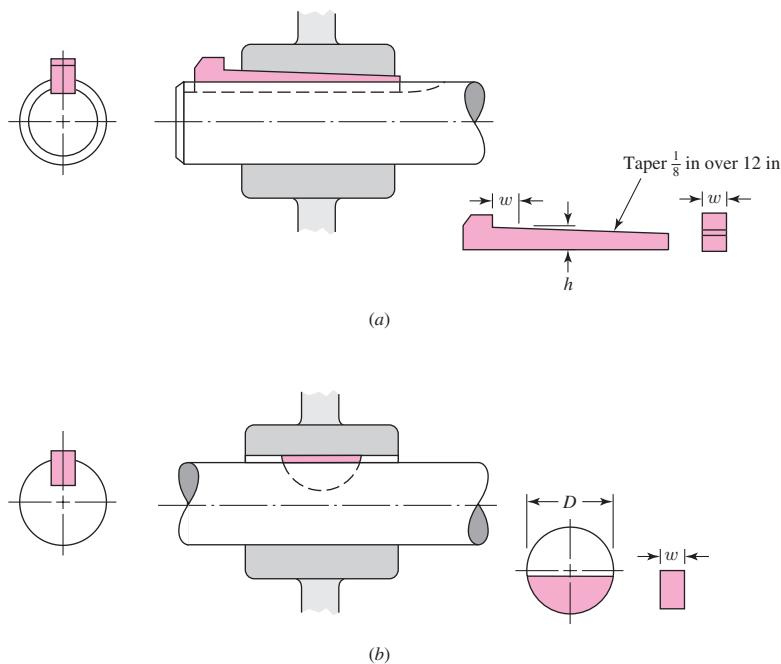
The square key, shown in Fig. 7–16a, is also available in rectangular sizes. Standard sizes of these, together with the range of applicable shaft diameters, are listed in Table 7–6. The shaft diameter determines standard sizes for width, height, and key depth. The designer chooses an appropriate key length to carry the torsional load. Failure of the key can be by direct shear, or by bearing stress. Example 7–6 demonstrates the process to size the length of a key. The maximum length of a key is limited by the hub length of the attached element, and should generally not exceed about 1.5 times the shaft diameter to avoid excessive twisting with the angular deflection of the shaft. Multiple keys may be used as necessary to carry greater loads, typically oriented at 90° from one another. Excessive safety factors should be avoided in key design, since it is desirable in an overload situation for the key to fail, rather than more costly components.

Stock key material is typically made from low carbon cold-rolled steel, and is manufactured such that its dimensions never exceed the nominal dimension. This allows standard cutter sizes to be used for the keyseats. A setscrew is sometimes used along with a key to hold the hub axially, and to minimize rotational backlash when the shaft rotates in both directions.

⁷See also Joseph E. Shigley, "Unthreaded Fasteners," Chap. 24. In Joseph E. Shigley, Charles R. Mischke, and Thomas H. Brown, Jr. (eds.), *Standard Handbook of Machine Design*, 3rd ed., McGraw-Hill, New York, 2004.

Figure 7-17

- (a) Gib-head key;
(b) Woodruff key.



The gib-head key, in Fig. 7-17a, is tapered so that, when firmly driven, it acts to prevent relative axial motion. This also gives the advantage that the hub position can be adjusted for the best axial location. The head makes removal possible without access to the other end, but the projection may be hazardous.

The Woodruff key, shown in Fig. 7-17b, is of general usefulness, especially when a wheel is to be positioned against a shaft shoulder, since the keyslot need not be machined into the shoulder stress concentration region. The use of the Woodruff key also yields better concentricity after assembly of the wheel and shaft. This is especially important at high speeds, as, for example, with a turbine wheel and shaft. Woodruff keys are particularly useful in smaller shafts where their deeper penetration helps prevent key rolling. Dimensions for some standard Woodruff key sizes can be found in Table 7-7, and Table 7-8 gives the shaft diameters for which the different keyseat widths are suitable.

Pilkey⁸ gives values for stress concentrations in an end-milled keyseat, as a function of the ratio of the radius r at the bottom of the groove and the shaft diameter d . For fillets cut by standard milling-machine cutters, with a ratio of $r/d = 0.02$, Peterson's charts give $K_t = 2.14$ for bending and $K_{ts} = 2.62$ for torsion without the key in place, or $K_{ts} = 3.0$ for torsion with the key in place. The stress concentration at the end of the keyseat can be reduced somewhat by using a sled-runner keyseat, eliminating the abrupt end to the keyseat, as shown in Fig. 7-17. It does, however, still have the sharp radius in the bottom of the groove on the sides. The sled-runner keyseat can only be used when definite longitudinal key positioning is not necessary. It is also not as suitable near a shoulder. Keeping the end of a keyseat at least a distance

⁸W. D. Pilkey, *Peterson's Stress-Concentration Factors*, 2nd ed., John Wiley & Sons, New York, 1997, pp. 408–409.

Table 7-7

Dimensions of Woodruff Keys—Inch Series

Key Size		Height	Offset	Keyseat Depth	
w	D	b	e	Shaft	Hub
$\frac{1}{16}$	$\frac{1}{4}$	0.109	$\frac{1}{64}$	0.0728	0.0372
$\frac{1}{16}$	$\frac{3}{8}$	0.172	$\frac{1}{64}$	0.1358	0.0372
$\frac{3}{32}$	$\frac{3}{8}$	0.172	$\frac{1}{64}$	0.1202	0.0529
$\frac{3}{32}$	$\frac{1}{2}$	0.203	$\frac{3}{64}$	0.1511	0.0529
$\frac{3}{32}$	$\frac{5}{8}$	0.250	$\frac{1}{16}$	0.1981	0.0529
$\frac{1}{8}$	$\frac{1}{2}$	0.203	$\frac{3}{64}$	0.1355	0.0685
$\frac{1}{8}$	$\frac{5}{8}$	0.250	$\frac{1}{16}$	0.1825	0.0685
$\frac{1}{8}$	$\frac{3}{4}$	0.313	$\frac{1}{16}$	0.2455	0.0685
$\frac{5}{32}$	$\frac{5}{8}$	0.250	$\frac{1}{16}$	0.1669	0.0841
$\frac{5}{32}$	$\frac{3}{4}$	0.313	$\frac{1}{16}$	0.2299	0.0841
$\frac{5}{32}$	$\frac{7}{8}$	0.375	$\frac{1}{16}$	0.2919	0.0841
$\frac{3}{16}$	$\frac{3}{4}$	0.313	$\frac{1}{16}$	0.2143	0.0997
$\frac{3}{16}$	$\frac{7}{8}$	0.375	$\frac{1}{16}$	0.2763	0.0997
$\frac{3}{16}$	1	0.438	$\frac{1}{16}$	0.3393	0.0997
$\frac{1}{4}$	$\frac{7}{8}$	0.375	$\frac{1}{16}$	0.2450	0.1310
$\frac{1}{4}$	1	0.438	$\frac{1}{16}$	0.3080	0.1310
$\frac{1}{4}$	$1\frac{1}{4}$	0.547	$\frac{5}{64}$	0.4170	0.1310
$\frac{5}{16}$	1	0.438	$\frac{1}{16}$	0.2768	0.1622
$\frac{5}{16}$	$1\frac{1}{4}$	0.547	$\frac{5}{64}$	0.3858	0.1622
$\frac{5}{16}$	$1\frac{1}{2}$	0.641	$\frac{7}{64}$	0.4798	0.1622
$\frac{3}{8}$	$1\frac{1}{4}$	0.547	$\frac{5}{64}$	0.3545	0.1935
$\frac{3}{8}$	$1\frac{1}{2}$	0.641	$\frac{7}{64}$	0.4485	0.1935

Table 7-8

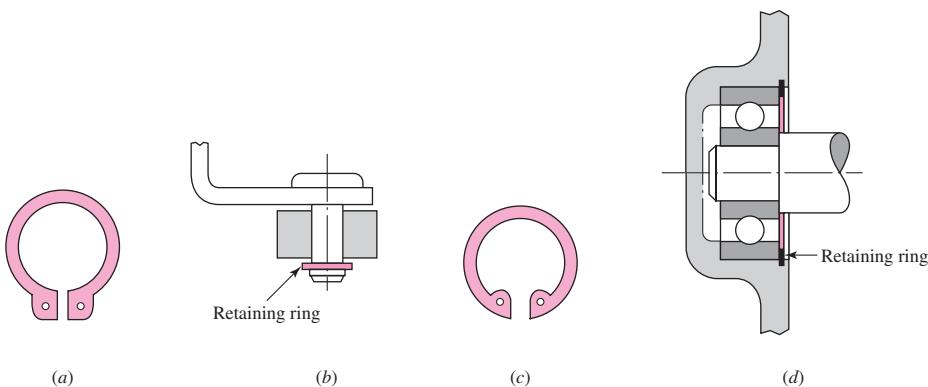
Sizes of Woodruff Keys

Suitable for Various
Shaft Diameters

Keyseat Width, in	From	Shaft Diameter, in To (inclusive)
$\frac{1}{16}$	$\frac{5}{16}$	$\frac{1}{2}$
$\frac{3}{32}$	$\frac{3}{8}$	$\frac{7}{8}$
$\frac{1}{8}$	$\frac{3}{8}$	$1\frac{1}{2}$
$\frac{5}{32}$	$\frac{1}{2}$	$1\frac{5}{8}$
$\frac{3}{16}$	$\frac{9}{16}$	2
$\frac{1}{4}$	$\frac{11}{16}$	$2\frac{1}{4}$
$\frac{5}{16}$	$\frac{3}{4}$	$2\frac{3}{8}$
$\frac{3}{8}$	1	$2\frac{5}{8}$

Figure 7-18

Typical uses for retaining rings.
(a) External ring and (b) its application; (c) internal ring and (d) its application.



of $d/10$ from the start of the shoulder fillet will prevent the two stress concentrations from combining with each other.⁹

Retaining Rings

A retaining ring is frequently used instead of a shaft shoulder or a sleeve to axially position a component on a shaft or in a housing bore. As shown in Fig. 7-18, a groove is cut in the shaft or bore to receive the spring retainer. For sizes, dimensions, and axial load ratings, the manufacturers' catalogs should be consulted.

Appendix Tables A-15-16 and A-15-17 give values for stress-concentration factors for flat-bottomed grooves in shafts, suitable for retaining rings. For the rings to seat nicely in the bottom of the groove, and support axial loads against the sides of the groove, the radius in the bottom of the groove must be reasonably sharp, typically about one-tenth of the groove width. This causes comparatively high values for stress-concentration factors, around 5 for bending and axial, and 3 for torsion. Care should be taken in using retaining rings, particularly in locations with high bending stresses.

EXAMPLE 7-6

A UNS G10350 steel shaft, heat-treated to a minimum yield strength of 75 kpsi, has a diameter of $1\frac{7}{16}$ in. The shaft rotates at 600 rev/min and transmits 40 hp through a gear. Select an appropriate key for the gear.

Solution

A $\frac{3}{8}$ -in square key is selected, UNS G10200 cold-drawn steel being used. The design will be based on a yield strength of 65 kpsi. A factor of safety of 2.80 will be employed in the absence of exact information about the nature of the load.

The torque is obtained from the horsepower equation

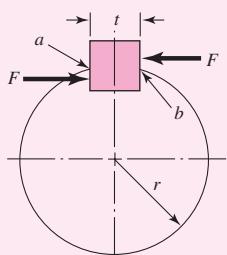
$$T = \frac{63025H}{n} = \frac{(63025)(40)}{600} = 4200 \text{ lbf} \cdot \text{in}$$

From Fig. 7-19, the force F at the surface of the shaft is

$$F = \frac{T}{r} = \frac{4200}{1.4375/2} = 5850 \text{ lbf}$$

By the distortion-energy theory, the shear strength is

$$S_{sy} = 0.577 S_y = (0.577)(65) = 37.5 \text{ kpsi}$$

**Figure 7-19**

⁹Ibid, p. 381.

Failure by shear across the area ab will create a stress of $\tau = F/tl$. Substituting the strength divided by the factor of safety for τ gives

$$\frac{S_{sy}}{n} = \frac{F}{tl} \quad \text{or} \quad \frac{37.5(10)^3}{2.80} = \frac{5850}{0.375l}$$

or $l = 1.16$ in. To resist crushing, the area of one-half the face of the key is used:

$$\frac{S_y}{n} = \frac{F}{tl/2} \quad \text{or} \quad \frac{65(10)^3}{2.80} = \frac{5850}{0.375l/2}$$

and $l = 1.34$ in. The hub length of a gear is usually greater than the shaft diameter, for stability. If the key, in this example, is made equal in length to the hub, it would therefore have ample strength, since it would probably be $1\frac{7}{16}$ in or longer.

7-8

Limits and Fits

The designer is free to adopt any geometry of fit for shafts and holes that will ensure the intended function. There is sufficient accumulated experience with commonly recurring situations to make standards useful. There are two standards for limits and fits in the United States, one based on inch units and the other based on metric units.¹⁰ These differ in nomenclature, definitions, and organization. No point would be served by separately studying each of the two systems. The metric version is the newer of the two and is well organized, and so here we present only the metric version but include a set of inch conversions to enable the same system to be used with either system of units.

In using the standard, *capital letters always refer to the hole; lowercase letters are used for the shaft*.

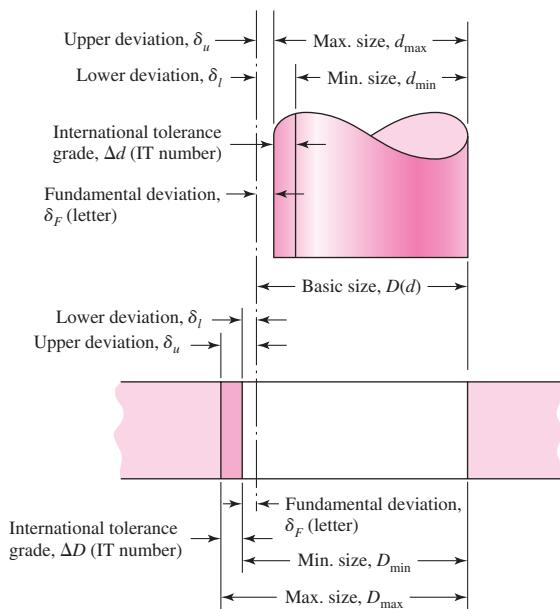
The definitions illustrated in Fig. 7-20 are explained as follows:

- *Basic size* is the size to which limits or deviations are assigned and is the same for both members of the fit.
- *Deviation* is the algebraic difference between a size and the corresponding basic size.
- *Upper deviation* is the algebraic difference between the maximum limit and the corresponding basic size.
- *Lower deviation* is the algebraic difference between the minimum limit and the corresponding basic size.
- *Fundamental deviation* is either the upper or the lower deviation, depending on which is closer to the basic size.
- *Tolerance* is the difference between the maximum and minimum size limits of a part.
- *International tolerance grade numbers (IT)* designate groups of tolerances such that the tolerances for a particular IT number have the same relative level of accuracy but vary depending on the basic size.
- *Hole basis* represents a system of fits corresponding to a basic hole size. The fundamental deviation is H.

¹⁰*Preferred Limits and Fits for Cylindrical Parts, ANSI B4.1-1967. Preferred Metric Limits and Fits, ANSI B4.2-1978.*

Figure 7-20

Definitions applied to a cylindrical fit.



- *Shaft basis* represents a system of fits corresponding to a basic shaft size. The fundamental deviation is h. The shaft-basis system is not included here.

The magnitude of the tolerance zone is the variation in part size and is the same for both the internal and the external dimensions. The tolerance zones are specified in international tolerance grade numbers, called IT numbers. The smaller grade numbers specify a smaller tolerance zone. These range from IT0 to IT16, but only grades IT6 to IT11 are needed for the preferred fits. These are listed in Tables A-11 to A-14 for basic sizes up to 16 in or 400 mm.

The standard uses *tolerance position letters*, with capital letters for internal dimensions (holes) and lowercase letters for external dimensions (shafts). As shown in Fig. 7-20, the fundamental deviation locates the tolerance zone relative to the basic size.

Table 7-9 shows how the letters are combined with the tolerance grades to establish a preferred fit. The ISO symbol for the hole for a sliding fit with a basic size of 32 mm is 32H7. Inch units are not a part of the standard. However, the designation $(1\frac{3}{8} \text{ in}) H7$ includes the same information and is recommended for use here. In both cases, the capital letter H establishes the fundamental deviation and the number 7 defines a tolerance grade of IT7.

For the sliding fit, the corresponding shaft dimensions are defined by the symbol 32g6 [$(1\frac{3}{8} \text{ in}) g6$].

The fundamental deviations for shafts are given in Tables A-11 and A-13. For letter codes c, d, f, g, and h,

$$\text{Upper deviation} = \text{fundamental deviation}$$

$$\text{Lower deviation} = \text{upper deviation} - \text{tolerance grade}$$

For letter codes k, n, p, s, and u, the deviations for shafts are

$$\text{Lower deviation} = \text{fundamental deviation}$$

$$\text{Upper deviation} = \text{lower deviation} + \text{tolerance grade}$$

Table 7-9

Descriptions of Preferred Fits Using the Basic Hole System
Source: Preferred Metric Limits and Fits, ANSI B4.2-1978. See also BS 4500.

	Type of Fit	Description	Symbol
Descriptions of Preferred Fits Using the Basic Hole System <i>Source: Preferred Metric Limits and Fits, ANSI B4.2-1978. See also BS 4500.</i>	Clearance	<i>Loose running fit:</i> for wide commercial tolerances or allowances on external members	H11/c11
		<i>Free running fit:</i> not for use where accuracy is essential, but good for large temperature variations, high running speeds, or heavy journal pressures	H9/d9
		<i>Close running fit:</i> for running on accurate machines and for accurate location at moderate speeds and journal pressures	H8/f7
		<i>Sliding fit:</i> where parts are not intended to run freely, but must move and turn freely and locate accurately	H7/g6
		<i>Locational clearance fit:</i> provides snug fit for location of stationary parts, but can be freely assembled and disassembled	H7/h6
Transition	Transition	<i>Locational transition fit:</i> for accurate location, a compromise between clearance and interference	H7/k6
		<i>Locational transition fit:</i> for more accurate location where greater interference is permissible	H7/n6
Interference	Interference	<i>Locational interference fit:</i> for parts requiring rigidity and alignment with prime accuracy of location but without special bore pressure requirements	H7/p6
		<i>Medium drive fit:</i> for ordinary steel parts or shrink fits on light sections, the tightest fit usable with cast iron	H7/s6
		<i>Force fit:</i> suitable for parts that can be highly stressed or for shrink fits where the heavy pressing forces required are impractical	H7/u6

The lower deviation H (for holes) is zero. For these, the upper deviation equals the tolerance grade.

As shown in Fig. 7-20, we use the following notation:

- D = basic size of hole
- d = basic size of shaft
- δ_u = upper deviation
- δ_l = lower deviation
- δ_F = fundamental deviation
- ΔD = tolerance grade for hole
- Δd = tolerance grade for shaft

Note that these quantities are all deterministic. Thus, for the hole,

$$D_{\max} = D + \Delta D \quad D_{\min} = D \quad (7-36)$$

For shafts with clearance fits c, d, f, g, and h,

$$d_{\max} = d + \delta_F \quad d_{\min} = d + \delta_F - \Delta d \quad (7-37)$$

For shafts with interference fits k, n, p, s, and u,

$$d_{\min} = d + \delta_F \quad d_{\max} = d + \delta_F + \Delta d \quad (7-38)$$

EXAMPLE 7-7 Find the shaft and hole dimensions for a loose running fit with a 34-mm basic size.

Solution From Table 7–9, the ISO symbol is 34H11/c11. From Table A–11, we find that tolerance grade IT11 is 0.160 mm. The symbol 34H11/c11 therefore says that $\Delta D = \Delta d = 0.160$ mm. Using Eq. (7–36) for the hole, we get

Answer $D_{\max} = D + \Delta D = 34 + 0.160 = 34.160 \text{ mm}$

Answer $D_{\min} = D = 34.000 \text{ mm}$

The shaft is designated as a 34c11 shaft. From Table A–12, the fundamental deviation is $\delta_F = -0.120$ mm. Using Eq. (7–37), we get for the shaft dimensions

Answer $d_{\max} = d + \delta_F = 34 + (-0.120) = 33.880 \text{ mm}$

Answer $d_{\min} = d + \delta_F - \Delta d = 34 + (-0.120) - 0.160 = 33.720 \text{ mm}$

EXAMPLE 7-8 Find the hole and shaft limits for a medium drive fit using a basic hole size of 2 in.

Solution The symbol for the fit, from Table 7–8, in inch units is (2 in)H7/s6. For the hole, we use Table A–13 and find the IT7 grade to be $\Delta D = 0.0010$ in. Thus, from Eq. (7–36),

Answer $D_{\max} = D + \Delta D = 2 + 0.0010 = 2.0010 \text{ in}$

Answer $D_{\min} = D = 2.0000 \text{ in}$

The IT6 tolerance for the shaft is $\Delta d = 0.0006$ in. Also, from Table A–14, the fundamental deviation is $\delta_F = 0.0017$ in. Using Eq. (7–38), we get for the shaft that

Answer $d_{\min} = d + \delta_F = 2 + 0.0017 = 2.0017 \text{ in}$

Answer $d_{\max} = d + \delta_F + \Delta d = 2 + 0.0017 + 0.0006 = 2.0023 \text{ in}$

Stress and Torque Capacity in Interference Fits

Interference fits between a shaft and its components can sometimes be used effectively to minimize the need for shoulders and keyways. The stresses due to an interference fit can be obtained by treating the shaft as a cylinder with a uniform external pressure, and the hub as a hollow cylinder with a uniform internal pressure. Stress equations for these situations were developed in Sec. 3–16, and will be converted here from radius terms into diameter terms to match the terminology of this section.

The pressure p generated at the interface of the interference fit, from Eq. (3–56) converted into terms of diameters, is given by

$$p = \frac{\delta}{\frac{d}{E_o} \left(\frac{d_o^2 + d^2}{d_o^2 - d^2} + v_o \right) + \frac{d}{E_i} \left(\frac{d^2 + d_i^2}{d^2 - d_i^2} - v_i \right)} \quad (7-39)$$

or, in the case where both members are of the same material,

$$p = \frac{E\delta}{2d^3} \left[\frac{(d_o^2 - d^2)(d^2 - d_i^2)}{d_o^2 - d_i^2} \right] \quad (7-40)$$

where d is the nominal shaft diameter, d_i is the inside diameter (if any) of the shaft, d_o is the outside diameter of the hub, E is Young's modulus, and v is Poisson's ratio, with subscripts o and i for the outer member (hub) and inner member (shaft), respectively. The term δ is the *diametral* interference between the shaft and hub, that is, the difference between the shaft outside diameter and the hub inside diameter.

$$\delta = d_{\text{shaft}} - d_{\text{hub}} \quad (7-41)$$

Since there will be tolerances on both diameters, the maximum and minimum pressures can be found by applying the maximum and minimum interferences. Adopting the notation from Fig. 7–20, we write

$$\delta_{\min} = d_{\min} - D_{\max} \quad (7-42)$$

$$\delta_{\max} = d_{\max} - D_{\min} \quad (7-43)$$

where the diameter terms are defined in Eqs. (7–36) and (7–38). The maximum interference should be used in Eq. (7–39) or (7–40) to determine the maximum pressure to check for excessive stress.

From Eqs. (3–58) and (3–59), with radii converted to diameters, the tangential stresses at the interface of the shaft and hub are

$$\sigma_{t, \text{shaft}} = -p \frac{d^2 + d_i^2}{d^2 - d_i^2} \quad (7-44)$$

$$\sigma_{t, \text{hub}} = p \frac{d_o^2 + d^2}{d_o^2 - d^2} \quad (7-45)$$

The radial stresses at the interface are simply

$$\sigma_{r, \text{shaft}} = -p \quad (7-46)$$

$$\sigma_{r, \text{hub}} = -p \quad (7-47)$$

The tangential and radial stresses are orthogonal, and should be combined using a failure theory to compare with the yield strength. If either the shaft or hub yields during assembly, the full pressure will not be achieved, diminishing the torque that can be transmitted. The interaction of the stresses due to the interference fit with the other stresses in the shaft due to shaft loading is not trivial. Finite-element analysis of the interface would be appropriate when warranted. A stress element on the surface of a rotating shaft will experience a completely reversed bending stress in the longitudinal direction, as well as the steady compressive stresses in the tangential and radial directions. This is a three-dimensional stress element. Shear stress due to torsion in shaft may also be present. Since the stresses due to the press fit are compressive, the fatigue situation is usually actually improved. For this reason, it may be acceptable to simplify the shaft analysis by ignoring

the steady compressive stresses due to the press fit. There is, however, a stress concentration effect in the shaft bending stress near the ends of the hub, due to the sudden change from compressed to uncompressed material. The design of the hub geometry, and therefore its uniformity and rigidity, can have a significant effect on the specific value of the stress-concentration factor, making it difficult to report generalized values. For first estimates, values are typically not greater than 2.

The amount of torque that can be transmitted through an interference fit can be estimated with a simple friction analysis at the interface. The friction force is the product of the coefficient of friction f and the normal force acting at the interface. The normal force can be represented by the product of the pressure p and the surface area A of interface. Therefore, the friction force F_f is

$$F_f = fN = f(pA) = f[p2\pi(d/2)l] = \pi f p l d \quad (7-48)$$

where l is the length of the hub. This friction force is acting with a moment arm of $d/2$ to provide the torque capacity of the joint, so

$$\begin{aligned} T &= F_f d/2 = \pi f p l d (d/2) \\ T &= (\pi/2) f p l d^2 \end{aligned} \quad (7-49)$$

The minimum interference, from Eq. (7-42), should be used to determine the minimum pressure to check for the maximum amount of torque that the joint should be designed to transmit without slipping.

PROBLEMS

Problems marked with an asterisk (*) are linked to problems in other chapters, as summarized in Table 1-1 of Sec. 1-16, p. 24.

7-1

A shaft is loaded in bending and torsion such that $M_a = 70 \text{ N}\cdot\text{m}$, $T_a = 45 \text{ N}\cdot\text{m}$, $M_m = 55 \text{ N}\cdot\text{m}$, and $T_m = 35 \text{ N}\cdot\text{m}$. For the shaft, $S_u = 700 \text{ MPa}$ and $S_y = 560 \text{ MPa}$, and a fully corrected endurance limit of $S_e = 210 \text{ MPa}$ is assumed. Let $K_f = 2.2$ and $K_{fs} = 1.8$. With a design factor of 2.0 determine the minimum acceptable diameter of the shaft using the

- (a) DE-Gerber criterion.
- (b) DE-elliptic criterion.
- (c) DE-Soderberg criterion.
- (d) DE-Goodman criterion.

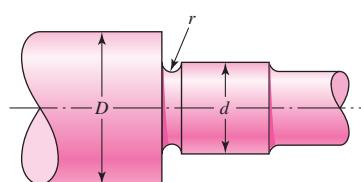
Discuss and compare the results.

7-2

The section of shaft shown in the figure is to be designed to approximate relative sizes of $d = 0.75D$ and $r = D/20$ with diameter d conforming to that of standard metric rolling-bearing bore sizes. The shaft is to be made of SAE 2340 steel, heat-treated to obtain minimum strengths in the shoulder area of 175 kpsi ultimate tensile strength and 160 kpsi yield strength with a Brinell hardness not less than 370. At the shoulder the shaft is subjected to a completely reversed bending moment of 600 lbf · in, accompanied by a steady torsion of 400 lbf · in. Use a design factor of 2.5 and size the shaft for an infinite life.

Problem 7-2

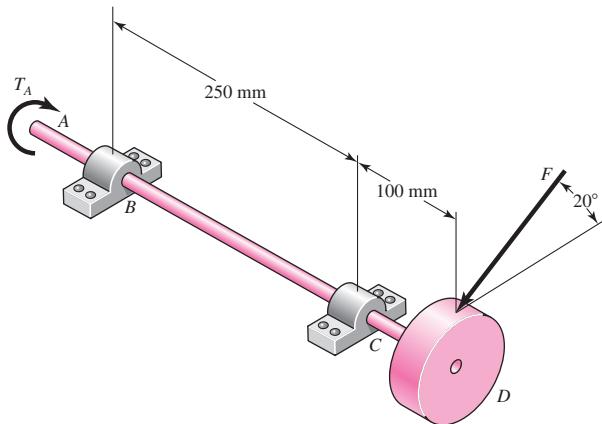
Section of a shaft containing a grinding-relief groove. Unless otherwise specified, the diameter at the root of the groove $d_r = d - 2r$, and though the section of diameter d is ground, the root of the groove is still a machined surface.



7-3

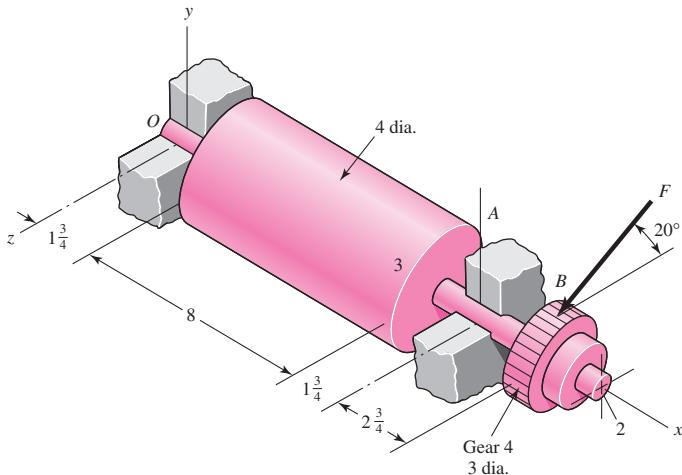
The rotating solid steel shaft is simply supported by bearings at points *B* and *C* and is driven by a gear (not shown) which meshes with the spur gear at *D*, which has a 150-mm pitch diameter. The force *F* from the drive gear acts at a pressure angle of 20° . The shaft transmits a torque to point *A* of $T_A = 340 \text{ N} \cdot \text{m}$. The shaft is machined from steel with $S_y = 420 \text{ MPa}$ and $S_{ut} = 560 \text{ MPa}$. Using a factor of safety of 2.5, determine the minimum allowable diameter of the 250-mm section of the shaft based on (a) a static yield analysis using the distortion energy theory and (b) a fatigue-failure analysis. Assume sharp fillet radii at the bearing shoulders for estimating stress-concentration factors.

Problem 7-3

**7-4**

A geared industrial roll shown in the figure is driven at 300 rev/min by a force *F* acting on a 3-in-diameter pitch circle as shown. The roll exerts a normal force of 30 lbf/in of roll length on the material being pulled through. The material passes under the roll. The coefficient of friction is 0.40. Develop the moment and shear diagrams for the shaft modeling the roll force as (a) a concentrated force at the center of the roll, and (b) a uniformly distributed force along the roll. These diagrams will appear on two orthogonal planes.

Problem 7-4
Material moves under the roll.
Dimensions in inches.

**7-5**

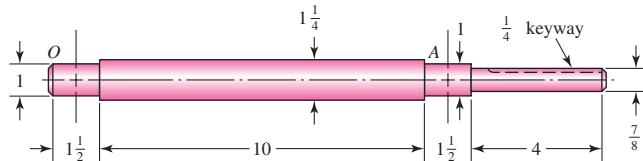
Design a shaft for the situation of the industrial roll of Prob. 7-4 with a design factor of 2 and a reliability goal of 0.999 against fatigue failure. Plan for a ball bearing on the left and a cylindrical roller on the right. For deformation use a factor of safety of 2.

7-6

The figure shows a proposed design for the industrial roll shaft of Prob. 7-4. Hydrodynamic film bearings are to be used. All surfaces are machined except the journals, which are ground and polished. The material is 1035 HR steel. Perform a design assessment. Is the design satisfactory?

Problem 7-6

Bearing shoulder fillets 0.030 in, others $\frac{1}{16}$ in. Sled-runner keyway is $\frac{3}{2}$ in long. Dimensions in inches.

**7-7* to
7-16***

For the problem specified in the table, build upon the results of the original problem to obtain a preliminary design of the shaft by performing the following tasks.

- Sketch a general shaft layout, including means to locate the components and to transmit the torque. Estimates for the component widths are acceptable at this point.
- Specify a suitable material for the shaft.
- Determine critical diameters of the shaft based on infinite fatigue life with a design factor of 1.5. Check for yielding.
- Make any other dimensional decisions necessary to specify all diameters and axial dimensions. Sketch the shaft to scale, showing all proposed dimensions.
- Check the deflections at the gears, and the slopes at the gears and the bearings for satisfaction of the recommended limits in Table 7-2. Assume the deflections for any pulleys are not likely to be critical. If any of the deflections exceed the recommended limits, make appropriate changes to bring them all within the limits.

Problem Number	Original Problem, Page Number
7-7*	3-68, 137
7-8*	3-69, 137
7-9*	3-70, 137
7-10*	3-71, 137
7-11*	3-72, 138
7-12*	3-73, 138
7-13*	3-74, 138
7-14*	3-76, 139
7-15*	3-77, 139
7-16*	3-79, 139

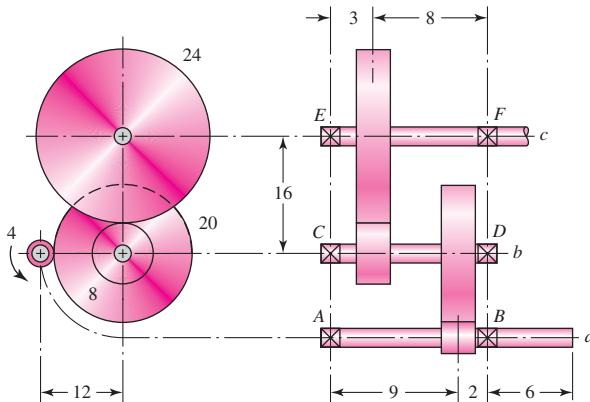
7-17

In the double-reduction gear train shown, shaft *a* is driven by a motor attached by a flexible coupling attached to the overhang. The motor provides a torque of 2500 lbf · in at a speed of 1200 rpm. The gears have 20° pressure angles, with diameters shown on the figure. Use an AISI 1020 cold-drawn steel. Design one of the shafts (as specified by the instructor) with a design factor of 1.5 by performing the following tasks.

- Sketch a general shaft layout, including means to locate the gears and bearings, and to transmit the torque.
- Perform a force analysis to find the bearing reaction forces, and generate shear and bending moment diagrams.
- Determine potential critical locations for stress design.

- (d) Determine critical diameters of the shaft based on fatigue and static stresses at the critical locations.
- (e) Make any other dimensional decisions necessary to specify all diameters and axial dimensions. Sketch the shaft to scale, showing all proposed dimensions.
- (f) Check the deflection at the gear, and the slopes at the gear and the bearings for satisfaction of the recommended limits in Table 7-2.
- (g) If any of the deflections exceed the recommended limits, make appropriate changes to bring them all within the limits.

Problem 7-17
Dimensions in inches.



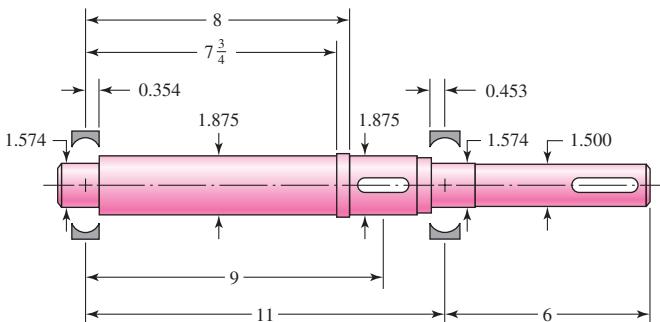
7-18

In the figure is a proposed shaft design to be used for the input shaft *a* in Prob. 7-17. A ball bearing is planned for the left bearing, and a cylindrical roller bearing for the right.

- (a) Determine the minimum fatigue factor of safety by evaluating at any critical locations. Use a fatigue failure criteria that is considered to be typical of the failure data, rather than one that is considered conservative. Also ensure that the shaft does not yield in the first load cycle.
- (b) Check the design for adequacy with respect to deformation, according to the recommendations in Table 7-2.

Problem 7-18

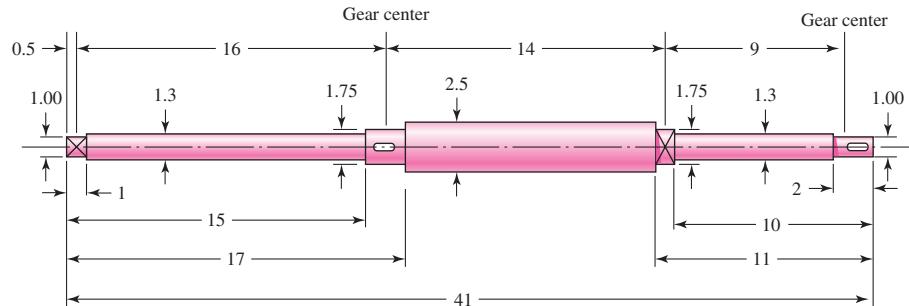
Shoulder fillets at bearing seat 0.030-in radius, others $\frac{1}{8}$ -in radius, except right-hand bearing seat transition, $\frac{1}{4}$ in. The material is 1030 HR. Keyways $\frac{3}{8}$ in wide by $\frac{3}{16}$ in deep. Dimensions in inches.



7-19*

The shaft shown in the figure is proposed for the application defined in Prob. 3-72, p. 138. The material is AISI 1018 cold-drawn steel. The gears seat against the shoulders, and have hubs with setscrews to lock them in place. The effective centers of the gears for force transmission are shown. The keyseats are cut with standard endmills. The bearings are press-fit against the shoulders. Determine the minimum fatigue factor of safety.

Problem 7-19*
All fillets $\frac{1}{16}$ in. Dimensions in inches.

**7-20***

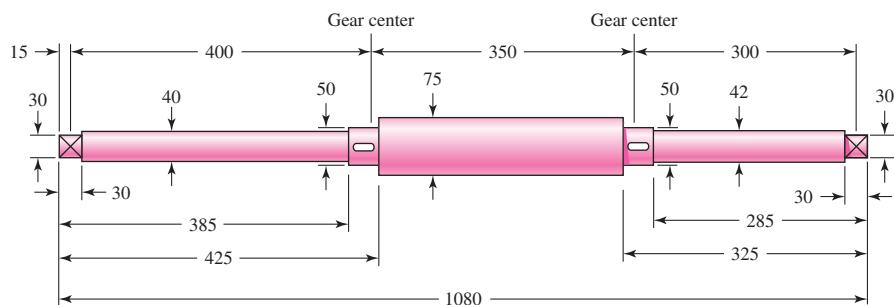
Continue Prob. 7-19 by checking that the deflections satisfy the suggested minimums for bearings and gears in Table 7-2. If any of the deflections exceed the recommended limits, make appropriate changes to bring them all within the limits.

7-21*

The shaft shown in the figure is proposed for the application defined in Prob. 3-73, p. 138. The material is AISI 1018 cold-drawn steel. The gears seat against the shoulders, and have hubs with setscrews to lock them in place. The effective centers of the gears for force transmission are shown. The keyseats are cut with standard endmills. The bearings are press-fit against the shoulders. Determine the minimum fatigue factor of safety.

Problem 7-21*

All fillets 2 mm. Dimensions in mm.

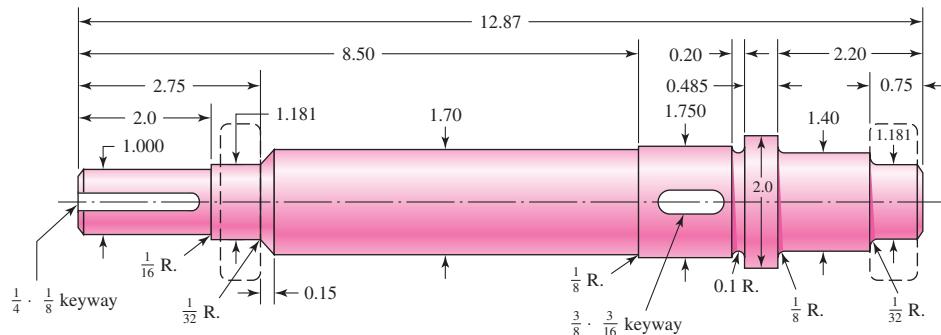
**7-22***

Continue Prob. 7-21 by checking that the deflections satisfy the suggested minimums for bearings and gears in Table 7-2. If any of the deflections exceed the recommended limits, make appropriate changes to bring them all within the limits.

7-23

The shaft shown in the figure is driven by a gear at the right keyway, drives a fan at the left keyway, and is supported by two deep-groove ball bearings. The shaft is made from AISI 1020 cold-drawn

Problem 7-23
Dimensions in inches.



steel. At steady-state speed, the gear transmits a radial load of 230 lbf and a tangential load of 633 lbf at a pitch diameter of 8 in.

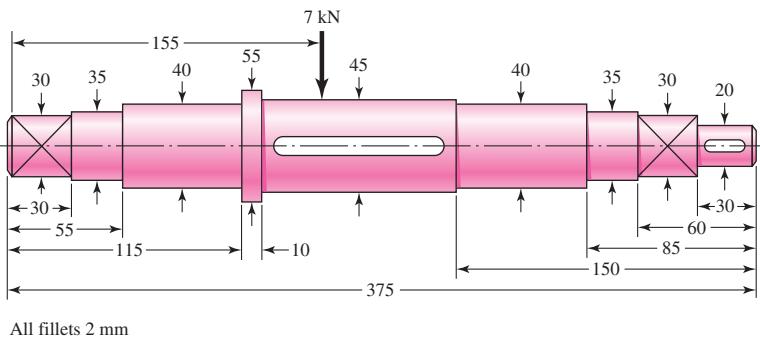
(a) Determine fatigue factors of safety at any potentially critical locations.

(b) Check that deflections satisfy the suggested minimums for bearings and gears.

7-24

An AISI 1020 cold-drawn steel shaft with the geometry shown in the figure carries a transverse load of 7 kN and a torque of 107 N · m. Examine the shaft for strength and deflection. If the largest allowable slope at the bearings is 0.001 rad and at the gear mesh is 0.0005 rad, what is the factor of safety guarding against damaging distortion? What is the factor of safety guarding against a fatigue failure? If the shaft turns out to be unsatisfactory, what would you recommend to correct the problem?

Problem 7-24
Dimensions in millimeters.

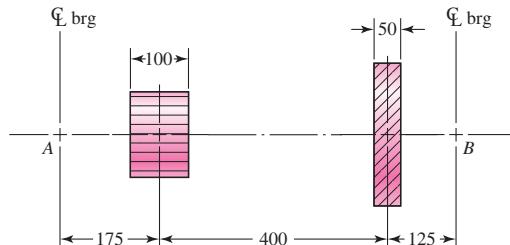


All fillets 2 mm

7-25

A shaft is to be designed to support the spur pinion and helical gear shown in the figure on two bearings spaced 700 mm center-to-center. Bearing *A* is a cylindrical roller and is to take only radial load; bearing *B* is to take the thrust load of 900 N produced by the helical gear and its share of the radial load. The bearing at *B* can be a ball bearing. The radial loads of both gears are in the same plane, and are 2.7 kN for the pinion and 900 N for the gear. The shaft speed is 1200 rev/min. Design the shaft. Make a sketch to scale of the shaft showing all fillet sizes, keyways, shoulders, and diameters. Specify the material and its heat treatment.

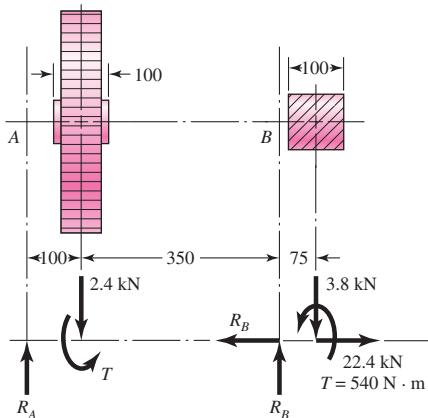
Problem 7-25
Dimensions in millimeters.



7-26

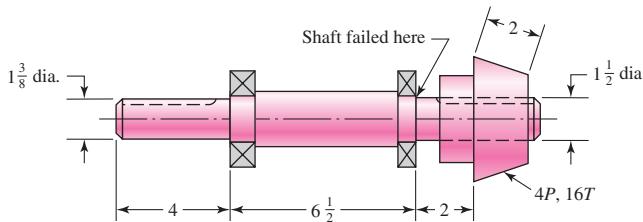
A heat-treated steel shaft is to be designed to support the spur gear and the overhanging worm shown in the figure. A bearing at *A* takes pure radial load. The bearing at *B* takes the worm-thrust load for either direction of rotation. The dimensions and the loading are shown in the figure; note that the radial loads are in the same plane. Make a complete design of the shaft, including a sketch of the shaft showing all dimensions. Identify the material and its heat treatment (if necessary). Provide an assessment of your final design. The shaft speed is 310 rev/min.

Problem 7-26
Dimensions in millimeters.

**7-27**

A bevel-gear shaft mounted on two 40-mm 02-series ball bearings is driven at 1720 rev/min by a motor connected through a flexible coupling. The figure shows the shaft, the gear, and the bearings. The shaft has been giving trouble—in fact, two of them have already failed—and the down time on the machine is so expensive that you have decided to redesign the shaft yourself rather than order replacements. A hardness check of the two shafts in the vicinity of the fracture of the two shafts showed an average of 198 Bhn for one and 204 Bhn of the other. As closely as you can estimate the two shafts failed at a life measure between 600 000 and 1 200 000 cycles of operation. The surfaces of the shaft were machined, but not ground. The fillet sizes were not measured, but they correspond with the recommendations for the ball bearings used. You know that the load is a pulsating or shock-type load, but you have no idea of the magnitude, because the shaft drives an indexing mechanism, and the forces are inertial. The keyways are $\frac{3}{8}$ in wide by $\frac{3}{16}$ in deep. The straight-toothed bevel pinion drives a 48-tooth bevel gear. Specify a new shaft in sufficient detail to ensure a long and trouble-free life.

Problem 7-27
Dimensions in inches.

**7-28**

A 25-mm-diameter uniform steel shaft is 600 mm long between bearings.

- Find the lowest critical speed of the shaft.
- If the goal is to double the critical speed, find the new diameter.
- A half-size model of the original shaft has what critical speed?

7-29

Demonstrate how rapidly Rayleigh's method converges for the uniform-diameter solid shaft of Prob. 7-28, by partitioning the shaft into first one, then two, and finally three elements.

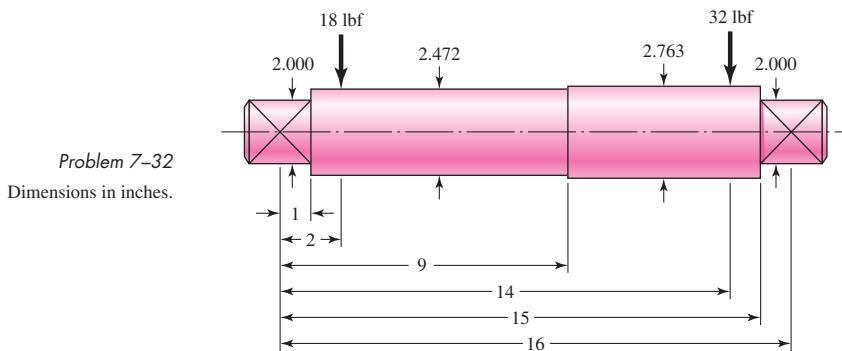
7-30

Compare Eq. (7-27) for the angular frequency of a two-disk shaft with Eq. (7-28), and note that the constants in the two equations are equal.

- Develop an expression for the second critical speed.
- Estimate the second critical speed of the shaft addressed in Ex. 7-5, parts *a* and *b*.

- 7-31** For a uniform-diameter shaft, does hollowing the shaft increase or decrease the critical speed?

- 7-32** The shaft shown in the figure carries a 18-lbf gear on the left and a 32-lbf gear on the right. Estimate the first critical speed due to the loads, the shaft's critical speed without the loads, and the critical speed of the combination.



- 7-33** A transverse drilled and reamed hole can be used in a solid shaft to hold a pin that locates and holds a mechanical element, such as the hub of a gear, in axial position, and allows for the transmission of torque. Since a small-diameter hole introduces high stress concentration, and a larger diameter hole erodes the area resisting bending and torsion, investigate the existence of a pin diameter with minimum adverse affect on the shaft. Then formulate a design rule. (*Hint:* Use Table A-16.)

- 7-34*** The shaft shown in Prob. 7-19 is proposed for the application defined in Prob. 3-72, p. 138. Specify a square key for gear *B*, using a factor of safety of 1.1.

- 7-35*** The shaft shown in Prob. 7-21 is proposed for the application defined in Prob. 3-73, p. 138. Specify a square key for gear *B*, using a factor of safety of 1.1.

- 7-36** A guide pin is required to align the assembly of a two-part fixture. The nominal size of the pin is 15 mm. Make the dimensional decisions for a 15-mm basic size locational clearance fit.

- 7-37** An interference fit of a cast-iron hub of a gear on a steel shaft is required. Make the dimensional decisions for a 1.75-in basic size medium drive fit.

- 7-38** A pin is required for forming a linkage pivot. Find the dimensions required for a 45-mm basic size pin and clevis with a sliding fit.

- 7-39** A journal bearing and bushing need to be described. The nominal size is 1.25 in. What dimensions are needed for a 1.25-in basic size with a close running fit if this is a lightly loaded journal and bushing assembly?

- 7-40** A ball bearing has been selected with the bore size specified in the catalog as 35.000 mm to 35.020 mm. Specify appropriate minimum and maximum shaft diameters to provide a locational interference fit.

- 7-41** A shaft diameter is carefully measured to be 1.5020 in. A bearing is selected with a catalog specification of the bore diameter range from 1.500 in to 1.501 in. Determine if this is an acceptable selection if a locational interference fit is desired.

7-42

A gear and shaft with nominal diameter of 35 mm are to be assembled with a *medium drive fit*, as specified in Table 7–9. The gear has a hub, with an outside diameter of 60 mm, and an overall length of 50 mm. The shaft is made from AISI 1020 CD steel, and the gear is made from steel that has been through hardened to provide $S_u = 700$ MPa and $S_y = 600$ MPa.

- (a) Specify dimensions with tolerances for the shaft and gear bore to achieve the desired fit.
- (b) Determine the minimum and maximum pressures that could be experienced at the interface with the specified tolerances.
- (c) Determine the worst-case static factors of safety guarding against yielding at assembly for the shaft and the gear based on the distortion energy failure theory.
- (d) Determine the maximum torque that the joint should be expected to transmit without slipping, i.e., when the interference pressure is at a minimum for the specified tolerances.

8

Screws, Fasteners, and the Design of Nonpermanent Joints

Chapter Outline

8-1	Thread Standards and Definitions	410
8-2	The Mechanics of Power Screws	414
8-3	Threaded Fasteners	422
8-4	Joints—Fastener Stiffness	424
8-5	Joints—Member Stiffness	427
8-6	Bolt Strength	432
8-7	Tension Joints—The External Load	435
8-8	Relating Bolt Torque to Bolt Tension	437
8-9	Statically Loaded Tension Joint with Preload	440
8-10	Gasketed Joints	444
8-11	Fatigue Loading of Tension Joints	444
8-12	Bolted and Riveted Joints Loaded in Shear	451

The helical-thread screw was undoubtably an extremely important mechanical invention. It is the basis of power screws, which change angular motion to linear motion to transmit power or to develop large forces (presses, jacks, etc.), and threaded fasteners, an important element in nonpermanent joints.

This book presupposes a knowledge of the elementary methods of fastening. Typical methods of fastening or joining parts use such devices as bolts, nuts, cap screws, setscrews, rivets, spring retainers, locking devices, pins, keys, welds, and adhesives. Studies in engineering graphics and in metal processes often include instruction on various joining methods, and the curiosity of any person interested in mechanical engineering naturally results in the acquisition of a good background knowledge of fastening methods. Contrary to first impressions, the subject is one of the most interesting in the entire field of mechanical design.

One of the key targets of current design for manufacture is to reduce the number of fasteners. However, there will always be a need for fasteners to facilitate disassembly for whatever purposes. For example, jumbo jets such as Boeing's 747 require as many as 2.5 million fasteners, some of which cost several dollars apiece. To keep costs down, aircraft manufacturers, and their subcontractors, constantly review new fastener designs, installation techniques, and tooling.

The number of innovations in the fastener field over any period you might care to mention has been tremendous. An overwhelming variety of fasteners are available for the designer's selection. Serious designers generally keep specific notebooks on fasteners alone. Methods of joining parts are extremely important in the engineering of a quality design, and it is necessary to have a thorough understanding of the performance of fasteners and joints under all conditions of use and design.

8-1

Thread Standards and Definitions

The terminology of screw threads, illustrated in Fig. 8-1, is explained as follows:

The *pitch* is the distance between adjacent thread forms measured parallel to the thread axis. The pitch in U.S. units is the reciprocal of the number of thread forms per inch N .

The *major diameter* d is the largest diameter of a screw thread.

The *minor (or root) diameter* d_r is the smallest diameter of a screw thread.

The *pitch diameter* d_p is a theoretical diameter between the major and minor diameters.

The *lead* l , not shown, is the distance the nut moves parallel to the screw axis when the nut is given one turn. For a single thread, as in Fig. 8-1, the lead is the same as the pitch.

A *multiple-threaded* product is one having two or more threads cut beside each other (imagine two or more strings wound side by side around a pencil). Standardized products such as screws, bolts, and nuts all have single threads; a *double-threaded* screw has a lead equal to twice the pitch, a *triple-threaded* screw has a lead equal to 3 times the pitch, and so on.

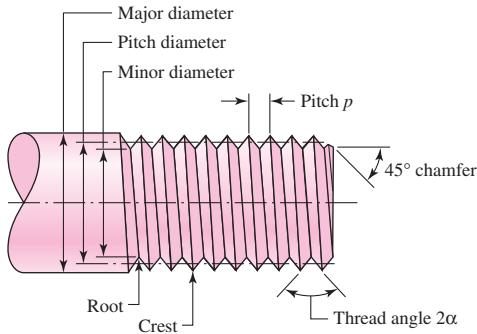
All threads are made according to the *right-hand rule* unless otherwise noted. That is, if the bolt is turned clockwise, the bolt advances toward the nut.

The *American National (Unified)* thread standard has been approved in this country and in Great Britain for use on all standard threaded products. The thread angle is 60° and the crests of the thread may be either flat or rounded.

Figure 8-2 shows the thread geometry of the metric M and MJ profiles. The M profile replaces the inch class and is the basic ISO 68 profile with 60° symmetric

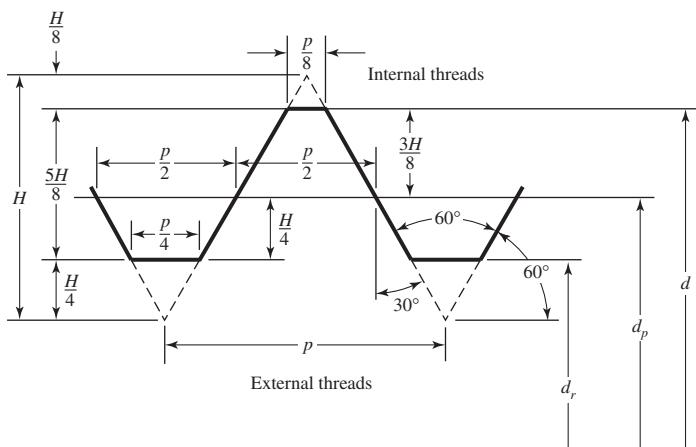
Figure 8-1

Terminology of screw threads. Sharp vee threads shown for clarity; the crests and roots are actually flattened or rounded during the forming operation.

**Figure 8-2**

Basic profile for metric M and MJ threads.
 d = major diameter
 d_r = minor diameter
 d_p = pitch diameter

p = pitch
 $H = \frac{\sqrt{3}}{2} p$



threads. The MJ profile has a rounded fillet at the root of the external thread and a larger minor diameter of both the internal and external threads. This profile is especially useful where high fatigue strength is required.

Tables 8-1 and 8-2 will be useful in specifying and designing threaded parts. Note that the thread size is specified by giving the pitch p for metric sizes and by giving the number of threads per inch N for the Unified sizes. The screw sizes in Table 8-2 with diameter under $\frac{1}{4}$ in are numbered or gauge sizes. The second column in Table 8-2 shows that a No. 8 screw has a nominal major diameter of 0.1640 in.

A great many tensile tests of threaded rods have shown that an unthreaded rod having a diameter equal to the mean of the pitch diameter and minor diameter will have the same tensile strength as the threaded rod. The area of this unthreaded rod is called the tensile-stress area A_t of the threaded rod; values of A_t are listed in both tables.

Two major Unified thread series are in common use: UN and UNR. The difference between these is simply that a root radius must be used in the UNR series. Because of reduced thread stress-concentration factors, UNR series threads have improved fatigue strengths. Unified threads are specified by stating the nominal major diameter, the number of threads per inch, and the thread series, for example, $\frac{5}{8}$ in-18 UNRF or 0.625 in-18 UNRF.

Metric threads are specified by writing the diameter and pitch in millimeters, in that order. Thus, M12 × 1.75 is a thread having a nominal major diameter of 12 mm and a pitch of 1.75 mm. Note that the letter M, which precedes the diameter, is the clue to the metric designation.

Table 8-1

Diameters and Areas of Coarse-Pitch and Fine-Pitch Metric Threads.*

Nominal Major Diameter <i>d</i> mm	Coarse-Pitch Series				Fine-Pitch Series			
	Pitch <i>p</i> mm	Tensile- Stress Area <i>A_f</i>, mm²	Minor- Diameter <i>d_r</i> mm	Pitch <i>p</i> mm	Tensile- Stress Area <i>A_f</i>, mm²	Minor- Diameter <i>d_r</i> mm		
1.6	0.35	1.27	1.07					
2	0.40	2.07	1.79					
2.5	0.45	3.39	2.98					
3	0.5	5.03	4.47					
3.5	0.6	6.78	6.00					
4	0.7	8.78	7.75					
5	0.8	14.2	12.7					
6	1	20.1	17.9					
8	1.25	36.6	32.8	1	39.2	36.0		
10	1.5	58.0	52.3	1.25	61.2	56.3		
12	1.75	84.3	76.3	1.25	92.1	86.0		
14	2	115	104	1.5	125	116		
16	2	157	144	1.5	167	157		
20	2.5	245	225	1.5	272	259		
24	3	353	324	2	384	365		
30	3.5	561	519	2	621	596		
36	4	817	759	2	915	884		
42	4.5	1120	1050	2	1260	1230		
48	5	1470	1380	2	1670	1630		
56	5.5	2030	1910	2	2300	2250		
64	6	2680	2520	2	3030	2980		
72	6	3460	3280	2	3860	3800		
80	6	4340	4140	1.5	4850	4800		
90	6	5590	5360	2	6100	6020		
100	6	6990	6740	2	7560	7470		
110				2	9180	9080		

*The equations and data used to develop this table have been obtained from ANSI B1.1-1974 and B18.3.1-1978. The minor diameter was found from the equation $d_r = d - 1.226869p$, and the pitch diameter from $d_p = d - 0.649519p$. The mean of the pitch diameter and the minor diameter was used to compute the tensile-stress area.

Square and Acme threads, whose profiles are shown in Fig. 8-3a and b, respectively, are used on screws when power is to be transmitted. Table 8-3 lists the preferred pitches for inch-series Acme threads. However, other pitches can be and often are used, since the need for a standard for such threads is not great.

Modifications are frequently made to both Acme and square threads. For instance, the square thread is sometimes modified by cutting the space between the teeth so as to have an included thread angle of 10 to 15°. This is not difficult, since these threads are usually cut with a single-point tool anyhow; the modification retains most of the high efficiency inherent in square threads and makes the cutting simpler. Acme threads

Table 8-2

Diameters and Area of Unified Screw Threads UNC and UNF*

Size Designation	Nominal Major Diameter in	Coarse Series—UNC			Fine Series—UNF		
		Threads per Inch N	Tensile-Stress Area A_f in ²	Minor-Diameter Area A_r in ²	Threads per Inch N	Tensile-Stress Area A_f in ²	Minor-Diameter Area A_r in ²
0	0.0600				80	0.001 80	0.001 51
1	0.0730	64	0.002 63	0.002 18	72	0.002 78	0.002 37
2	0.0860	56	0.003 70	0.003 10	64	0.003 94	0.003 39
3	0.0990	48	0.004 87	0.004 06	56	0.005 23	0.004 51
4	0.1120	40	0.006 04	0.004 96	48	0.006 61	0.005 66
5	0.1250	40	0.007 96	0.006 72	44	0.008 80	0.007 16
6	0.1380	32	0.009 09	0.007 45	40	0.010 15	0.008 74
8	0.1640	32	0.014 0	0.011 96	36	0.014 74	0.012 85
10	0.1900	24	0.017 5	0.014 50	32	0.020 0	0.017 5
12	0.2160	24	0.024 2	0.020 6	28	0.025 8	0.022 6
$\frac{1}{4}$	0.2500	20	0.031 8	0.026 9	28	0.036 4	0.032 6
$\frac{5}{16}$	0.3125	18	0.052 4	0.045 4	24	0.058 0	0.052 4
$\frac{3}{8}$	0.3750	16	0.077 5	0.067 8	24	0.087 8	0.080 9
$\frac{7}{16}$	0.4375	14	0.106 3	0.093 3	20	0.118 7	0.109 0
$\frac{1}{2}$	0.5000	13	0.141 9	0.125 7	20	0.159 9	0.148 6
$\frac{9}{16}$	0.5625	12	0.182	0.162	18	0.203	0.189
$\frac{5}{8}$	0.6250	11	0.226	0.202	18	0.256	0.240
$\frac{3}{4}$	0.7500	10	0.334	0.302	16	0.373	0.351
$\frac{7}{8}$	0.8750	9	0.462	0.419	14	0.509	0.480
1	1.0000	8	0.606	0.551	12	0.663	0.625
$1\frac{1}{4}$	1.2500	7	0.969	0.890	12	1.073	1.024
$1\frac{1}{2}$	1.5000	6	1.405	1.294	12	1.581	1.521

*This table was compiled from ANSI B1.1-1974. The minor diameter was found from the equation $d_r = d - 1.299 038p$, and the pitch diameter from $d_p = d - 0.649 519p$. The mean of the pitch diameter and the minor diameter was used to compute the tensile-stress area.

Figure 8-3

(a) Square thread; (b) Acme thread.

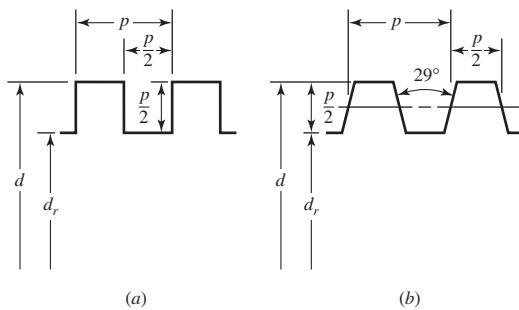


Table 8-3

Preferred Pitches for
Acme Threads

<i>d</i> , in	$\frac{1}{4}$	$\frac{5}{16}$	$\frac{3}{8}$	$\frac{1}{2}$	$\frac{5}{8}$	$\frac{3}{4}$	$\frac{7}{8}$	1	$1\frac{1}{4}$	$1\frac{1}{2}$	$1\frac{3}{4}$	2	$2\frac{1}{2}$	3
<i>p</i> , in	$\frac{1}{16}$	$\frac{1}{14}$	$\frac{1}{12}$	$\frac{1}{10}$	$\frac{1}{8}$	$\frac{1}{6}$	$\frac{1}{5}$	$\frac{1}{5}$	$\frac{1}{4}$	$\frac{1}{4}$	$\frac{1}{3}$	$\frac{1}{4}$	$\frac{1}{3}$	$\frac{1}{2}$

are sometimes modified to a stub form by making the teeth shorter. This results in a larger minor diameter and a somewhat stronger screw.

8-2

The Mechanics of Power Screws

A power screw is a device used in machinery to change angular motion into linear motion, and, usually, to transmit power. Familiar applications include the lead screws of lathes, and the screws for vises, presses, and jacks.

An application of power screws to a power-driven jack is shown in Fig. 8-4. You should be able to identify the worm, the worm gear, the screw, and the nut. Is the worm gear supported by one bearing or two?

Figure 8-4

The Joyce worm-gear screw jack. (*Courtesy Joyce-Dayton Corp., Dayton, Ohio.*)

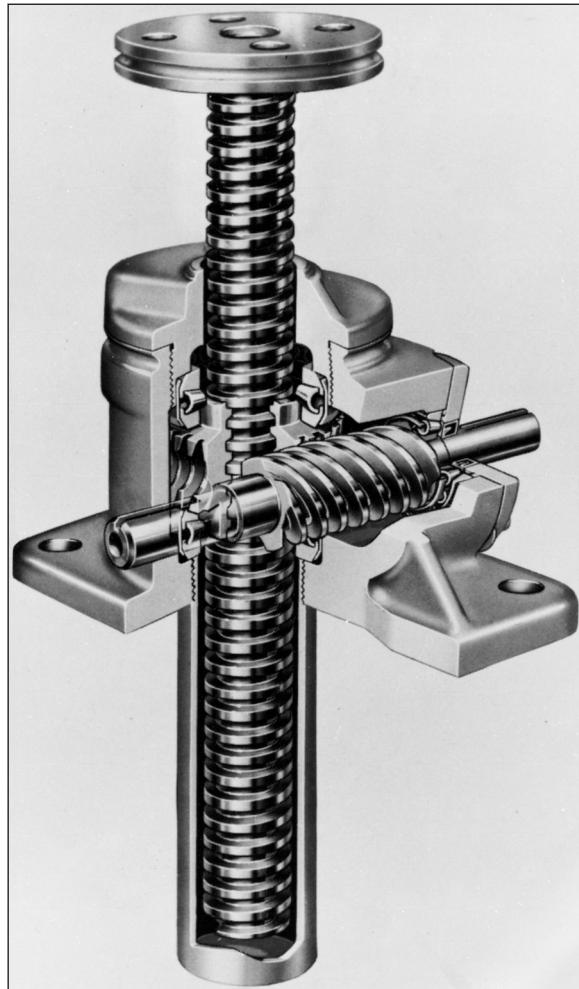
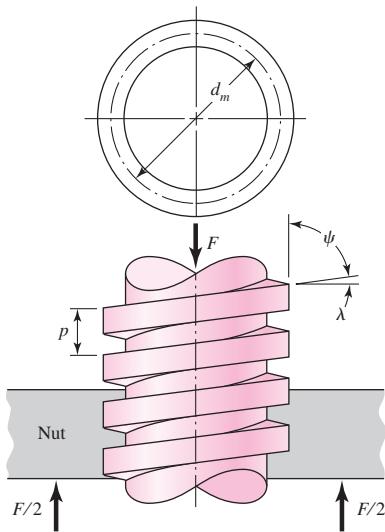
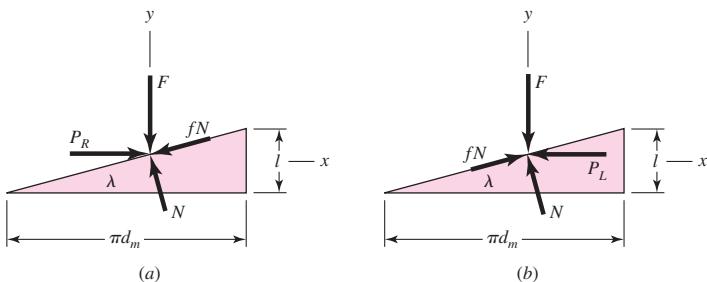


Figure 8-5

Portion of a power screw.

**Figure 8-6**

Force diagrams: (a) lifting the load; (b) lowering the load.



In Fig. 8-5 a square-threaded power screw with single thread having a mean diameter d_m , a pitch p , a lead angle λ , and a helix angle ψ is loaded by the axial compressive force F . We wish to find an expression for the torque required to raise this load, and another expression for the torque required to lower the load.

First, imagine that a single thread of the screw is unrolled or developed (Fig. 8-6) for exactly a single turn. Then one edge of the thread will form the hypotenuse of a right triangle whose base is the circumference of the mean-thread-diameter circle and whose height is the lead. The angle λ , in Figs. 8-5 and 8-6, is the lead angle of the thread. We represent the summation of all the axial forces acting upon the normal thread area by F . To raise the load, a force P_R acts to the right (Fig. 8-6a), and to lower the load, P_L acts to the left (Fig. 8-6b). The friction force is the product of the coefficient of friction f with the normal force N , and acts to oppose the motion. The system is in equilibrium under the action of these forces, and hence, for raising the load, we have

$$\sum F_x = P_R - N \sin \lambda - fN \cos \lambda = 0 \quad (a)$$

$$\sum F_y = -F - fN \sin \lambda + N \cos \lambda = 0$$

In a similar manner, for lowering the load, we have

$$\sum F_x = -P_L - N \sin \lambda + fN \cos \lambda = 0 \quad (b)$$

$$\sum F_y = -F + fN \sin \lambda + N \cos \lambda = 0$$

Since we are not interested in the normal force N , we eliminate it from each of these sets of equations and solve the result for P . For raising the load, this gives

$$P_R = \frac{F(\sin \lambda + f \cos \lambda)}{\cos \lambda - f \sin \lambda} \quad (c)$$

and for lowering the load,

$$P_L = \frac{F(f \cos \lambda - \sin \lambda)}{\cos \lambda + f \sin \lambda} \quad (d)$$

Next, divide the numerator and the denominator of these equations by $\cos \lambda$ and use the relation $\tan \lambda = l/\pi d_m$ (Fig. 8–6). We then have, respectively,

$$P_R = \frac{F[(l/\pi d_m) + f]}{1 - (f l / \pi d_m)} \quad (e)$$

$$P_L = \frac{F[f - (l/\pi d_m)]}{1 + (f l / \pi d_m)} \quad (f)$$

Finally, noting that the torque is the product of the force P and the mean radius $d_m/2$, for raising the load we can write

$$T_R = \frac{Fd_m}{2} \left(\frac{l + \pi f d_m}{\pi d_m - f l} \right) \quad (8-1)$$

where T_R is the torque required for two purposes: to overcome thread friction and to raise the load.

The torque required to lower the load, from Eq. (f), is found to be

$$T_L = \frac{Fd_m}{2} \left(\frac{\pi f d_m - l}{\pi d_m + f l} \right) \quad (8-2)$$

This is the torque required to overcome a part of the friction in lowering the load. It may turn out, in specific instances where the lead is large or the friction is low, that the load will lower itself by causing the screw to spin without any external effort. In such cases, the torque T_L from Eq. (8–2) will be negative or zero. When a positive torque is obtained from this equation, the screw is said to be *self-locking*. Thus the condition for self-locking is

$$\pi f d_m > l$$

Now divide both sides of this inequality by πd_m . Recognizing that $l/\pi d_m = \tan \lambda$, we get

$$f > \tan \lambda \quad (8-3)$$

This relation states that self-locking is obtained whenever the coefficient of thread friction is equal to or greater than the tangent of the thread lead angle.

An expression for efficiency is also useful in the evaluation of power screws. If we let $f = 0$ in Eq. (8–1), we obtain

$$T_0 = \frac{Fl}{2\pi} \quad (g)$$

which, since thread friction has been eliminated, is the torque required only to raise the load. The efficiency is therefore

$$e = \frac{T_0}{T_R} = \frac{Fl}{2\pi T_R} \quad (8-4)$$

The preceding equations have been developed for square threads where the normal thread loads are parallel to the axis of the screw. In the case of Acme or other threads, the normal thread load is inclined to the axis because of the thread angle 2α and the lead angle λ . Since lead angles are small, this inclination can be neglected and only the effect of the thread angle (Fig. 8-7a) considered. The effect of the angle α is to increase the frictional force by the wedging action of the threads. Therefore the frictional terms in Eq. (8-1) must be divided by $\cos \alpha$. For raising the load, or for tightening a screw or bolt, this yields

$$T_R = \frac{Fd_m}{2} \left(\frac{l + \pi f d_m \sec \alpha}{\pi d_m - fl \sec \alpha} \right) \quad (8-5)$$

In using Eq. (8-5), remember that it is an approximation because the effect of the lead angle has been neglected.

For power screws, the Acme thread is not as efficient as the square thread, because of the additional friction due to the wedging action, but it is often preferred because it is easier to machine and permits the use of a split nut, which can be adjusted to take up for wear.

Usually a third component of torque must be applied in power-screw applications. When the screw is loaded axially, a thrust or collar bearing must be employed between the rotating and stationary members in order to carry the axial component. Figure 8-7b shows a typical thrust collar in which the load is assumed to be concentrated at the mean collar diameter d_c . If f_c is the coefficient of collar friction, the torque required is

$$T_c = \frac{F f_c d_c}{2} \quad (8-6)$$

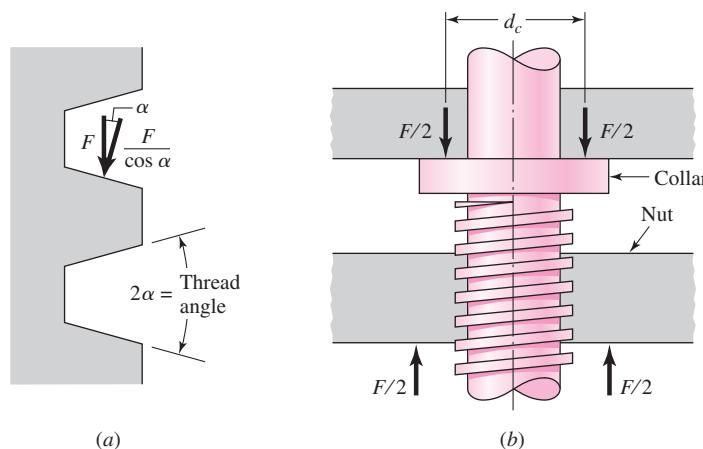
For large collars, the torque should probably be computed in a manner similar to that employed for disk clutches.

Nominal body stresses in power screws can be related to thread parameters as follows. The maximum nominal shear stress τ in torsion of the screw body can be expressed as

$$\tau = \frac{16T}{\pi d_r^3} \quad (8-7)$$

Figure 8-7

- (a) Normal thread force is increased because of angle α ;
- (b) thrust collar has frictional diameter d_c .



The axial stress σ in the body of the screw due to load F is

$$\sigma = \frac{F}{A} = \frac{4F}{\pi d_r^2} \quad (8-8)$$

in the absence of column action. For a short column the J. B. Johnson buckling formula is given by Eq. (4-43), which is

$$\left(\frac{F}{A}\right)_{\text{crit}} = S_y - \left(\frac{S_y}{2\pi k}\right)^2 \frac{1}{CE} \quad (8-9)$$

Nominal thread stresses in power screws can be related to thread parameters as follows. The bearing stress in Fig. 8-8, σ_B , is

$$\sigma_B = -\frac{F}{\pi d_m n_t p / 2} = -\frac{2F}{\pi d_m n_t p} \quad (8-10)$$

where n_t is the number of engaged threads. The bending stress at the root of the thread σ_b is found from

$$Z = \frac{I}{c} = \frac{(\pi d_r n_t) (p/2)^2}{6} = \frac{\pi}{24} d_r n_t p^2 \quad M = \frac{Fp}{4}$$

so

$$\sigma_b = \frac{M}{Z} = \frac{Fp}{4} \frac{24}{\pi d_r n_t p^2} = \frac{6F}{\pi d_r n_t p} \quad (8-11)$$

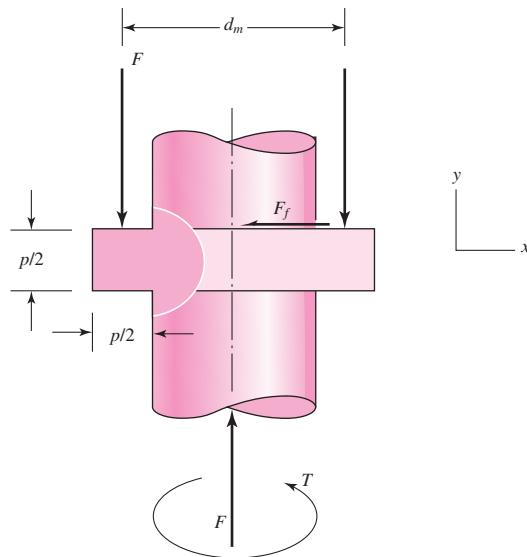
The transverse shear stress τ at the center of the root of the thread due to load F is

$$\tau = \frac{3V}{2A} = \frac{3}{2} \frac{F}{\pi d_r n_t p / 2} = \frac{3F}{\pi d_r n_t p} \quad (8-12)$$

and at the top of the root it is zero. The von Mises stress σ' at the top of the root “plane” is found by first identifying the orthogonal normal stresses and the shear stresses. From

Figure 8-8

Geometry of square thread useful in finding bending and transverse shear stresses at the thread root.



the coordinate system of Fig. 8–8, we note

$$\begin{aligned}\sigma_x &= \frac{6F}{\pi d_r n_t p} & \tau_{xy} &= 0 \\ \sigma_y &= -\frac{4F}{\pi d_r^2} & \tau_{yz} &= \frac{16T}{\pi d_r^3} \\ \sigma_z &= 0 & \tau_{zx} &= 0\end{aligned}$$

then use Eq. (5–14) of Sec. 5–5.

The screw-thread form is complicated from an analysis viewpoint. Remember the origin of the tensile-stress area A_t , which comes from experiment. A power screw lifting a load is in compression and its thread pitch is *shortened* by elastic deformation. Its engaging nut is in tension and its thread pitch is *lengthened*. The engaged threads cannot share the load equally. Some experiments show that the first engaged thread carries 0.38 of the load, the second 0.25, the third 0.18, and the seventh is free of load. In estimating thread stresses by the equations above, substituting $0.38F$ for F and setting n_t to 1 will give the largest level of stresses in the thread-nut combination.

EXAMPLE 8–1

A square-thread power screw has a major diameter of 32 mm and a pitch of 4 mm with double threads, and it is to be used in an application similar to that in Fig. 8–4. The given data include $f = f_c = 0.08$, $d_c = 40$ mm, and $F = 6.4$ kN per screw.

- (a) Find the thread depth, thread width, pitch diameter, minor diameter, and lead.
- (b) Find the torque required to raise and lower the load.
- (c) Find the efficiency during lifting the load.
- (d) Find the body stresses, torsional and compressive.
- (e) Find the bearing stress.
- (f) Find the thread bending stress at the root of the thread.
- (g) Determine the von Mises stress at the root of the thread.
- (h) Determine the maximum shear stress at the root of the thread.

Solution

- (a) From Fig. 8–3a the thread depth and width are the same and equal to half the pitch, or 2 mm. Also

$$d_m = d - p/2 = 32 - 4/2 = 30 \text{ mm}$$

Answer

$$d_r = d - p = 32 - 4 = 28 \text{ mm}$$

$$l = np = 2(4) = 8 \text{ mm}$$

- (b) Using Eqs. (8–1) and (8–6), the torque required to turn the screw against the load is

$$\begin{aligned}T_R &= \frac{Fd_m}{2} \left(\frac{l + \pi f d_m}{\pi d_m - fl} \right) + \frac{F f_c d_c}{2} \\ &= \frac{6.4(30)}{2} \left[\frac{8 + \pi(0.08)(30)}{\pi(30) - 0.08(8)} \right] + \frac{6.4(0.08)40}{2} \\ &= 15.94 + 10.24 = 26.18 \text{ N} \cdot \text{m}\end{aligned}$$

Answer

Using Eqs. (8–2) and (8–6), we find the load-lowering torque is

$$\begin{aligned} T_L &= \frac{Fd_m}{2} \left(\frac{\pi f d_m - l}{\pi d_m + fl} \right) + \frac{F f_c d_c}{2} \\ &= \frac{6.4(30)}{2} \left[\frac{\pi(0.08)30 - 8}{\pi(30) + 0.08(8)} \right] + \frac{6.4(0.08)(40)}{2} \\ &= -0.466 + 10.24 = 9.77 \text{ N} \cdot \text{m} \end{aligned}$$

Answer

The minus sign in the first term indicates that the screw alone is not self-locking and would rotate under the action of the load except for the fact that the collar friction is present and must be overcome, too. Thus the torque required to rotate the screw “with” the load is less than is necessary to overcome collar friction alone.

(c) The overall efficiency in raising the load is

Answer

$$\epsilon = \frac{Fl}{2\pi T_R} = \frac{6.4(8)}{2\pi(26.18)} = 0.311$$

(d) The body shear stress τ due to torsional moment T_R at the outside of the screw body is

Answer

$$\tau = \frac{16T_R}{\pi d_r^3} = \frac{16(26.18)(10^3)}{\pi(28^3)} = 6.07 \text{ MPa}$$

The axial nominal normal stress σ is

Answer

$$\sigma = -\frac{4F}{\pi d_r^2} = -\frac{4(6.4)10^3}{\pi(28^2)} = -10.39 \text{ MPa}$$

(e) The bearing stress σ_B is, with one thread carrying $0.38F$,

Answer

$$\sigma_B = -\frac{2(0.38F)}{\pi d_m(1)p} = -\frac{2(0.38)(6.4)10^3}{\pi(30)(1)(4)} = -12.9 \text{ MPa}$$

(f) The thread-root bending stress σ_b with one thread carrying $0.38F$ is

Answer

$$\sigma_b = \frac{6(0.38F)}{\pi d_r(1)p} = \frac{6(0.38)(6.4)10^3}{\pi(28)(1)4} = 41.5 \text{ MPa}$$

(g) The transverse shear at the extreme of the root cross section due to bending is zero. However, there is a circumferential shear stress at the extreme of the root cross section of the thread as shown in part (d) of 6.07 MPa . The three-dimensional stresses, after Fig. 8–8, noting the y coordinate is into the page, are

$$\sigma_x = 41.5 \text{ MPa} \quad \tau_{xy} = 0$$

$$\sigma_y = -10.39 \text{ MPa} \quad \tau_{yz} = 6.07 \text{ MPa}$$

$$\sigma_z = 0 \quad \tau_{zx} = 0$$

For the von Mises stress, Eq. (5–14) of Sec. 5–5 can be written as

Answer

$$\begin{aligned} \sigma' &= \frac{1}{\sqrt{2}} \{ (41.5 - 0)^2 + [0 - (-10.39)]^2 + (-10.39 - 41.5)^2 + 6(6.07)^2 \}^{1/2} \\ &= 48.7 \text{ MPa} \end{aligned}$$

Alternatively, you can determine the principal stresses and then use Eq. (5–12) to find the von Mises stress. This would prove helpful in evaluating τ_{\max} as well. The principal stresses can be found from Eq. (3–15); however, sketch the stress element and note that there are no shear stresses on the x face. This means that σ_x is a principal stress. The remaining stresses can be transformed by using the plane stress equation, Eq. (3–13). Thus, the remaining principal stresses are

$$\frac{-10.39}{2} \pm \sqrt{\left(\frac{-10.39}{2}\right)^2 + 6.07^2} = 2.79, -13.18 \text{ MPa}$$

Ordering the principal stresses gives $\sigma_1, \sigma_2, \sigma_3 = 41.5, 2.79, -13.18$ MPa. Substituting these into Eq. (5–12) yields

Answer

$$\begin{aligned}\sigma' &= \left\{ \frac{[41.5 - 2.79]^2 + [2.79 - (-13.18)]^2 + [-13.18 - 41.5]^2}{2} \right\}^{1/2} \\ &= 48.7 \text{ MPa}\end{aligned}$$

(h) The maximum shear stress is given by Eq. (3–16), where $\tau_{\max} = \tau_{1/3}$, giving

Answer

$$\tau_{\max} = \frac{\sigma_1 - \sigma_3}{2} = \frac{41.5 - (-13.18)}{2} = 27.3 \text{ MPa}$$

Table 8–4

Screw Bearing

Pressure p_b

Source: H. A. Rothbart and T. H. Brown, Jr., *Mechanical Design Handbook*, 2nd ed., McGraw-Hill, New York, 2006.

	Screw Material	Nut Material	Safe p_b, psi	Notes
Screw Bearing Pressure p_b	Steel	Bronze	2500–3500	Low speed
	Steel	Bronze	1600–2500	≤ 10 fpm
		Cast iron	1800–2500	≤ 8 fpm
	Steel	Bronze	800–1400	20–40 fpm
		Cast iron	600–1000	20–40 fpm
	Steel	Bronze	150–240	≥ 50 fpm

Ham and Ryan¹ showed that the coefficient of friction in screw threads is independent of axial load, practically independent of speed, decreases with heavier lubricants, shows little variation with combinations of materials, and is best for steel on bronze. Sliding coefficients of friction in power screws are about 0.10–0.15.

Table 8–4 shows safe bearing pressures on threads, to protect the moving surfaces from abnormal wear. Table 8–5 shows the coefficients of sliding friction for

¹Ham and Ryan, *An Experimental Investigation of the Friction of Screw-threads*, Bulletin 247, University of Illinois Experiment Station, Champaign-Urbana, Ill., June 7, 1932.

Table 8-5

Coefficients of Friction f
for Threaded Pairs

Source: H. A. Rothbart and
T. H. Brown, Jr., *Mechanical
Design Handbook*, 2nd ed.,
McGraw-Hill, New York, 2006.

Screw Material	Nut Material			
	Steel	Bronze	Brass	Cast Iron
Steel, dry	0.15–0.25	0.15–0.23	0.15–0.19	0.15–0.25
Steel, machine oil	0.11–0.17	0.10–0.16	0.10–0.15	0.11–0.17
Bronze	0.08–0.12	0.04–0.06	—	0.06–0.09

Table 8-6

Thrust-Collar Friction
Coefficients

Source: H. A. Rothbart and
T. H. Brown, Jr., *Mechanical
Design Handbook*, 2nd ed.,
McGraw-Hill, New York, 2006.

Combination	Running	Starting
Soft steel on cast iron	0.12	0.17
Hard steel on cast iron	0.09	0.15
Soft steel on bronze	0.08	0.10
Hard steel on bronze	0.06	0.08

common material pairs. Table 8-6 shows coefficients of starting and running friction for common material pairs.

8-3 Threaded Fasteners

As you study the sections on threaded fasteners and their use, be alert to the stochastic and deterministic viewpoints. In most cases the threat is from overproof loading of fasteners, and this is best addressed by statistical methods. The threat from fatigue is lower, and deterministic methods can be adequate.

Figure 8-9 is a drawing of a standard hexagon-head bolt. Points of stress concentration are at the fillet, at the start of the threads (runout), and at the thread-root fillet in the plane of the nut when it is present. See Table A-29 for dimensions. The diameter of the washer face is the same as the width across the flats of the hexagon. The thread length of inch-series bolts, where d is the nominal diameter, is

$$L_T = \begin{cases} 2d + \frac{1}{4} \text{ in} & L \leq 6 \text{ in} \\ 2d + \frac{1}{2} \text{ in} & L > 6 \text{ in} \end{cases} \quad (8-13)$$

and for metric bolts is

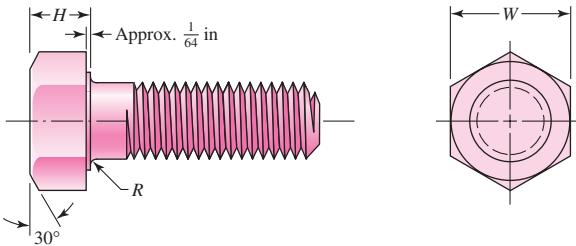
$$L_T = \begin{cases} 2d + 6 & L \leq 125 \quad d \leq 48 \\ 2d + 12 & 125 < L \leq 200 \\ 2d + 25 & L > 200 \end{cases} \quad (8-14)$$

where the dimensions are in millimeters. The ideal bolt length is one in which only one or two threads project from the nut after it is tightened. Bolt holes may have burrs or sharp edges after drilling. These could bite into the fillet and increase stress concentration. Therefore, washers must always be used under the bolt head to prevent this. They should be of hardened steel and loaded onto the bolt so that the rounded edge of the stamped hole faces the washer face of the bolt. Sometimes it is necessary to use washers under the nut too.

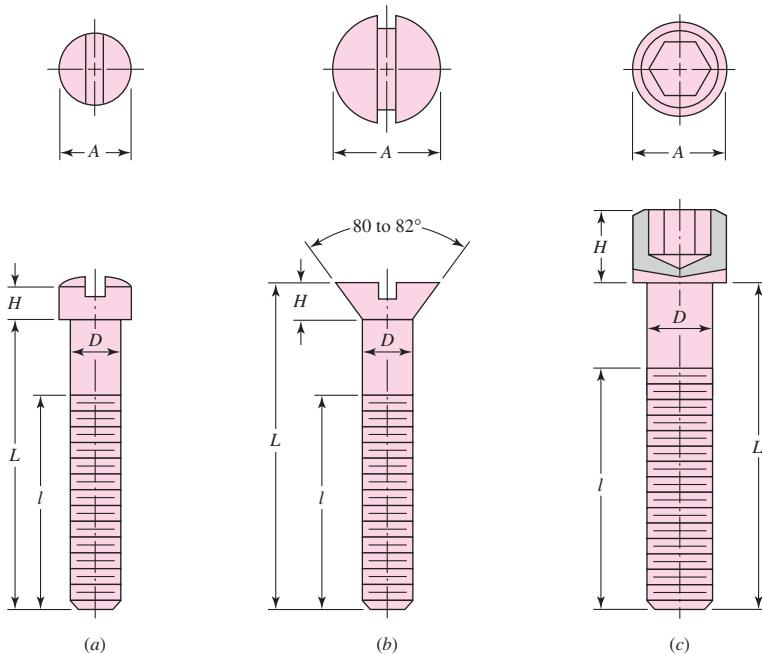
The purpose of a bolt is to clamp two or more parts together. The clamping load stretches or elongates the bolt; the load is obtained by twisting the nut until the bolt

Figure 8-9

Hexagon-head bolt; note the washer face, the fillet under the head, the start of threads, and the chamfer on both ends. Bolt lengths are always measured from below the head.

**Figure 8-10**

Typical cap-screw heads:
(a) fillister head; (b) flat head;
(c) hexagonal socket head. Cap
screws are also manufactured
with hexagonal heads similar to
the one shown in Fig. 8-9, as
well as a variety of other head
styles. This illustration uses
one of the conventional
methods of representing
threads.



has elongated almost to the elastic limit. If the nut does not loosen, this bolt tension remains as the preload or clamping force. When tightening, the mechanic should, if possible, hold the bolt head stationary and twist the nut; in this way the bolt shank will not feel the thread-friction torque.

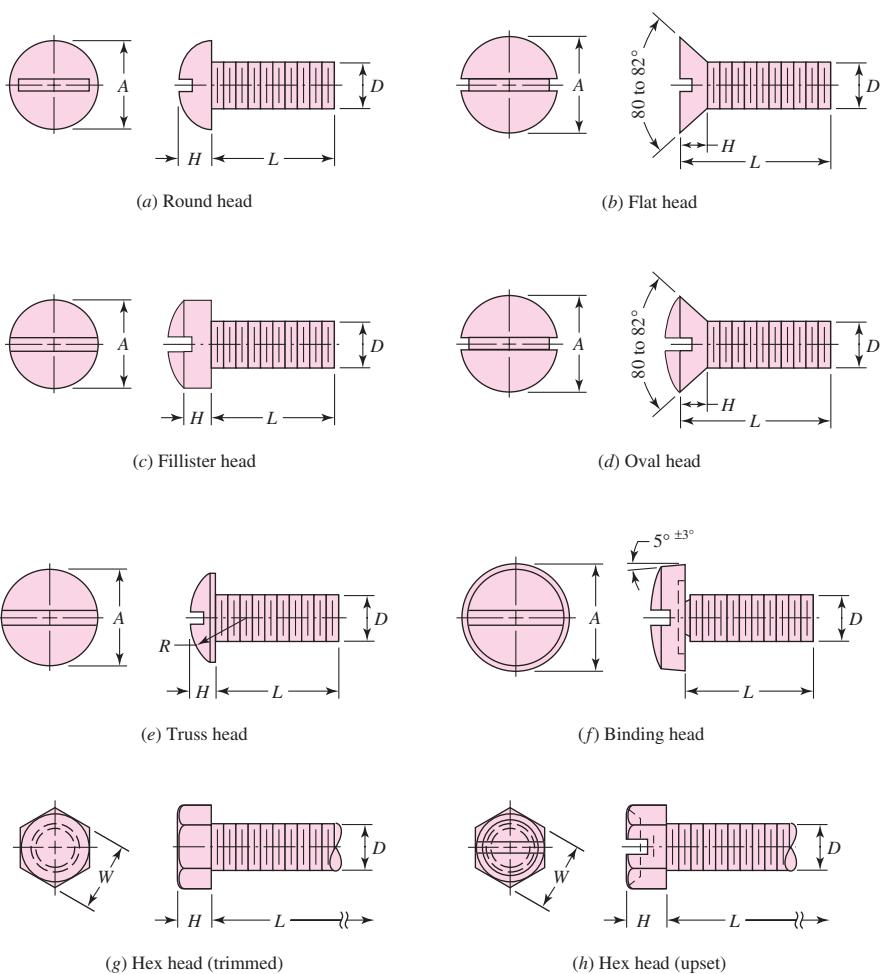
The head of a hexagon-head cap screw is slightly thinner than that of a hexagon-head bolt. Dimensions of hexagon-head cap screws are listed in Table A-30. Hexagon-head cap screws are used in the same applications as bolts and also in applications in which one of the clamped members is threaded. Three other common cap-screw head styles are shown in Fig. 8-10.

A variety of machine-screw head styles are shown in Fig. 8-11. Inch-series machine screws are generally available in sizes from No. 0 to about $\frac{3}{8}$ in.

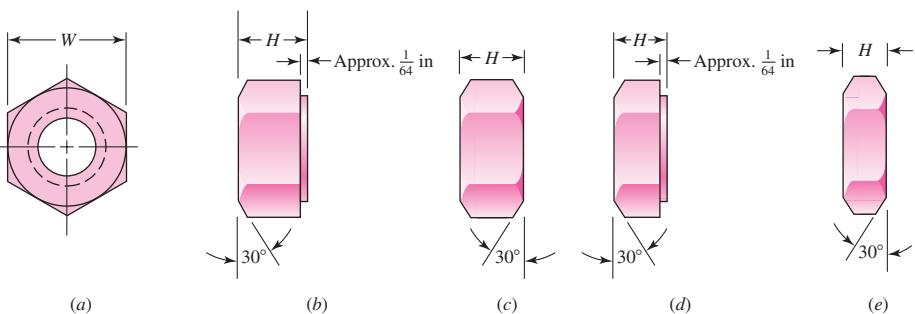
Several styles of hexagonal nuts are illustrated in Fig. 8-12; their dimensions are given in Table A-31. The material of the nut must be selected carefully to match that of the bolt. During tightening, the first thread of the nut tends to take the entire load; but yielding occurs, with some strengthening due to the cold work that takes place, and the load is eventually divided over about three nut threads. For this reason you should never reuse nuts; in fact, it can be dangerous to do so.

Figure 8-11

Types of heads used on machine screws.

**Figure 8-12**

Hexagonal nuts: (a) end view, general; (b) washer-faced regular nut; (c) regular nut chamfered on both sides; (d) jam nut with washer face; (e) jam nut chamfered on both sides.



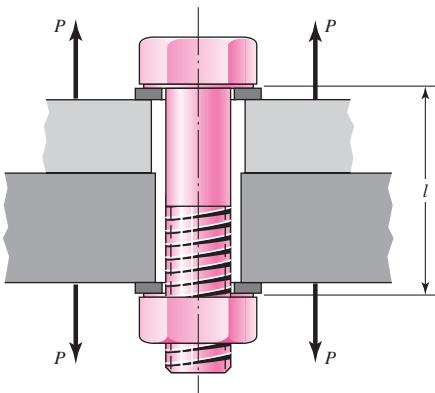
8-4

Joints—Fastener Stiffness

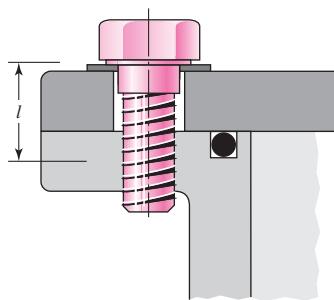
When a connection is desired that can be disassembled without destructive methods and that is strong enough to resist external tensile loads, moment loads, and shear loads, or a combination of these, then the simple bolted joint using hardened-steel washers is a good solution. Such a joint can also be dangerous unless it is properly designed and assembled by a *trained* mechanic.

Figure 8-13

A bolted connection loaded in tension by the forces P . Note the use of two washers. Note how the threads extend into the body of the connection. This is usual and is desired. l is the grip of the connection.

**Figure 8-14**

Section of cylindrical pressure vessel. Hexagon-head cap screws are used to fasten the cylinder head to the body. Note the use of an O-ring seal. l is the effective grip of the connection (see Table 8-7).



A section through a tension-loaded bolted joint is illustrated in Fig. 8-13. Notice the clearance space provided by the bolt holes. Notice, too, how the bolt threads extend into the body of the connection.

As noted previously, the purpose of the bolt is to clamp the two, or more, parts together. Twisting the nut stretches the bolt to produce the clamping force. This clamping force is called the *pretension* or *bolt preload*. It exists in the connection after the nut has been properly tightened no matter whether the external tensile load P is exerted or not.

Of course, since the members are being clamped together, the clamping force that produces tension in the bolt induces compression in the members.

Figure 8-14 shows another tension-loaded connection. This joint uses cap screws threaded into one of the members. An alternative approach to this problem (of not using a nut) would be to use studs. A stud is a rod threaded on both ends. The stud is screwed into the lower member first; then the top member is positioned and fastened down with hardened washers and nuts. The studs are regarded as permanent, and so the joint can be disassembled merely by removing the nut and washer. Thus the threaded part of the lower member is not damaged by reusing the threads.

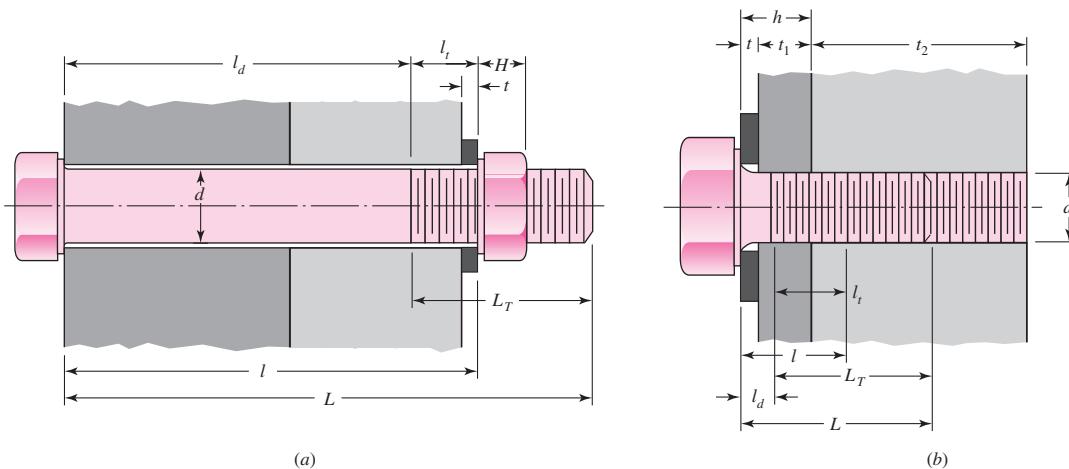
The *spring rate* is a limit as expressed in Eq. (4-1). For an elastic member such as a bolt, as we learned in Eq. (4-2), it is the ratio between the force applied to the member and the deflection produced by that force. We can use Eq. (4-4) and the results of Prob. 4-1 to find the stiffness constant of a fastener in any bolted connection.

The *grip l* of a connection is the total thickness of the clamped material. In Fig. 8-13 the grip is the sum of the thicknesses of both members and both washers. In Fig. 8-14 the effective grip is given in Table 8-7.

The stiffness of the portion of a bolt or screw within the clamped zone will generally consist of two parts, that of the unthreaded shank portion and that of the

Table 8-7

Suggested Procedure for Finding Fastener Stiffness



Given fastener diameter d and pitch p in mm or number of threads per inch

Washer thickness: t from Table A-32 or A-33

Nut thickness [Fig. (a) only]: H from Table A-31

Grip length:

For Fig. (a): l = thickness of all material squeezed between face of bolt and face of nut

$$\text{For Fig. (b): } l = \begin{cases} h + t_2/2, & t_2 < d \\ h + d/2, & t_2 > d \end{cases}$$

Fastener length (round up using Table A-17*):

For Fig. (a): $L > l + H$

For Fig. (b): $L \geq h + 1.5d$

Threaded length L_T : Inch series:

$$L_T = \begin{cases} 2d + \frac{1}{4} \text{ in,} & L \leq 6 \text{ in} \\ 2d + \frac{1}{2} \text{ in,} & L > 6 \text{ in} \end{cases}$$

Metric series:

$$L_T = \begin{cases} 2d + 6 \text{ mm}, & L \leq 125 \text{ mm}, d \leq 48 \text{ mm} \\ 2d + 12 \text{ mm}, & 125 < L \leq 200 \text{ mm} \\ 2d + 25 \text{ mm}, & L > 200 \text{ mm} \end{cases}$$

Length of unthreaded portion in grip: $l_d \equiv L - L_T$

Length of threaded portion in grip: $l_t \equiv l = l_d$

Area of unthreaded portion: $A_d \equiv \pi d^2/4$

Area of threaded portion: A_t from Table 8-1 or 8-2

$$k_b = \frac{A_d A_t E}{A_d l_t + A_t l_d}$$

*Bolts and cap screws may not be available in all the preferred lengths listed in Table A-17. Large fasteners may not be available in fractional inches or in millimeter lengths ending in a nonzero digit. Check with your bolt supplier for availability.

threaded portion. Thus the stiffness constant of the bolt is equivalent to the stiffnesses of two springs in series. Using the results of Prob. 4-1, we find

$$\frac{1}{k} = \frac{1}{k_1} + \frac{1}{k_2} \quad \text{or} \quad k = \frac{k_1 k_2}{k_1 + k_2} \quad (8-15)$$

for two springs in series. From Eq. (4-4), the spring rates of the threaded and unthreaded portions of the bolt in the clamped zone are, respectively,

$$k_t = \frac{A_t E}{l_t} \quad k_d = \frac{A_d E}{l_d} \quad (8-16)$$

where A_t = tensile-stress area (Tables 8-1, 8-2)

l_t = length of threaded portion of grip

A_d = major-diameter area of fastener

l_d = length of unthreaded portion in grip

Substituting these stiffnesses in Eq. (8-15) gives

$$k_b = \frac{A_d A_t E}{A_d l_t + A_t l_d} \quad (8-17)$$

where k_b is the estimated effective stiffness of the bolt or cap screw in the clamped zone. For short fasteners, the one in Fig. 8-14, for example, the unthreaded area is small and so the first of the expressions in Eq. (8-16) can be used to find k_b . For long fasteners, the threaded area is relatively small, and so the second expression in Eq. (8-16) can be used. Table 8-7 is useful.

8-5 Joints—Member Stiffness

In the previous section, we determined the stiffness of the fastener in the clamped zone. In this section, we wish to study the stiffnesses of the members in the clamped zone. Both of these stiffnesses must be known in order to learn what happens when the assembled connection is subjected to an external tensile loading.

There may be more than two members included in the grip of the fastener. All together these act like compressive springs in series, and hence the total spring rate of the members is

$$\frac{1}{k_m} = \frac{1}{k_1} + \frac{1}{k_2} + \frac{1}{k_3} + \cdots + \frac{1}{k_i} \quad (8-18)$$

If one of the members is a soft gasket, its stiffness relative to the other members is usually so small that for all practical purposes the others can be neglected and only the gasket stiffness used.

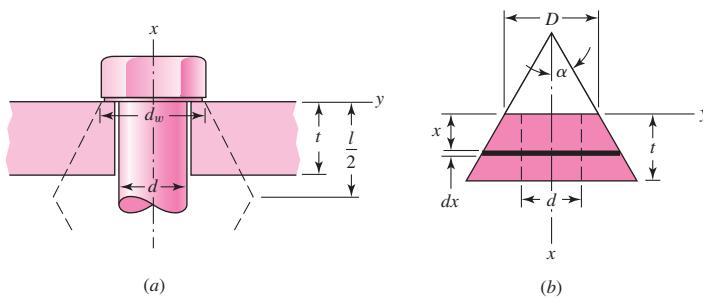
If there is no gasket, the stiffness of the members is rather difficult to obtain, except by experimentation, because the compression region spreads out between the bolt head and the nut and hence the area is not uniform. There are, however, some cases in which this area can be determined.

Ito² has used ultrasonic techniques to determine the pressure distribution at the member interface. The results show that the pressure stays high out to about 1.5 bolt radii.

²Y. Ito, J. Toyoda, and S. Nagata, "Interface Pressure Distribution in a Bolt-Flange Assembly," ASME paper no. 77-WA/DE-11, 1977.

Figure 8-15

Compression of a member with the equivalent elastic properties represented by a frustum of a hollow cone. Here, l represents the grip length.



The pressure, however, falls off farther away from the bolt. Thus Ito suggests the use of Rotscher's pressure-cone method for stiffness calculations with a variable cone angle. This method is quite complicated, and so here we choose to use a simpler approach using a fixed cone angle.

Figure 8-15 illustrates the general cone geometry using a half-apex angle α . An angle $\alpha = 45^\circ$ has been used, but Little³ reports that this overestimates the clamping stiffness. When loading is restricted to a washer-face annulus (hardened steel, cast iron, or aluminum), the proper apex angle is smaller. Osgood⁴ reports a range of $25^\circ \leq \alpha \leq 33^\circ$ for most combinations. In this book we shall use $\alpha = 30^\circ$ except in cases in which the material is insufficient to allow the frusta to exist.

Referring now to Fig. 8-15b, the contraction of an element of the cone of thickness dx subjected to a compressive force P is, from Eq. (4-3),

$$d\delta = \frac{P dx}{EA} \quad (a)$$

The area of the element is

$$\begin{aligned} A &= \pi(r_o^2 - r_i^2) = \pi \left[\left(x \tan \alpha + \frac{D}{2} \right)^2 - \left(\frac{d}{2} \right)^2 \right] \\ &= \pi \left(x \tan \alpha + \frac{D+d}{2} \right) \left(x \tan \alpha + \frac{D-d}{2} \right) \end{aligned} \quad (b)$$

Substituting this in Eq. (a) and integrating gives a total contraction of

$$\delta = \frac{P}{\pi E} \int_0^t \frac{dx}{[x \tan \alpha + (D+d)/2][x \tan \alpha + (D-d)/2]} \quad (c)$$

Using a table of integrals, we find the result to be

$$\delta = \frac{P}{\pi Ed \tan \alpha} \ln \frac{(2t \tan \alpha + D - d)(D + d)}{(2t \tan \alpha + D + d)(D - d)} \quad (d)$$

Thus the spring rate or stiffness of this frustum is

$$k = \frac{P}{\delta} = \frac{\pi Ed \tan \alpha}{\ln \frac{(2t \tan \alpha + D - d)(D + d)}{(2t \tan \alpha + D + d)(D - d)}} \quad (8-19)$$

³R. E. Little, "Bolted Joints: How Much Give?" *Machine Design*, Nov. 9, 1967.

⁴C. C. Osgood, "Saving Weight on Bolted Joints," *Machine Design*, Oct. 25, 1979.

With $\alpha = 30^\circ$, this becomes

$$k = \frac{0.5774\pi Ed}{\ln \frac{(1.155t + D - d)(D + d)}{(1.155t + D + d)(D - d)}} \quad (8-20)$$

Equation (8–20), or (8–19), must be solved separately for each frustum in the joint. Then individual stiffnesses are assembled to obtain k_m using Eq. (8–18).

If the members of the joint have the same Young's modulus E with symmetrical frusta back to back, then they act as two identical springs in series. From Eq. (8–18) we learn that $k_m = k/2$. Using the grip as $l = 2t$ and d_w as the diameter of the washer face, from Eq. (8–19) we find the spring rate of the members to be

$$k_m = \frac{\pi Ed \tan \alpha}{2 \ln \frac{(l \tan \alpha + d_w - d)(d_w + d)}{(l \tan \alpha + d_w + d)(d_w - d)}} \quad (8-21)$$

The diameter of the washer face is about 50 percent greater than the fastener diameter for standard hexagon-head bolts and cap screws. Thus we can simplify Eq. (8–21) by letting $d_w = 1.5d$. If we also use $\alpha = 30^\circ$, then Eq. (8–21) can be written as

$$k_m = \frac{0.5774\pi Ed}{2 \ln \left(5 \frac{0.5774l + 0.5d}{0.5774l + 2.5d} \right)} \quad (8-22)$$

It is easy to program the numbered equations in this section, and you should do so. The time spent in programming will save many hours of formula plugging.

To see how good Eq. (8–21) is, solve it for k_m/Ed :

$$\frac{k_m}{Ed} = \frac{\pi \tan \alpha}{2 \ln \left[\frac{(l \tan \alpha + d_w - d)(d_w + d)}{(l \tan \alpha + d_w + d)(d_w - d)} \right]}$$

Earlier in the section use of $\alpha = 30^\circ$ was recommended for hardened steel, cast iron, or aluminum members. Wileman, Choudury, and Green⁵ conducted a finite element study of this problem. The results, which are depicted in Fig. 8–16, agree with the $\alpha = 30^\circ$ recommendation, coinciding exactly at the aspect ratio $d/l = 0.4$. Additionally, they offered an exponential curve-fit of the form

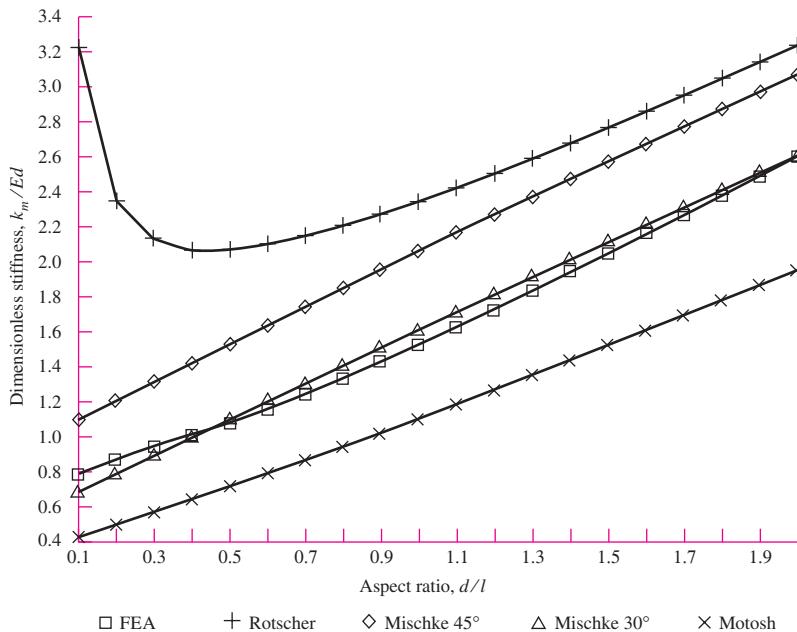
$$\frac{k_m}{Ed} = A \exp(Bd/l) \quad (8-23)$$

with constants A and B defined in Table 8–8. Equation (8–23) offers a simple calculation for member stiffness k_m . However, it is very important to note that the *entire joint* must be made up of the *same material*. For departure from these conditions, Eq. (8–20) remains the basis for approaching the problem.

⁵J. Wileman, M. Choudury, and I. Green, "Computation of Member Stiffness in Bolted Connections," *Trans. ASME, J. Mech. Design*, vol. 113, December 1991, pp. 432–437.

Figure 8-16

The dimensionless plot of stiffness versus aspect ratio of the members of a bolted joint, showing the relative accuracy of methods of Rotscher, Mischke, and Motosh, compared to a finite-element analysis (FEA) conducted by Wileman, Choudury, and Green.

**Table 8-8**

Stiffness Parameters of Various Member Materials[†]

[†]Source: J. Wileman, M. Choudury, and I. Green, "Computation of Member Stiffness in Bolted Connections," *Trans. ASME, J. Mech. Design*, vol. 113, December 1991, pp. 432–437.

Material Used	Poisson Ratio	Elastic GPa	Modulus Mpsi	A	B
Steel	0.291	207	30.0	0.787 15	0.628 73
Aluminum	0.334	71	10.3	0.796 70	0.638 16
Copper	0.326	119	17.3	0.795 68	0.635 53
Gray cast iron	0.211	100	14.5	0.778 71	0.616 16
General expression				0.789 52	0.629 14

EXAMPLE 8-2

As shown in Fig. 8-17a, two plates are clamped by washer-faced $\frac{1}{2}$ in-20 UNF \times $1\frac{1}{2}$ in SAE grade 5 bolts each with a standard $\frac{1}{2}$ N steel plain washer.

- (a) Determine the member spring rate k_m if the top plate is steel and the bottom plate is gray cast iron.
- (b) Using the method of conical frusta, determine the member spring rate k_m if both plates are steel.
- (c) Using Eq. (8-23), determine the member spring rate k_m if both plates are steel. Compare the results with part (b).
- (d) Determine the bolt spring rate k_b .

Solution

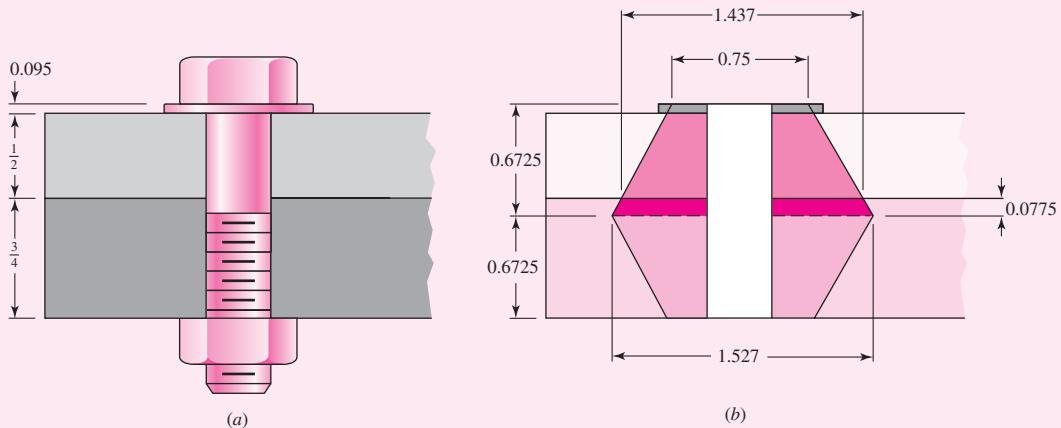
From Table A-32, the thickness of a standard $\frac{1}{2}$ N plain washer is 0.095 in.

- (a) As shown in Fig. 8-17b, the frusta extend halfway into the joint the distance

$$\frac{1}{2}(0.5 + 0.75 + 0.095) = 0.6725 \text{ in}$$

Figure 8-17

Dimensions in inches.



The distance between the joint line and the dotted frusta line is $0.6725 - 0.5 - 0.095 = 0.0775$ in. Thus, the top frusta consist of the steel washer, steel plate, and 0.0775 in of the cast iron. Since the washer and top plate are both steel with $E = 30(10^6)$ psi, they can be considered a single frustum of 0.595 in thick. The outer diameter of the frustum of the steel member at the joint interface is $0.75 + 2(0.595) \tan 30^\circ = 1.437$ in. The outer diameter at the midpoint of the entire joint is $0.75 + 2(0.6725) \tan 30^\circ = 1.527$ in. Using Eq. (8-20), the spring rate of the steel is

$$k_1 = \frac{0.5774\pi(30)(10^6)0.5}{\ln\left\{\frac{[1.155(0.595) + 0.75 - 0.5](0.75 + 0.5)}{[1.155(0.595) + 0.75 + 0.5](0.75 - 0.5)}\right\}} = 30.80(10^6) \text{ lbf/in}$$

For the upper cast-iron frustum

$$k_2 = \frac{0.5774\pi(14.5)(10^6)0.5}{\ln\left\{\frac{[1.155(0.0775) + 1.437 - 0.5](1.437 + 0.5)}{[1.155(0.0775) + 1.437 + 0.5](1.437 - 0.5)}\right\}} = 285.5(10^6) \text{ lbf/in}$$

For the lower cast-iron frustum

$$k_3 = \frac{0.5774\pi(14.5)(10^6)0.5}{\ln\left\{\frac{[1.155(0.6725) + 0.75 - 0.5](0.75 + 0.5)}{[1.155(0.6725) + 0.75 + 0.5](0.75 - 0.5)}\right\}} = 14.15(10^6) \text{ lbf/in}$$

The three frusta are in series, so from Eq. (8-18)

$$\frac{1}{k_m} = \frac{1}{30.80(10^6)} + \frac{1}{285.5(10^6)} + \frac{1}{14.15(10^6)}$$

Answer This results in $k_m = 9.378(10^6)$ lbf/in.

(b) If the entire joint is steel, Eq. (8–22) with $l = 2(0.6725) = 1.345$ in gives

Answer

$$k_m = \frac{0.5774\pi(30.0)(10^6)0.5}{2 \ln \left\{ 5 \left[\frac{0.5774(1.345) + 0.5(0.5)}{0.5774(1.345) + 2.5(0.5)} \right] \right\}} = 14.64(10^6) \text{ lbf/in.}$$

(c) From Table 8–8, $A = 0.787\ 15$, $B = 0.628\ 73$. Equation (8–23) gives

Answer

$$k_m = 30(10^6)(0.5)(0.787\ 15) \exp[0.628\ 73(0.5)/1.345] = 14.92(10^6) \text{ lbf/in}$$

For this case, the difference between the results for Eqs. (8–22) and (8–23) is less than 2 percent.

(d) Following the procedure of Table 8–7, the threaded length of a 0.5-in bolt is $L_T = 2(0.5) + 0.25 = 1.25$ in. The length of the unthreaded portion is $l_d = 1.5 - 1.25 = 0.25$ in. The length of the unthreaded portion in grip is $l_t = 1.345 - 0.25 = 1.095$ in. The major diameter area is $A_d = (\pi/4)(0.5^2) = 0.196\ 3 \text{ in}^2$. From Table 8–2, the tensile-stress area is $A_t = 0.159\ 9 \text{ in}^2$. From Eq. (8–17)

Answer

$$k_b = \frac{0.196\ 3(0.159\ 9)30(10^6)}{0.196\ 3(1.095) + 0.159\ 9(0.25)} = 3.69(10^6) \text{ lbf/in}$$

8–6

Bolt Strength

In the specification standards for bolts, the strength is specified by stating SAE or ASTM minimum quantities, the *minimum proof strength*, or *minimum proof load*, and the *minimum tensile strength*. The *proof load* is the maximum load (force) that a bolt can withstand without acquiring a permanent set. The *proof strength* is the quotient of the proof load and the tensile-stress area. The proof strength thus corresponds roughly to the proportional limit and corresponds to 0.0001-in permanent set in the fastener (first measurable deviation from elastic behavior). Tables 8–9, 8–10, and 8–11 provide *minimum* strength specifications for steel bolts. The values of the mean proof strength, the mean tensile strength, and the corresponding standard deviations are not part of the specification codes, so it is the designer's responsibility to obtain these values, perhaps by laboratory testing, if designing to a reliability specification.

The SAE specifications are found in Table 8–9. The bolt grades are numbered according to the tensile strengths, with decimals used for variations at the same strength level. Bolts and screws are available in all grades listed. Studs are available in grades 1, 2, 4, 5, 8, and 8.1. Grade 8.1 is not listed.

ASTM specifications are listed in Table 8–10. ASTM threads are shorter because ASTM deals mostly with structures; structural connections are generally loaded in shear, and the decreased thread length provides more shank area.

Specifications for metric fasteners are given in Table 8–11.

It is worth noting that all specification-grade bolts made in this country bear a manufacturer's mark or logo, in addition to the grade marking, on the bolt head. Such marks confirm that the bolt meets or exceeds specifications. If such marks are missing, the bolt may be imported; for imported bolts there is no obligation to meet specifications.

Bolts in fatigue axial loading fail at the fillet under the head, at the thread runout, and at the first thread engaged in the nut. If the bolt has a standard shoulder under the head, it has a value of K_f from 2.1 to 2.3, and this shoulder fillet is protected

Table 8-9

SAE Specifications for Steel Bolts

SAE Grade No.	Size Range Inclusive, in	Minimum Proof Strength,* kpsi	Minimum Tensile Strength,* kpsi	Minimum Yield Strength,* kpsi	Material	Head Marking
1	$\frac{1}{4}$ – $1\frac{1}{2}$	33	60	36	Low or medium carbon	
2	$\frac{1}{4}$ – $\frac{3}{4}$	55	74	57	Low or medium carbon	
	$\frac{7}{8}$ – $1\frac{1}{2}$	33	60	36		
4	$\frac{1}{4}$ – $1\frac{1}{2}$	65	115	100	Medium carbon, cold-drawn	
5	$\frac{1}{4}$ –1	85	120	92	Medium carbon, Q&T	
	$1\frac{1}{8}$ – $1\frac{1}{2}$	74	105	81		
5.2	$\frac{1}{4}$ –1	85	120	92	Low-carbon martensite, Q&T	
7	$\frac{1}{4}$ – $1\frac{1}{2}$	105	133	115	Medium-carbon alloy, Q&T	
8	$\frac{1}{4}$ – $1\frac{1}{2}$	120	150	130	Medium-carbon alloy, Q&T	
8.2	$\frac{1}{4}$ –1	120	150	130	Low-carbon martensite, Q&T	

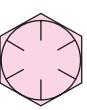
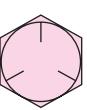
*Minimum strengths are strengths exceeded by 99 percent of fasteners.

from scratching or scoring by a washer. If the thread runout has a 15° or less half-cone angle, the stress is higher at the first engaged thread in the nut. Bolts are sized by examining the loading at the plane of the washer face of the nut. This is the weakest part of the bolt *if and only if* the conditions above are satisfied (washer protection of the shoulder fillet and thread runout $\leq 15^\circ$). Inattention to this requirement has led to a record of 15 percent fastener fatigue failure under the head, 20 percent at thread runout, and 65 percent where the designer is focusing attention. It does little good to concentrate on the plane of the nut washer face if it is not the weakest location.

Nuts are graded so that they can be mated with their corresponding grade of bolt. The purpose of the nut is to have its threads deflect to distribute the load of the bolt more evenly to the nut. The nut's properties are controlled in order to accomplish this. The grade of the nut should be the grade of the bolt.

Table 8-10

ASTM Specifications for Steel Bolts

ASTM Designation	Size Range, Inclusive,	Minimum Proof Strength,* kpsi	Minimum Tensile Strength,* kpsi	Minimum Yield Strength,* kpsi	Material	Head Marking
	No.	in	kpsi	kpsi	kpsi	
A307		$\frac{1}{4}$ - $1\frac{1}{2}$	33	60	36	Low carbon
						
A325, type 1		$\frac{1}{2}$ -1 $1\frac{1}{8}$ - $1\frac{1}{2}$	85 74	120 105	92 81	Medium carbon, Q&T
						
A325, type 2		$\frac{1}{2}$ -1 $1\frac{1}{8}$ - $1\frac{1}{2}$	85 74	120 105	92 81	Low-carbon, martensite, Q&T
						
A325, type 3		$\frac{1}{2}$ -1 $1\frac{1}{8}$ - $1\frac{1}{2}$	85 74	120 105	92 81	Weathering steel, Q&T
						
A354, grade BC		$\frac{1}{4}$ - $2\frac{1}{2}$ $2\frac{3}{4}$ -4	105 95	125 115	109 99	Alloy steel, Q&T
						
A354, grade BD		$\frac{1}{4}$ -4	120	150	130	Alloy steel, Q&T
						
A449		$\frac{1}{4}$ -1 $1\frac{1}{8}$ - $1\frac{1}{2}$ $1\frac{3}{4}$ -3	85 74 55	120 105 90	92 81 58	Medium-carbon, Q&T
						
A490, type 1		$\frac{1}{2}$ - $1\frac{1}{2}$	120	150	130	Alloy steel, Q&T
						
A490, type 3		$\frac{1}{2}$ - $1\frac{1}{2}$	120	150	130	Weathering steel, Q&T
						

*Minimum strengths are strengths exceeded by 99 percent of fasteners.

Table 8-11

Metric Mechanical-Property Classes for Steel Bolts, Screws, and Studs*

Property Class	Size Range, Inclusive	Minimum Proof Strength, [†] MPa	Minimum Tensile Strength, [†] MPa	Minimum Yield Strength, [†] MPa	Material	Head Marking
4.6	M5–M36	225	400	240	Low or medium carbon	 4.6
4.8	M1.6–M16	310	420	340	Low or medium carbon	 4.8
5.8	M5–M24	380	520	420	Low or medium carbon	 5.8
8.8	M16–M36	600	830	660	Medium carbon, Q&T	 8.8
9.8	M1.6–M16	650	900	720	Medium carbon, Q&T	 9.8
10.9	M5–M36	830	1040	940	Low-carbon martensite, Q&T	 10.9
12.9	M1.6–M36	970	1220	1100	Alloy, Q&T	 12.9

*The thread length for bolts and cap screws is

$$L_T = \begin{cases} 2d + 6 & L \leq 125 \\ 2d + 12 & 125 < L \leq 200 \\ 2d + 25 & L > 200 \end{cases}$$

where L is the bolt length. The thread length for structural bolts is slightly shorter than given above.

†Minimum strengths are strengths exceeded by 99 percent of fasteners.

8-7 Tension Joints—The External Load

Let us now consider what happens when an external tensile load P , as in Fig. 8-13, is applied to a bolted connection. It is to be assumed, of course, that the clamping force, which we will call the *preload* F_i , has been correctly applied by tightening the nut *before* P is applied. The nomenclature used is:

$$F_i = \text{preload}$$

P_{total} = Total external tensile load applied to the joint

P = external tensile load per bolt

P_b = portion of P taken by bolt

P_m = portion of P taken by members

$F_b = P_b + F_i$ = resultant bolt load

$F_m = P_m - F_i$ = resultant load on members

C = fraction of external load P carried by bolt

$1 - C$ = fraction of external load P carried by members

N = Number of bolts in the joint

If N bolts equally share the total external load, then

$$P = P_{\text{total}}/N \quad (\text{a})$$

The load P is tension, and it causes the connection to stretch, or elongate, through some distance δ . We can relate this elongation to the stiffnesses by recalling that k is the force divided by the deflection. Thus

$$\delta = \frac{P_b}{k_b} \quad \text{and} \quad \delta = \frac{P_m}{k_m} \quad (\text{b})$$

or

$$P_m = P_b \frac{k_m}{k_b} \quad (\text{c})$$

Since $P = P_b + P_m$, we have

$$P_b = \frac{k_b P}{k_b + k_m} = C P \quad (\text{d})$$

and

$$P_m = P - P_b = (1 - C)P \quad (\text{e})$$

where

$$C = \frac{k_b}{k_b + k_m} \quad (\text{f})$$

is called the *stiffness constant of the joint*. The resultant bolt load is

$$F_b = P_b + F_i = C P + F_i \quad F_m < 0 \quad (\text{8-24})$$

and the resultant load on the connected members is

$$F_m = P_m - F_i = (1 - C)P - F_i \quad F_m < 0 \quad (\text{8-25})$$

Of course, these results are valid only as long as some clamping load remains in the members; this is indicated by the qualifier in the equations.

Table 8-12 is included to provide some information on the relative values of the stiffnesses encountered. The grip contains only two members, both of steel, and no

Table 8-12

Computation of Bolt and Member Stiffnesses.
Steel members clamped using a $\frac{1}{2}$ in-13 NC steel bolt. $C = \frac{k_b}{k_b + k_m}$

Bolt Grip, in	Stiffnesses, M lbf/in			
	k_b	k_m	C	$1 - C$
2	2.57	12.69	0.168	0.832
3	1.79	11.33	0.136	0.864
4	1.37	10.63	0.114	0.886

washers. The ratios C and $1 - C$ are the coefficients of P in Eqs. (8–24) and (8–25), respectively. They describe the proportion of the external load taken by the bolt and by the members, respectively. In all cases, the members take over 80 percent of the external load. Think how important this is when fatigue loading is present. Note also that making the grip longer causes the members to take an even greater percentage of the external load.

8-8

Relating Bolt Torque to Bolt Tension

Having learned that a high preload is very desirable in important bolted connections, we must next consider means of ensuring that the preload is actually developed when the parts are assembled.

If the overall length of the bolt can actually be measured with a micrometer when it is assembled, the bolt elongation due to the preload F_i can be computed using the formula $\delta = F_i l / (AE)$. Then the nut is simply tightened until the bolt elongates through the distance δ . This ensures that the desired preload has been attained.

The elongation of a screw cannot usually be measured, because the threaded end is often in a blind hole. It is also impractical in many cases to measure bolt elongation. In such cases the wrench torque required to develop the specified preload must be estimated. Then torque wrenching, pneumatic-impact wrenching, or the turn-of-the-nut method may be used.

The torque wrench has a built-in dial that indicates the proper torque.

With impact wrenching, the air pressure is adjusted so that the wrench stalls when the proper torque is obtained, or in some wrenches, the air automatically shuts off at the desired torque.

The turn-of-the-nut method requires that we first define the meaning of snug-tight. The *snug-tight* condition is the tightness attained by a few impacts of an impact wrench, or the full effort of a person using an ordinary wrench. When the snug-tight condition is attained, all additional turning develops useful tension in the bolt. The turn-of-the-nut method requires that you compute the fractional number of turns necessary to develop the required preload from the snug-tight condition. For example, for heavy hexagonal structural bolts, the turn-of-the-nut specification states that the nut should be turned a minimum of 180° from the snug-tight condition under optimum conditions. Note that this is also about the correct rotation for the wheel nuts of a passenger car. Problems 8–15 to 8–17 illustrate the method further.

Although the coefficients of friction may vary widely, we can obtain a good estimate of the torque required to produce a given preload by combining Eqs. (8–5) and (8–6):

$$T = \frac{F_i d_m}{2} \left(\frac{l + \pi f d_m \sec \alpha}{\pi d_m - f l \sec \alpha} \right) + \frac{F_i f_c d_c}{2} \quad (a)$$

Table 8-13

Distribution of Preload F_i for 20 Tests of Unlubricated Bolts Torqued to 90 N · m	23.6, 34.7, 27.6, 35.6, 28.0, 35.6, 29.4, 37.4, 30.3, 37.8, 30.7, 37.8, 32.9, 39.2, 33.8, 40.0, 33.8, 40.5, 33.8, 42.7
	Mean value $\bar{F}_i = 34.3$ kN. Standard deviation, $\hat{\sigma} = 4.91$ kN.

where d_m is the average of the major and minor diameters. Since $\tan \lambda = l/\pi d_m$, we divide the numerator and denominator of the first term by πd_m and get

$$T = \frac{F_i d_m}{2} \left(\frac{\tan \lambda + f \sec \alpha}{1 - f \tan \lambda \sec \alpha} \right) + \frac{F_i f_c d_c}{2} \quad (b)$$

The diameter of the washer face of a hexagonal nut is the same as the width across flats and equal to $1\frac{1}{2}$ times the nominal size. Therefore the mean collar diameter is $d_c = (d + 1.5d)/2 = 1.25d$. Equation (b) can now be arranged to give

$$T = \left[\left(\frac{d_m}{2d} \right) \left(\frac{\tan \lambda + f \sec \alpha}{1 - f \tan \lambda \sec \alpha} \right) + 0.625 f_c \right] F_i d \quad (c)$$

We now define a *torque coefficient K* as the term in brackets, and so

$$K = \left(\frac{d_m}{2d} \right) \left(\frac{\tan \lambda + f \sec \alpha}{1 - f \tan \lambda \sec \alpha} \right) + 0.625 f_c \quad (8-26)$$

Equation (c) can now be written

$$T = K F_i d \quad (8-27)$$

The coefficient of friction depends upon the surface smoothness, accuracy, and degree of lubrication. On the average, both f and f_c are about 0.15. The interesting fact about Eq. (8-26) is that $K \doteq 0.20$ for $f = f_c = 0.15$ no matter what size bolts are employed and no matter whether the threads are coarse or fine.

Blake and Kurtz have published results of numerous tests of the torquing of bolts.⁶ By subjecting their data to a statistical analysis, we can learn something about the distribution of the torque coefficients and the resulting preload. Blake and Kurtz determined the preload in quantities of unlubricated and lubricated bolts of size $\frac{1}{2}$ in-20 UNF when torqued to 800 lbf · in. This corresponds roughly to an M12 × 1.25 bolt torqued to 90 N · m. The statistical analyses of these two groups of bolts, converted to SI units, are displayed in Tables 8-13 and 8-14.

We first note that both groups have about the same mean preload, 34 kN. The unlubricated bolts have a standard deviation of 4.9 kN and a COV of about 0.15. The lubricated bolts have a standard deviation of 3 kN and a COV of about 0.9.

The means obtained from the two samples are nearly identical, approximately 34 kN; using Eq. (8-27), we find, for both samples, $K = 0.208$.

Bowman Distribution, a large manufacturer of fasteners, recommends the values shown in Table 8-15. In this book we shall use these values and use $K = 0.2$ when the bolt condition is not stated.

⁶J. C. Blake and H. J. Kurtz, "The Uncertainties of Measuring Fastener Preload," *Machine Design*, vol. 37, Sept. 30, 1965, pp. 128–131.

Table 8-14

Distribution of Preload F_i for 10 Tests of Lubricated Bolts Torqued to 90 N · m

30.3,	32.5,	32.5,	32.9,	32.9,	33.8,	34.3,	34.7,	37.4,	40.5
-------	-------	-------	-------	-------	-------	-------	-------	-------	------

Mean value, $\bar{F}_i = 34.18$ kN. Standard deviation, $\hat{\sigma} = 2.88$ kN.

Table 8-15

Torque Factors K for Use with Eq. (8-27)

Bolt Condition	K
Nonplated, black finish	0.30
Zinc-plated	0.20
Lubricated	0.18
Cadmium-plated	0.16
With Bowman Anti-Seize	0.12
With Bowman-Grip nuts	0.09

EXAMPLE 8-3

A $\frac{3}{4}$ in-16 UNF $\times 2\frac{1}{2}$ in SAE grade 5 bolt is subjected to a load P of 6 kip in a tension joint. The initial bolt tension is $F_i = 25$ kip. The bolt and joint stiffnesses are $k_b = 6.50$ and $k_m = 13.8$ Mlbf/in, respectively.

- (a) Determine the preload and service load stresses in the bolt. Compare these to the SAE minimum proof strength of the bolt.
- (b) Specify the torque necessary to develop the preload, using Eq. (8-27).
- (c) Specify the torque necessary to develop the preload, using Eq. (8-26) with $f = f_c = 0.15$.

Solution

From Table 8-2, $A_t = 0.373$ in 2 .

- (a) The preload stress is

Answer

$$\sigma_i = \frac{F_i}{A_t} = \frac{25}{0.373} = 67.02 \text{ ksi}$$

The stiffness constant is

$$C = \frac{k_b}{k_b + k_m} = \frac{6.5}{6.5 + 13.8} = 0.320$$

From Eq. (8-24), the stress under the service load is

Answer

$$\begin{aligned} \sigma_b &= \frac{F_b}{A_t} = \frac{CP + F_i}{A_t} = C \frac{P}{A_t} + \sigma_i \\ &= 0.320 \frac{6}{0.373} + 67.02 = 72.17 \text{ ksi} \end{aligned}$$

From Table 8-9, the SAE minimum proof strength of the bolt is $S_p = 85$ ksi. The preload and service load stresses are respectively 21 and 15 percent less than the proof strength.

(b) From Eq. (8–27), the torque necessary to achieve the preload is

Answer

$$T = K F_i d = 0.2(25)(10^3)(0.75) = 3750 \text{ lbf} \cdot \text{in}$$

(c) The minor diameter can be determined from the minor area in Table 8–2. Thus $d_r = \sqrt{4A_r/\pi} = \sqrt{4(0.351)/\pi} = 0.6685$ in. Thus, the mean diameter is $d_m = (0.75 + 0.6685)/2 = 0.7093$ in. The lead angle is

$$\lambda = \tan^{-1} \frac{l}{\pi d_m} = \tan^{-1} \frac{1}{\pi d_m N} = \tan^{-1} \frac{1}{\pi(0.7093)(16)} = 1.6066^\circ$$

For $\alpha = 30^\circ$, Eq. (8–26) gives

$$\begin{aligned} T &= \left\{ \left[\frac{0.7093}{2(0.75)} \right] \left[\frac{\tan 1.6066^\circ + 0.15(\sec 30^\circ)}{1 - 0.15(\tan 1.6066^\circ)(\sec 30^\circ)} \right] + 0.625(0.15) \right\} 25(10^3)(0.75) \\ &= 3551 \text{ lbf} \cdot \text{in} \end{aligned}$$

which is 5.3 percent less than the value found in part (b).

8–9

Statically Loaded Tension Joint with Preload

Equations (8–24) and (8–25) represent the forces in a bolted joint with preload. The tensile stress in the bolt can be found as in Ex. 8–3 as

$$\sigma_b = \frac{F_b}{A_t} = \frac{CP + F_i}{A_t} \quad (a)$$

Thus, the yielding factor of safety guarding against the static stress exceeding the proof strength is

$$n_p = \frac{S_p}{\sigma_b} = \frac{S_p}{(CP + F_i)/A_t} \quad (b)$$

or

$$n_p = \frac{S_p A_t}{CP + F_i} \quad (8-28)$$

Since it is common to load a bolt close to the proof strength, the yielding factor of safety is often not much greater than unity. Another indicator of yielding that is sometimes used is a *load factor*, which is applied only to the load P as a guard against overloading. Applying such a load factor to the load P in Eq. (a), and equating it to the proof strength gives

$$\frac{C n_L P + F_i}{A_t} = S_p \quad (c)$$

Solving for the load factor gives

$$n_L = \frac{S_p A_t - F_i}{CP} \quad (8-29)$$

It is also essential for a safe joint that the external load be smaller than that needed to cause the joint to separate. If separation does occur, then the entire external load

will be imposed on the bolt. Let P_0 be the value of the external load that would cause joint separation. At separation, $F_m = 0$ in Eq. (8–25), and so

$$(1 - C)P_0 - F_i = 0 \quad (d)$$

Let the factor of safety against joint separation be

$$n_0 = \frac{P_0}{P} \quad (e)$$

Substituting $P_0 = n_0 P$ in Eq. (d), we find

$$n_0 = \frac{F_i}{P(1 - C)} \quad (8-30)$$

as a load factor guarding against joint separation.

Figure 8–18 is the stress-strain diagram of a good-quality bolt material. Notice that there is no clearly defined yield point and that the diagram progresses smoothly up to fracture, which corresponds to the tensile strength. This means that no matter how much preload is given the bolt, it will retain its load-carrying capacity. This is what keeps the bolt tight and determines the joint strength. The pretension is the “muscle” of the joint, and its magnitude is determined by the bolt strength. If the full bolt strength is not used in developing the pretension, then money is wasted and the joint is weaker.

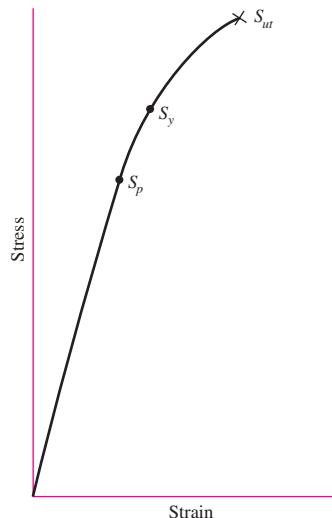
Good-quality bolts can be preloaded into the plastic range to develop more strength. Some of the bolt torque used in tightening produces torsion, which increases the principal tensile stress. However, this torsion is held only by the friction of the bolt head and nut; in time it relaxes and lowers the bolt tension slightly. Thus, as a rule, a bolt will either fracture during tightening, or not at all.

Above all, do not rely too much on wrench torque; it is not a good indicator of preload. Actual bolt elongation should be used whenever possible—especially with fatigue loading. In fact, if high reliability is a requirement of the design, then preload should always be determined by bolt elongation.

Russell, Burdsall & Ward Inc. (RB&W) recommendations for preload are 60 kpsi for SAE grade 5 bolts for nonpermanent connections, and that A325 bolts (equivalent to SAE grade 5) used in structural applications be tightened to proof load or beyond

Figure 8-18

Typical stress-strain diagram for bolt materials showing proof strength S_p , yield strength S_y , and ultimate tensile strength S_{ut} .



(85 kpsi up to a diameter of 1 in).⁷ Bowman⁸ recommends a preload of 75 percent of proof load, which is about the same as the RB&W recommendations for reused bolts. In view of these guidelines, it is recommended for both static and fatigue loading that the following be used for preload:

$$F_i = \begin{cases} 0.75F_p & \text{for nonpermanent connections, reused fasteners} \\ 0.90F_p & \text{for permanent connections} \end{cases} \quad (8-31)$$

where F_p is the proof load, obtained from the equation

$$F_p = A_t S_p \quad (8-32)$$

Here S_p is the proof strength obtained from Tables 8–9 to 8–11. For other materials, an approximate value is $S_p = 0.85S_y$. Be very careful not to use a soft material in a threaded fastener. For high-strength steel bolts used as structural steel connectors, if advanced tightening methods are used, tighten to yield.

You can see that the RB&W recommendations on preload are in line with what we have encountered in this chapter. The purposes of development were to give the reader the perspective to appreciate Eqs. (8–31) and a methodology with which to handle cases more specifically than the recommendations.

EXAMPLE 8-4

Figure 8–19 is a cross section of a grade 25 cast-iron pressure vessel. A total of N bolts are to be used to resist a separating force of 36 kip.

(a) Determine k_b , k_m , and C .

(b) Find the number of bolts required for a load factor of 2 where the bolts may be reused when the joint is taken apart.

(c) With the number of bolts obtained in part (b), determine the realized load factor for overload, the yielding factor of safety, and the load factor for joint separation.

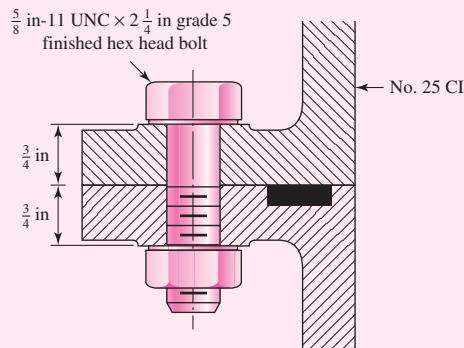
Solution

(a) The grip is $l = 1.50$ in. From Table A–31, the nut thickness is $\frac{35}{64}$ in. Adding two threads beyond the nut of $\frac{2}{11}$ in gives a bolt length of

$$L = \frac{35}{64} + 1.50 + \frac{2}{11} = 2.229 \text{ in}$$

From Table A–17 the next fraction size bolt is $L = 2\frac{1}{4}$ in. From Eq. (8–13), the thread length is $L_T = 2(0.625) + 0.25 = 1.50$ in. Thus, the length of the unthreaded portion

| Figure 8-19



⁷Russell, Burdsall & Ward Inc., *Helpful Hints for Fastener Design and Application*, Mentor, Ohio, 1965, p. 42.

⁸Bowman Distribution–Barnes Group, *Fastener Facts*, Cleveland, 1985, p. 90.

in the grip is $l_d = 2.25 - 1.50 = 0.75$ in. The threaded length in the grip is $l_t = l - l_d = 0.75$ in. From Table 8–2, $A_t = 0.226$ in². The major-diameter area is $A_d = \pi(0.625)^2/4 = 0.3068$ in². The bolt stiffness is then

$$\begin{aligned} \text{Answer} \quad k_b &= \frac{A_d A_t E}{A_d l_t + A_t l_d} = \frac{0.3068(0.226)(30)}{0.3068(0.75) + 0.226(0.75)} \\ &= 5.21 \text{ Mlbf/in} \end{aligned}$$

From Table A–24, for no. 25 cast iron we will use $E = 14$ Mpsi. The stiffness of the members, from Eq. (8–22), is

$$\begin{aligned} \text{Answer} \quad k_m &= \frac{0.5774\pi Ed}{2 \ln \left(5 \frac{0.5774l + 0.5d}{0.5774l + 2.5d} \right)} = \frac{0.5774\pi(14)(0.625)}{2 \ln \left[5 \frac{0.5774(1.5) + 0.5(0.625)}{0.5774(1.5) + 2.5(0.625)} \right]} \\ &= 8.95 \text{ Mlbf/in} \end{aligned}$$

If you are using Eq. (8–23), from Table 8–8, $A = 0.778$ 71 and $B = 0.616$ 16, and

$$\begin{aligned} k_m &= EdA \exp(Bd/l) \\ &= 14(0.625)(0.778 71) \exp[0.616 16(0.625)/1.5] \\ &= 8.81 \text{ Mlbf/in} \end{aligned}$$

which is only 1.6 percent lower than the previous result.

From the first calculation for k_m , the stiffness constant C is

$$\text{Answer} \quad C = \frac{k_b}{k_b + k_m} = \frac{5.21}{5.21 + 8.95} = 0.368$$

(b) From Table 8–9, $S_p = 85$ kpsi. Then, using Eqs. (8–31) and (8–32), we find the recommended preload to be

$$F_i = 0.75A_t S_p = 0.75(0.226)(85) = 14.4 \text{ kip}$$

For N bolts, Eq. (8–29) can be written

$$n_L = \frac{S_p A_t - F_i}{C(P_{\text{total}}/N)} \quad (1)$$

or

$$N = \frac{C n_L P_{\text{total}}}{S_p A_t - F_i} = \frac{0.368(2)(36)}{85(0.226) - 14.4} = 5.52$$

Answer

Six bolts should be used to provide the specified load factor.

(c) With six bolts, the load factor actually realized is

$$\text{Answer} \quad n_L = \frac{85(0.226) - 14.4}{0.368(36/6)} = 2.18$$

From Eq. (8–28), the yielding factor of safety is

$$\text{Answer} \quad n_p = \frac{S_p A_t}{C(P_{\text{total}}/N) + F_i} = \frac{85(0.226)}{0.368(36/6) + 14.4} = 1.16$$

From Eq. (8–30), the load factor guarding against joint separation is

$$\text{Answer} \quad n_0 = \frac{F_i}{(P_{\text{total}}/N)(1 - C)} = \frac{14.4}{(36/6)(1 - 0.368)} = 3.80$$

8-10 Gasketed Joints

If a full gasket is present in the joint, the gasket pressure p is found by dividing the force in the member by the gasket area per bolt. Thus, for N bolts,

$$p = -\frac{F_m}{A_g/N} \quad (a)$$

With a load factor n , Eq. (8-25) can be written as

$$F_m = (1 - C)nP - F_i \quad (b)$$

Substituting this into Eq. (a) gives the gasket pressure as

$$p = [F_i - nP(1 - C)] \frac{N}{A_g} \quad (8-33)$$

In full-gasketed joints uniformity of pressure on the gasket is important. To maintain adequate uniformity of pressure adjacent bolts should not be placed more than six nominal diameters apart on the bolt circle. To maintain wrench clearance, bolts should be placed at least three diameters apart. A rough rule for bolt spacing around a bolt circle is

$$3 \leq \frac{\pi D_b}{Nd} \leq 6 \quad (8-34)$$

where D_b is the diameter of the bolt circle and N is the number of bolts.

8-11 Fatigue Loading of Tension Joints

Tension-loaded bolted joints subjected to fatigue action can be analyzed directly by the methods of Chap. 6. Table 8-16 lists average fatigue stress-concentration factors for the fillet under the bolt head and also at the beginning of the threads on the bolt shank. These are already corrected for notch sensitivity and for surface finish. Designers should be aware that situations may arise in which it would be advisable to investigate these factors more closely, since they are only average values. In fact, Peterson⁹ observes that the distribution of typical bolt failures is about 15 percent under the head, 20 percent at the end of the thread, and 65 percent in the thread at the nut face.

Use of rolled threads is the predominant method of thread-forming in screw fasteners, where Table 8-16 applies. In thread-rolling, the amount of cold work and strain-strengthening is unknown to the designer; therefore, fully corrected (including K_f) axial endurance strength is reported in Table 8-17. For cut threads, the methods of Chap. 6 are useful. Anticipate that the endurance strengths will be considerably lower.

Table 8-16

Fatigue Stress-Concentration Factors K_f for Threaded Elements

	SAE Grade	Metric Grade	Rolled Threads	Cut Threads	Fillet
	0 to 2	3.6 to 5.8	2.2	2.8	2.1
	4 to 8	6.6 to 10.9	3.0	3.8	2.3

⁹W. D. Pilkey, *Peterson's Stress-Concentration Factors*, 2nd ed., John Wiley & Sons, New York, 1997, p. 387.

Table 8-17

Fully Corrected
Endurance Strengths for
Bolts and Screws with
Rolled Threads*

Grade or Class	Size Range	Endurance Strength
SAE 5	$\frac{1}{4}$ –1 in	18.6 kpsi
	$1\frac{1}{8}$ – $1\frac{1}{2}$ in	16.3 kpsi
SAE 7	$\frac{1}{4}$ – $1\frac{1}{2}$ in	20.6 kpsi
SAE 8	$\frac{1}{4}$ – $1\frac{1}{2}$ in	23.2 kpsi
ISO 8.8	M16–M36	129 MPa
ISO 9.8	M1.6–M16	140 MPa
ISO 10.9	M5–M36	162 MPa
ISO 12.9	M1.6–M36	190 MPa

*Repeatedly applied, axial loading, fully corrected.

For a general case with a constant preload, and an external load on a per bolt basis fluctuating between P_{\min} and P_{\max} , a bolt will experience fluctuating forces such that

$$F_{b\min} = CP_{\min} + F_i \quad (a)$$

$$F_{b\max} = CP_{\max} + F_i \quad (b)$$

The alternating stress experienced by a bolt is

$$\sigma_a = \frac{(F_{b\max} - F_{b\min})/2}{A_t} = \frac{(CP_{\max} + F_i) - (CP_{\min} + F_i)}{2A_t}$$

$$\sigma_a = \frac{C(P_{\max} - P_{\min})}{2A_t} \quad (8-35)$$

The midrange stress experienced by a bolt is

$$\sigma_m = \frac{(F_{b\max} + F_{b\min})/2}{A_t} = \frac{(CP_{\max} + F_i) + (CP_{\min} + F_i)}{2A_t}$$

$$\sigma_m = \frac{C(P_{\max} + P_{\min})}{2A_t} + \frac{F_i}{A_t} \quad (8-36)$$

A load line typically experienced by a bolt is shown in Fig. 8-20, where the stress starts from the preload stress and increases with a constant slope of $\sigma_a/(\sigma_m - \sigma_i)$. The Goodman failure line is also shown in Fig. 8-20. The fatigue factor of safety can be found by intersecting the load line and the Goodman line to find the intersection point (S_m , S_a). The load line is given by

$$\text{Load line: } S_a = \frac{\sigma_a}{\sigma_m - \sigma_i}(S_m - \sigma_i) \quad (a)$$

The Goodman line, rearranging Eq. (6-40), p. 306, is

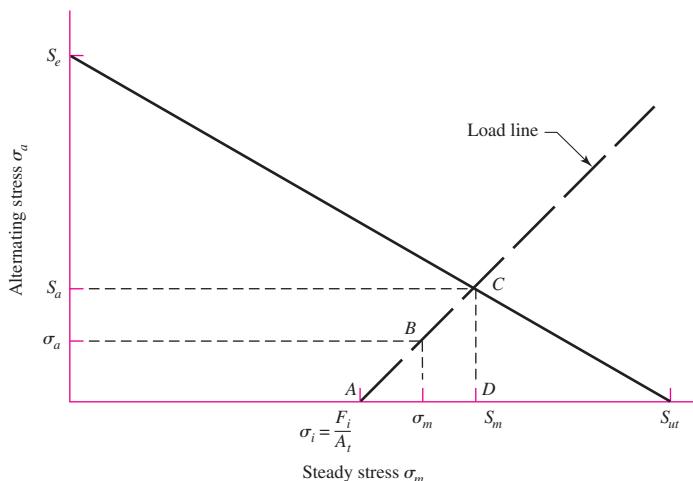
$$\text{Goodman line: } S_a = S_e - \frac{S_e}{S_{ut}}S_m \quad (b)$$

Equating Eqs. (a) and (b), solving for S_m , then substituting S_m back into Eq. (b) yields

$$S_a = \frac{S_e \sigma_a (S_{ut} - \sigma_i)}{S_{ut} \sigma_a + S_e (\sigma_m - \sigma_i)} \quad (c)$$

Figure 8–20

Designer's fatigue diagram showing a Goodman failure line and a commonly used load line for a constant preload and a fluctuating load.



The fatigue factor of safety is given by

$$n_f = \frac{S_a}{\sigma_a} \quad (8-37)$$

Substituting Eq. (c) into Eq. (8-37) gives

$$n_f = \frac{S_e(S_{ut} - \sigma_i)}{S_{ut}\sigma_a + S_e(\sigma_m - \sigma_i)} \quad (8-38)$$

The same approach can be used for the other failure curves, though the algebra is a bit more tedious to put in equation form such as Eq. (8-38). An easier approach would be to solve in stages numerically, first S_m , then S_a , and finally n_f .

Often, the type of fatigue loading encountered in the analysis of bolted joints is one in which the externally applied load fluctuates between zero and some maximum force P . This would be the situation in a pressure cylinder, for example, where a pressure either exists or does not exist. For such cases, Eqs. (8-35) and (8-36) can be simplified by setting $P_{\max} = P$ and $P_{\min} = 0$, resulting in

$$\sigma_a = \frac{CP}{2A_t} \quad (8-39)$$

$$\sigma_m = \frac{CP}{2A_t} + \frac{F_i}{A_t} \quad (8-40)$$

Note that Eq. (8-40) can be viewed as the sum of the alternating stress and the preload stress. If the preload is considered to be constant, the load line relationship between the alternating and midrange stresses can be treated as

$$\sigma_m = \sigma_a + \sigma_i \quad (8-41)$$

This load line has a slope of unity, and is a special case of the load line shown in Fig. 8-20. With the simplifications in the algebra, we can now proceed as before to obtain the fatigue factor of safety using each of the typical failure criteria, duplicated here from Eqs. (6-40), (6-41), and (6-42).

Goodman:

$$\frac{S_a}{S_e} + \frac{S_m}{S_{ut}} = 1 \quad (8-42)$$

Gerber:

$$\frac{S_a}{S_e} + \left(\frac{S_m}{S_{ut}} \right)^2 = 1 \quad (8-43)$$

ASME-elliptic:

$$\left(\frac{S_a}{S_e} \right)^2 + \left(\frac{S_m}{S_p} \right)^2 = 1 \quad (8-44)$$

Now if we intersect Eq. (8-41) and each of Eqs. (8-42) to (8-44) to solve for S_a , and apply Eq. (8-37), we obtain fatigue factors of safety for each failure criteria in a repeated loading situation.

Goodman:

$$n_f = \frac{S_e(S_{ut} - \sigma_i)}{\sigma_a(S_{ut} + S_e)} \quad (8-45)$$

Gerber:

$$n_f = \frac{1}{2\sigma_a S_e} \left[S_{ut} \sqrt{S_{ut}^2 + 4S_e(S_e + \sigma_i)} - S_{ut}^2 - 2\sigma_i S_e \right] \quad (8-46)$$

ASME-elliptic:

$$n_f = \frac{S_e}{\sigma_a(S_p^2 + S_e^2)} \left(S_p \sqrt{S_p^2 + S_e^2 - \sigma_i^2} - \sigma_i S_e \right) \quad (8-47)$$

Note that Eqs. (8-45) to (8-47) are only applicable for repeated loads. Be sure to use K_f for both σ_a and σ_m . Otherwise, the slope of the load line will not remain 1 to 1.

If desired, σ_a from Eq. (8-39) and $\sigma_i = F_i/A_t$ can be directly substituted into any of Eqs. (8-45) to (8-47). If we do so for the Goodman criteria in Eq. (8-45), we obtain

$$n_f = \frac{2S_e(S_{ut}A_t - F_i)}{CP(S_{ut} + S_e)} \quad (8-48)$$

when preload F_i is present. With no preload, $C = 1$, $F_i = 0$, and Eq. (8-48) becomes

$$n_{f0} = \frac{2S_e S_{ut} A_t}{P(S_{ut} + S_e)} \quad (8-49)$$

Preload is beneficial for resisting fatigue when n_f/n_{f0} is greater than unity. For Goodman, Eqs. (8-48) and (8-49) with $n_f/n_{f0} \geq 1$ puts an upper bound on the preload F_i of

$$F_i \leq (1 - C)S_{ut}A_t \quad (8-50)$$

If this cannot be achieved, and n_f is unsatisfactory, use the Gerber or ASME-elliptic criterion to obtain a less conservative assessment. If the design is still not satisfactory, additional bolts and/or a different size bolt may be called for.

Bolts loosen, as they are friction devices, and cyclic loading and vibration as well as other effects allow the fasteners to lose tension with time. How does one fight loosening? Within strength limitations, the higher the preload the better. A rule of thumb is that pre-loads of 60 percent of proof load rarely loosen. If more is better, how much more? Well, not enough to create reused fasteners as a future threat. Alternatively, fastener-locking schemes can be employed.

After solving for the fatigue factor of safety, you should also check the possibility of yielding, using the proof strength

$$n_p = \frac{S_p}{\sigma_m + \sigma_a} \quad (8-51)$$

which is equivalent to Eq. (8-28).

EXAMPLE 8-5

Figure 8-21 shows a connection using cap screws. The joint is subjected to a fluctuating force whose maximum value is 5 kip per screw. The required data are: cap screw, 5/8 in-11 NC, SAE 5; hardened-steel washer, $t_w = \frac{1}{16}$ in thick; steel cover plate, $t_1 = \frac{5}{8}$ in, $E_s = 30$ Mpsi; and cast-iron base, $t_2 = \frac{5}{8}$ in, $E_{ci} = 16$ Mpsi.

- (a) Find k_b , k_m , and C using the assumptions given in the caption of Fig. 8-21.
- (b) Find all factors of safety and explain what they mean.

Solution

(a) For the symbols of Figs. 8-15 and 8-21, $h = t_1 + t_w = 0.6875$ in, $l = h + d/2 = 1$ in, and $D_2 = 1.5d = 0.9375$ in. The joint is composed of three frusta; the upper two frusta are steel and the lower one is cast iron.

For the upper frustum: $t = l/2 = 0.5$ in, $D = 0.9375$ in, and $E = 30$ Mpsi. Using these values in Eq. (8-20) gives $k_1 = 46.46$ Mlbf/in.

For the middle frustum: $t = h - l/2 = 0.1875$ in and $D = 0.9375 + 2(l - h) \tan 30^\circ = 1.298$ in. With these and $E_s = 30$ Mpsi, Eq. (8-20) gives $k_2 = 197.43$ Mlbf/in.

The lower frustum has $D = 0.9375$ in, $t = l - h = 0.3125$ in, and $E_{ci} = 16$ Mpsi. The same equation yields $k_3 = 32.39$ Mlbf/in.

Substituting these three stiffnesses into Eq. (8-18) gives $k_m = 17.40$ Mlbf/in. The cap screw is short and threaded all the way. Using $l = 1$ in for the grip and $A_t = 0.226$ in² from Table 8-2, we find the stiffness to be $k_b = A_t E / l = 6.78$ Mlbf/in. Thus the joint constant is

$$C = \frac{k_b}{k_b + k_m} = \frac{6.78}{6.78 + 17.40} = 0.280$$

Answer

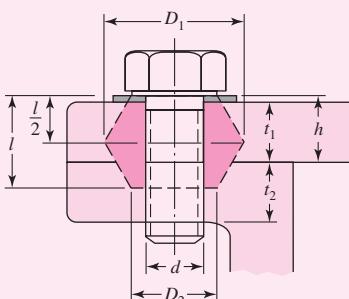


Figure 8-21

Pressure-cone frustum member model for a cap screw. For this model the significant sizes are

$$l = \begin{cases} h + t_2/2 & t_2 < d \\ h + d/2 & t_2 \geq d \end{cases}$$

$$D_1 = d_w + l \tan \alpha = 1.5d + 0.577l$$

$$D_2 = d_w = 1.5d$$

where l = effective grip. The

solutions are for $\alpha = 30^\circ$ and $d_w = 1.5d$.

(b) Equation (8–30) gives the preload as

$$F_i = 0.75F_p = 0.75A_t S_p = 0.75(0.226)(85) = 14.4 \text{ kip}$$

where from Table 8–9, $S_p = 85$ kpsi for an SAE grade 5 cap screw. Using Eq. (8–28), we obtain the load factor as the yielding factor of safety is

Answer

$$n_p = \frac{S_p A_t}{CP + F_i} = \frac{85(0.226)}{0.280(5) + 14.4} = 1.22$$

This is the traditional factor of safety, which compares the maximum bolt stress to the proof strength.

Using Eq. (8–29),

Answer

$$n_L = \frac{S_p A_t - F_i}{CP} = \frac{85(0.226) - 14.4}{0.280(5)} = 3.44$$

This factor is an indication of the overload on P that can be applied without exceeding the proof strength.

Next, using Eq. (8–30), we have

Answer

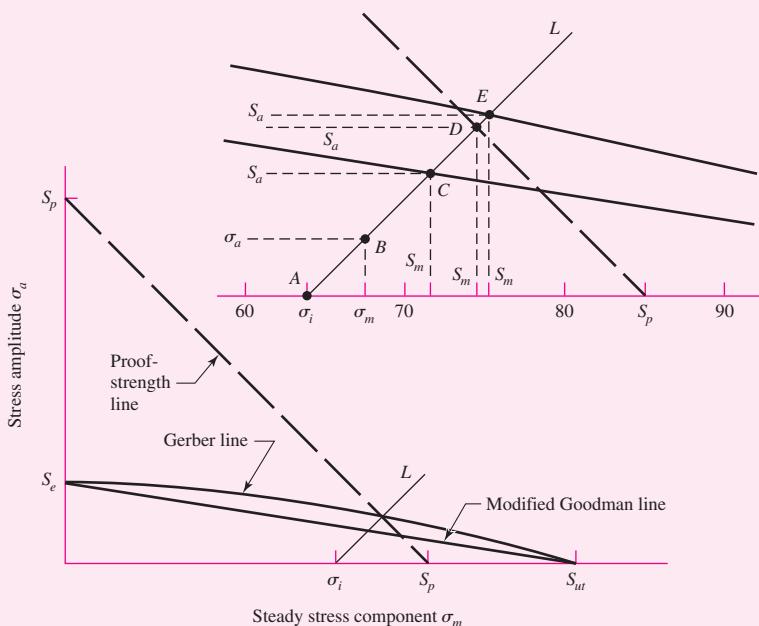
$$n_0 = \frac{F_i}{P(1 - C)} = \frac{14.4}{5(1 - 0.280)} = 4.00$$

If the force P gets too large, the joint will separate and the bolt will take the entire load. This factor guards against that event.

For the remaining factors, refer to Fig. 8–22. This diagram contains the modified Goodman line, the Gerber line, and the proof-strength line. The intersection

Figure 8–22

Designer's fatigue diagram for preloaded bolts, drawn to scale, showing the modified Goodman line, the Gerber line, and the Langer proof-strength line, with an exploded view of the area of interest. The strengths used are $S_p = 85$ kpsi, $S_e = 18.6$ kpsi, and $S_{ut} = 120$ kpsi. The coordinates are A , $\sigma_i = 63.72$ kpsi; B , $\sigma_a = 3.10$ kpsi, $\sigma_m = 66.82$ kpsi; C , $S_a = 7.55$ kpsi, $S_m = 71.29$ kpsi; D , $S_a = 10.64$ kpsi, $S_m = 74.36$ kpsi; E , $S_a = 11.32$ kpsi, $S_m = 75.04$ kpsi.



of the load line L with the respective failure lines at points C , D , and E defines a set of strengths S_a and S_m at each intersection. Point B represents the stress state σ_a , σ_m . Point A is the preload stress σ_i . Therefore the load line begins at A and makes an angle having a unit slope. This angle is 45° only when both stress axes have the same scale.

The factors of safety are found by dividing the distances AC , AD , and AE by the distance AB . Note that this is the same as dividing S_a for each theory by σ_a .

The quantities shown in the caption of Fig. 8–22 are obtained as follows:

Point A

$$\sigma_i = \frac{F_i}{A_t} = \frac{14.4}{0.226} = 63.72 \text{ kpsi}$$

Point B

$$\sigma_a = \frac{CP}{2A_t} = \frac{0.280(5)}{2(0.226)} = 3.10 \text{ kpsi}$$

$$\sigma_m = \sigma_a + \sigma_i = 3.10 + 63.72 = 66.82 \text{ kpsi}$$

Point C

This is the modified Goodman criteria. From Table 8–17, we find $S_e = 18.6$ kpsi. Then, using Eq. (8–45), the factor of safety is found to be

Answer

$$n_f = \frac{S_e(S_{ut} - \sigma_i)}{\sigma_a(S_{ut} + S_e)} = \frac{18.6(120 - 63.72)}{3.10(120 + 18.6)} = 2.44$$

Point D

This is on the proof-strength line where

$$S_m + S_a = S_p \quad (1)$$

In addition, the horizontal projection of the load line AD is

$$S_m = \sigma_i + S_a \quad (2)$$

Solving Eqs. (1) and (2) simultaneously results in

$$S_a = \frac{S_p - \sigma_i}{2} = \frac{85 - 63.72}{2} = 10.64 \text{ kpsi}$$

The factor of safety resulting from this is

Answer

$$n_p = \frac{S_a}{\sigma_a} = \frac{10.64}{3.10} = 3.43$$

which, of course, is identical to the result previously obtained by using Eq. (8–29).

A similar analysis of a fatigue diagram could have been done using yield strength instead of proof strength. Though the two strengths are somewhat related, proof strength is a much better and more positive indicator of a fully loaded bolt than is the yield strength. It is also worth remembering that proof-strength values are specified in design codes; yield strengths are not.

We found $n_f = 2.44$ on the basis of fatigue and the modified Goodman line, and $n_p = 3.43$ on the basis of proof strength. Thus the danger of failure is by fatigue, not by overproof loading. These two factors should always be compared to determine where the greatest danger lies.

Point E

For the Gerber criterion, from Eq. (8–46), the safety factor is

$$\begin{aligned}\text{Answer} \quad n_f &= \frac{1}{2\sigma_a S_e} \left[S_{ut} \sqrt{S_{ut}^2 + 4S_e(S_e + \sigma_i)} - S_{ut}^2 - 2\sigma_i S_e \right] \\ &= \frac{1}{2(3.10)(18.6)} \left[120 \sqrt{120^2 + 4(18.6)(18.6 + 63.72)} - 120^2 - 2(63.72)(18.6) \right] \\ &= 3.65\end{aligned}$$

which is greater than $n_p = 3.43$ and contradicts the conclusion earlier that the danger of failure is fatigue. Figure 8–22 clearly shows the conflict where point *D* lies between points *C* and *E*. Again, the conservative nature of the Goodman criterion explains the discrepancy and the designer must form his or her own conclusion.

8–12 Bolted and Riveted Joints Loaded in Shear¹⁰

Riveted and bolted joints loaded in shear are treated exactly alike in design and analysis.

Figure 8–23a shows a riveted connection loaded in shear. Let us now study the various means by which this connection might fail.

Figure 8–23b shows a failure by bending of the rivet or of the riveted members. The bending moment is approximately $M = Ft/2$, where F is the shearing force and t is the grip of the rivet, that is, the total thickness of the connected parts. The bending stress in the members or in the rivet is, neglecting stress concentration,

$$\sigma = \frac{M}{I/c} \quad (8-52)$$

where I/c is the section modulus for the weakest member or for the rivet or rivets, depending upon which stress is to be found. The calculation of the bending stress in this manner is an assumption, because we do not know exactly how the load is distributed to the rivet or the relative deformations of the rivet and the members. Although this equation can be used to determine the bending stress, it is seldom used in design; instead its effect is compensated for by an increase in the factor of safety.

In Fig. 8–23c failure of the rivet by pure shear is shown; the stress in the rivet is

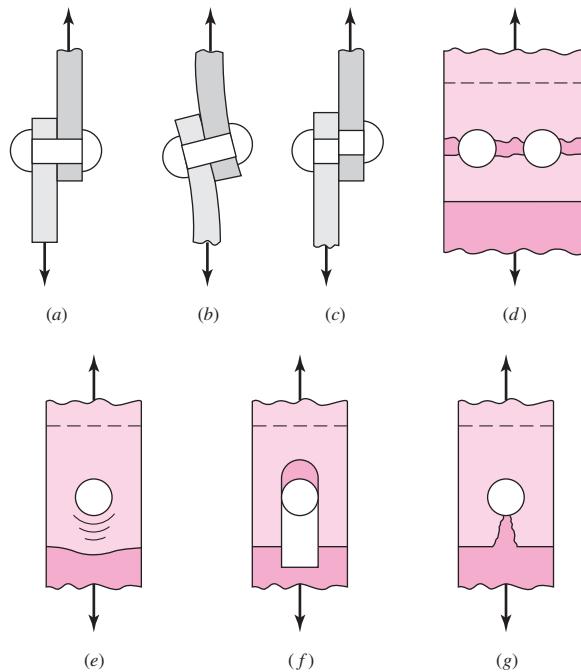
$$\tau = \frac{F}{A} \quad (8-53)$$

where A is the cross-sectional area of all the rivets in the group. It may be noted that it is standard practice in structural design to use the nominal diameter of the rivet rather than the diameter of the hole, even though a hot-driven rivet expands and nearly fills up the hole.

¹⁰The design of bolted and riveted connections for boilers, bridges, buildings, and other structures in which danger to human life is involved is strictly governed by various construction codes. When designing these structures, the engineer should refer to the *American Institute of Steel Construction Handbook*, the American Railway Engineering Association specifications, or the Boiler Construction Code of the American Society of Mechanical Engineers.

Figure 8–23

Modes of failure in shear loading of a bolted or riveted connection: (a) shear loading; (b) bending of rivet; (c) shear of rivet; (d) tensile failure of members; (e) bearing of rivet on members or bearing of members on rivet; (f) shear tear-out; (g) tensile tear-out.



Rupture of one of the connected members or plates by pure tension is illustrated in Fig. 8–23d. The tensile stress is

$$\sigma = \frac{F}{A} \quad (8-54)$$

where A is the net area of the plate, that is, the area reduced by an amount equal to the area of all the rivet holes. For brittle materials and static loads and for either ductile or brittle materials loaded in fatigue, the stress-concentration effects must be included. It is true that the use of a bolt with an initial preload and, sometimes, a rivet will place the area around the hole in compression and thus tend to nullify the effects of stress concentration, but unless definite steps are taken to ensure that the preload does not relax, it is on the conservative side to design as if the full stress-concentration effect were present. The stress-concentration effects are not considered in structural design, because the loads are static and the materials ductile.

In calculating the area for Eq. (8–54), the designer should, of course, use the combination of rivet or bolt holes that gives the smallest area.

Figure 8–23e illustrates a failure by crushing of the rivet or plate. Calculation of this stress, which is usually called a *bearing stress*, is complicated by the distribution of the load on the cylindrical surface of the rivet. The exact values of the forces acting upon the rivet are unknown, and so it is customary to assume that the components of these forces are uniformly distributed over the projected contact area of the rivet. This gives for the stress

$$\sigma = -\frac{F}{A} \quad (8-55)$$

where the projected area for a single rivet is $A = td$. Here, t is the thickness of the thinnest plate and d is the rivet or bolt diameter.

Edge shearing, or tearing, of the margin is shown in Fig. 8-23*f* and *g*, respectively. In structural practice this failure is avoided by spacing the rivets at least $1\frac{1}{2}$ diameters away from the edge. Bolted connections usually are spaced an even greater distance than this for satisfactory appearance, and hence this type of failure may usually be neglected.

In a rivet joint, the rivets all share the load in shear, bearing in the rivet, bearing in the member, and shear in the rivet. Other failures are participated in by only some of the joint. In a bolted joint, shear is taken by clamping friction, and bearing does not exist. When bolt preload is lost, one bolt begins to carry the shear and bearing until yielding slowly brings other fasteners in to share the shear and bearing. Finally, all participate, and this is the basis of most bolted-joint analysis if loss of bolt preload is complete. The usual analysis involves

- Bearing in the bolt (all bolts participate)
- Bearing in members (all holes participate)
- Shear of bolt (all bolts participate eventually)
- Distinguishing between thread and shank shear
- Edge shearing and tearing of member (edge bolts participate)
- Tensile yielding of member across bolt holes
- Checking member capacity

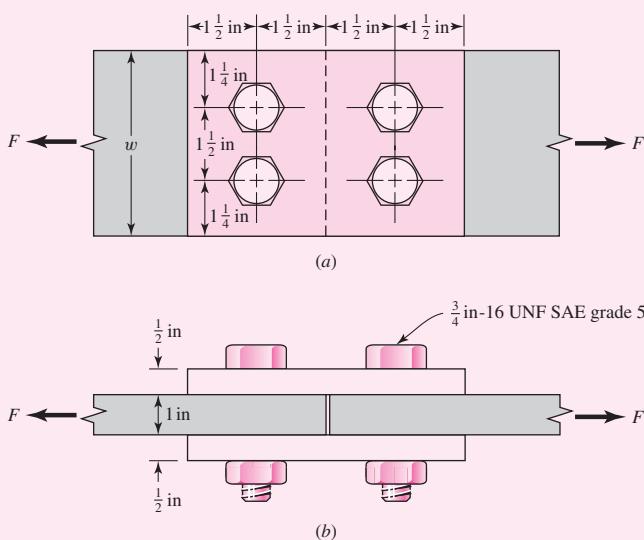
EXAMPLE 8-6

Two 1- by 4-in 1018 cold-rolled steel bars are butt-spliced with two $\frac{1}{2}$ - by 4-in 1018 cold-rolled splice plates using four $\frac{3}{4}$ in-16 UNF grade 5 bolts as depicted in Fig. 8-24. For a design factor of $n_d = 1.5$ estimate the static load F that can be carried if the bolts lose preload.

Solution

From Table A-20, minimum strengths of $S_y = 54$ kpsi and $S_{ut} = 64$ kpsi are found for the members, and from Table 8-9 minimum strengths of $S_p = 85$ kpsi and $S_{ut} = 120$ kpsi for the bolts are found.

| Figure 8-24



$F/2$ is transmitted by each of the splice plates, but since the areas of the splice plates are half those of the center bars, the stresses associated with the plates are the same. So for stresses associated with the plates, the force and areas used will be those of the center plates.

Bearing in bolts, all bolts loaded:

$$\sigma = \frac{F}{2td} = \frac{S_p}{n_d}$$

$$F = \frac{2tdS_p}{n_d} = \frac{2(1)(\frac{3}{4})85}{1.5} = 85 \text{ kip}$$

Bearing in members, all bolts active:

$$\sigma = \frac{F}{2td} = \frac{(S_y)_{mem}}{n_d}$$

$$F = \frac{2td(S_y)_{mem}}{n_d} = \frac{2(1)(\frac{3}{4})54}{1.5} = 54 \text{ kip}$$

Shear of bolt, all bolts active: If the bolt threads do not extend into the shear planes for four shanks:

$$\tau = \frac{F}{4\pi d^2/4} = 0.577 \frac{S_p}{n_d}$$

$$F = 0.577\pi d^2 \frac{S_p}{n_d} = 0.577\pi(0.75)^2 \frac{85}{1.5} = 57.8 \text{ kip}$$

If the bolt threads extend into a shear plane:

$$\tau = \frac{F}{4A_r} = 0.577 \frac{S_p}{n_d}$$

$$F = \frac{0.577(4)A_rS_p}{n_d} = \frac{0.577(4)0.351(85)}{1.5} = 45.9 \text{ kip}$$

Edge shearing of member at two margin bolts: From Fig. 8-25,

$$\tau = \frac{F}{4at} = \frac{0.577(S_y)_{mem}}{n_d}$$

$$F = \frac{4at0.577(S_y)_{mem}}{n_d} = \frac{4(1.125)(1)0.577(54)}{1.5} = 93.5 \text{ kip}$$

Tensile yielding of members across bolt holes:

$$\sigma = \frac{F}{[4 - 2(\frac{3}{4})]t} = \frac{(S_y)_{mem}}{n_d}$$

$$F = \frac{[4 - 2(\frac{3}{4})]t(S_y)_{mem}}{n_d} = \frac{[4 - 2(\frac{3}{4})](1)54}{1.5} = 90 \text{ kip}$$

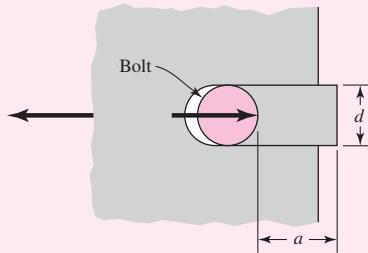
Member yield:

$$F = \frac{wt(S_y)_{\text{mem}}}{n_d} = \frac{4(1)54}{1.5} = 144 \text{ kip}$$

On the basis of bolt shear, the limiting value of the force is 45.9 kip, assuming the threads extend into a shear plane. However, it would be poor design to allow the threads to extend into a shear plane. So, assuming a *good* design based on bolt shear, the limiting value of the force is 57.8 kip. For the members, the bearing stress limits the load to 54 kip.

Figure 8-25

Edge shearing of member.



Shear Joints with Eccentric Loading

In the previous example, the load distributed equally to the bolts since the load acted along a line of symmetry of the fasteners. The analysis of a shear joint undergoing eccentric loading requires locating the center of relative motion between the two members. In Fig. 8-26 let A_1 to A_5 be the respective cross-sectional areas of a group of five pins, or hot-driven rivets, or tight-fitting shoulder bolts. Under this assumption the rotational pivot point lies at the centroid of the cross-sectional area pattern of the pins, rivets, or bolts. Using statics, we learn that the centroid G is located by the coordinates \bar{x} and \bar{y} , where x_i and y_i are the distances to the i th area center:

$$\bar{x} = \frac{A_1x_1 + A_2x_2 + A_3x_3 + A_4x_4 + A_5x_5}{A_1 + A_2 + A_3 + A_4 + A_5} = \frac{\sum_1^n A_i x_i}{\sum_1^n A_i}$$

$$\bar{y} = \frac{A_1y_1 + A_2y_2 + A_3y_3 + A_4y_4 + A_5y_5}{A_1 + A_2 + A_3 + A_4 + A_5} = \frac{\sum_1^n A_i y_i}{\sum_1^n A_i} \quad (8-56)$$

Figure 8-26

Centroid of pins, rivets, or bolts.

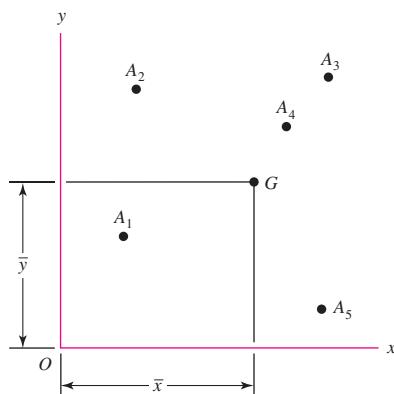
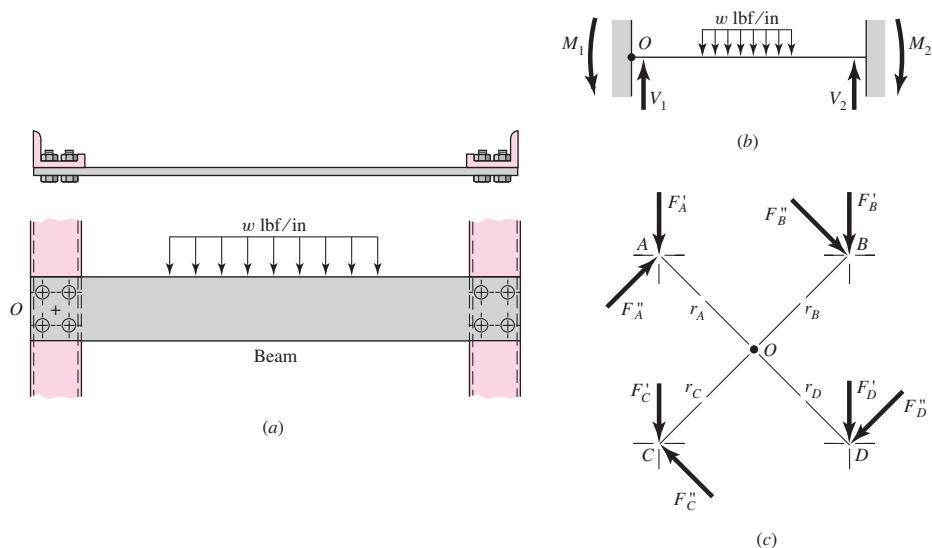


Figure 8-27

(a) Beam bolted at both ends with distributed load; (b) free-body diagram of beam; (c) enlarged view of bolt group centered at O showing primary and secondary resultant shear forces.



In many instances the centroid can be located by symmetry.

An example of eccentric loading of fasteners is shown in Fig. 8-27. This is a portion of a machine frame containing a beam subjected to the action of a bending load. In this case, the beam is fastened to vertical members at the ends with specially prepared load-sharing bolts. You will recognize the schematic representation in Fig. 8-27b as a statically indeterminate beam with both ends fixed and with moment and shear reactions at each end.

For convenience, the centers of the bolts at the left end of the beam are drawn to a larger scale in Fig. 8-27c. Point O represents the centroid of the group, and it is assumed in this example that all the bolts are of the same diameter. Note that the forces shown in Fig. 8-27c are the *resultant* forces acting on the pins with a net force and moment equal and opposite to the *reaction* loads V_1 and M_1 acting at O . The total load taken by each bolt will be calculated in three steps. In the first step the shear V_1 is divided equally among the bolts so that each bolt takes $F' = V_1/n$, where n refers to the number of bolts in the group and the force F' is called the *direct load*, or *primary shear*.

It is noted that an equal distribution of the direct load to the bolts assumes an absolutely rigid member. The arrangement of the bolts or the shape and size of the members sometimes justifies the use of another assumption as to the division of the load. The direct loads F'_n are shown as vectors on the loading diagram (Fig. 8-27c).

The *moment load*, or *secondary shear*, is the additional load on each bolt due to the moment M_1 . If r_A , r_B , r_C , etc., are the radial distances from the centroid to the center of each bolt, the moment and moment loads are related as follows:

$$M_1 = F''_A r_A + F''_B r_B + F''_C r_C + \dots \quad (a)$$

where the F'' are the moment loads. The force taken by each bolt depends upon its radial distance from the centroid; that is, the bolt farthest from the centroid takes the greatest load, while the nearest bolt takes the smallest. We can therefore write

$$\frac{F''_A}{r_A} = \frac{F''_B}{r_B} = \frac{F''_C}{r_C} \quad (b)$$

where again, the diameters of the bolts are assumed equal. If not, then one replaces F'' in Eq. (b) with the shear stresses $\tau'' = 4F''/\pi d^2$ for each bolt. Solving Eqs. (a) and (b) simultaneously, we obtain

$$F_n'' = \frac{M_1 r_n}{r_A^2 + r_B^2 + r_C^2 + \dots} \quad (8-57)$$

where the subscript n refers to the particular bolt whose load is to be found. These moment loads are also shown as vectors on the loading diagram.

In the third step the direct and moment loads are added vectorially to obtain the resultant load on each bolt. Since all the bolts or rivets are usually the same size, only that bolt having the maximum load need be considered. When the maximum load is found, the strength may be determined by using the various methods already described.

EXAMPLE 8-7

Shown in Fig. 8-28 is a 15- by 200-mm rectangular steel bar cantilevered to a 250-mm steel channel using four tightly fitted bolts located at A , B , C , and D .

For a $F = 16$ kN load find

- (a) The resultant load on each bolt
- (b) The maximum shear stress in each bolt
- (c) The maximum bearing stress
- (d) The critical bending stress in the bar

Solution

(a) Point O , the centroid of the bolt group in Fig. 8-28, is found by symmetry. If a free-body diagram of the beam were constructed, the shear reaction V would pass through O and the moment reactions M would be about O . These reactions are

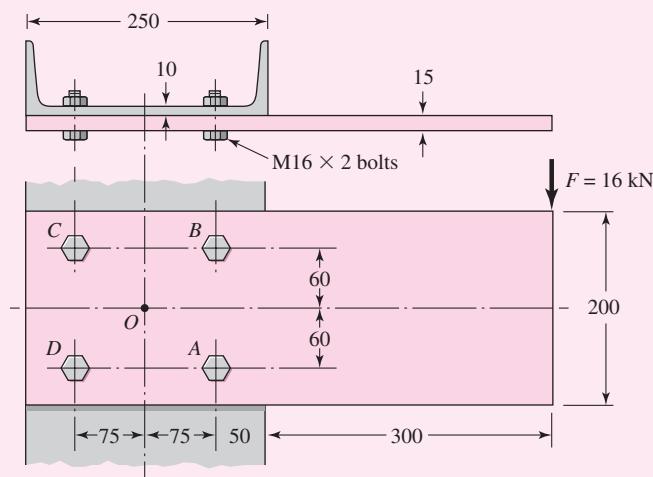
$$V = 16 \text{ kN} \quad M = 16(425) = 6800 \text{ N} \cdot \text{m}$$

In Fig. 8-29, the bolt group has been drawn to a larger scale and the reactions are shown. The distance from the centroid to the center of each bolt is

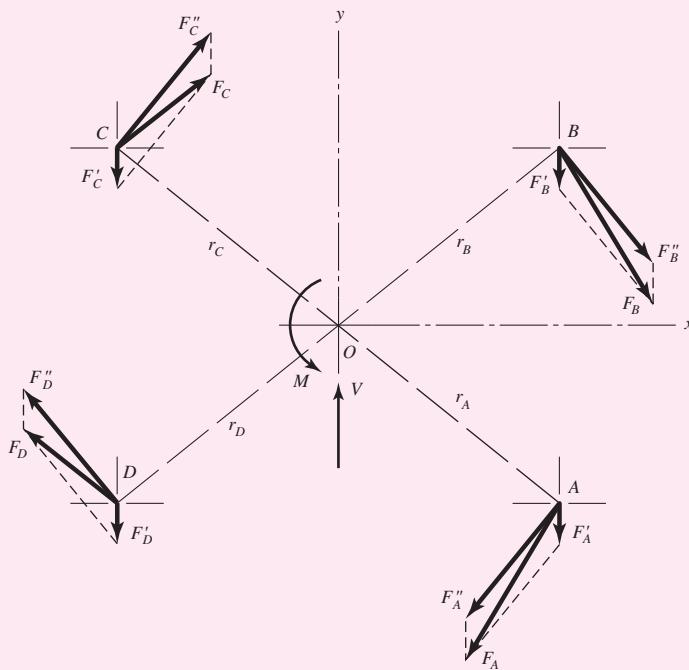
$$r = \sqrt{(60)^2 + (75)^2} = 96.0 \text{ mm}$$

Figure 8-28

Dimensions in millimeters.



| Figure 8-29



The primary shear load per bolt is

$$F' = \frac{V}{n} = \frac{16}{4} = 4 \text{ kN}$$

Since the secondary shear forces are equal, Eq. (8-57) becomes

$$F'' = \frac{Mr}{4r^2} = \frac{M}{4r} = \frac{6800}{4(96.0)} = 17.7 \text{ kN}$$

The primary and secondary shear forces are plotted to scale in Fig. 8-29 and the resultants obtained by using the parallelogram rule. The magnitudes are found by measurement (or analysis) to be

Answer

$$F_A = F_B = 21.0 \text{ kN}$$

Answer

$$F_C = F_D = 14.8 \text{ kN}$$

(b) Bolts A and B are critical because they carry the largest shear load. Does this shear act on the threaded portion of the bolt, or on the unthreaded portion? The bolt length will be 25 mm plus the height of the nut plus about 2 mm for a washer. Table A-31 gives the nut height as 14.8 mm. Including two threads beyond the nut, this adds up to a length of 43.8 mm, and so a bolt 46 mm long will be needed. From Eq. (8-14) we compute the thread length as $L_T = 38$ mm. Thus the unthreaded portion of the bolt is $46 - 38 = 8$ mm long. This is less than the 15 mm for the plate in Fig. 8-28, and so the bolt will tend to shear across its minor diameter. Therefore the shear-stress area is $A_s = 144 \text{ mm}^2$, and so the shear stress is

Answer

$$\tau = \frac{F}{A_s} = \frac{21.0(10)^3}{144} = 146 \text{ MPa}$$

(c) The channel is thinner than the bar, and so the largest bearing stress is due to the pressing of the bolt against the channel web. The bearing area is $A_b = td = 10(16) = 160 \text{ mm}^2$. Thus the bearing stress is

Answer

$$\sigma = -\frac{F}{A_b} = -\frac{21.0(10)^3}{160} = -131 \text{ MPa}$$

(d) The critical bending stress in the bar is assumed to occur in a section parallel to the y axis and through bolts A and B . At this section the bending moment is

$$M = 16(300 + 50) = 5600 \text{ N} \cdot \text{m}$$

The second moment of area through this section is obtained by the use of the transfer formula, as follows:

$$\begin{aligned} I &= I_{\text{bar}} - 2(I_{\text{holes}} + \bar{d}^2 A) \\ &= \frac{15(200)^3}{12} - 2 \left[\frac{15(16)^3}{12} + (60)^2(15)(16) \right] = 8.26(10)^6 \text{ mm}^4 \end{aligned}$$

Then

Answer

$$\sigma = \frac{Mc}{I} = \frac{5600(100)}{8.26(10)^6}(10)^3 = 67.8 \text{ MPa}$$

PROBLEMS

8-1

A power screw is 25 mm in diameter and has a thread pitch of 5 mm.

- (a) Find the thread depth, the thread width, the mean and root diameters, and the lead, provided square threads are used.
- (b) Repeat part (a) for Acme threads.

8-2

Using the information in the footnote of Table 8-1, show that the tensile-stress area is

$$A_t = \frac{\pi}{4}(d - 0.938194p)^2$$

8-3

Show that for zero collar friction the efficiency of a square-thread screw is given by the equation

$$e = \tan \lambda \frac{1 - f \tan \lambda}{\tan \lambda + f}$$

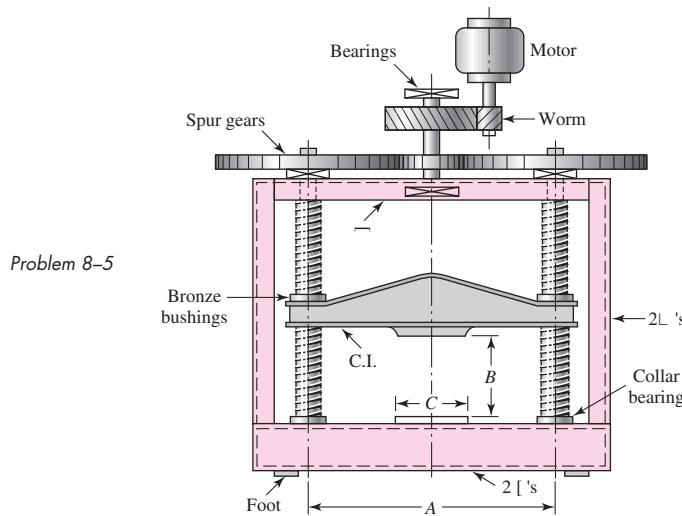
Plot a curve of the efficiency for lead angles up to 45° . Use $f = 0.08$.

8-4

A single-threaded 25-mm power screw is 25 mm in diameter with a pitch of 5 mm. A vertical load on the screw reaches a maximum of 5 kN. The coefficients of friction are 0.06 for the collar and 0.09 for the threads. The frictional diameter of the collar is 45 mm. Find the overall efficiency and the torque to “raise” and “lower” the load.

8-5

The machine shown in the figure can be used for a tension test but not for a compression test. Why? Can both screws have the same hand?

**8-6**

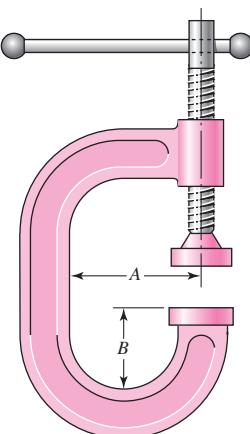
The press shown for Prob. 8-5 has a rated load of 5000 lbf. The twin screws have Acme threads, a diameter of 2 in, and a pitch of $\frac{1}{4}$ in. Coefficients of friction are 0.05 for the threads and 0.08 for the collar bearings. Collar diameters are 3.5 in. The gears have an efficiency of 95 percent and a speed ratio of 60:1. A slip clutch, on the motor shaft, prevents overloading. The full-load motor speed is 1720 rev/min.

- When the motor is turned on, how fast will the press head move?
- What should be the horsepower rating of the motor?

8-7

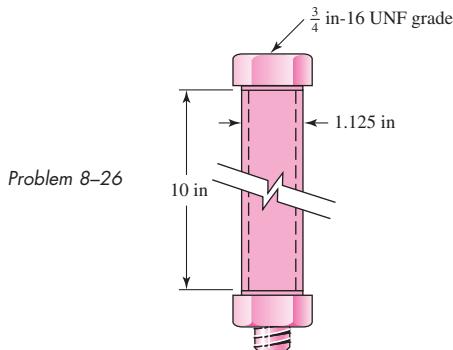
A screw clamp similar to the one shown in the figure has a handle with diameter $\frac{3}{8}$ in made of cold-drawn AISI 1006 steel. The overall length is 4.25 in. The screw is $\frac{3}{4}$ in-10 UNC and is 8 in long, overall. Distance A is 3 in. The clamp will accommodate parts up to 6 in high.

- What screw torque will cause the handle to bend permanently?
- What clamping force will the answer to part (a) cause if the collar friction is neglected and if the thread friction is 0.15?
- What clamping force will cause the screw to buckle?
- Are there any other stresses or possible failures to be checked?

Problem 8-7

- 8-8** The C clamp shown in the figure for Prob. 8-7 uses a $\frac{3}{4}$ in-6 Acme thread. The frictional coefficients are 0.15 for the threads and for the collar. The collar, which in this case is the anvil striker's swivel joint, has a friction diameter of 1 in. Calculations are to be based on a maximum force of 8 lbf applied to the handle at a radius of $3\frac{1}{2}$ in from the screw centerline. Find the clamping force.
- 8-9** Find the power required to drive a 1.5-in power screw having double square threads with a pitch of $\frac{1}{4}$ in. The nut is to move at a velocity of 2 in/s and move a load of $F = 2.2$ kips. The frictional coefficients are 0.10 for the threads and 0.15 for the collar. The frictional diameter of the collar is 2.25 in.
- 8-10** A single square-thread power screw has an input power of 3 kW at a speed of 1 rev/s. The screw has a diameter of 40 mm and a pitch of 8 mm. The frictional coefficients are 0.14 for the threads and 0.09 for the collar, with a collar friction radius of 50 mm. Find the axial resisting load F and the combined efficiency of the screw and collar.
- 8-11** An M14 \times 2 hex-head bolt with a nut is used to clamp together two 15-mm steel plates.
(a) Determine a suitable length for the bolt, rounded up to the nearest 5 mm.
(b) Determine the bolt stiffness.
(c) Determine the stiffness of the members.
- 8-12** Repeat Prob. 8-11 with the addition of one 14R metric plain washer under the nut.
- 8-13** Repeat Prob. 8-11 with one of the plates having a threaded hole to eliminate the nut.
- 8-14** A 2-in steel plate and a 1-in cast-iron plate are compressed with one bolt and nut. The bolt is $\frac{1}{2}$ in-13 UNC.
(a) Determine a suitable length for the bolt, rounded up to the nearest $\frac{1}{4}$ in.
(b) Determine the bolt stiffness.
(c) Determine the stiffness of the members.
- 8-15** Repeat Prob. 8-14 with the addition of one $\frac{1}{2}$ N American Standard plain washer under the head of the bolt, and another identical washer under the nut.
- 8-16** Repeat Prob. 8-14 with the cast-iron plate having a threaded hole to eliminate the nut.
- 8-17** Two identical aluminum plates are each 2 in thick, and are compressed with one bolt and nut. Washers are used under the head of the bolt and under the nut.
Washer properties: steel; ID = 0.531 in; OD = 1.062 in; thickness = 0.095 in
Nut properties: steel; height = $\frac{7}{16}$ in
Bolt properties: $\frac{1}{2}$ in-13 UNC grade 8
Plate properties: aluminum; $E = 10.3$ GPa; $S_u = 47$ ksi; $S_y = 25$ ksi
(a) Determine a suitable length for the bolt, rounded up to the nearest $\frac{1}{4}$ in.
(b) Determine the bolt stiffness.
(c) Determine the stiffness of the members.
- 8-18** Repeat Prob. 8-17 with no washer under the head of the bolt, and two washers stacked under the nut.
- 8-19** A 30-mm thick AISI 1020 steel plate is sandwiched between two 10-mm thick 2024-T3 aluminum plates and compressed with a bolt and nut with no washers. The bolt is M10 \times 1.5, property class 5.8.
(a) Determine a suitable length for the bolt, rounded up to the nearest 5 mm.
(b) Determine the bolt stiffness.
(c) Determine the stiffness of the members.

- 8-20** Repeat Prob. 8-19 with the bottom aluminum plate replaced by one that is 20 mm thick.
- 8-21** Repeat Prob. 8-19 with the bottom aluminum plate having a threaded hole to eliminate the nut.
- 8-22** Two 20-mm steel plates are to be clamped together with a bolt and nut. Specify a bolt to provide a joint constant C between 0.2 and 0.3.
- 8-23** A 2-in steel plate and a 1-in cast-iron plate are to be compressed with one bolt and nut. Specify a bolt to provide a joint constant C between 0.2 and 0.3.
- 8-24** An aluminum bracket with a $\frac{1}{2}$ -in thick flange is to be clamped to a steel column with a $\frac{3}{4}$ -in wall thickness. A cap screw passes through a hole in the bracket flange, and threads into a tapped hole through the column wall. Specify a cap screw to provide a joint constant C between 0.2 and 0.3.
- 8-25** An M14 \times 2 hex-head bolt with a nut is used to clamp together two 20-mm steel plates. Compare the results of finding the overall member stiffness by use of Eqs. (8-20), (8-22), and (8-23).
- 8-26** A $\frac{3}{4}$ in-16 UNF series SAE grade 5 bolt has a $\frac{3}{4}$ -in ID steel tube 10 in long, clamped between washer faces of bolt and nut by turning the nut snug and adding one-third of a turn. The tube OD is the washer-face diameter $d_w = 1.5d = 1.5(0.75) = 1.125$ in = OD.



- (a) Determine the bolt stiffness, the tube stiffness, and the joint constant C .
(b) When the one-third turn-of-nut is applied, what is the initial tension F_i in the bolt?

- 8-27** From your experience with Prob. 8-26, generalize your solution to develop a turn-of-nut equation

$$N_t = \frac{\theta}{360^\circ} = \left(\frac{k_b + k_m}{k_b k_m} \right) F_i N$$

where N_t = turn of the nut from snug tight

θ = turn of the nut in degrees

N = number of thread/in (1/p where p is pitch)

F_i = initial preload

k_b, k_m = spring rates of the bolt and members, respectively

Use this equation to find the relation between torque-wrench setting T and turn-of-nut N_t . (“Snug tight” means the joint has been tightened to perhaps half the intended preload to flatten asperities on the washer faces and the members. Then the nut is loosened and retightened finger tight, and the nut is rotated the number of degrees indicated by the equation. Properly done, the result is competitive with torque wrenching.)

8-28

RB&W¹¹ recommends turn-of-nut from snug fit to preload as follows: 1/3 turn for bolt grips of 1–4 diameters, 1/2 turn for bolt grips 4–8 diameters, and 2/3 turn for grips of 8–12 diameters. These recommendations are for structural steel fabrication (permanent joints), producing preloads of 100 percent of proof strength and beyond. Machinery fabricators with fatigue loadings and possible joint disassembly have much smaller turns-of-nut. The RB&W recommendation enters the nonlinear plastic deformation zone.

For Ex. 8-4, use Eq. (8-27) with $K = 0.2$ to estimate the torque necessary to establish the desired preload. Then, using the results from Prob. 8-27, determine the turn of the nut in degrees. How does this compare with the RB&W recommendations?

8-29

For a bolted assembly with six bolts, the stiffness of each bolt is $k_b = 3 \text{ Mlbf/in}$ and the stiffness of the members is $k_m = 12 \text{ Mlbf/in}$ per bolt. An external load of 80 kips is applied to the entire joint. Assume the load is equally distributed to all the bolts. It has been determined to use $\frac{1}{2} \text{ in-13 UNC grade 8}$ bolts with rolled threads. Assume the bolts are preloaded to 75 percent of the proof load.

- (a) Determine the yielding factor of safety.
- (b) Determine the overload factor of safety.
- (c) Determine the factor of safety based on joint separation.

8-30

For the bolted assembly of Prob. 8-29, it is desired to find the range of torque that a mechanic could apply to initially preload the bolts without expecting failure once the joint is loaded. Assume a torque coefficient of $K = 0.2$.

- (a) Determine the maximum bolt preload that can be applied without exceeding the proof strength of the bolts.
- (b) Determine the minimum bolt preload that can be applied while avoiding joint separation.
- (c) Determine the value of torque in units of $\text{lbf} \cdot \text{ft}$ that should be specified for preloading the bolts if it is desired to preload to the midpoint of the values found in parts (a) and (b).

8-31

For a bolted assembly with eight bolts, the stiffness of each bolt is $k_b = 1.0 \text{ MN/mm}$ and the stiffness of the members is $k_m = 2.6 \text{ MN/mm}$ per bolt. The joint is subject to occasional disassembly for maintenance and should be preloaded accordingly. Assume the external load is equally distributed to all the bolts. It has been determined to use $M6 \times 1$ class 5.8 bolts with rolled threads.

- (a) Determine the maximum external load P_{\max} that can be applied to the entire joint without exceeding the proof strength of the bolts.
- (b) Determine the maximum external load P_{\max} that can be applied to the entire joint without causing the members to come out of compression.

8-32

For a bolted assembly, the stiffness of each bolt is $k_b = 4 \text{ Mlbf/in}$ and the stiffness of the members is $k_m = 12 \text{ Mlbf/in}$ per bolt. The joint is subject to occasional disassembly for maintenance and should be preloaded accordingly. A fluctuating external load is applied to the entire joint with $P_{\max} = 80 \text{ kips}$ and $P_{\min} = 20 \text{ kips}$. Assume the load is equally distributed to all the bolts. It has been determined to use $\frac{1}{2} \text{ in-13 UNC grade 8}$ bolts with rolled threads.

- (a) Determine the minimum number of bolts necessary to avoid yielding of the bolts.
- (b) Determine the minimum number of bolts necessary to avoid joint separation.

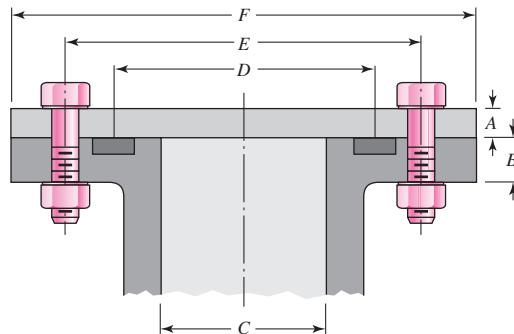
**8-33 to
8-36**

The figure illustrates the connection of a steel cylinder head to a grade 30 cast-iron pressure vessel using N bolts. A confined gasket seal has an effective sealing diameter D . The cylinder stores gas at a maximum pressure p_g . For the specifications given in the table for the specific

¹¹Russell, Burdsall & Ward, Inc., Metal Forming Specialists, Mentor, Ohio.

problem assigned, select a suitable bolt length from the preferred sizes in Table A-17, then determine the yielding factor of safety n_p , the load factor n_L , and the joint separation factor n_0 .

Problems 8-33 to 8-36



Problem Number	8-33	8-34	8-35	8-36
A	20 mm	$\frac{1}{2}$ in	20 mm	$\frac{3}{8}$ in
B	20 mm	$\frac{5}{8}$ in	25 mm	$\frac{1}{2}$ in
C	100 mm	3.5 in	0.8 m	3.25 in
D	150 mm	4.25 in	0.9 m	3.5 in
E	200 mm	6 in	1.0 m	5.5 in
F	300 mm	8 in	1.1 m	7 in
N	10	10	36	8
p_g	6 MPa	1500 psi	550 kPa	1200 psi
Bolt grade	ISO 9.8	SAE 5	ISO 10.9	SAE 8
Bolt spec.	M12 × 1.75	$\frac{1}{2}$ in-13	M10 × 1.5	$\frac{7}{16}$ in-14

**8-37 to
8-40**

Repeat the requirements for the problem specified in the table if the bolts and nuts are replaced with cap screws that are threaded into tapped holes in the cast-iron cylinder.

Problem Number	Originating Problem Number
8-37	8-33
8-38	8-34
8-39	8-35
8-40	8-36

**8-41 to
8-44**

For the pressure vessel defined in the problem specified in the table, redesign the bolt specifications to satisfy all of the following requirements.

- Use coarse-thread bolts selecting a class from Table 8-11 for Probs. 8-41 and 8-43, or a grade from Table 8-9 for Probs. 8-42 and 8-44.
- To ensure adequate gasket sealing around the bolt circle, use enough bolts to provide a maximum center-to-center distance between bolts of four bolt diameters.

- Obtain a joint stiffness constant C between 0.2 and 0.3 to ensure most of the pressure load is carried by the members.
- The bolts may be reused, so the yielding factor of safety should be at least 1.1.
- The overload factor and the joint separation factor should allow for the pressure to exceed the expected pressure by 15 percent.

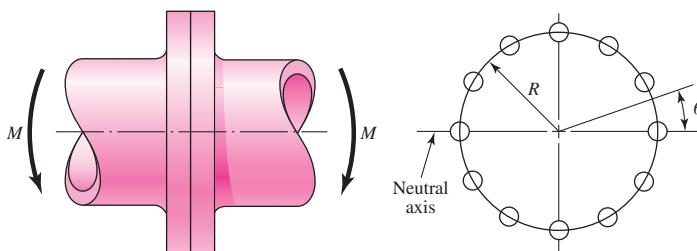
Problem Number	Originating Problem Number
8-41	8-33
8-42	8-34
8-43	8-35
8-44	8-36

8-45

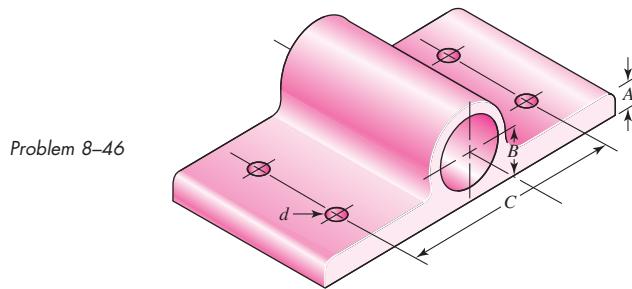
Bolts distributed about a bolt circle are often called upon to resist an external bending moment as shown in the figure. The external moment is 12 kip · in and the bolt circle has a diameter of 8 in. The neutral axis for bending is a diameter of the bolt circle. What needs to be determined is the most severe external load seen by a bolt in the assembly.

- (a) View the effect of the bolts as placing a line load around the bolt circle whose intensity F'_b , in pounds per inch, varies linearly with the distance from the neutral axis according to the relation $F'_b = F'_{b,\max} R \sin \theta$. The load on any particular bolt can be viewed as the effect of the line load over the arc associated with the bolt. For example, there are 12 bolts shown in the figure. Thus each bolt load is assumed to be distributed on a 30° arc of the bolt circle. Under these conditions, what is the largest bolt load?
- (b) View the largest load as the intensity $F'_{b,\max}$ multiplied by the arc length associated with each bolt and find the largest bolt load.
- (c) Express the load on any bolt as $F = F_{\max} \sin \theta$, sum the moments due to all the bolts, and estimate the largest bolt load. Compare the results of these three approaches to decide how to attack such problems in the future.

Problem 8-45
Bolted connection subjected to bending.

**8-46**

The figure shows a cast-iron bearing block that is to be bolted to a steel ceiling joist and is to support a gravity load of 18 kN. Bolts used are M24 ISO 8.8 with coarse threads and with 4.6-mm-thick steel washers under the bolt head and nut. The joist flanges are 20 mm in thickness, and the dimension A , shown in the figure, is 20 mm. The modulus of elasticity of the bearing block is 135 GPa.



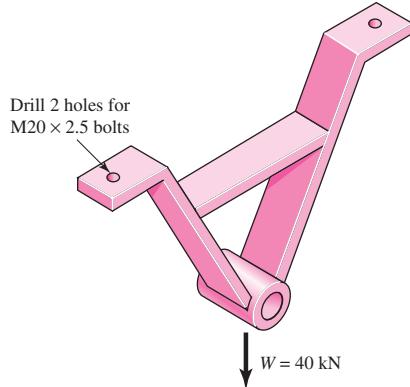
- (a) Find the wrench torque required if the fasteners are lubricated during assembly and the joint is to be permanent.
 (b) Determine the factors of safety guarding against yielding, overload, and joint separation.

8-47

The upside-down steel A frame shown in the figure is to be bolted to steel beams on the ceiling of a machine room using ISO grade 8.8 bolts. This frame is to support the 40-kN radial load as illustrated. The total bolt grip is 48 mm, which includes the thickness of the steel beam, the A-frame feet, and the steel washers used. The bolts are size M20 × 2.5.

- (a) What tightening torque should be used if the connection is permanent and the fasteners are lubricated?
 (b) Determine the factors of safety guarding against yielding, overload, and joint separation.

Problem 8-47

**8-48**

For the bolted assembly in Prob. 8-29, assume the external load is a repeated load. Determine the fatigue factor of safety for the bolts using the following failure criteria:

- Goodman.
- Gerber.
- ASME-elliptic.

8-49

For a bolted assembly with eight bolts, the stiffness of each bolt is $k_b = 1.0 \text{ MN/mm}$ and the stiffness of the members is $k_m = 2.6 \text{ MN/mm}$ per bolt. The bolts are preloaded to 75 percent of proof strength. Assume the external load is equally distributed to all the bolts. The bolts are M6 × 1 class 5.8 with rolled threads. A fluctuating external load is applied to the entire joint with $P_{\max} = 60 \text{ kN}$ and $P_{\min} = 20 \text{ kN}$.

- Determine the yielding factor of safety.
- Determine the overload factor of safety.

- (c) Determine the factor of safety based on joint separation.
- (d) Determine the fatigue factor of safety using the Goodman criterion.

8-50

For the bolted assembly in Prob. 8-32, assume 10 bolts are used. Determine the fatigue factor of safety using the Goodman criterion.

8-51 to**8-54**

For the pressure cylinder defined in the problem specified in the table, the gas pressure is cycled between zero and p_g . Determine the fatigue factor of safety for the bolts using the following failure criteria:

- (a) Goodman.
- (b) Gerber.
- (c) ASME-elliptic.

Problem Number	Originating Problem Number
8-51	8-33
8-52	8-34
8-53	8-35
8-54	8-36

8-55 to**8-58**

For the pressure cylinder defined in the problem specified in the table, the gas pressure is cycled between p_g and $p_g/2$. Determine the fatigue factor of safety for the bolts using the Goodman criterion.

Problem Number	Originating Problem Number
8-55	8-33
8-56	8-34
8-57	8-35
8-58	8-36

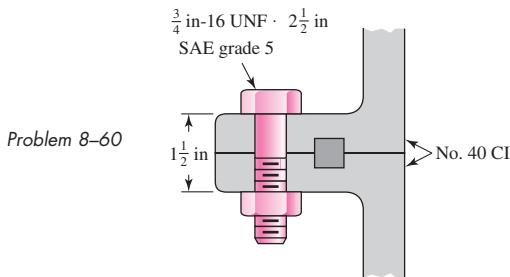
8-59

A 1-in-diameter hot-rolled AISI 1144 steel rod is hot-formed into an eyebolt similar to that shown in the figure for Prob. 3-122, with an inner 3-in-diameter eye. The threads are 1 in-12 UNF and are die-cut.

- (a) For a repeatedly applied load collinear with the thread axis, using the Gerber criterion, is fatigue failure more likely in the thread or in the eye?
- (b) What can be done to strengthen the bolt at the weaker location?
- (c) If the factor of safety guarding against a fatigue failure is $n_f = 2$, what repeatedly applied load can be applied to the eye?

8-60

The section of the sealed joint shown in the figure is loaded by a force cycling between 4 and 6 kips. The members have $E = 16$ Mpsi. All bolts have been carefully preloaded to $F_i = 25$ kip each.

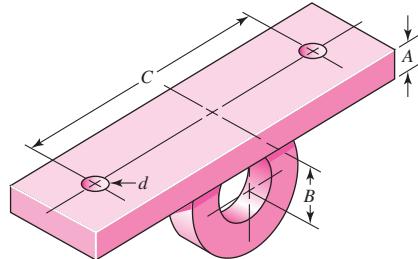


- Determine the yielding factor of safety.
- Determine the overload factor of safety.
- Determine the factor of safety based on joint separation.
- Determine the fatigue factor of safety using the Goodman criterion.

8-61

Suppose the welded steel bracket shown in the figure is bolted underneath a structural-steel ceiling beam to support a fluctuating vertical load imposed on it by a pin and yoke. The bolts are $\frac{1}{2}$ -in coarse-thread SAE grade 8, tightened to recommended preload for nonpermanent assembly. The stiffnesses have already been computed and are $k_b = 4$ Mlb/in and $k_m = 16$ Mlb/in.

Problem 8-61



- Assuming that the bolts, rather than the welds, govern the strength of this design, determine the safe repeated load that can be imposed on this assembly using the Goodman criterion with the load line in Fig. 8-20 and a fatigue design factor of 2.
- Compute the static load factors based on the load found in part (a).

8-62

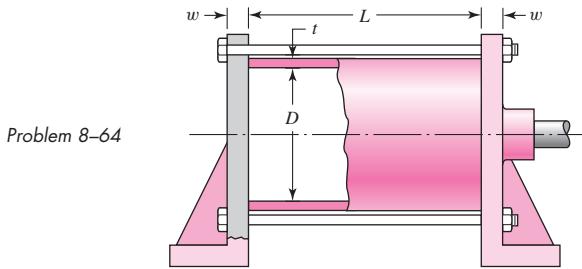
Using the Gerber fatigue criterion and a fatigue-design factor of 2, determine the external repeated load P that a $1\frac{1}{4}$ -in SAE grade 5 coarse-thread bolt can take compared with that for a fine-thread bolt. The joint constants are $C = 0.30$ for coarse- and 0.32 for fine-thread bolts.

8-63

An M30 \times 3.5 ISO 8.8 bolt is used in a joint at recommended preload, and the joint is subject to a repeated tensile fatigue load of $P = 65$ kN per bolt. The joint constant is $C = 0.28$. Find the static load factors and the factor of safety guarding against a fatigue failure based on the Gerber fatigue criterion.

8-64

The figure shows a fluid-pressure linear actuator (hydraulic cylinder) in which $D = 4$ in, $t = \frac{3}{8}$ in, $L = 12$ in, and $w = \frac{3}{4}$ in. Both brackets as well as the cylinder are of steel. The actuator has been designed for a working pressure of 2000 psi. Six $\frac{3}{8}$ -in SAE grade 5 coarse-thread bolts are used, tightened to 75 percent of proof load.



Problem 8-64

- Find the stiffnesses of the bolts and members, assuming that the entire cylinder is compressed uniformly and that the end brackets are perfectly rigid.
- Using the Gerber fatigue criterion, find the factor of safety guarding against a fatigue failure.
- What pressure would be required to cause total joint separation?

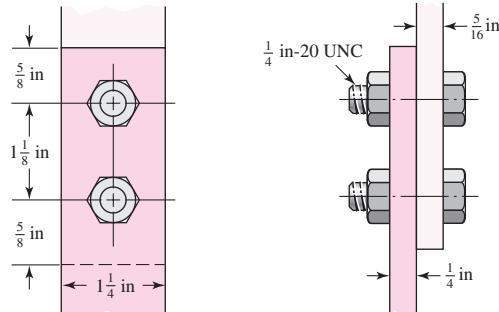
8-65

Using the Goodman fatigue criterion, repeat Prob. 8-64 with the working pressure cycling between 1200 psi and 2000 psi.

8-66

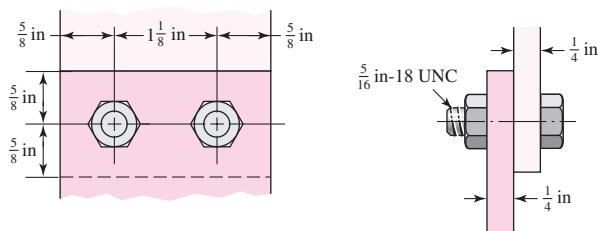
The figure shows a bolted lap joint that uses SAE grade 5 bolts. The members are made of cold-drawn AISI 1020 steel. Find the safe tensile shear load F that can be applied to this connection to provide a minimum factor of safety of 2 for the following failure modes: shear of bolts, bearing on bolts, bearing on members, and tension of members.

Problem 8-66

**8-67**

The bolted connection shown in the figure uses SAE grade 8 bolts. The members are hot-rolled AISI 1040 steel. A tensile shear load $F = 5000$ lbf is applied to the connection. Find the factor of safety for all possible modes of failure.

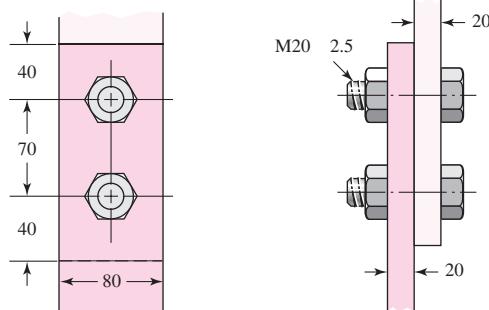
Problem 8-67

**8-68**

A bolted lap joint using ISO class 5.8 bolts and members made of cold-drawn SAE 1040 steel is shown in the figure. Find the tensile shear load F that can be applied to this connection to provide a minimum factor of safety of 2.5 for the following failure modes: shear of bolts, bearing on bolts, bearing on members, and tension of members.

Problem 8-68

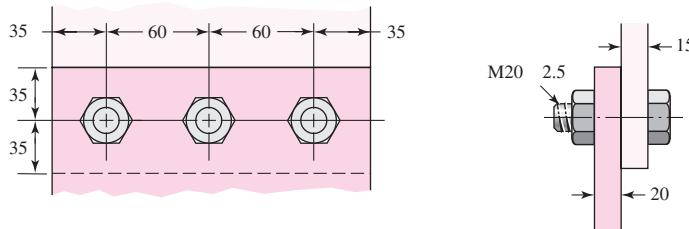
Dimensions in millimeters.

**8-69**

The bolted connection shown in the figure is subjected to a tensile shear load of 90 kN. The bolts are ISO class 5.8 and the material is cold-drawn AISI 1015 steel. Find the factor of safety of the connection for all possible modes of failure.

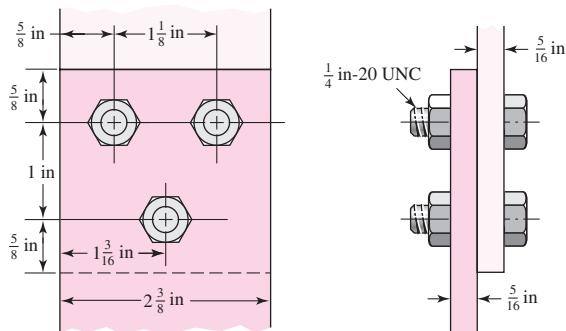
Problem 8-69

Dimensions in millimeters.

**8-70**

The figure shows a connection that employs three SAE grade 4 bolts. The tensile shear load on the joint is 5000 lbf. The members are cold-drawn bars of AISI 1020 steel. Find the factor of safety for each possible mode of failure.

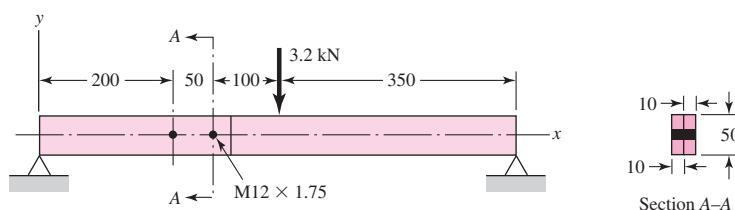
Problem 8-70

**8-71**

A beam is made up by bolting together two cold-drawn bars of AISI 1018 steel as a lap joint, as shown in the figure. The bolts used are ISO 5.8. Ignoring any twisting, determine the factor of safety of the connection.

Problem 8-71

Dimensions in millimeters.



8-72

Standard design practice, as exhibited by the solutions to Probs. 8-66 to 8-70, is to assume that the bolts, or rivets, share the shear equally. For many situations, such an assumption may lead to an unsafe design. Consider the yoke bracket of Prob. 8-61, for example. Suppose this bracket is bolted to a wide-flange *column* with the centerline through the two bolts in the vertical direction. A vertical load through the yoke-pin hole at distance B from the column flange would place a shear load on the bolts as well as a tensile load. The tensile load comes about because the bracket tends to pry itself about the bottom corner, much like a claw hammer, exerting a large tensile load on the upper bolt. In addition, it is almost certain that both the spacing of the bolt holes and their diameters will be slightly different on the column flange from what they are on the yoke bracket. Thus, unless yielding occurs, only one of the bolts will take the shear load. The designer has no way of knowing which bolt this will be.

In this problem the bracket is 8 in long, $A = \frac{1}{2}$ in, $B = 3$ in, $C = 6$ in, and the column flange is $\frac{1}{2}$ in thick. The bolts are $\frac{1}{2}$ -in UNC SAE grade 4. The nuts are tightened to 75 percent of proof load. The vertical yoke-pin load is 2500 lbf. If the upper bolt takes all the shear load as well as the tensile load, how closely does the bolt stress approach the proof strength?

8-73

The bearing of Prob. 8-46 is bolted to a vertical surface and supports a horizontal shaft. The bolts used have coarse threads and are M20 ISO 5.8. The joint constant is $C = 0.25$, and the dimensions are $A = 20$ mm, $B = 50$ mm, and $C = 160$ mm. The bearing base is 240 mm long. The bearing load is 14 kN. If the bolts are tightened to 75 percent of proof load, will the bolt stress exceed the proof strength? Use worst-case loading, as discussed in Prob. 8-72.

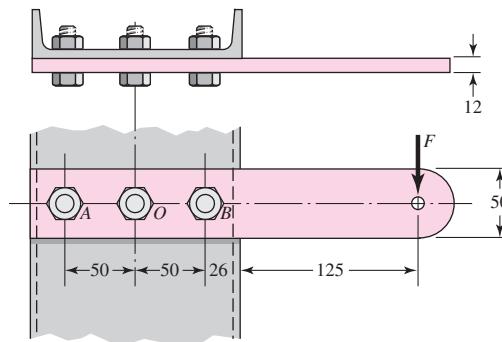
8-74

A split-ring clamp-type shaft collar such as is described in Prob. 5-67 must resist an axial load of 1000 lbf. Using a design factor of $n = 3$ and a coefficient of friction of 0.12, specify an SAE Grade 5 cap screw using fine threads. What wrench torque should be used if a lubricated screw is used?

8-75

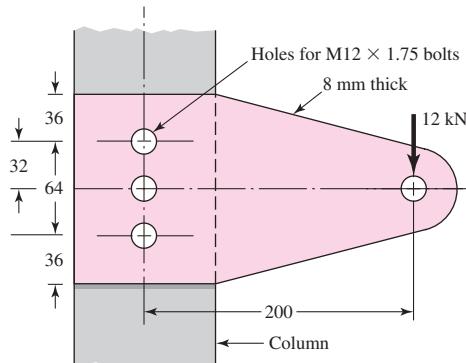
A vertical channel 152×76 (see Table A-7) has a cantilever beam bolted to it as shown. The channel is hot-rolled AISI 1006 steel. The bar is of hot-rolled AISI 1015 steel. The shoulder bolts are M10 \times 1.5 ISO 5.8. For a design factor of 2.0, find the safe force F that can be applied to the cantilever.

Problem 8-75
Dimensions in millimeters.

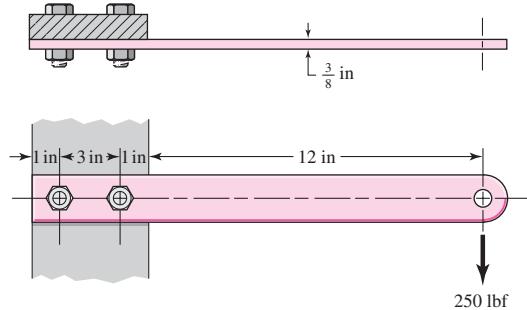
**8-76**

The cantilever bracket is bolted to a column with three M12 \times 1.75 ISO 5.8 bolts. The bracket is made from AISI 1020 hot-rolled steel. Find the factors of safety for the following failure modes: shear of bolts, bearing of bolts, bearing of bracket, and bending of bracket.

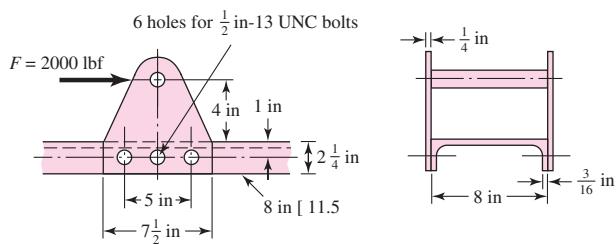
Problem 8-76
Dimensions in millimeters.

**8-77**

A $\frac{3}{8}$ -in \times 2-in AISI 1018 cold-drawn steel bar is cantilevered to support a static load of 250 lbf as illustrated. The bar is secured to the support using two $\frac{3}{8}$ in-16 UNC SAE grade 4 bolts. Find the factor of safety for the following modes of failure: shear of bolt, bearing on bolt, bearing on member, and strength of member.

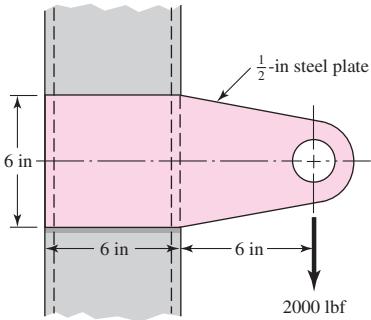
Problem 8-77**8-78**

The figure shows a welded fitting which has been tentatively designed to be bolted to a channel so as to transfer the 2000-lbf load into the channel. The channel and the two fitting plates are of hot-rolled stock having a minimum S_y of 42 kpsi. The fitting is to be bolted using six SAE grade 4 shoulder bolts. Check the strength of the design by computing the factor of safety for all possible modes of failure.

Problem 8-78**8-79**

A cantilever is to be attached to the flat side of a 6-in, 13.0-lbf/in channel used as a column. The cantilever is to carry a load as shown in the figure. To a designer the choice of a bolt array is usually an a priori decision. Such decisions are made from a background of knowledge of the effectiveness of various patterns.

Problem 8-79



- (a) If two fasteners are used, should the array be arranged vertically, horizontally, or diagonally? How would you decide?
- (b) If three fasteners are used, should a linear or triangular array be used? For a triangular array, what should be the orientation of the triangle? How would you decide?

8-80 Using your experience with Prob. 8-79, specify an optimal bolt pattern for two bolts for the bracket in Prob. 8-79 and size the bolts.

8-81 Using your experience with Prob. 8-79, specify an optimal bolt pattern for three bolts for the bracket in Prob. 8-79 and size the bolts.

This page intentionally left blank

9

Welding, Bonding, and the Design of Permanent Joints

Chapter Outline

- 9-1** Welding Symbols **476**
- 9-2** Butt and Fillet Welds **478**
- 9-3** Stresses in Welded Joints in Torsion **482**
- 9-4** Stresses in Welded Joints in Bending **487**
- 9-5** The Strength of Welded Joints **489**
- 9-6** Static Loading **492**
- 9-7** Fatigue Loading **496**
- 9-8** Resistance Welding **498**
- 9-9** Adhesive Bonding **498**

Form can more readily pursue function with the help of joining processes such as welding, brazing, soldering, cementing, and gluing—processes that are used extensively in manufacturing today. Whenever parts have to be assembled or fabricated, there is usually good cause for considering one of these processes in preliminary design work. Particularly when sections to be joined are thin, one of these methods may lead to significant savings. The elimination of individual fasteners, with their holes and assembly costs, is an important factor. Also, some of the methods allow rapid machine assembly, furthering their attractiveness.

Riveted permanent joints were common as the means of fastening rolled steel shapes to one another to form a permanent joint. The childhood fascination of seeing a cherry-red hot rivet thrown with tongs across a building skeleton to be unerringly caught by a person with a conical bucket, to be hammered pneumatically into its final shape, is all but gone. Two developments relegated riveting to lesser prominence. The first was the development of high-strength steel bolts whose preload could be controlled. The second was the improvement of welding, competing both in cost and in latitude of possible form.

9-1

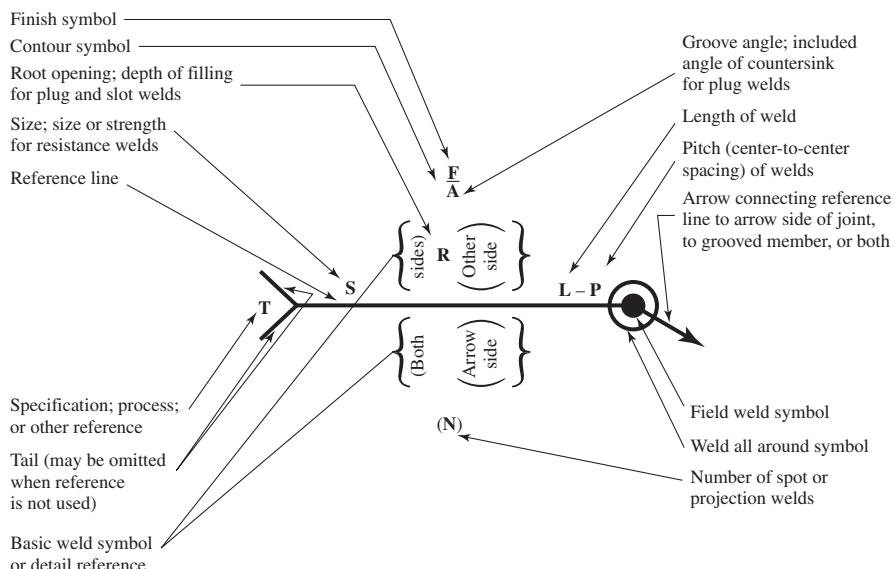
Welding Symbols

A weldment is fabricated by welding together a collection of metal shapes, cut to particular configurations. During welding, the several parts are held securely together, often by clamping or jigging. The welds must be precisely specified on working drawings, and this is done by using the welding symbol, shown in Fig. 9-1, as standardized by the American Welding Society (AWS). The arrow of this symbol points to the joint to be welded. The body of the symbol contains as many of the following elements as are deemed necessary:

- Reference line
- Arrow

Figure 9-1

The AWS standard welding symbol showing the location of the symbol elements.



- Basic weld symbols as in Fig. 9–2
- Dimensions and other data
- Supplementary symbols
- Finish symbols
- Tail
- Specification or process

The *arrow side* of a joint is the line, side, area, or near member to which the arrow points. The side opposite the arrow side is the *other side*.

Figures 9–3 to 9–6 illustrate the types of welds used most frequently by designers. For general machine elements most welds are fillet welds, though butt welds are used a great deal in designing pressure vessels. Of course, the parts to be joined must be arranged so that there is sufficient clearance for the welding operation. If unusual joints are required because of insufficient clearance or because of the section shape, the design may be a poor one and the designer should begin again and endeavor to synthesize another solution.

Since heat is used in the welding operation, there are metallurgical changes in the parent metal in the vicinity of the weld. Also, residual stresses may be introduced because of clamping or holding or, sometimes, because of the order of welding. Usually these

Figure 9–2

Arc- and gas-weld symbols.

		Type of weld							
Bead	Fillet	Plug or slot	Groove					J	
			Square	V	Bevel	U	J		
				▽	▽	U	J		

Figure 9–3

Fillet welds. (a) The number indicates the leg size; the arrow should point only to one weld when both sides are the same. (b) The symbol indicates that the welds are intermittent and staggered 60 mm along on 200-mm centers.

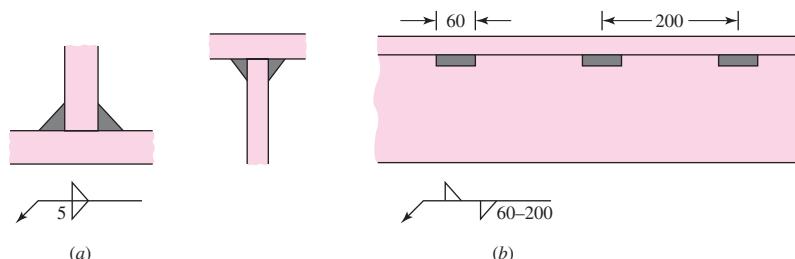


Figure 9–4

The circle on the weld symbol indicates that the welding is to go all around.

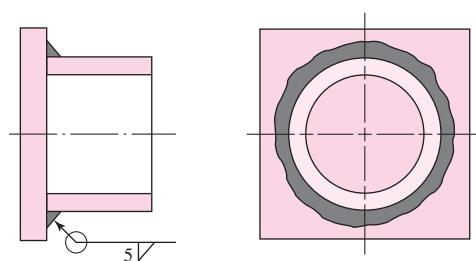
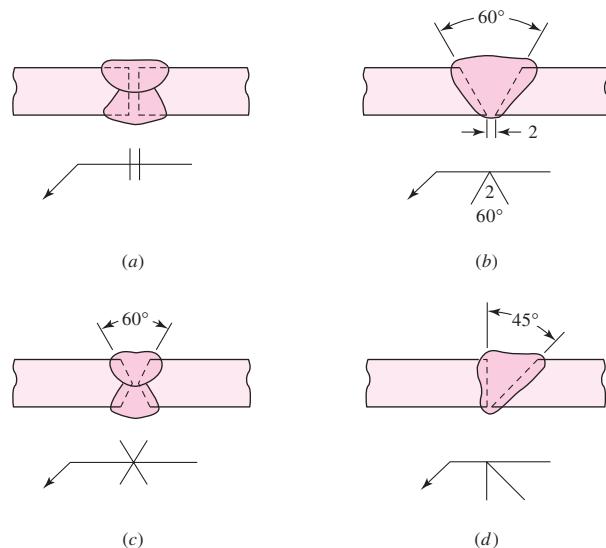


Figure 9–5

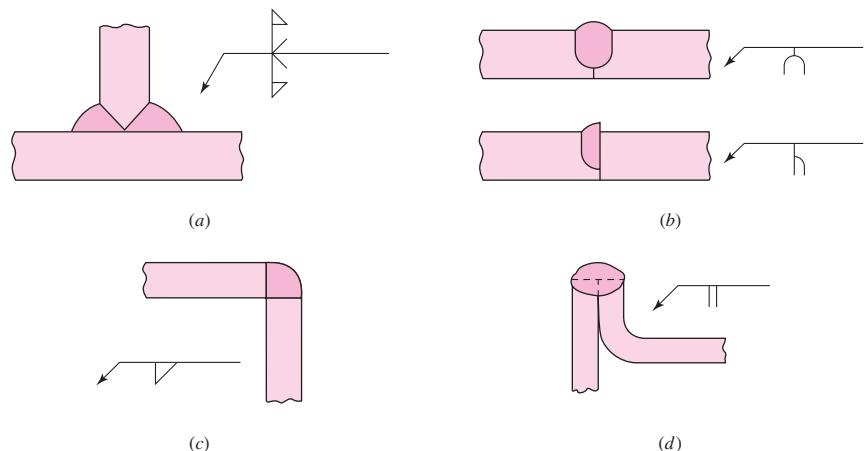
Butt or groove welds:

- (a) square butt-welded on both sides; (b) single V with 60° bevel and root opening of 2 mm; (c) double V; (d) single bevel.

**Figure 9–6**

Special groove welds:

- (a) T joint for thick plates;
 (b) U and J welds for thick plates; (c) corner weld (may also have a bead weld on inside for greater strength but should not be used for heavy loads);
 (d) edge weld for sheet metal and light loads.



residual stresses are not severe enough to cause concern; in some cases a light heat treatment after welding has been found helpful in relieving them. When the parts to be welded are thick, a preheating will also be of benefit. If the reliability of the component is to be quite high, a testing program should be established to learn what changes or additions to the operations are necessary to ensure the best quality.

9–2

Butt and Fillet Welds

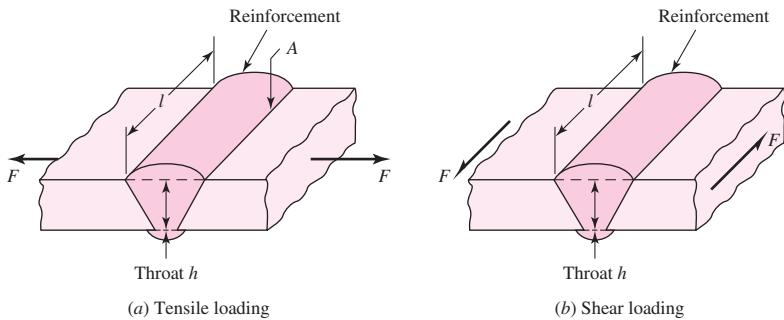
Figure 9–7a shows a single V-groove weld loaded by the tensile force F . For either tension or compression loading, the average normal stress is

$$\sigma = \frac{F}{hl} \quad (9-1)$$

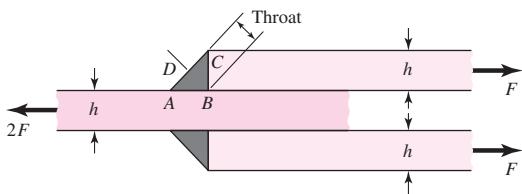
where h is the weld throat and l is the length of the weld, as shown in the figure. Note that the value of h does not include the reinforcement. The reinforcement can be desirable, but it varies somewhat and does produce stress concentration at point A in the figure. If fatigue loads exist, it is good practice to grind or machine off the reinforcement.

Figure 9-7

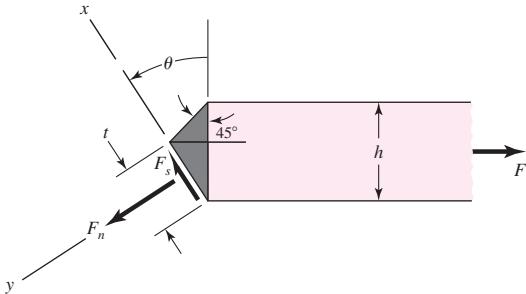
A typical butt joint.

**Figure 9-8**

A transverse fillet weld.

**Figure 9-9**

Free body from Fig. 9-8.



The average stress in a butt weld due to shear loading (Fig. 9-7b) is

$$\tau = \frac{F}{hl} \quad (9-2)$$

Figure 9-8 illustrates a typical transverse fillet weld. In Fig. 9-9 a portion of the welded joint has been isolated from Fig. 9-8 as a free body. At angle θ the forces on each weldment consist of a normal force F_n and a shear force F_s . Summing forces in the x and y directions gives

$$F_s = F \sin \theta \quad (a)$$

$$F_n = F \cos \theta \quad (b)$$

Using the law of sines for the triangle in Fig. 9-9 yields

$$\frac{t}{\sin 45^\circ} = \frac{h}{\sin(180^\circ - 45^\circ - \theta)} = \frac{h}{\sin(135^\circ - \theta)} = \frac{\sqrt{2}h}{\cos \theta + \sin \theta}$$

Solving for the throat thickness t gives

$$t = \frac{h}{\cos \theta + \sin \theta} \quad (c)$$

The nominal stresses at the angle θ in the weldment, τ and σ , are

$$\tau = \frac{F_s}{A} = \frac{F \sin \theta (\cos \theta + \sin \theta)}{hl} = \frac{F}{hl} (\sin \theta \cos \theta + \sin^2 \theta) \quad (d)$$

$$\sigma = \frac{F_n}{A} = \frac{F \cos \theta (\cos \theta + \sin \theta)}{hl} = \frac{F}{hl} (\cos^2 \theta + \sin \theta \cos \theta) \quad (e)$$

The von Mises stress σ' at angle θ is

$$\sigma' = (\sigma^2 + 3\tau^2)^{1/2} = \frac{F}{hl} [(\cos^2 \theta + \sin \theta \cos \theta)^2 + 3(\sin^2 \theta + \sin \theta \cos \theta)^2]^{1/2} \quad (f)$$

The largest von Mises stress occurs at $\theta = 62.5^\circ$ with a value of $\sigma' = 2.16F/(hl)$. The corresponding values of τ and σ are $\tau = 1.196F/(hl)$ and $\sigma = 0.623F/(hl)$.

The maximum shear stress can be found by differentiating Eq. (d) with respect to θ and equating to zero. The stationary point occurs at $\theta = 67.5^\circ$ with a corresponding $\tau_{\max} = 1.207F/(hl)$ and $\sigma = 0.5F/(hl)$.

There are some experimental and analytical results that are helpful in evaluating Eqs. (d) through (f) and consequences. A model of the transverse fillet weld of Fig. 9–8 is easily constructed for photoelastic purposes and has the advantage of a balanced loading condition. Norris constructed such a model and reported the stress distribution along the sides AB and BC of the weld.¹ An approximate graph of the results he obtained is shown as Fig. 9–10a. Note that stress concentration exists at A and B on the horizontal leg and at B on the vertical leg. Norris states that he could not determine the stresses at A and B with any certainty.

Salakian² presents data for the stress distribution across the throat of a fillet weld (Fig. 9–10b). This graph is of particular interest because we have just learned that it is the throat stresses that are used in design. Again, the figure shows stress concentration at point B . Note that Fig. 9–10a applies either to the weld metal or to the parent metal, and that Fig. 9–10b applies only to the weld metal.

Equations (a) through (f) and their consequences seem familiar, and we can become comfortable with them. The net result of photoelastic and finite element analysis of transverse fillet weld geometry is more like that shown in Fig. 9–10 than those given by mechanics of materials or elasticity methods. The most important concept here is that we have *no analytical approach that predicts the existing stresses*. The geometry of the fillet is crude by machinery standards, and even if it were ideal, the macrogeometry is too abrupt and complex for our methods. There are also subtle bending stresses due to eccentricities. Still, in the absence of robust analysis, weldments must be specified and the resulting joints must be safe. The approach has been to use a simple *and conservative* model, verified by testing as conservative. The approach has been to

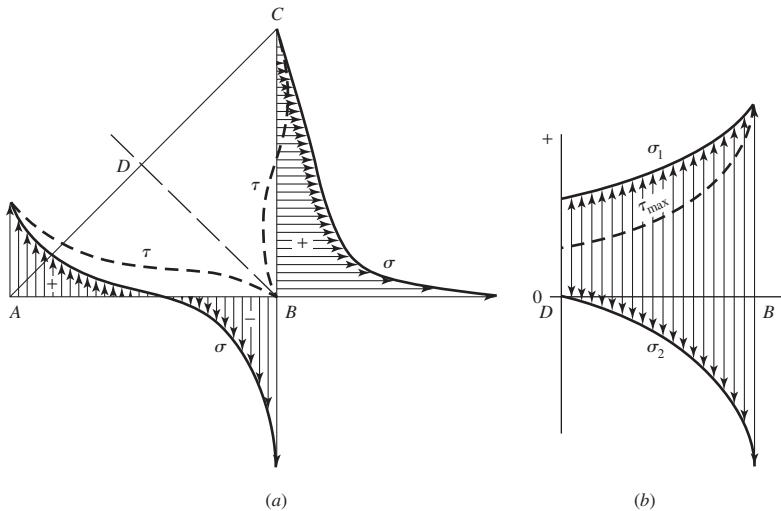
- Consider the external loading to be carried by shear forces on the throat area of the weld. By ignoring the normal stress on the throat, the shearing stresses are inflated sufficiently to render the model conservative.

¹C. H. Norris, "Photoelastic Investigation of Stress Distribution in Transverse Fillet Welds," *Welding J.*, vol. 24, 1945, p. 557s.

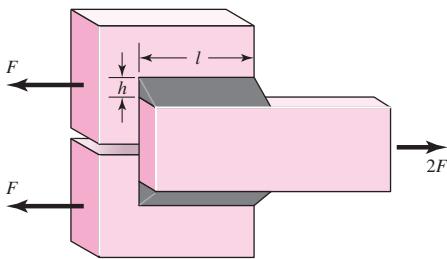
²A. G. Salakian and G. E. Claussen, "Stress Distribution in Fillet Welds: A Review of the Literature," *Welding J.*, vol. 16, May 1937, pp. 1–24.

Figure 9-10

Stress distribution in fillet welds: (a) stress distribution on the legs as reported by Norris; (b) distribution of principal stresses and maximum shear stress as reported by Salakian.

**Figure 9-11**

Parallel fillet welds.



- Use distortion energy for significant stresses.
- Circumscribe typical cases by code.

For this model, the basis for weld analysis or design employs

$$\tau = \frac{F}{0.707hl} = \frac{1.414F}{hl} \quad (9-3)$$

which assumes the entire force F is accounted for by a shear stress in the minimum throat area. Note that this inflates the maximum estimated shear stress by a factor of $1.414/1.207 = 1.17$. Further, consider the parallel fillet welds shown in Fig. 9-11 where, as in Fig. 9-8, each weld transmits a force F . However, in the case of Fig. 9-11, the maximum shear stress is at the minimum throat area and corresponds to Eq. (9-3).

Under circumstances of combined loading we

- Examine primary shear stresses due to external forces.
- Examine secondary shear stresses due to torsional and bending moments.
- Estimate the strength(s) of the parent metal(s).
- Estimate the strength of deposited weld metal.
- Estimate permissible load(s) for parent metal(s).
- Estimate permissible load for deposited weld metal.

9-3 Stresses in Welded Joints in Torsion

Figure 9–12 illustrates a cantilever of length l welded to a column by two fillet welds. The reaction at the support of a cantilever always consists of a shear force V and a moment M . The shear force produces a *primary shear* in the welds of magnitude

$$\tau' = \frac{V}{A} \quad (9-4)$$

where A is the throat area of all the welds.

The moment at the support produces *secondary shear* or *torsion* of the welds, and this stress is given by the equation

$$\tau'' = \frac{Mr}{J} \quad (9-5)$$

where r is the distance from the centroid of the weld group to the point in the weld of interest and J is the second polar moment of area of the weld group about the centroid of the group. When the sizes of the welds are known, these equations can be solved and the results combined to obtain the maximum shear stress. Note that r is usually the farthest distance from the centroid of the weld group.

Figure 9–13 shows two welds in a group. The rectangles represent the throat areas of the welds. Weld 1 has a throat thickness $t_1 = 0.707h_1$, and weld 2 has a throat thickness $t_2 = 0.707h_2$. Note that h_1 and h_2 are the respective weld sizes. The throat area of both welds together is

$$A = A_1 + A_2 = t_1 d + t_2 d \quad (a)$$

This is the area that is to be used in Eq. (9–4).

The x axis in Fig. 9–13 passes through the centroid G_1 of weld 1. The second moment of area about this axis is

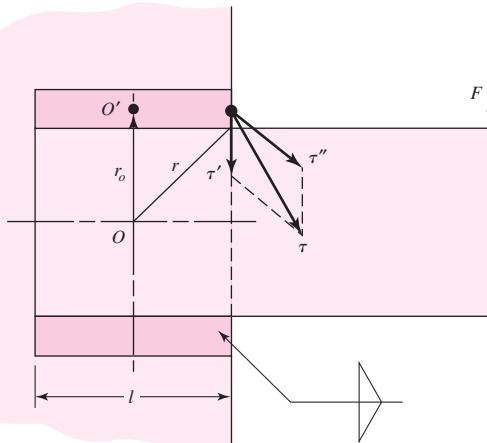
$$I_x = \frac{t_1 d^3}{12}$$

Similarly, the second moment of area about an axis through G_1 parallel to the y axis is

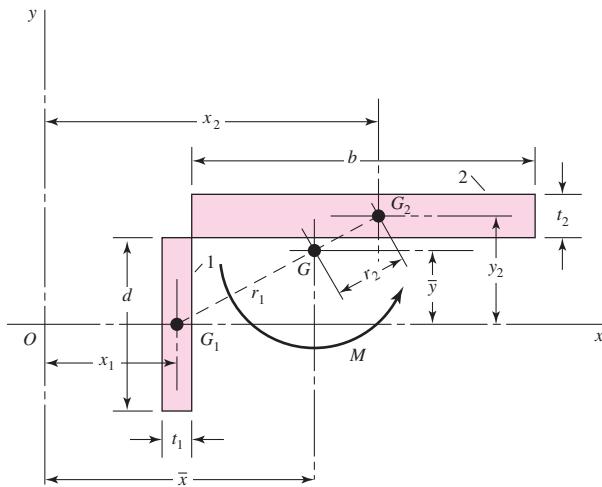
$$I_y = \frac{dt_1^3}{12}$$

Figure 9–12

This is a *moment connection*; such a connection produces *torsion* in the welds. The shear stresses shown are resultant stresses.



| Figure 9-13



Thus the second polar moment of area of weld 1 about its own centroid is

$$J_{G1} = I_x + I_y = \frac{t_1 d^3}{12} + \frac{dt_1^3}{12} \quad (b)$$

In a similar manner, the second polar moment of area of weld 2 about its centroid is

$$J_{G2} = \frac{bt_2^3}{12} + \frac{t_2 b^3}{12} \quad (c)$$

The centroid G of the weld group is located at

$$\bar{x} = \frac{A_1 x_1 + A_2 x_2}{A} \quad \bar{y} = \frac{A_1 y_1 + A_2 y_2}{A}$$

Using Fig. 9-13 again, we see that the distances r_1 and r_2 from G_1 and G_2 to G , respectively, are

$$r_1 = [(\bar{x} - x_1)^2 + \bar{y}^2]^{1/2} \quad r_2 = [(y_2 - \bar{y})^2 + (x_2 - \bar{x})^2]^{1/2}$$

Now, using the parallel-axis theorem, we find the second polar moment of area of the weld group to be

$$J = (J_{G1} + A_1 r_1^2) + (J_{G2} + A_2 r_2^2) \quad (d)$$

This is the quantity to be used in Eq. (9-5). The distance r must be measured from G and the moment M computed about G .

The reverse procedure is that in which the allowable shear stress is given and we wish to find the weld size. The usual procedure is to estimate a probable weld size and then to use iteration.

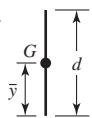
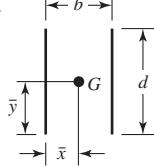
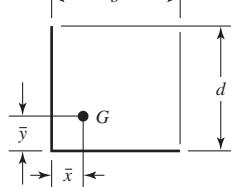
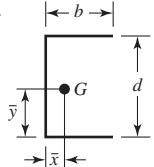
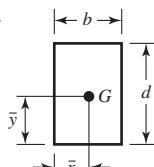
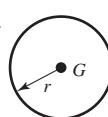
Observe in Eqs. (b) and (c) the quantities t_1^3 and t_2^3 , respectively, which are the cubes of the weld thicknesses. These quantities are small and can be neglected. This leaves the terms $t_1 d^3 / 12$ and $t_2 b^3 / 12$, which make J_{G1} and J_{G2} linear in the weld width. Setting the weld thicknesses t_1 and t_2 to unity leads to the idea of treating each fillet weld as a line. The resulting second moment of area is then a *unit second polar moment of area*. The advantage of treating the weld size as a line is that the value of J_u is the same regardless of the weld size. Since the throat width of a fillet weld is $0.707h$, the relationship between J and the unit value is

$$J = 0.707h J_u \quad (9-6)$$

in which J_u is found by conventional methods for an area having unit width. The transfer formula for J_u must be employed when the welds occur in groups, as in Fig. 9–12. Table 9–1 lists the throat areas and the unit second polar moments of area for the most common fillet welds encountered. The example that follows is typical of the calculations normally made.

Table 9–1

Torsional Properties of Fillet Welds*

Weld	Throat Area	Location of G	Unit Second Polar Moment of Area
1. 	$A = 0.707 hd$	$\bar{x} = 0$ $\bar{y} = d/2$	$J_u = d^3/12$
2. 	$A = 1.414 hd$	$\bar{x} = b/2$ $\bar{y} = d/2$	$J_u = \frac{d(3b^2 + d^2)}{6}$
3. 	$A = 0.707h(b + d)$	$\bar{x} = \frac{b^2}{2(b + d)}$ $\bar{y} = \frac{d^2}{2(b + d)}$	$J_u = \frac{(b + d)^4 - 6b^2d^2}{12(b + d)}$
4. 	$A = 0.707h(2b + d)$	$\bar{x} = \frac{b^2}{2b + d}$ $\bar{y} = d/2$	$J_u = \frac{8b^3 + 6bd^2 + d^3}{12} - \frac{b^4}{2b + d}$
5. 	$A = 1.414h(b + d)$	$\bar{x} = b/2$ $\bar{y} = d/2$	$J_u = \frac{(b + d)^3}{6}$
6. 	$A = 1.414 \pi hr$		$J_u = 2\pi r^3$

*G is centroid of weld group; h is weld size; plane of torque couple is in the plane of the paper; all welds are of unit width.

EXAMPLE 9-1

A 50-kN load is transferred from a welded fitting into a 200-mm steel channel as illustrated in Fig. 9-14. Estimate the maximum stress in the weld.

Solution³

(a) Label the ends and corners of each weld by letter. See Fig. 9-15. Sometimes it is desirable to label each weld of a set by number.

(b) Estimate the primary shear stress τ' . As shown in Fig. 9-14, each plate is welded to the channel by means of three 6-mm fillet welds. Figure 9-15 shows that we have divided the load in half and are considering only a single plate. From case 4 of Table 9-1 we find the throat area as

$$A = 0.707(6)[2(56) + 190] = 1280 \text{ mm}^2$$

Then the primary shear stress is

$$\tau' = \frac{V}{A} = \frac{25(10)^3}{1280} = 19.5 \text{ MPa}$$

(c) Draw the τ' stress, to scale, at each lettered corner or end. See Fig. 9-16.

(d) Locate the centroid of the weld pattern. Using case 4 of Table 9-1, we find

$$\bar{x} = \frac{(56)^2}{2(56) + 190} = 10.4 \text{ mm}$$

This is shown as point O on Figs. 9-15 and 9-16.

(e) Find the distances r_i (see Fig. 9-16):

$$r_A = r_B = [(190/2)^2 + (56 - 10.4)^2]^{1/2} = 105 \text{ mm}$$

$$r_C = r_D = [(190/2)^2 + (10.4)^2]^{1/2} = 95.6 \text{ mm}$$

These distances can also be scaled from the drawing.

Figure 9-14

Dimensions in millimeters.

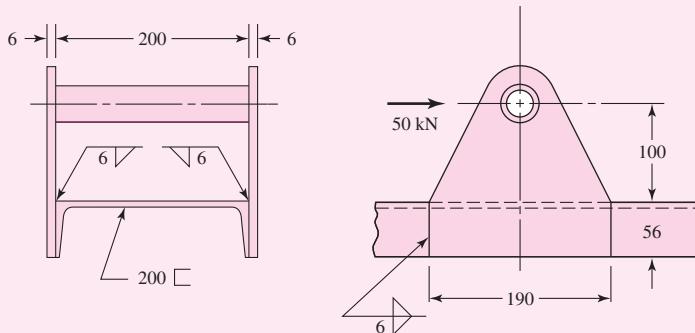
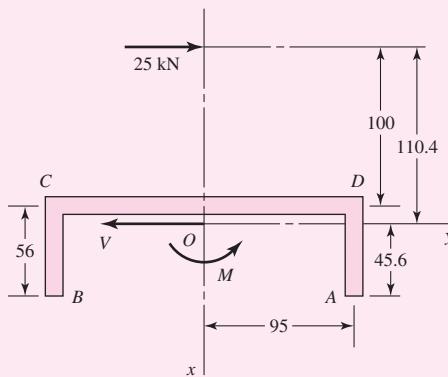
**Figure 9-15**

Diagram showing the weld geometry on a single plate; all dimensions in millimeters.

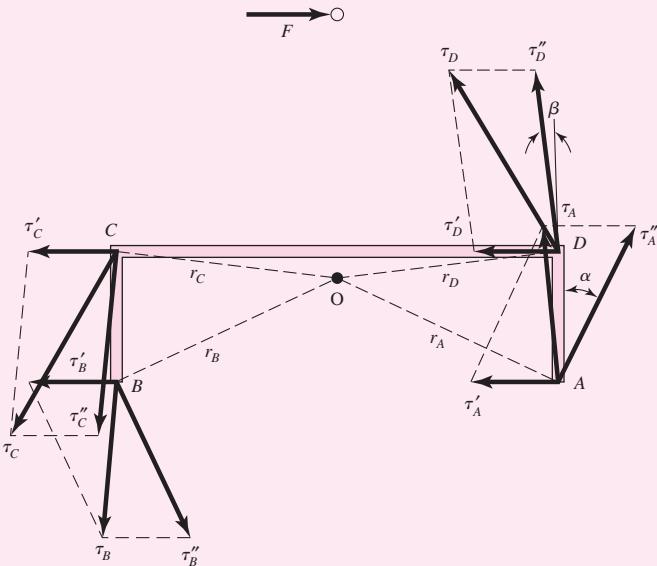
Note that V and M represent the reaction loads applied by the welds to the plate.



³We are indebted to Professor George Piotrowski of the University of Florida for the detailed steps, presented here, of his method of weld analysis R.G.B., J.K.N.

Figure 9–16

Free-body diagram of one of the side plates.



(f) Find J . Using case 4 of Table 9–1 again, with Eq. (9–6), we get

$$J = 0.707(6) \left[\frac{8(56)^3 + 6(56)(190)^2 + (190)^3}{12} - \frac{(56)^4}{2(56) + 190} \right] \\ = 7.07(10)^6 \text{ mm}^4$$

(g) Find M :

$$M = Fl = 25(100 + 10.4) = 2760 \text{ N} \cdot \text{m}$$

(h) Estimate the secondary shear stresses τ'' at each lettered end or corner:

$$\tau_A'' = \tau_B'' = \frac{Mr}{J} = \frac{2760(10)^3(105)}{7.07(10)^6} = 41.0 \text{ MPa}$$

$$\tau_C'' = \tau_D'' = \frac{2760(10)^3(95.6)}{7.07(10)^6} = 37.3 \text{ MPa}$$

(i) Draw the τ'' stress at each corner and end. See Fig. 9–16. Note that this is a free-body diagram of one of the side plates, and therefore the τ' and τ'' stresses represent what the channel is doing to the plate (through the welds) to hold the plate in equilibrium.

(j) At each point labeled, combine the two stress components as vectors (since they apply to the same area). At point A, the angle that τ_A'' makes with the vertical, α , is also the angle r_A makes with the horizontal, which is $\alpha = \tan^{-1}(45.6/95) = 25.64^\circ$. This angle also applies to point B. Thus

$$\tau_A = \tau_B = \sqrt{(19.5 - 41.0 \sin 25.64^\circ)^2 + (41.0 \cos 25.64^\circ)^2} = 37.0 \text{ MPa}$$

Similarly, for C and D, $\beta = \tan^{-1}(10.4/95) = 6.25^\circ$. Thus

$$\tau_C = \tau_D = \sqrt{(19.5 + 37.3 \sin 6.25^\circ)^2 + (37.3 \cos 6.25^\circ)^2} = 43.9 \text{ MPa}$$

(k) Identify the most highly stressed point:

Answer

$$\tau_{\max} = \tau_C = \tau_D = 43.9 \text{ MPa}$$

9-4 Stresses in Welded Joints in Bending

Figure 9-17a shows a cantilever welded to a support by fillet welds at top and bottom. A free-body diagram of the beam would show a shear-force reaction V and a moment reaction M . The shear force produces a primary shear in the welds of magnitude

$$\tau' = \frac{V}{A} \quad (a)$$

where A is the total throat area.

The moment M induces a horizontal shear stress component in the welds. Treating the two welds of Fig. 9-17b as lines we find the unit second moment of area to be

$$I_u = \frac{bd^2}{2} \quad (b)$$

The second moment of area I , based on weld throat area, is

$$I = 0.707hI_u = 0.707h \frac{bd^2}{2} \quad (c)$$

The nominal throat shear stress is now found to be

$$\tau'' = \frac{Mc}{I} = \frac{Md/2}{0.707hbd^2/2} = \frac{1.414M}{bdh} \quad (d)$$

The model gives the coefficient of 1.414, in contrast to the predictions of Sec. 9-2 of 1.197 from distortion energy, or 1.207 from maximum shear. The conservatism of the model's 1.414 is not that it is simply larger than either 1.196 or 1.207, but the tests carried out to validate the model show that it is large enough.

The second moment of area in Eq. (d) is based on the distance d between the two welds. If this moment is found by treating the two welds as having rectangular footprints, the distance between the weld throat centroids is approximately $(d + h)$. This would produce a slightly larger second moment of area, and result in a smaller level of stress. This method of treating welds as a line does not interfere with the conservatism of the model. It also makes Table 9-2 possible with all the conveniences that ensue.

The vertical (primary) shear of Eq. (a) and the horizontal (secondary) shear of Eq. (d) are then combined as vectors to give

$$\tau = (\tau'^2 + \tau''^2)^{1/2} \quad (e)$$

Figure 9-17

A rectangular cross-section cantilever welded to a support at the top and bottom edges.

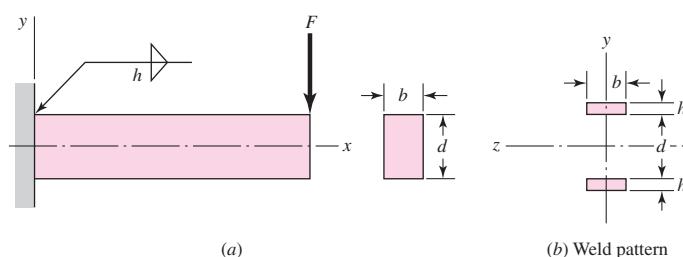


Table 9–2

Bending Properties of Fillet Welds*

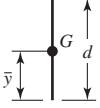
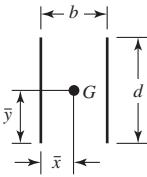
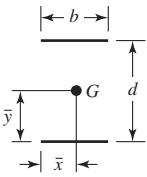
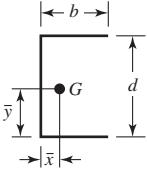
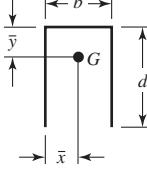
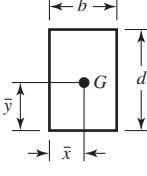
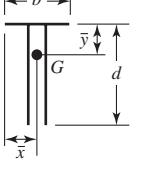
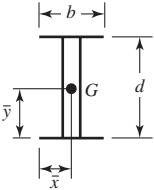
Weld	Throat Area	Location of G	Unit Second Moment of Area
1.		$A = 0.707hd$	$\bar{x} = 0$ $\bar{y} = d/2$ $I_u = \frac{d^3}{12}$
2.		$A = 1.414hd$	$\bar{x} = b/2$ $\bar{y} = d/2$ $I_u = \frac{d^3}{6}$
3.		$A = 1.414hb$	$\bar{x} = b/2$ $\bar{y} = d/2$ $I_u = \frac{bd^2}{2}$
4.		$A = 0.707h(2b + d)$	$\bar{x} = \frac{b^2}{2b + d}$ $\bar{y} = d/2$ $I_u = \frac{d^2}{12}(6b + d)$
5.		$A = 0.707h(b + 2d)$	$\bar{x} = b/2$ $\bar{y} = \frac{d^2}{b + 2d}$ $I_u = \frac{2d^3}{3} - 2d^2\bar{y} + (b + 2d)\bar{y}^2$
6.		$A = 1.414h(b + d)$	$\bar{x} = b/2$ $\bar{y} = d/2$ $I_u = \frac{d^2}{6}(3b + d)$
7.		$A = 0.707h(b + 2d)$	$\bar{x} = b/2$ $\bar{y} = \frac{d^2}{b + 2d}$ $I_u = \frac{2d^3}{3} - 2d^2\bar{y} + (b + 2d)\bar{y}^2$

Table 9-2

Continued

Weld	Throat Area	Location of G	Unit Second Moment of Area
8.	 $A = 1.414h(b + d)$	$\bar{x} = b/2$ $\bar{y} = d/2$	$I_u = \frac{d^2}{6}(3b + d)$
9.	 $A = 1.414\pi hr$		$I_u = \pi r^3$

* I_u , unit second moment of area, is taken about a horizontal axis through G , the centroid of the weld group, h is weld size; the plane of the bending couple is normal to the plane of the paper and parallel to the y -axis; all welds are of the same size.

9-5 The Strength of Welded Joints

The matching of the electrode properties with those of the parent metal is usually not so important as speed, operator appeal, and the appearance of the completed joint. The properties of electrodes vary considerably, but Table 9-3 lists the minimum properties for some electrode classes.

It is preferable, in designing welded components, to select a steel that will result in a fast, economical weld even though this may require a sacrifice of other qualities such as machinability. Under the proper conditions, all steels can be welded, but best results will be obtained if steels having a UNS specification between G10140 and G10230 are chosen. All these steels have a tensile strength in the hot-rolled condition in the range of 60 to 70 kpsi.

The designer can choose factors of safety or permissible working stresses with more confidence if he or she is aware of the values of those used by others. One of the best standards to use is the American Institute of Steel Construction (AISC) code for building construction.⁴ The permissible stresses are now based on the yield strength of the material instead of the ultimate strength, and the code permits the use of a variety of ASTM structural steels having yield strengths varying from 33 to 50 kpsi. Provided the loading is the same, the code permits the same stress in the weld metal as in the parent metal. For these ASTM steels, $S_y = 0.5S_u$. Table 9-4 lists the formulas specified by the code for calculating these permissible stresses for various loading conditions. The factors of safety implied by this code are easily calculated. For tension, $n = 1/0.60 = 1.67$. For shear, $n = 0.577/0.40 = 1.44$, using the distortion-energy theory as the criterion of failure.

It is important to observe that the electrode material is often the strongest material present. If a bar of AISI 1010 steel is welded to one of 1018 steel, the weld metal is actually a mixture of the electrode material and the 1010 and 1018 steels. Furthermore,

⁴For a copy, either write the AISC, 400 N. Michigan Ave., Chicago, IL 60611, or contact on the Internet at www.aisc.org.

Table 9–3

Minimum Weld-Metal Properties

AWS Electrode Number*	Tensile Strength kpsi (MPa)	Yield Strength, kpsi (MPa)	Percent Elongation
E60xx	62 (427)	50 (345)	17–25
E70xx	70 (482)	57 (393)	22
E80xx	80 (551)	67 (462)	19
E90xx	90 (620)	77 (531)	14–17
E100xx	100 (689)	87 (600)	13–16
E120xx	120 (827)	107 (737)	14

*The American Welding Society (AWS) specification code numbering system for electrodes. This system uses an E prefixed to a four- or five-digit numbering system in which the first two or three digits designate the approximate tensile strength. The last digit includes variables in the welding technique, such as current supply. The next-to-last digit indicates the welding position, as, for example, flat, or vertical, or overhead. The complete set of specifications may be obtained from the AWS upon request.

Table 9–4

Stresses Permitted by the AISC Code for Weld Metal

Type of Loading	Type of Weld	Permissible Stress	<i>n</i> *
Tension	Butt	0.60S _y	1.67
Bearing	Butt	0.90S _y	1.11
Bending	Butt	0.60–0.66S _y	1.52–1.67
Simple compression	Butt	0.60S _y	1.67
Shear	Butt or fillet	0.30S _{ut} [†]	

*The factor of safety *n* has been computed by using the distortion-energy theory.

[†]Shear stress on base metal should not exceed 0.40S_y of base metal.

a welded cold-drawn bar has its cold-drawn properties replaced with the hot-rolled properties in the vicinity of the weld. Finally, remembering that the weld metal is usually the strongest, do check the stresses in the parent metals.

The AISC code, as well as the AWS code, for bridges includes permissible stresses when fatigue loading is present. The designer will have no difficulty in using these codes, but their empirical nature tends to obscure the fact that they have been established by means of the same knowledge of fatigue failure already discussed in Chap. 6. Of course, for structures covered by these codes, the actual stresses *cannot* exceed the permissible stresses; otherwise the designer is legally liable. But in general, codes tend to conceal the actual margin of safety involved.

The fatigue stress-concentration factors listed in Table 9–5 are suggested for use. These factors should be used for the parent metal as well as for the weld metal. Table 9–6 gives steady-load information and minimum fillet sizes.

Table 9–5

Fatigue Stress-Concentration Factors, *K_{fs}*

Type of Weld	<i>K_{fs}</i>
Reinforced butt weld	1.2
Toe of transverse fillet weld	1.5
End of parallel fillet weld	2.7
T-butt joint with sharp corners	2.0

Table 9-6

Allowable Steady Loads and Minimum Fillet Weld Sizes

Schedule A: Allowable Load for Various Sizes of Fillet Welds								Schedule B: Minimum Fillet Weld Size, h		
Strength Level of Weld Metal (EXX)										
	60*	70*	80	90*	100	110*	120			
Allowable shear stress on throat, ksi (1000 psi) of fillet weld or partial penetration groove weld										
$\tau =$	18.0	21.0	24.0	27.0	30.0	33.0	36.0			
Allowable Unit Force on Fillet Weld, kip/linear in										
$^{\dagger}f =$	12.73 h	14.85 h	16.97 h	19.09 h	21.21 h	23.33 h	25.45 h			
Leg Size h , in	Allowable Unit Force for Various Sizes of Fillet Welds kip/linear in									
1	12.73	14.85	16.97	19.09	21.21	23.33	25.45			
7/8	11.14	12.99	14.85	16.70	18.57	20.41	22.27			
3/4	9.55	11.14	12.73	14.32	15.92	17.50	19.09			
5/8	7.96	9.28	10.61	11.93	13.27	14.58	15.91			
1/2	6.37	7.42	8.48	9.54	10.61	11.67	12.73			
7/16	5.57	6.50	7.42	8.35	9.28	10.21	11.14			
3/8	4.77	5.57	6.36	7.16	7.95	8.75	9.54			
5/16	3.98	4.64	5.30	5.97	6.63	7.29	7.95			
1/4	3.18	3.71	4.24	4.77	5.30	5.83	6.36			
3/16	2.39	2.78	3.18	3.58	3.98	4.38	4.77			
1/8	1.59	1.86	2.12	2.39	2.65	2.92	3.18			
1/16	0.795	0.930	1.06	1.19	1.33	1.46	1.59			

*Fillet welds actually tested by the joint AISC-AWS Task Committee.

 $^{\dagger}f = 0.707h \tau_{all}$.

Material Thickness of Thicker Part Joined, in	Weld Size, in
*To $\frac{1}{4}$ incl.	$\frac{1}{8}$
Over $\frac{1}{4}$	To $\frac{1}{2}$
Over $\frac{1}{2}$	To $\frac{3}{4}$
[†] Over $\frac{3}{4}$	To $1\frac{1}{2}$
Over $1\frac{1}{2}$	To $2\frac{1}{4}$
Over $2\frac{1}{4}$	To 6
Over 6	$\frac{5}{8}$

Not to exceed the thickness of the thinner part.

*Minimum size for bridge application does not go below $\frac{3}{16}$ in.[†]For minimum fillet weld size, schedule does not go above $\frac{5}{16}$ in fillet weld for every $\frac{3}{4}$ in material.Source: From Omer W. Blodgett (ed.), *Stress Allowables Affect Weldment Design*, D412, The James F. Lincoln Arc Welding Foundation, Cleveland, May 1991, p. 3. Reprinted by permission of Lincoln Electric Company.

9–6 Static Loading

Some examples of statically loaded joints are useful in comparing and contrasting the conventional method of analysis and the welding code methodology.

EXAMPLE 9–2

A $\frac{1}{2}$ -in by 2-in rectangular-cross-section 1015 bar carries a static load of 16.5 kip. It is welded to a gusset plate with a $\frac{3}{8}$ -in fillet weld 2 in long on both sides with an E70XX electrode as depicted in Fig. 9–18. Use the welding code method.

- (a) Is the weld metal strength satisfactory?
- (b) Is the attachment strength satisfactory?

Solution

(a) From Table 9–6, allowable force per unit length for a $\frac{3}{8}$ -in E70 electrode metal is 5.57 kip/in of weldment; thus

$$F = 5.57l = 5.57(4) = 22.28 \text{ kip}$$

Since $22.28 > 16.5$ kip, weld metal strength is satisfactory.

(b) Check shear in attachment adjacent to the welds. From Table A–20, $S_y = 27.5$ kpsi. Then, from Table 9–4, the allowable attachment shear stress is

$$\tau_{\text{all}} = 0.4S_y = 0.4(27.5) = 11 \text{ kpsi}$$

The shear stress τ on the base metal adjacent to the weld is

$$\tau = \frac{F}{2hl} = \frac{16.5}{2(0.375)2} = 11 \text{ kpsi}$$

Since $\tau_{\text{all}} \geq \tau$, the attachment is satisfactory near the weld beads. The tensile stress in the shank of the attachment σ is

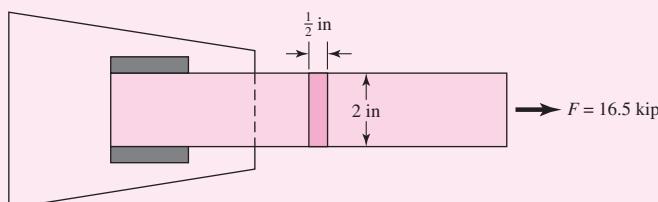
$$\sigma = \frac{F}{tl} = \frac{16.5}{(1/2)2} = 16.5 \text{ kpsi}$$

The allowable tensile stress σ_{all} , from Table 9–4, is $0.6S_y$ and, with welding code safety level preserved,

$$\sigma_{\text{all}} = 0.6S_y = 0.6(27.5) = 16.5 \text{ kpsi}$$

Since $\sigma \leq \sigma_{\text{all}}$, the shank tensile stress is satisfactory.

| Figure 9–18



EXAMPLE 9-3

A specially rolled A36 structural steel section for the attachment has a cross section as shown in Fig. 9-19 and has yield and ultimate tensile strengths of 36 and 58 kpsi, respectively. It is statically loaded through the attachment centroid by a load of $F = 24$ kip. Unsymmetrical weld tracks can compensate for eccentricity such that there is no moment to be resisted by the welds. Specify the weld track lengths l_1 and l_2 for a $\frac{5}{16}$ -in fillet weld using an E70XX electrode. This is part of a design problem in which the design variables include weld lengths and the fillet leg size.

Solution

The y coordinate of the section centroid of the attachment is

$$\bar{y} = \frac{\sum y_i A_i}{\sum A_i} = \frac{1(0.75)2 + 3(0.375)2}{0.75(2) + 0.375(2)} = 1.67 \text{ in}$$

Summing moments about point B to zero gives

$$\sum M_B = 0 = -F_1 b + F \bar{y} = -F_1(4) + 24(1.67)$$

from which

$$F_1 = 10 \text{ kip}$$

It follows that

$$F_2 = 24 - 10.0 = 14.0 \text{ kip}$$

The weld throat areas have to be in the ratio $14/10 = 1.4$, that is, $l_2 = 1.4l_1$. The weld length design variables are coupled by this relation, so l_1 is the weld length design variable. The other design variable is the fillet weld leg size h , which has been decided by the problem statement. From Table 9-4, the allowable shear stress on the throat τ_{all} is

$$\tau_{\text{all}} = 0.3(70) = 21 \text{ kpsi}$$

The shear stress τ on the 45° throat is

$$\begin{aligned} \tau &= \frac{F}{(0.707)h(l_1 + l_2)} = \frac{F}{(0.707)h(l_1 + 1.4l_1)} \\ &= \frac{F}{(0.707)h(2.4l_1)} = \tau_{\text{all}} = 21 \text{ kpsi} \end{aligned}$$

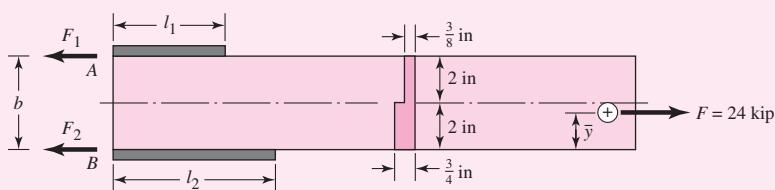
from which the weld length l_1 is

$$l_1 = \frac{24}{21(0.707)0.3125(2.4)} = 2.16 \text{ in}$$

and

$$l_2 = 1.4l_1 = 1.4(2.16) = 3.02 \text{ in}$$

| **Figure 9-19**



These are the weld-bead lengths required by weld metal strength. The attachment shear stress allowable in the base metal, from Table 9–4, is

$$\tau_{\text{all}} = 0.4S_y = 0.4(36) = 14.4 \text{ kpsi}$$

The shear stress τ in the base metal adjacent to the weld is

$$\tau = \frac{F}{h(l_1 + l_2)} = \frac{F}{h(l_1 + 1.4l_1)} = \frac{F}{h(2.4l_1)} = \tau_{\text{all}} = 14.4 \text{ kpsi}$$

from which

$$l_1 = \frac{F}{14.4h(2.4)} = \frac{24}{14.4(0.3125)2.4} = 2.22 \text{ in}$$

$$l_2 = 1.4l_1 = 1.4(2.22) = 3.11 \text{ in}$$

These are the weld-bead lengths required by base metal (attachment) strength. The base metal controls the weld lengths. For the allowable tensile stress σ_{all} in the shank of the attachment, the AISC allowable for tension members is $0.6S_y$; therefore,

$$\sigma_{\text{all}} = 0.6S_y = 0.6(36) = 21.6 \text{ kpsi}$$

The nominal tensile stress σ is *uniform* across the attachment cross section because of the load application at the centroid. The stress σ is

$$\sigma = \frac{F}{A} = \frac{24}{0.75(2) + 2(0.375)} = 10.7 \text{ kpsi}$$

Since $\sigma \leq \sigma_{\text{all}}$, the shank section is satisfactory. With l_1 set to a nominal $2\frac{1}{4}$ in, l_2 should be $1.4(2.25) = 3.15$ in.

Decision Set $l_1 = 2\frac{1}{4}$ in, $l_2 = 3\frac{1}{4}$ in. The small magnitude of the departure from $l_2/l_1 = 1.4$ is not serious. The joint is essentially moment-free.

EXAMPLE 9–4

Perform an adequacy assessment of the statically loaded welded cantilever carrying 500 lbf depicted in Fig. 9–20. The cantilever is made of AISI 1018 HR steel and welded with a $\frac{3}{8}$ -in fillet weld as shown in the figure. An E6010 electrode was used, and the design factor was 3.0.

- (a) Use the conventional method for the weld metal.
- (b) Use the conventional method for the attachment (cantilever) metal.
- (c) Use a welding code for the weld metal.

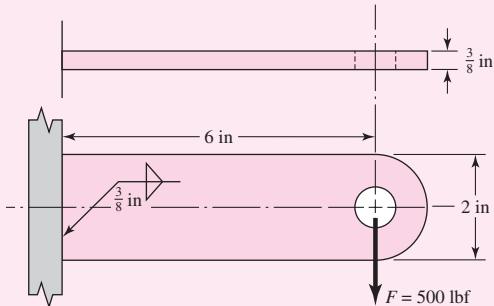
Solution

(a) From Table 9–3, $S_y = 50$ kpsi, $S_{ut} = 62$ kpsi. From Table 9–2, second pattern, $b = 0.375$ in, $d = 2$ in, so

$$A = 1.414hd = 1.414(0.375)2 = 1.06 \text{ in}^2$$

$$I_u = d^3/6 = 2^3/6 = 1.33 \text{ in}^3$$

$$I = 0.707hI_u = 0.707(0.375)1.33 = 0.353 \text{ in}^4$$

| Figure 9–20

Primary shear:

$$\tau' = \frac{F}{A} = \frac{500(10^{-3})}{1.06} = 0.472 \text{ kpsi}$$

Secondary shear:

$$\tau'' = \frac{Mr}{I} = \frac{500(10^{-3})(6)(1)}{0.353} = 8.50 \text{ kpsi}$$

The shear magnitude τ is the Pythagorean combination

$$\tau = (\tau'^2 + \tau''^2)^{1/2} = (0.472^2 + 8.50^2)^{1/2} = 8.51 \text{ kpsi}$$

The factor of safety based on a minimum strength and the distortion-energy criterion is

Answer $n = \frac{S_{sy}}{\tau} = \frac{0.577(50)}{8.51} = 3.39$

Since $n \geq n_d$, that is, $3.39 \geq 3.0$, the weld metal has satisfactory strength.

(b) From Table A–20, minimum strengths are $S_u = 58 \text{ kpsi}$ and $S_y = 32 \text{ kpsi}$. Then

$$\sigma = \frac{M}{I/c} = \frac{M}{bd^2/6} = \frac{500(10^{-3})6}{0.375(2^2)/6} = 12 \text{ kpsi}$$

Answer $n = \frac{S_y}{\sigma} = \frac{32}{12} = 2.67$

Since $n < n_d$, that is, $2.67 < 3.0$, the joint is unsatisfactory as to the attachment strength.

(c) From part (a), $\tau = 8.51 \text{ kpsi}$. For an E6010 electrode Table 9–6 gives the allowable shear stress τ_{all} as 18 kpsi . Since $\tau < \tau_{all}$, the weld is satisfactory. Since the code already has a design factor of $0.577(50)/18 = 1.6$ included at the equality, the corresponding factor of safety to part (a) is

Answer $n = 1.6 \frac{18}{8.51} = 3.38$

which is consistent.

9-7 Fatigue Loading

The conventional methods will be provided here. In fatigue, the Gerber criterion is best; however, you will find that the Goodman criterion is in common use. For the surface factor of Eq. 6-19, an as-forged surface should always be assumed for weldments unless a superior finish is specified and obtained.

Some examples of fatigue loading of welded joints follow.

EXAMPLE 9-5

The 1018 steel strap of Fig. 9-21 has a 1000 lbf, completely reversed load applied. Determine the factor of safety of the weldment for infinite life.

Solution

From Table A-20 for the 1018 attachment metal the strengths are $S_{ut} = 58$ kpsi and $S_y = 32$ kpsi. For the E6010 electrode, from Table 9-3 $S_{ut} = 62$ kpsi and $S_y = 50$ kpsi. The fatigue stress-concentration factor, from Table 9-5, is $K_{fs} = 2.7$. From Table 6-2, p. 288, $k_a = 39.9(58)^{-0.995} = 0.702$. For case 2 of Table 9-5, the shear area is:

$$A = 1.414(0.375)(2) = 1.061 \text{ in}^2$$

For a uniform shear stress on the throat, $k_b = 1$.

From Eq. (6-26), p. 290, for torsion (shear),

$$k_c = 0.59 \quad k_d = k_e = k_f = 1$$

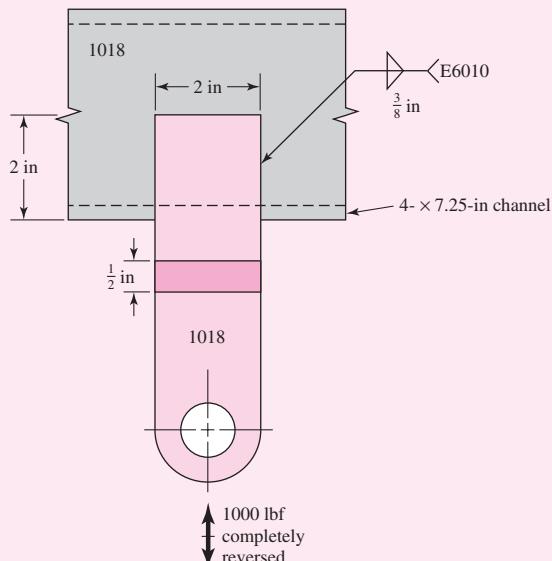
From Eqs. (6-8), p. 282, and (6-18), p. 287,

$$S_{se} = 0.702(1)0.59(1)(1)(1)0.5(58) = 12.0 \text{ kpsi}$$

From Table 9-5, $K_{fs} = 2.7$. Only primary shear is present. So, with $F_a = 1000$ lbf and $F_m = 0$

$$\tau'_a = \frac{K_{fs} F_a}{A} = \frac{2.7(1000)}{1.061} = 2545 \text{ psi} \quad \tau'_m = 0 \text{ psi}$$

| Figure 9-21



In the absence of a midrange component, the fatigue factor of safety n_f is given by

Answer

$$n_f = \frac{S_{se}}{\tau'_a} = \frac{12\,000}{2545} = 4.72$$

EXAMPLE 9–6

The 1018 steel strap of Fig. 9–22 has a repeatedly applied load of 2000 lbf ($F_a = F_m = 1000$ lbf). Determine the fatigue factor of safety fatigue strength of the weldment.

Solution

From Table 6–2, p. 288, $k_a = 39.9(58)^{-0.995} = 0.702$. From case 2 of Table 9–2

$$A = 1.414(0.375)(2) = 1.061 \text{ in}^2$$

For uniform shear stress on the throat $k_b = 1$.

From Eq. (6–26), p. 290, $k_c = 0.59$. From Eqs. (6–8), p. 282, and (6–18), p. 287,

$$S_{se} = 0.702(1)0.59(1)(1)(1)0.5(58) = 12.0 \text{ kpsi}$$

From Table 9–5, $K_{fs} = 2$. Only primary shear is present:

$$\tau'_a = \tau'_m = \frac{K_{fs}F_a}{A} = \frac{2(1000)}{1.061} = 1885 \text{ psi}$$

From Eq. (6–54), p. 317, $S_{su} \doteq 0.67S_{ut}$. This, together with the Gerber fatigue failure criterion for shear stresses from Table 6–7, p. 307, gives

$$n_f = \frac{1}{2} \left(\frac{0.67S_{ut}}{\tau_m} \right)^2 \frac{\tau_a}{S_{se}} \left[-1 + \sqrt{1 + \left(\frac{2\tau_m S_{se}}{0.67S_{ut}\tau_a} \right)^2} \right]$$

Answer

$$n_f = \frac{1}{2} \left[\frac{0.67(58)}{1.885} \right]^2 \frac{1.885}{12.0} \left\{ -1 + \sqrt{1 + \left[\frac{2(1.885)12.0}{0.67(58)1.885} \right]^2} \right\} = 5.85$$

| **Figure 9–22**

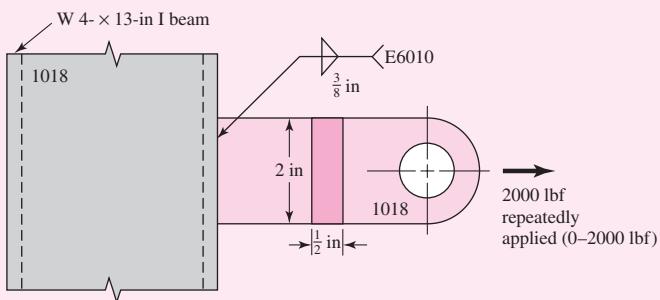
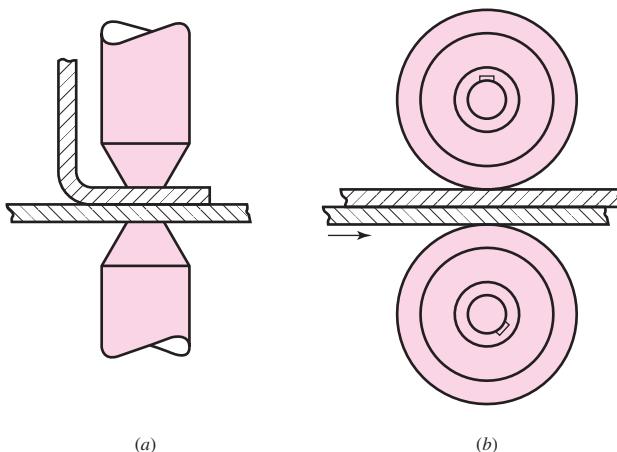


Figure 9-23

(a) Spot welding; (b) seam welding.



9-8 Resistance Welding

The heating and consequent welding that occur when an electric current is passed through several parts that are pressed together is called *resistance welding*. *Spot welding* and *seam welding* are forms of resistance welding most often used. The advantages of resistance welding over other forms are the speed, the accurate regulation of time and heat, the uniformity of the weld, and the mechanical properties that result. In addition the process is easy to automate, and filler metal and fluxes are not needed.

The spot- and seam-welding processes are illustrated schematically in Fig. 9-23. Seam welding is actually a series of overlapping spot welds, since the current is applied in pulses as the work moves between the rotating electrodes.

Failure of a resistance weld occurs either by shearing of the weld or by tearing of the metal around the weld. Because of the possibility of tearing, it is good practice to avoid loading a resistance-welded joint in tension. Thus, for the most part, design so that the spot or seam is loaded in pure shear. The shear stress is then simply the load divided by the area of the spot. Because the thinner sheet of the pair being welded may tear, the strength of spot welds is often specified by stating the load per spot based on the thickness of the thinnest sheet. Such strengths are best obtained by experiment.

Somewhat larger factors of safety should be used when parts are fastened by spot welding rather than by bolts or rivets, to account for the metallurgical changes in the materials due to the welding.

9-9 Adhesive Bonding⁵

The use of polymeric adhesives to join components for structural, semistructural, and non-structural applications has expanded greatly in recent years as a result of the unique advantages adhesives may offer for certain assembly processes and the development of new adhesives with improved robustness and environmental acceptability. The increasing complexity of modern assembled structures and the diverse types of materials used have led to many joining applications that would not be possible with more conventional joining techniques. Adhesives are also being used either in conjunction with or to replace

⁵For a more extensive discussion of this topic, see J. E. Shigley and C. R. Mischke, *Mechanical Engineering Design*, 6th ed., McGraw-Hill, New York, 2001, Sec. 9-11. This section was prepared with the assistance of Professor David A. Dillard, Professor of Engineering Science and Mechanics and Director of the Center for Adhesive and Sealant Science, Virginia Polytechnic Institute and State University, Blacksburg, Virginia, and with the encouragement and technical support of the Bonding Systems Division of 3M, Saint Paul, Minnesota.

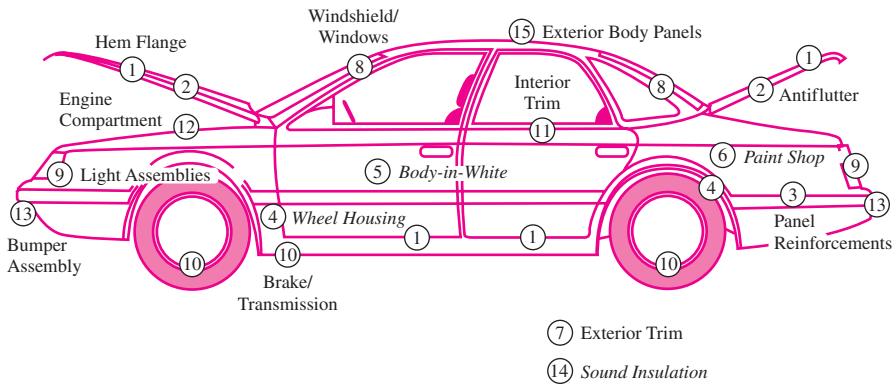


Figure 9-24

Diagram of an automobile body showing at least 15 locations at which adhesives and sealants could be used or are being used. Particular note should be made of the windshield (8), which is considered a load-bearing structure in modern automobiles and is adhesively bonded. Also attention should be paid to hem flange bonding (1), in which adhesives are used to bond and seal. Adhesives are used to bond friction surfaces in brakes and clutches (10). Antiflutter adhesive bonding (2) helps control deformation of hood and trunk lids under wind shear. Thread-sealing adhesives are used in engine applications (12). (From A. V. Pocius, *Adhesion and Adhesives Technology*, 2nd edition, Hanser Publishers, Munich, 2002. Reprinted by permission.)

mechanical fasteners and welds. Reduced weight, sealing capabilities, and reduced part count and assembly time, as well as improved fatigue and corrosion resistance, all combine to provide the designer with opportunities for customized assembly. The worldwide size of the adhesive and sealant industry is approximately 40 billion Euro dollars, and the United States market is about 12 billion US dollars.⁶ At the current exchange rates, the global market is therefore approximately \$57 billion. Figure 9-24 illustrates the numerous places where adhesives are used on a modern automobile. Indeed, the fabrication of many modern vehicles, devices, and structures is dependent on adhesives.

In well-designed joints and with proper processing procedures, use of adhesives can result in significant reductions in weight. Eliminating mechanical fasteners eliminates the weight of the fasteners, and also may permit the use of thinner-gauge materials because stress concentrations associated with the holes are eliminated. The capability of polymeric adhesives to dissipate energy can significantly reduce noise, vibration, and harshness (NVH), crucial in modern automobile performance. Adhesives can be used to assemble heat-sensitive materials or components that might be damaged by drilling holes for mechanical fasteners. They can be used to join dissimilar materials or thin-gauge stock that cannot be joined through other means.

Types of Adhesive

There are numerous adhesive types for various applications. They may be classified in a variety of ways depending on their chemistry (e.g., epoxies, polyurethanes, polyimides), their form (e.g., paste, liquid, film, pellets, tape), their type (e.g., hot melt, reactive hot melt, thermosetting, pressure sensitive, contact), or their load-carrying capability (structural, semistructural, or nonstructural).

Structural adhesives are relatively strong adhesives that are normally used well below their glass transition temperature; common examples include epoxies and certain acrylics. Such adhesives can carry significant stresses, and they lend themselves to structural applications. For many engineering applications, semistructural applications (where

⁶From E. M. Petrie, *Handbook of Adhesives and Sealants*, 2nd ed., McGraw-Hill, New York, 2007.

failure would be less critical) and nonstructural applications (of headliners, etc., for aesthetic purposes) are also of significant interest to the design engineer, providing cost-effective means required for assembly of finished products. These include *contact adhesives*, where a solution or emulsion containing an elastomeric adhesive is coated onto both adherends, the solvent is allowed to evaporate, and then the two adherends are brought into contact. Examples include rubber cement and adhesives used to bond laminates to countertops. *Pressure-sensitive adhesives* are very low modulus elastomers that deform easily under small pressures, permitting them to wet surfaces. When the substrate and adhesive are brought into intimate contact, van der Waals forces are sufficient to maintain the contact and provide relatively durable bonds. Pressure-sensitive adhesives are normally purchased as tapes or labels for nonstructural applications, although there are also double-sided foam tapes that can be used in semistructural applications. As the name implies, *hot melts* become liquid when heated, wetting the surfaces and then cooling into a solid polymer. These materials are increasingly applied in a wide array of engineering applications by more sophisticated versions of the glue guns in popular use. *Anaerobic adhesives* cure within narrow spaces deprived of oxygen; such materials have been widely used in mechanical engineering applications to lock bolts or bearings in place. Cure in other adhesives may be induced by exposure to ultraviolet light or electron beams, or it may be catalyzed by certain materials that are ubiquitous on many surfaces, such as water.

Table 9–7 presents important strength properties of commonly used adhesives.

Table 9–7

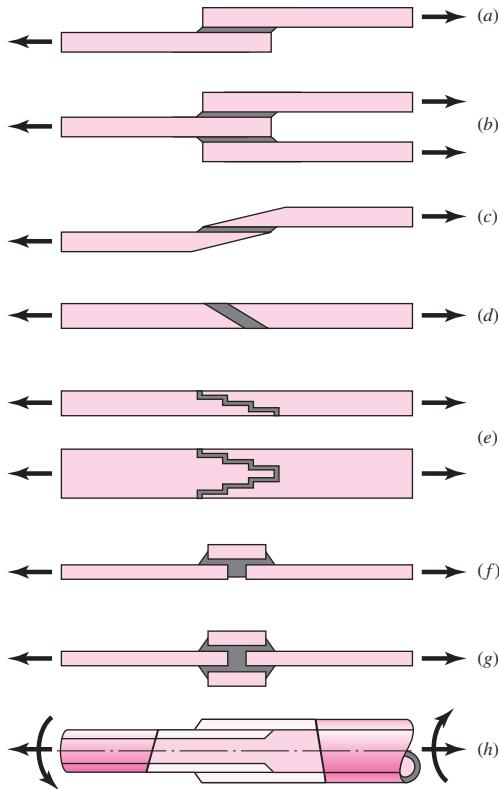
Mechanical Performance of Various Types of Adhesives

Adhesive Chemistry or Type	Room Temperature Lap-Shear Strength, MPa (psi)	Peel Strength per Unit Width, kN/m (lbf/in)
Pressure-sensitive	0.01–0.07 (2–10)	0.18–0.88 (1–5)
Starch-based	0.07–0.7 (10–100)	0.18–0.88 (1–5)
Cellosics	0.35–3.5 (50–500)	0.18–1.8 (1–10)
Rubber-based	0.35–3.5 (50–500)	1.8–7 (10–40)
Formulated hot melt	0.35–4.8 (50–700)	0.88–3.5 (5–20)
Synthetically designed hot melt	0.7–6.9 (100–1000)	0.88–3.5 (5–20)
PVAc emulsion (white glue)	1.4–6.9 (200–1000)	0.88–1.8 (5–10)
Cyanoacrylate	6.9–13.8 (1000–2000)	0.18–3.5 (1–20)
Protein-based	6.9–13.8 (1000–2000)	0.18–1.8 (1–10)
Anaerobic acrylic	6.9–13.8 (1000–2000)	0.18–1.8 (1–10)
Urethane	6.9–17.2 (1000–2500)	1.8–8.8 (10–50)
Rubber-modified acrylic	13.8–24.1 (2000–3500)	1.8–8.8 (10–50)
Modified phenolic	13.8–27.6 (2000–4000)	3.6–7 (20–40)
Unmodified epoxy	10.3–27.6 (1500–4000)	0.35–1.8 (2–10)
Bis-maleimide	13.8–27.6 (2000–4000)	0.18–3.5 (1–20)
Polyimide	13.8–27.6 (2000–4000)	0.18–0.88 (1–5)
Rubber-modified epoxy	20.7–41.4 (3000–6000)	4.4–14 (25–80)

Source: From A. V. Pocius, *Adhesion and Adhesives Technology*, 2nd ed., Hanser Gardner Publishers, Ohio, 2002. Reprinted by permission.

Figure 9–25

Common types of lap joints used in mechanical design:
 (a) single lap; (b) double lap;
 (c) scarf; (d) bevel; (e) step;
 (f) butt strap; (g) double butt
 strap; (h) tubular lap. (Adapted
 from R. D. Adams, J. Comyn,
 and W. C. Wake, Structural
 Adhesive Joints in Engineering,
 2nd ed., Chapman and Hall,
 New York, 1997.)



Stress Distributions

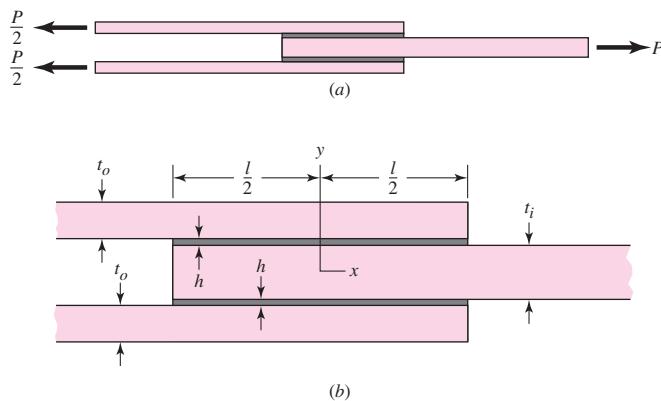
Good design practice normally requires that adhesive joints be constructed in such a manner that the adhesive carries the load in shear rather than tension. Bonds are typically much stronger when loaded in shear rather than in tension across the bond plate. Lap-shear joints represent an important family of joints, both for test specimens to evaluate adhesive properties and for actual incorporation into practical designs. Generic types of lap joints that commonly arise are illustrated in Fig. 9–25.

The simplest analysis of lap joints suggests the applied load is uniformly distributed over the bond area. Lap joint test results, such as those obtained following the ASTM D1002 for single-lap joints, report the “apparent shear strength” as the breaking load divided by the bond area. Although this simple analysis can be adequate for stiff adherends bonded with a soft adhesive over a relatively short bond length, significant peaks in shear stress occur except for the most flexible adhesives. In an effort to point out the problems associated with such practice, ASTM D4896 outlines some of the concerns associated with taking this simplistic view of stresses within lap joints.

In 1938, O. Volkersen presented an analysis of the lap joint, known as the *shear-lag model*. It provides valuable insights into the shear-stress distributions in a host of lap joints. Bending induced in the single-lap joint due to eccentricity significantly complicates the analysis, so here we will consider a symmetric double-lap joint to

Figure 9–26

Double-lap joint.



illustrate the principles. The shear-stress distribution for the double lap joint of Fig. 9–26 is given by

$$\tau(x) = \frac{P\omega}{4b \sinh(\omega l/2)} \cosh(\omega x) + \left[\frac{P\omega}{4b \cosh(\omega l/2)} \left(\frac{2E_o t_o - E_i t_i}{2E_o t_o + E_i t_i} \right) + \frac{(\alpha_i - \alpha_o) \Delta T \omega}{(1/E_o t_o + 2/E_i t_i) \cosh(\omega l/2)} \right] \sinh(\omega x) \quad (9-7)$$

where

$$\omega = \sqrt{\frac{G}{h} \left(\frac{1}{E_o t_o} + \frac{2}{E_i t_i} \right)}$$

and E_o , t_o , α_o , and E_i , t_i , α_i , are the modulus, thickness, coefficient of thermal expansion for the outer and inner adherend, respectively; G , h , b , and l are the shear modulus, thickness, width, and length of the adhesive, respectively; and ΔT is a change in temperature of the joint. If the adhesive is cured at an elevated temperature such that the stress-free temperature of the joint differs from the service temperature, the mismatch in thermal expansion of the outer and inner adherends induces a thermal shear across the adhesive.

EXAMPLE 9–7

The double-lap joint depicted in Fig. 9–26 consists of aluminum outer adherends and an inner steel adherend. The assembly is cured at 250°F and is stress-free at 200°F. The completed bond is subjected to an axial load of 2000 lbf at a service temperature of 70°F. The width b is 1 in, the length of the bond l is 1 in. Additional information is tabulated below:

	G, psi	E, psi	α, in/(in · °F)	Thickness, in
Adhesive	$0.2(10^6)$		$55(10^{-6})$	0.020
Outer adherend		$10(10^6)$	$13.3(10^{-6})$	0.150
Inner adherend		$30(10^6)$	$6.0(10^{-6})$	0.100

Sketch a plot of the shear stress as a function of the length of the bond due to (a) thermal stress, (b) load-induced stress, and (c) the sum of stresses in *a* and *b*; and (d) find where the largest shear stress is maximum.

Solution

In Eq. (9–7) the parameter ω is given by

$$\begin{aligned}\omega &= \sqrt{\frac{G}{h} \left(\frac{1}{E_o t_o} + \frac{2}{E_i t_i} \right)} \\ &= \sqrt{\frac{0.2(10^6)}{0.020} \left[\frac{1}{10(10^6)0.15} + \frac{2}{30(10^6)0.10} \right]} = 3.65 \text{ in}^{-1}\end{aligned}$$

(a) For the thermal component, $\alpha_i - \alpha_o = 6(10^{-6}) - 13.3(10^{-6}) = -7.3(10^{-6})$ in/(in \cdot $^{\circ}$ F), $\Delta T = 70 - 200 = -130$ $^{\circ}$ F,

$$\begin{aligned}\tau_{th}(x) &= \frac{(\alpha_i - \alpha_o)\Delta T \omega \sinh(\omega x)}{(1/E_o t_o + 2/E_i t_i) \cosh(\omega l/2)} \\ \tau_{th}(x) &= \frac{-7.3(10^{-6})(-130)3.65 \sinh(3.65x)}{\left[\frac{1}{10(10^6)0.150} + \frac{2}{30(10^6)0.100} \right] \cosh\left[\frac{3.65(1)}{2}\right]} \\ &= 816.4 \sinh(3.65x)\end{aligned}$$

The thermal stress is plotted in Fig. (9–27) and tabulated at $x = -0.5, 0$, and 0.5 in the table below.

(b) The bond is “balanced” ($E_o t_o = E_i t_i/2$), so the load-induced stress is given by

$$\tau_P(x) = \frac{P \omega \cosh(\omega x)}{4b \sinh(\omega l/2)} = \frac{2000(3.65) \cosh(3.65x)}{4(1)3.0208} = 604.1 \cosh(3.65x) \quad (1)$$

The load-induced stress is plotted in Fig. (9–27) and tabulated at $x = -0.5, 0$, and 0.5 in the table below.

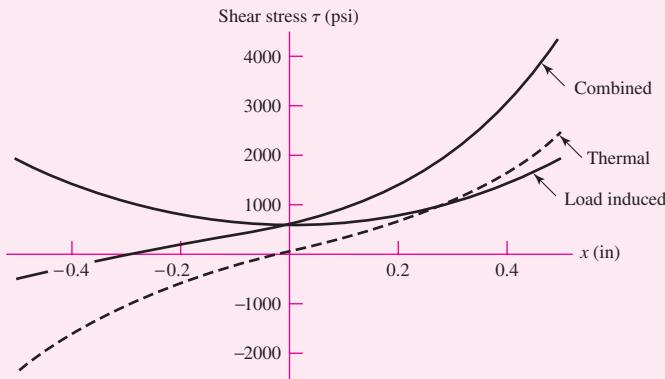
(c) Total stress table (in psi):

	$\tau(-0.5)$	$\tau(0)$	$\tau(0.5)$
Thermal only	-2466	0	2466
Load-induced only	1922	604	1922
Combined	-544	604	4388

(d) The maximum shear stress predicted by the shear-lag model will always occur at the ends. See the plot in Fig. 9–27. Since the residual stresses are always present, significant shear stresses may already exist prior to application of the load. The large stresses present for the combined-load case could result in local yielding of a ductile adhesive or failure of a more brittle one. The significance of the thermal stresses serves as a caution against joining dissimilar adherends when large temperature changes are involved. Note also that the average shear stress due to the load is

Figure 9–27

Plot for Ex. 9–7.



$\tau_{\text{avg}} = P/(2bl) = 1000$ psi. Equation (1) produced a maximum of 1922 psi, almost double the average.

Although design considerations for single-lap joints are beyond the scope of this chapter, one should note that the load eccentricity is an important aspect in the stress state of single-lap joints. Adherend bending can result in shear stresses that may be as much as double those given for the double-lap configuration (for a given total bond area). In addition, peel stresses can be quite large and often account for joint failure. Finally, plastic bending of the adherends can lead to high strains, which less ductile adhesives cannot withstand, leading to bond failure as well. Bending stresses in the adherends at the end of the overlap can be four times greater than the average stress within the adherend; thus, they must be considered in the design. Figure 9–28 shows the shear and peel stresses present in a typical single-lap joint that corresponds to the ASTM D1002 test specimen. Note that the shear stresses are significantly larger than predicted by the Volkersen analysis, a result of the increased adhesive strains associated with adherend bending.

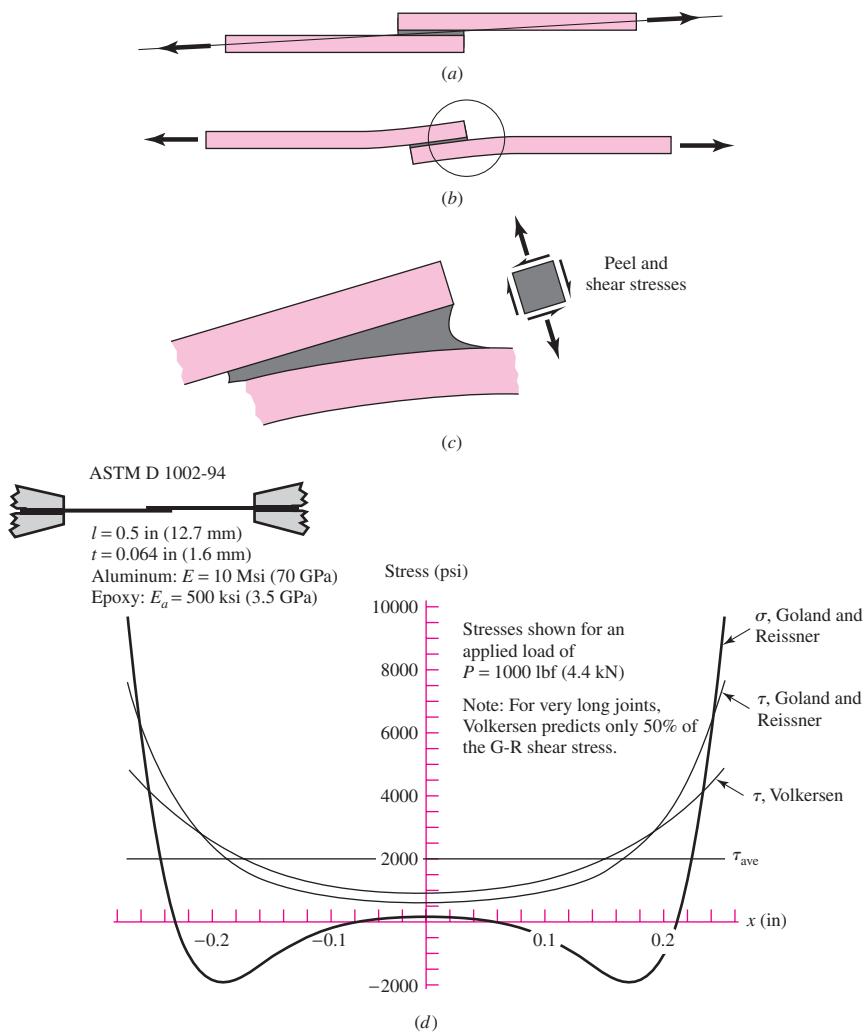
Joint Design

Some basic guidelines that should be used in adhesive joint design include:

- Design to place bondline in shear, not peel. Beware of peel stresses focused at bond terminations. When necessary, reduce peel stresses through tapering the adherend ends, increasing bond area where peel stresses occur, or utilizing rivets at bond terminations where peel stresses can initiate failures.
- Where possible, use adhesives with adequate ductility. The ability of an adhesive to yield reduces the stress concentrations associated with the ends of joints and increases the toughness to resist debond propagation.
- Recognize environmental limitations of adhesives and surface preparation methods. Exposure to water, solvents, and other diluents can significantly degrade adhesive performance in some situations, through displacing the adhesive from the surface or degrading the polymer. Certain adhesives may be susceptible to environmental stress cracking in the presence of certain solvents. Exposure to ultraviolet light can also degrade adhesives.

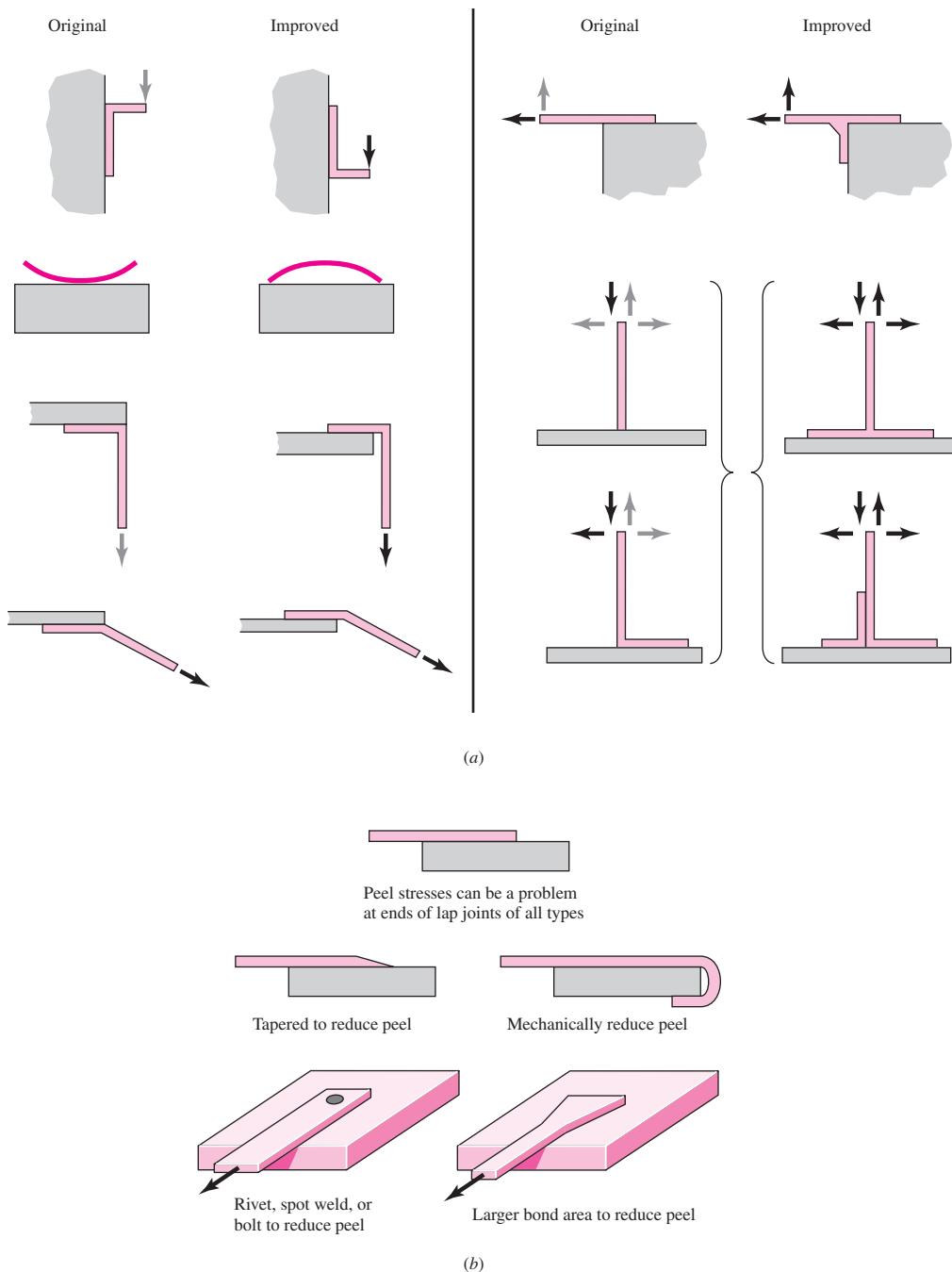
Figure 9–28

Stresses within a single-lap joint. (a) Lap-joint tensile forces have a line of action that is not initially parallel to the adherend sides. (b) As the load increases the adherends and bond bend. (c) In the locality of the end of an adherend peel and shear stresses appear, and the peel stresses often induce joint failure. (d) The seminal Goland and Reissner stress predictions (*J. Appl. Mech.*, vol. 77, 1944) are shown. (Note that the predicted shear-stress maximum is higher than that predicted by the Volkersen shear-lag model because of adherend bending.)



- Design in a way that permits or facilitates inspections of bonds where possible. A missing rivet or bolt is often easy to detect, but debonds or unsatisfactory adhesive bonds are not readily apparent.
- Allow for sufficient bond area so that the joint can tolerate some debonding before going critical. This increases the likelihood that debonds can be detected. Having some regions of the overall bond at relatively low stress levels can significantly improve durability and reliability.
- Where possible, bond to multiple surfaces to offer support to loads in any direction. Bonding an attachment to a single surface can place peel stresses on the bond, whereas bonding to several adjacent planes tends to permit arbitrary loads to be carried predominantly in shear.
- Adhesives can be used in conjunction with spot welding. The process is known as *weld bonding*. The spot welds serve to fixture the bond until it is cured.

Figure 9–29 presents examples of improvements in adhesive bonding.

**Figure 9-29**

Design practices that improve adhesive bonding. (a) Gray load vectors are to be avoided as resulting strength is poor. (b) Means to reduce peel stresses in lap-type joints.

References

Good references are available for analyzing and designing adhesive bonds, including the following:

- R. D. Adams, J. Comyn, and W. C. Wake, *Structural Adhesive Joints in Engineering*, 2nd ed., Chapman and Hall, New York, 1997.
- G. P. Anderson, S. J. Bennett, and K. L. DeVries, *Analysis and Testing of Adhesive Bonds*, Academic Press, New York, 1977.
- H. F. Brinson (ed.), *Engineered Materials Handbook, vol. 3: Adhesives and Sealants*, ASM International, Metals Park, Ohio, 1990.
- A. J. Kinloch, *Adhesion and Adhesives: Science and Technology*, Chapman and Hall, New York, 1987.
- A. J. Kinloch (ed.), *Durability of Structural Adhesives*, Applied Science Publishers, New York, 1983.
- R. W. Messler, Jr., *Joining of Materials and Structures*, Elsevier Butterworth-Heinemann, Mass., 2004.
- E. M. Petrie, *Handbook of Adhesives and Sealants*, 2nd ed., McGraw-Hill, New York, 2007.
- A. V. Pocius, *Adhesion and Adhesives Technology: An Introduction*, 2nd ed., Hanser Gardner, Ohio, 1997.

The Internet is also a good source of information. For example, try this website: www.3m.com/adhesives.

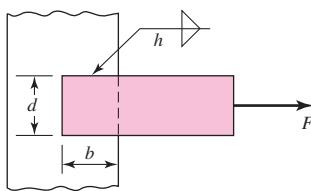
PROBLEMS

9-1 to 9-4

The figure shows a horizontal steel bar of thickness h loaded in steady tension and welded to a vertical support. Find the load F that will cause an allowable shear stress, τ_{allow} , in the throats of the welds.

Problem Number	b	d	h	τ_{allow}
9-1	50 mm	50 mm	5 mm	140 MPa
9-2	2 in	2 in	$\frac{5}{16}$ in	25 kpsi
9-3	50 mm	30 mm	5 mm	140 MPa
9-4	4 in	2 in	$\frac{5}{16}$ in	25 kpsi

Problems 9-1 to 9-4



9-5 to 9-8

For the weldments of Probs. 9-1 to 9-4, the electrodes are specified in the table. For the electrode metal indicated, what is the allowable load on the weldment?

Problem Number	Reference Problem	Electrode
9-5	9-1	E7010
9-6	9-2	E6010
9-7	9-3	E7010
9-8	9-4	E6010

**9-9 to
9-12**

The materials for the members being joined in Probs. 9-1 to 9-4 are specified below. What load on the weldment is allowable because member metal is incorporated in the welds?

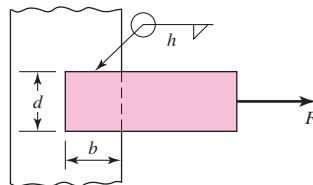
Problem Number	Reference Problem	Bar	Vertical Support
9-9	9-1	1018 CD	1018 HR
9-10	9-2	1020 CD	1020 CD
9-11	9-3	1035 HR	1035 CD
9-12	9-4	1035 HR	1020 CD

**9-13 to
9-16**

A steel bar of thickness h is welded to a vertical support as shown in the figure. What is the shear stress in the throat of the welds due to the force F ?

Problem Number	b	d	h	F
9-13	50 mm	50 mm	5 mm	100 kN
9-14	2 in	2 in	$\frac{5}{16}$ in	40 kip
9-15	50 mm	30 mm	5 mm	100 kN
9-16	4 in	2 in	$\frac{5}{16}$ in	40 kip

Problems 9-13 to 9-16

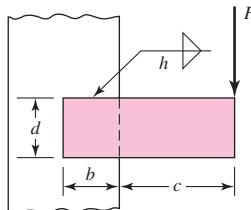
**9-17 to
9-20**

A steel bar of thickness h , to be used as a beam, is welded to a vertical support by two fillet welds as shown in the figure.

- (a) Find the safe bending force F if the allowable shear stress in the welds is τ_{allow} .
- (b) In part a, you found a simple expression for F in terms of the allowable shear stress. Find the allowable load if the electrode is E7010, the bar is hot-rolled 1020, and the support is hot-rolled 1015.

Problem Number	b	c	d	h	τ_{allow}
9-17	50 mm	150 mm	50 mm	5 mm	140 MPa
9-18	2 in	6 in	2 in	$\frac{5}{16}$ in	25 ksi
9-19	50 mm	150 mm	30 mm	5 mm	140 MPa
9-20	4 in	6 in	2 in	$\frac{5}{16}$ in	25 ksi

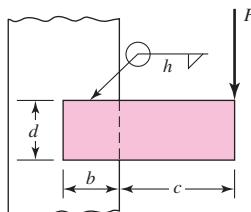
Problems 9-17 to 9-20

**9-21 to
9-24**

The figure shows a weldment just like that for Probs. 9-17 to 9-20 except there are four welds instead of two. Find the safe bending force F if the allowable shear stress in the welds is τ_{allow} .

Problem Number	b	c	d	h	τ_{allow}
9-21	50 mm	150 mm	50 mm	5 mm	140 MPa
9-22	2 in	6 in	2 in	$\frac{5}{16}$ in	25 ksi
9-23	50 mm	150 mm	30 mm	5 mm	140 MPa
9-24	4 in	6 in	2 in	$\frac{5}{16}$ in	25 ksi

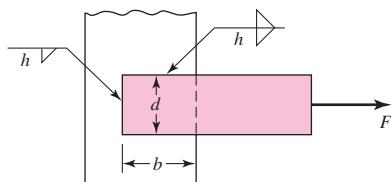
Problems 9-21 to 9-24

**9-25 to
9-28**

The weldment shown in the figure is subjected to an alternating force F . The hot-rolled steel bar has a thickness h and is of AISI 1010 steel. The vertical support is likewise AISI 1010 HR steel. The electrode given in the table below. Estimate the fatigue load F the bar will carry if three fillet welds are used.

Problem Number	b	d	h	Electrode
9-25	50 mm	50 mm	5 mm	E6010
9-26	2 in	2 in	$\frac{5}{16}$ in	E6010
9-27	50 mm	30 mm	5 mm	E7010
9-28	4 in	2 in	$\frac{5}{16}$ in	E7010

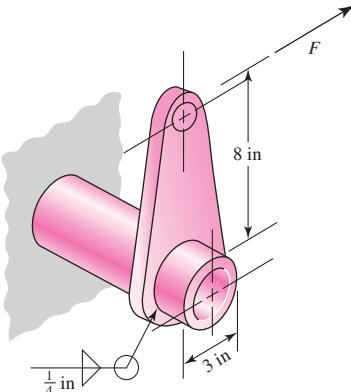
Problems 9-25 to 9-28



9-29

The permissible shear stress for the weldment illustrated is 20 kpsi. Estimate the load, F , that will cause this stress in the weldment throat.

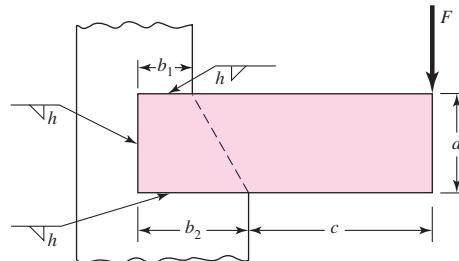
Problem 9-29

**9-30 to
9-31**

A steel bar of thickness h is subjected to a bending force F . The vertical support is stepped such that the horizontal welds are b_1 and b_2 long. Determine F if the maximum allowable shear stress is τ_{allow} .

Problem Number	b_1	b_2	c	d	h	τ_{allow}
9-30	2 in	4 in	6 in	4 in	5/16 in	25 kpsi
9-31	30 mm	50 mm	150 mm	50 mm	5 mm	140 MPa

Problems 9-30 to 9-31

**9-32**

In the design of weldments in torsion it is helpful to have a hierarchical perception of the relative efficiency of common patterns. For example, the weld-bead patterns shown in Table 9-1 can be ranked for desirability. Assume the space available is an $a \times a$ square. Use a formal figure of merit that is directly proportional to J and inversely proportional to the volume of weld metal laid down:

$$\text{fom} = \frac{J}{\text{vol}} = \frac{0.707hJ_u}{(h^2/2)l} = 1.414 \frac{J_u}{hl}$$

A tactical figure of merit could omit the constant, that is, $\text{fom}' = J_u/(hl)$. Rank the six patterns of Table 9-1 from most to least efficient.

9-33

The space available for a weld-bead pattern subject to bending is $a \times a$. Place the patterns of Table 9-2 in hierarchical order of efficiency of weld metal placement to resist bending. A formal figure of merit can be directly proportion to I and inversely proportional to the volume of weld metal laid down:

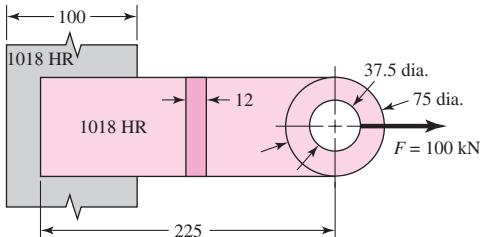
$$\text{fom} = \frac{I}{\text{vol}} = \frac{0.707hI_u}{(h^2/2)l} = 1.414 \frac{I_u}{hl}$$

The tactical figure of merit can omit the constant 1.414, that is, $f_{om'} = I_u/(hl)$. Omit the patterns intended for T beams and I beams. Rank the remaining seven.

9-34

The attachment shown in the figure is made of 1018 HR steel 12 mm thick. The static force is 100 kN. The member is 75 mm wide. Specify the weldment (give the pattern, electrode number, type of weld, length of weld, and leg size).

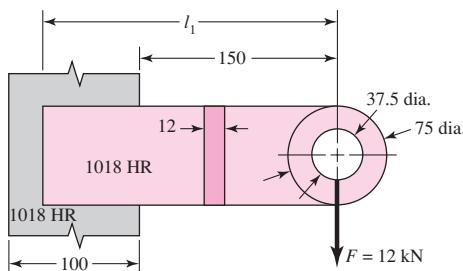
Problem 9-34
Dimensions in millimeters.



9-35

The attachment shown carries a static bending load of 12 kN. The attachment length, l_1 , is 225 mm. Specify the weldment (give the pattern, electrode number, type of weld, length of weld, and leg size).

Problem 9-35
Dimensions in millimeters.



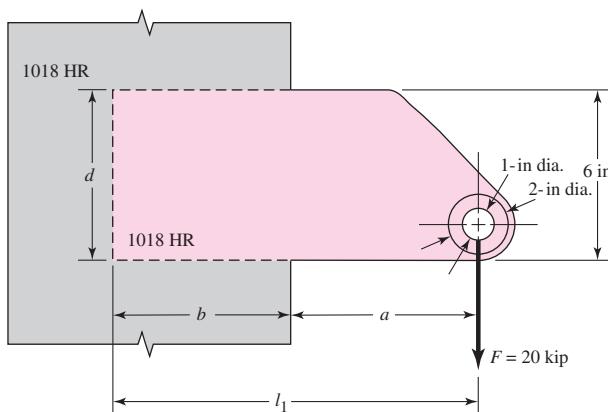
9-36

The attachment in Prob. 9-35 has not had its length determined. The static force is 12 kN. Specify the weldment (give the pattern, electrode number, type of weld, length of bead, and leg size). Specify the attachment length.

9-37

A vertical column of 1018 hot-rolled steel is 10 in wide. An attachment has been designed to the point shown in the figure. The static load of 20 kip is applied, and the clearance a of 6.25 in has to be equaled or exceeded. The attachment is also 1018 hot-rolled steel, to be made from $\frac{1}{2}$ -in plate with weld-on bosses when all dimensions are known. Specify the weldment (give the pattern, electrode number, type of weld, length of weld bead, and leg size). Specify also the length l_1 for the attachment.

Problem 9-37



9-38

Write a computer program to assist with a task such as that of Prob. 9-37 with a rectangular weld-bead pattern for a torsional shear joint. In doing so solicit the force F , the clearance a , and the largest allowable shear stress. Then, as part of an iterative loop, solicit the dimensions b and d of the rectangle. These can be your design variables. Output all the parameters after the leg size has been determined by computation. In effect this will be your adequacy assessment when you stop iterating. Include the figure of merit $J_u/(hl)$ in the output. The fom and the leg size h with available width will give you a useful insight into the nature of this class of welds. Use your program to verify your solutions to Prob. 9-37.

9-39

Fillet welds in joints resisting bending are interesting in that they can be simpler than those resisting torsion. From Prob. 9-33 you learned that your objective is to place weld metal as far away from the weld-bead centroid as you can, but distributed in an orientation parallel to the x axis. Furthermore, placement on the top and bottom of the built-in end of a cantilever with rectangular cross section results in parallel weld beads, each element of which is in the ideal position. The object of this problem is to study the full weld bead and the interrupted weld-bead pattern. Consider the case of Fig. 9-17, p. 487, with $F = 10$ kips, the beam length is 10 in, $b = 8$ in, and $d = 8$ in. For the second case, for the interrupted weld consider a centered gap of $b_1 = 2$ in existing in the top and bottom welds. Study the two cases with $\tau_{\text{all}} = 12.8$ kpsi. What do you notice about τ , σ , and τ_{\max} ? Compare the fom'.

9-40

For a rectangular weld-bead track resisting bending, develop the necessary equations to treat cases of vertical welds, horizontal welds, and weld-all-around patterns with depth d and width b and allowing central gaps in parallel beads of length b_1 and d_1 . Do this by superposition of parallel tracks, vertical tracks subtracting out the gaps. Then put the two together for a rectangular weld bead with central gaps of length b_1 and d_1 . Show that the results are

$$A = 1.414(b - b_1 + d - d_1)h$$

$$I_u = \frac{(b - b_1)d^2}{2} + \frac{d^3 - d_1^3}{6}$$

$$I = 0.707hI_u$$

$$l = 2(b - b_1) + 2(d - d_1)$$

$$\text{fom} = \frac{I_u}{hl}$$

9-41

Write a computer program based on the Prob. 9-40 protocol. Solicit the largest allowable shear stress, the force F , and the clearance a , as well as the dimensions b and d . Begin an iterative loop by soliciting b_1 and d_1 . Either or both of these can be your design variables. Program to find the leg size corresponding to a shear-stress level at the maximum allowable at a corner. Output all your parameters including the figure of merit. Use the program to check any previous problems to which it is applicable. Play with it in a “what if” mode and learn from the trends in your parameters.

9-42

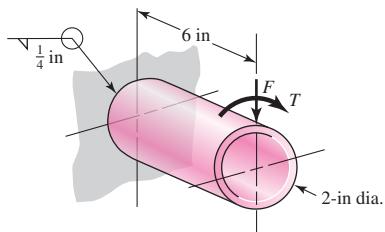
When comparing two different weldment patterns it is useful to observe the resistance to bending or torsion and the volume of weld metal deposited. Measure of effectiveness, defined as second moment of area divided by weld-metal volume, is useful. If a 3-in by 6-in section of a cantilever carries a static bending moment of 100 kip · in in the weldment plane, with an allowable shear stress of 12 kpsi realized, compare horizontal weldments with vertical weldments. The horizontal beads are to be 3 in long and the vertical beads, 6 in long.

9-43 to 9-45

A 2-in dia. steel bar is subjected to the loading indicated. Locate and estimate the maximum shear stress in the weld throat.

Problem Number	F	T
9–43	0	15 kip · in
9–44	2 kips	0
9–45	2 kips	15 kip · in

Problems 9–43 to 9–45



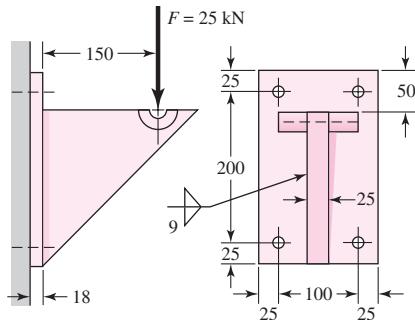
9-46

For Prob. 9–45, determine the weld size if the maximum allowable shear stress is 20 kpsi.

9-47

Find the maximum shear stress in the throat of the weld metal in the figure.

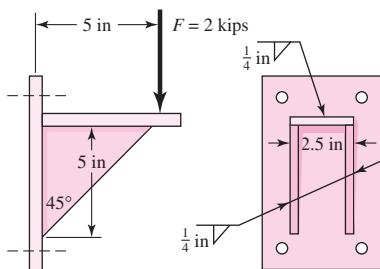
Problem 9-47



9-48

The figure shows a welded steel bracket loaded by a static force F . Estimate the factor of safety if the allowable shear stress in the weld throat is 18 kpsi.

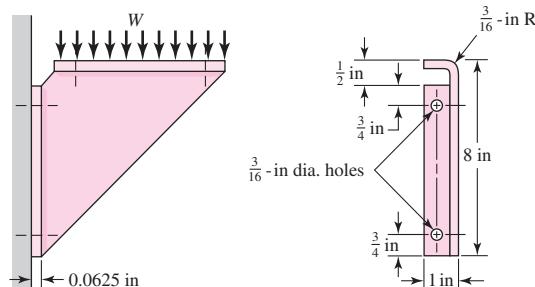
Problem 9-48



9-49

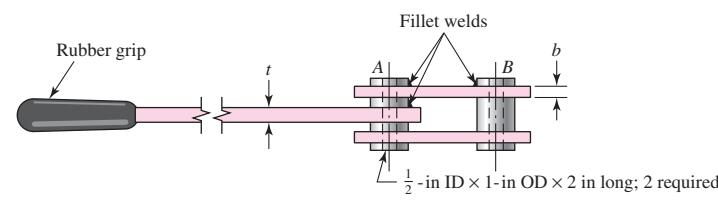
The figure shows a formed sheet-steel bracket. Instead of securing it to the support with machine screws, welding has been proposed. If the combined shear stress in the weld metal is limited to 1.5 kpsi, estimate the total load W the bracket will support. The dimensions of the top flange are the same as the mounting flange.

Problem 9-49
Structural support is 1030 HR steel, bracket is 1020 press cold-formed steel. The weld electrode is E6010.

**9-50**

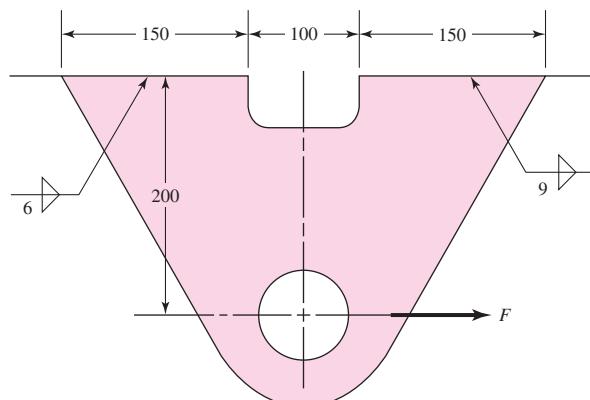
Without bracing, a machinist can exert only about 100 lbf on a wrench or tool handle. The lever shown in the figure has $t = \frac{1}{2}$ in and $w = 2$ in. We wish to specify the fillet-weld size to secure the lever to the tubular part at A. Both parts are of steel, and the shear stress in the weld throat should not exceed 3000 psi. Find a safe weld size.

Problem 9-50

**9-51**

Estimate the safe static load F for the weldment shown in the figure if an E6010 electrode is used and the design factor is to be 2. The steel members are 1015 hot-rolled steel. Use conventional analysis.

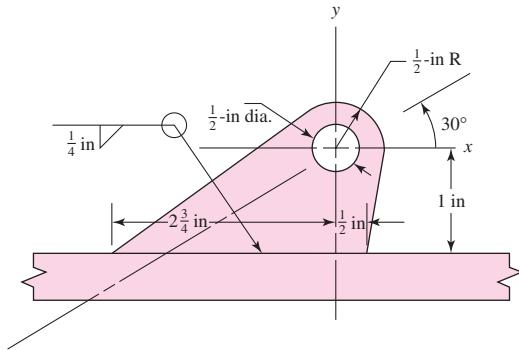
Problem 9-51
Dimensions in millimeters.



9-52

Brackets, such as the one shown, are used in mooring small watercraft. Failure of such brackets is usually caused by bearing pressure of the mooring clip against the side of the hole. Our purpose here is to get an idea of the static and dynamic margins of safety involved. We use a bracket 1/4 in thick made of hot-rolled 1018 steel. We then assume wave action on the boat will create force F no greater than 1200 lbf.

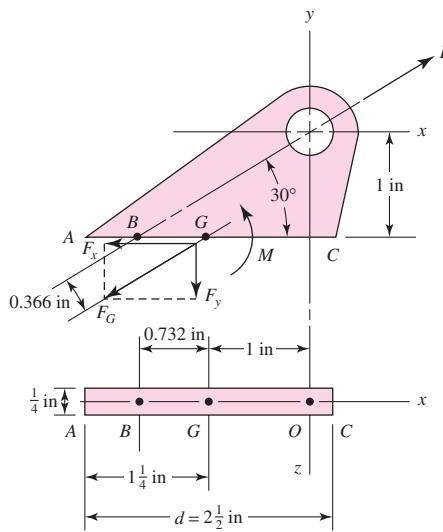
- Identify the moment M that produces a shear stress on the throat resisting bending action with a "tension" at A and "compression" at C .
- Find the force component F_y that produces a shear stress at the throat resisting a "tension" throughout the weld.
- Find the force component F_x that produces an in-line shear throughout the weld.
- Find A , I_u , and I using Table 9-2, in part.
- Find the shear stress τ_1 at A due to F_y and M , the shear stress τ_2 due to F_x , and combine to find τ .
- Find the factor of safety guarding against shear yielding in the weldment.
- Find the factor of safety guarding against a static failure in the parent metal at the weld.
- Find the factor of safety guarding against a fatigue failure in the weld metal using a Gerber failure criterion.



(a)

Problem 9-52

Small watercraft mooring bracket.



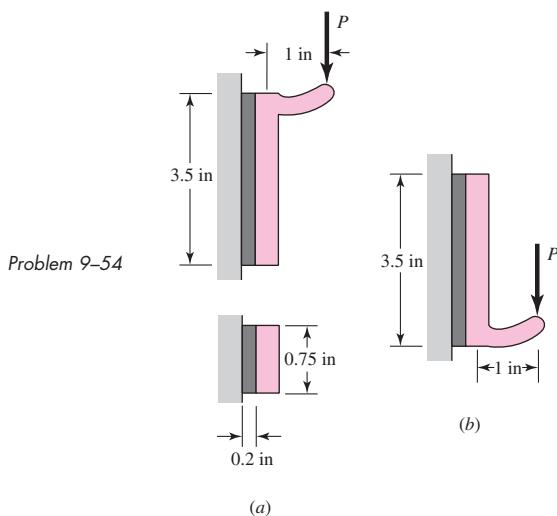
(b)

9-53

For the sake of perspective it is always useful to look at the matter of scale. Double all dimensions in Prob. 9-18 and find the allowable load. By what factor has it increased? First make a guess, then carry out the computation. Would you expect the same ratio if the load had been variable?

9-54

Hardware stores often sell plastic hooks that can be mounted on walls with pressure-sensitive adhesive foam tape. Two designs are shown in (a) and (b) of the figure. Indicate which one you would buy and why.

**9-55**

For a balanced double-lap joint cured at room temperature, Volkersen's equation simplifies to

$$\tau(x) = \frac{P\omega \cosh(\omega x)}{4b \sinh(\omega l/2)} = A_1 \cosh(\omega x)$$

- (a) Show that the average stress $\bar{\tau}$ is $P/(2bl)$.
- (b) Show that the largest shear stress is $P\omega/[4b \tanh(\omega l/2)]$.
- (c) Define a stress-augmentation factor K such that

$$\tau(l/2) = K\bar{\tau}$$

and it follows that

$$K = \frac{P\omega}{4b \tanh(\omega l/2)} \frac{2bl}{P} = \frac{\omega l/2}{\tanh(\omega l/2)} = \frac{\omega l}{2} \frac{\exp(\omega l/2) + \exp(-\omega l/2)}{\exp(\omega l/2) - \exp(-\omega l/2)}$$

9-56

Program the shear-lag solution for the shear-stress state into your computer using Eq. (9-7). Determine the maximum shear stress for each of the following scenarios:

Part	E_a , psi	t_o , in	t_i , in	E_o , psi	E_i , psi	h , in
a	$0.2(10^6)$	0.125	0.250	$30(10^6)$	$30(10^6)$	0.005
b	$0.2(10^6)$	0.125	0.250	$30(10^6)$	$30(10^6)$	0.015
c	$0.2(10^6)$	0.125	0.125	$30(10^6)$	$30(10^6)$	0.005
d	$0.2(10^6)$	0.125	0.250	$30(10^6)$	$10(10^6)$	0.005

Provide plots of the actual stress distributions predicted by this analysis. You may omit thermal stresses from the calculations, assuming that the service temperature is similar to the stress-free temperature. If the allowable shear stress is 800 psi and the load to be carried is 300 lbf, estimate the respective factors of safety for each geometry. Let $l = 1.25$ in and $b = 1$ in.

10

Mechanical Springs

Chapter Outline

10-1	Stresses in Helical Springs	518
10-2	The Curvature Effect	519
10-3	Deflection of Helical Springs	520
10-4	Compression Springs	520
10-5	Stability	522
10-6	Spring Materials	523
10-7	Helical Compression Spring Design for Static Service	528
10-8	Critical Frequency of Helical Springs	534
10-9	Fatigue Loading of Helical Compression Springs	536
10-10	Helical Compression Spring Design for Fatigue Loading	539
10-11	Extension Springs	542
10-12	Helical Coil Torsion Springs	550
10-13	Belleville Springs	557
10-14	Miscellaneous Springs	558
10-15	Summary	560

When a designer wants rigidity, negligible deflection is an acceptable approximation as long as it does not compromise function. Flexibility is sometimes needed and is often provided by metal bodies with cleverly controlled geometry. These bodies can exhibit flexibility to the degree the designer seeks. Such flexibility can be linear or nonlinear in relating deflection to load. These devices allow controlled application of force or torque; the storing and release of energy can be another purpose. Flexibility allows temporary distortion for access and the immediate restoration of function. Because of machinery's value to designers, springs have been intensively studied; moreover, they are mass-produced (and therefore low cost), and ingenious configurations have been found for a variety of desired applications. In this chapter we will discuss the more frequently used types of springs, their necessary parametric relationships, and their design.

In general, springs may be classified as wire springs, flat springs, or special-shaped springs, and there are variations within these divisions. Wire springs include helical springs of round or square wire, made to resist and deflect under tensile, compressive, or torsional loads. Flat springs include cantilever and elliptical types, wound motor- or clock-type power springs, and flat spring washers, usually called Belleville springs.

10-1

Stresses in Helical Springs

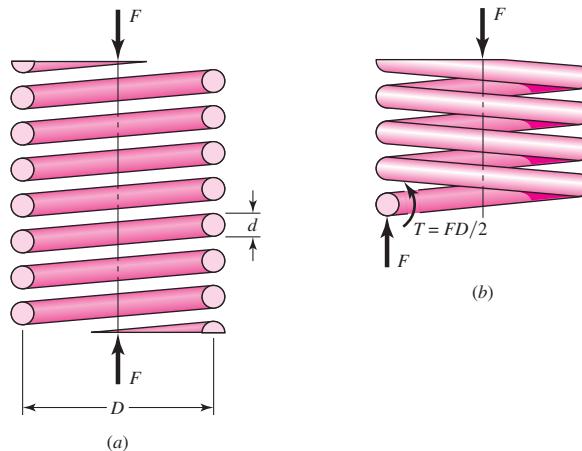
Figure 10-1a shows a round-wire helical compression spring loaded by the axial force F . We designate D as the *mean coil diameter* and d as the *wire diameter*. Now imagine that the spring is cut at some point (Fig. 10-1b), a portion of it removed, and the effect of the removed portion replaced by the net internal reactions. Then, as shown in the figure, from equilibrium the cut portion would contain a direct shear force F and a torsion $T = FD/2$.

The maximum stress in the wire may be computed by superposition of the direct shear stress given by Eq. (3-23), p. 89, with $V = F$ and the torsional shear stress given by Eq. (3-37), p. 101. The result is

$$\tau_{\max} = \frac{Tr}{J} + \frac{F}{A} \quad (a)$$

Figure 10-1

(a) Axially loaded helical spring; (b) free-body diagram showing that the wire is subjected to a direct shear and a torsional shear.



at the *inside* fiber of the spring. Substitution of $\tau_{\max} = \tau$, $T = FD/2$, $r = d/2$, $J = \pi d^4/32$, and $A = \pi d^2/4$ gives

$$\tau = \frac{8FD}{\pi d^3} + \frac{4F}{\pi d^2} \quad (b)$$

Now we define the *spring index*

$$C = \frac{D}{d} \quad (10-1)$$

which is a measure of coil curvature. The preferred value of C ranges from 4 to 12.¹ With this relation, Eq. (b) can be rearranged to give

$$\tau = K_s \frac{8FD}{\pi d^3} \quad (10-2)$$

where K_s is a *shear stress-correction factor* and is defined by the equation

$$K_s = \frac{2C + 1}{2C} \quad (10-3)$$

The use of square or rectangular wire is not recommended for springs unless space limitations make it necessary. Springs of special wire shapes are not made in large quantities, unlike those of round wire; they have not had the benefit of refining development and hence may not be as strong as springs made from round wire. When space is severely limited, the use of nested round-wire springs should always be considered. They may have an economical advantage over the special-section springs, as well as a strength advantage.

10-2 The Curvature Effect

Equation (10-2) is based on the wire being straight. However, the curvature of the wire increases the stress on the inside of the spring but decreases it only slightly on the outside. This curvature stress is primarily important in fatigue because the loads are lower and there is no opportunity for localized yielding. For static loading, these stresses can normally be neglected because of strain-strengthening with the first application of load.

Unfortunately, it is necessary to find the curvature factor in a roundabout way. The reason for this is that the published equations also include the effect of the direct shear stress. Suppose K_s in Eq. (10-2) is replaced by another K factor, which corrects for both curvature and direct shear. Then this factor is given by either of the equations

$$K_W = \frac{4C - 1}{4C - 4} + \frac{0.615}{C} \quad (10-4)$$

$$K_B = \frac{4C + 2}{4C - 3} \quad (10-5)$$

The first of these is called the *Wahl factor*, and the second, the *Bergsträsser factor*.² Since the results of these two equations differ by the order of 1 percent, Eq. (10-6) is preferred. The curvature correction factor can now be obtained by canceling out the

¹Design Handbook: Engineering Guide to Spring Design, Associated Spring-Barnes Group Inc., Bristol, CT, 1987.

²Cyril Samónov, "Some Aspects of Design of Helical Compression Springs," *Int. Symp. Design and Synthesis*, Tokyo, 1984.

effect of the direct shear. Thus, using Eq. (10–5) with Eq. (10–3), the curvature correction factor is found to be

$$K_c = \frac{K_B}{K_s} = \frac{2C(4C + 2)}{(4C - 3)(2C + 1)} \quad (10-6)$$

Now, K_s , K_B or K_W , and K_c are simply stress-correction factors applied multiplicatively to Tr/J at the critical location to estimate a particular stress. There is no stress-concentration factor. In this book we will use

$$\tau = K_B \frac{8FD}{\pi d^3} \quad (10-7)$$

to predict the largest shear stress.

10–3

Deflection of Helical Springs

The deflection-force relations are quite easily obtained by using Castigliano's theorem. The total strain energy for a helical spring is composed of a torsional component and a shear component. From Eqs. (4–18) and (4–20), p. 162, the strain energy is

$$U = \frac{T^2 l}{2GJ} + \frac{F^2 l}{2AG} \quad (a)$$

Substituting $T = FD/2$, $l = \pi DN$, $J = \pi d^4/32$, and $A = \pi d^2/4$ results in

$$U = \frac{4F^2 D^3 N}{d^4 G} + \frac{2F^2 D N}{d^2 G} \quad (b)$$

where $N = N_a$ = number of active coils. Then using Castigliano's theorem, Eq. (4–26), p. 165, to find total deflection y gives

$$y = \frac{\partial U}{\partial F} = \frac{8FD^3 N}{d^4 G} + \frac{4FDN}{d^2 G} \quad (c)$$

Since $C = D/d$, Eq. (c) can be rearranged to yield

$$y = \frac{8FD^3 N}{d^4 G} \left(1 + \frac{1}{2C^2}\right) \doteq \frac{8FD^3 N}{d^4 G} \quad (10-8)$$

The spring rate, also called the *scale* of the spring, is $k = F/y$, and so

$$k \doteq \frac{d^4 G}{8D^3 N} \quad (10-9)$$

10–4

Compression Springs

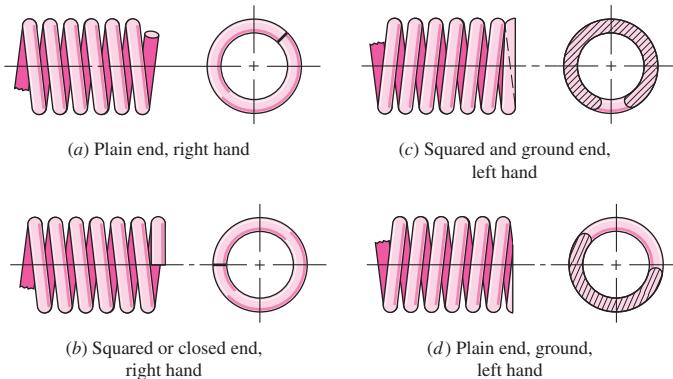
The four types of ends generally used for compression springs are illustrated in Fig. 10–2. A spring with *plain ends* has a noninterrupted helicoid; the ends are the same as if a long spring had been cut into sections. A spring with plain ends that are *squared* or *closed* is obtained by deforming the ends to a zero-degree helix angle. Springs should always be both squared and ground for important applications, because a better transfer of the load is obtained.

Table 10–1 shows how the type of end used affects the number of coils and the spring length.³ Note that the digits 0, 1, 2, and 3 appearing in Table 10–1 are often

³For a thorough discussion and development of these relations, see Cyril Samónov, "Computer-Aided Design of Helical Compression Springs," ASME paper No. 80-DET-69, 1980.

Figure 10-2

Types of ends for compression springs: (a) both ends plain; (b) both ends squared; (c) both ends squared and ground; (d) both ends plain and ground.

**Table 10-1**

Formulas for the Dimensional Characteristics of Compression-Springs. (N_a = Number of Active Coils)

Source: From *Design Handbook*, 1987, p. 32.
Courtesy of Associated Spring.

Term	Plain	Type of Spring Ends		
		Plain and Ground	Squared or Closed	Squared and Ground
End coils, N_e	0	1	2	2
Total coils, N_t	N_a	$N_a + 1$	$N_a + 2$	$N_a + 2$
Free length, L_0	$pN_a + d$	$p(N_a + 1)$	$pN_a + 3d$	$pN_a + 2d$
Solid length, L_s	$d(N_t + 1)$	dN_t	$d(N_t + 1)$	dN_t
Pitch, p	$(L_0 - d)/N_a$	$L_0/(N_a + 1)$	$(L_0 - 3d)/N_a$	$(L_0 - 2d)/N_a$

used without question. Some of these need closer scrutiny as they may not be integers. This depends on how a springmaker forms the ends. Forsy⁴ pointed out that squared and ground ends give a solid length L_s of

$$L_s = (N_t - a)d$$

where a varies, with an average of 0.75, so the entry dN_t in Table 10-1 may be overstated. The way to check these variations is to take springs from a particular springmaker, close them solid, and measure the solid height. Another way is to look at the spring and count the wire diameters in the solid stack.

Set removal or *presetting* is a process used in the manufacture of compression springs to induce useful residual stresses. It is done by making the spring longer than needed and then compressing it to its solid height. This operation *sets* the spring to the required final free length and, since the torsional yield strength has been exceeded, induces residual stresses opposite in direction to those induced in service. Springs to be preset should be designed so that 10 to 30 percent of the initial free length is removed during the operation. If the stress at the solid height is greater than 1.3 times the torsional yield strength, distortion may occur. If this stress is much less than 1.1 times, it is difficult to control the resulting free length.

Set removal increases the strength of the spring and so is especially useful when the spring is used for energy-storage purposes. However, set removal should not be used when springs are subject to fatigue.

⁴Edward L. Forsy, "Accurate Spring Heights," *Machine Design*, vol. 56, no. 2, January 26, 1984.

10-5 Stability

In Chap. 4 we learned that a column will buckle when the load becomes too large. Similarly, compression coil springs may buckle when the deflection becomes too large. The critical deflection is given by the equation

$$y_{\text{cr}} = L_0 C'_1 \left[1 - \left(1 - \frac{C'_2}{\lambda_{\text{eff}}^2} \right)^{1/2} \right] \quad (10-10)$$

where y_{cr} is the deflection corresponding to the onset of instability. Samónov⁵ states that this equation is cited by Wahl⁶ and verified experimentally by Haringx.⁷ The quantity λ_{eff} in Eq. (10-10) is the *effective slenderness ratio* and is given by the equation

$$\lambda_{\text{eff}} = \frac{\alpha L_0}{D} \quad (10-11)$$

C'_1 and C'_2 are elastic constants defined by the equations

$$C'_1 = \frac{E}{2(E - G)}$$

$$C'_2 = \frac{2\pi^2(E - G)}{2G + E}$$

Equation (10-11) contains the *end-condition constant* α . This depends upon how the ends of the spring are supported. Table 10-2 gives values of α for usual end conditions. Note how closely these resemble the end conditions for columns.

Absolute stability occurs when, in Eq. (10-10), the term $C'_2/\lambda_{\text{eff}}^2$ is greater than unity. This means that the condition for absolute stability is that

$$L_0 < \frac{\pi D}{\alpha} \left[\frac{2(E - G)}{2G + E} \right]^{1/2} \quad (10-12)$$

Table 10-2

	End Condition	Constant α
End-Condition Constants α for Helical Compression Springs*		
Spring supported between flat parallel surfaces (fixed ends)		0.5
One end supported by flat surface perpendicular to spring axis (fixed); other end pivoted (hinged)		0.707
Both ends pivoted (hinged)		1
One end clamped; other end free		2

*Ends supported by flat surfaces must be squared and ground.

⁵Cyril Samónov “Computer-Aided Design,” op. cit.

⁶A. M. Wahl, *Mechanical Springs*, 2d ed., McGraw-Hill, New York, 1963.

⁷J. A. Haringx, “On Highly Compressible Helical Springs and Rubber Rods and Their Application for Vibration-Free Mountings,” I and II, *Philips Res. Rep.*, vol. 3, December 1948, pp. 401–449, and vol. 4, February 1949, pp. 49–80.

For steels, this turns out to be

$$L_0 < 2.63 \frac{D}{\alpha} \quad (10-13)$$

For squared and ground ends $\alpha = 0.5$ and $L_0 < 5.26D$.

10-6 Spring Materials

Springs are manufactured either by hot- or cold-working processes, depending upon the size of the material, the spring index, and the properties desired. In general, pre-hardened wire should not be used if $D/d < 4$ or if $d > \frac{1}{4}$ in. Winding of the spring induces residual stresses through bending, but these are normal to the direction of the torsional working stresses in a coil spring. Quite frequently in spring manufacture, they are relieved, after winding, by a mild thermal treatment.

A great variety of spring materials are available to the designer, including plain carbon steels, alloy steels, and corrosion-resisting steels, as well as nonferrous materials such as phosphor bronze, spring brass, beryllium copper, and various nickel alloys. Descriptions of the most commonly used steels will be found in Table 10-3. The UNS steels listed in Appendix A should be used in designing hot-worked, heavy-coil springs, as well as flat springs, leaf springs, and torsion bars.

Spring materials may be compared by an examination of their tensile strengths; these vary so much with wire size that they cannot be specified until the wire size is known. The material and its processing also, of course, have an effect on tensile strength. It turns out that the graph of tensile strength versus wire diameter is almost a straight line for some materials when plotted on log-log paper. Writing the equation of this line as

$$S_{ut} = \frac{A}{d^m} \quad (10-14)$$

furnishes a good means of estimating minimum tensile strengths when the intercept A and the slope m of the line are known. Values of these constants have been worked out from recent data and are given for strengths in units of kpsi and MPa in Table 10-4. In Eq. (10-14) when d is measured in millimeters, then A is in $\text{MPa} \cdot \text{mm}^m$ and when d is measured in inches, then A is in $\text{kpsi} \cdot \text{in}^m$.

Although the torsional yield strength is needed to design the spring and to analyze the performance, spring materials customarily are tested only for tensile strength—perhaps because it is such an easy and economical test to make. A very rough estimate of the torsional yield strength can be obtained by assuming that the tensile yield strength is between 60 and 90 percent of the tensile strength. Then the distortion-energy theory can be employed to obtain the torsional yield strength ($S_{sy} = 0.577S_y$). This approach results in the range

$$0.35S_{ut} \leq S_{sy} \leq 0.52S_{ut} \quad (10-15)$$

for steels.

For wires listed in Table 10-5, the maximum allowable shear stress in a spring can be seen in column 3. Music wire and hard-drawn steel spring wire have a low end of range $S_{sy} = 0.45S_{ut}$. Valve spring wire, Cr-Va, Cr-Si, and other (not shown) hardened and tempered carbon and low-alloy steel wires as a group have $S_{sy} \geq 0.50S_{ut}$. Many nonferrous materials (not shown) as a group have $S_{sy} \geq 0.35S_{ut}$. In view of this,

Table 10-3**High-Carbon and Alloy Spring Steels**

Source: From Harold C. R. Carlson, "Selection and Application of Spring Materials," *Mechanical Engineering*, vol. 78, 1956, pp. 331-334.

Name of Material	Similar Specifications	Description
Music wire, 0.80–0.95C	UNS G10850 AISI 1085 ASTM A228-51	This is the best, toughest, and most widely used of all spring materials for small springs. It has the highest tensile strength and can withstand higher stresses under repeated loading than any other spring material. Available in diameters 0.12 to 3 mm (0.005 to 0.125 in). Do not use above 120°C (250°F) or at subzero temperatures.
Oil-tempered wire, 0.60–0.70C	UNS G10650 AISI 1065 ASTM 229-41	This general-purpose spring steel is used for many types of coil springs where the cost of music wire is prohibitive and in sizes larger than available in music wire. Not for shock or impact loading. Available in diameters 3 to 12 mm (0.125 to 0.500 in), but larger and smaller sizes may be obtained. Not for use above 180°C (350°F) or at subzero temperatures.
Hard-drawn wire, 0.60–0.70C	UNS G10660 AISI 1066 ASTM A227-47	This is the cheapest general-purpose spring steel and should be used only where life, accuracy, and deflection are not too important. Available in diameters 0.8 to 12 mm (0.031 to 0.500 in). Not for use above 120°C (250°F) or at subzero temperatures.
Chrome-vanadium	UNS G61500 AISI 6150 ASTM 231-41	This is the most popular alloy spring steel for conditions involving higher stresses than can be used with the high-carbon steels and for use where fatigue resistance and long endurance are needed. Also good for shock and impact loads. Widely used for aircraft-engine valve springs and for temperatures to 220°C (425°F). Available in annealed or pretempered sizes 0.8 to 12 mm (0.031 to 0.500 in) in diameter.
Chrome-silicon	UNS G92540 AISI 9254	This alloy is an excellent material for highly stressed springs that require long life and are subjected to shock loading. Rockwell hardnesses of C50 to C53 are quite common, and the material may be used up to 250°C (475°F). Available from 0.8 to 12 mm (0.031 to 0.500 in) in diameter.

Table 10-4

Constants A and m of $S_{ut} = A/d^m$ for Estimating Minimum Tensile Strength of Common Spring Wires

Source: From *Design Handbook*, 1987, p. 19. Courtesy of Associated Spring.

Material	ASTM No.	Exponent m	Diameter, in	A, kpsi · in ^m	Diameter, mm	A, MPa · mm ^m	Relative Cost of Wire
Music wire*	A228	0.145	0.004–0.256	201	0.10–6.5	2211	2.6
OQ&T wire†	A229	0.187	0.020–0.500	147	0.5–12.7	1855	1.3
Hard-drawn wire‡	A227	0.190	0.028–0.500	140	0.7–12.7	1783	1.0
Chrome-vanadium wire§	A232	0.168	0.032–0.437	169	0.8–11.1	2005	3.1
Chrome-silicon wire	A401	0.108	0.063–0.375	202	1.6–9.5	1974	4.0
302 Stainless wire#	A313	0.146	0.013–0.10	169	0.3–2.5	1867	7.6–11
		0.263	0.10–0.20	128	2.5–5	2065	
		0.478	0.20–0.40	90	5–10	2911	
Phosphor-bronze wire**	B159	0	0.004–0.022	145	0.1–0.6	1000	8.0
		0.028	0.022–0.075	121	0.6–2	913	
		0.064	0.075–0.30	110	2–7.5	932	

*Surface is smooth, free of defects, and has a bright, lustrous finish.

†Has a slight heat-treating scale which must be removed before plating.

‡Surface is smooth and bright with no visible marks.

§Aircraft-quality tempered wire, can also be obtained annealed.

||Tempered to Rockwell C49, but may be obtained untempered.

#Type 302 stainless steel.

**Temper CA510.

Joerres⁸ uses the maximum allowable torsional stress for static application shown in Table 10-6. For specific materials for which you have torsional yield information use this table as a guide. Joerres provides set-removal information in Table 10-6, that $S_{sy} \geq 0.65S_{ut}$ increases strength through cold work, but at the cost of an additional operation by the springmaker. Sometimes the additional operation can be done by the manufacturer during assembly. Some correlations with carbon steel springs show that the tensile yield strength of spring wire in torsion can be estimated from $0.75S_{ut}$. The corresponding estimate of the yield strength in shear based on distortion energy theory is $S_{sy} = 0.577(0.75)S_{ut} = 0.433S_{ut} \doteq 0.45S_{ut}$. Samónov discusses the problem of allowable stress and shows that

$$S_{sy} = \tau_{all} = 0.56S_{ut} \quad (10-16)$$

for high-tensile spring steels, which is close to the value given by Joerres for hardened alloy steels. He points out that this value of allowable stress is specified by Draft Standard 2089 of the German Federal Republic when Eq. (10-2) is used without stress-correction factor.

⁸Robert E. Joerres, "Springs," Chap. 6 in Joseph E. Shigley, Charles R. Mischke, and Thomas H. Brown, Jr. (eds.), *Standard Handbook of Machine Design*, 3rd ed., McGraw-Hill, New York, 2004.

Table 10-5

Mechanical Properties of Some Spring Wires

Material	Elastic Limit, Percent of S_{ut} Tension Torsion		Diameter d , in	E Mpsi	E GPa	G Mpsi	G GPa
Music wire A228	65–75	45–60	<0.032	29.5	203.4	12.0	82.7
			0.033–0.063	29.0	200	11.85	81.7
			0.064–0.125	28.5	196.5	11.75	81.0
			>0.125	28.0	193	11.6	80.0
HD spring A227	60–70	45–55	<0.032	28.8	198.6	11.7	80.7
			0.033–0.063	28.7	197.9	11.6	80.0
			0.064–0.125	28.6	197.2	11.5	79.3
			>0.125	28.5	196.5	11.4	78.6
Oil tempered A239	85–90	45–50		28.5	196.5	11.2	77.2
Valve spring A230	85–90	50–60		29.5	203.4	11.2	77.2
Chrome-vanadium A231	88–93	65–75		29.5	203.4	11.2	77.2
A232	88–93			29.5	203.4	11.2	77.2
Chrome-silicon A401	85–93	65–75		29.5	203.4	11.2	77.2
Stainless steel							
A313*	65–75	45–55		28	193	10	69.0
17-7PH	75–80	55–60		29.5	208.4	11	75.8
414	65–70	42–55		29	200	11.2	77.2
420	65–75	45–55		29	200	11.2	77.2
431	72–76	50–55		30	206	11.5	79.3
Phosphor-bronze B159	75–80	45–50		15	103.4	6	41.4
Beryllium-copper B197	70	50		17	117.2	6.5	44.8
	75	50–55		19	131	7.3	50.3
Inconel alloy X-750	65–70	40–45		31	213.7	11.2	77.2

*Also includes 302, 304, and 316.

Note: See Table 10-6 for allowable torsional stress design values.

Table 10-6

Maximum Allowable
Torsional Stresses for
Helical Compression
Springs in Static
Applications

Source: Robert E. Joerres,
“Springs,” Chap. 6 in Joseph
E. Shigley, Charles R. Mischke,
and Thomas H. Brown, Jr. (eds.),
*Standard Handbook of Machine
Design*, 3rd ed., McGraw-Hill,
New York, 2004.

Material	Maximum Percent of Tensile Strength	
	Before Set Removed (includes K_w or K_B)	After Set Removed (includes K_s)
Music wire and cold-drawn carbon steel	45	60–70
Hardened and tempered carbon and low-alloy steel	50	65–75
Austenitic stainless steels	35	55–65
Nonferrous alloys	35	55–65

EXAMPLE 10-1

A helical compression spring is made of no. 16 music wire. The outside coil diameter of the spring is $\frac{7}{16}$ in. The ends are squared and there are $12\frac{1}{2}$ total turns.

- Estimate the torsional yield strength of the wire.
- Estimate the static load corresponding to the yield strength.
- Estimate the scale of the spring.
- Estimate the deflection that would be caused by the load in part (b).
- Estimate the solid length of the spring.
- What length should the spring be to ensure that when it is compressed solid and then released, there will be no permanent change in the free length?
- Given the length found in part (f), is buckling a possibility?
- What is the pitch of the body coil?

Solution

(a) From Table A-28, the wire diameter is $d = 0.037$ in. From Table 10-4, we find $A = 201 \text{ kpsi} \cdot \text{in}^m$ and $m = 0.145$. Therefore, from Eq. (10-14)

$$S_{ut} = \frac{A}{d^m} = \frac{201}{0.037^{0.145}} = 324 \text{ kpsi}$$

Then, from Table 10-6,

Answer

$$S_{sy} = 0.45S_{ut} = 0.45(324) = 146 \text{ kpsi}$$

(b) The mean spring coil diameter is $D = \frac{7}{16} - 0.037 = 0.400$ in, and so the spring index is $C = 0.400/0.037 = 10.8$. Then, from Eq. (10-6),

$$K_B = \frac{4C + 2}{4C - 3} = \frac{4(10.8) + 2}{4(10.8) - 3} = 1.124$$

Now rearrange Eq. (10-7) replacing τ with S_{sy} , and solve for F :

Answer

$$F = \frac{\pi d^3 S_{sy}}{8K_B D} = \frac{\pi(0.037^3)146(10^3)}{8(1.124)0.400} = 6.46 \text{ lbf}$$

(c) From Table 10-1, $N_a = 12.5 - 2 = 10.5$ turns. In Table 10-5, $G = 11.85 \text{ Mpsi}$, and the scale of the spring is found to be, from Eq. (10-9),

Answer

$$k = \frac{d^4 G}{8D^3 N_a} = \frac{0.037^4 (11.85)10^6}{8(0.400^3)10.5} = 4.13 \text{ lbf/in}$$

Answer

(d)

$$y = \frac{F}{k} = \frac{6.46}{4.13} = 1.56 \text{ in}$$

(e) From Table 10-1,

Answer

$$L_s = (N_t + 1)d = (12.5 + 1)0.037 = 0.500 \text{ in}$$

Answer

(f)

$$L_0 = y + L_s = 1.56 + 0.500 = 2.06 \text{ in.}$$

(g) To avoid buckling, Eq. (10-13) and Table 10-2 give

$$L_0 < 2.63 \frac{D}{\alpha} = 2.63 \frac{0.400}{0.5} = 2.10 \text{ in}$$

Mathematically, a free length of 2.06 in is less than 2.10 in, and buckling is unlikely. However, the forming of the ends will control how close α is to 0.5. This has to be investigated and an inside rod or exterior tube or hole may be needed.

(h) Finally, from Table 10–1, the pitch of the body coil is

Answer

$$p = \frac{L_0 - 3d}{N_a} = \frac{2.06 - 3(0.037)}{10.5} = 0.186 \text{ in}$$

10–7

Helical Compression Spring Design for Static Service

The preferred range of spring index is $4 \leq C \leq 12$, with the lower indexes being more difficult to form (because of the danger of surface cracking) and springs with higher indexes tending to tangle often enough to require individual packing. This can be the first item of the design assessment. The recommended range of active turns is $3 \leq N_a \leq 15$. To maintain linearity when a spring is about to close, it is necessary to avoid the gradual touching of coils (due to nonperfect pitch). A helical coil spring force-deflection characteristic is ideally linear. Practically, it is nearly so, but not at each end of the force-deflection curve. The spring force is not reproducible for very small deflections, and near closure, nonlinear behavior begins as the number of active turns diminishes as coils begin to touch. The designer confines the spring's operating point to the central 75 percent of the curve between no load, $F = 0$, and closure, $F = F_s$. Thus, the maximum operating force should be limited to $F_{\max} \leq \frac{7}{8}F_s$. Defining the fractional overrun to closure as ξ , where

$$F_s = (1 + \xi)F_{\max} \quad (10-17)$$

it follows that

$$F_s = (1 + \xi)F_{\max} = (1 + \xi)\left(\frac{7}{8}\right)F_s$$

From the outer equality $\xi = 1/7 = 0.143 \doteq 0.15$. Thus, it is recommended that $\xi \geq 0.15$.

In addition to the relationships and material properties for springs, we now have some recommended design conditions to follow, namely:

$$4 \leq C \leq 12 \quad (10-18)$$

$$3 \leq N_a \leq 15 \quad (10-19)$$

$$\xi \geq 0.15 \quad (10-20)$$

$$n_s \geq 1.2 \quad (10-21)$$

where n_s is the factor of safety at closure (solid height).

When considering designing a spring for high volume production, the figure of merit can be the cost of the wire from which the spring is wound. The fom would be proportional to the relative material cost, weight density, and volume:

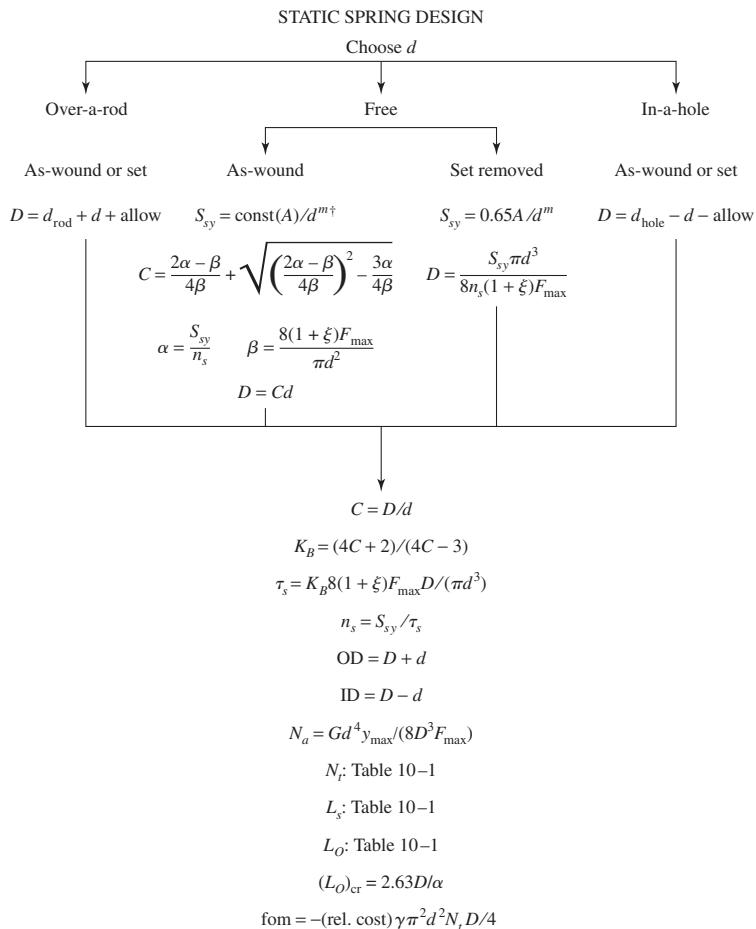
$$\text{fom} = -(\text{relative material cost}) \frac{\gamma \pi^2 d^2 N_a D}{4} \quad (10-22)$$

For comparisons between steels, the specific weight γ can be omitted.

Spring design is an open-ended process. There are many decisions to be made, and many possible solution paths as well as solutions. In the past, charts, nomographs, and "spring design slide rules" were used by many to simplify the spring design problem. Today, the computer enables the designer to create programs in many different formats—direct programming, spreadsheet, MATLAB, etc. Commercial programs are

Figure 10–3

Helical coil compression spring design flowchart for static loading.



Print or display: d , D , C , OD, ID, N_a , N_t , L_s , L_O , $(L_O)_{cr}$, n_s , fom

Build a table, conduct design assessment by inspection

Eliminate infeasible designs by showing active constraints

Choose among satisfactory designs using the figure of merit

[†]const is found from Table 10–6.

also available.⁹ There are almost as many ways to create a spring-design program as there are programmers. Here, we will suggest one possible design approach.

Design Strategy

Make the a priori decisions, with hard-drawn steel wire the first choice (relative material cost is 1.0). Choose a wire size d . With all decisions made, generate a column of parameters: d , D , C , OD or ID, N_a , L_s , L_O , $(L_O)_{cr}$, n_s , and fom. By incrementing wire sizes available, we can scan the table of parameters and apply the design recommendations by inspection. After wire sizes are eliminated, choose the spring design with the highest figure of merit. This will give the optimal design despite the presence of a discrete design variable d and aggregation of equality and inequality constraints. The column vector of information can be generated by using the flowchart displayed in Fig. 10–3. It is general enough to accommodate to the situations of as-wound and

⁹For example, see *Advanced Spring Design*, a program developed jointly between the Spring Manufacturers Institute (SMI), www.smihq.org, and Universal Technical Systems, Inc. (UTS), www.uts.com.

set-removed springs, operating over a rod, or in a hole free of rod or hole. In as-wound springs the controlling equation must be solved for the spring index as follows. From Eq. (10–3) with $\tau = S_{sy}/n_s$, $C = D/d$, K_B from Eq. (10–6), and Eq. (10–17),

$$\frac{S_{sy}}{n_s} = K_B \frac{8F_s D}{\pi d^3} = \frac{4C + 2}{4C - 3} \left[\frac{8(1 + \xi) F_{max} C}{\pi d^2} \right] \quad (a)$$

Let

$$\alpha = \frac{S_{sy}}{n_s} \quad (b)$$

$$\beta = \frac{8(1 + \xi) F_{max}}{\pi d^2} \quad (c)$$

Substituting Eqs. (b) and (c) into (a) and simplifying yields a quadratic equation in C . The larger of the two solutions will yield the spring index

$$C = \frac{2\alpha - \beta}{4\beta} + \sqrt{\left(\frac{2\alpha - \beta}{4\beta} \right)^2 - \frac{3\alpha}{4\beta}} \quad (10-23)$$

EXAMPLE 10-2

A music wire helical compression spring is needed to support a 20-lbf load after being compressed 2 in. Because of assembly considerations the solid height cannot exceed 1 in and the free length cannot be more than 4 in. Design the spring.

Solution

The a priori decisions are

- Music wire, A228; from Table 10–4, $A = 201\ 000 \text{ psi-in}^m$; $m = 0.145$; from Table 10–5, $E = 28.5 \text{ Mpsi}$, $G = 11.75 \text{ Mpsi}$ (expecting $d > 0.064 \text{ in}$)
- Ends squared and ground
- Function: $F_{max} = 20 \text{ lbf}$, $y_{max} = 2 \text{ in}$
- Safety: use design factor at solid height of $(n_s)_d = 1.2$
- Robust linearity: $\xi = 0.15$
- Use as-wound spring (cheaper), $S_{sy} = 0.45S_{ut}$ from Table 10–6
- Decision variable: $d = 0.080 \text{ in}$, music wire gage #30, Table A–28. From Fig. 10–3 and Table 10–6,

$$S_{sy} = 0.45 \frac{201\ 000}{0.080^{0.145}} = 130\ 455 \text{ psi}$$

From Fig. 10–3 or Eq. (10–23)

$$\alpha = \frac{S_{sy}}{n_s} = \frac{130\ 455}{1.2} = 108\ 713 \text{ psi}$$

$$\beta = \frac{8(1 + \xi) F_{max}}{\pi d^2} = \frac{8(1 + 0.15) 20}{\pi (0.080^2)} = 9151.4 \text{ psi}$$

$$C = \frac{2(108\ 713) - 9151.4}{4(9151.4)} + \sqrt{\left[\frac{2(108\ 713) - 9151.4}{4(9151.4)} \right]^2 - \frac{3(108\ 713)}{4(9151.4)}} = 10.53$$

Continuing with Fig. 10–3:

$$D = Cd = 10.53(0.080) = 0.8424 \text{ in}$$

$$K_B = \frac{4(10.53) + 2}{4(10.53) - 3} = 1.128$$

$$\tau_s = 1.128 \frac{8(1 + 0.15)20(0.8424)}{\pi(0.080)^3} = 108\ 700 \text{ psi}$$

$$n_s = \frac{130\ 445}{108\ 700} = 1.2$$

$$\text{OD} = 0.843 + 0.080 = 0.923 \text{ in}$$

$$N_a = \frac{11.75(10^6)0.080^4(2)}{8(0.843)^320} = 10.05 \text{ turns}$$

$$N_t = 10.05 + 2 = 12.05 \text{ total turns}$$

$$L_s = 0.080(12.05) = 0.964 \text{ in}$$

$$L_0 = 0.964 + (1 + 0.15)2 = 3.264 \text{ in}$$

$$(L)_{\text{cr}} = 2.63(0.843/0.5) = 4.43 \text{ in}$$

$$\text{fom} = -2.6\pi^2(0.080)^212.05(0.843)/4 = -0.417$$

Repeat the above for other wire diameters and form a table (easily accomplished with a spreadsheet program):

<i>d</i>	0.063	0.067	0.071	0.075	0.080	0.085	0.090	0.095
<i>D</i>	0.391	0.479	0.578	0.688	0.843	1.017	1.211	1.427
<i>C</i>	6.205	7.153	8.143	9.178	10.53	11.96	13.46	15.02
OD	0.454	0.546	0.649	0.763	0.923	1.102	1.301	1.522
<i>N_a</i>	39.1	26.9	19.3	14.2	10.1	7.3	5.4	4.1
<i>L_s</i>	2.587	1.936	1.513	1.219	0.964	0.790	0.668	0.581
<i>L₀</i>	4.887	4.236	3.813	3.519	3.264	3.090	2.968	2.881
(<i>L₀</i>) _{cr}	2.06	2.52	3.04	3.62	4.43	5.35	6.37	7.51
<i>n_s</i>	1.2	1.2	1.2	1.2	1.2	1.2	1.2	1.2
fom	-0.409	-0.399	-0.398	-0.404	-0.417	-0.438	-0.467	-0.505

Now examine the table and perform the adequacy assessment. The shading of the table indicates values outside the range of recommended or specified values. The spring index constraint $4 \leq C \leq 12$ rules out diameters larger than 0.085 in. The constraint $3 \leq N_a \leq 15$ rules out wire diameters less than 0.075 in. The $L_s \leq 1$ constraint rules out diameters less than 0.080 in. The $L_0 \leq 4$ constraint rules out diameters less than 0.071 in. The buckling criterion rules out free lengths longer than $(L_0)_{\text{cr}}$, which rules out diameters less than 0.075 in. The factor of safety n_s is exactly 1.20 because the

mathematics forced it. Had the spring been in a hole or over a rod, the helix diameter would be chosen without reference to $(n_s)_d$. The result is that there are only two springs in the feasible domain, one with a wire diameter of 0.080 in and the other with a wire diameter of 0.085. The figure of merit decides and the decision is the design with 0.080 in wire diameter.

Having designed a spring, will we have it made to our specifications? Not necessarily. There are vendors who stock literally thousands of music wire compression springs. By browsing their catalogs, we will usually find several that are close. Maximum deflection and maximum load are listed in the display of characteristics. Check to see if this allows soliding without damage. Often it does not. Spring rates may only be close. At the very least this situation allows a small number of springs to be ordered “off the shelf” for testing. The decision often hinges on the economics of special order versus the acceptability of a close match.

Spring design is not a closed-form approach and requires iteration. Example 10–2 provided an iterative approach to spring design for static service by first selecting the wire diameter. The diameter selection can be rather arbitrary. In the next example, we will first select a value for the spring index C , which is within the recommended range.

EXAMPLE 10–3

Design a compression spring with plain ends using hard-drawn wire. The deflection is to be 2.25 in when the force is 18 lbf and to close solid when the force is 24 lbf. Upon closure, use a design factor of 1.2 guarding against yielding. Select the smallest gauge W&M (Washburn & Moen) wire.

Solution

Instead of starting with a trial wire diameter, we will start with an acceptable spring index for C after some preliminaries. From Eq. (10–14) and Table 10–6 the shear strength, in kpsi, is

$$S_{sy} = 0.45S_{ut} = 0.45 \left(\frac{A}{d^m} \right) \quad (1)$$

The shear stress is given by Eq. (10–7) replacing τ and F with τ_{\max} and F_{\max} , respectively, gives

$$\tau_{\max} = K_B \frac{8F_{\max}D}{\pi d^3} = K_B \frac{8F_{\max}C}{\pi d^2} \quad (2)$$

where the Bergsträsser factor, K_B , from Eq. (10–5) is

$$K_B = \frac{4C + 2}{4C - 3} \quad (3)$$

Dividing Eq. (1) by the design factor n and equating this to Eq. (2), in kpsi, gives

$$\frac{0.45}{n} \left(\frac{A}{d^m} \right) = K_B \frac{8F_{\max}C}{\pi d^2} (10^{-3}) \quad (4)$$

For the problem $F_{\max} = 24$ lbf and $n = 1.2$. Solving for d gives

$$d = \left(0.163 \frac{K_B C}{A}\right)^{1/(2-m)} \quad (5)$$

Try a trial spring index of $C = 10$. From Eq. (3)

$$K_B = \frac{4(10) + 2}{4(10) - 3} = 1.135$$

From Table 10–4, $m = 0.190$ and $A = 140$ kpsi · in^{0.190}. Thus, Eq. (5) gives

$$d = \left(0.163 \frac{1.135(10)}{140}\right)^{1/(2-0.190)} = 0.09160 \text{ in}$$

From Table A–28, a 12-gauge W&M wire, $d = 0.105$ 5 in, is selected. Checking the resulting factor of safety, from Eq. (4) with $F_{\max} = 24$ lbf

$$\begin{aligned} n &= 7.363 \frac{Ad^{2-m}}{K_B C} \\ &= 7.363 \frac{140(0.105 5^{2-0.190})}{1.135(10)} = 1.55 \end{aligned} \quad (6)$$

which is pretty conservative. If we had selected the 13-gauge wire, $d = 0.091$ 5 in, the factor of safety would be $n = 1.198$, which rounds to 1.2. Taking a little liberty here we will select the W&M 13-gauge wire.

To continue with the design, the spring rate is

$$k = \frac{F}{y} = \frac{18}{2.25} = 8 \text{ lbf/in}$$

From Eq. (10–9) solving for the active number of coils

$$N_a = \frac{d^4 G}{8kD^3} = \frac{dG}{8kC^3} = \frac{0.0915(11.5)10^6}{8(8)10^3} = 16.4 \text{ turns}$$

This exceeds the recommended range of $3 \leq N_a \leq 15$. To decrease N_a , increase C . Repeating the process with $C = 12$ gives $K_B = 1.111$ and $d = 0.100$ 1 in. Selecting a 12-gauge W&M wire, $d = 0.105$ 5 in. From Eq. (6), this gives $n = 1.32$, which is acceptable. The number of active coils is

$$N_a = \frac{dG}{8kC^3} = \frac{0.1055(11.5)10^6}{8(8)12^3} = 10.97 = 11 \text{ turns}$$

which is acceptable. From Table 10–1, for plain ends, the total number of coils is $N_t = N_a = 11$ turns. The deflection from free length to solid length of the spring is given by

$$y_s = \frac{F_{\max}}{k} = \frac{24}{8} = 3 \text{ in}$$

From Table 10–1, the solid length is

$$L_s = d(N_t + 1) = 0.1055(11 + 1) = 1.266 \text{ in}$$

The free length of the spring is then

$$L_0 = L_s + y_s = 1.266 + 3 = 4.266 \text{ in}$$

The mean coil diameter of the spring is

$$D = Cd = 12(0.1055) = 1.266 \text{ in}$$

and the outside coil diameter of the spring is $OD = D + d = 1.266 + 0.1055 = 1.372 \text{ in.}$

To avoid buckling, Eq. (10–13) gives

$$\alpha < 2.63 \frac{D}{L_0} = 2.63 \frac{1.266}{4.266} = 0.780$$

From Table 10–2, the spring is stable provided it is supported between either fixed-fixed or fixed-hinged ends.

The final results are:

Answer

W&M wire size: 12 gauge, $d = 0.1055 \text{ in}$

Outside coil diameter: $OD = 1.372 \text{ in}$

Total number of coils: $N_t = 11 \text{ turns with plain ends}$

Free length: $L_0 = 4.266 \text{ in}$

10–8

Critical Frequency of Helical Springs

If a wave is created by a disturbance at one end of a swimming pool, this wave will travel down the length of the pool, be reflected back at the far end, and continue in this back-and-forth motion until it is finally damped out. The same effect occurs in helical springs, and it is called *spring surge*. If one end of a compression spring is held against a flat surface and the other end is disturbed, a compression wave is created that travels back and forth from one end to the other exactly like the swimming-pool wave.

Spring manufacturers have taken slow-motion movies of automotive valve-spring surge. These pictures show a very violent surging, with the spring actually jumping out of contact with the end plates. Figure 10–4 is a photograph of a failure caused by such surging.

When helical springs are used in applications requiring a rapid reciprocating motion, the designer must be certain that the physical dimensions of the spring are not such as to create a natural vibratory frequency close to the frequency of the applied force; otherwise, resonance may occur, resulting in damaging stresses, since the internal damping of spring materials is quite low.

The governing equation for the translational vibration of a spring is the wave equation

$$\frac{\partial^2 u}{\partial x^2} = \frac{W}{kg l^2} \frac{\partial^2 u}{\partial t^2} \quad (10-24)$$

where k = spring rate

g = acceleration due to gravity

l = length of spring

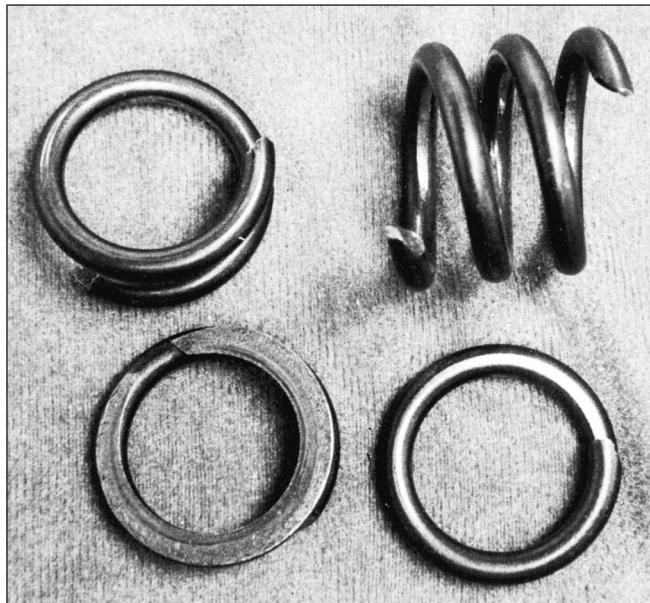
W = weight of spring

x = coordinate along length of spring

u = motion of any particle at distance x

Figure 10-4

Valve-spring failure in an overrevved engine. Fracture is along the 45° line of maximum principal stress associated with pure torsional loading.



The solution to this equation is harmonic and depends on the given physical properties as well as the end conditions of the spring. The harmonic, *natural*, frequencies for a spring placed between two flat and parallel plates, in radians per second, are

$$\omega = m\pi \sqrt{\frac{kg}{W}} \quad m = 1, 2, 3, \dots$$

where the fundamental frequency is found for $m = 1$, the second harmonic for $m = 2$, and so on. We are usually interested in the frequency in cycles per second; since $\omega = 2\pi f$, we have, for the fundamental frequency in hertz,

$$f = \frac{1}{2} \sqrt{\frac{kg}{W}} \quad (10-25)$$

assuming the spring ends are always in contact with the plates.

Wolford and Smith¹⁰ show that the frequency is

$$f = \frac{1}{4} \sqrt{\frac{kg}{W}} \quad (10-26)$$

where the spring has one end against a flat plate and the other end free. They also point out that Eq. (10-25) applies when one end is against a flat plate and the other end is driven with a sine-wave motion.

The weight of the active part of a helical spring is

$$W = AL\gamma = \frac{\pi d^2}{4}(\pi DN_a)(\gamma) = \frac{\pi^2 d^2 D N_a \gamma}{4} \quad (10-27)$$

where γ is the specific weight.

¹⁰J. C. Wolford and G. M. Smith, "Surge of Helical Springs," *Mech. Eng. News*, vol. 13, no. 1, February 1976, pp. 4-9.

The fundamental critical frequency should be greater than 15 to 20 times the frequency of the force or motion of the spring in order to avoid resonance with the harmonics. If the frequency is not high enough, the spring should be redesigned to increase k or decrease W .

10-9

Fatigue Loading of Helical Compression Springs

Springs are almost always subject to fatigue loading. In many instances the number of cycles of required life may be small, say, several thousand for a padlock spring or a toggle-switch spring. But the valve spring of an automotive engine must sustain millions of cycles of operation without failure; so it must be designed for infinite life.

To improve the fatigue strength of dynamically loaded springs, shot peening can be used. It can increase the torsional fatigue strength by 20 percent or more. Shot size is about $\frac{1}{64}$ in, so spring coil wire diameter and pitch must allow for complete coverage of the spring surface.

The best data on the torsional endurance limits of spring steels are those reported by Zimmerli.¹¹ He discovered the surprising fact that size, material, and tensile strength have no effect on the endurance limits (infinite life only) of spring steels in sizes under $\frac{3}{8}$ in (10 mm). We have already observed that endurance limits tend to level out at high tensile strengths (Fig. 6-17), p. 283, but the reason for this is not clear. Zimmerli suggests that it may be because the original surfaces are alike or because plastic flow during testing makes them the same. Unpeened springs were tested from a minimum torsional stress of 20 kpsi to a maximum of 90 kpsi and peened springs in the range 20 kpsi to 135 kpsi. The corresponding endurance strength components for infinite life were found to be

Unpeened:

$$S_{sa} = 35 \text{ kpsi (241 MPa)} \quad S_{sm} = 55 \text{ kpsi (379 MPa)} \quad (10-28)$$

Peened:

$$S_{sa} = 57.5 \text{ kpsi (398 MPa)} \quad S_{sm} = 77.5 \text{ kpsi (534 MPa)} \quad (10-29)$$

For example, given an unpeened spring with $S_{su} = 211.5$ kpsi, the Gerber ordinate intercept for shear, from Eq. (6-42), p. 306, is

$$S_{se} = \frac{S_{sa}}{1 - \left(\frac{S_{sm}}{S_{su}} \right)^2} = \frac{35}{1 - \left(\frac{55}{211.5} \right)^2} = 37.5 \text{ kpsi}$$

For the Goodman failure criterion, the intercept would be 47.3 kpsi. Each possible wire size would change these numbers, since S_{su} would change.

An extended study¹² of available literature regarding torsional fatigue found that for polished, notch-free, cylindrical specimens subjected to torsional shear stress, the maximum alternating stress that may be imposed without causing failure is *constant* and independent of the mean stress in the cycle provided that the maximum stress range does not equal or exceed the torsional yield strength of the metal. With notches and abrupt section changes this consistency is not found. Springs are free of notches and surfaces are often very smooth. This failure criterion is known as the *Sines failure criterion* in torsional fatigue.

¹¹F. P. Zimmerli, "Human Failures in Spring Applications," *The Mainspring*, no. 17, Associated Spring Corporation, Bristol, Conn., August–September 1957.

¹²Oscar J. Horger (ed.), *Metals Engineering: Design Handbook*, McGraw-Hill, New York, 1953, p. 84.

In constructing certain failure criteria on the designers' torsional fatigue diagram, the torsional modulus of rupture S_{su} is needed. We shall continue to employ Eq. (6–54), p. 317, which is

$$S_{su} = 0.67 S_{ut} \quad (10-30)$$

In the case of shafts and many other machine members, fatigue loading in the form of completely reversed stresses is quite ordinary. Helical springs, on the other hand, are never used as both compression and extension springs. In fact, they are usually assembled with a preload so that the working load is additional. Thus the stress-time diagram of Fig. 6–23d, p. 301, expresses the usual condition for helical springs. The worst condition, then, would occur when there is no preload, that is, when $\tau_{\min} = 0$.

Now, we define

$$F_a = \frac{F_{\max} - F_{\min}}{2} \quad (10-31a)$$

$$F_m = \frac{F_{\max} + F_{\min}}{2} \quad (10-31b)$$

where the subscripts have the same meaning as those of Fig. 6–23d when applied to the axial spring force F . Then the shear stress amplitude is

$$\tau_a = K_B \frac{8F_a D}{\pi d^3} \quad (10-32)$$

where K_B is the Bergsträsser factor, obtained from Eq. (10–5), and corrects for both direct shear and the curvature effect. As noted in Sec. 10–2, the Wahl factor K_W can be used instead, if desired.

The midrange shear stress is given by the equation

$$\tau_m = K_B \frac{8F_m D}{\pi d^3} \quad (10-33)$$

EXAMPLE 10–4

An as-wound helical compression spring, made of music wire, has a wire size of 0.092 in, an outside coil diameter of $\frac{9}{16}$ in, a free length of $4\frac{3}{8}$ in, 21 active coils, and both ends squared and ground. The spring is unpeened. This spring is to be assembled with a preload of 5 lbf and will operate with a maximum load of 35 lbf during use.

- (a) Estimate the factor of safety guarding against fatigue failure using a torsional Gerber fatigue failure criterion with Zimmerli data.
- (b) Repeat part (a) using the Sines torsional fatigue criterion (steady stress component has no effect), with Zimmerli data.
- (c) Repeat using a torsional Goodman failure criterion with Zimmerli data.
- (d) Estimate the critical frequency of the spring.

Solution

The mean coil diameter is $D = 0.5625 - 0.092 = 0.4705$ in. The spring index is $C = D/d = 0.4705/0.092 = 5.11$. Then

$$K_B = \frac{4C + 2}{4C - 3} = \frac{4(5.11) + 2}{4(5.11) - 3} = 1.287$$

From Eqs. (10–31),

$$F_a = \frac{35 - 5}{2} = 15 \text{ lbf} \quad F_m = \frac{35 + 5}{2} = 20 \text{ lbf}$$

The alternating shear-stress component is found from Eq. (10–32) to be

$$\tau_a = K_B \frac{8F_a D}{\pi d^3} = (1.287) \frac{8(15)0.4705}{\pi(0.092)^3} (10^{-3}) = 29.7 \text{ kpsi}$$

Equation (10–33) gives the midrange shear-stress component

$$\tau_m = K_B \frac{8F_m D}{\pi d^3} = 1.287 \frac{8(20)0.4705}{\pi(0.092)^3} (10^{-3}) = 39.6 \text{ kpsi}$$

From Table 10–4 we find $A = 201 \text{ kpsi} \cdot \text{in}^m$ and $m = 0.145$. The ultimate tensile strength is estimated from Eq. (10–14) as

$$S_{ut} = \frac{A}{d^m} = \frac{201}{0.092^{0.145}} = 284.1 \text{ kpsi}$$

Also the shearing ultimate strength is estimated from

$$S_{su} = 0.67S_{ut} = 0.67(284.1) = 190.3 \text{ kpsi}$$

The load-line slope $r = \tau_a/\tau_m = 29.7/39.6 = 0.75$.

(a) The Gerber ordinate intercept for the Zimmerli data, Eq. (10–28), is

$$S_{se} = \frac{S_{sa}}{1 - (S_{sm}/S_{su})^2} = \frac{35}{1 - (55/190.3)^2} = 38.2 \text{ kpsi}$$

The amplitude component of strength S_{sa} , from Table 6–7, p. 307, is

$$\begin{aligned} S_{sa} &= \frac{r^2 S_{su}^2}{2S_{se}} \left[-1 + \sqrt{1 + \left(\frac{2S_{se}}{rS_{su}} \right)^2} \right] \\ &= \frac{0.75^2 190.3^2}{2(38.2)} \left\{ -1 + \sqrt{1 + \left[\frac{2(38.2)}{0.75(190.3)} \right]^2} \right\} = 35.8 \text{ kpsi} \end{aligned}$$

and the fatigue factor of safety n_f is given by

Answer

$$n_f = \frac{S_{sa}}{\tau_a} = \frac{35.8}{29.7} = 1.21$$

(b) The Sines failure criterion ignores S_{sm} so that, for the Zimmerli data with $S_{sa} = 35 \text{ kpsi}$,

Answer

$$n_f = \frac{S_{sa}}{\tau_a} = \frac{35}{29.7} = 1.18$$

(c) The ordinate intercept S_{se} for the Goodman failure criterion with the Zimmerli data is

$$S_{se} = \frac{S_{sa}}{1 - (S_{sm}/S_{su})} = \frac{35}{1 - (55/190.3)} = 49.2 \text{ kpsi}$$

The amplitude component of the strength S_{sa} for the Goodman criterion, from Table 6–6, p. 307, is

$$S_{sa} = \frac{r S_{se} S_{su}}{r S_{su} + S_{se}} = \frac{0.75(49.2)190.3}{0.75(190.3) + 49.2} = 36.6 \text{ kpsi}$$

The fatigue factor of safety is given by

Answer

$$n_f = \frac{S_{sa}}{\tau_a} = \frac{36.6}{29.7} = 1.23$$

(d) Using Eq. (10–9) and Table 10–5, we estimate the spring rate as

$$k = \frac{d^4 G}{8D^3 N_a} = \frac{0.092^4 [11.75(10^6)]}{8(0.4705)^3 21} = 48.1 \text{ lbf/in}$$

From Eq. (10–27) we estimate the spring weight as

$$W = \frac{\pi^2 (0.092^2) 0.4705 (21) 0.284}{4} = 0.0586 \text{ lbf}$$

and from Eq. (10–25) the frequency of the fundamental wave is

Answer

$$f_n = \frac{1}{2} \left[\frac{48.1(386)}{0.0586} \right]^{1/2} = 281 \text{ Hz}$$

If the operating or exciting frequency is more than $281/20 = 14.1$ Hz, the spring may have to be redesigned.

We used three approaches to estimate the fatigue factor of safety in Ex. 10–4. The results, in order of smallest to largest, were 1.18 (Sines), 1.21 (Gerber), and 1.23 (Goodman). Although the results were very close to one another, using the Zimmerli data as we have, the Sines criterion will always be the most conservative and the Goodman the least. If we perform a fatigue analysis using strength properties as was done in Chap. 6, different results would be obtained, but here the Goodman criterion would be more conservative than the Gerber criterion. Be prepared to see designers or design software using any one of these techniques. This is why we cover them. Which criterion is correct? Remember, we are performing *estimates* and only testing will reveal the truth—*statistically*.

10–10 Helical Compression Spring Design for Fatigue Loading

Let us begin with the statement of a problem. In order to compare a static spring to a dynamic spring, we shall design the spring in Ex. 10–2 for dynamic service.

EXAMPLE 10–5

A music wire helical compression spring with infinite life is needed to resist a dynamic load that varies from 5 to 20 lbf at 5 Hz while the end deflection varies from $\frac{1}{2}$ to 2 in. Because of assembly considerations, the solid height cannot exceed 1 in and the free length cannot be more than 4 in. The springmaker has the following wire sizes in stock: 0.069, 0.071, 0.080, 0.085, 0.090, 0.095, 0.105, and 0.112 in.

Solution The a priori decisions are:

- Material and condition: for music wire, $A = 201 \text{ kpsi} \cdot \text{in}^m$, $m = 0.145$, $G = 11.75(10^6) \text{ psi}$; relative cost is 2.6
- Surface treatment: unpeened
- End treatment: squared and ground
- Robust linearity: $\xi = 0.15$
- Set: use in as-wound condition
- Fatigue-safe: $n_f = 1.5$ using the Sines-Zimmerli fatigue-failure criterion
- Function: $F_{\min} = 5 \text{ lbf}$, $F_{\max} = 20 \text{ lbf}$, $y_{\min} = 0.5 \text{ in}$, $y_{\max} = 2 \text{ in}$, spring operates free (no rod or hole)
- Decision variable: wire size d

The figure of merit will be the volume of wire to wind the spring, Eq. (10–22). The design strategy will be to set wire size d , build a table, inspect the table, and choose the satisfactory spring with the highest figure of merit.

Solution Set $d = 0.112 \text{ in}$. Then

$$F_a = \frac{20 - 5}{2} = 7.5 \text{ lbf} \quad F_m = \frac{20 + 5}{2} = 12.5 \text{ lbf}$$

$$k = \frac{F_{\max}}{y_{\max}} = \frac{20}{2} = 10 \text{ lbf/in}$$

$$S_{ut} = \frac{201}{0.112^{0.145}} = 276.1 \text{ kpsi}$$

$$S_{su} = 0.67(276.1) = 185.0 \text{ kpsi}$$

$$S_{sy} = 0.45(276.1) = 124.2 \text{ kpsi}$$

From Eq. (10–28), with the Sines criterion, $S_{se} = S_{sa} = 35 \text{ kpsi}$. Equation (10–23) can be used to determine C with S_{se} , n_f , and F_a in place of S_{sy} , n_s , and $(1 + \xi)F_{\max}$, respectively. Thus,

$$\alpha = \frac{S_{se}}{n_f} = \frac{35\,000}{1.5} = 23\,333 \text{ psi}$$

$$\beta = \frac{8F_a}{\pi d^2} = \frac{8(7.5)}{\pi(0.112^2)} = 1522.5 \text{ psi}$$

$$C = \frac{2(23\,333) - 1522.5}{4(1522.5)} + \sqrt{\left[\frac{2(23\,333) - 1522.5}{4(1522.5)} \right]^2 - \frac{3(23\,333)}{4(1522.5)}} = 14.005$$

$$D = Cd = 14.005(0.112) = 1.569 \text{ in}$$

$$F_s = (1 + \xi)F_{\max} = (1 + 0.15)20 = 23 \text{ lbf}$$

$$N_a = \frac{d^4 G}{8D^3 k} = \frac{0.112^4 (11.75)(10^6)}{8(1.569)^3 10} = 5.98 \text{ turns}$$

$$N_t = N_a + 2 = 5.98 + 2 = 7.98 \text{ turns}$$

$$L_s = dN_t = 0.112(7.98) = 0.894 \text{ in}$$

$$L_0 = L_s + \frac{F_s}{k} = 0.894 + \frac{23}{10} = 3.194 \text{ in}$$

$$\text{ID} = 1.569 - 0.112 = 1.457 \text{ in}$$

$$\text{OD} = 1.569 + 0.112 = 1.681 \text{ in}$$

$$y_s = L_0 - L_s = 3.194 - 0.894 = 2.30 \text{ in}$$

$$(L_0)_{\text{cr}} < \frac{2.63D}{\alpha} = 2.63 \frac{(1.569)}{0.5} = 8.253 \text{ in}$$

$$K_B = \frac{4(14.005) + 2}{4(14.005) - 3} = 1.094$$

$$W = \frac{\pi^2 d^2 D N_a \gamma}{4} = \frac{\pi^2 0.112^2 (1.569) 5.98 (0.284)}{4} = 0.0825 \text{ lbf}$$

$$f_n = 0.5 \sqrt{\frac{386k}{W}} = 0.5 \sqrt{\frac{386(10)}{0.0825}} = 108 \text{ Hz}$$

$$\tau_a = K_B \frac{8F_a D}{\pi d^3} = 1.094 \frac{8(7.5)1.569}{\pi 0.112^3} = 23\ 334 \text{ psi}$$

$$\tau_m = \tau_a \frac{F_m}{F_a} = 23\ 334 \frac{12.5}{7.5} = 38\ 890 \text{ psi}$$

$$\tau_s = \tau_a \frac{F_s}{F_a} = 23\ 334 \frac{23}{7.5} = 71\ 560 \text{ psi}$$

$$n_f = \frac{S_{sa}}{\tau_a} = \frac{35\ 000}{23\ 334} = 1.5$$

$$n_s = \frac{S_{sy}}{\tau_s} = \frac{124\ 200}{71\ 560} = 1.74$$

$$\text{fom} = -(\text{relative material cost}) \pi^2 d^2 N_t D / 4$$

$$= -2.6\pi^2(0.112^2)(7.98)1.569/4 = -1.01$$

Inspection of the results shows that all conditions are satisfied except for $4 \leq C \leq 12$. Repeat the process using the other available wire sizes and develop the following table:

d:	0.069	0.071	0.080	0.085	0.090	0.095	0.105	0.112
D	0.297	0.332	0.512	0.632	0.767	0.919	1.274	1.569
ID	0.228	0.261	0.432	0.547	0.677	0.824	1.169	1.457
OD	0.366	0.403	0.592	0.717	0.857	1.014	1.379	1.681
C	4.33	4.67	6.40	7.44	8.53	9.67	12.14	14.00
N_a	127.2	102.4	44.8	30.5	21.3	15.4	8.63	6.0
L_s	8.916	7.414	3.740	2.750	2.100	1.655	1.116	0.895
L_0	11.216	9.714	6.040	5.050	4.400	3.955	3.416	3.195
$(L_0)_{cr}$	1.562	1.744	2.964	3.325	4.036	4.833	6.703	8.250
n_f	1.50	1.50	1.50	1.50	1.50	1.50	1.50	1.50
n_s	1.86	1.85	1.82	1.81	1.79	1.78	1.75	1.74
f_n	87.5	89.7	96.9	99.7	101.9	103.8	106.6	108
fom	-1.17	-1.12	-0.983	-0.948	-0.930	-0.927	-0.958	-1.01

The problem-specific inequality constraints are

$$L_s \leq 1 \text{ in}$$

$$L_0 \leq 4 \text{ in}$$

$$f_n \geq 5(20) = 100 \text{ Hz}$$

The general constraints are

$$3 \leq N_a \leq 15$$

$$4 \leq C \leq 12$$

$$(L_0)_{cr} > L_0$$

We see that none of the diameters satisfy the given constraints. The 0.105-in-diameter wire is the closest to satisfying all requirements. The value of $C = 12.14$ is not a serious deviation and can be tolerated. However, the tight constraint on L_s needs to be addressed. If the assembly conditions can be relaxed to accept a solid height of 1.116 in, we have a solution. If not, the only other possibility is to use the 0.112-in diameter and accept a value $C = 14$, individually package the springs, and possibly reconsider supporting the spring in service.

10-11

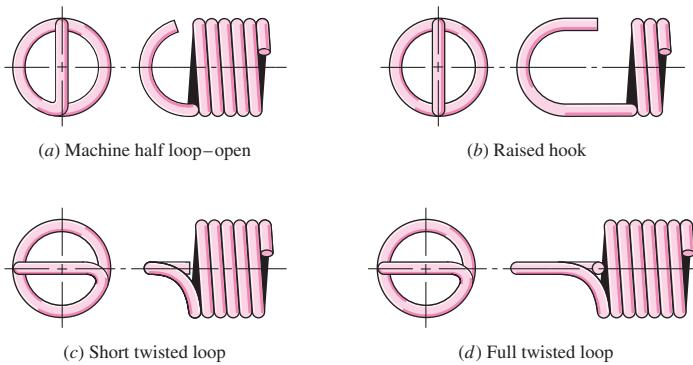
Extension Springs

Extension springs differ from compression springs in that they carry tensile loading, they require some means of transferring the load from the support to the body of the spring, and the spring body is wound with an initial tension. The load transfer can be done with a threaded plug or a swivel hook; both of these add to the cost of the finished product, and so one of the methods shown in Fig. 10-5 is usually employed.

Stresses in the body of the extension spring are handled the same as compression springs. In designing a spring with a hook end, bending and torsion in the hook

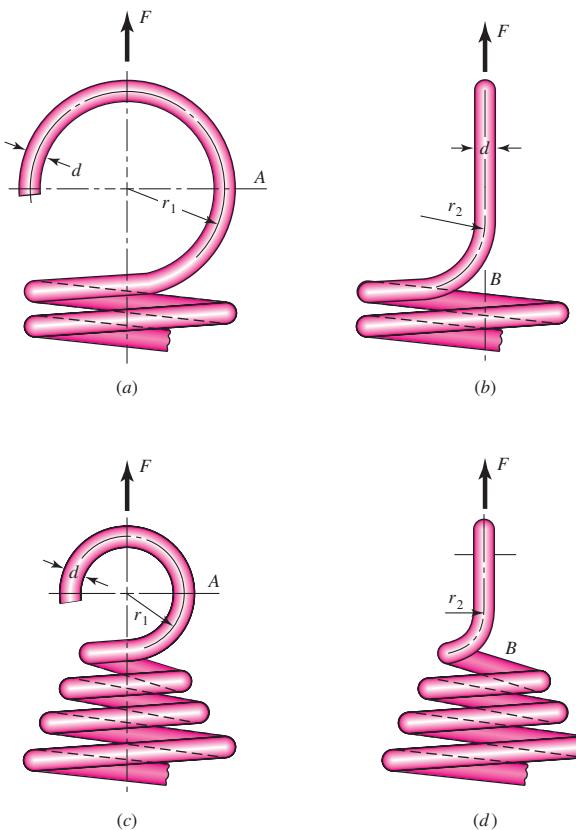
Figure 10-5

Types of ends used on extension springs. (Courtesy of Associated Spring.)

**Figure 10-6**

Ends for extension springs.

(a) Usual design; stress at A is due to combined axial force and bending moment. (b) Side view of part a; stress is mostly torsion at B. (c) Improved design; stress at A is due to combined axial force and bending moment. (d) Side view of part c; stress at B is mostly torsion.



Note: Radius r_1 is in the plane of the end coil for curved beam bending stress. Radius r_2 is at a right angle to the end coil for torsional shear stress.

must be included in the analysis. In Fig. 10-6a and b a commonly used method of designing the end is shown. The maximum tensile stress at A, due to bending and axial loading, is given by

$$\sigma_A = F \left[(K)_A \frac{16D}{\pi d^3} + \frac{4}{\pi d^2} \right] \quad (10-34)$$

where $(K)_A$ is a bending stress-correction factor for curvature, given by

$$(K)_A = \frac{4C_1^2 - C_1 - 1}{4C_1(C_1 - 1)} \quad C_1 = \frac{2r_1}{d} \quad (10-35)$$

The maximum torsional stress at point B is given by

$$\tau_B = (K)_B \frac{8FD}{\pi d^3} \quad (10-36)$$

where the stress-correction factor for curvature, $(K)_B$, is

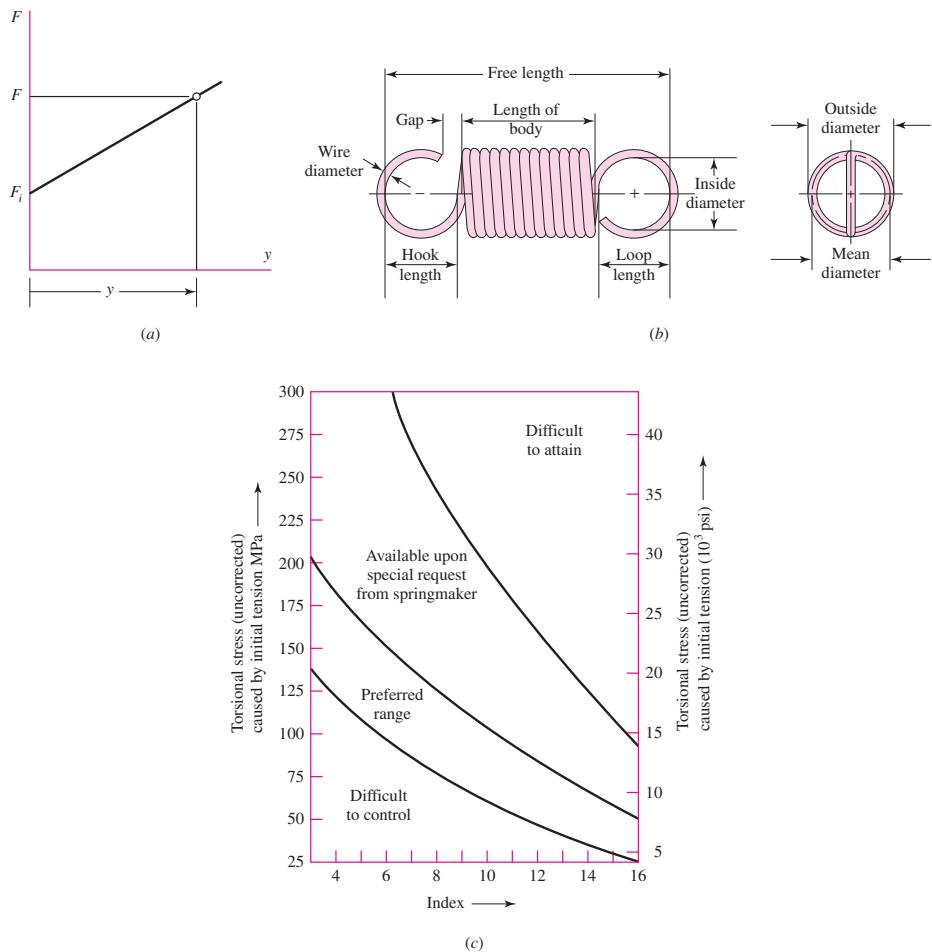
$$(K)_B = \frac{4C_2 - 1}{4C_2 - 4} \quad C_2 = \frac{2r_2}{d} \quad (10-37)$$

Figure 10–6c and d show an improved design due to a reduced coil diameter.

When extension springs are made with coils in contact with one another, they are said to be *close-wound*. Spring manufacturers prefer some initial tension in close-wound springs in order to hold the free length more accurately. The corresponding load-deflection curve is shown in Fig. 10–7a, where y is the extension beyond the free length

Figure 10–7

- (a) Geometry of the force F and extension y curve of an extension spring;
- (b) geometry of the extension spring; and
- (c) torsional stresses due to initial tension as a function of spring index C in helical extension springs.



L_0 and F_i is the initial tension in the spring that must be exceeded before the spring deflects. The load-deflection relation is then

$$F = F_i + ky \quad (10-38)$$

where k is the spring rate. The free length L_0 of a spring measured inside the end loops or hooks as shown in Fig. 10-7b can be expressed as

$$L_0 = 2(D - d) + (N_b + 1)d = (2C - 1 + N_b)d \quad (10-39)$$

where D is the mean coil diameter, N_b is the number of body coils, and C is the spring index. With ordinary twisted end loops as shown in Fig. 10-7b, to account for the deflection of the loops in determining the spring rate k , the equivalent number of active helical turns N_a for use in Eq. (10-9) is

$$N_a = N_b + \frac{G}{E} \quad (10-40)$$

where G and E are the shear and tensile moduli of elasticity, respectively (see Prob. 10-38).

The initial tension in an extension spring is created in the winding process by twisting the wire as it is wound onto the mandrel. When the spring is completed and removed from the mandrel, the initial tension is locked in because the spring cannot get any shorter. The amount of initial tension that a springmaker can routinely incorporate is as shown in Fig. 10-7c. The preferred range can be expressed in terms of the *uncorrected torsional stress* τ_i as

$$\tau_i = \frac{33\,500}{\exp(0.105C)} \pm 1000 \left(4 - \frac{C - 3}{6.5}\right) \text{ psi} \quad (10-41)$$

where C is the spring index.

Guidelines for the maximum allowable corrected stresses for static applications of extension springs are given in Table 10-7.

Table 10-7

Maximum Allowable Stresses (K_W or K_B corrected) for Helical Extension Springs in Static Applications

Source: From *Design Handbook*, 1987, p. 52.
Courtesy of Associated Spring.

Materials	Percent of Tensile Strength		
	In Torsion Body	In Torsion End	In Bending End
Patented, cold-drawn or hardened and tempered carbon and low-alloy steels	45–50	40	75
Austenitic stainless steel and nonferrous alloys	35	30	55

This information is based on the following conditions: set not removed and low temperature heat treatment applied. For springs that require high initial tension, use the same percent of tensile strength as for end.

EXAMPLE 10-6

A hard-drawn steel wire extension spring has a wire diameter of 0.035 in, an outside coil diameter of 0.248 in, hook radii of $r_1 = 0.106$ in and $r_2 = 0.089$ in, and an initial tension of 1.19 lbf. The number of body turns is 12.17. From the given information:

- Determine the physical parameters of the spring.
- Check the initial preload stress conditions.
- Find the factors of safety under a static 5.25-lbf load.

Solution

(a)

$$D = OD - d = 0.248 - 0.035 = 0.213 \text{ in}$$

$$C = \frac{D}{d} = \frac{0.213}{0.035} = 6.086$$

$$K_B = \frac{4C + 2}{4C - 3} = \frac{4(6.086) + 2}{4(6.086) - 3} = 1.234$$

Eq. (10-40) and Table 10-5:

$$N_a = N_b + G/E = 12.17 + 11.6/28.7 = 12.57 \text{ turns}$$

$$\text{Eq. (10-9): } k = \frac{d^4 G}{8D^3 N_a} = \frac{0.035^4 (11.6) 10^6}{8(0.213^3) 12.57} = 17.91 \text{ lbf/in}$$

$$\text{Eq. (10-39): } L_0 = (2C - 1 + N_b)d = [2(6.086) - 1 + 12.17] 0.035 = 0.817 \text{ in}$$

The deflection under the service load is

$$y_{\max} = \frac{F_{\max} - F_i}{k} = \frac{5.25 - 1.19}{17.91} = 0.227 \text{ in}$$

where the spring length becomes $L = L_0 + y = 0.817 + 0.227 = 1.044$ in.

(b) The uncorrected initial stress is given by Eq. (10-2) without the correction factor. That is,

$$(\tau_i)_{\text{uncorr}} = \frac{8F_i D}{\pi d^3} = \frac{8(1.19)0.213(10^{-3})}{\pi(0.035^3)} = 15.1 \text{ ksi}$$

The preferred range is given by Eq. (10-41) and for this case is

$$\begin{aligned} (\tau_i)_{\text{pref}} &= \frac{33.500}{\exp(0.105C)} \pm 1000 \left(4 - \frac{C - 3}{6.5} \right) \\ &= \frac{33.500}{\exp[0.105(6.086)]} \pm 1000 \left(4 - \frac{6.086 - 3}{6.5} \right) \\ &= 17.681 \pm 3525 = 21.2, 14.2 \text{ ksi} \end{aligned}$$

Answer

Thus, the initial tension of 15.1 ksi is in the preferred range.

(c) For hard-drawn wire, Table 10-4 gives $m = 0.190$ and $A = 140 \text{ ksi} \cdot \text{in}^m$. From Eq. (10-14)

$$S_{ut} = \frac{A}{d^m} = \frac{140}{0.035^{0.190}} = 264.7 \text{ ksi}$$

For torsional shear in the main body of the spring, from Table 10-7,

$$S_{sy} = 0.45 S_{ut} = 0.45(264.7) = 119.1 \text{ ksi}$$

The shear stress under the service load is

$$\tau_{\max} = \frac{8K_B F_{\max} D}{\pi d^3} = \frac{8(1.234)5.25(0.213)}{\pi(0.035^3)}(10^{-3}) = 82.0 \text{ kpsi}$$

Thus, the factor of safety is

Answer

$$n = \frac{S_{sy}}{\tau_{\max}} = \frac{119.1}{82.0} = 1.45$$

For the end-hook bending at A,

$$C_1 = 2r_1/d = 2(0.106)/0.035 = 6.057$$

From Eq. (10–35)

$$(K)_A = \frac{4C_1^2 - C_1 - 1}{4C_1(C_1 - 1)} = \frac{4(6.057^2) - 6.057 - 1}{4(6.057)(6.057 - 1)} = 1.14$$

From Eq. (10–34)

$$\begin{aligned} \sigma_A &= F_{\max} \left[(K)_A \frac{16D}{\pi d^3} + \frac{4}{\pi d^2} \right] \\ &= 5.25 \left[1.14 \frac{16(0.213)}{\pi(0.035^3)} + \frac{4}{\pi(0.035^2)} \right] (10^{-3}) = 156.9 \text{ kpsi} \end{aligned}$$

The yield strength, from Table 10–7, is given by

$$S_y = 0.75S_{ut} = 0.75(264.7) = 198.5 \text{ kpsi}$$

The factor of safety for end-hook bending at A is then

Answer

$$n_A = \frac{S_y}{\sigma_A} = \frac{198.5}{156.9} = 1.27$$

For the end-hook in torsion at B, from Eq. (10–37)

$$C_2 = 2r_2/d = 2(0.089)/0.035 = 5.086$$

$$(K)_B = \frac{4C_2 - 1}{4C_2 - 4} = \frac{4(5.086) - 1}{4(5.086) - 4} = 1.18$$

and the corresponding stress, given by Eq. (10–36), is

$$\tau_B = (K)_B \frac{8F_{\max} D}{\pi d^3} = 1.18 \frac{8(5.25)0.213}{\pi(0.035^3)} (10^{-3}) = 78.4 \text{ kpsi}$$

Using Table 10–7 for yield strength, the factor of safety for end-hook torsion at B is

Answer

$$n_B = \frac{(S_{sy})_B}{\tau_B} = \frac{0.4(264.7)}{78.4} = 1.35$$

Yield due to bending of the end hook will occur first.

Next, let us consider a fatigue problem.

EXAMPLE 10-7

The helical coil extension spring of Ex. 10-6 is subjected to a dynamic loading from 1.5 to 5 lbf. Estimate the factors of safety using the Gerber failure criterion for (a) coil fatigue, (b) coil yielding, (c) end-hook bending fatigue at point A of Fig. 10-6a, and (d) end-hook torsional fatigue at point B of Fig. 10-6b.

Solution

A number of quantities are the same as in Ex. 10-6: $d = 0.035$ in, $S_{ut} = 264.7$ kpsi, $D = 0.213$ in, $r_1 = 0.106$ in, $C = 6.086$, $K_B = 1.234$, $(K)_A = 1.14$, $(K)_B = 1.18$, $N_b = 12.17$ turns, $L_0 = 0.817$ in, $k = 17.91$ lbf/in, $F_i = 1.19$ lbf, and $(\tau_i)_{uncorr} = 15.1$ kpsi. Then

$$F_a = (F_{\max} - F_{\min})/2 = (5 - 1.5)/2 = 1.75 \text{ lbf}$$

$$F_m = (F_{\max} + F_{\min})/2 = (5 + 1.5)/2 = 3.25 \text{ lbf}$$

The strengths from Ex. 10-6 include $S_{ut} = 264.7$ kpsi, $S_y = 198.5$ kpsi, and $S_{sy} = 119.1$ kpsi. The ultimate shear strength is estimated from Eq. (10-30) as

$$S_{su} = 0.67S_{ut} = 0.67(264.7) = 177.3 \text{ kpsi}$$

(a) Body-coil fatigue:

$$\tau_a = \frac{8K_B F_a D}{\pi d^3} = \frac{8(1.234)1.75(0.213)}{\pi(0.035^3)}(10^{-3}) = 27.3 \text{ kpsi}$$

$$\tau_m = \frac{F_m}{F_a} \tau_a = \frac{3.25}{1.75} 27.3 = 50.7 \text{ kpsi}$$

Using the Zimmerli data of Eq. (10-28) gives

$$S_{se} = \frac{S_{sa}}{1 - \left(\frac{S_{sm}}{S_{su}}\right)^2} = \frac{35}{1 - \left(\frac{55}{177.3}\right)^2} = 38.7 \text{ kpsi}$$

From Table 6-7, p. 307, the Gerber fatigue criterion for shear is

Answer

$$(n_f)_{\text{body}} = \frac{1}{2} \left(\frac{S_{su}}{\tau_m} \right)^2 \frac{\tau_a}{S_{se}} \left[-1 + \sqrt{1 + \left(2 \frac{\tau_m}{S_{su}} \frac{S_{se}}{\tau_a} \right)^2} \right]$$

$$= \frac{1}{2} \left(\frac{177.3}{50.7} \right)^2 \frac{27.3}{38.7} \left[-1 + \sqrt{1 + \left(2 \frac{50.7}{177.3} \frac{38.7}{27.3} \right)^2} \right] = 1.24$$

(b) The load-line for the coil body begins at $S_{sm} = \tau_i$ and has a slope $r = \tau_a / (\tau_m - \tau_i)$. It can be shown that the intersection with the yield line is given by $(S_{sa})_y = [r/(r+1)](S_{sy} - \tau_i)$. Consequently, $\tau_i = (F_i/F_a)\tau_a = (1.19/1.75)27.3 = 18.6$ kpsi, $r = 27.3/(50.7 - 18.6) = 0.850$, and

$$(S_{sa})_y = \frac{0.850}{0.850 + 1}(119.1 - 18.6) = 46.2 \text{ kpsi}$$

Thus,

Answer

$$(n_y)_{\text{body}} = \frac{(S_{sa})_y}{\tau_a} = \frac{46.2}{27.3} = 1.69$$

(c) End-hook bending fatigue: using Eqs. (10–34) and (10–35) gives

$$\begin{aligned}\sigma_a &= F_a \left[(K)_A \frac{16D}{\pi d^3} + \frac{4}{\pi d^2} \right] \\ &= 1.75 \left[1.14 \frac{16(0.213)}{\pi(0.035^3)} + \frac{4}{\pi(0.035^2)} \right] (10^{-3}) = 52.3 \text{ kpsi} \\ \sigma_m &= \frac{F_m}{F_a} \sigma_a = \frac{3.25}{1.75} 52.3 = 97.1 \text{ kpsi}\end{aligned}$$

To estimate the tensile endurance limit using the distortion-energy theory,

$$S_e = S_{se}/0.577 = 38.7/0.577 = 67.1 \text{ kpsi}$$

Using the Gerber criterion for tension gives

$$\begin{aligned}\text{Answer } (n_f)_A &= \frac{1}{2} \left(\frac{S_{ut}}{\sigma_m} \right)^2 \frac{\sigma_a}{S_e} \left[-1 + \sqrt{1 + \left(2 \frac{\sigma_m}{S_{ut}} \frac{S_e}{\sigma_a} \right)^2} \right] \\ &= \frac{1}{2} \left(\frac{264.7}{97.1} \right)^2 \frac{52.3}{67.1} \left[-1 + \sqrt{1 + \left(2 \frac{97.1}{264.7} \frac{67.1}{52.3} \right)^2} \right] = 1.08\end{aligned}$$

(d) End-hook torsional fatigue: from Eq. (10–36)

$$\begin{aligned}(\tau_a)_B &= (K)_B \frac{8F_a D}{\pi d^3} = 1.18 \frac{8(1.75)0.213}{\pi(0.035^3)} (10^{-3}) = 26.1 \text{ kpsi} \\ (\tau_m)_B &= \frac{F_m}{F_a} (\tau_a)_B = \frac{3.25}{1.75} 26.1 = 48.5 \text{ kpsi}\end{aligned}$$

Then, again using the Gerber criterion, we obtain

$$\begin{aligned}\text{Answer } (n_f)_B &= \frac{1}{2} \left(\frac{S_{su}}{\tau_m} \right)^2 \frac{\tau_a}{S_{se}} \left[-1 + \sqrt{1 + \left(2 \frac{\tau_m}{S_{su}} \frac{S_{se}}{\tau_a} \right)^2} \right] \\ &= \frac{1}{2} \left(\frac{177.3}{48.5} \right)^2 \frac{26.1}{38.7} \left[-1 + \sqrt{1 + \left(2 \frac{48.5}{177.3} \frac{38.7}{26.1} \right)^2} \right] = 1.30\end{aligned}$$

The analyses in Exs. 10–6 and 10–7 show how extension springs differ from compression springs. The end hooks are usually the weakest part, with bending usually controlling. We should also appreciate that a fatigue failure separates the extension spring under load. Flying fragments, lost load, and machine shutdown are threats to personal safety as well as machine function. For these reasons higher design factors are used in extension-spring design than in the design of compression springs.

In Ex. 10–7 we estimated the endurance limit for the hook in bending using the Zimmerli data, which are based on torsion in compression springs and the distortion theory. An alternative method is to use Table 10–8, which is based on a stress-ratio of $R = \tau_{\min}/\tau_{\max} = 0$. For this case, $\tau_a = \tau_m = \tau_{\max}/2$. Label the strength values of

Table 10–8

Maximum Allowable Stresses for ASTM A228 and Type 302 Stainless Steel Helical Extension Springs in Cyclic Applications

Source: From *Design Handbook*, 1987, p. 52.
Courtesy of Associated Spring.

Number of Cycles	Percent of Tensile Strength		
	In Torsion Body	In Torsion End	In Bending End
10^5	36	34	51
10^6	33	30	47
10^7	30	28	45

This information is based on the following conditions: not shot-peened, no surging and ambient environment with a low temperature heat treatment applied.
Stress ratio = 0.

Table 10–8 as S_r for bending or S_{sr} for torsion. Then for torsion, for example, $S_{sa} = S_{sm} = S_{sr}/2$ and the Gerber ordinate intercept, given by Eq. (6–42) for shear, is

$$S_{se} = \frac{S_{sa}}{1 - (S_{sm}/S_{su})^2} = \frac{S_{sr}/2}{1 - \left(\frac{S_{sr}/2}{S_{su}}\right)^2} \quad (10-42)$$

So in Ex. 10–7 an estimate for the bending endurance limit from Table 10–8 would be

$$S_r = 0.45S_{ut} = 0.45(264.7) = 119.1 \text{ kpsi}$$

and from Eq. (10–42)

$$S_e = \frac{S_r/2}{1 - [S_r / (2S_{ut})]^2} = \frac{119.1/2}{1 - \left(\frac{119.1/2}{264.7}\right)^2} = 62.7 \text{ kpsi}$$

Using this in place of 67.1 kpsi in Ex. 10–7 results in $(n_f)_A = 1.03$, a reduction of 5 percent.

10–12

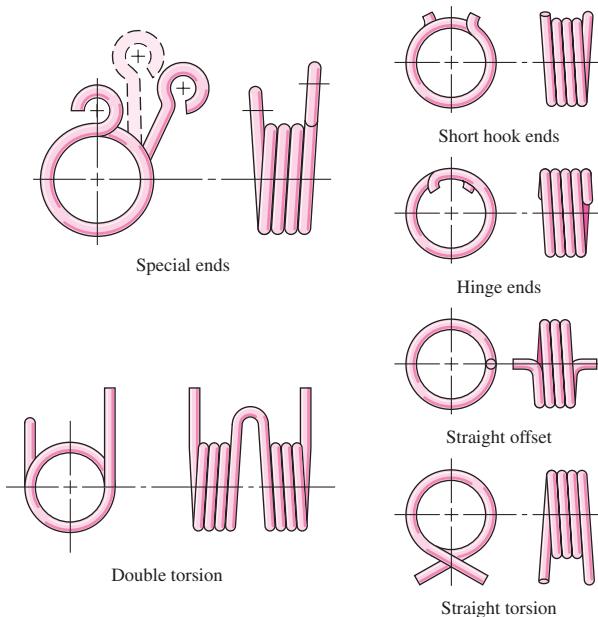
Helical Coil Torsion Springs

When a helical coil spring is subjected to end torsion, it is called a *torsion spring*. It is usually close-wound, as is a helical coil extension spring, but with negligible initial tension. There are single-bodied and double-bodied types as depicted in Fig. 10–8. As shown in the figure, torsion springs have ends configured to apply torsion to the coil body in a convenient manner, with short hook, hinged straight offset, straight torsion, and special ends. The ends ultimately connect a force at a distance from the coil axis to apply a torque. The most frequently encountered (and least expensive) end is the straight torsion end. If intercoil friction is to be avoided completely, the spring can be wound with a pitch that just separates the body coils. Helical coil torsion springs are usually used with a rod or arbor for reactive support when ends cannot be built in, to maintain alignment, and to provide buckling resistance if necessary.

The wire in a torsion spring is in bending, in contrast to the torsion encountered in helical coil compression and extension springs. The springs are designed to wind tighter in service. As the applied torque increases, the inside diameter of the coil decreases. Care must be taken so that the coils do not interfere with the pin, rod, or arbor. The bending mode in the coil might seem to invite square- or rectangular-cross-section wire, but cost, range of materials, and availability discourage its use.

Figure 10–8

Torsion springs. (Courtesy of Associated Spring.)

**Table 10–9**

End Position Tolerances
for Helical Coil Torsion
Springs (for D/d Ratios
up to and Including 16)

Source: From *Design Handbook*, 1987, p. 52.
Courtesy of Associated Spring.

Total Coils	Tolerance: \pm Degrees*
Up to 3	8
Over 3–10	10
Over 10–20	15
Over 20–30	20
Over 30	25

*Closer tolerances available on request.

Torsion springs are familiar in clothespins, window shades, and animal traps, where they may be seen around the house, and out of sight in counterbalance mechanisms, ratchets, and a variety of other machine components. There are many stock springs that can be purchased off-the-shelf from a vendor. This selection can add economy of scale to small projects, avoiding the cost of custom design and small-run manufacture.

Describing the End Location

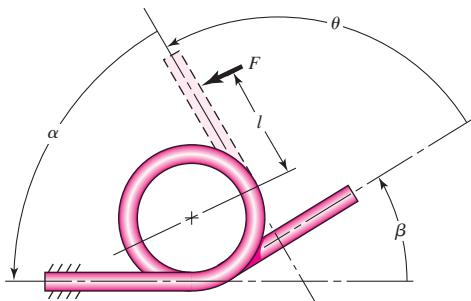
In specifying a torsion spring, the ends must be located relative to each other. Commercial tolerances on these relative positions are listed in Table 10–9. The simplest scheme for expressing the initial unloaded location of one end with respect to the other is in terms of an angle β defining the partial turn present in the coil body as $N_p = \beta/360^\circ$, as shown in Fig. 10–9. For analysis purposes the nomenclature of Fig. 10–9 can be used. Communication with a springmaker is often in terms of the back-angle α .

The number of body turns N_b is the number of turns in the free spring body by count. The body-turn count is related to the initial position angle β by

$$N_b = \text{integer} + \frac{\beta}{360^\circ} = \text{integer} + N_p$$

Figure 10-9

The free-end location angle is β . The rotational coordinate θ is proportional to the product Fl . Its back angle is α . For all positions of the moving end $\theta + \alpha = \Sigma = \text{constant}$.



where N_p is the number of partial turns. The above equation means that N_b takes on noninteger, discrete values such as 5.3, 6.3, 7.3, . . . , with successive differences of 1 as possibilities in designing a specific spring. This consideration will be discussed later.

Bending Stress

A torsion spring has bending induced in the coils, rather than torsion. This means that residual stresses built in during winding are in the same direction but of opposite sign to the working stresses that occur during use. The strain-strengthening locks in residual stresses opposing working stresses *provided* the load is always applied in the winding sense. Torsion springs can operate at bending stresses exceeding the yield strength of the wire from which it was wound.

The bending stress can be obtained from curved-beam theory expressed in the form

$$\sigma = K \frac{Mc}{I}$$

where K is a stress-correction factor. The value of K depends on the shape of the wire cross section and whether the stress sought is at the inner or outer fiber. Wahl analytically determined the values of K to be, for round wire,

$$K_i = \frac{4C^2 - C - 1}{4C(C - 1)} \quad K_o = \frac{4C^2 + C - 1}{4C(C + 1)} \quad (10-43)$$

where C is the spring index and the subscripts i and o refer to the inner and outer fibers, respectively. In view of the fact that K_o is always less than unity, we shall use K_i to estimate the stresses. When the bending moment is $M = Fr$ and the section modulus $I/c = d^3/32$, we express the bending equation as

$$\sigma = K_i \frac{32Fr}{\pi d^3} \quad (10-44)$$

which gives the bending stress for a round-wire torsion spring.

Deflection and Spring Rate

For torsion springs, angular deflection can be expressed in radians or revolutions (turns). If a term contains revolution units the term will be expressed with a prime sign. The spring rate k' is expressed in units of torque/revolution (lbf · in/rev or N · mm/rev) and moment is proportional to angle θ' expressed in turns rather than radians. The spring rate, if linear, can be expressed as

$$k' = \frac{M_1}{\theta'_1} = \frac{M_2}{\theta'_2} = \frac{M_2 - M_1}{\theta'_2 - \theta'_1} \quad (10-45)$$

where the moment M can be expressed as Fl or Fr .

The angle subtended by the end deflection of a cantilever, when viewed from the built-in ends, is y/l rad. From Table A-9-1,

$$\theta_e = \frac{y}{l} = \frac{Fl^2}{3EI} = \frac{Fl^2}{3E(\pi d^4/64)} = \frac{64Ml}{3\pi d^4 E} \quad (10-46)$$

For a straight torsion end spring, end corrections such as Eq. (10-46) must be added to the body-coil deflection. The strain energy in bending is, from Eq. (4-23),

$$U = \int \frac{M^2 dx}{2EI}$$

For a torsion spring, $M = Fl = Fr$, and integration must be accomplished over the length of the body-coil wire. The force F will deflect through a distance $r\theta$ where θ is the angular deflection of the coil body, in radians. Applying Castiglione's theorem gives

$$r\theta = \frac{\partial U}{\partial F} = \int_0^{\pi DN_b} \frac{\partial}{\partial F} \left(\frac{F^2 r^2 dx}{2EI} \right) = \int_0^{\pi DN_b} \frac{Fr^2 dx}{EI}$$

Substituting $I = \pi d^4/64$ for round wire and solving for θ gives

$$\theta = \frac{64FrDN_b}{d^4 E} = \frac{64MDN_b}{d^4 E}$$

The total angular deflection in radians is obtained by adding Eq. (10-46) for each end of lengths l_1, l_2 :

$$\theta_t = \frac{64MDN_b}{d^4 E} + \frac{64Ml_1}{3\pi d^4 E} + \frac{64Ml_2}{3\pi d^4 E} = \frac{64MD}{d^4 E} \left(N_b + \frac{l_1 + l_2}{3\pi D} \right) \quad (10-47)$$

The equivalent number of active turns N_a is expressed as

$$N_a = N_b + \frac{l_1 + l_2}{3\pi D} \quad (10-48)$$

The spring rate k in torque per radian is

$$k = \frac{Fr}{\theta_t} = \frac{M}{\theta_t} = \frac{d^4 E}{64DN_a} \quad (10-49)$$

The spring rate may also be expressed as torque per turn. The expression for this is obtained by multiplying Eq. (10-49) by 2π rad/turn. Thus spring rate k' (units torque/turn) is

$$k' = \frac{2\pi d^4 E}{64DN_a} = \frac{d^4 E}{10.2DN_a} \quad (10-50)$$

Tests show that the effect of friction between the coils and arbor is such that the constant 10.2 should be increased to 10.8. The equation above becomes

$$k' = \frac{d^4 E}{10.8DN_a} \quad (10-51)$$

(units torque per turn). Equation (10-51) gives better results. Also Eq. (10-47) becomes

$$\theta'_t = \frac{10.8MD}{d^4 E} \left(N_b + \frac{l_1 + l_2}{3\pi D} \right) \quad (10-52)$$

Torsion springs are frequently used over a round bar or pin. When the load is applied to a torsion spring, the spring winds up, causing a decrease in the inside diameter of the coil body. It is necessary to ensure that the inside diameter of the coil never becomes equal to or less than the diameter of the pin, in which case loss of spring function would ensue. The helix diameter of the coil D' becomes

$$D' = \frac{N_b D}{N_b + \theta'_c} \quad (10-53)$$

where θ'_c is the angular deflection of the body of the coil in number of turns, given by

$$\theta'_c = \frac{10.8 M D N_b}{d^4 E} \quad (10-54)$$

The new inside diameter $D'_i = D' - d$ makes the diametral clearance Δ between the body coil and the pin of diameter D_p equal to

$$\Delta = D' - d - D_p = \frac{N_b D}{N_b + \theta'_c} - d - D_p \quad (10-55)$$

Equation (10-55) solved for N_b is

$$N_b = \frac{\theta'_c(\Delta + d + D_p)}{D - \Delta - d - D_p} \quad (10-56)$$

which gives the number of body turns corresponding to a specified diametral clearance of the arbor. This angle may not be in agreement with the necessary partial-turn remainder. Thus the diametral clearance may be exceeded but not equaled.

Static Strength

First column entries in Table 10-6 can be divided by 0.577 (from distortion-energy theory) to give

$$S_y = \begin{cases} 0.78 S_{ut} & \text{Music wire and cold-drawn carbon steels} \\ 0.87 S_{ut} & \text{OQ&T carbon and low-alloy steels} \\ 0.61 S_{ut} & \text{Austenitic stainless steel and nonferrous alloys} \end{cases} \quad (10-57)$$

Fatigue Strength

Since the spring wire is in bending, the Sines equation is not applicable. The Sines model is in the presence of pure torsion. Since Zimmerli's results were for compression springs (wire in pure torsion), we will use the repeated bending stress ($R = 0$) values provided by Associated Spring in Table 10-10. As in Eq. (10-40) we will use the Gerber fatigue-failure criterion incorporating the Associated Spring $R = 0$ fatigue strength S_r :

$$S_e = \frac{S_r / 2}{1 - \left(\frac{S_r / 2}{S_{ut}} \right)^2} \quad (10-58)$$

The value of S_r (and S_e) has been corrected for size, surface condition, and type of loading, but not for temperature or miscellaneous effects. The Gerber fatigue criterion is now defined. The strength-amplitude component is given by Table 6-7, p. 307, as

$$S_a = \frac{r^2 S_{ut}^2}{2 S_e} \left[-1 + \sqrt{1 + \left(\frac{2 S_e}{r S_{ut}} \right)^2} \right] \quad (10-59)$$

Table 10-10

Maximum Recommended Bending Stresses (K_B Corrected) for Helical Torsion Springs in Cyclic Applications as Percent of S_{ut}

Source: Courtesy of Associated Spring.

Fatigue Life, Cycles	ASTM A228 and Type 302 Stainless Steel		ASTM A230 and A232	
	Not Shot-Peened	Shot-Peened*	Not Shot-Peened	Shot-Peened*
10^5	53	62	55	64
10^6	50	60	53	62

This information is based on the following conditions: no surging, springs are in the "as-stress-relieved" condition.

*Not always possible.

where the slope of the load line is $r = M_a/M_m$. The load line is radial through the origin of the designer's fatigue diagram. The factor of safety guarding against fatigue failure is

$$n_f = \frac{S_a}{\sigma_a} \quad (10-60)$$

Alternatively, we can find n_f directly by using Table 6-7, p. 307:

$$n_f = \frac{1}{2} \frac{\sigma_a}{S_e} \left(\frac{S_{ut}}{\sigma_m} \right)^2 \left[-1 + \sqrt{1 + \left(2 \frac{\sigma_m}{S_{ut}} \frac{S_e}{\sigma_a} \right)^2} \right] \quad (10-61)$$

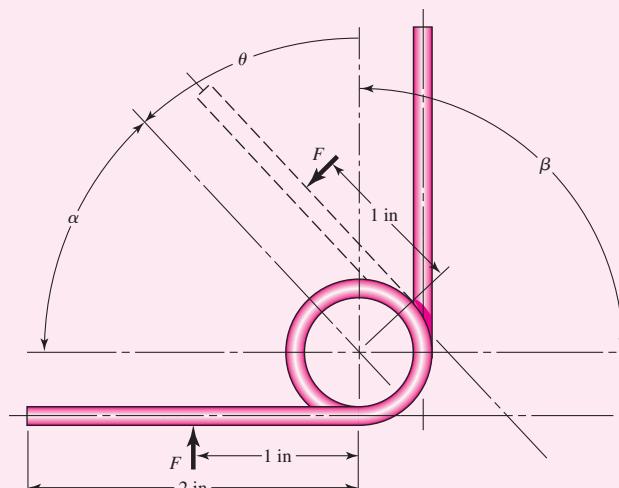
EXAMPLE 10-8

A stock spring is shown in Fig. 10-10. It is made from 0.072-in-diameter music wire and has $4\frac{1}{4}$ body turns with straight torsion ends. It works over a pin of 0.400 in diameter. The coil outside diameter is $\frac{19}{32}$ in.

- (a) Find the maximum operating torque and corresponding rotation for static loading.
- (b) Estimate the inside coil diameter and pin diametral clearance when the spring is subjected to the torque in part (a).

Figure 10-10

Angles α , β , and θ are measured between the straight-end centerline translated to the coil axis. Coil OD is $\frac{19}{32}$ in.



(c) Estimate the fatigue factor of safety n_f if the applied moment varies between $M_{\min} = 1$ to $M_{\max} = 5$ lbf · in.

Solution

(a) For music wire, from Table 10–4 we find that $A = 201$ kpsi · in^m and $m = 0.145$. Therefore,

$$S_{ut} = \frac{A}{d^m} = \frac{201}{(0.072)^{0.145}} = 294.4 \text{ kpsi}$$

Using Eq. (10–57) gives

$$S_y = 0.78S_{ut} = 0.78(294.4) = 229.6 \text{ kpsi}$$

The mean coil diameter is $D = 19/32 - 0.072 = 0.5218$ in. The spring index $C = D/d = 0.5218/0.072 = 7.247$. The bending stress-correction factor K_i from Eq. (10–43), is

$$K_i = \frac{4(7.247)^2 - 7.247 - 1}{4(7.247)(7.247 - 1)} = 1.115$$

Now rearrange Eq. (10–44), substitute S_y for σ , and solve for the maximum torque Fr to obtain

$$M_{\max} = (Fr)_{\max} = \frac{\pi d^3 S_y}{32 K_i} = \frac{\pi (0.072)^3 229.600}{32(1.115)} = 7.546 \text{ lbf} \cdot \text{in}$$

Note that no factor of safety has been used. Next, from Eq. (10–54) and Table 10–5, the number of turns of the coil body θ'_c is

$$\theta'_c = \frac{10.8 M D N_b}{d^4 E} = \frac{10.8(7.546)0.5218(4.25)}{0.072^4(28.5)10^6} = 0.236 \text{ turn}$$

Answer

$$(\theta'_c)_{\deg} = 0.236(360^\circ) = 85.0^\circ$$

The active number of turns N_a , from Eq. (10–48), is

$$N_a = N_b + \frac{l_1 + l_2}{3\pi D} = 4.25 + \frac{1 + 1}{3\pi(0.5218)} = 4.657 \text{ turns}$$

The spring rate of the complete spring, from Eq. (10–51), is

$$k' = \frac{0.072^4(28.5)10^6}{10.8(0.5218)4.657} = 29.18 \text{ lbf} \cdot \text{in/turn}$$

The number of turns of the complete spring θ' is

$$\theta' = \frac{M}{k'} = \frac{7.546}{29.18} = 0.259 \text{ turn}$$

Answer

$$(\theta'_s)_{\deg} = 0.259(360^\circ) = 93.24^\circ$$

(b) With no load, the mean coil diameter of the spring is 0.5218 in. From Eq. (10–53),

$$D' = \frac{N_b D}{N_b + \theta'_c} = \frac{4.25(0.5218)}{4.25 + 0.236} = 0.494 \text{ in}$$

The diametral clearance between the inside of the spring coil and the pin at load is

Answer

$$\Delta = D' - d - D_p = 0.494 - 0.072 - 0.400 = 0.022 \text{ in}$$

(c) Fatigue:

$$M_a = (M_{\max} - M_{\min})/2 = (5 - 1)/2 = 2 \text{ lbf} \cdot \text{in}$$

$$M_m = (M_{\max} + M_{\min})/2 = (5 + 1)/2 = 3 \text{ lbf} \cdot \text{in}$$

$$r = \frac{M_a}{M_m} = \frac{2}{3}$$

$$\sigma_a = K_i \frac{32M_a}{\pi d^3} = 1.115 \frac{32(2)}{\pi 0.072^3} = 60\,857 \text{ psi}$$

$$\sigma_m = \frac{M_m}{M_a} \sigma_a = \frac{3}{2}(60\,857) = 91\,286 \text{ psi}$$

From Table 10–10, $S_r = 0.50S_{ut} = 0.50(294.4) = 147.2$ kpsi. Then

$$S_e = \frac{147.2/2}{1 - \left(\frac{147.2/2}{294.4}\right)^2} = 78.51 \text{ kpsi}$$

The amplitude component of the strength S_a , from Eq. (10–59), is

$$S_a = \frac{(2/3)^2 294.4^2}{2(78.51)} \left[-1 + \sqrt{1 + \left(\frac{2}{2/3} \frac{78.51}{294.4}\right)^2} \right] = 68.85 \text{ kpsi}$$

The fatigue factor of safety is

Answer

$$n_f = \frac{S_a}{\sigma_a} = \frac{68.85}{60.86} = 1.13$$

10–13 Belleville Springs

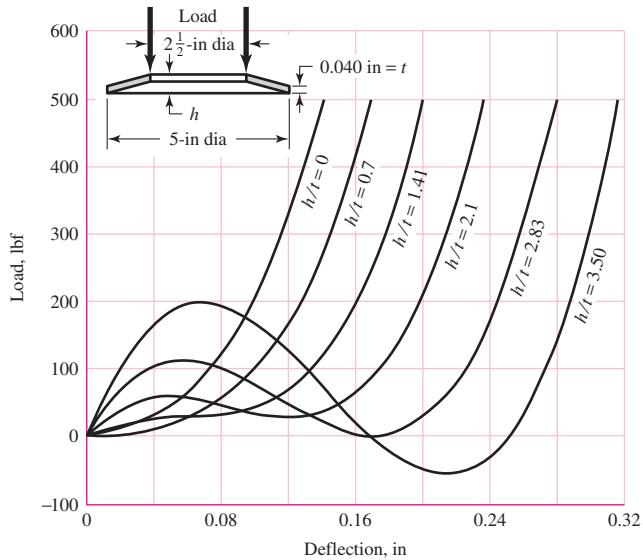
The inset of Fig. 10–11 shows the cross-section of a coned-disk spring, commonly called a *Belleville spring*. Although the mathematical treatment is beyond the scope of this book, you should at least become familiar with the remarkable characteristics of these springs.

Aside from the obvious advantage that a Belleville spring occupies only a small space, variation in the h/t ratio will produce a wide variety of load-deflection curve shapes, as illustrated in Fig. 10–11. For example, using an h/t ratio of 2.83 or larger gives an S curve that might be useful for snap-acting mechanisms. A reduction of the ratio to a value between 1.41 and 2.1 causes the central portion of the curve to become horizontal, which means that the load is constant over a considerable deflection range.

A higher load for a given deflection may be obtained by nesting, that is, by stacking the springs in parallel. On the other hand, stacking in series provides a larger deflection for the same load, but in this case there is danger of instability.

Figure 10-11

Load-deflection curves for Belleville springs. (Courtesy of Associated Spring.)



10-14 Miscellaneous Springs

The extension spring shown in Fig. 10-12 is made of slightly curved strip steel, not flat, so that the force required to uncoil it remains constant; thus it is called a *constant-force spring*. This is equivalent to a zero spring rate. Such springs can also be manufactured having either a positive or a negative spring rate.

A *volute spring*, shown in Fig. 10-13a, is a wide, thin strip, or "flat," of material wound on the flat so that the coils fit inside one another. Since the coils do not stack, the solid height of the spring is the width of the strip. A variable-spring scale, in a compression volute spring, is obtained by permitting the coils to contact the support. Thus, as the deflection increases, the number of active coils decreases. The volute spring has another important advantage that cannot be obtained with round-wire springs: if the coils are wound so as to contact or slide on one another during action, the sliding friction will serve to damp out vibrations or other unwanted transient disturbances.

A *conical spring*, as the name implies, is a coil spring wound in the shape of a cone (see Prob. 10-28). Most conical springs are compression springs and are wound with round wire. But a volute spring is a conical spring too. Probably the principal advantage of this type of spring is that it can be wound so that the solid height is only a single wire diameter.

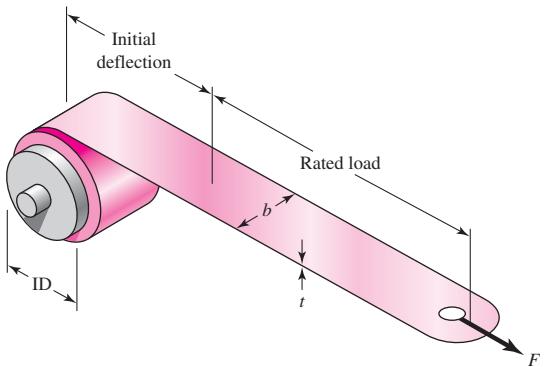
Flat stock is used for a great variety of springs, such as clock springs, power springs, torsion springs, cantilever springs, and hair springs; frequently it is specially shaped to create certain spring actions for fuse clips, relay springs, spring washers, snap rings, and retainers.

In designing many springs of flat stock or strip material, it is often economical and of value to proportion the material so as to obtain a constant stress throughout the spring material. A uniform-section cantilever spring has a stress

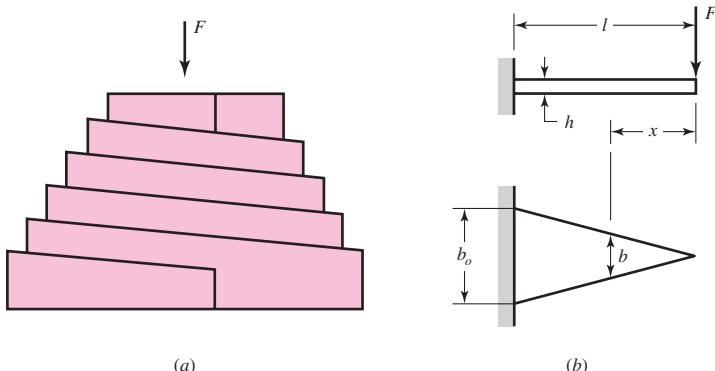
$$\sigma = \frac{M}{I/c} = \frac{Fx}{I/c} \quad (a)$$

Figure 10-12

Constant-force spring.
(Courtesy of Vulcan Spring & Mfg. Co., Telford, PA.
www.vulcanspring.com)

**Figure 10-13**

(a) A volute spring; (b) a flat triangular spring.



which is proportional to the distance x if I/c is a constant. But there is no reason why I/c need be a constant. For example, one might design such a spring as that shown in Fig. 10-13b, in which the thickness h is constant but the width b is permitted to vary. Since, for a rectangular section, $I/c = bh^2/6$, we have, from Eq. (a),

$$\frac{bh^2}{6} = \frac{Fx}{\sigma}$$

or

$$b = \frac{6Fx}{h^2\sigma} \quad (10-62)$$

Since b is linearly related to x , the width b_o at the base of the spring is

$$b_o = \frac{6Fl}{h^2\sigma} \quad (10-62)$$

Good approximations for deflections can be found easily by using Castiglione's theorem. To demonstrate this, assume that deflection of the triangular flat spring is primarily due to bending and we can neglect the transverse shear force.¹³ The bending moment as a function of x is $M = -Fx$ and the beam width at x can be expressed

¹³Note that, because of shear, the width of the beam cannot be zero at $x = 0$. So, there is already some simplification in the design model. All of this can be accounted for in a more sophisticated model.

as $b = b_o x/l$. Thus, the deflection of F is given by Eq. (4–31), p. 166, as

$$\begin{aligned} y &= \int_0^l \frac{M(\partial M/\partial F)}{EI} dx = \frac{1}{E} \int_0^l \frac{-Fx(-x)}{\frac{1}{12}(b_o x/l)h^3} dx \\ &= \frac{12Fl}{b_o h^3 E} \int_0^l x dx = \frac{6Fl^3}{b_o h^3 E} \end{aligned} \quad (10-63)$$

Thus the spring constant, $k = F/y$, is estimated as

$$k = \frac{b_o h^3 E}{6l^3} \quad (10-64)$$

The methods of stress and deflection analysis illustrated in previous sections of this chapter have served to illustrate that springs may be analyzed and designed by using the fundamentals discussed in the earlier chapters of this book. This is also true for most of the miscellaneous springs mentioned in this section, and you should now experience no difficulty in reading and understanding the literature of such springs.

10-15 Summary

In this chapter we have considered helical coil springs in considerable detail in order to show the importance of viewpoint in approaching engineering problems, their analysis, and design. For compression springs undergoing static and fatigue loads, the complete design process was presented. This was not done for extension and torsion springs, as the process is the same, although the governing conditions are not. The governing conditions, however, were provided and extension to the design process from what was provided for the compression spring should be straightforward. Problems are provided at the end of the chapter, and it is hoped that the reader will develop additional, similar, problems to tackle.

Stochastic considerations are notably missing in this chapter. The complexity and nuances of the deterministic approach alone are enough to handle in a first presentation of spring design. Springmakers offer a vast array of information concerning tolerances on springs.¹⁴ This, together with the material in Chaps. 5, 6, and 20, should provide the reader with ample ability to advance and incorporate statistical analyses in their design evaluations.

As spring problems become more computationally involved, programmable calculators and computers must be used. Spreadsheet programming is very popular for repetitive calculations. As mentioned earlier, commercial programs are available. With these programs, backsolving can be performed; that is, when the final objective criteria are entered, the program determines the input values.

PROBLEMS

10-1

Within the range of recommended values of the spring index, C , determine the maximum and minimum percentage difference between the Bergsträsser factor, K_B , and the Wahl factor, K_W .

¹⁴See, for example, Associated Spring–Barnes Group, *Design Handbook*, Bristol, Conn., 1987.

10-2

It is instructive to examine the question of the units of the parameter A of Eq. (10-14). Show that for U.S. customary units the units for A_{uscu} are $\text{kpsi} \cdot \text{in}^m$ and for SI units are $\text{MPa} \cdot \text{mm}^m$ for A_{SI} , which make the dimensions of both A_{uscu} and A_{SI} different for every material to which Eq. (10-14) applies. Also show that the conversion from A_{uscu} to A_{SI} is given by

$$A_{\text{SI}} = 6.895(25.40)^m A_{\text{uscu}}$$

10-3

A helical compression spring is wound using 2.5-mm-diameter music wire. The spring has an outside diameter of 31 mm with plain ground ends, and 14 total coils.

- (a) What should the free length be to ensure that when the spring is compressed solid the torsional stress does not exceed the yield strength, that is, that it is solid-safe?
- (b) What force is needed to compress this spring to closure?
- (c) Estimate the spring rate.
- (d) Is there a possibility that the spring might buckle in service?

10-4

The spring in Prob. 10-3 is to be used with a static load of 130 N. Perform a design assessment represented by Eqs. (10-13) and (10-18) through (10-21) if the spring is closed to solid height.

10-5

A helical compression spring is made with oil-tempered wire with wire diameter of 0.2 in, mean coil diameter of 2 in, a total of 12 coils, a free length of 5 in, with squared ends.

- (a) Find the solid length.
- (b) Find the force necessary to deflect the spring to its solid length.
- (c) Find the factor of safety guarding against yielding when the spring is compressed to its solid length.

10-6

A helical compression spring is to be made of oil-tempered wire of 4-mm diameter with a spring index of $C = 10$. The spring is to operate inside a hole, so buckling is not a problem and the ends can be left plain. The free length of the spring should be 80 mm. A force of 50 N should deflect the spring 15 mm.

- (a) Determine the spring rate.
- (b) Determine the minimum hole diameter for the spring to operate in.
- (c) Determine the total number of coils needed.
- (d) Determine the solid length.
- (e) Determine a static factor of safety based on the yielding of the spring if it is compressed to its solid length.

10-7

A helical compression spring is made of hard-drawn spring steel wire 0.080-in in diameter and has an outside diameter of 0.880 in. The ends are plain and ground, and there are 8 total coils.

- (a) The spring is wound to a free length, which is the largest possible with a solid-safe property. Find this free length.
- (b) What is the pitch of this spring?
- (c) What force is needed to compress the spring to its solid length?
- (d) Estimate the spring rate.
- (e) Will the spring buckle in service?

10-8

The spring of Prob. 10-7 is to be used with a static load of 16.5 lbf. Perform a design assessment represented by Eqs. (10-13) and (10-18) through (10-21) if the spring closed to solid height.

**10-9 to
10-19**

Listed in the tables are six springs described in customary units and five springs described in SI units. Investigate these squared-and-ground-ended helical compression springs to see if they are solid-safe. If not, what is the largest free length to which they can be wound using $n_s = 1.2$?

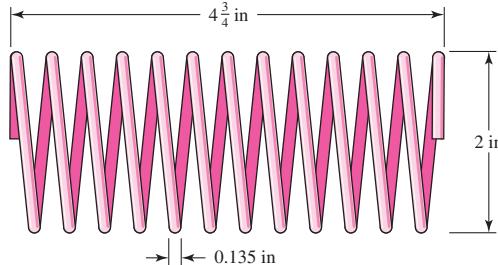
Problem Number	d , in	OD, in	L_0 , in	N ,	Material
10-9	0.007	0.038	0.58	38	A228 music wire
10-10	0.014	0.128	0.50	16	B159 phosphor-bronze
10-11	0.050	0.250	0.68	11.2	A313 stainless steel
10-12	0.148	2.12	2.5	5.75	A227 hard-drawn steel
10-13	0.138	0.92	2.86	12	A229 OQ&T steel
10-14	0.185	2.75	7.5	8	A232 chrome-vanadium
	d , mm	OD, mm	L_0 , mm	N ,	Material
10-15	0.25	0.95	12.1	38	A313 stainless steel
10-16	1.2	6.5	15.7	10.2	A228 music wire
10-17	3.5	50.6	75.5	5.5	A229 OQ&T spring steel
10-18	3.8	31.4	71.4	12.8	B159 phosphor-bronze
10-19	4.5	69.2	215.6	8.2	A232 chrome-vanadium

10-20

Consider the steel spring in the illustration.

- (a) Find the pitch, solid height, and number of active turns.
- (b) Find the spring rate. Assume the material is A227 HD steel.
- (c) Find the force F_s required to close the spring solid.
- (d) Find the shear stress in the spring due to the force F_s .

Problem 10-20

**10-21**

A static service music wire helical compression spring is needed to support a 20-lbf load after being compressed 2 in. The solid height of the spring cannot exceed $1\frac{1}{2}$ in. The free length must not exceed 4 in. The static factor of safety must equal or exceed 1.2. For robust linearity use a fractional overrun to closure ξ of 0.15. There are two springs to be designed. Start with a wire diameter of 0.075 in.

- (a) The spring must operate over a $\frac{3}{4}$ -in rod. A 0.050-in diametral clearance allowance should be adequate to avoid interference between the rod and the spring due to out-of-round coils. Design the spring.
- (b) The spring must operate in a 1-in-diameter hole. A 0.050-in diametral clearance allowance should be adequate to avoid interference between the spring and the hole due to swelling of the spring diameter as the spring is compressed and out-of-round coils. Design the spring.

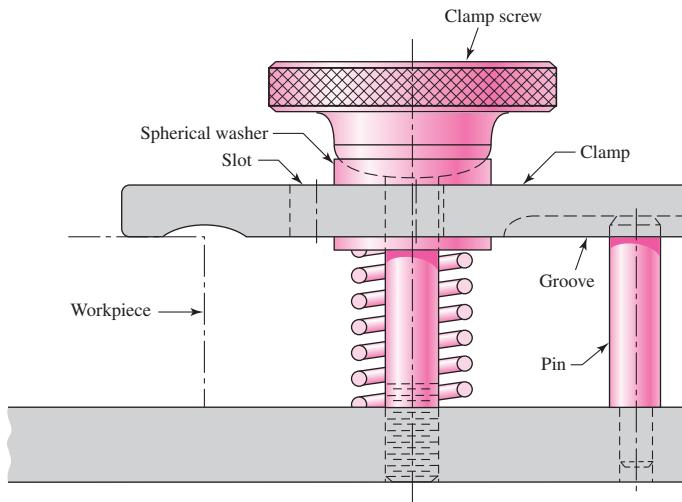
10-22

Solve Prob. 10-21 by iterating with an initial value of $C = 10$. If you have already solved Prob. 10-21, compare the steps and the results.

10-23

A holding fixture for a workpiece 37.5 mm thick at the clamp locations is being designed. The detail of one of the clamps is shown in the figure. A spring is required to drive the clamp upward when removing the workpiece with a starting force of 45 N. The clamp screw has an M10 × 1.25 thread. Allow a diametral clearance of 1.25 mm between it and the uncompressed spring. It is further specified that the free length of the spring should be $L_0 \leq 48$ mm, the solid height $L_s \leq 31.5$ mm, and the safety factor when closed solid should be $n_s \geq 1.2$. Starting with $d = 2$ mm, design a suitable helical coil compression spring for this fixture. Wire diameters are available in 0.2-mm increments between 0.2 to 3.2 mm.

*Problem 10-23
Clamping fixture.*

**10-24**

Solve Prob. 10-23 by iterating with an initial value of $C = 8$. If you have already solved Prob. 10-23, compare the steps and the results.

10-25

Your instructor will provide you with a stock spring supplier's catalog, or pages reproduced from it. Accomplish the task of Prob. 10-23 by selecting an available stock spring. (This is design by *selection*.)

10-26

A compression spring is needed to fit over a 0.5-in diameter rod. To allow for some clearance, the inside diameter of the spring is to be 0.6 in. To ensure a reasonable coil, use a spring index of 10. The spring is to be used in a machine by compressing it from a free length of 5 in through a stroke of 3 in to its solid length. The spring should have squared and ground ends, unpeened, and is to be made from cold-drawn wire.

- (a) Determine a suitable wire diameter.
- (b) Determine a suitable total number of coils.
- (c) Determine the spring constant.
- (d) Determine the static factor of safety when compressed to solid length.
- (e) Determine the fatigue factor of safety when repeatedly cycled from free length to solid length.

10-27

A compression spring is needed to fit within a 1-in diameter hole. To allow for some clearance, the outside diameter of the spring is to be no larger than 0.9 in. To ensure a reasonable coil, use a spring index of 8. The spring is to be used in a machine by compressing it from a

free length of 3 in to a solid length of 1 in. The spring should have squared ends, and is unpeened, and is to be made from music wire.

- (a) Determine a suitable wire diameter.
- (b) Determine a suitable total number of coils.
- (c) Determine the spring constant.
- (d) Determine the static factor of safety when compressed to solid length.
- (e) Determine the fatigue factor of safety when repeatedly cycled from free length to solid length.

10-28

A helical compression spring is to be cycled between 150 lbf and 300 lbf with a 1-in stroke. The number of cycles is low, so fatigue is not an issue. The coil must fit in a 2.1-in diameter hole with a 0.1-in clearance all the way around the spring. Use unpeened music wire with squared and ground ends.

- (a) Determine a suitable wire diameter, using a spring index of $C = 7$.
- (b) Determine a suitable mean coil diameter.
- (c) Determine the necessary spring constant.
- (d) Determine a suitable total number of coils.
- (e) Determine the necessary free length so that if the spring were compressed to its solid length, there would be no yielding.

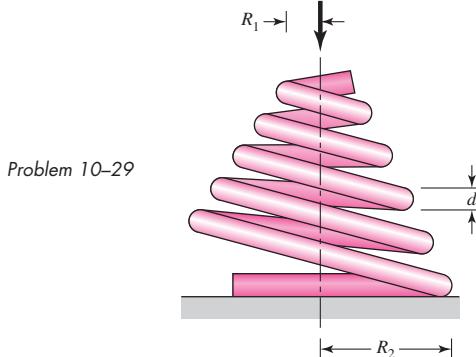
10-29

The figure shows a conical compression helical coil spring where R_1 and R_2 are the initial and final coil radii, respectively, d is the diameter of the wire, and N_a is the total number of active coils. The wire cross section primarily transmits a torsional moment, which changes with the coil radius. Let the coil radius be given by

$$R = R_1 + \frac{R_2 - R_1}{2\pi N_a} \theta$$

where θ is in radians. Use Castigliano's method to estimate the spring rate as

$$k = \frac{d^4 G}{16N_a(R_2 + R_1)(R_2^2 + R_1^2)}$$

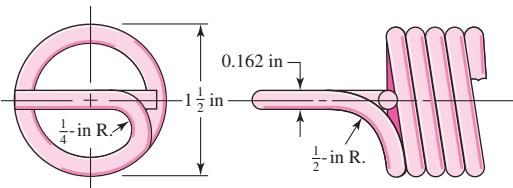


10-30

A helical coil compression spring is needed for food service machinery. The load varies from a minimum of 4 lbf to a maximum of 18 lbf. The spring rate k is to be 9.5 lbf/in. The outside diameter of the spring cannot exceed $2\frac{1}{2}$ in. The springmaker has available suitable dies for drawing 0.080-, 0.0915-, 0.1055-, and 0.1205-in-diameter wire. Using a fatigue design factor n_f of 1.5, and the Gerber-Zimmerli fatigue-failure criterion, design a suitable spring.

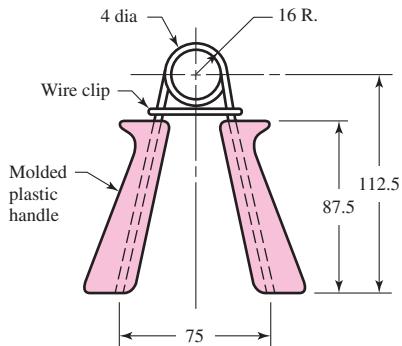
- 10-31** Solve Prob. 10-30 using the Goodman-Zimmerli fatigue-failure criterion.
- 10-32** Solve Prob. 10-30 using the Sines-Zimmerli fatigue-failure criterion.
- 10-33** Design the spring of Ex. 10-5 using the Gerber fatigue-failure criterion.
- 10-34** Solve Prob. 10-33 using the Goodman-Zimmerli fatigue-failure criterion.
- 10-35** A hard-drawn spring steel extension spring is to be designed to carry a static load of 18 lbf with an extension of $\frac{1}{2}$ in using a design factor of $n_y = 1.5$ in bending. Use full-coil end hooks with the fullest bend radius of $r = D/2$ and $r_2 = 2d$. The free length must be less than 3 in, and the body turns must be fewer than 30. Integer and half-integer body turns allow end hooks to be placed in the same plane. This adds extra cost and is done only when necessary.
- 10-36** The extension spring shown in the figure has full-twisted loop ends. The material is AISI 1065 OQ&T wire. The spring has 84 coils and is close-wound with a preload of 16 lbf.
 (a) Find the closed length of the spring.
 (b) Find the torsional stress in the spring corresponding to the preload.
 (c) Estimate the spring rate.
 (d) What load would cause permanent deformation?
 (e) What is the spring deflection corresponding to the load found in part *d*?

Problem 10-36



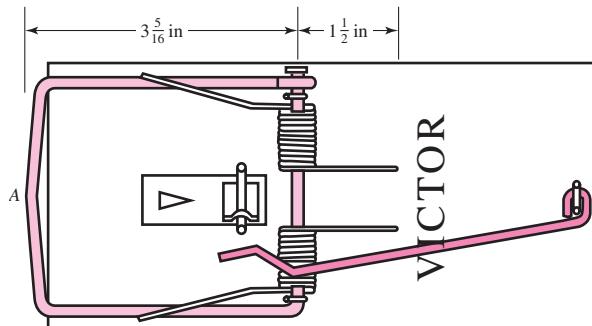
- 10-37** Design an infinite-life helical coil extension spring with full end loops and generous loop-bend radii for a minimum load of 9 lbf and a maximum load of 18 lbf, with an accompanying stretch of $\frac{1}{4}$ in. The spring is for food-service equipment and must be stainless steel. The outside diameter of the coil cannot exceed 1 in, and the free length cannot exceed $2\frac{1}{2}$ in. Using a fatigue design factor of $n_f = 2$, complete the design.
- 10-38** Prove Eq. (10-40). *Hint:* Using Castiglione's theorem, determine the deflection due to bending of an end hook alone as if the hook were fixed at the end connecting it to the body of the spring. Consider the wire diameter d small as compared to the mean radius of the hook, $R = D/2$. Add the deflections of the end hooks to the deflection of the main body to determine the final spring constant, then equate it to Eq. (10-9).
- 10-39** The figure shows a finger exerciser used by law-enforcement officers and athletes to strengthen their grip. It is formed by winding A227 hard-drawn steel wire around a mandrel to obtain $2\frac{1}{2}$ turns when the grip is in the closed position. After winding, the wire is cut to leave the two legs as handles. The plastic handles are then molded on, the grip is squeezed together, and a wire clip is placed around the legs to obtain initial "tension" and to space the handles for the best initial gripping position. The clip is formed like a figure 8 to prevent it from coming off. When the grip is in the closed position, the stress in the spring should not exceed the permissible stress.
 (a) Determine the configuration of the spring before the grip is assembled.
 (b) Find the force necessary to close the grip.

Problem 10-39
Dimensions in millimeters.

**10-40**

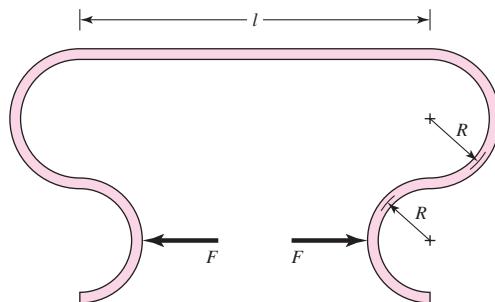
The rat trap shown in the figure uses two opposite-image torsion springs. The wire has a diameter of 0.081 in, and the outside diameter of the spring in the position shown is $\frac{1}{2}$ in. Each spring has 11 turns. Use of a fish scale revealed a force of about 8 lbf is needed to set the trap.

- Find the probable configuration of the spring prior to assembly.
- Find the maximum stress in the spring when the trap is set.

Problem 10-40**10-41**

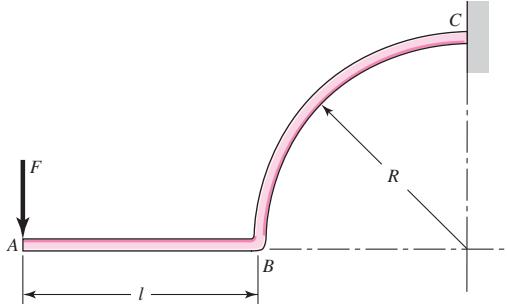
Wire form springs can be made in a variety of shapes. The clip shown operates by applying a force F . The wire diameter is d , the length of the straight section is l , and Young's modulus is E . Consider the effects of bending only, with $d \ll R$.

- Use Castigiano's theorem to determine the spring rate k .
- Determine the spring rate if the clip is made from 2-mm diameter A227 hard-drawn steel wire with $R = 6$ mm and $l = 25$ mm.
- Estimate the value of the load F , which will cause the wire to yield.

Problem 10-41

- 10-42** For the wire form shown, the wire diameter is d , the length of the straight section is l , and Young's modulus is E . Consider the effects of bending only, with $d \ll R$.
- Use Castiglano's method to determine the spring rate k .
 - Determine the spring rate if the form is made from 0.063-in diameter A313 stainless wire with $R = \frac{5}{8}$ in and $l = \frac{1}{2}$ in.
 - For part (b), estimate the value of the load F , which will cause the wire to yield.

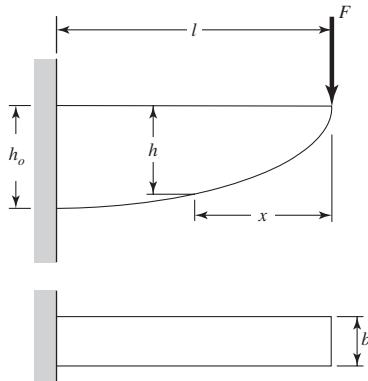
Problem 10-42



- 10-43** Figure 10-13b shows a spring of constant thickness and constant stress. A constant stress spring can be designed where the width b is constant as shown.

- Determine how h varies as a function of x .
- Given Young's modulus E , determine the spring rate k in terms of E , l , b , and h_o . Verify the units of k .

Problem 10-43



- 10-44** Using the experience gained with Prob. 10-30, write a computer program that would help in the design of helical coil compression springs.

- 10-45** Using the experience gained with Prob. 10-37, write a computer program that would help in the design of a helical coil extension spring.

This page intentionally left blank

11

Rolling-Contact Bearings

Chapter Outline

11-1	Bearing Types	570
11-2	Bearing Life	573
11-3	Bearing Load Life at Rated Reliability	574
11-4	Bearing Survival: Reliability versus Life	576
11-5	Relating Load, Life, and Reliability	577
11-6	Combined Radial and Thrust Loading	579
11-7	Variable Loading	584
11-8	Selection of Ball and Cylindrical Roller Bearings	588
11-9	Selection of Tapered Roller Bearings	590
11-10	Design Assessment for Selected Rolling-Contact Bearings	599
11-11	Lubrication	603
11-12	Mounting and Enclosure	604

The terms *rolling-contact bearing*, *antifriction bearing*, and *rolling bearing* are all used to describe that class of bearing in which the main load is transferred through elements in rolling contact rather than in sliding contact. In a rolling bearing the starting friction is about twice the running friction, but still it is negligible in comparison with the starting friction of a sleeve bearing. Load, speed, and the operating viscosity of the lubricant do affect the frictional characteristics of a rolling bearing. It is probably a mistake to describe a rolling bearing as “antifriction,” but the term is used generally throughout the industry.

From the mechanical designer’s standpoint, the study of antifriction bearings differs in several respects when compared with the study of other topics because the bearings they specify have already been designed. The specialist in antifriction-bearing design is confronted with the problem of designing a group of elements that compose a rolling bearing: these elements must be designed to fit into a space whose dimensions are specified; they must be designed to receive a load having certain characteristics; and finally, these elements must be designed to have a satisfactory life when operated under the specified conditions. Bearing specialists must therefore consider such matters as fatigue loading, friction, heat, corrosion resistance, kinematic problems, material properties, lubrication, machining tolerances, assembly, use, and cost. From a consideration of all these factors, bearing specialists arrive at a compromise that, in their judgment, is a good solution to the problem as stated.

We begin with an overview of bearing types; then we note that bearing life cannot be described in deterministic form. We introduce the invariant, the statistical distribution of life, which is strongly Weibullian.¹ There are some useful deterministic equations addressing load versus life at constant reliability, and we introduce the catalog rating at rating life.

The reliability-life relationship involves Weibullian statistics. The load-life-reliability relationship, combines statistical and deterministic relationships giving the designer a way to move from the desired load and life to the catalog rating in one equation.

Ball bearings also resist thrust, and a unit of thrust does different damage per revolution than a unit of radial load, so we must find the equivalent pure radial load that does the same damage as the existing radial and thrust loads. Next, variable loading, stepwise and continuous, is approached, and the equivalent pure radial load doing the same damage is quantified. Oscillatory loading is mentioned.

With this preparation we have the tools to consider the selection of ball and cylindrical roller bearings. The question of misalignment is quantitatively approached.

Tapered roller bearings have some complications, and our experience so far contributes to understanding them.

Having the tools to find the proper catalog ratings, we make decisions (selections), we perform a design assessment, and the bearing reliability is quantified. Lubrication and mounting conclude our introduction. Vendors’ manuals should be consulted for specific details relating to bearings of their manufacture.

11-1

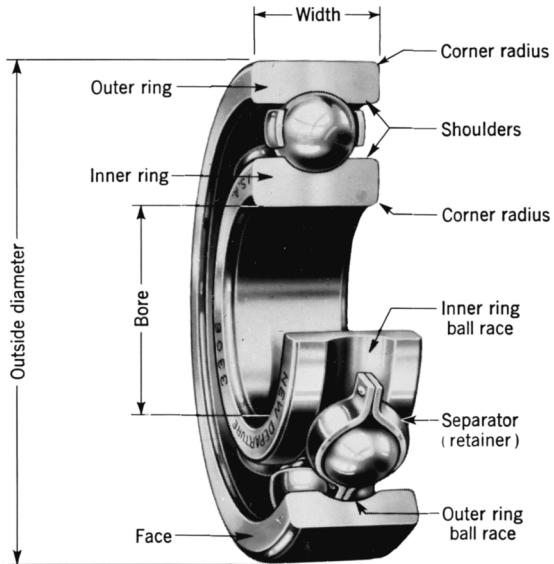
Bearing Types

Bearings are manufactured to take pure radial loads, pure thrust loads, or a combination of the two kinds of loads. The nomenclature of a ball bearing is illustrated in Fig. 11-1, which also shows the four essential parts of a bearing. These are the outer ring, the inner ring, the balls or rolling elements, and the separator. In low-priced bearings, the

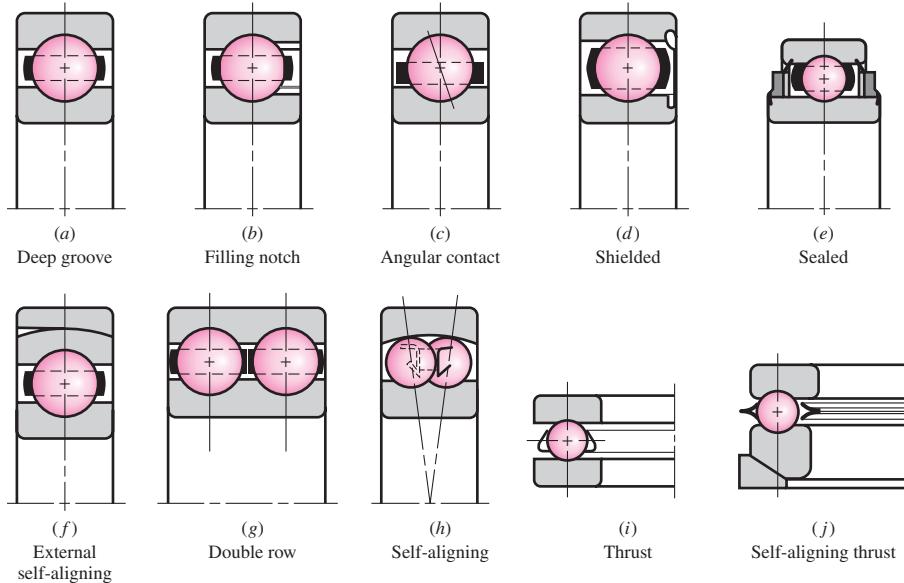
¹To completely understand the statistical elements of this chapter, the reader is urged to review Chap. 20, Secs. 20-1 through 20-3.

Figure 11-1

Nomenclature of a ball bearing.
(General Motors Corp. Used with permission, GM Media Archives.)

**Figure 11-2**

Various types of ball bearings.



separator is sometimes omitted, but it has the important function of separating the elements so that rubbing contact will not occur.

In this section we include a selection from the many types of standardized bearings that are manufactured. Most bearing manufacturers provide engineering manuals and brochures containing lavish descriptions of the various types available. In the small space available here, only a meager outline of some of the most common types can be given. So you should include a survey of bearing manufacturers' literature in your studies of this section.

Some of the various types of standardized bearings that are manufactured are shown in Fig. 11-2. The single-row deep-groove bearing will take radial load as well as some thrust load. The balls are inserted into the grooves by moving the inner ring

to an eccentric position. The balls are separated after loading, and the separator is then inserted. The use of a filling notch (Fig. 11–2b) in the inner and outer rings enables a greater number of balls to be inserted, thus increasing the load capacity. The thrust capacity is decreased, however, because of the bumping of the balls against the edge of the notch when thrust loads are present. The angular-contact bearing (Fig. 11–2c) provides a greater thrust capacity.

All these bearings may be obtained with shields on one or both sides. The shields are not a complete closure but do offer a measure of protection against dirt. A variety of bearings are manufactured with seals on one or both sides. When the seals are on both sides, the bearings are lubricated at the factory. Although a sealed bearing is supposed to be lubricated for life, a method of relubrication is sometimes provided.

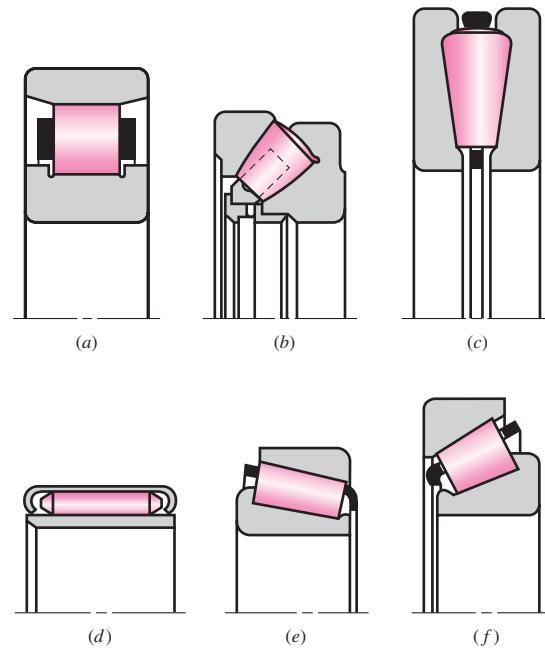
Single-row bearings will withstand a small amount of shaft misalignment of deflection, but where this is severe, self-aligning bearings may be used. Double-row bearings are made in a variety of types and sizes to carry heavier radial and thrust loads. Sometimes two single-row bearings are used together for the same reason, although a double-row bearing will generally require fewer parts and occupy less space. The one-way ball thrust bearings (Fig. 11–2i) are made in many types and sizes.

Some of the large variety of standard roller bearings available are illustrated in Fig. 11–3. Straight roller bearings (Fig. 11–3a) will carry a greater radial load than ball bearings of the same size because of the greater contact area. However, they have the disadvantage of requiring almost perfect geometry of the raceways and rollers. A slight misalignment will cause the rollers to skew and get out of line. For this reason, the retainer must be heavy. Straight roller bearings will not, of course, take thrust loads.

Helical rollers are made by winding rectangular material into rollers, after which they are hardened and ground. Because of the inherent flexibility, they will take considerable misalignment. If necessary, the shaft and housing can be used for raceways instead of separate inner and outer races. This is especially important if radial space is limited.

Figure 11–3

Types of roller bearings:
 (a) straight roller; (b) spherical roller, thrust; (c) tapered roller, thrust; (d) needle; (e) tapered roller; (f) steep-angle tapered roller. (*Courtesy of The Timken Company.*)



The spherical-roller thrust bearing (Fig. 11–3b) is useful where heavy loads and misalignment occur. The spherical elements have the advantage of increasing their contact area as the load is increased.

Needle bearings (Fig. 11–3d) are very useful where radial space is limited. They have a high load capacity when separators are used, but may be obtained without separators. They are furnished both with and without races.

Tapered roller bearings (Fig. 11–3e, f) combine the advantages of ball and straight roller bearings, since they can take either radial or thrust loads or any combination of the two, and in addition, they have the high load-carrying capacity of straight roller bearings. The tapered roller bearing is designed so that all elements in the roller surface and the raceways intersect at a common point on the bearing axis.

The bearings described here represent only a small portion of the many available for selection. Many special-purpose bearings are manufactured, and bearings are also made for particular classes of machinery. Typical of these are:

- Instrument bearings, which are high-precision and are available in stainless steel and high-temperature materials
- Nonprecision bearings, usually made with no separator and sometimes having split or stamped sheet-metal races
- Ball bushings, which permit either rotation or sliding motion or both
- Bearings with flexible rollers

11-2

Bearing Life

When the ball or roller of rolling-contact bearings rolls, contact stresses occur on the inner ring, the rolling element, and on the outer ring. Because the curvature of the contacting elements in the axial direction is different from that in the radial direction, the equations for these stresses are more involved than in the Hertz equations presented in Chap. 3. If a bearing is clean and properly lubricated, is mounted and sealed against the entrance of dust and dirt, is maintained in this condition, and is operated at reasonable temperatures, then metal fatigue will be the only cause of failure. Inasmuch as metal fatigue implies many millions of stress applications successfully endured, we need a quantitative life measure. Common life measures are

- Number of revolutions of the inner ring (outer ring stationary) until the first tangible evidence of fatigue
- Number of hours of use at a standard angular speed until the first tangible evidence of fatigue

The commonly used term is *bearing life*, which is applied to either of the measures just mentioned. It is important to realize, as in all fatigue, life as defined above is a stochastic variable and, as such, has both a distribution and associated statistical parameters. The life measure of an individual bearing is defined as the total number of revolutions (or hours at a constant speed) of bearing operation until the failure criterion is developed. Under ideal conditions, the fatigue failure consists of spalling of the load-carrying surfaces. The American Bearing Manufacturers Association (ABMA) standard states that the failure criterion is the first evidence of fatigue. The fatigue criterion used by the Timken Company laboratories is the spalling or pitting of an area of 0.01 in². Timken also observes that the useful life of the bearing may extend considerably beyond this point. This is an operational definition of fatigue failure in rolling bearings.

The *rating life* is a term sanctioned by the ABMA and used by most manufacturers. The rating life of a group of nominally identical ball or roller bearings is defined as the number of revolutions (or hours at a constant speed) that 90 percent of a group of bearings will achieve or exceed before the failure criterion develops. The terms *minimum life*, L_{10} *life*, and B_{10} *life* are also used as synonyms for rating life. The rating life is the 10th percentile location of the bearing group's revolutions-to-failure distribution.

Median life is the 50th percentile life of a group of bearings. The term *average life* has been used as a synonym for median life, contributing to confusion. When many groups of bearings are tested, the median life is between 4 and 5 times the L_{10} life.

Each bearing manufacturer will choose a specific rating life for which load ratings of its bearings are reported. The most commonly used rating life is 10^6 revolutions. The Timken Company is a well-known exception, rating its bearings at 3 000 hours at 500 rev/min, which is $90(10^6)$ revolutions. These levels of rating life are actually quite low for today's bearings, but since rating life is an arbitrary reference point, the traditional values have generally been maintained.

11-3

Bearing Load Life at Rated Reliability

When nominally identical groups are tested to the life-failure criterion at different loads, the data are plotted on a graph as depicted in Fig. 11-4 using a log-log transformation. To establish a single point, load F_1 and the rating life of group one (L_{10}^1) are the coordinates that are logarithmically transformed. The reliability associated with this point, and all other points, is 0.90. Thus we gain a glimpse of the load-life function at 0.90 reliability. Using a regression equation of the form

$$FL^{1/a} = \text{constant} \quad (11-1)$$

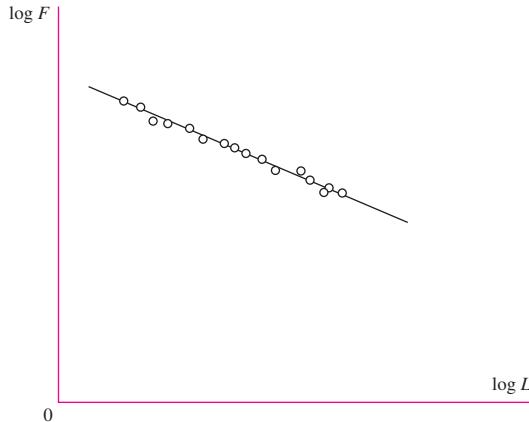
the result of many tests for various kinds of bearings result in

- $a = 3$ for ball bearings
- $a = 10/3$ for roller bearings (cylindrical and tapered roller)

A *catalog load rating* is defined as the radial load that causes 10 percent of a group of bearings to fail at the bearing manufacturer's rating life. We shall denote the catalog load rating as C_{10} . The catalog load rating is often referred to as a *Basic Dynamic Load Rating*, or sometimes just *Basic Load Rating*, if the manufacturer's rating life is 10^6 revolutions. The radial load that would be necessary to cause failure at such a low life would be unrealistically high. Consequently, the Basic Load Rating should be viewed as a reference value, and not as an actual load to be achieved by a bearing.

Figure 11-4

Typical bearing load-life log-log curve.



In selecting a bearing for a given application, it is necessary to relate the desired load and life requirements to the published catalog load rating corresponding to the catalog rating life. From Eq. (11-1) we can write

$$F_1 L_1^{1/a} = F_2 L_2^{1/a} \quad (11-2)$$

where the subscripts 1 and 2 can refer to any set of load and life conditions. Letting F_1 and L_1 correlate with the catalog load rating and rating life, and F_2 and L_2 correlate with desired load and life for the application, we can express Eq. (11-2) as

$$F_R L_R^{1/a} = F_D L_D^{1/a} \quad (a)$$

where the units of L_R and L_D are revolutions, and the subscripts R and D stand for Rated and Desired.

It is sometimes convenient to express the life in hours at a given speed. Accordingly, any life L in revolutions can be expressed as

$$L = 60 \mathcal{L}n \quad (b)$$

where \mathcal{L} is in hours, n is in rev/min, and 60 min/h is the appropriate conversion factor.

Incorporating Eq. (b) into Eq. (a),

$$F_R (\mathcal{L}_R n_R 60)^{1/a} = F_D (\mathcal{L}_D n_D 60)^{1/a} \quad (c)$$

Solving Eq. (c) for F_R , and noting that it is simply an alternate notation for the catalog load rating C_{10} , we obtain an expression for a catalog load rating as a function of the desired load, desired life, and catalog rating life.

$$C_{10} = F_R = F_D \left(\frac{L_D}{L_R} \right)^{1/a} = F_D \left(\frac{\mathcal{L}_D n_D 60}{\mathcal{L}_R n_R 60} \right)^{1/a} \quad (11-3)$$

It is sometimes convenient to define $x_D = L_D / L_R$ as a dimensionless *multiple of rating life*.

EXAMPLE 11-1

Consider SKF, which rates its bearings for 1 million revolutions. If you desire a life of 5000 h at 1725 rev/min with a load of 400 lbf with a reliability of 90 percent, for which catalog rating would you search in an SKF catalog?

Solution The rating life is $L_{10} = L_R = \mathcal{L}_R n_R 60 = 10^6$ revolutions. From Eq. (11-3),

$$\text{Answer} \quad C_{10} = F_D \left(\frac{\mathcal{L}_D n_D 60}{\mathcal{L}_R n_R 60} \right)^{1/a} = 400 \left[\frac{5000(1725)60}{10^6} \right]^{1/3} = 3211 \text{ lbf} = 14.3 \text{ kN}$$

11-4 Bearing Survival: Reliability versus Life

At constant load, the life measure distribution is right skewed. Candidates for a distributional curve fit include lognormal and Weibull. The Weibull is by far the most popular, largely because of its ability to adjust to varying amounts of skewness. If the life measure is expressed in dimensionless form as $x = L/L_{10}$, then the reliability can be expressed as [see Eq. (20-24), p. 990]

$$R = \exp \left[- \left(\frac{x - x_0}{\theta - x_0} \right)^b \right] \quad (11-4)$$

where R = reliability

x = life measure dimensionless variate, L/L_{10}

x_0 = guaranteed, or “minimum,” value of the variate

θ = characteristic parameter corresponding to the 63.211 percentile value of the variate

b = shape parameter that controls the skewness

Because there are three distributional parameters, x_0 , θ , and b , the Weibull has a robust ability to conform to a data string. Also, in Eq. (11-4) an explicit expression for the cumulative distribution function is possible:

$$F = 1 - R = 1 - \exp \left[- \left(\frac{x - x_0}{\theta - x_0} \right)^b \right] \quad (11-5)$$

EXAMPLE 11-2

Construct the distributional properties of a 02-30 millimeter deep-groove ball bearing if the Weibull parameters are $x_0 = 0.02$, $(\theta - x_0) = 4.439$, and $b = 1.483$. Find the mean, median, 10th percentile life, standard deviation, and coefficient of variation.

Solution

From Eq. (20-28), p. 991, the mean dimensionless life μ_x is

Answer
$$\mu_x = x_0 + (\theta - x_0) \Gamma \left(1 + \frac{1}{b} \right) = 0.02 + 4.439 \Gamma \left(1 + \frac{1}{1.483} \right) = 4.033$$

The median dimensionless life is, from Eq. (20-26) where $R = 0.5$,

Answer
$$x_{0.50} = x_0 + (\theta - x_0) \left(\ln \frac{1}{R} \right)^{1/b} = 0.02 + 4.439 \left(\ln \frac{1}{0.5} \right)^{1/1.483}$$

$$= 3.487$$

The 10th percentile value of the dimensionless life x is

Answer
$$x_{0.10} = 0.02 + 4.439 \left(\ln \frac{1}{0.90} \right)^{1/1.483} \doteq 1 \quad (\text{as it should be})$$

The standard deviation of the dimensionless life is given by Eq. (20–29):

$$\begin{aligned}\text{Answer} \quad \hat{\sigma}_x &= (\theta - x_0) \left[\Gamma \left(1 + \frac{2}{b} \right) - \Gamma^2 \left(1 + \frac{1}{b} \right) \right]^{1/2} \\ &= 4.439 \left[\Gamma \left(1 + \frac{2}{1.483} \right) - \Gamma^2 \left(1 + \frac{1}{1.483} \right) \right]^{1/2} = 2.753\end{aligned}$$

The coefficient of variation of the dimensionless life is

$$\text{Answer} \quad C_x = \frac{\hat{\sigma}_x}{\mu_x} = \frac{2.753}{4.033} = 0.683$$

11–5 Relating Load, Life, and Reliability

This is the designer's problem. The desired load is not the manufacturer's test load or catalog entry. The desired speed is different from the vendor's test speed, and the reliability expectation is typically much higher than the 0.90 accompanying the catalog entry. Figure 11–5 shows the situation. The catalog information is plotted as point A, whose coordinates are (the logs of) C_{10} and $x_{10} = L_{10}/L_{10} = 1$, a point on the 0.90 reliability contour. The design point is at D, with the coordinates (the logs of) F_D and x_D , a point that is on the $R = R_D$ reliability contour. The designer must move from point D to point A via point B as follows. Along a constant reliability contour (BD), Eq. (11–2) applies:

$$F_B x_B^{1/a} = F_D x_D^{1/a}$$

from which

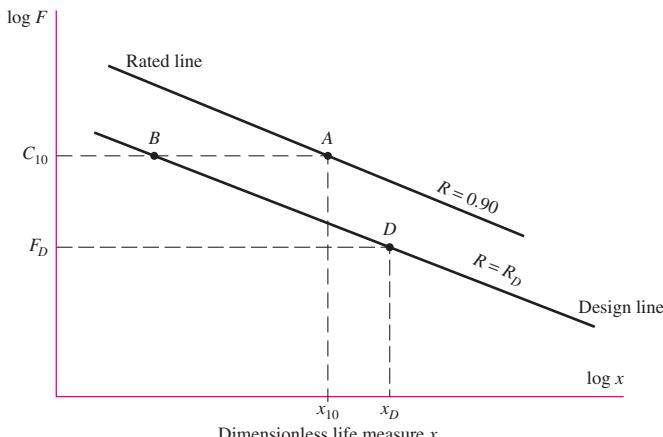
$$F_B = F_D \left(\frac{x_D}{x_B} \right)^{1/a} \quad (a)$$

Along a constant load line (AB), Eq. (11–4) applies:

$$R_D = \exp \left[- \left(\frac{x_B - x_0}{\theta - x_0} \right)^b \right]$$

Figure 11–5

Constant reliability contours. Point A represents the catalog rating C_{10} at $x = L/L_{10} = 1$. Point B is on the target reliability design line R_D , with a load of C_{10} . Point D is a point on the desired reliability contour exhibiting the design life $x_D = L_D/L_{10}$ at the design load F_D .



Solving for x_B gives

$$x_B = x_0 + (\theta - x_0) \left(\ln \frac{1}{R_D} \right)^{1/b}$$

Now substitute this in Eq. (a) to obtain

$$F_B = F_D \left(\frac{x_D}{x_B} \right)^{1/a} = F_D \left[\frac{x_D}{x_0 + (\theta - x_0)(\ln 1/R_D)^{1/b}} \right]^{1/a}$$

Noting that $F_B = C_{10}$, and including an application factor a_f with the design load,

$$C_{10} = a_f F_D \left[\frac{x_D}{x_0 + (\theta - x_0)(\ln 1/R_D)^{1/b}} \right]^{1/a} \quad (11-6)$$

The application factor serves as a factor of safety to increase the design load to take into account overload, dynamic loading, and uncertainty. Typical load application factors for certain types of applications will be discussed shortly.

Eq. (11-6) can be simplified slightly for calculator entry by noting that

$$\ln \frac{1}{R_D} = \ln \frac{1}{1 - p_f} = \ln(1 + p_f + \dots) \doteq p_f = 1 - R_D$$

where p_f is the probability for failure. Equation (11-6) can be written as

$$C_{10} \doteq a_f F_D \left[\frac{x_D}{x_0 + (\theta - x_0)(1 - R_D)^{1/b}} \right]^{1/a} \quad R \geq 0.90 \quad (11-7)$$

Either Eq. (11-6) or Eq. (11-7) may be used to convert from a design situation with a desired load, life, and reliability to a catalog load rating based on a rating life at 90 percent reliability. Note that when $R_D = 0.90$, the denominator is equal to one, and the equation reduces to Eq. (11-3). The Weibull parameters are usually provided in the manufacturer's catalog. Typical values are given on p. 608 at the beginning of the end-of-chapter problems.

EXAMPLE 11-3

The design load on a ball bearing is 413 lbf and an application factor of 1.2 is appropriate. The speed of the shaft is to be 300 rev/min, the life to be 30 kh with a reliability of 0.99. What is the C_{10} catalog entry to be sought (or exceeded) when searching for a deep-groove bearing in a manufacturer's catalog on the basis of 10^6 revolutions for rating life? The Weibull parameters are $x_0 = 0.02$, $(\theta - x_0) = 4.439$, and $b = 1.483$.

Solution

$$x_D = \frac{L_D}{L_R} = \frac{60\mathcal{L}_D n_D}{L_{10}} = \frac{60(30\,000)300}{10^6} = 540$$

Thus, the design life is 540 times the L_{10} life. For a ball bearing, $a = 3$. Then, from Eq. (11-7),

$$\text{Answer} \quad C_{10} = (1.2)(413) \left[\frac{540}{0.02 + 4.439(1 - 0.99)^{1/1.483}} \right]^{1/3} = 6696 \text{ lbf}$$

Shafts generally have two bearings. Often these bearings are different. If the bearing reliability of the shaft with its pair of bearings is to be R , then R is related to the individual bearing reliabilities R_A and R_B by

$$R = R_A R_B$$

First, we observe that if the product $R_A R_B$ equals R , then, in general, R_A and R_B are both greater than R . Since the failure of either or both of the bearings results in the shutdown of the shaft, then A or B or both can create a failure. Second, in sizing bearings one can begin by making R_A and R_B equal to the square root of the reliability goal, \sqrt{R} . In Ex. 11–3, if the bearing was one of a pair, the reliability goal would be $\sqrt{0.99}$, or 0.995. The bearings selected are discrete in their reliability property in your problem, so the selection procedure “rounds up,” and the overall reliability exceeds the goal R . Third, it may be possible, if $R_A > \sqrt{R}$, to round down on B yet have the product $R_A R_B$ still exceed the goal R .

11–6 Combined Radial and Thrust Loading

A ball bearing is capable of resisting radial loading and a thrust loading. Furthermore, these can be combined. Consider F_a and F_r to be the axial thrust and radial loads, respectively, and F_e to be the *equivalent radial load* that does the same damage as the combined radial and thrust loads together. A rotation factor V is defined such that $V = 1$ when the inner ring rotates and $V = 1.2$ when the outer ring rotates. Two dimensionless groups can now be formed: F_e/VF_r and F_a/VF_r . When these two dimensionless groups are plotted as in Fig. 11–6, the data fall in a gentle curve that is well approximated by two straight-line segments. The abscissa e is defined by the intersection of the two lines. The equations for the two lines shown in Fig. 11–6 are

$$\frac{F_e}{VF_r} = 1 \quad \text{when } \frac{F_a}{VF_r} \leq e \quad (11-8a)$$

$$\frac{F_e}{VF_r} = X + Y \frac{F_a}{VF_r} \quad \text{when } \frac{F_a}{VF_r} > e \quad (11-8b)$$

Figure 11–6

The relationship of dimensionless group $F_e/(VF_r)$ and $F_a/(VF_r)$ and the straight-line segments representing the data.

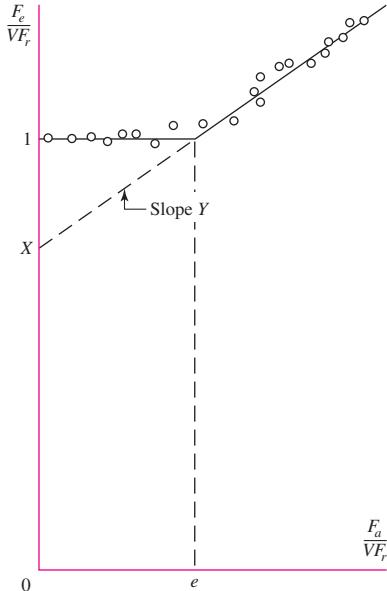


Table 11-1

Equivalent Radial Load Factors for Ball Bearings	F_a/C_0	e	$F_a/(VF_r) \leq e$		$F_a/(VF_r) > e$	
			X_1	Y_1	X_2	Y_2
	0.014*	0.19	1.00	0	0.56	2.30
	0.021	0.21	1.00	0	0.56	2.15
	0.028	0.22	1.00	0	0.56	1.99
	0.042	0.24	1.00	0	0.56	1.85
	0.056	0.26	1.00	0	0.56	1.71
	0.070	0.27	1.00	0	0.56	1.63
	0.084	0.28	1.00	0	0.56	1.55
	0.110	0.30	1.00	0	0.56	1.45
	0.17	0.34	1.00	0	0.56	1.31
	0.28	0.38	1.00	0	0.56	1.15
	0.42	0.42	1.00	0	0.56	1.04
	0.56	0.44	1.00	0	0.56	1.00

*Use 0.014 if $F_a/C_0 < 0.014$.

where, as shown, X is the ordinate intercept and Y is the slope of the line for $F_a/VF_r > e$. It is common to express Eqs. (11–8a) and (11–8b) as a single equation,

$$F_e = X_i VF_r + Y_i F_a \quad (11-9)$$

where $i = 1$ when $F_a/VF_r \leq e$ and $i = 2$ when $F_a/VF_r > e$. The X and Y factors depend upon the geometry and construction of the specific bearing. Table 11–1 lists representative values of X_1 , Y_1 , X_2 , and Y_2 as a function of e , which in turn is a function of F_a/C_0 , where C_0 is the basic static load rating. The *basic static load rating* is the load that will produce a total permanent deformation in the raceway and rolling element at any contact point of 0.0001 times the diameter of the rolling element. The basic static load rating is typically tabulated, along with the basic dynamic load rating C_{10} , in bearing manufacturers' publications. See Table 11–2, for example.

In these equations, the rotation factor V is intended to correct for the rotating-ring conditions. The factor of 1.2 for outer-ring rotation is simply an acknowledgment that the fatigue life is reduced under these conditions. Self-aligning bearings are an exception: they have $V = 1$ for rotation of either ring.

Since straight or cylindrical roller bearings will take no axial load, or very little, the Y factor is always zero.

The ABMA has established standard boundary dimensions for bearings, which define the bearing bore, the outside diameter (OD), the width, and the fillet sizes on the shaft and housing shoulders. The basic plan covers all ball and straight roller bearings in the metric sizes. The plan is quite flexible in that, for a given bore, there is an assortment of widths and outside diameters. Furthermore, the outside diameters selected are such that, for a particular outside diameter, one can usually find a variety of bearings having different bores and widths.

This basic ABMA plan is illustrated in Fig. 11–7. The bearings are identified by a two-digit number called the *dimension-series code*. The first number in the code is from the *width series*, 0, 1, 2, 3, 4, 5, and 6. The second number is from the *diameter series* (outside), 8, 9, 0, 1, 2, 3, and 4. Figure 11–7 shows the variety of bearings that may be obtained with a particular bore. Since the dimension-series code does not reveal the

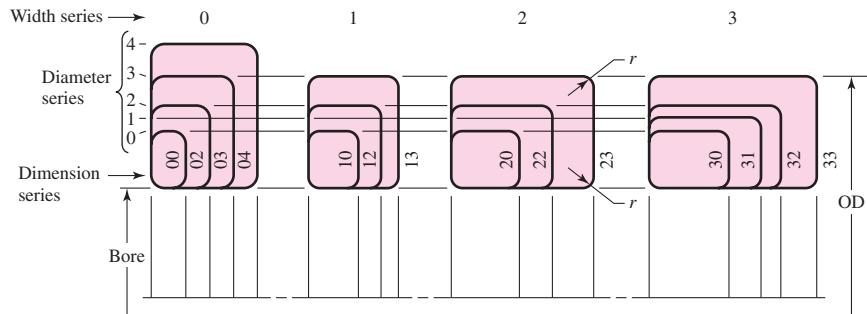
Table 11-2

Dimensions and Load Ratings for Single-Row 02-Series Deep-Groove and Angular-Contact Ball Bearings

Bore, mm	OD, mm	Width, mm	Fillet	Shoulder		Load Ratings, kN		Angular Contact	
			Radius, mm	Diameter, mm	d_s	d_H	Deep Groove	C_{10}	C_0
10	30	9	0.6	12.5	27		5.07	2.24	4.94
12	32	10	0.6	14.5	28		6.89	3.10	7.02
15	35	11	0.6	17.5	31		7.80	3.55	8.06
17	40	12	0.6	19.5	34		9.56	4.50	9.95
20	47	14	1.0	25	41		12.7	6.20	13.3
25	52	15	1.0	30	47		14.0	6.95	14.8
30	62	16	1.0	35	55		19.5	10.0	20.3
35	72	17	1.0	41	65		25.5	13.7	27.0
40	80	18	1.0	46	72		30.7	16.6	31.9
45	85	19	1.0	52	77		33.2	18.6	35.8
50	90	20	1.0	56	82		35.1	19.6	37.7
55	100	21	1.5	63	90		43.6	25.0	46.2
60	110	22	1.5	70	99		47.5	28.0	55.9
65	120	23	1.5	74	109		55.9	34.0	63.7
70	125	24	1.5	79	114		61.8	37.5	68.9
75	130	25	1.5	86	119		66.3	40.5	71.5
80	140	26	2.0	93	127		70.2	45.0	80.6
85	150	28	2.0	99	136		83.2	53.0	90.4
90	160	30	2.0	104	146		95.6	62.0	106
95	170	32	2.0	110	156		108	69.5	121

Figure 11-7

The basic ABMA plan for boundary dimensions. These apply to ball bearings, straight roller bearings, and spherical roller bearings, but not to inch-series ball bearings or tapered roller bearings. The contour of the corner is not specified. It may be rounded or chamfered, but it must be small enough to clear the fillet radius specified in the standards.

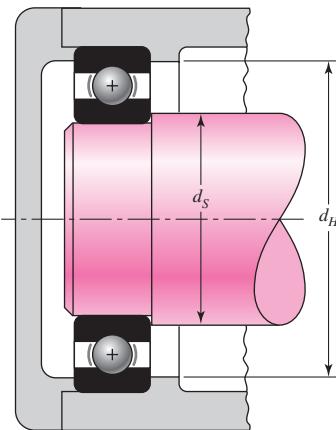


dimensions directly, it is necessary to resort to tabulations. The 02 series is used here as an example of what is available. See Table 11-2.

The housing and shaft shoulder diameters listed in the tables should be used whenever possible to secure adequate support for the bearing and to resist the maximum thrust loads (Fig. 11-8). Table 11-3 lists the dimensions and load ratings of some straight roller bearings.

Figure 11-8

Shaft and housing shoulder diameters d_S and d_H should be adequate to ensure good bearing support.

**Table 11-3**

Dimensions and Basic Load Ratings for Cylindrical Roller Bearings

02-Series					03-Series			
Bore, mm	OD, mm	Width, mm	Load Rating, C_{10}	C_0	OD, mm	Width, mm	Load Rating, C_{10}	C_0
25	52	15	16.8	8.8	62	17	28.6	15.0
30	62	16	22.4	12.0	72	19	36.9	20.0
35	72	17	31.9	17.6	80	21	44.6	27.1
40	80	18	41.8	24.0	90	23	56.1	32.5
45	85	19	44.0	25.5	100	25	72.1	45.4
50	90	20	45.7	27.5	110	27	88.0	52.0
55	100	21	56.1	34.0	120	29	102	67.2
60	110	22	64.4	43.1	130	31	123	76.5
65	120	23	76.5	51.2	140	33	138	85.0
70	125	24	79.2	51.2	150	35	151	102
75	130	25	93.1	63.2	160	37	183	125
80	140	26	106	69.4	170	39	190	125
85	150	28	119	78.3	180	41	212	149
90	160	30	142	100	190	43	242	160
95	170	32	165	112	200	45	264	189
100	180	34	183	125	215	47	303	220
110	200	38	229	167	240	50	391	304
120	215	40	260	183	260	55	457	340
130	230	40	270	193	280	58	539	408
140	250	42	319	240	300	62	682	454
150	270	45	446	260	320	65	781	502

Table 11–4

Bearing-Life
Recommendations
for Various Classes
of Machinery

Type of Application	Life, kh
Instruments and apparatus for infrequent use	Up to 0.5
Aircraft engines	0.5–2
Machines for short or intermittent operation where service interruption is of minor importance	4–8
Machines for intermittent service where reliable operation is of great importance	8–14
Machines for 8-h service that are not always fully utilized	14–20
Machines for 8-h service that are fully utilized	20–30
Machines for continuous 24-h service	50–60
Machines for continuous 24-h service where reliability is of extreme importance	100–200

Table 11–5

Load-Application Factors

Type of Application	Load Factor
Precision gearing	1.0–1.1
Commercial gearing	1.1–1.3
Applications with poor bearing seals	1.2
Machinery with no impact	1.0–1.2
Machinery with light impact	1.2–1.5
Machinery with moderate impact	1.5–3.0

To assist the designer in the selection of bearings, most of the manufacturers' handbooks contain data on bearing life for many classes of machinery, as well as information on load-application factors. Such information has been accumulated the hard way, that is, by experience, and the beginner designer should utilize this information until he or she gains enough experience to know when deviations are possible. Table 11–4 contains recommendations on bearing life for some classes of machinery. The load-application factors in Table 11–5 serve the same purpose as factors of safety; use them to increase the equivalent load before selecting a bearing.

EXAMPLE 11–4

An SKF 6210 angular-contact ball bearing has an axial load F_a of 400 lbf and a radial load F_r of 500 lbf applied with the outer ring stationary. The basic static load rating C_0 is 4450 lbf and the basic load rating C_{10} is 7900 lbf. Estimate the \mathcal{L}_{10} life at a speed of 720 rev/min.

Solution

$V = 1$ and $F_a/C_0 = 400/4450 = 0.090$. Interpolate for e in Table 11–1:

F_a/C_0	e
0.084	0.28
0.090	e from which $e = 0.285$
0.110	0.30

$F_a/(VF_r) = 400/[(1)500] = 0.8 > 0.285$. Thus, interpolate for Y_2 :

F_a/C_0	Y_2
0.084	1.55
0.090	Y_2 from which $Y_2 = 1.527$
0.110	1.45

From Eq. (11-9),

$$F_e = X_2 V F_r + Y_2 F_a = 0.56(1)500 + 1.527(400) = 890.8 \text{ lbf}$$

With $\mathcal{L}_D = \mathcal{L}_{10}$ and $F_D = F_e$, solving Eq. (11-3) for \mathcal{L}_{10} gives

Answer
$$\mathcal{L}_{10} = \frac{60\mathcal{L}_R n_R}{60n_D} \left(\frac{C_{10}}{F_e} \right)^a = \frac{10^6}{60(720)} \left(\frac{7900}{890.8} \right)^3 = 16\,150 \text{ h}$$

We now know how to combine a steady radial load and a steady thrust load into an equivalent steady radial load F_e that inflicts the same damage per revolution as the radial–thrust combination.

11-7

Variable Loading

Bearing loads are frequently variable and occur in some identifiable patterns:

- Piecewise constant loading in a cyclic pattern
- Continuously variable loading in a repeatable cyclic pattern
- Random variation

Equation (11-1) can be written as

$$F^a L = \text{constant} = K \quad (a)$$

Note that F may already be an equivalent steady radial load for a radial–thrust load combination. Figure 11-9 is a plot of F^a as ordinate and L as abscissa for Eq. (a). If

Figure 11-9

Plot of F^a as ordinate and L as abscissa for $F^a L = \text{constant}$. The linear damage hypothesis says that in the case of load F_1 , the area under the curve from $L = 0$ to $L = L_A$ is a measure of the damage $D = F_1^a L_A$. The complete damage to failure is measured by $C_{10}^a L_B$.

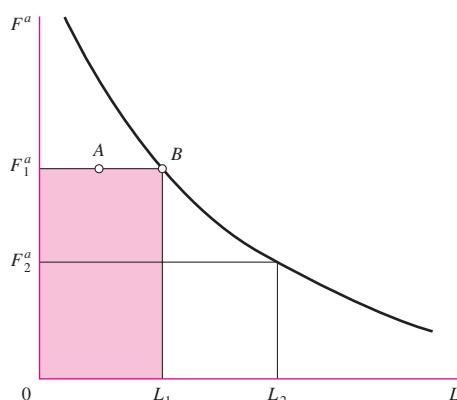
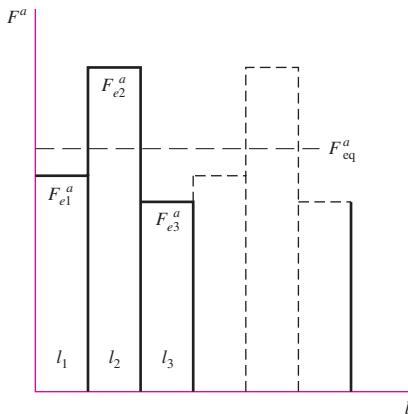


Figure 11-10

A three-part piecewise-continuous periodic loading cycle involving loads F_{e1} , F_{e2} , and F_{e3} . F_{eq} is the equivalent steady load inflicting the same damage when run for $l_1 + l_2 + l_3$ revolutions, doing the same damage D per period.



a load level of F_1 is selected and run to the failure criterion, then the area under the F_1-L_1 trace is numerically equal to K . The same is true for a load level F_2 ; that is, the area under the F_2-L_2 trace is numerically equal to K . The linear damage theory says that in the case of load level F_1 , the area from $L = 0$ to $L = L_A$ does damage measured by $F_1^a L_A = D$.

Consider the piecewise continuous cycle depicted in Fig. 11-10. The loads F_{ei} are equivalent steady radial loads for combined radial-thrust loads. The damage done by loads F_{e1} , F_{e2} , and F_{e3} is

$$D = F_{e1}^a l_1 + F_{e2}^a l_2 + F_{e3}^a l_3 \quad (b)$$

where l_i is the number of revolutions at life L_i . The equivalent steady load F_{eq} when run for $l_1 + l_2 + l_3$ revolutions does the same damage D . Thus

$$D = F_{eq}^a (l_1 + l_2 + l_3) \quad (c)$$

Equating Eqs. (b) and (c), and solving for F_{eq} , we get

$$F_{eq} = \left[\frac{F_{e1}^a l_1 + F_{e2}^a l_2 + F_{e3}^a l_3}{l_1 + l_2 + l_3} \right]^{1/a} = \left[\sum f_i F_{ei}^a \right]^{1/a} \quad (11-10)$$

where f_i is the fraction of revolution run up under load F_{ei} . Since l_i can be expressed as $n_i t_i$, where n_i is the rotational speed at load F_{ei} and t_i is the duration of that speed, then it follows that

$$F_{eq} = \left[\frac{\sum n_i t_i F_{ei}^a}{\sum n_i t_i} \right]^{1/a} \quad (11-11)$$

The character of the individual loads can change, so an application factor (a_f) can be prefixed to each F_{ei} as $(a_f F_{ei})^a$; then Eq. (11-10) can be written

$$F_{eq} = \left[\sum f_i (a_f F_{ei})^a \right]^{1/a} \quad L_{eq} = \frac{K}{F_{eq}^a} \quad (11-12)$$

EXAMPLE 11-5

A ball bearing is run at four piecewise continuous steady loads as shown in the following table. Columns (1), (2), and (5) to (8) are given.

(1) Time Fraction	(2) Speed, rev/min	(3) Product, Column (1) × (2)	(4) Turns Fraction, (3)/ $\sum(3)$	(5) F_{fir} lbf	(6) F_{air} lbf	(7) F_{ei} lbf	(8) a_{fi}	(9) $a_{fi} F_{ei}$, lbf
0.1	2000	200	0.077	600	300	794	1.10	873
0.1	3000	300	0.115	300	300	626	1.25	795
0.3	3000	900	0.346	750	300	878	1.10	966
0.5	2400	1200	0.462	375	300	668	1.25	835
		2600	1.000					

Columns 1 and 2 are multiplied to obtain column 3. The column 3 entry is divided by the sum of column 3, 2600, to give column 4. Columns 5, 6, and 7 are the radial, axial, and equivalent loads respectively. Column 8 is the appropriate application factor. Column 9 is the product of columns 7 and 8.

Solution

From Eq. (11-10), with $a = 3$, the equivalent radial load F_e is

Answer
$$F_e = [0.077(873)^3 + 0.115(795)^3 + 0.346(966)^3 + 0.462(835)^3]^{1/3} = 884 \text{ lbf}$$

Sometimes the question after several levels of loading is: How much life is left if the next level of stress is held until failure? Failure occurs under the linear damage hypothesis when the damage D equals the constant $K = F^a L$. Taking the first form of Eq. (11-10), we write

$$F_{eq}^a L_{eq} = F_{e1}^a l_1 + F_{e2}^a l_2 + F_{e3}^a l_3$$

and note that

$$K = F_{e1}^a L_1 = F_{e2}^a L_2 = F_{e3}^a L_3$$

and K also equals

$$K = F_{e1}^a l_1 + F_{e2}^a l_2 + F_{e3}^a l_3 = \frac{K}{L_1} l_1 + \frac{K}{L_2} l_2 + \frac{K}{L_3} l_3 = K \sum \frac{l_i}{L_i}$$

From the outer parts of the preceding equation we obtain

$$\sum \frac{l_i}{L_i} = 1 \quad (11-13)$$

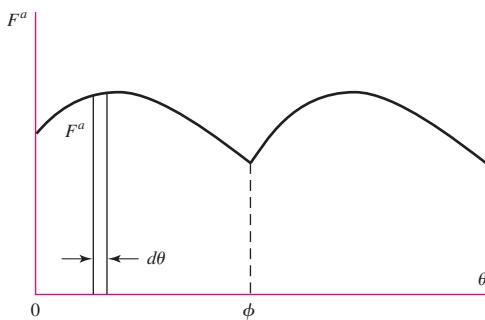
This equation was advanced by Palmgren in 1924, and again by Miner in 1945. See Eq. (6-58), p. 323.

The second kind of load variation mentioned is continuous, periodic variation, depicted by Fig. 11-11. The differential damage done by F^a during rotation through the angle $d\theta$ is

$$dD = F^a d\theta$$

Figure 11-11

A continuous load variation of a cyclic nature whose period is ϕ .



An example of this would be a cam whose bearings rotate with the cam through the angle $d\theta$. The total damage during a complete cam rotation is given by

$$D = \int dD = \int_0^\phi F^a d\theta = F_{eq}^a \phi$$

from which, solving for the equivalent load, we obtain

$$F_{eq} = \left[\frac{1}{\phi} \int_0^\phi F^a d\theta \right]^{1/a} \quad L_{eq} = \frac{K}{F_{eq}^a} \quad (11-14)$$

The value of ϕ is often 2π , although other values occur. Numerical integration is often useful to carry out the indicated integration, particularly when a is not an integer and trigonometric functions are involved. We have now learned how to find the steady equivalent load that does the same damage as a continuously varying cyclic load.

EXAMPLE 11-6

The operation of a particular rotary pump involves a power demand of $P = \bar{P} + A' \sin \theta$ where \bar{P} is the average power. The bearings feel the same variation as $F = \bar{F} + A \sin \theta$. Develop an application factor a_f for this application of ball bearings.

Solution From Eq. (11-14), with $a = 3$,

$$\begin{aligned} F_{eq} &= \left(\frac{1}{2\pi} \int_0^{2\pi} F^a d\theta \right)^{1/3} = \left(\frac{1}{2\pi} \int_0^{2\pi} (\bar{F} + A \sin \theta)^3 d\theta \right)^{1/3} \\ &= \left[\frac{1}{2\pi} \left(\int_0^{2\pi} \bar{F}^3 d\theta + 3\bar{F}^2 A \int_0^{2\pi} \sin \theta d\theta + 3\bar{F}A^2 \int_0^{2\pi} \sin^2 \theta d\theta \right. \right. \\ &\quad \left. \left. + A^3 \int_0^{2\pi} \sin^3 \theta d\theta \right) \right]^{1/3} \\ F_{eq} &= \left[\frac{1}{2\pi} (2\pi \bar{F}^3 + 0 + 3\pi \bar{F}A^2 + 0) \right]^{1/3} = \bar{F} \left[1 + \frac{3}{2} \left(\frac{A}{\bar{F}} \right)^2 \right]^{1/3} \end{aligned}$$

In terms of \bar{F} , the application factor is

$$a_f = \left[1 + \frac{3}{2} \left(\frac{A}{\bar{F}} \right)^2 \right]^{1/3}$$

Answer

We can present the result in tabular form:

A/F	a_f
0	1
0.2	1.02
0.4	1.07
0.6	1.15
0.8	1.25
1.0	1.36

11-8 Selection of Ball and Cylindrical Roller Bearings

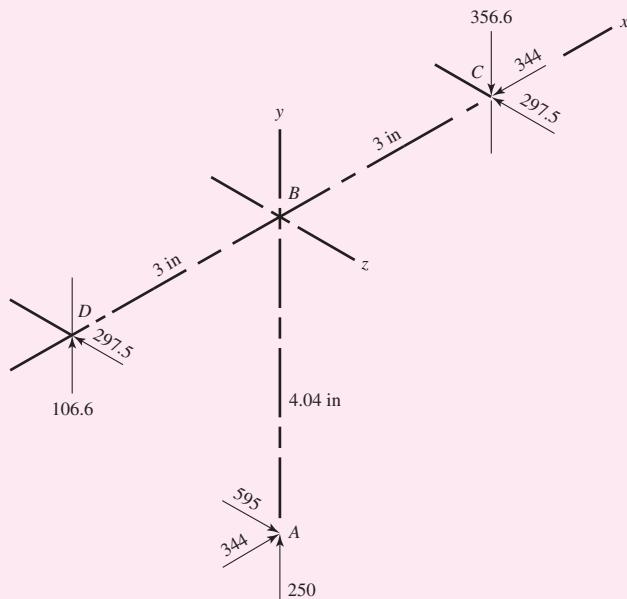
We have enough information concerning the loading of rolling-contact ball and roller bearings to develop the steady equivalent radial load that will do as much damage to the bearing as the existing loading. Now let's put it to work.

EXAMPLE 11-7

The second shaft on a parallel-shaft 25-hp foundry crane speed reducer contains a helical gear with a pitch diameter of 8.08 in. Helical gears transmit components of force in the tangential, radial, and axial directions (see Chap. 13). The components of the gear force transmitted to the second shaft are shown in Fig. 11-12, at point A. The bearing reactions at C and D, assuming simple-supports, are also shown. A ball bearing is to be selected for location C to accept the thrust, and a cylindrical roller bearing is to be utilized at location D. The life goal of the speed reducer is 10 kh, with a reliability factor for the ensemble of all four bearings (both shafts) to equal or exceed 0.96 for the Weibull parameters of Ex. 11-3. The application factor is to be 1.2.

Figure 11-12

Forces in pounds applied to the second shaft of the helical gear speed reducer of Ex. 11-7.



- (a) Select the roller bearing for location *D*.
 (b) Select the ball bearing (angular contact) for location *C*, assuming the inner ring rotates.

Solution The torque transmitted is $T = 595(4.04) = 2404 \text{ lbf} \cdot \text{in}$. The speed at the rated horsepower, given by Eq. (3-42), p. 102, is

$$n_D = \frac{63\ 025 H}{T} = \frac{63\ 025(25)}{2404} = 655.4 \text{ rev/min}$$

The radial load at *D* is $\sqrt{106.6^2 + 297.5^2} = 316.0 \text{ lbf}$, and the radial load at *C* is $\sqrt{356.6^2 + 297.5^2} = 464.4 \text{ lbf}$. The individual bearing reliabilities, if equal, must be at least $\sqrt[4]{0.96} = 0.98985 \doteq 0.99$. The dimensionless design life for both bearings is

$$x_D = \frac{L_D}{L_{10}} = \frac{60 \mathcal{L}_D n_D}{L_{10}} = \frac{60(10\ 000)655.4}{10^6} = 393.2$$

(a) From Eq. (11-7), the Weibull parameters of Ex. 11-3, an application factor of 1.2, and $a = 10/3$ for the roller bearing at *D*, the catalog rating should be equal to or greater than

$$\begin{aligned} C_{10} &= a_f F_D \left[\frac{x_D}{x_0 + (\theta - x_0)(1 - R_D)^{1/b}} \right]^{1/a} \\ &= 1.2(316.0) \left[\frac{393.2}{0.02 + 4.439(1 - 0.99)^{1/1.483}} \right]^{3/10} = 3591 \text{ lbf} = 16.0 \text{ kN} \end{aligned}$$

Answer The absence of a thrust component makes the selection procedure simple. Choose a 02-25 mm series, or a 03-25 mm series cylindrical roller bearing from Table 11-3.

(b) The ball bearing at *C* involves a thrust component. This selection procedure requires an iterative procedure. Assuming $F_a/(VF_r) > e$,

- 1 Choose Y_2 from Table 11-1.
- 2 Find C_{10} .
- 3 Tentatively identify a suitable bearing from Table 11-2, note C_0 .
- 4 Using F_a/C_0 enter Table 11-1 to obtain a new value of Y_2 .
- 5 Find C_{10} .
- 6 If the same bearing is obtained, stop.
- 7 If not, take next bearing and go to step 4.

As a first approximation, take the middle entry from Table 11-1:

$$X_2 = 0.56 \quad Y_2 = 1.63.$$

From Eq. (11-9), with $V = 1$,

$$F_e = XVF_r + YF_a = 0.56(1)(464.4) + 1.63(344) = 821 \text{ lbf} = 3.65 \text{ kN}$$

From Eq. (11-7), with $a = 3$,

$$C_{10} = 1.2(3.65) \left[\frac{393.2}{0.02 + 4.439(1 - 0.99)^{1/1.483}} \right]^{1/3} = 53.2 \text{ kN}$$

From Table 11-2, angular-contact bearing 02-60 mm has $C_{10} = 55.9 \text{ kN}$. C_0 is 35.5 kN. Step 4 becomes, with F_a in kN,

$$\frac{F_a}{C_0} = \frac{344(4.45)10^{-3}}{35.5} = 0.0431$$

which makes e from Table 11–1 approximately 0.24. Now $F_a/[VF_r] = 344/[(1)464.4] = 0.74$, which is greater than 0.24, so we find Y_2 by interpolation:

F_a/C_0	Y_2
0.042	1.85
0.043	Y_2 from which $Y_2 = 1.84$
0.056	1.71

From Eq. (11–9),

$$F_e = 0.56(1)(464.4) + 1.84(344) = 893 \text{ lbf} = 3.97 \text{ kN}$$

The prior calculation for C_{10} changes only in F_e , so

$$C_{10} = \frac{3.97}{3.65}53.2 = 57.9 \text{ kN}$$

From Table 11–2 an angular contact bearing 02-65 mm has $C_{10} = 63.7$ kN and C_0 of 41.5 kN. Again,

$$\frac{F_a}{C_0} = \frac{344(4.45)10^{-3}}{41.5} = 0.0369$$

making e approximately 0.23. Now from before, $F_a/VF_r = 0.74$, which is greater than 0.23. We find Y_2 again by interpolation:

F_a/C_0	Y_2
0.028	1.99
0.0369	Y_2 from which $Y_2 = 1.90$
0.042	1.85

From Eq. (11–9),

$$F_e = 0.56(1)(464.4) + 1.90(344) = 914 \text{ lbf} = 4.07 \text{ kN}$$

The prior calculation for C_{10} changes only in F_e , so

$$C_{10} = \frac{4.07}{3.65}53.2 = 59.3 \text{ kN}$$

Answer From Table 11–2 an angular-contact 02-65 mm is still selected, so the iteration is complete.

11–9

Selection of Tapered Roller Bearings

Tapered roller bearings have a number of features that make them complicated. As we address the differences between tapered roller and ball and cylindrical roller bearings, note that the underlying fundamentals are the same, but that there are differences in detail. Moreover, bearing and cup combinations are not necessarily priced in proportion to capacity. Any catalog displays a mix of high-production, low-production, and successful special-order designs. Bearing suppliers have computer programs that will take your problem descriptions, give intermediate design assessment information, and list a number of satisfactory cup-and-cone combinations in order of decreasing cost.

Company sales offices provide access to comprehensive engineering services to help designers select and apply their bearings. At a large original equipment manufacturer's plant, there may be a resident bearing company representative.

Bearing suppliers provide a wealth of engineering information and detail in their catalogs and engineering guides, both in print and online. It is strongly recommended that the designer become familiar with the specifics of the supplier. It will usually utilize a similar approach as presented here, but may include various modifying factors for such things as temperature and lubrication. Many of the suppliers will provide online software tools to aid in bearing selection. The engineer will always benefit from a general understanding of the theory utilized in such software tools. Our goal here is to introduce the vocabulary, show congruence to fundamentals that were learned earlier, offer examples, and develop confidence. Finally, problems should reinforce the learning experience.

The four components of a tapered roller bearing assembly are the

- Cone (inner ring)
- Cup (outer ring)
- Tapered rollers
- Cage (spacer-retainer)

The assembled bearing consists of two separable parts: (1) the cone assembly: the cone, the rollers, and the cage; and (2) the cup. Bearings can be made as single-row, two-row, four-row, and thrust-bearing assemblies. Additionally, auxiliary components such as spacers and closures can be used. Figure 11–13 shows the nomenclature of a tapered roller bearing, and the point G through which radial and axial components of load act.

A tapered roller bearing can carry both radial and thrust (axial) loads, or any combination of the two. However, even when an external thrust load is not present, the radial

Figure 11–13

Nomenclature of a tapered roller bearing. Point G is the location of the effective load center; use this point to estimate the radial bearing load. (Courtesy of The Timken Company.)

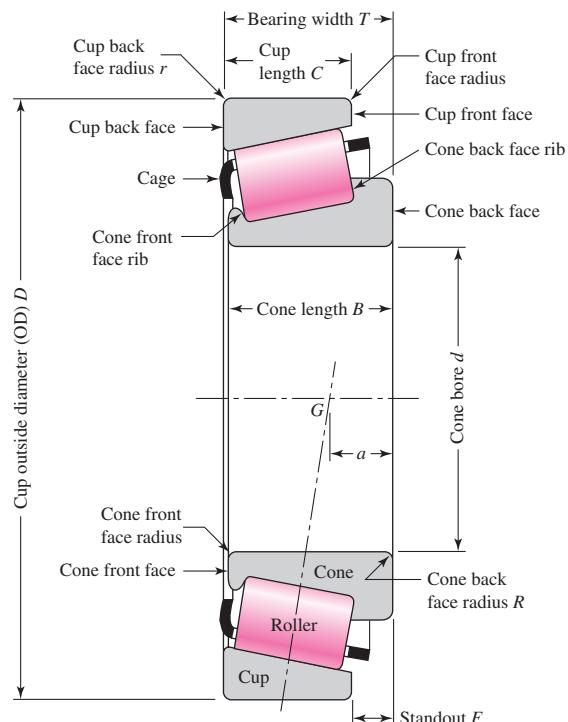
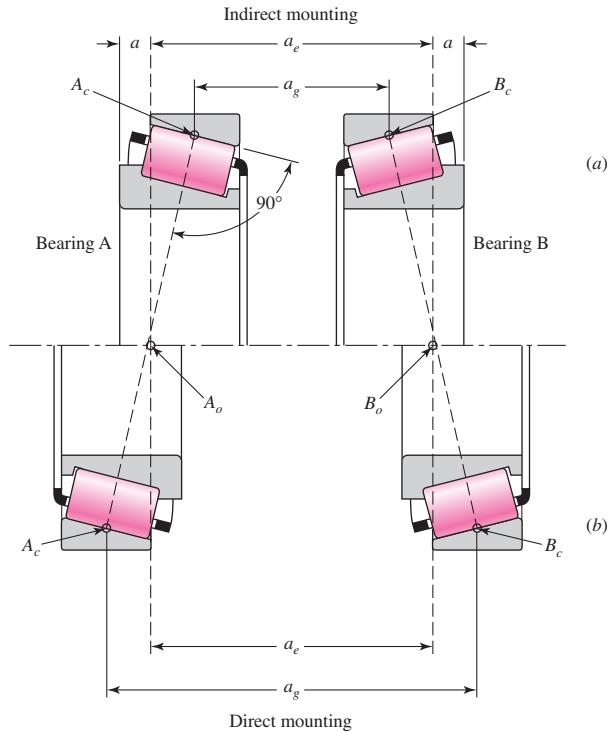


Figure 11-14

Comparison of mounting stability between indirect and direct mountings. (Courtesy of The Timken Company.)



load will induce a thrust reaction within the bearing because of the taper. To avoid the separation of the races and the rollers, this thrust must be resisted by an equal and opposite force. One way of generating this force is to always use at least two tapered roller bearings on a shaft. Two bearings can be mounted with the cone backs facing each other, in a configuration called *direct mounting*, or with the cone fronts facing each other, in what is called *indirect mounting*.

Figure 11-14 shows a pair of tapered roller bearings mounted directly (b) and indirectly (a) with the bearing reaction locations A_0 and B_0 shown for the shaft. For the shaft as a beam, the span is a_e , the effective spread. It is through points A_0 and B_0 that the radial loads act perpendicular to the shaft axis, and the thrust loads act along the shaft axis. The geometric spread a_g for the direct mounting is greater than for the indirect mounting. With indirect mounting the bearings are closer together compared to the direct mounting; however, the system stability is the same (a_e is the same in both cases). Thus direct and indirect mounting involve space and compactness needed or desired, but with the same system stability.

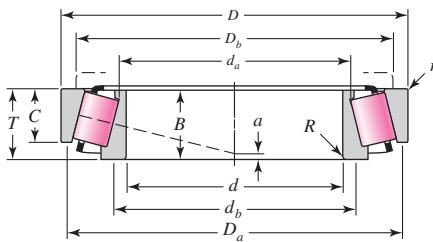
In addition to the usual ratings and geometry information, catalog data for tapered roller bearings will include the location of the effective force center. Two sample pages from a Timken catalog are shown in Fig. 11-15.

A radial load on a tapered roller bearing will induce a thrust reaction. The *load zone* includes about half the rollers and subtends an angle of approximately 180°. Using the symbol F_i for the induced thrust load from a radial load with a 180° load zone, Timken provides the equation

$$F_i = \frac{0.47F_r}{K} \quad (11-15)$$

where the K factor is geometry-specific, and is the ratio of the radial load rating to the thrust load rating. The K factor can be first approximated with 1.5 for a radial

SINGLE-ROW STRAIGHT BORE



bore d	outside diameter D	width T	rating at 500 rpm for 3000 hours L ₁₀				factor K	part numbers		max shaft fillet radius R ^①	width B	cone		cup		max housing fillet radius r ^①	width C	backing shoulder diameters		
			one- row radial N lbf	thrust N lbf	eff. load center a ^②			cone	cup			d _b	d _a	D _b	D _a					
25.000 0.9843	52.000 2.0472	16.250 0.6398	8190 1840	5260 1180	1.56 -0.14	-3.6 -0.14	◆30205	◆30205	1.0 0.04	15.000 0.5906	30.5 1.20	29.0 1.14	1.0 0.04	13.000 0.5118	46.0 1.81	48.5 1.91				
25.000 0.9843	52.000 2.0472	19.250 0.7579	9520 2140	9510 2140	1.00 -0.12	-3.0 -0.12	◆32205-B	◆32205-B	1.0 0.04	18.000 0.7087	34.0 1.34	31.0 1.22	1.0 0.04	15.000 0.5906	43.5 1.71	49.5 1.95				
25.000 0.9843	52.000 2.0472	22.000 0.8661	13200 2980	7960 1790	1.66 -0.30	-7.6 -0.30	◆33205	◆33205	1.0 0.04	22.000 0.8661	34.0 1.34	30.5 1.20	1.0 0.04	18.000 0.7087	44.5 1.75	49.0 1.93				
25.000 0.9843	62.000 2.4409	18.250 0.7185	13000 2930	6680 1500	1.95 -0.20	-5.1 -0.20	◆30305	◆30305	1.5 0.06	17.000 0.6693	32.5 1.28	30.0 1.18	1.5 0.06	15.000 0.5906	55.0 2.17	57.0 2.24				
25.000 0.9843	62.000 2.4409	25.250 0.9941	17400 3910	8930 2010	1.95 -0.38	-9.7 -0.38	◆32305	◆32305	1.5 0.06	24.000 0.9449	35.0 1.38	31.5 1.24	1.5 0.06	20.000 0.7874	54.0 2.13	57.0 2.24				
25.159 0.9905	50.005 1.9687	13.495 0.5313	6990 1570	4810 1080	1.45 -0.11	-2.8 -0.11	07096	07196	1.5 0.06	14.260 0.5614	31.5 1.24	29.5 1.16	1.0 0.04	9.525 0.3750	44.5 1.75	47.0 1.85				
25.400 1.0000	50.005 1.9687	13.495 0.5313	6990 1570	4810 1080	1.45 -0.11	-2.8 -0.11	07100	07196	1.0 0.04	14.260 0.5614	30.5 1.20	29.5 1.16	1.0 0.04	9.525 0.3750	44.5 1.75	47.0 1.85				
25.400 1.0000	50.005 1.9687	13.495 0.5313	6990 1570	4810 1080	1.45 -0.11	-2.8 -0.11	07100-S	07196	1.5 0.06	14.260 0.5614	31.5 1.24	29.5 1.16	1.0 0.04	9.525 0.3750	44.5 1.75	47.0 1.85				
25.400 1.0000	50.292 1.9800	14.224 0.5600	7210 1620	4620 1040	1.56 -0.13	-3.3 -0.13	L44642	L44610	3.5 0.14	14.732 0.5800	36.0 1.42	29.5 1.16	1.3 0.05	10.668 0.4200	44.5 1.75	47.0 1.85				
25.400 1.0000	50.292 1.9800	14.224 0.5600	7210 1620	4620 1040	1.56 -0.13	-3.3 -0.13	L44643	L44610	1.3 0.05	14.732 0.5800	31.5 1.24	29.5 1.16	1.3 0.05	10.668 0.4200	44.5 1.75	47.0 1.85				
25.400 1.0000	51.994 2.0470	15.011 0.5910	6990 1570	4810 1080	1.45 -0.11	-2.8 -0.11	07100	07204	1.0 0.04	14.260 0.5614	30.5 1.20	29.5 1.16	1.3 0.05	12.700 0.5000	45.0 1.77	48.0 1.89				
25.400 1.0000	56.896 2.2400	19.368 0.7625	10900 2450	5740 1290	1.90 -0.27	-6.9 -0.27	1780	1729	0.8 0.03	19.837 0.7810	30.5 1.20	30.0 1.18	1.3 0.05	15.875 0.6250	49.0 1.93	51.0 2.01				
25.400 1.0000	57.150 2.2500	19.431 0.7650	11700 2620	10900 2450	1.07 -0.12	-3.0 -0.12	M84548	M84510	1.5 0.06	19.431 0.7650	36.0 1.42	33.0 1.30	1.5 0.06	14.732 0.5800	48.5 1.91	54.0 2.13				
25.400 1.0000	58.738 2.3125	19.050 0.7500	11600 2610	6560 1470	1.77 -0.23	-5.8 -0.23	1986	1932	1.3 0.05	19.355 0.7620	32.5 1.28	30.5 1.20	1.3 0.05	15.080 0.5937	52.0 2.05	54.0 2.13				
25.400 1.0000	59.530 2.3437	23.368 0.9200	13900 3140	13000 2930	1.07 -0.20	-5.1 -0.20	M84249	M84210	0.8 0.03	23.114 0.9100	36.0 1.42	32.5 1.27	1.5 0.06	18.288 0.7200	49.5 1.95	56.0 2.20				
25.400 1.0000	60.325 2.3750	19.842 0.7812	11000 2480	6550 1470	1.69 -0.20	-5.1 -0.20	15578	15523	1.3 0.05	17.462 0.6875	32.5 1.28	30.5 1.20	1.5 0.06	15.875 0.6250	51.0 2.01	54.0 2.13				
25.400 1.0000	61.912 2.4375	19.050 0.7500	12100 2730	7280 1640	1.67 -0.23	-5.8 -0.23	15101	15243	0.8 0.03	20.638 0.8125	32.5 1.28	31.5 1.24	2.0 0.08	14.288 0.5625	54.0 2.13	58.0 2.28				
25.400 1.0000	62.000 2.4409	19.050 0.7500	12100 2730	7280 1640	1.67 -0.23	-5.8 -0.23	15100	15245	3.5 0.14	20.638 0.8125	38.0 1.50	31.5 1.24	1.3 0.05	14.288 0.5625	55.0 2.17	58.0 2.28				
25.400 1.0000	62.000 2.4409	19.050 0.7500	12100 2730	7280 1640	1.67 -0.23	-5.8 -0.23	15101	15245	0.8 0.03	20.638 0.8125	32.5 1.28	31.5 1.24	1.3 0.05	14.288 0.5625	55.0 2.17	58.0 2.28				

Figure 11-15 (Continued on next page)

Catalog entry of single-row straight-bore Timken roller bearings, in part. (Courtesy of The Timken Company.)

SINGLE-ROW STRAIGHT BORE

bore	outside diameter	width	rating at 500 rpm for 3000 hours L ₁₀		factor	eff. load center	part numbers		max shaft fillet radius	width	backing shoulder diameters		max housing fillet radius	width	cup			
			one-row radial	thrust			cone	cup					d _b	d _a	R ^①	B		
			N lbf	N lbf							cone	cup			K	a②		
d	D	T									R ^①	B	d _b	d _a	r ^①	C	D _b	D _a
25.400 1.0000	62.000 2.4409	19.050 0.7500	12100 2730	7280 1640	1.67 -0.23	-5.8 -0.23	15102	15245	1.5 0.06	20.638 0.8125	34.0 1.34	31.5 1.24	1.3 0.05	14.288 0.5625	55.0 2.17	58.0 2.28		
25.400 1.0000	62.000 2.4409	20.638 0.8125	12100 2730	7280 1640	1.67 -0.23	-5.8 -0.23	15101	15244	0.8 0.03	20.638 0.8125	32.5 1.28	31.5 1.24	1.3 0.05	15.875 0.6250	55.0 2.17	58.0 2.28		
25.400 1.0000	63.500 2.5000	20.638 0.8125	12100 2730	7280 1640	1.67 -0.23	-5.8 -0.23	15101	15250	0.8 0.03	20.638 0.8125	32.5 1.28	31.5 1.24	1.3 0.05	15.875 0.6250	56.0 2.20	59.0 2.32		
25.400 1.0000	63.500 2.5000	20.638 0.8125	12100 2730	7280 1640	1.67 -0.23	-5.8 -0.23	15101	15250X	0.8 0.03	20.638 0.8125	32.5 1.28	31.5 1.24	1.5 0.06	15.875 0.6250	55.0 2.17	59.0 2.32		
25.400 1.0000	64.292 2.5312	21.433 0.8438	14500 3250	13500 3040	1.07 -0.13	-3.3 -0.13	M86643	M86610	1.5 0.06	21.433 0.8438	38.0 1.50	36.5 1.44	1.5 0.06	16.670 0.6563	54.0 2.13	61.0 2.40		
25.400 1.0000	65.088 2.5625	22.225 0.8750	13100 2950	16400 3690	0.80 -0.09	-2.3 -0.09	23100	23256	1.5 0.06	21.463 0.8450	39.0 1.54	34.5 1.36	1.5 0.06	15.875 0.6250	53.0 2.09	63.0 2.48		
25.400 1.0000	66.421 2.6150	23.812 0.9375	18400 4140	8000 1800	2.30 -0.37	-9.4 -0.37	2687	2631	1.3 0.05	25.433 1.0013	33.5 1.32	31.5 1.24	1.3 0.05	19.050 0.7500	58.0 2.28	60.0 2.36		
25.400 1.0000	68.262 2.6875	22.225 0.8750	15300 3440	10900 2450	1.40 -0.20	-5.1 -0.20	02473	02420	0.8 0.03	22.225 0.8750	34.5 1.36	33.5 1.32	1.5 0.06	17.462 0.6875	59.0 2.32	63.0 2.48		
25.400 1.0000	72.233 2.8438	25.400 1.0000	18400 4140	17200 3870	1.07 -0.18	-4.6 -0.18	HM88630	HM88610	0.8 0.03	25.400 1.0000	39.5 1.56	39.5 1.56	2.3 0.09	19.842 0.7812	60.0 2.36	69.0 2.72		
25.400 1.0000	72.626 2.8593	30.162 1.1875	22700 5110	13000 2910	1.76 -0.40	-10.2 -0.40	3189	3120	0.8 0.03	29.997 1.1810	35.5 1.40	35.0 1.38	3.3 0.13	23.812 0.9375	61.0 2.40	67.0 2.64		
26.157 1.0298	62.000 2.4409	19.050 0.7500	12100 2730	7280 1640	1.67 -0.23	-5.8 -0.23	15103	15245	0.8 0.03	20.638 0.8125	33.0 1.30	32.5 1.28	1.3 0.05	14.288 0.5625	55.0 2.17	58.0 2.28		
26.162 1.0300	63.100 2.4843	23.812 0.9375	18400 4140	8000 1800	2.30 -0.37	-9.4 -0.37	2682	2630	1.5 0.06	25.433 1.0013	34.5 1.36	32.0 1.26	0.8 0.03	19.050 0.7500	57.0 2.24	59.0 2.32		
26.162 1.0300	66.421 2.6150	23.812 0.9375	18400 4140	8000 1800	2.30 -0.37	-9.4 -0.37	2682	2631	1.5 0.06	25.433 1.0013	34.5 1.36	32.0 1.26	1.3 0.05	19.050 0.7500	58.0 2.28	60.0 2.36		
26.975 1.0620	58.738 2.3125	19.050 0.7500	11600 2610	6560 1470	1.77 -0.23	-5.8 -0.23	1987	1932	0.8 0.03	19.355 0.7620	32.5 1.28	31.5 1.24	1.3 0.05	15.080 0.5937	52.0 2.05	54.0 2.13		
† 26.988 † 1.0625	50.292 1.9800	14.224 0.5600	7210 1620	4620 1040	1.56 -0.13	-3.3 -0.13	L44649	L44610	3.5 0.14	14.732 0.5800	37.5 1.48	31.0 1.22	1.3 0.05	10.668 0.4200	44.5 1.75	47.0 1.85		
† 26.988 † 1.0625	60.325 2.3750	19.842 0.7812	11000 2480	6550 1470	1.69 -0.20	-5.1 -0.20	15580	15523	3.5 0.14	17.462 0.6875	38.5 1.52	32.0 1.26	1.5 0.06	15.875 0.6250	51.0 2.01	54.0 2.13		
† 26.988 † 1.0625	62.000 2.4409	19.050 0.7500	12100 2730	7280 1640	1.67 -0.23	-5.8 -0.23	15106	15245	0.8 0.03	20.638 0.8125	33.5 1.32	33.0 1.30	1.3 0.05	14.288 0.5625	55.0 2.17	58.0 2.28		
† 26.988 † 1.0625	66.421 2.6150	23.812 0.9375	18400 4140	8000 1800	2.30 -0.37	-9.4 -0.37	2688	2631	1.5 0.06	25.433 1.0013	35.0 1.38	33.0 1.30	1.3 0.05	19.050 0.7500	58.0 2.28	60.0 2.36		
28.575 1.1250	56.896 2.2400	19.845 0.7813	11600 2610	6560 1470	1.77 -0.23	-5.8 -0.23	1985	1930	0.8 0.03	19.355 0.7620	34.0 1.34	33.5 1.32	0.8 0.03	15.875 0.6250	51.0 2.01	54.0 2.11		
28.575 1.1250	57.150 2.2500	17.462 0.6875	11000 2480	6550 1470	1.69 -0.20	-5.1 -0.20	15590	15520	3.5 0.14	17.462 0.6875	39.5 1.56	33.5 1.32	1.5 0.06	13.495 0.5313	51.0 2.01	53.0 2.09		
28.575 1.1250	58.738 2.3125	19.050 0.7500	11600 2610	6560 1470	1.77 -0.23	-5.8 -0.23	1985	1932	0.8 0.03	19.355 0.7620	34.0 1.34	33.5 1.32	1.3 0.05	15.080 0.5937	52.0 2.05	54.0 2.13		
28.575 1.1250	58.738 2.3125	19.050 0.7500	11600 2610	6560 1470	1.77 -0.23	-5.8 -0.23	1988	1932	3.5 0.14	19.355 0.7620	39.5 1.56	33.5 1.32	1.3 0.05	15.080 0.5937	52.0 2.05	54.0 2.13		
28.575 1.1250	60.325 2.3750	19.842 0.7812	11000 2480	6550 1470	1.69 -0.20	-5.1 -0.20	15590	15523	3.5 0.14	17.462 0.6875	39.5 1.56	33.5 1.32	1.5 0.06	15.875 0.6250	51.0 2.01	54.0 2.13		
28.575 1.1250	60.325 2.3750	19.842 0.7812	11000 2480	6550 1470	1.69 -0.20	-5.1 -0.20	1985	1931	0.5 0.03	19.355 0.7620	34.0 1.34	33.5 1.32	1.3 0.05	15.875 0.6250	52.0 2.05	55.0 2.17		

① These maximum fillet radii will be cleared by the bearing corners.

② Minus value indicates center is inside cone backface.

† For standard class **ONLY**, the maximum metric size is a whole mm value.

* For "J" part tolerances—see metric tolerances, page 73, and fitting practice, page 65.

◆ ISO cone and cup combinations are designated with a common part number and should be purchased as an assembly.

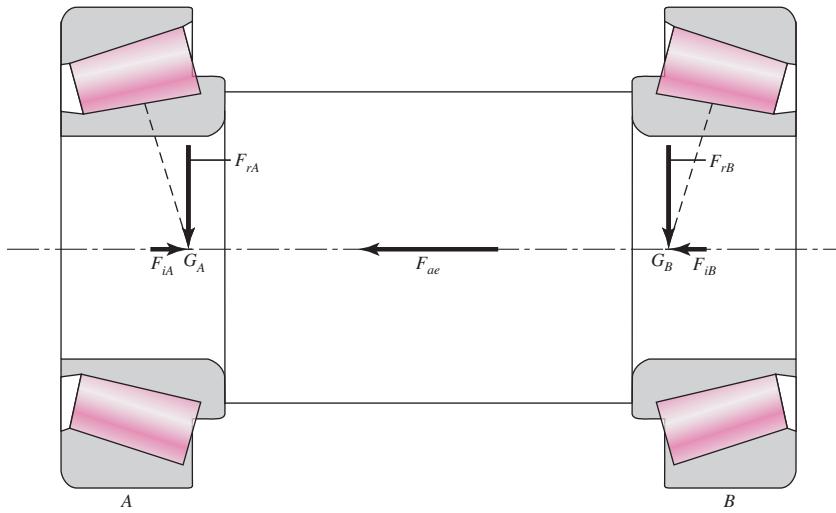
For ISO bearing tolerances—see metric tolerances, page 73, and fitting practice, page 65.

Figure 11-15

(Continued)

Figure 11-16

Direct-mounted tapered roller bearings, showing radial, induced thrust, and external thrust loads.



bearing and 0.75 for a steep angle bearing in the preliminary selection process. After a possible bearing is identified, the exact value of K for each bearing can be found in the bearing catalog.

A shaft supported by a pair of direct-mounted tapered roller bearings is shown in Fig. 11-16. Force vectors are shown as applied to the shaft. F_{rA} and F_{rB} are the radial loads carried by the bearings, applied at the effective force centers G_A and G_B . The induced loads F_{iA} and F_{iB} due to the effect of the radial loads on the tapered bearings are also shown. Additionally, there may be an externally applied thrust load F_{ae} on the shaft from some other source, such as the axial load on a helical gear. Since the bearings experience both radial and thrust loads, it is necessary to determine equivalent radial loads. Following the form of Eq. (11-9), where $F_e = XVF_r + YF_a$, Timken recommends using $X = 0.4$ and $V = 1$ for all cases, and using the K factor for the specific bearing for Y . This gives an equation of the form

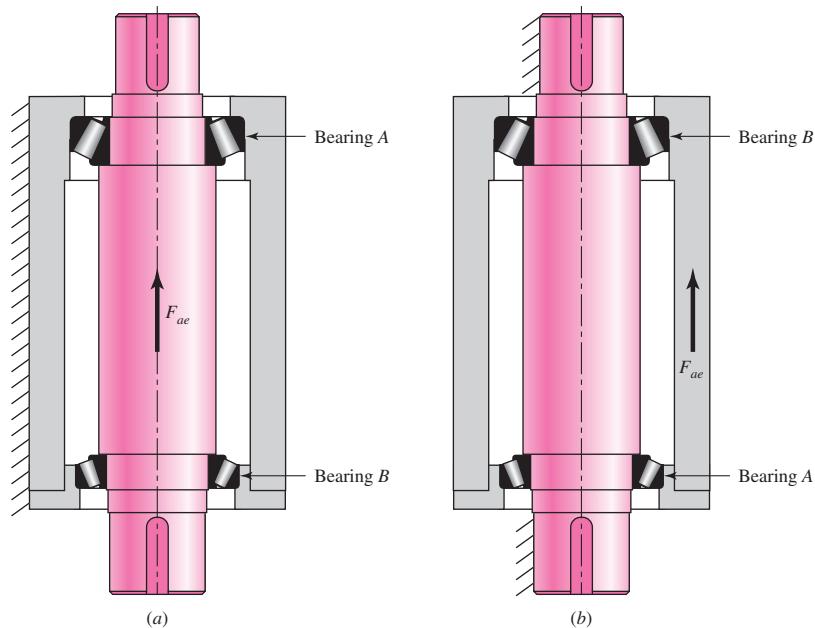
$$F_e = 0.4F_r + KF_a \quad (a)$$

The axial load F_a is the net axial load carried by the bearing due to the combination of the induced axial load from the other bearing and the external axial load. However, only one of the bearings will carry the net axial load, and which one it is depends on the direction the bearings are mounted, the relative magnitudes of the induced loads, the direction of the external load, and whether the shaft or the housing is the moving part. Timken handles it with a table containing each of the configurations and a sign convention on the external loads. It further requires the application to be oriented horizontally with left and right bearings that must match the left and right sign conventions. Here, we will present a method that gives equivalent results, but that is perhaps more conducive to visualizing and understanding the logic behind it.

First, determine visually which bearing is being “squeezed” by the external thrust load, and label it as bearing A. Label the other bearing as bearing B. For example, in Fig. 11-16, the external thrust F_{ae} causes the shaft to push to the left against the cone of the left bearing, squeezing it against the rollers and the cup. On the other hand, it tends to pull apart the cup from the right bearing. The left bearing is therefore labeled as bearing A. If the direction of F_{ae} were reversed, then the right bearing would be labeled as bearing A. This approach to labeling the bearing being squeezed by the

Figure 11-17

Examples of determining which bearing carries the external thrust load. In each case, the compressed bearing is labeled as bearing A.
(a) External thrust applied to rotating shaft; (b) External thrust applied to rotating cylinder.



external thrust is applied similarly regardless of whether the bearings are mounted directly or indirectly, regardless of whether the shaft or the housing carries the external thrust, and regardless of the orientation of the assembly. To clarify by example, consider the vertical shaft and cylinder in Fig. 11-17 with direct-mounted bearings. In Fig. 11-17a, an external load is applied in the upward direction to a rotating shaft, compressing the top bearing, which should be labeled as bearing A. On the other hand, in Fig. 11-17b, an upward external load is applied to a rotating outer cylinder with a stationary shaft. In this case, the lower bearing is being squeezed and should be labeled as bearing A. If there is no external thrust, then either bearing can arbitrarily be labeled as bearing A.

Second, determine which bearing actually carries the net axial load. Generally, it would be expected that bearing A would carry the axial load, since the external thrust F_{ae} is directed toward A, along with the induced thrust F_{iB} from bearing B. However, if the induced thrust F_{iA} from bearing A happens to be larger than the combination of the external thrust and the thrust induced by bearing B, then bearing B will carry the net thrust load. We will use Eq. (a) for the bearing carrying the thrust load. Timken recommends leaving the other bearing at its original radial load, rather than reducing it due to the negative net thrust load. The results are presented in equation form below, where the induced thrusts are defined by Eq. (11-15).

$$\text{If } F_{iA} \leq (F_{iB} + F_{ae}) \quad \begin{cases} F_{eA} = 0.4F_{rA} + K_A(F_{iB} + F_{ae}) \\ F_{eB} = F_{rB} \end{cases} \quad (11-16a) \quad (11-16b)$$

$$\text{If } F_{iA} > (F_{iB} + F_{ae}) \quad \begin{cases} F_{eB} = 0.4F_{rB} + K_B(F_{iA} - F_{ae}) \\ F_{eA} = F_{rA} \end{cases} \quad (11-17a) \quad (11-17b)$$

In any case, if the equivalent radial load is ever less than the original radial load, then the original radial load should be used.

Once the equivalent radial loads are determined, they should be used to find the catalog rating load using any of Eqs. (11–3), (11–6), or (11–7) as before. Timken uses a two-parameter Weibell model with $x_0 = 0$, $\theta = 4.48$, and $b = 3/2$. Note that since K_A and K_B are dependent on the specific bearing chosen, it may be necessary to iterate the process.

EXAMPLE 11–8

The shaft depicted in Fig. 11–18a carries a helical gear with a tangential force of 3980 N, a radial force of 1770 N, and a thrust force of 1690 N at the pitch cylinder with directions shown. The pitch diameter of the gear is 200 mm. The shaft runs at a speed of 800 rev/min, and the span (effective spread) between the direct-mount bearings is 150 mm. The design life is to be 5000 h and an application factor of 1 is appropriate. If the reliability of the bearing set is to be 0.99, select suitable single-row tapered-roller Timken bearings.

Solution

The reactions in the xz plane from Fig. 11–18b are

$$R_{zA} = \frac{3980(50)}{150} = 1327 \text{ N}$$

$$R_{zB} = \frac{3980(100)}{150} = 2653 \text{ N}$$

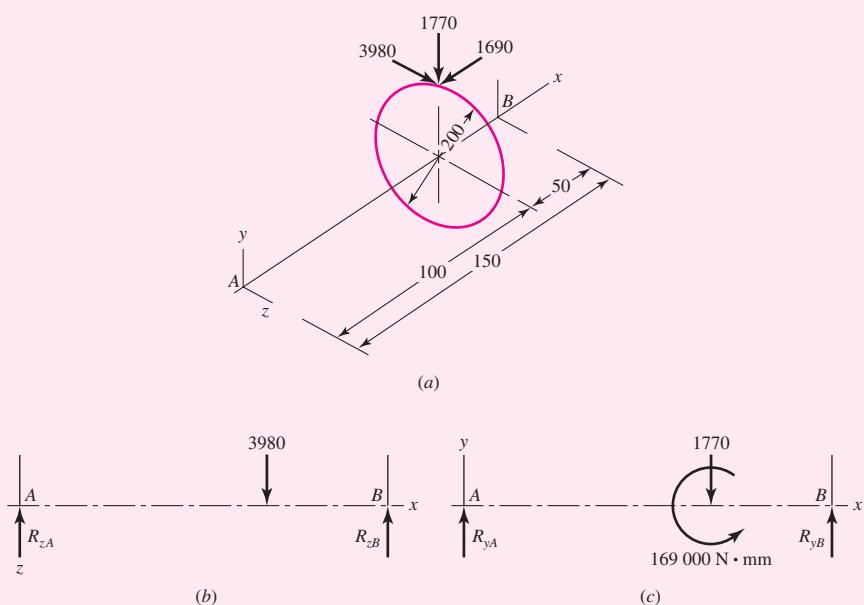
The reactions in the xy plane from Fig. 11–18c are

$$R_{yA} = \frac{1770(50)}{150} + \frac{169\,000}{150} = 1716.7 = 1717 \text{ N}$$

$$R_{yB} = \frac{1770(100)}{150} - \frac{169\,000}{150} = 53.3 \text{ N}$$

Figure 11–18

Essential geometry of helical gear and shaft. Length dimensions in mm, loads in N, couple in N · mm. (a) Sketch (not to scale) showing thrust, radial, and tangential forces. (b) Forces in xz plane. (c) Forces in xy plane.



The radial loads F_{rA} and F_{rB} are the vector additions of R_{yA} and R_{zA} , and R_{yB} and R_{zB} , respectively:

$$F_{rA} = (R_{zA}^2 + R_{yA}^2)^{1/2} = (1327^2 + 1717^2)^{1/2} = 2170 \text{ N}$$

$$F_{rB} = (R_{zB}^2 + R_{yB}^2)^{1/2} = (2653^2 + 53.3^2)^{1/2} = 2654 \text{ N}$$

Trial 1: With direct mounting of the bearings and application of the external thrust to the shaft, the squeezed bearing is bearing A as labeled in Fig. 11–18a. Using K of 1.5 as the initial guess for each bearing, the induced loads from the bearings are

$$F_{iA} = \frac{0.47F_{rA}}{K_A} = \frac{0.47(2170)}{1.5} = 680 \text{ N}$$

$$F_{iB} = \frac{0.47F_{rB}}{K_B} = \frac{0.47(2654)}{1.5} = 832 \text{ N}$$

Since F_{iA} is clearly less than $F_{iB} + F_{ae}$, bearing A carries the net thrust load, and Eq. (11–16) is applicable. Therefore, the dynamic equivalent loads are

$$F_{eA} = 0.4F_{rA} + K_A(F_{iB} + F_{ae}) = 0.4(2170) + 1.5(832 + 1690) = 4651 \text{ N}$$

$$F_{eB} = F_{rB} = 2654 \text{ N}$$

The multiple of rating life is

$$x_D = \frac{L_D}{L_R} = \frac{\mathcal{L}_D n_D 60}{L_R} = \frac{(5000)(800)(60)}{90(10^6)} = 2.67$$

Estimate R_D as $\sqrt{0.99} = 0.995$ for each bearing. For bearing A, from Eq. (11–7) the catalog entry C_{10} should equal or exceed

$$C_{10} = (1)(4651) \left[\frac{2.67}{(4.48)(1 - 0.995)^{2/3}} \right]^{3/10} = 11\,486 \text{ N}$$

From Fig. 11–15, tentatively select type TS 15100 cone and 15245 cup, which will work: $K_A = 1.67$, $C_{10} = 12\,100 \text{ N}$.

For bearing B, from Eq. (11–7), the catalog entry C_{10} should equal or exceed

$$C_{10} = (1)2654 \left[\frac{2.67}{(4.48)(1 - 0.995)^{2/3}} \right]^{3/10} = 6554 \text{ N}$$

Tentatively select the bearing identical to bearing A, which will work: $K_B = 1.67$, $C_{10} = 12\,100 \text{ N}$.

Trial 2: Repeat the process with $K_A = K_B = 1.67$ from tentative bearing selection.

$$F_{iA} = \frac{0.47F_{rA}}{K_A} = \frac{0.47(2170)}{1.67} = 611 \text{ N}$$

$$F_{iB} = \frac{0.47F_{rB}}{K_B} = \frac{0.47(2654)}{1.67} = 747 \text{ N}$$

Since F_{iA} is still less than $F_{iB} + F_{ae}$, Eq. (11–16) is still applicable.

$$F_{eA} = 0.4F_{rA} + K_A(F_{iB} + F_{ae}) = 0.4(2170) + 1.67(747 + 1690) = 4938 \text{ N}$$

$$F_{eB} = F_{rB} = 2654 \text{ N}$$

For bearing A, from Eq. (11–7) the corrected catalog entry C_{10} should equal or exceed

$$C_{10} = (1)(4938) \left[\frac{2.67}{(4.48)(1 - 0.995)^{2/3}} \right]^{3/10} = 12\,195 \text{ N}$$

Although this catalog entry exceeds slightly the tentative selection for bearing A, we will keep it since the reliability of bearing B exceeds 0.995. In the next section we will quantitatively show that the combined reliability of bearing A and B will exceed the reliability goal of 0.99.

For bearing B, $F_{eB} = F_{rB} = 2654 \text{ N}$. From Eq. (11–7),

$$C_{10} = (1)2654 \left[\frac{2.67}{(4.48)(1 - 0.995)^{2/3}} \right]^{3/10} = 6554 \text{ N}$$

Select cone and cup 15100 and 15245, respectively, for both bearing A and B. Note from Fig. 11–14 the effective load center is located at $a = -5.8 \text{ mm}$, that is, 5.8 mm into the cup from the back. Thus the shoulder-to-shoulder dimension should be $150 - 2(5.8) = 138.4 \text{ mm}$. Note that in each iteration of Eq. (11–7) to find the catalog load rating, the bracketed portion of the equation is identical and need not be re-entered on a calculator each time.

11–10

Design Assessment for Selected Rolling-Contact Bearings

In textbooks machine elements typically are treated singly. This can lead the reader to the presumption that a design assessment involves only that element, in this case a rolling-contact bearing. The immediately adjacent elements (the shaft journal and the housing bore) have immediate influence on the performance. Other elements, further removed (gears producing the bearing load), also have influence. Just as some say, “If you pull on something in the environment, you find that it is attached to everything else.” This should be intuitively obvious to those involved with machinery. How, then, can one check shaft attributes that aren’t mentioned in a problem statement? Possibly, because the bearing hasn’t been designed yet (in fine detail). All this points out the necessary iterative nature of designing, say, a speed reducer. If power, speed, and reduction are stipulated, then gear sets can be roughed in, their sizes, geometry, and location estimated, shaft forces and moments identified, bearings tentatively selected, seals identified; the bulk is beginning to make itself evident, the housing and lubricating scheme as well as the cooling considerations become clearer, shaft overhangs and coupling accommodations appear. It is time to iterate, now addressing each element again, knowing much more about all of the others. When you have completed the necessary iterations, you will know what you need for the design assessment for the bearings. In the meantime you do as much of the design assessment as you can, avoiding bad selections, even if tentative. Always keep in mind that you eventually have to do it all in order to pronounce your completed design satisfactory.

An outline of a design assessment for a rolling contact bearing includes, at a minimum,

- Bearing reliability for the load imposed and life expected
- Shouldering on shaft and housing satisfactory
- Journal finish, diameter and tolerance compatible
- Housing finish, diameter and tolerance compatible
- Lubricant type according to manufacturer's recommendations; lubricant paths and volume supplied to keep operating temperature satisfactory
- Preloads, if required, are supplied

Since we are focusing on rolling-contact bearings, we can address bearing reliability quantitatively, as well as shouldering. Other quantitative treatment will have to wait until the materials for shaft and housing, surface quality, and diameters and tolerances are known.

Bearing Reliability

Equation (11-6) can be solved for the reliability R_D in terms of C_{10} , the basic load rating of the selected bearing:

$$R = \exp \left(- \left\{ \frac{x_D \left(\frac{a_f F_D}{C_{10}} \right)^a - x_0}{\theta - x_0} \right\}^b \right) \quad (11-18)$$

Equation (11-7) can likewise be solved for R_D :

$$R \doteq 1 - \left\{ \frac{x_D \left(\frac{a_f F_D}{C_{10}} \right)^a - x_0}{\theta - x_0} \right\}^b \quad R \geq 0.90 \quad (11-19)$$

EXAMPLE 11-9

In Ex. 11-3, the minimum required load rating for 99 percent reliability, at $x_D = L_D/L_{10} = 540$, is $C_{10} = 6696$ lbf = 29.8 kN. From Table 11-2 a 02-40 mm deep-groove ball bearing would satisfy the requirement. If the bore in the application had to be 70 mm or larger (selecting a 02-70 mm deep-groove ball bearing), what is the resulting reliability?

Solution

From Table 11-2, for a 02-70 mm deep-groove ball bearing, $C_{10} = 61.8$ kN = 13 888 lbf. Using Eq. (11-19), recalling from Ex. 11-3 that $a_f = 1.2$, $F_D = 413$ lbf, $x_0 = 0.02$, $(\theta - x_0) = 4.439$, and $b = 1.483$, we can write

Answer

$$R \doteq 1 - \left\{ \frac{\left[540 \left[\frac{1.2(413)}{13888} \right]^3 - 0.02 \right]}{4.439} \right\}^{1.483} = 0.999963$$

which, as expected, is much higher than 0.99 from Ex. 11-3.

In tapered roller bearings, or other bearings for a two-parameter Weibull distribution, Eq. (11–18) becomes, for $x_0 = 0$, $\theta = 4.48$, $b = \frac{3}{2}$,

$$\begin{aligned} R &= \exp \left\{ - \left[\frac{x_D}{\theta [C_{10}/(a_f F_D)]^a} \right]^b \right\} \\ &= \exp \left\{ - \left[\frac{x_D}{4.48 [C_{10}/(a_f F_D)]^{10/3}} \right]^{3/2} \right\} \end{aligned} \quad (11-20)$$

and Eq. (11–19) becomes

$$R \doteq 1 - \left\{ \frac{x_D}{\theta [C_{10}/(a_f F_D)]^a} \right\}^b = 1 - \left\{ \frac{x_D}{4.48 [C_{10}/(a_f F_D)]^{10/3}} \right\}^{3/2} \quad (11-21)$$

EXAMPLE 11-10

In Ex. 11–8 bearings *A* and *B* (cone 15100 and cup 15245) have $C_{10} = 12\ 100$ N. What is the reliability of the pair of bearings *A* and *B*?

Solution

The desired life x_D was $5000(800)60/[90(10^6)] = 2.67$ rating lives. Using Eq. (11–21) for bearing *A*, where from Ex. 11–8, $F_D = F_{eA} = 4938$ N, and $a_f = 1$, gives

$$R_A \doteq 1 - \left\{ \frac{2.67}{4.48 [12\ 100/(1 \times 4938)]^{10/3}} \right\}^{3/2} = 0.994\ 791$$

which is less than 0.995, as expected. Using Eq. (11–21) for bearing *B* with $F_D = F_{eB} = 2654$ N gives

$$R_B \doteq 1 - \left\{ \frac{2.67}{4.48 [12\ 100/(1 \times 2654)]^{10/3}} \right\}^{3/2} = 0.999\ 766$$

Answer

The reliability of the bearing pair is

$$R = R_A R_B = 0.994\ 791(0.999\ 766) = 0.994\ 558$$

which is greater than the overall reliability goal of 0.99. When two bearings are made identical for simplicity, or reducing the number of spares, or other stipulation, and the loading is not the same, both can be made smaller and still meet a reliability goal. If the loading is disparate, then the more heavily loaded bearing can be chosen for a reliability goal just slightly larger than the overall goal.

An additional example is useful to show what happens in cases of pure thrust loading.

EXAMPLE 11-11

Consider a constrained housing as depicted in Fig. 11–19 with two direct-mount tapered roller bearings resisting an external thrust F_{ae} of 8000 N. The shaft speed is 950 rev/min, the desired life is 10 000 h, the expected shaft diameter is approximately 1 in. The reliability goal is 0.95. The application factor is appropriately $a_f = 1$.

- Choose a suitable tapered roller bearing for A.
- Choose a suitable tapered roller bearing for B.
- Find the reliabilities R_A , R_B , and R .

Solution

(a) By inspection, note that the left bearing carries the axial load and is properly labeled as bearing A. The bearing reactions at A are

$$F_{rA} = F_{rB} = 0$$

$$F_{aA} = F_{ae} = 8000 \text{ N}$$

Since bearing B is unloaded, we will start with $R = R_A = 0.95$.

With no radial loads, there are no induced thrust loads. Eq. (11–16) is applicable.

$$F_{eA} = 0.4F_{rA} + K_A(F_{iB} + F_{ae}) = K_A F_{ae}$$

If we set $K_A = 1$, we can find C_{10} in the thrust column and avoid iteration:

$$F_{eA} = (1)8000 = 8000 \text{ N}$$

$$F_{eB} = F_{rB} = 0$$

The multiple of rating life is

$$x_D = \frac{L_D}{L_R} = \frac{\mathcal{L}_D n_D 60}{L_R} = \frac{(10\,000)(950)(60)}{90(10^6)} = 6.333$$

Then, from Eq. (11–7), for bearing A

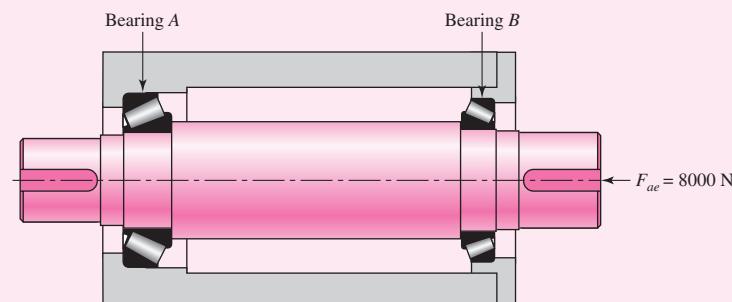
$$\begin{aligned} C_{10} &= a_f F_{eA} \left[\frac{x_D}{4.48(1 - R_D)^{2/3}} \right]^{3/10} \\ &= (1)8000 \left[\frac{6.33}{4.48(1 - 0.95)^{2/3}} \right]^{3/10} = 16\,159 \text{ N} \end{aligned}$$

Answer

Figure 11–15 presents one possibility in the 1-in bore (25.4-mm) size: cone, HM88630, cup HM88610 with a thrust rating (C_{10})_a = 17 200 N.

Figure 11-19

The constrained housing of Ex. 11-11.



Answer

(b) Bearing *B* experiences no load, and the cheapest bearing of this bore size will do, including a ball or roller bearing.

(c) The actual reliability of bearing *A*, from Eq. (11–21), is

Answer

$$R_A \doteq 1 - \left\{ \frac{x_D}{4.48[C_{10}/(a_f F_D)]^{10/3}} \right\}^{3/2}$$

$$\doteq 1 - \left\{ \frac{6.333}{4.48[17\ 200/(1 \times 8000)]^{10/3}} \right\}^{3/2} = 0.963$$

which is greater than 0.95, as one would expect. For bearing *B*,

Answer

$$F_D = F_{eB} = 0$$

$$R_B \doteq 1 - \left[\frac{6.333}{0.85(17\ 200/0)^{10/3}} \right]^{3/2} = 1 - 0 = 1$$

as one would expect. The combined reliability of bearings *A* and *B* as a pair is

Answer

$$R = R_A R_B = 0.963(1) = 0.963$$

which is greater than the reliability goal of 0.95, as one would expect.

Matters of Fit

Table 11–2 (and Fig. 11–8), which shows the rating of single-row, 02-series, deep-groove and angular-contact ball bearings, includes shoulder diameters recommended for the shaft seat of the inner ring and the shoulder diameter of the outer ring, denoted d_S and d_H , respectively. The shaft shoulder can be greater than d_S but not enough to obstruct the annulus. It is important to maintain concentricity and perpendicularity with the shaft centerline, and to that end the shoulder diameter should equal or exceed d_S . The housing shoulder diameter d_H is to be equal to or less than d_H to maintain concentricity and perpendicularity with the housing bore axis. Neither the shaft shoulder nor the housing shoulder features should allow interference with the free movement of lubricant through the bearing annulus.

In a tapered roller bearing (Fig. 11–15), the cup housing shoulder diameter should be equal to or less than D_b . The shaft shoulder for the cone should be equal to or greater than d_b . Additionally, free lubricant flow is not to be impeded by obstructing any of the annulus. In splash lubrication, common in speed reducers, the lubricant is thrown to the housing cover (ceiling) and is directed in its draining by ribs to a bearing. In direct mounting, a tapered roller bearing pumps oil from outboard to inboard. An oil passageway to the outboard side of the bearing needs to be provided. The oil returns to the sump as a consequence of bearing pump action. With an indirect mount, the oil is directed to the inboard annulus, the bearing pumping it to the outboard side. An oil passage from the outboard side to the sump has to be provided.

11–11

Lubrication

The contacting surfaces in rolling bearings have a relative motion that is both rolling and sliding, and so it is difficult to understand exactly what happens. If the relative velocity of the sliding surfaces is high enough, then the lubricant action is

hydrodynamic (see Chap. 12). *Elastohydrodynamic lubrication* (EHD) is the phenomenon that occurs when a lubricant is introduced between surfaces that are in pure rolling contact. The contact of gear teeth and that found in rolling bearings and in cam-and-follower surfaces are typical examples. When a lubricant is trapped between two surfaces in rolling contact, a tremendous increase in the pressure within the lubricant film occurs. But viscosity is exponentially related to pressure, and so a very large increase in viscosity occurs in the lubricant that is trapped between the surfaces. Leibensperger² observes that the change in viscosity in and out of contact pressure is equivalent to the difference between cold asphalt and light sewing machine oil.

The purposes of an antifriction-bearing lubricant may be summarized as follows:

- 1** To provide a film of lubricant between the sliding and rolling surfaces
- 2** To help distribute and dissipate heat
- 3** To prevent corrosion of the bearing surfaces
- 4** To protect the parts from the entrance of foreign matter

Either oil or grease may be employed as a lubricant. The following rules may help in deciding between them.

Use Grease When	Use Oil When
<ol style="list-style-type: none"> 1. The temperature is not over 200°F. 2. The speed is low. 3. Unusual protection is required from the entrance of foreign matter. 4. Simple bearing enclosures are desired. 5. Operation for long periods without attention is desired. 	<ol style="list-style-type: none"> 1. Speeds are high. 2. Temperatures are high. 3. Oiltight seals are readily employed. 4. Bearing type is not suitable for grease lubrication. 5. The bearing is lubricated from a central supply which is also used for other machine parts.

11-12 Mounting and Enclosure

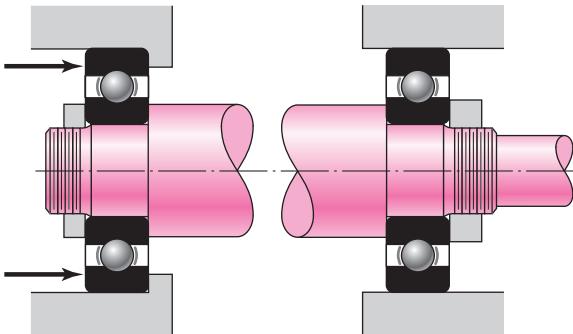
There are so many methods of mounting antifriction bearings that each new design is a real challenge to the ingenuity of the designer. The housing bore and shaft outside diameter must be held to very close limits, which of course is expensive. There are usually one or more counterboring operations, several facing operations and drilling, tapping, and threading operations, all of which must be performed on the shaft, housing, or cover plate. Each of these operations contributes to the cost of production, so that the designer, in ferreting out a trouble-free and low-cost mounting, is faced with a difficult and important problem. The various bearing manufacturers' handbooks give many mounting details in almost every design area. In a text of this nature, however, it is possible to give only the barest details.

The most frequently encountered mounting problem is that which requires one bearing at each end of a shaft. Such a design might use one ball bearing at each end, one tapered roller bearing at each end, or a ball bearing at one end and a straight roller bearing at the other. One of the bearings usually has the added function of

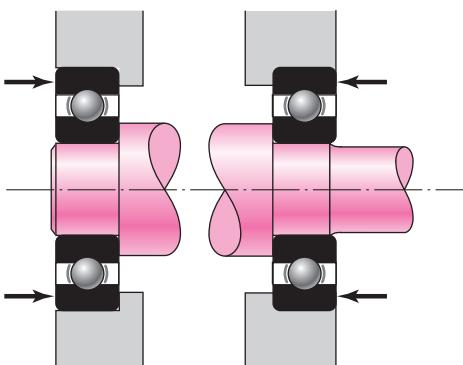
²R. L. Leibensperger, "When Selecting a Bearing," *Machine Design*, vol. 47, no. 8, April 3, 1975, pp. 142–147.

Figure 11-20

A common bearing mounting.

**Figure 11-21**

An alternative bearing mounting to that in Fig. 11-20.



positioning or axially locating the shaft. Figure 11-20 shows a very common solution to this problem. The inner rings are backed up against the shaft shoulders and are held in position by round nuts threaded onto the shaft. The outer ring of the left-hand bearing is backed up against a housing shoulder and is held in position by a device that is not shown. The outer ring of the right-hand bearing floats in the housing.

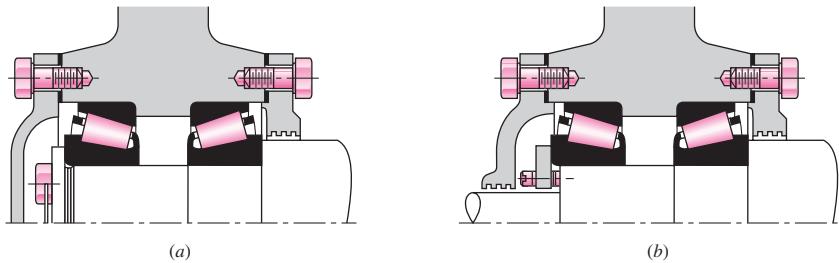
There are many variations possible on the method shown in Fig. 11-20. For example, the function of the shaft shoulder may be performed by retaining rings, by the hub of a gear or pulley, or by spacing tubes or rings. The round nuts may be replaced by retaining rings or by washers locked in position by screws, cotters, or taper pins. The housing shoulder may be replaced by a retaining ring; the outer ring of the bearing may be grooved for a retaining ring, or a flanged outer ring may be used. The force against the outer ring of the left-hand bearing is usually applied by the cover plate, but if no thrust is present, the ring may be held in place by retaining rings.

Figure 11-21 shows an alternative method of mounting in which the inner races are backed up against the shaft shoulders as before but no retaining devices are required. With this method the outer races are completely retained. This eliminates the grooves or threads, which cause stress concentration on the overhanging end, but it requires accurate dimensions in an axial direction or the employment of adjusting means. This method has the disadvantage that if the distance between the bearings is great, the temperature rise during operation may expand the shaft enough to destroy the bearings.

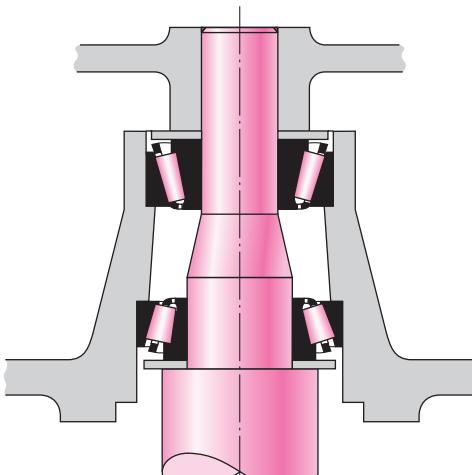
It is frequently necessary to use two or more bearings at one end of a shaft. For example, two bearings could be used to obtain additional rigidity or increased load capacity or to cantilever a shaft. Several two-bearing mountings are shown in Fig. 11-22. These may be used with tapered roller bearings, as shown, or with ball bearings. In either case it should be noted that the effect of the mounting is to preload the bearings in an axial direction.

Figure 11-22

Two-bearing mountings.
(Courtesy of The Timken Company.)

**Figure 11-23**

Mounting for a washing-machine spindle. (Courtesy of The Timken Company.)

**Figure 11-24**

Arrangements of angular ball bearings. (a) DF mounting; (b) DB mounting; (c) DT mounting. (Courtesy of The Timken Company.)

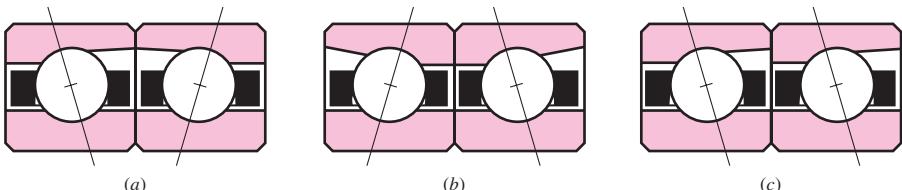
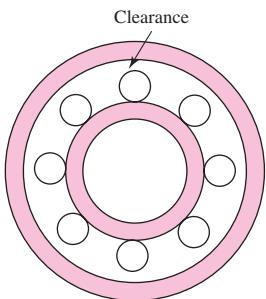


Figure 11-23 shows another two-bearing mounting. Note the use of washers against the cone backs.

When maximum stiffness and resistance to shaft misalignment is desired, pairs of angular-contact ball bearings (Fig. 11-2) are often used in an arrangement called *duplexing*. Bearings manufactured for duplex mounting have their rings ground with an offset, so that when a pair of bearings is tightly clamped together, a preload is automatically established. As shown in Fig. 11-24, three mounting arrangements are used. The face-to-face mounting, called DF, will take heavy radial loads and thrust loads from either direction. The DB mounting (back to back) has the greatest aligning stiffness and is also good for heavy radial loads and thrust loads from either direction. The tandem arrangement, called the DT mounting, is used where the thrust is always in the same direction; since the two bearings have their thrust functions in the same direction, a preload, if required, must be obtained in some other manner.

Bearings are usually mounted with the rotating ring a press fit, whether it be the inner or outer ring. The stationary ring is then mounted with a push fit. This permits the stationary ring to creep in its mounting slightly, bringing new portions of the ring into the load-bearing zone to equalize wear.

**Figure 11-25**

Clearance in an off-the-shelf bearing, exaggerated for clarity.

Preloading

The object of preloading is to remove the internal clearance usually found in bearings, to increase the fatigue life, and to decrease the shaft slope at the bearing. Figure 11–25 shows a typical bearing in which the clearance is exaggerated for clarity.

Preloading of straight roller bearings may be obtained by:

- 1 Mounting the bearing on a tapered shaft or sleeve to expand the inner ring
- 2 Using an interference fit for the outer ring
- 3 Purchasing a bearing with the outer ring preshrunk over the rollers

Ball bearings are usually preloaded by the axial load built in during assembly. However, the bearings of Fig. 11–24a and b are preloaded in assembly because of the differences in widths of the inner and outer rings.

It is always good practice to follow manufacturers' recommendations in determining preload, since too much will lead to early failure.

Alignment

The permissible misalignment in bearings depends on the type of bearing and the geometric and material properties of the specific bearing. Manufacturers' catalogs should be referenced for detailed specifications on a given bearing. In general, cylindrical and tapered roller bearings require alignments that are closer than deep-groove ball bearings. Spherical ball bearings and self-aligning bearings are the most forgiving. Table 7–2, p. 379, gives typical maximum ranges for each type of bearing. The life of the bearing decreases significantly when the misalignment exceeds the allowable limits.

Additional protection against misalignment is obtained by providing the full shoulders (see Fig. 11–8) recommended by the manufacturer. Also, if there is any misalignment at all, it is good practice to provide a safety factor of around 2 to account for possible increases during assembly.

Enclosures

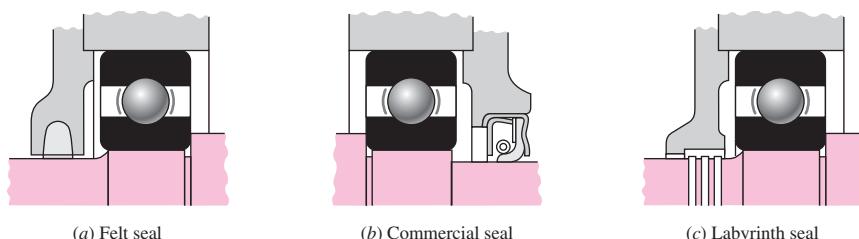
To exclude dirt and foreign matter and to retain the lubricant, the bearing mountings must include a seal. The three principal methods of sealings are the felt seal, the commercial seal, and the labyrinth seal (Fig. 11–26).

Felt seals may be used with grease lubrication when the speeds are low. The rubbing surfaces should have a high polish. Felt seals should be protected from dirt by placing them in machined grooves or by using metal stampings as shields.

The *commercial seal* is an assembly consisting of the rubbing element and, generally, a spring backing, which are retained in a sheet-metal jacket. These seals are usually made by press fitting them into a counterbored hole in the bearing cover. Since they obtain the sealing action by rubbing, they should not be used for high speeds.

Figure 11-26

Typical sealing methods.
(General Motors Corp. Used with permission, GM Media Archives.)



The *labyrinth seal* is especially effective for high-speed installations and may be used with either oil or grease. It is sometimes used with flingers. At least three grooves should be used, and they may be cut on either the bore or the outside diameter. The clearance may vary from 0.010 to 0.040 in, depending upon the speed and temperature.

PROBLEMS

Problems marked with an asterisk (*) are linked to problems in other chapters, as summarized in Table 1–1 of Sec. 1–16, p. 24.

Since each bearing manufacturer makes individual decisions with respect to materials, treatments, and manufacturing processes, manufacturers' experiences with bearing life distribution differ. In solving the following problems, we will use the experience of two manufacturers, tabulated as follows:

Manufacturer	Rating Life, Revolutions	Weibull Parameters		
		x_0	θ	b
1	$90(10^6)$	0	4.48	1.5
2	$1(10^6)$	0.02	4.459	1.483

Tables 11–2 and 11–3 are based on manufacturer 2.

11–1

A certain application requires a ball bearing with the inner ring rotating, with a design life of 25 kh at a speed of 350 rev/min. The radial load is 2.5 kN and an application factor of 1.2 is appropriate. The reliability goal is 0.90. Find the multiple of rating life required, x_D , and the catalog rating C_{10} with which to enter a bearing table. Choose a 02-series deep-groove ball bearing from Table 11–2, and estimate the reliability in use.

11–2

An angular-contact, inner ring rotating, 02-series ball bearing is required for an application in which the life requirement is 40 kh at 520 rev/min. The design radial load is 725 lbf. The application factor is 1.4. The reliability goal is 0.90. Find the multiple of rating life x_D required and the catalog rating C_{10} with which to enter Table 11–2. Choose a bearing and estimate the existing reliability in service.

11–3

The other bearing on the shaft of Prob. 11–2 is to be a 03-series cylindrical roller bearing with inner ring rotating. For a 2235-lbf radial load, find the catalog rating C_{10} with which to enter Table 11–3. The reliability goal is 0.90. Choose a bearing and estimate its reliability in use.

11–4

Problems 11–2 and 11–3 raise the question of the reliability of the bearing pair on the shaft. Since the combined reliabilities R is $R_1 R_2$, what is the reliability of the two bearings (probability that either or both will not fail) as a result of your decisions in Probs. 11–2 and 11–3? What does this mean in setting reliability goals for each of the bearings of the pair on the shaft?

11–5

Combine Probs. 11–2 and 11–3 for an overall reliability of $R = 0.90$. Reconsider your selections, and meet this overall reliability goal.

11–6

A straight (cylindrical) roller bearing is subjected to a radial load of 20 kN. The life is to be 8000 h at a speed of 950 rev/min and exhibit a reliability of 0.95. What basic load rating should be used in selecting the bearing from a catalog of manufacturer 2?

11–7

Two ball bearings from different manufacturers are being considered for a certain application. Bearing A has a catalog rating of 2.0 kN based on a catalog rating system of 3 000 hours

at 500 rev/min. Bearing *B* has a catalog rating of 7.0 kN based on a catalog that rates at 10^6 cycles. For a given application, determine which bearing can carry the larger load.

**11-8 to
11-13**

For the bearing application specifications given in the table for the assigned problem, determine the Basic Load Rating for a ball bearing with which to enter a bearing catalog.

Problem Number	Radial Load	Design Life	Desired Reliability
11-8	2 kN	10^9 rev	90%
11-9	800 lbf	12 kh, 350 rev/min	90%
11-10	4 kN	8 kh, 500 rev/min	90%
11-11	650 lbf	5 yrs, 40 h/week, 400 rev/min	95%
11-12	9 kN	10^8 rev	99%
11-13	11 kips	20 kh, 200 rev/min	99%

**11-14* to
11-17***

For the problem specified in the table, build upon the results of the original problem to obtain a Basic Load Rating for a ball bearing at *C* with a 95 percent reliability. The shaft rotates at 1200 rev/min, and the desired bearing life is 15 kh. Use an application factor of 1.2.

Problem Number	Original Problem, Page Number
11-14*	3-68, 137
11-15*	3-69, 137
11-16*	3-70, 137
11-17*	3-71, 137

11-18*

For the shaft application defined in Prob. 3-77, p. 139, the input shaft *EG* is driven at a constant speed of 191 rev/min. Obtain a Basic Load Rating for a ball bearing at *A* for a life of 12 kh with a 95 percent reliability.

11-19*

For the shaft application defined in Prob. 3-79, p. 139, the input shaft *EG* is driven at a constant speed of 280 rev/min. Obtain a Basic Load Rating for a cylindrical roller bearing at *A* for a life of 14 kh with a 98 percent reliability.

11-20

An 02-series single-row deep-groove ball bearing with a 65-mm bore (see Tables 11-1 and 11-2 for specifications) is loaded with a 3-kN axial load and a 7-kN radial load. The outer ring rotates at 500 rev/min.

- (a) Determine the equivalent radial load that will be experienced by this particular bearing.
- (b) Determine whether this bearing should be expected to carry this load with a 95 percent reliability for 10 kh.

11-21

An 02-series single-row deep-groove ball bearing with a 30-mm bore (see Tables 11-1 and 11-2 for specifications) is loaded with a 2-kN axial load and a 5-kN radial load. The inner ring rotates at 400 rev/min.

- (a) Determine the equivalent radial load that will be experienced by this particular bearing.
- (b) Determine the predicted life (in revolutions) that this bearing could be expected to give in this application with a 99 percent reliability.

**11-22 to
11-26**

An 02-series single-row deep-groove ball bearing is to be selected from Table 11-2 for the application conditions specified in the table. Assume Table 11-1 is applicable if needed. Specify the smallest bore size from Table 11-2 that can satisfy these conditions.

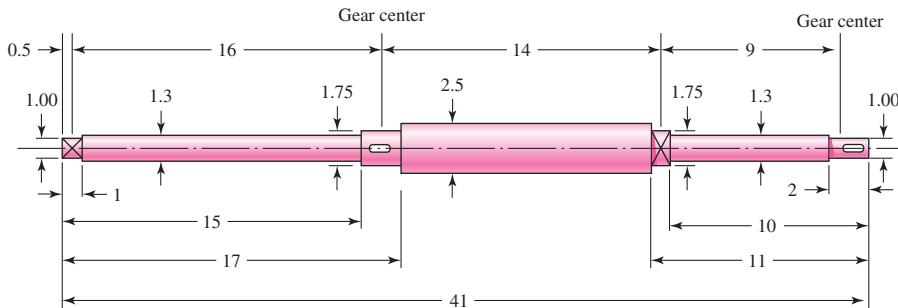
Problem Number	Radial Load	Axial Load	Design Life	Ring Rotating	Desired Reliability
11-22	8 kN	0 kN	10^9 rev	Inner	90%
11-23	8 kN	2 kN	10 kh, 400 rev/min	Inner	99%
11-24	8 kN	3 kN	10^8 rev	Outer	90%
11-25	10 kN	5 kN	12 kh, 300 rev/min	Inner	95%
11-26	9 kN	3 kN	10^9 rev	Outer	99%

11-27*

The shaft shown in the figure is proposed as a preliminary design for the application defined in Prob. 3-72, p. 138. The effective centers of the gears for force transmission are shown. The dimensions for the bearing surfaces (indicated with cross markings) have been estimated. The shaft rotates at 1200 rev/min, and the desired bearing life is 15 kh with a 95 percent reliability. Use an application factor of 1.2.

- (a) Obtain a Basic Load Rating for a ball bearing at the right end.
- (b) Use an online bearing catalog to find a specific bearing that satisfies the needed Basic Load Rating and the geometry requirements. If necessary, indicate appropriate adjustments to the dimensions of the bearing surface.

*Problem 11-27**
All fillets $\frac{1}{16}$ in. Dimensions in inches.

**11-28***

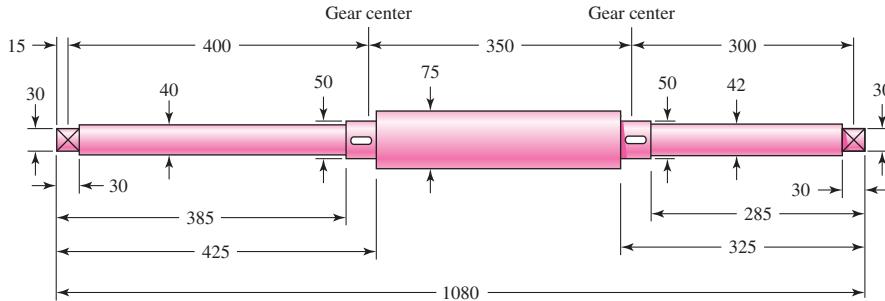
Repeat the requirements of Prob. 11-27 for the bearing at the left end of the shaft.

11-29*

The shaft shown in the figure is proposed as a preliminary design for the application defined in Prob. 3-73, p. 138. The effective centers of the gears for force transmission are shown. The dimensions for the bearing surfaces (indicated with cross markings) have been estimated. The shaft rotates at 900 rev/min, and the desired bearing life is 12 kh with a 98 percent reliability. Use an application factor of 1.2.

- (a) Obtain a Basic Load Rating for a ball bearing at the right end.
- (b) Use an online bearing catalog to find a specific bearing that satisfies the needed Basic Load Rating and the geometry requirements. If necessary, indicate appropriate adjustments to the dimensions of the bearing surface.

*Problem 11-29**
All fillets 2 mm. Dimensions in millimeters.



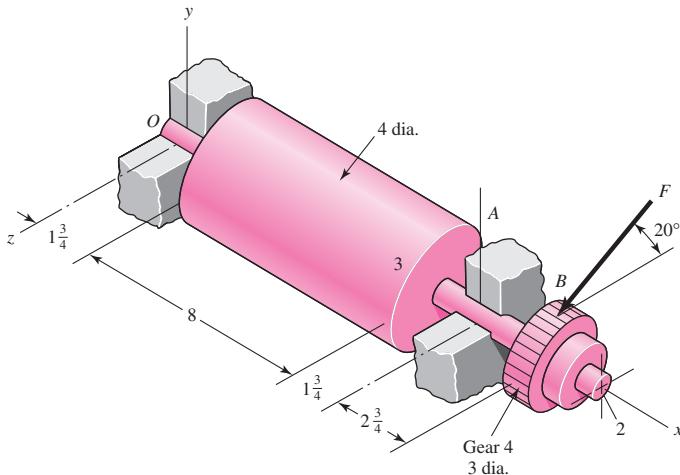
11-30*

Repeat the requirements of Prob. 11-29 for the bearing at the left end of the shaft.

11-31

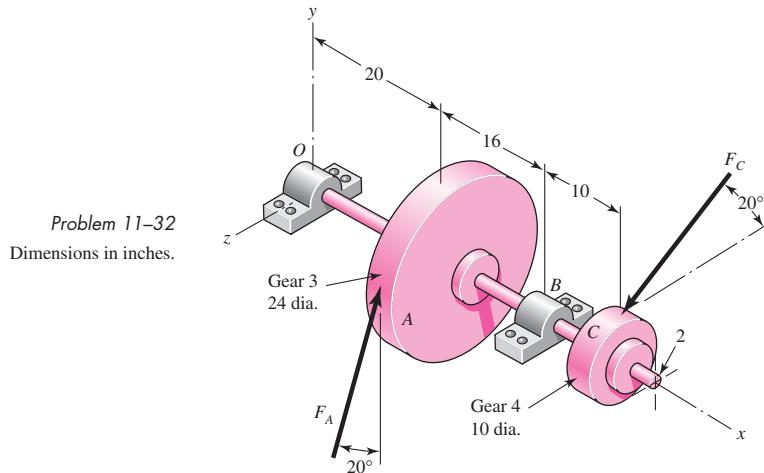
Shown in the figure is a gear-driven squeeze roll that mates with an idler roll. The roll is designed to exert a normal force of 35 lbf/in of roll length and a pull of 28 lbf/in on the material being processed. The roll speed is 350 rev/min, and a design life of 35 kh is desired. Use an application factor of 1.2, and select a pair of angular-contact 02-series ball bearings from Table 11-2 to be mounted at 0 and A. Use the same size bearings at both locations and a combined reliability of at least 0.92.

Problem 11-31
Dimensions in inches.

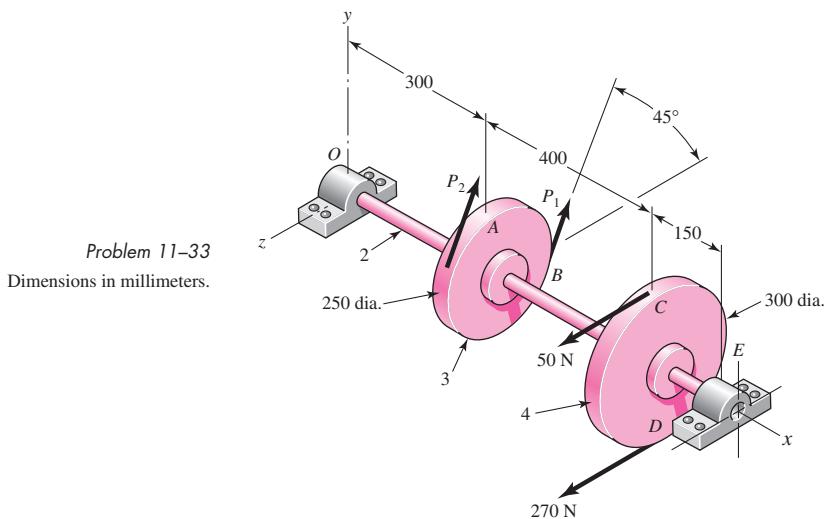


11-32

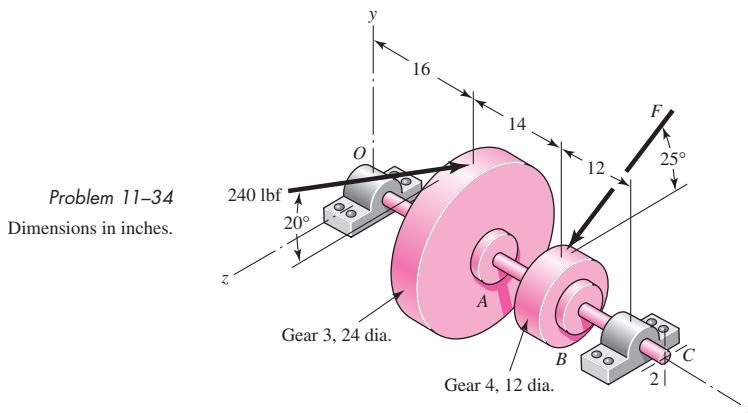
The figure shown is a geared countershaft with an overhanging pinion at C. Select an angular-contact ball bearing from Table 11-2 for mounting at O and a straight roller bearing from Table 11-3 for mounting at B. The force on gear A is $F_A = 600 \text{ lbf}$, and the shaft is to run at a speed of 420 rev/min. Solution of the statics problem gives force of bearings against the shaft at O as $\mathbf{R}_O = -387\mathbf{j} + 467\mathbf{k} \text{ lbf}$, and at B as $\mathbf{R}_B = 316\mathbf{j} - 1615\mathbf{k} \text{ lbf}$. Specify the bearings required, using an application factor of 1.2, a desired life of 40 kh, and a combined reliability goal of 0.95.

**11-33**

The figure is a schematic drawing of a countershaft that supports two V-belt pulleys. The countershaft runs at 1500 rev/min and the bearings are to have a life of 60 kh at a combined reliability of 0.98. The belt tension on the loose side of pulley A is 15 percent of the tension on the tight side. Select deep-groove bearings from Table 11-2 for use at O and E, using an application factor of unity.

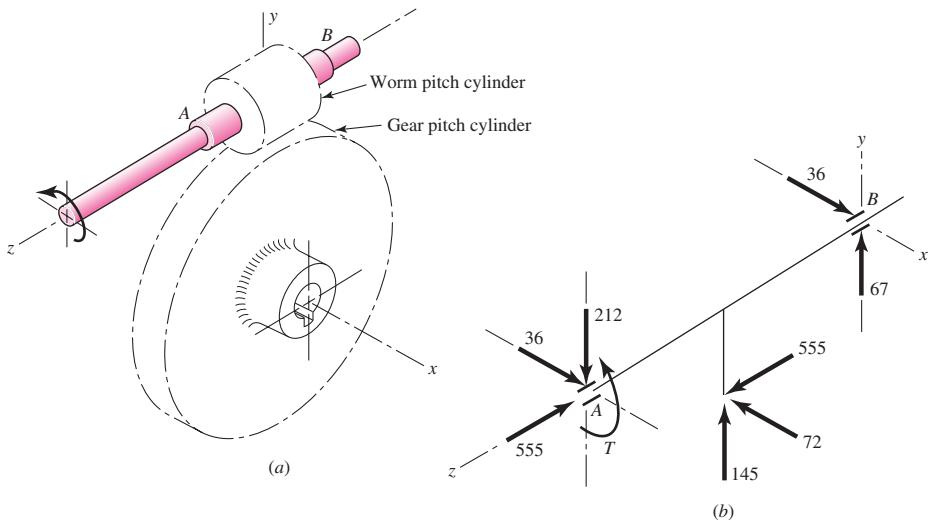
**11-34**

A gear-reduction unit uses the countershaft depicted in the figure. Find the two bearing reactions. The bearings are to be angular-contact ball bearings, having a desired life of 50 kh when used at 300 rev/min. Use 1.2 for the application factor and a reliability goal for the bearing pair of 0.96. Select the bearings from Table 11-2.

**11-35**

The worm shaft shown in part *a* of the figure transmits 1.2 hp at 500 rev/min. A static force analysis gave the results shown in part *b* of the figure. Bearing *A* is to be an angular-contact ball bearing mounted to take the 555-lbf thrust load. The bearing at *B* is to take only the radial load, so a straight roller bearing will be employed. Use an application factor of 1.2, a desired life of 30 kh, and a reliability goal, combined, of 0.99. Specify each bearing.

Problem 11-35
(*a*) Worm and worm gear;
(*b*) force analysis of worm shaft,
forces in pounds.

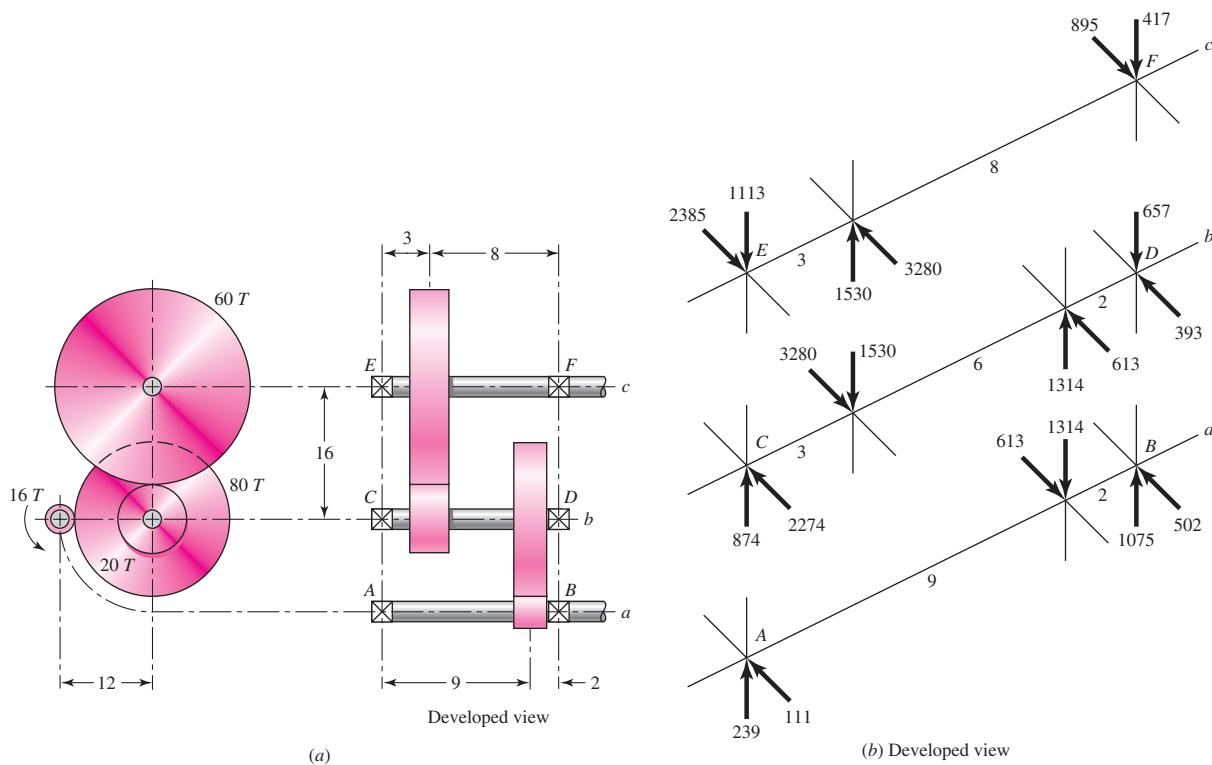
**11-36**

In bearings tested at 2000 rev/min with a steady radial load of 18 kN, a set of bearings showed an L_{10} life of 115 h and an L_{80} life of 600 h. The basic load rating of this bearing is 39.6 kN. Estimate the Weibull shape factor b and the characteristic life θ for a two-parameter model. This manufacturer rates ball bearings at 1 million revolutions.

11-37

A 16-tooth pinion drives the double-reduction spur-gear train in the figure. All gears have 25° pressure angles. The pinion rotates ccw at 1200 rev/min and transmits power to the gear train. The shaft has not yet been designed, but the free bodies have been generated. The shaft speeds are 1200 rev/min, 240 rev/min, and 80 rev/min. A bearing study is commencing with a 10-kh

life and a gearbox bearing ensemble reliability of 0.99. An application factor of 1.2 is appropriate. Specify the six bearings.



Problem 11-37

(a) Drive detail; (b) force analysis on shafts. Forces in pounds; linear dimensions in inches.

11-38

Estimate the remaining life in revolutions of an 02-30 mm angular-contact ball bearing already subjected to 200 000 revolutions with a radial load of 18 kN, if it is now to be subjected to a change in load to 30 kN.

11-39

The same 02-30 angular-contact ball bearing as in Prob. 11-38 is to be subjected to a two-step loading cycle of 4 min with a loading of 18 kN, and one of 6 min with a loading of 30 kN. This cycle is to be repeated until failure. Estimate the total life in revolutions, hours, and loading cycles.

11-40

A countershaft is supported by two tapered roller bearings using an indirect mounting. The radial bearing loads are 560 lbf for the left-hand bearing and 1095 for the right-hand bearing. An axial load of 200 lbf is carried by the left bearing. The shaft rotates at 400 rev/min and is to have a desired life of 40 kh. Use an application factor of 1.4 and a combined reliability goal of 0.90. Using an initial $K = 1.5$, find the required radial rating for each bearing. Select the bearings from Fig. 11-15.

11-41*

For the shaft application defined in Prob. 3-74, p. 138, perform a preliminary specification for tapered roller bearings at C and D . A bearing life of 10^8 revolutions is desired with a 90 percent combined reliability for the bearing set. Should the bearings be oriented with direct mounting or indirect mounting for the axial thrust to be carried by the bearing at C ? Assuming bearings are available with $K = 1.5$, find the required radial rating for each bearing. For this preliminary design, assume an application factor of one.

11-42*

For the shaft application defined in Prob. 3–76, p. 139, perform a preliminary specification for tapered roller bearings at *A* and *B*. A bearing life of 500 million revolutions is desired with a 90 percent combined reliability for the bearing set. Should the bearings be oriented with direct mounting or indirect mounting for the axial thrust to be carried by the bearing at *A*? Assuming bearings are available with $K = 1.5$, find the required radial rating for each bearing. For this preliminary design, assume an application factor of one.

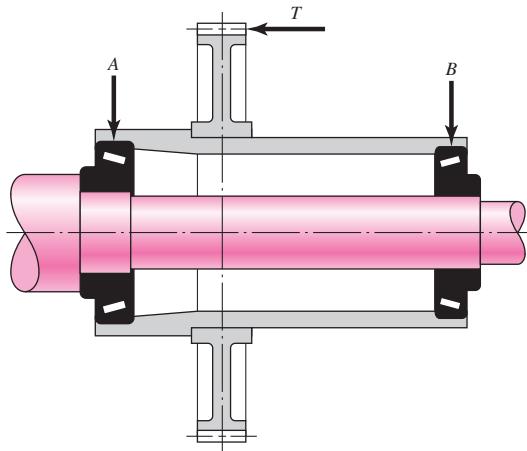
11-43

An outer hub rotates around a stationary shaft, supported by two tapered roller bearings as shown in Fig. 11–23. The device is to operate at 250 rev/min, 8 hours per day, 5 days per week, for 5 years, before bearing replacement is necessary. A reliability of 90 percent on each bearing is acceptable. A free body analysis determines the radial force carried by the upper bearing to be 12 kN and the radial force at the lower bearing to be 25 kN. In addition, the outer hub applies a downward force of 5 kN. Assuming bearings are available with $K = 1.5$, find the required radial rating for each bearing. Assume an application factor of 1.2.

11-44

The gear-reduction unit shown has a gear that is press fit onto a cylindrical sleeve that rotates around a stationary shaft. The helical gear transmits an axial thrust load *T* of 250 lbf as shown in the figure. Tangential and radial loads (not shown) are also transmitted through the gear, producing radial ground reaction forces at the bearings of 875 lbf for bearing *A* and 625 lbf for bearing *B*. The desired life for each bearing is 90 kh at a speed of 150 rev/min with a 90 percent reliability. The first iteration of the shaft design indicates approximate diameters of $1\frac{1}{8}$ in at *A* and 1 in at *B*. Select suitable tapered roller bearings from Fig. 11–15.

Problem 11-44
(Courtesy of The Timken Company.)



This page intentionally left blank

12

Lubrication and Journal Bearings

Chapter Outline

12-1	Types of Lubrication	618
12-2	Viscosity	619
12-3	Petroff's Equation	621
12-4	Stable Lubrication	623
12-5	Thick-Film Lubrication	624
12-6	Hydrodynamic Theory	625
12-7	Design Considerations	629
12-8	The Relations of the Variables	631
12-9	Steady-State Conditions in Self-Contained Bearings	645
12-10	Clearance	648
12-11	Pressure-Fed Bearings	650
12-12	Loads and Materials	656
12-13	Bearing Types	658
12-14	Thrust Bearings	659
12-15	Boundary-Lubricated Bearings	660

The object of lubrication is to reduce friction, wear, and heating of machine parts that move relative to each other. A lubricant is any substance that, when inserted between the moving surfaces, accomplishes these purposes. In a sleeve bearing, a shaft, or *journal*, rotates or oscillates within a sleeve, or *bushing*, and the relative motion is sliding. In an antifriction bearing, the main relative motion is rolling. A follower may either roll or slide on the cam. Gear teeth mate with each other by a combination of rolling and sliding. Pistons slide within their cylinders. All these applications require lubrication to reduce friction, wear, and heating.

The field of application for journal bearings is immense. The crankshaft and connecting-rod bearings of an automotive engine must operate for thousands of miles at high temperatures and under varying load conditions. The journal bearings used in the steam turbines of power-generating stations are said to have reliabilities approaching 100 percent. At the other extreme there are thousands of applications in which the loads are light and the service relatively unimportant; a simple, easily installed bearing is required, using little or no lubrication. In such cases an antifriction bearing might be a poor answer because of the cost, the elaborate enclosures, the close tolerances, the radial space required, the high speeds, or the increased inertial effects. Instead, a nylon bearing requiring no lubrication, a powder-metallurgy bearing with the lubrication "built in," or a bronze bearing with ring oiling, wick feeding, or solid-lubricant film or grease lubrication might be a very satisfactory solution. Recent metallurgy developments in bearing materials, combined with increased knowledge of the lubrication process, now make it possible to design journal bearings with satisfactory lives and very good reliabilities.

Much of the material we have studied thus far in this book has been based on fundamental engineering studies, such as statics, dynamics, the mechanics of solids, metal processing, mathematics, and metallurgy. In the study of lubrication and journal bearings, additional fundamental studies, such as chemistry, fluid mechanics, thermodynamics, and heat transfer, must be utilized in developing the material. While we shall not utilize all of them in the material to be included here, you can now begin to appreciate better how the study of mechanical engineering design is really an integration of most of your previous studies and a directing of this total background toward the resolution of a single objective.

12-1 Types of Lubrication

Five distinct forms of lubrication may be identified:

- 1 Hydrodynamic
- 2 Hydrostatic
- 3 Elastohydrodynamic
- 4 Boundary
- 5 Solid film

Hydrodynamic lubrication means that the load-carrying surfaces of the bearing are separated by a relatively thick film of lubricant, so as to prevent metal-to-metal contact, and that the stability thus obtained can be explained by the laws of fluid mechanics. Hydrodynamic lubrication does not depend upon the introduction of the lubricant under pressure, though that may occur; but it does require the existence of an adequate supply at all times. The film pressure is created by the moving surface itself pulling the lubricant into a wedge-shaped zone at a velocity sufficiently high to create the pressure necessary to separate the surfaces against the load on the bearing. Hydrodynamic lubrication is also called *full-film*, or *fluid, lubrication*.

Hydrostatic lubrication is obtained by introducing the lubricant, which is sometimes air or water, into the load-bearing area at a pressure high enough to separate the surfaces with a relatively thick film of lubricant. So, unlike hydrodynamic lubrication, this kind of lubrication does not require motion of one surface relative to another. We shall not deal with hydrostatic lubrication in this book, but the subject should be considered in designing bearings where the velocities are small or zero and where the frictional resistance is to be an absolute minimum.

Elastohydrodynamic lubrication is the phenomenon that occurs when a lubricant is introduced between surfaces that are in rolling contact, such as mating gears or rolling bearings. The mathematical explanation requires the Hertzian theory of contact stress and fluid mechanics.

Insufficient surface area, a drop in the velocity of the moving surface, a lessening in the quantity of lubricant delivered to a bearing, an increase in the bearing load, or an increase in lubricant temperature resulting in a decrease in viscosity—any one of these—may prevent the buildup of a film thick enough for full-film lubrication. When this happens, the highest asperities may be separated by lubricant films only several molecular dimensions in thickness. This is called *boundary lubrication*. The change from hydrodynamic to boundary lubrication is not at all a sudden or abrupt one. It is probable that a mixed hydrodynamic- and boundary-type lubrication occurs first, and as the surfaces move closer together, the boundary-type lubrication becomes predominant. The viscosity of the lubricant is not of as much importance with boundary lubrication as is the chemical composition.

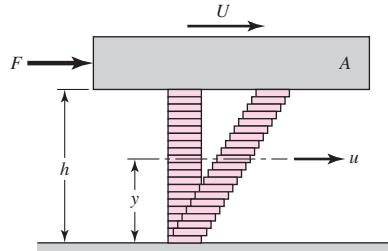
When bearings must be operated at extreme temperatures, a *solid-film lubricant* such as graphite or molybdenum disulfide must be used because the ordinary mineral oils are not satisfactory. Much research is currently being carried out in an effort, too, to find composite bearing materials with low wear rates as well as small frictional coefficients.

12-2 Viscosity

In Fig. 12-1 let plate A be moving with a velocity U on a film of lubricant of thickness h . We imagine the film as composed of a series of horizontal layers and the force F causing these layers to deform or slide on one another just like a deck of cards. The layers in contact with the moving plate are assumed to have a velocity U ; those in contact with the stationary surface are assumed to have a zero velocity. Intermediate layers have velocities that depend upon their distances y from the stationary surface. Newton's viscous effect states that the shear stress in the fluid is proportional to the rate of change of velocity with respect to y . Thus

$$\tau = \frac{F}{A} = \mu \frac{du}{dy} \quad (12-1)$$

| Figure 12-1



where μ is the constant of proportionality and defines *absolute viscosity*, also called *dynamic viscosity*. The derivative du/dy is the rate of change of velocity with distance and may be called the rate of shear, or the velocity gradient. The viscosity μ is thus a measure of the internal frictional resistance of the fluid. For most lubricating fluids, the rate of shear is constant, and $du/dy = U/h$. Thus, from Eq. (12-1),

$$\tau = \frac{F}{A} = \mu \frac{U}{h} \quad (12-2)$$

Fluids exhibiting this characteristic are said to be *Newtonian fluids*. The unit of viscosity in the ips system is seen to be the pound-force-second per square inch; this is the same as stress or pressure multiplied by time. The ips unit is called the *reyn*, in honor of Sir Osborne Reynolds.

The absolute viscosity is measured by the pascal-second ($\text{Pa} \cdot \text{s}$) in SI; this is the same as a Newton-second per square meter. The conversion from ips units to SI is the same as for stress. For example, multiply the absolute viscosity in reyns by 6890 to convert to units of $\text{Pa} \cdot \text{s}$.

The American Society of Mechanical Engineers (ASME) has published a list of cgs units that are not to be used in ASME documents.¹ This list results from a recommendation by the International Committee of Weights and Measures (CIPM) that the use of cgs units with special names be discouraged. Included in this list is a unit of force called the *dyne* (dyn), a unit of dynamic viscosity called the *poise* (P), and a unit of kinematic viscosity called the *stoke* (St). All of these units have been, and still are, used extensively in lubrication studies.

The poise is the cgs unit of dynamic or absolute viscosity, and its unit is the dyne-second per square centimeter ($\text{dyn} \cdot \text{s}/\text{cm}^2$). It has been customary to use the centipoise (cP) in analysis, because its value is more convenient. When the viscosity is expressed in centipoises, it is designated by Z . The conversion from cgs units to SI and ips units is as follows:

$$\mu(\text{Pa} \cdot \text{s}) = (10)^{-3} Z \text{ (cP)}$$

$$\mu(\text{reyn}) = \frac{Z \text{ (cP)}}{6.89(10)^6}$$

$$\mu(\text{mPa} \cdot \text{s}) = 6.89 \mu'(\mu\text{reyn})$$

In using ips units, the microreyn (μreyn) is often more convenient. The symbol μ' will be used to designate viscosity in μreyn such that $\mu = \mu'/(10^6)$.

The ASTM standard method for determining viscosity uses an instrument called the Saybolt Universal Viscosimeter. The method consists of measuring the time in seconds for 60 mL of lubricant at a specified temperature to run through a tube 17.6 mm in diameter and 12.25 mm long. The result is called the *kinematic viscosity*, and in the past the unit of the square centimeter per second has been used. One square centimeter per second is defined as a *stoke*. By the use of the *Hagen-Poiseuille law*, the kinematic viscosity based upon seconds Saybolt, also called *Saybolt Universal viscosity* (SUV) in seconds, is

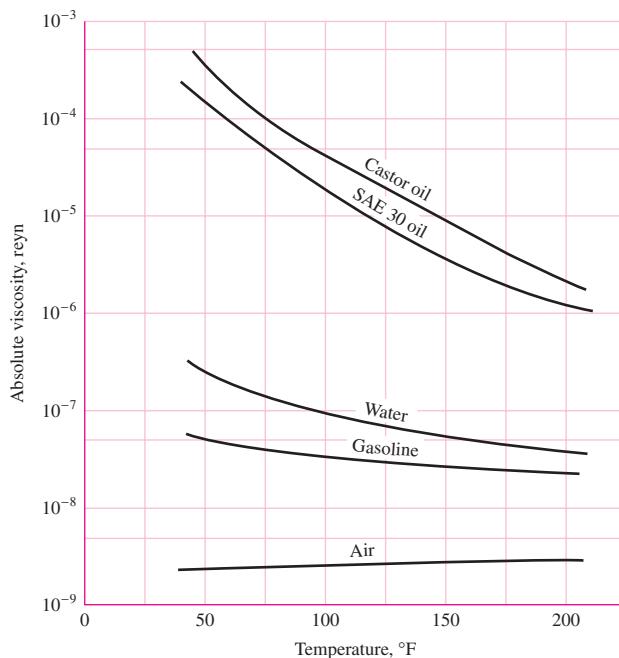
$$Z_k = \left(0.22t - \frac{180}{t} \right) \quad (12-3)$$

where Z_k is in centistokes (cSt) and t is the number of seconds Saybolt.

¹ASME *Orientation and Guide for Use of Metric Units*, 2nd ed., American Society of Mechanical Engineers, 1972, p. 13.

Figure 12-2

A comparison of the viscosities of various fluids.



In SI, the kinematic viscosity ν has the unit of the square meter per second (m^2/s), and the conversion is

$$\nu(\text{m}^2/\text{s}) = 10^{-6} Z_k (\text{cSt})$$

Thus, Eq. (12-3) becomes

$$\nu = \left(0.22t - \frac{180}{t} \right) (10^{-6}) \quad (12-4)$$

To convert to dynamic viscosity, we multiply ν by the density in SI units. Designating the density as ρ with the unit of the kilogram per cubic meter, we have

$$\mu = \rho \left(0.22t - \frac{180}{t} \right) (10^{-6}) \quad (12-5)$$

where μ is in pascal-seconds.

Figure 12-2 shows the absolute viscosity in the ips system of a number of fluids often used for lubrication purposes and their variation with temperature.

12-3

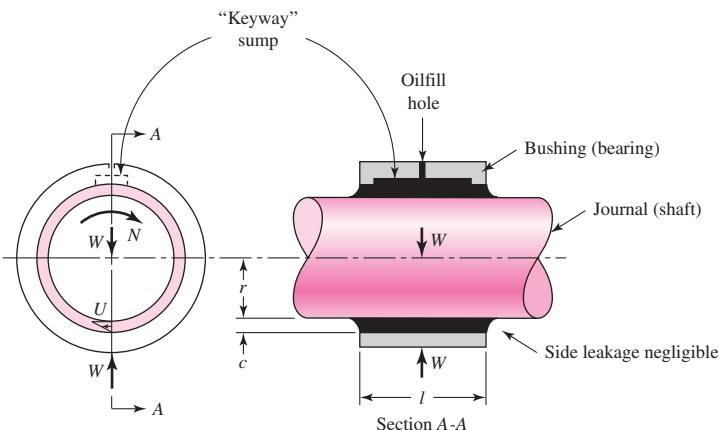
Petroff's Equation

The phenomenon of bearing friction was first explained by Petroff on the assumption that the shaft is concentric. Though we shall seldom make use of Petroff's method of analysis in the material to follow, it is important because it defines groups of dimensionless parameters and because the coefficient of friction predicted by this law turns out to be quite good even when the shaft is not concentric.

Let us now consider a vertical shaft rotating in a guide bearing. It is assumed that the bearing carries a very small load, that the clearance space is completely filled with oil, and that leakage is negligible (Fig. 12-3). We denote the radius of the shaft by r ,

Figure 12-3

Petroff's lightly loaded journal bearing consisting of a shaft journal and a bushing with an axial-groove internal lubricant reservoir. The linear velocity gradient is shown in the end view. The clearance c is several thousandths of an inch and is grossly exaggerated for presentation purposes.



the radial clearance by c , and the length of the bearing by l , all dimensions being in inches. If the shaft rotates at N rev/s, then its surface velocity is $U = 2\pi r N$ in/s. Since the shearing stress in the lubricant is equal to the velocity gradient times the viscosity, from Eq. (12-2) we have

$$\tau = \mu \frac{U}{h} = \frac{2\pi r \mu N}{c} \quad (a)$$

where the radial clearance c has been substituted for the distance h . The force required to shear the film is the stress times the area. The torque is the force times the lever arm r . Thus

$$T = (\tau A)(r) = \left(\frac{2\pi r \mu N}{c} \right) (2\pi rl)(r) = \frac{4\pi^2 r^3 l \mu N}{c} \quad (b)$$

If we now designate a small force on the bearing by W , in pounds-force, then the pressure P , in pounds-force per square inch of projected area, is $P = W/2rl$. The frictional force is fW , where f is the coefficient of friction, and so the frictional torque is

$$T = fWr = (f)(2rlP)(r) = 2r^2 f l P \quad (c)$$

Substituting the value of the torque from Eq. (c) in Eq. (b) and solving for the coefficient of friction, we find

$$f = 2\pi^2 \frac{\mu N}{P} \frac{r}{c} \quad (12-6)$$

Equation (12-6) is called *Petroff's equation* and was first published in 1883. The two quantities $\mu N/P$ and r/c are very important parameters in lubrication. Substitution of the appropriate dimensions in each parameter will show that they are dimensionless.

The *bearing characteristic number*, or the *Sommerfeld number*, is defined by the equation

$$S = \left(\frac{r}{c} \right)^2 \frac{\mu N}{P} \quad (12-7)$$

The Sommerfeld number is very important in lubrication analysis because it contains many of the parameters that are specified by the designer. Note that it is also dimensionless. The quantity r/c is called the *radial clearance ratio*. If we multiply both sides

of Eq. (12–6) by this ratio, we obtain the interesting relation

$$f \frac{r}{c} = 2\pi^2 \frac{\mu N}{P} \left(\frac{r}{c} \right)^2 = 2\pi^2 S \quad (12-8)$$

12-4

Stable Lubrication

The difference between boundary and hydrodynamic lubrication can be explained by reference to Fig. 12–4. This plot of the change in the coefficient of friction versus the bearing characteristic $\mu N/P$ was obtained by the McKee brothers in an actual test of friction.² The plot is important because it defines stability of lubrication and helps us to understand hydrodynamic and boundary, or thin-film, lubrication.

Recall Petroff's bearing model in the form of Eq. (12–6) predicts that f is proportional to $\mu N/P$, that is, a straight line from the origin in the first quadrant. On the coordinates of Fig. 12–4 the locus to the right of point C is an example. Petroff's model presumes thick-film lubrication, that is, no metal-to-metal contact, the surfaces being completely separated by a lubricant film.

The McKee abscissa was ZN/P (centipoise \times rev/min/psi) and the value of abscissa B in Fig. 12–4 was 30. The corresponding $\mu N/P$ (reyn \times rev/s/psi) is $0.33(10^{-6})$. Designers keep $\mu N/P \geq 1.7(10^{-6})$, which corresponds to $ZN/P \geq 150$. A design constraint to keep thick-film lubrication is to be sure that

$$\frac{\mu N}{P} \geq 1.7(10^{-6}) \quad (a)$$

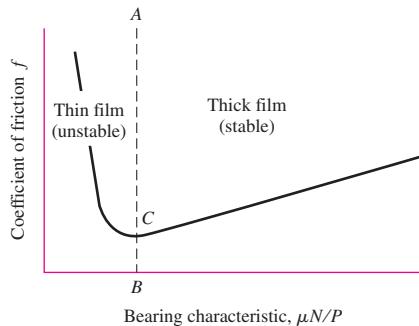
Suppose we are operating to the right of line BA and something happens, say, an increase in lubricant temperature. This results in a lower viscosity and hence a smaller value of $\mu N/P$. The coefficient of friction decreases, not as much heat is generated in shearing the lubricant, and consequently the lubricant temperature drops. Thus the region to the right of line BA defines *stable lubrication* because variations are self-correcting.

To the left of line BA , a decrease in viscosity would increase the friction. A temperature rise would ensue, and the viscosity would be reduced still more. The result would be compounded. Thus the region to the left of line BA represents *unstable lubrication*.

It is also helpful to see that a small viscosity, and hence a small $\mu N/P$, means that the lubricant film is very thin and that there will be a greater possibility of some

Figure 12–4

The variation of the coefficient of friction f with $\mu N/P$.



²S. A. McKee and T. R. McKee, "Journal Bearing Friction in the Region of Thin Film Lubrication," *SAE J.*, vol. 31, 1932, pp. (T)371–377.

metal-to-metal contact, and hence of more friction. Thus, point *C* represents what is probably the beginning of metal-to-metal contact as $\mu N/P$ becomes smaller.

12–5 Thick-Film Lubrication

Let us now examine the formation of a lubricant film in a journal bearing. Figure 12–5*a* shows a journal that is just beginning to rotate in a clockwise direction. Under starting conditions, the bearing will be dry, or at least partly dry, and hence the journal will climb or roll up the right side of the bearing as shown in Fig. 12–5*a*.

Now suppose a lubricant is introduced into the top of the bearing as shown in Fig. 12–5*b*. The action of the rotating journal is to pump the lubricant around the bearing in a clockwise direction. The lubricant is pumped into a wedge-shaped space and forces the journal over to the other side. A *minimum film thickness* h_0 occurs, not at the bottom of the journal, but displaced clockwise from the bottom as in Fig. 12–5*b*. This is explained by the fact that a film pressure in the converging half of the film reaches a maximum somewhere to the left of the bearing center.

Figure 12–5 shows how to decide whether the journal, under hydrodynamic lubrication, is eccentrically located on the right or on the left side of the bearing. Visualize the journal beginning to rotate. Find the side of the bearing upon which the journal tends to roll. Then, if the lubrication is hydrodynamic, mentally place the journal on the opposite side.

The nomenclature of a journal bearing is shown in Fig. 12–6. The dimension *c* is the *radial clearance* and is the difference in the radii of the bushing and journal. In

Figure 12–5

Formation of a film.

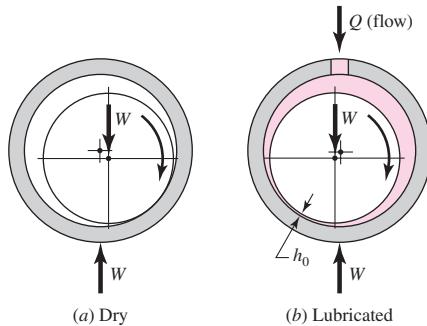


Figure 12–6

Nomenclature of a partial journal bearing.

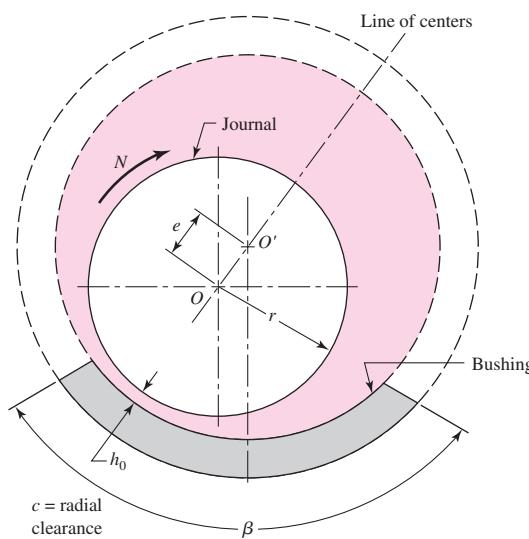


Fig. 12–6 the center of the journal is at O and the center of the bearing at O' . The distance between these centers is the *eccentricity* and is denoted by e . The *minimum film thickness* is designated by h_0 , and it occurs at the line of centers. The film thickness at any other point is designated by h . We also define an *eccentricity ratio* ϵ as

$$\epsilon = \frac{e}{c}$$

The bearing shown in the figure is known as a *partial bearing*. If the radius of the bushing is the same as the radius of the journal, it is known as a *fitted bearing*. If the bushing encloses the journal, as indicated by the dashed lines, it becomes a *full bearing*. The angle β describes the angular length of a partial bearing. For example, a 120° partial bearing has the angle β equal to 120°.

12–6

Hydrodynamic Theory

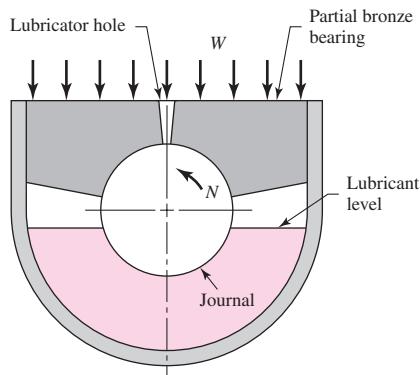
The present theory of hydrodynamic lubrication originated in the laboratory of Beauchamp Tower in the early 1880s in England. Tower had been employed to study the friction in railroad journal bearings and learn the best methods of lubricating them. It was an accident or error, during the course of this investigation, that prompted Tower to look at the problem in more detail and that resulted in a discovery that eventually led to the development of the theory.

Figure 12–7 is a schematic drawing of the journal bearing that Tower investigated. It is a partial bearing, having a diameter of 4 in, a length of 6 in, and a bearing arc of 157°, and having bath-type lubrication, as shown. The coefficients of friction obtained by Tower in his investigations on this bearing were quite low, which is now not surprising. After testing this bearing, Tower later drilled a $\frac{1}{2}$ -in-diameter lubricator hole through the top. But when the apparatus was set in motion, oil flowed out of this hole. In an effort to prevent this, a cork stopper was used, but this popped out, and so it was necessary to drive a wooden plug into the hole. When the wooden plug was pushed out too, Tower, at this point, undoubtedly realized that he was on the verge of discovery. A pressure gauge connected to the hole indicated a pressure of more than twice the unit bearing load. Finally, he investigated the bearing film pressures in detail throughout the bearing width and length and reported a distribution similar to that of Fig. 12–8.³

The results obtained by Tower had such regularity that Osborne Reynolds concluded that there must be a definite equation relating the friction, the pressure, and the

Figure 12–7

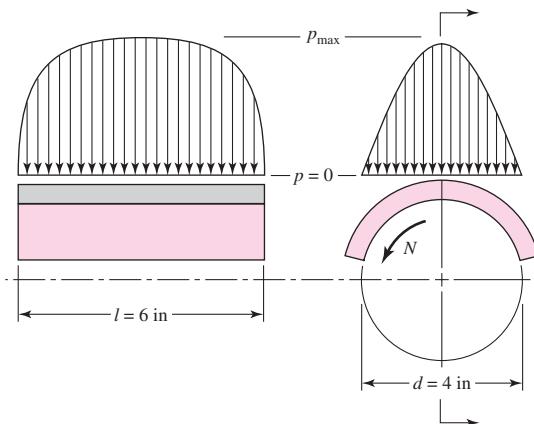
Schematic representation of the partial bearing used by Tower.



³Beauchamp Tower, "First Report on Friction Experiments," *Proc. Inst. Mech. Eng.*, November 1883, pp. 632–666; "Second Report," ibid., 1885, pp. 58–70; "Third Report," ibid., 1888, pp. 173–205; "Fourth Report," ibid., 1891, pp. 111–140.

Figure 12-8

Approximate pressure-distribution curves obtained by Tower.



velocity. The present mathematical theory of lubrication is based upon Reynolds' work following the experiment by Tower.⁴ The original differential equation, developed by Reynolds, was used by him to explain Tower's results. The solution is a challenging problem that has interested many investigators ever since then, and it is still the starting point for lubrication studies.

Reynolds pictured the lubricant as adhering to both surfaces and being pulled by the moving surface into a narrowing, wedge-shaped space so as to create a fluid or film pressure of sufficient intensity to support the bearing load. One of the important simplifying assumptions resulted from Reynolds' realization that the fluid films were so thin in comparison with the bearing radius that the curvature could be neglected. This enabled him to replace the curved partial bearing with a flat bearing, called a *plane slider bearing*. Other assumptions made were:

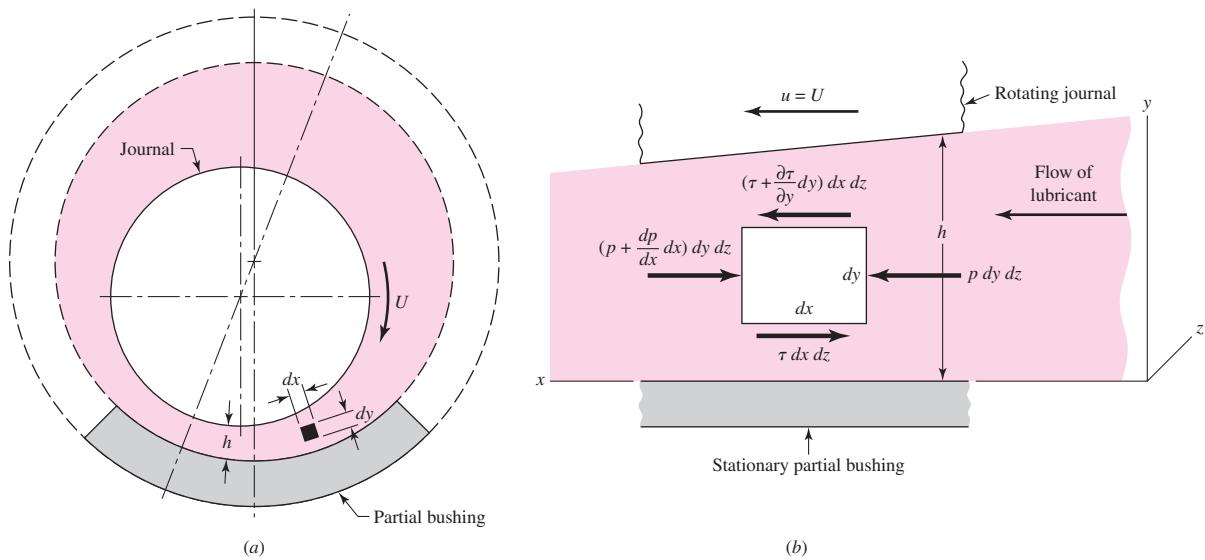
- 1 The lubricant obeys Newton's viscous effect, Eq. (12-1).
- 2 The forces due to the inertia of the lubricant are neglected.
- 3 The lubricant is assumed to be incompressible.
- 4 The viscosity is assumed to be constant throughout the film.
- 5 The pressure does not vary in the axial direction.

Figure 12-9a shows a journal rotating in the clockwise direction supported by a film of lubricant of variable thickness h on a partial bearing, which is fixed. We specify that the journal has a constant surface velocity U . Using Reynolds' assumption that curvature can be neglected, we fix a right-handed xyz reference system to the stationary bearing. We now make the following additional assumptions:

- 6 The bushing and journal extend infinitely in the z direction; this means there can be no lubricant flow in the z direction.
- 7 The film pressure is constant in the y direction. Thus the pressure depends only on the coordinate x .
- 8 The velocity of any particle of lubricant in the film depends only on the coordinates x and y .

We now select an element of lubricant in the film (Fig. 12-9a) of dimensions dx , dy , and dz , and compute the forces that act on the sides of this element. As shown in Fig. 12-9b, normal forces, due to the pressure, act upon the right and left sides of the

⁴Osborne Reynolds, "Theory of Lubrication, Part I," *Phil. Trans. Roy. Soc. London*, 1886.



| Figure 12-9

element, and shear forces, due to the viscosity and to the velocity, act upon the top and bottom sides. Summing the forces in the x direction gives

$$\sum F_x = p dy dz - \left(p + \frac{dp}{dx} dy \right) dy dz - \tau dx dz + \left(\tau + \frac{\partial \tau}{\partial y} dy \right) dx dz = 0 \quad (a)$$

This reduces to

$$\frac{dp}{dx} = \frac{\partial \tau}{\partial y} \quad (b)$$

From Eq. (12-1), we have

$$\tau = \mu \frac{\partial u}{\partial y} \quad (c)$$

where the partial derivative is used because the velocity u depends upon both x and y . Substituting Eq. (c) in Eq. (b), we obtain

$$\frac{dp}{dx} = \mu \frac{\partial^2 u}{\partial y^2} \quad (d)$$

Holding x constant, we now integrate this expression twice with respect to y . This gives

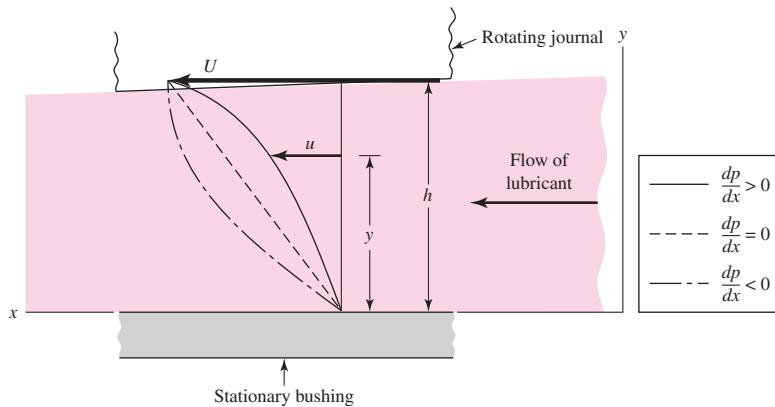
$$\begin{aligned} \frac{\partial u}{\partial y} &= \frac{1}{\mu} \frac{dp}{dx} y + C_1 \\ u &= \frac{1}{2\mu} \frac{dp}{dx} y^2 + C_1 y + C_2 \end{aligned} \quad (e)$$

Note that the act of holding x constant means that C_1 and C_2 can be functions of x . We now assume that there is no slip between the lubricant and the boundary surfaces. This gives two sets of boundary conditions for evaluating the constants C_1 and C_2 :

$$\begin{aligned} \text{At } y = 0, u &= 0 \\ \text{At } y = h, u &= U \end{aligned} \quad (f)$$

Figure 12-10

Velocity of the lubricant.



Notice, in the second condition, that h is a function of x . Substituting these conditions in Eq. (e) and solving for the constants gives

$$C_1 = \frac{U}{h} - \frac{h}{2\mu} \frac{dp}{dx} \quad C_2 = 0$$

or

$$u = \frac{1}{2\mu} \frac{dp}{dx} (y^2 - hy) + \frac{U}{h} y \quad (12-9)$$

This equation gives the velocity distribution of the lubricant in the film as a function of the coordinate y and the pressure gradient dp/dx . The equation shows that the velocity distribution across the film (from $y = 0$ to $y = h$) is obtained by superposing a parabolic distribution onto a linear distribution. Figure 12-10 shows the superposition of these distributions to obtain the velocity for particular values of x and dp/dx . In general, the parabolic term may be additive or subtractive to the linear term, depending upon the sign of the pressure gradient. When the pressure is maximum, $dp/dx = 0$ and the velocity is

$$u = \frac{U}{h} y \quad (g)$$

which is a linear relation.

We next define Q as the volume of lubricant flowing in the x direction per unit time. By using a width of unity in the z direction, the volume may be obtained by the expression

$$Q = \int_0^h u dy \quad (h)$$

Substituting the value of u from Eq. (12-9) and integrating gives

$$Q = \frac{Uh}{2} - \frac{h^3}{12\mu} \frac{dp}{dx} \quad (i)$$

The next step uses the assumption of an incompressible lubricant and states that the flow is the same for any cross section. Thus

$$\frac{dQ}{dx} = 0$$

From Eq. (i),

$$\frac{dQ}{dx} = \frac{U}{2} \frac{dh}{dx} - \frac{d}{dx} \left(\frac{h^3}{12\mu} \frac{dp}{dx} \right) = 0$$

or

$$\frac{d}{dx} \left(\frac{h^3}{\mu} \frac{dp}{dx} \right) = 6U \frac{dh}{dx} \quad (12-10)$$

which is the classical Reynolds equation for one-dimensional flow. It neglects side leakage, that is, flow in the z direction. A similar development is used when side leakage is not neglected. The resulting equation is

$$\frac{\partial}{\partial x} \left(\frac{h^3}{\mu} \frac{\partial p}{\partial x} \right) + \frac{\partial}{\partial z} \left(\frac{h^3}{\mu} \frac{\partial p}{\partial z} \right) = 6U \frac{\partial h}{\partial x} \quad (12-11)$$

There is no general analytical solution to Eq. (12-11); approximate solutions have been obtained by using electrical analogies, mathematical summations, relaxation methods, and numerical and graphical methods. One of the important solutions is due to Sommerfeld⁵ and may be expressed in the form

$$\frac{r}{c} f = \phi \left[\left(\frac{r}{c} \right)^2 \frac{\mu N}{P} \right] \quad (12-12)$$

where ϕ indicates a functional relationship. Sommerfeld found the functions for half-bearings and full bearings by using the assumption of no side leakage.

12-7 Design Considerations

We may distinguish between two groups of variables in the design of sliding bearings. In the first group are those whose values either are given or are under the control of the designer. These are:

- 1 The viscosity μ
- 2 The load per unit of projected bearing area, P
- 3 The speed N
- 4 The bearing dimensions r, c, β , and l

Of these four variables, the designer usually has no control over the speed, because it is specified by the overall design of the machine. Sometimes the viscosity is specified in advance, as, for example, when the oil is stored in a sump and is used for lubricating and cooling a variety of bearings. The remaining variables, and sometimes the viscosity, may be controlled by the designer and are therefore the *decisions* the designer makes. In other words, when these four decisions are made, the design is complete.

In the second group are the dependent variables. The designer cannot control these except indirectly by changing one or more of the first group. These are:

- 1 The coefficient of friction f
- 2 The temperature rise ΔT
- 3 The volume flow rate of oil Q
- 4 The minimum film thickness h_0

⁵A. Sommerfeld, "Zur Hydrodynamischen Theorie der Schmiermittel-Reibung" ("On the Hydrodynamic Theory of Lubrication"), *Z. Math. Physik*, vol. 50, 1904, pp. 97–155.

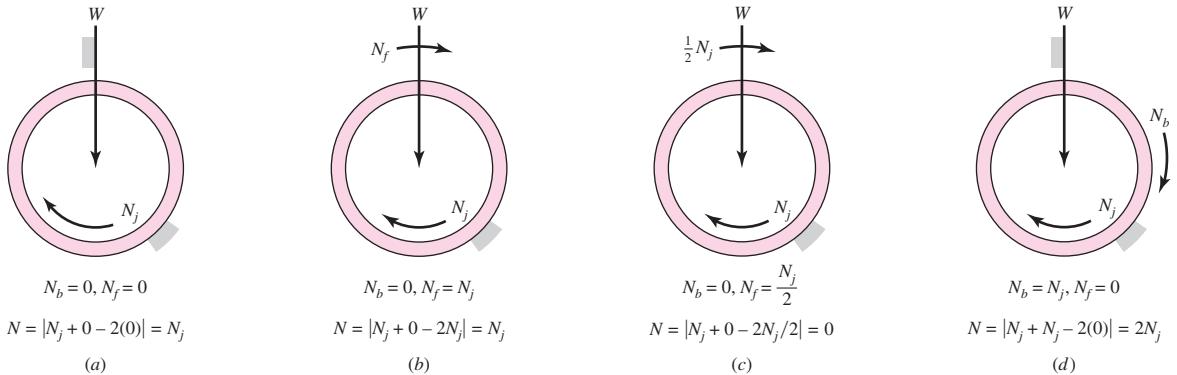


Figure 12-11

How the significant speed varies. (a) Common bearing case. (b) Load vector moves at the same speed as the journal. (c) Load vector moves at half journal speed, no load can be carried. (d) Journal and bushing move at same speed, load vector stationary, capacity halved.

This group of variables tells us how well the bearing is performing, and hence we may regard them as *performance factors*. Certain limitations on their values must be imposed by the designer to ensure satisfactory performance. These limitations are specified by the characteristics of the bearing materials and of the lubricant. The fundamental problem in bearing design, therefore, is to define satisfactory limits for the second group of variables and then to decide upon values for the first group such that these limitations are not exceeded.

Significant Angular Speed

In the next section we will examine several important charts relating key variables to the Sommerfeld number. To this point we have assumed that only the journal rotates and it is the journal rotational speed that is used in the Sommerfeld number. It has been discovered that the angular speed N that is significant to hydrodynamic film bearing performance is⁶

$$N = |N_i + N_b - 2N_f| \quad (12-13)$$

where N_i = journal angular speed, rev/s

N_b = bearing angular speed, rev/s

N_f = load vector angular speed, rev/s

When determining the Sommerfeld number for a general bearing, use Eq. (12-13) when entering N . Figure 12-11 shows several situations for determining N .

Trumpler's Design Criteria for Journal Bearings

Because the bearing assembly creates the lubricant pressure to carry a load, it reacts to loading by changing its eccentricity, which reduces the minimum film thickness h_0 until the load is carried. What is the limit of smallness of h_0 ? Close examination reveals that the moving adjacent surfaces of the journal and bushing are not smooth but consist of a series of asperities that pass one another, separated by a lubricant film. In starting a

⁶Paul Robert Trumpler, *Design of Film Bearings*, Macmillan, New York, 1966, pp. 103–119.

bearing under load from rest there is metal-to-metal contact and surface asperities are broken off, free to move and circulate with the oil. Unless a filter is provided, this debris accumulates. Such particles have to be free to tumble at the section containing the minimum film thickness without snagging in a togglelike configuration, creating additional damage and debris. Trumpler, an accomplished bearing designer, provides a throat of at least 200μ in to pass particles from ground surfaces.⁷ He also provides for the influence of size (tolerances tend to increase with size) by stipulating

$$h_0 \geq 0.0002 + 0.0004d \text{ in} \quad (a)$$

where d is the journal diameter in inches.

A lubricant is a mixture of hydrocarbons that reacts to increasing temperature by vaporizing the lighter components, leaving behind the heavier. This process (bearings have lots of time) slowly increases the viscosity of the remaining lubricant, which increases heat generation rate and elevates lubricant temperatures. This sets the stage for future failure. For light oils, Trumpler limits the maximum film temperature T_{\max} to

$$T_{\max} \leq 250^{\circ}\text{F} \quad (b)$$

Some oils can operate at slightly higher temperatures. Always check with the lubricant manufacturer.

A journal bearing often consists of a ground steel journal working against a softer, usually nonferrous, bushing. In starting under load there is metal-to-metal contact, abrasion, and the generation of wear particles, which, over time, can change the geometry of the bushing. The starting load divided by the projected area is limited to

$$\frac{W_{st}}{lD} \leq 300 \text{ psi} \quad (c)$$

If the load on a journal bearing is suddenly increased, the increase in film temperature in the annulus is immediate. Since ground vibration due to passing trucks, trains, and earth tremors is often present, Trumpler used a design factor of 2 or more on the running load, but not on the starting load of Eq. (c):

$$n_d \geq 2 \quad (d)$$

Many of Trumpler's designs are operating today, long after his consulting career is over; clearly they constitute good advice to the beginning designer.

12-8 The Relations of the Variables

Before proceeding to the problem of design, it is necessary to establish the relationships between the variables. Albert A. Raimondi and John Boyd, of Westinghouse Research Laboratories, used an iteration technique to solve Reynolds' equation on the digital computer.⁸ This is the first time such extensive data have been available for use by designers, and consequently we shall employ them in this book.⁹

⁷Op. cit., pp. 192–194.

⁸A. A. Raimondi and John Boyd, "A Solution for the Finite Journal Bearing and Its Application to Analysis and Design, Parts I, II, and III," *Trans. ASLE*, vol. 1, no. 1, in *Lubrication Science and Technology*, Pergamon, New York, 1958, pp. 159–209.

⁹See also the earlier companion paper, John Boyd and Albert A. Raimondi, "Applying Bearing Theory to the Analysis and Design of Journal Bearings, Part I and II," *J. Appl. Mechanics*, vol. 73, 1951, pp. 298–316.

The Raimondi and Boyd papers were published in three parts and contain 45 detailed charts and 6 tables of numerical information. In all three parts, charts are used to define the variables for length-diameter (l/d) ratios of 1:4, 1:2, and 1 and for beta angles of 60 to 360°. Under certain conditions the solution to the Reynolds equation gives negative pressures in the diverging portion of the oil film. Since a lubricant cannot usually support a tensile stress, Part III of the Raimondi-Boyd papers assumes that the oil film is ruptured when the film pressure becomes zero. Part III also contains data for the infinitely long bearing; since it has no ends, this means that there is no side leakage. The charts appearing in this book are from Part III of the papers, and are for full journal bearings ($\beta = 360^\circ$) only. Space does not permit the inclusion of charts for partial bearings. This means that you must refer to the charts in the original papers when beta angles of less than 360° are desired. The notation is very nearly the same as in this book, and so no problems should arise.

Viscosity Charts (Figs. 12-12 to 12-14)

One of the most important assumptions made in the Raimondi-Boyd analysis is that *viscosity of the lubricant is constant as it passes through the bearing*. But since work is done on the lubricant during this flow, the temperature of the oil is higher when it leaves the loading zone than it was on entry. And the viscosity charts clearly indicate that the viscosity drops off significantly with a rise in temperature. Since the analysis is based on a constant viscosity, our problem now is to determine the value of viscosity to be used in the analysis.

Some of the lubricant that enters the bearing emerges as a side flow, which carries away some of the heat. The balance of the lubricant flows through the load-bearing zone and carries away the balance of the heat generated. In determining the viscosity to be used we shall employ a temperature that is the average of the inlet and outlet temperatures, or

$$T_{av} = T_1 + \frac{\Delta T}{2} \quad (12-14)$$

where T_1 is the inlet temperature and ΔT is the temperature rise of the lubricant from inlet to outlet. Of course, the viscosity used in the analysis must correspond to T_{av} .

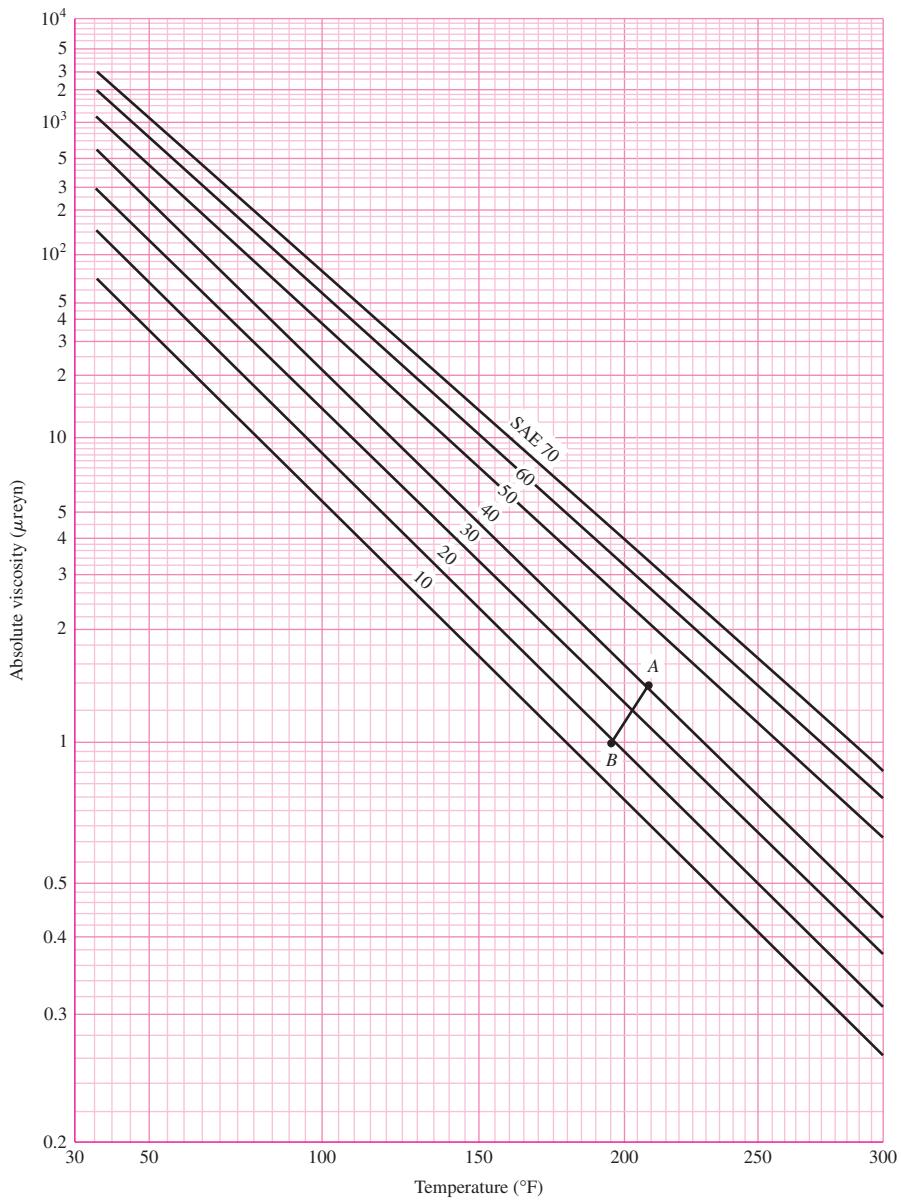
Viscosity varies considerably with temperature in a nonlinear fashion. The ordinates in Figs. 12-12 to 12-14 are not logarithmic, as the decades are of differing vertical length. These graphs represent the temperature versus viscosity functions for common grades of lubricating oils in both customary engineering and SI units. We have the temperature versus viscosity function only in graphical form, unless curve fits are developed. See Table 12-1.

One of the objectives of lubrication analysis is to determine the oil outlet temperature when the oil and its inlet temperature are specified. This is a trial-and-error type of problem. In an analysis, the temperature rise will first be estimated. This allows for the viscosity to be determined from the chart. With the value of the viscosity, the analysis is performed where the temperature rise is then computed. With this, a new estimate of the temperature rise is established. This process is continued until the estimated and computed temperatures agree.

To illustrate, suppose we have decided to use SAE 30 oil in an application in which the oil inlet temperature is $T_1 = 180^\circ\text{F}$. We begin by estimating that the temperature rise

Figure 12-12

Viscosity-temperature chart in U.S. customary units.
(Raimondi and Boyd.)



will be $\Delta T = 30^{\circ}\text{F}$. Then, from Eq. (12-14),

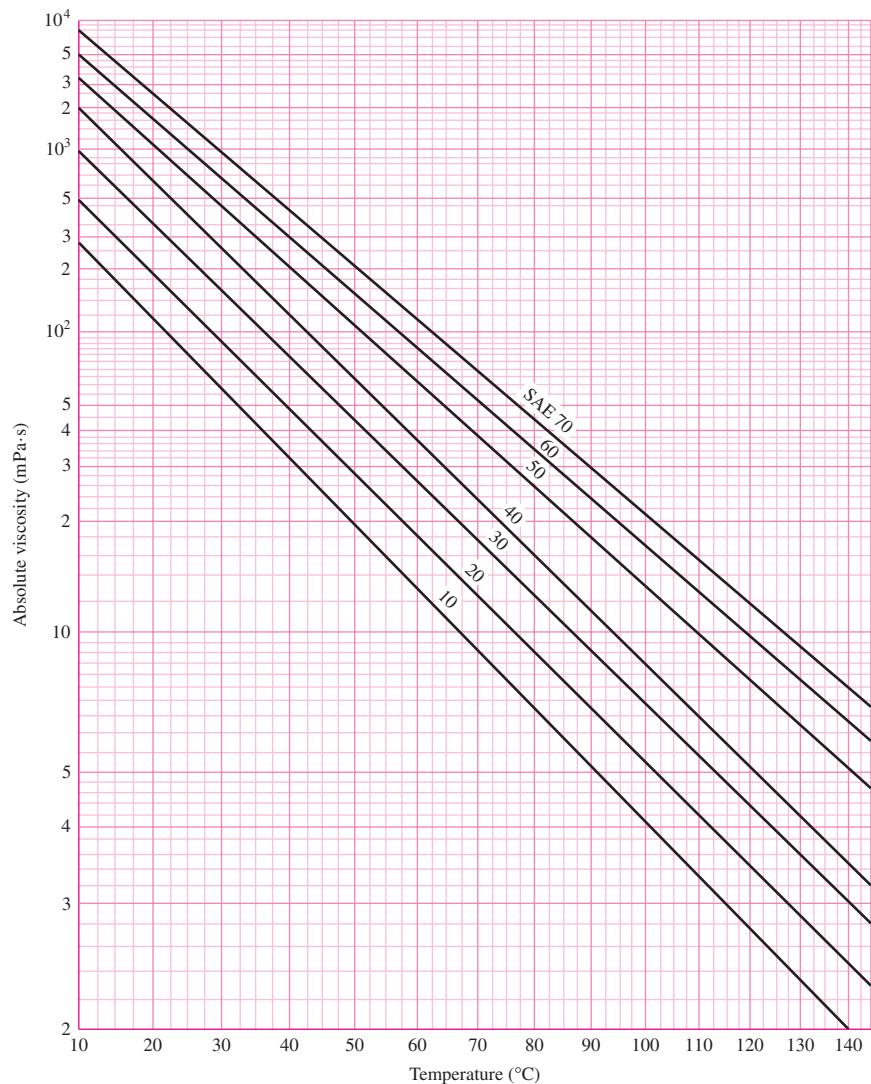
$$T_{\text{av}} = T_1 + \frac{\Delta T}{2} = 180 + \frac{30}{2} = 195^{\circ}\text{F}$$

From Fig. 12-12 we follow the SAE 30 line and find that $\mu = 1.40 \mu\text{reyn}$ at 195°F . So we use this viscosity (in an analysis to be explained in detail later) and find that the temperature rise is actually $\Delta T = 54^{\circ}\text{F}$. Thus Eq. (12-14) gives

$$T_{\text{av}} = 180 + \frac{54}{2} = 207^{\circ}\text{F}$$

Figure 12-13

Viscosity–temperature chart in SI units. (Adapted from Fig. 12-12.)



This corresponds to point *A* on Fig. 12-12, which is above the SAE 30 line and indicates that the viscosity used in the analysis was too high.

For a second guess, try $\mu = 1.00 \text{ } \mu\text{reyn}$. Again we run through an analysis and this time find that $\Delta T = 30^\circ\text{F}$. This gives an average temperature of

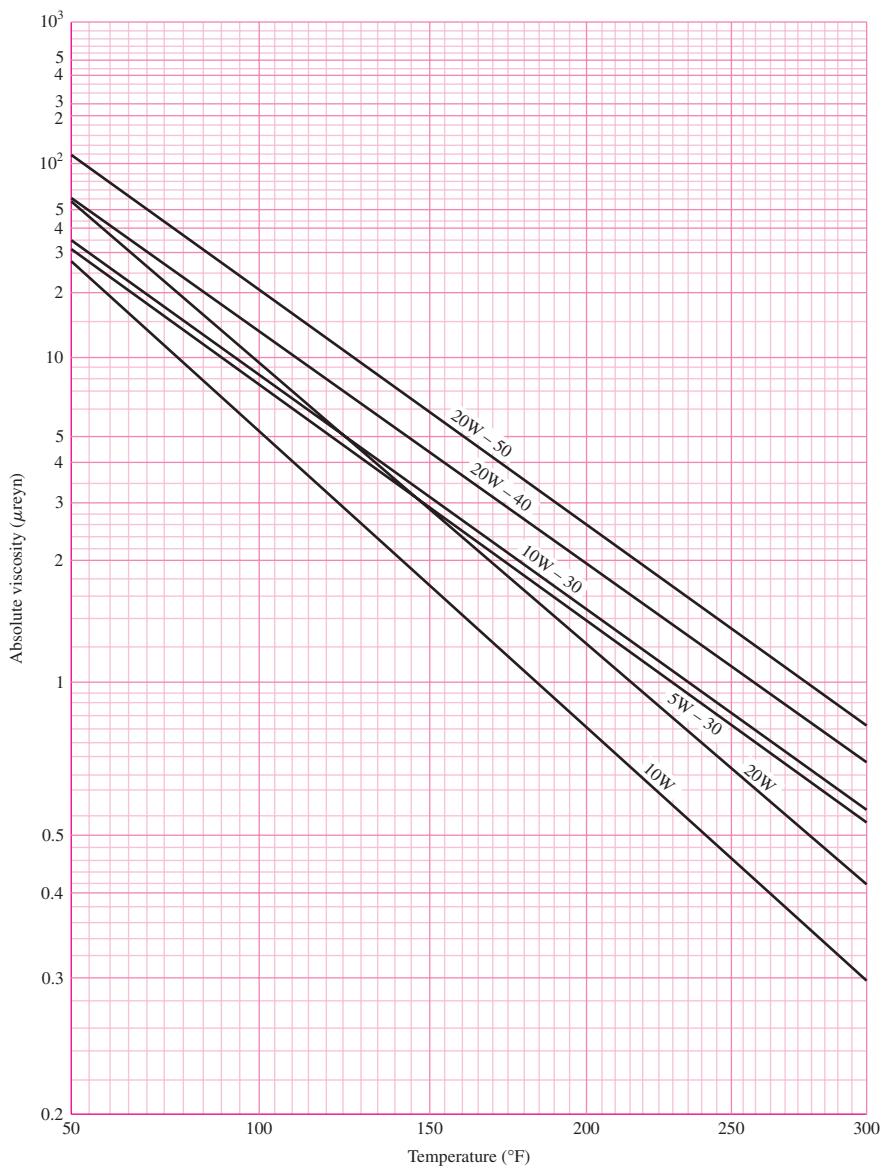
$$T_{av} = 180 + \frac{30}{2} = 195^\circ\text{F}$$

and locates point *B* on Fig. 12-12.

If points *A* and *B* are fairly close to each other and on opposite sides of the SAE 30 line, a straight line can be drawn between them with the intersection locating the correct values of viscosity and average temperature to be used in the analysis. For this illustration, we see from the viscosity chart that they are $T_{av} = 203^\circ\text{F}$ and $\mu = 1.20 \text{ } \mu\text{reyn}$.

Figure 12-14

Chart for multiviscosity lubricants. This chart was derived from known viscosities at two points, 100 and 210°F, and the results are believed to be correct for other temperatures.

**Table 12-1**

Curve Fits* to Approximate the Viscosity versus Temperature Functions for SAE Grades 10 to 60

Source: A. S. Seireg and S. Dandage, "Empirical Design Procedure for the Thermodynamic Behavior of Journal Bearings," *J. Lubrication Technology*, vol. 104, April 1982, pp. 135–148.

Oil Grade, SAE	Viscosity μ_0 , reyn	Constant b , °F
10	$0.0158(10^{-6})$	1157.5
20	$0.0136(10^{-6})$	1271.6
30	$0.0141(10^{-6})$	1360.0
40	$0.0121(10^{-6})$	1474.4
50	$0.0170(10^{-6})$	1509.6
60	$0.0187(10^{-6})$	1564.0

* $\mu = \mu_0 \exp [b/(T + 95)]$, T in °F.

Figure 12-15

Polar diagram of the film-pressure distribution showing the notation used.
(Raimondi and Boyd.)

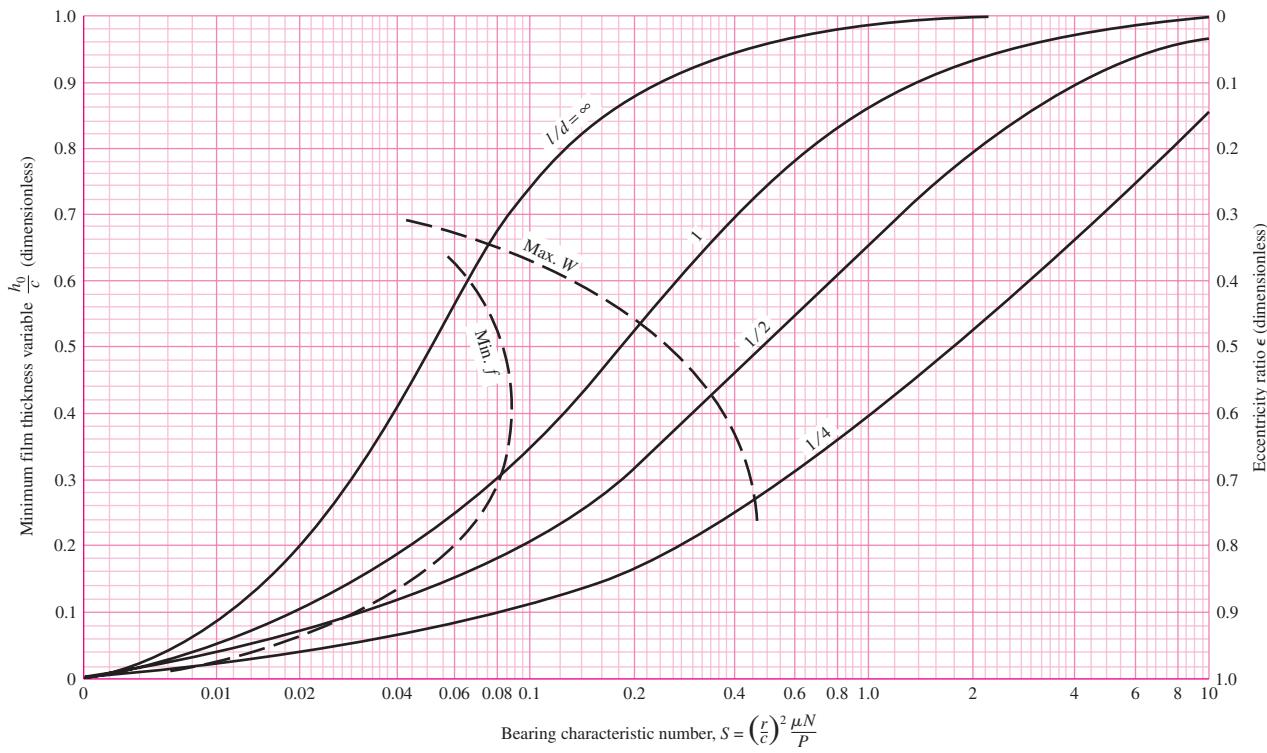
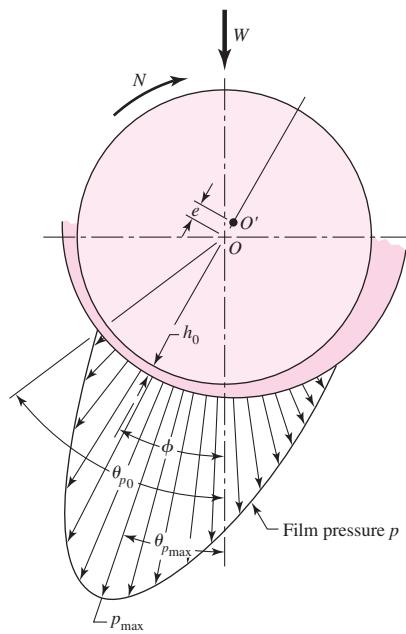
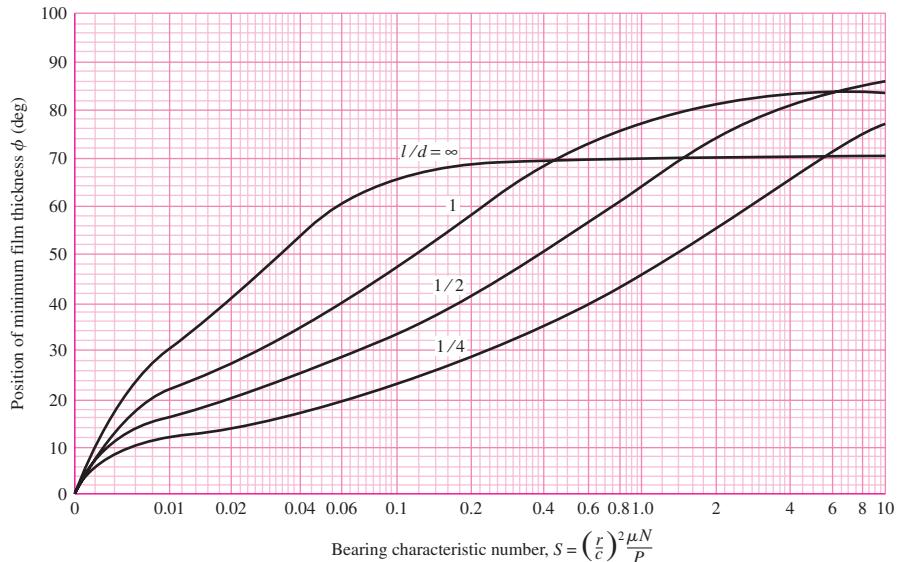
**Figure 12-16**

Chart for minimum film thickness variable and eccentricity ratio. The left boundary of the zone defines the optimal h_0 for minimum friction; the right boundary is optimum h_0 for load. (Raimondi and Boyd.)

Figure 12-17

Chart for determining the position of the minimum film thickness h_0 . (Raimondi and Boyd.)



The remaining charts from Raimondi and Boyd relate several variables to the Sommerfeld number. These variables are

- Minimum film thickness (Figs. 12-16 and 12-17)
- Coefficient of friction (Fig. 12-18)
- Lubricant flow (Figs. 12-19 and 12-20)
- Film pressure (Figs. 12-21 and 12-22)

Figure 12-15 shows the notation used for the variables. We will describe the use of these curves in a series of four examples using the same set of given parameters.

Minimum Film Thickness

In Fig. 12-16, the minimum film thickness variable h_0/c and eccentricity ratio $\epsilon = e/c$ are plotted against the Sommerfeld number S with contours for various values of l/d . The corresponding angular position of the minimum film thickness is found in Fig. 12-17.

EXAMPLE 12-1

Determine h_0 and e using the following given parameters: $\mu = 4 \text{ } \mu\text{reyn}$, $N = 30 \text{ rev/s}$, $W = 500 \text{ lbf}$ (bearing load), $r = 0.75 \text{ in}$, $c = 0.0015 \text{ in}$, and $l = 1.5 \text{ in}$.

Solution

The nominal bearing pressure (in projected area of the journal) is

$$P = \frac{W}{2rl} = \frac{500}{2(0.75)1.5} = 222 \text{ psi}$$

The Sommerfeld number is, from Eq. (12-7), where $N = N_j = 30 \text{ rev/s}$,

$$S = \left(\frac{r}{c}\right)^2 \left(\frac{\mu N}{P}\right) = \left(\frac{0.75}{0.0015}\right)^2 \left[\frac{4(10^{-6})30}{222}\right] = 0.135$$

Also, $l/d = 1.50/[2(0.75)] = 1$. Entering Fig. 12-16 with $S = 0.135$ and $l/d = 1$ gives $h_0/c = 0.42$ and $\epsilon = 0.58$. The quantity h_0/c is called the *minimum film thickness*.

variable. Since $c = 0.0015$ in, the minimum film thickness h_0 is

$$h_0 = 0.42(0.0015) = 0.00063 \text{ in}$$

We can find the angular location ϕ of the minimum film thickness from the chart of Fig. 12–17. Entering with $S = 0.135$ and $l/d = 1$ gives $\phi = 53^\circ$.

The eccentricity ratio is $\epsilon = e/c = 0.58$. This means the eccentricity e is

$$e = 0.58(0.0015) = 0.00087 \text{ in}$$

Note that if the journal is centered in the bushing, $e = 0$ and $h_0 = c$, corresponding to a very light (zero) load. Since $e = 0$, $\epsilon = 0$. As the load is increased the journal displaces downward; the limiting position is reached when $h_0 = 0$ and $e = c$, that is, when the journal touches the bushing. For this condition the eccentricity ratio is unity. Since $h_0 = c - e$, dividing both sides by c , we have

$$\frac{h_0}{c} = 1 - \epsilon$$

Design optima are sometimes *maximum load*, which is a load-carrying characteristic of the bearing, and sometimes *minimum parasitic power loss* or *minimum coefficient of friction*. Dashed lines appear on Fig. 12–16 for maximum load and minimum coefficient of friction, so you can easily favor one of maximum load or minimum coefficient of friction, but not both. The zone between the two dashed-line contours might be considered a desirable location for a design point.

Coefficient of Friction

The friction chart, Fig. 12–18, has the *friction variable* $(r/c)f$ plotted against Sommerfeld number S with contours for various values of the l/d ratio.

EXAMPLE 12–2

Using the parameters given in Ex. 12–1, determine the coefficient of friction, the torque to overcome friction, and the power loss to friction.

Solution

We enter Fig. 12–18 with $S = 0.135$ and $l/d = 1$ and find $(r/c)f = 3.50$. The coefficient of friction f is

$$f = 3.50 c/r = 3.50(0.0015/0.75) = 0.0070$$

The friction torque on the journal is

$$T = f Wr = 0.007(500)0.75 = 2.62 \text{ lbf} \cdot \text{in}$$

The power loss in horsepower is

$$(hp)_{\text{loss}} = \frac{TN}{1050} = \frac{2.62(30)}{1050} = 0.075 \text{ hp}$$

or, expressed in Btu/s,

$$H = \frac{2\pi TN}{778(12)} = \frac{2\pi(2.62)30}{778(12)} = 0.0529 \text{ Btu/s}$$

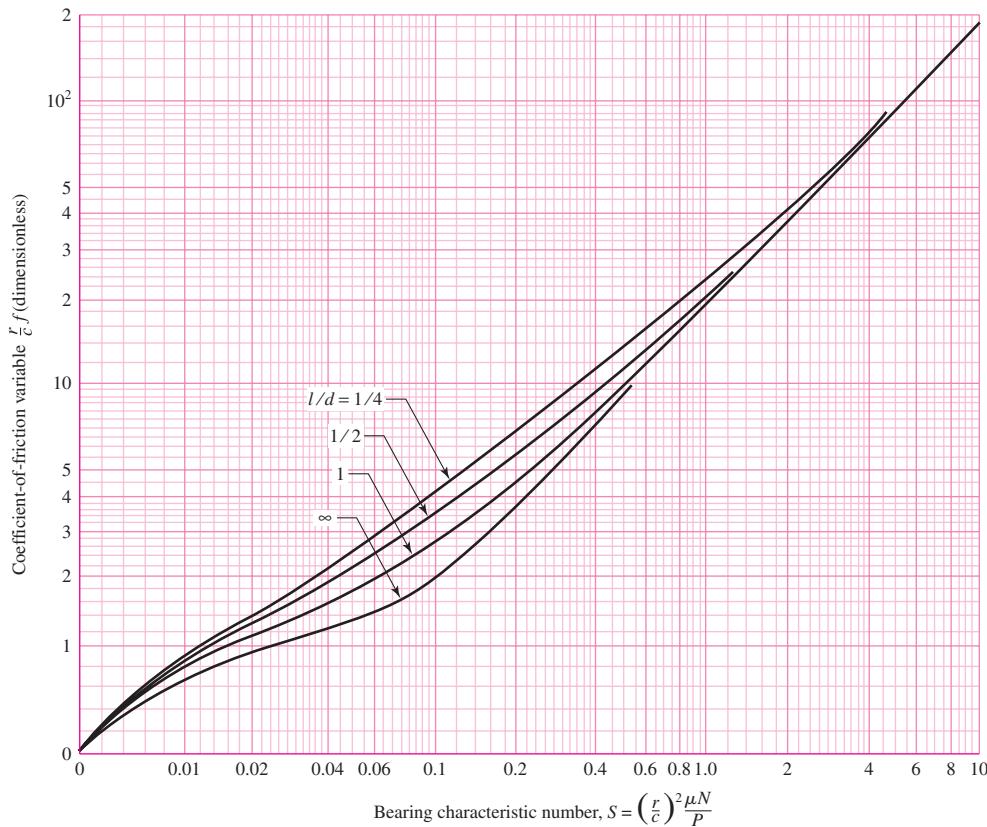


Figure 12-18

Chart for coefficient-of-friction variable; note that Petroff's equation is the asymptote. (Raimondi and Boyd.)

Lubricant Flow

Figures 12-19 and 12-20 are used to determine the lubricant flow and side flow.

EXAMPLE 12-3

Continuing with the parameters of Ex. 12-1, determine the total volumetric flow rate Q and the side flow rate Q_s .

Solution

To estimate the lubricant flow, enter Fig. 12-19 with $S = 0.135$ and $l/d = 1$ to obtain $Q/(rcNl) = 4.28$. The total volumetric flow rate is

$$Q = 4.28rcNl = 4.28(0.75)0.0015(30)1.5 = 0.217 \text{ in}^3/\text{s}$$

From Fig. 12-20 we find the flow ratio $Q_s/Q = 0.655$ and Q_s is

$$Q_s = 0.655Q = 0.655(0.217) = 0.142 \text{ in}^3/\text{s}$$

Figure 12-19

Chart for flow variable.

Note: Not for pressure-fed bearings. (Raimondi and Boyd.)

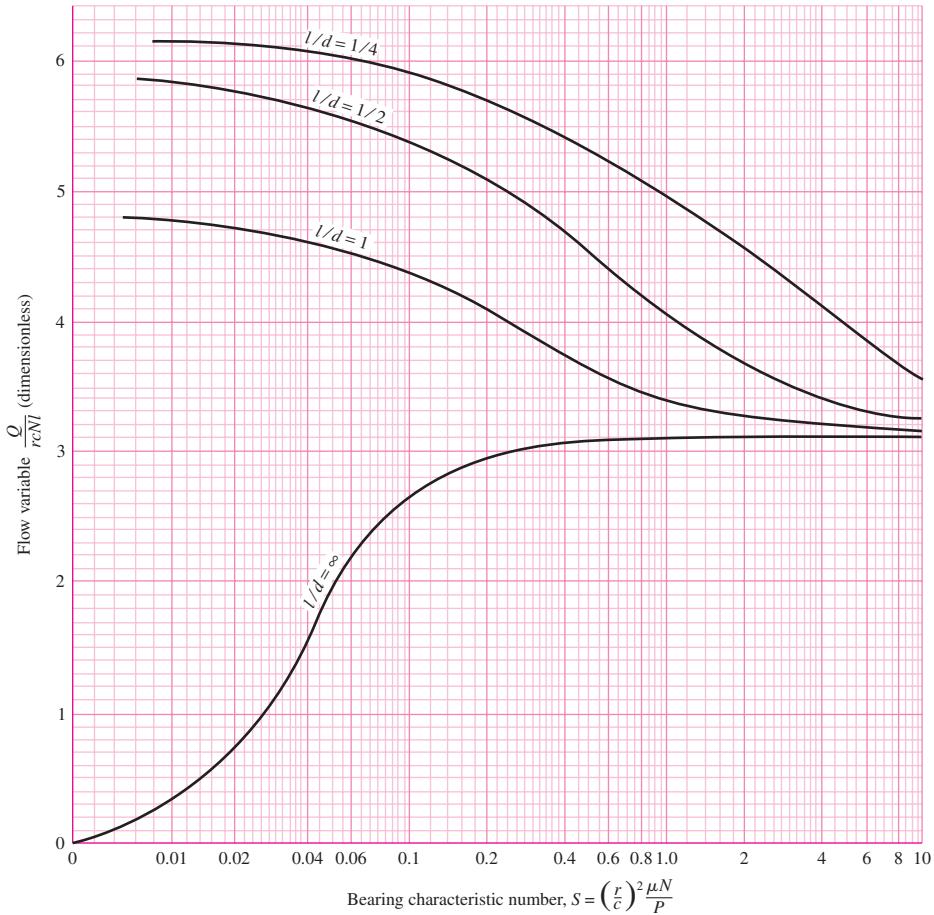
**Figure 12-20**

Chart for determining the ratio of side flow to total flow.

(Raimondi and Boyd.)

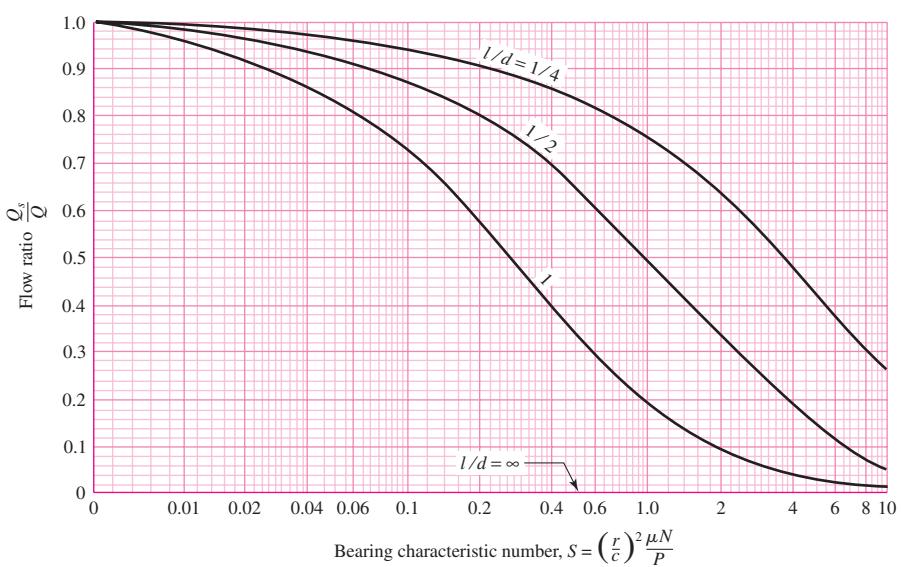
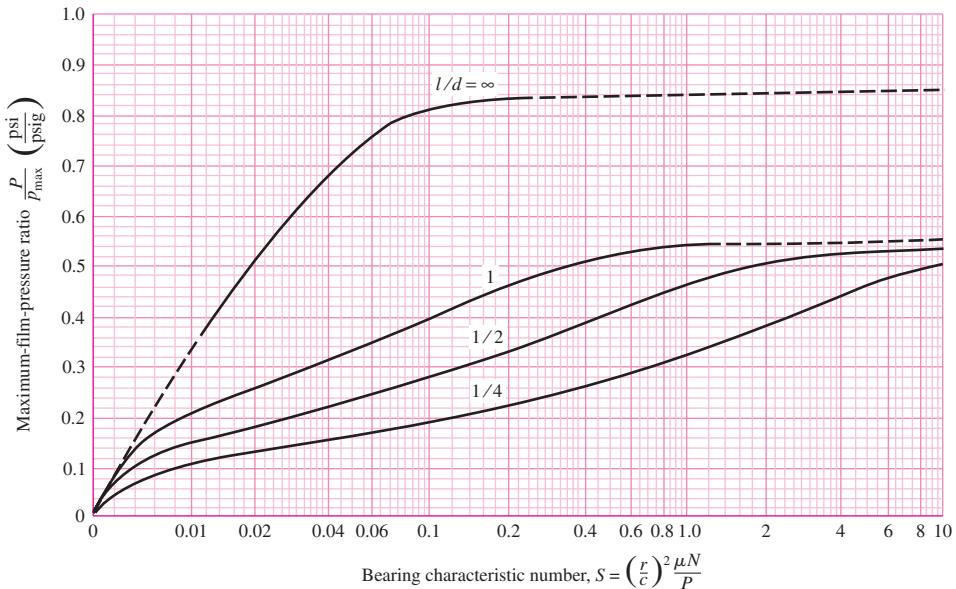


Figure 12-21

Chart for determining the maximum film pressure.
Note: Not for pressure-fed bearings. (Raimondi and Boyd)



The side leakage Q_s is from the lower part of the bearing, where the internal pressure is above atmospheric pressure. The leakage forms a fillet at the journal-bushing external junction, and it is carried by journal motion to the top of the bushing, where the internal pressure is below atmospheric pressure and the gap is much larger, to be “sucked in” and returned to the lubricant sump. That portion of side leakage that leaks away from the bearing has to be made up by adding oil to the bearing sump periodically by maintenance personnel.

Film Pressure

The maximum pressure developed in the film can be estimated by finding the pressure ratio P/p_{\max} from the chart in Fig. 12-21. The locations where the terminating and maximum pressures occur, as defined in Fig. 12-22, are determined from Fig. 12-22.

EXAMPLE 12-4

Using the parameters given in Ex. 12-1, determine the maximum film pressure and the locations of the maximum and terminating pressures.

Solution

Entering Fig. 12-21 with $S = 0.135$ and $l/d = 1$, we find $P/p_{\max} = 0.42$. The maximum pressure p_{\max} is therefore

$$p_{\max} = \frac{P}{0.42} = \frac{222}{0.42} = 529 \text{ psi}$$

With $S = 0.135$ and $l/d = 1$, from Fig. 12-22, $\theta_{p_{\max}} = 18.5^\circ$ and the terminating position θ_{p_0} is 75° .

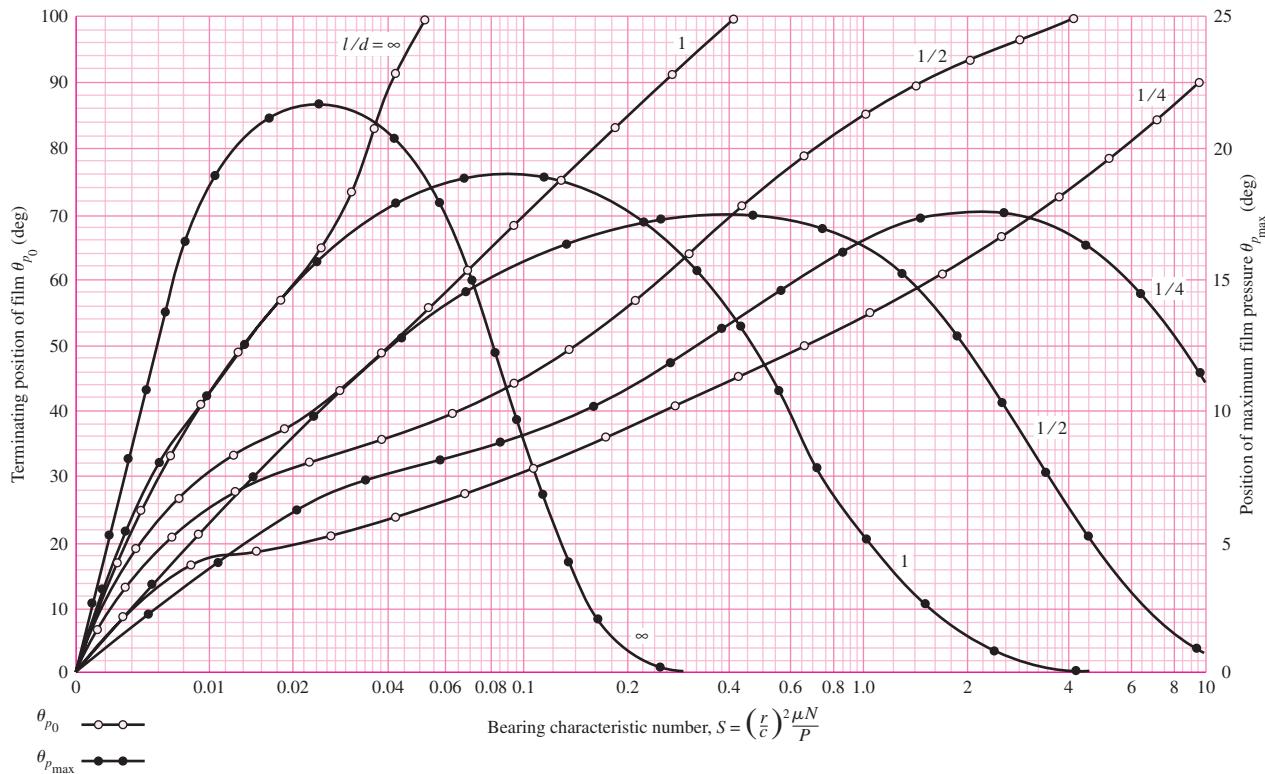


Figure 12-22

Chart for finding the terminating position of the lubricant film and the position of maximum film pressure. (Raimondi and Boyd.)

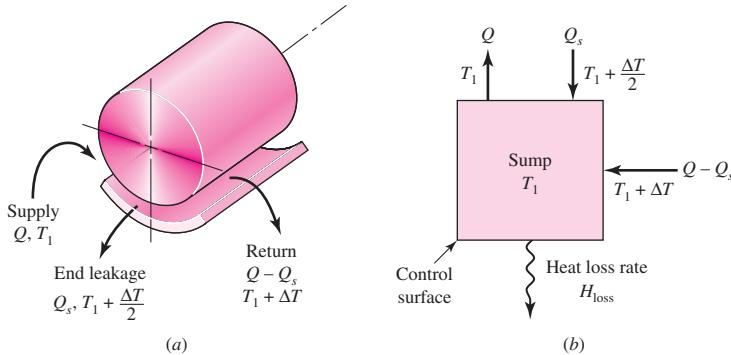
Examples 12–1 to 12–4 demonstrate how the Raimondi and Boyd charts are used. It should be clear that we do not have journal-bearing parametric relations as equations, but in the form of charts. Moreover, the examples were simple because the steady-state equivalent viscosity was given. We will now show how the average film temperature (and the corresponding viscosity) is found from energy considerations.

Lubricant Temperature Rise

The temperature of the lubricant rises until the rate at which work is done by the journal on the film through fluid shear is the same as the rate at which heat is transferred to the greater surroundings. The specific arrangement of the bearing plumbing affects the quantitative relationships. See Fig. 12–23. A lubricant sump (internal or external to the bearing housing) supplies lubricant at sump temperature T_s to the bearing annulus at temperature $T_s = T_1$. The lubricant passes once around the bushing and is delivered at a higher lubricant temperature $T_1 + \Delta T$ to the sump. Some of the lubricant leaks out of the bearing at a mixing-cup temperature of $T_1 + \Delta T/2$ and is returned to the sump. The sump may be a keyway-like groove in the bearing cap or a larger chamber up to half the bearing circumference. It can occupy “all” of the bearing cap of a split bearing. In such a bearing the side leakage occurs from the lower portion and is sucked back in, into the ruptured film arc. The sump could be well removed from the journal-bushing interface.

Figure 12-23

Schematic of a journal bearing with an external sump with cooling; lubricant makes one pass before returning to the sump.



Let

$$Q = \text{volumetric oil-flow rate into the bearing, in}^3/\text{s}$$

$$Q_s = \text{volumetric side-flow leakage rate out of the bearing and to the sump, in}^3/\text{s}$$

$$Q - Q_s = \text{volumetric oil-flow discharge from annulus to sump, in}^3/\text{s}$$

$$T_1 = \text{oil inlet temperature (equal to sump temperature } T_s), ^\circ\text{F}$$

$$\Delta T = \text{temperature rise in oil between inlet and outlet, } ^\circ\text{F}$$

$$\rho = \text{lubricant density, lbm/in}^3$$

$$C_p = \text{specific heat capacity of lubricant, Btu/(lbm} \cdot ^\circ\text{F)}$$

$$J = \text{Joulean heat equivalent, in} \cdot \text{lbf/Btu}$$

$$H = \text{heat rate, Btu/s}$$

Using the sump as a control region, we can write an enthalpy balance. Using T_1 as the datum temperature gives

$$H_{\text{loss}} = \rho C_p Q_s \Delta T / 2 + \rho C_p (Q - Q_s) \Delta T = \rho C_p Q \Delta T \left(1 - \frac{1}{2} \frac{Q_s}{Q} \right) \quad (a)$$

The thermal energy loss at steady state H_{loss} is equal to the rate the journal does work on the film is $H_{\text{loss}} = \dot{W} = 2\pi T N/J$. The torque $T = f Wr$, the load in terms of pressure is $W = 2Prl$, and multiplying numerator and denominator by the clearance c gives

$$H_{\text{loss}} = \frac{4\pi PrlNc rf}{J c} \quad (b)$$

Equating Eqs. (a) and (b) and rearranging results in

$$\frac{J\rho C_p \Delta T}{4\pi P} = \frac{rf/c}{(1 - 0.5Q_s/Q)[Q/(rcNl)]} \quad (c)$$

For common petroleum lubricants $\rho = 0.0311 \text{ lbm/in}^3$, $C_p = 0.42 \text{ Btu/(lbm} \cdot ^\circ\text{F)}$, and $J = 778(12) = 9336 \text{ in} \cdot \text{lbf/Btu}$; therefore the left term of Eq. (c) is

$$\frac{J\rho C_p \Delta T}{4\pi P} = \frac{9336(0.0311)0.42\Delta T_F}{4\pi P_{\text{psi}}} = 9.70 \frac{\Delta T_F}{P_{\text{psi}}}$$

thus

$$\frac{9.70\Delta T_F}{P_{\text{psi}}} = \frac{rf/c}{(1 - \frac{1}{2}Q_s/Q)[Q/(rcNl)]} \quad (12-15)$$

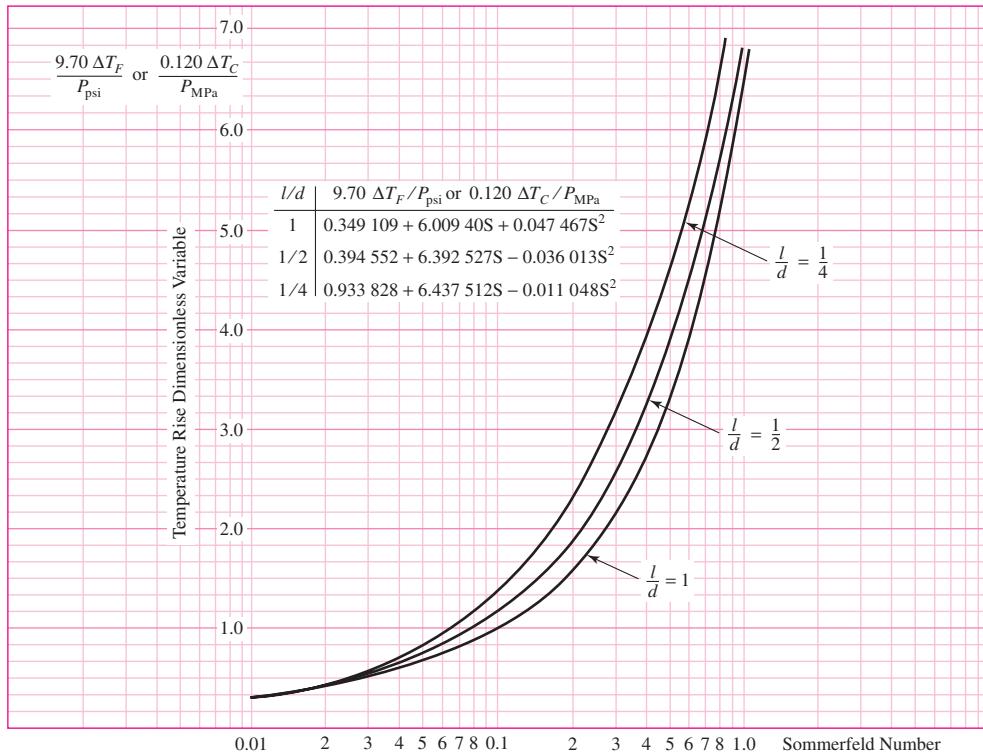


Figure 12-24

Figures 12–18, 12–19, and 12–20 combined to reduce iterative table look-up. (Source: Chart based on work of Raimondi and Boyd boundary condition (2), i.e., no negative lubricant pressure developed. Chart is for full journal bearing using single lubricant pass, side flow emerges with temperature rise $\Delta T/2$, thru flow emerges with temperature rise ΔT , and entire flow is supplied at datum sump temperature.)

where ΔT_F is the temperature rise in $^{\circ}\text{F}$ and P_{psi} is the bearing pressure in psi. The right side of Eq. (12–15) can be evaluated from Figs. 12–18, 12–19, and 12–20 for various Sommerfeld numbers and l/d ratios to give Fig. 12–24. It is easy to show that the left side of Eq. (12–15) can be expressed as $0.120\Delta T_C / P_{\text{MPa}}$ where ΔT_C is expressed in $^{\circ}\text{C}$ and the pressure P_{MPa} is expressed in MPa. The ordinate in Fig. 12–24 is either $9.70 \Delta T_F / P_{\text{psi}}$ or $0.120 \Delta T_C / P_{\text{MPa}}$, which is not surprising since both are dimensionless in proper units and *identical in magnitude*. Since solutions to bearing problems involve iteration and reading many graphs can introduce errors, Fig. 12–24 reduces three graphs to one, a step in the proper direction.

Interpolation

For l/d ratios other than the ones given in the charts, Raimondi and Boyd have provided the following interpolation equation

$$y = \frac{1}{(l/d)^3} \left[-\frac{1}{8} \left(1 - \frac{l}{d}\right) \left(1 - 2\frac{l}{d}\right) \left(1 - 4\frac{l}{d}\right) y_\infty + \frac{1}{3} \left(1 - 2\frac{l}{d}\right) \left(1 - 4\frac{l}{d}\right) y_1 \right. \\ \left. - \frac{1}{4} \left(1 - \frac{l}{d}\right) \left(1 - 4\frac{l}{d}\right) y_{1/2} + \frac{1}{24} \left(1 - \frac{l}{d}\right) \left(1 - 2\frac{l}{d}\right) y_{1/4} \right] \quad (12-16)$$

where y is the desired variable within the interval $\infty > l/d > \frac{1}{4}$ and y_∞ , y_1 , $y_{1/2}$, and $y_{1/4}$ are the variables corresponding to l/d ratios of ∞ , 1 , $\frac{1}{2}$, and $\frac{1}{4}$, respectively.

12-9

Steady-State Conditions in Self-Contained Bearings

The case in which the lubricant carries away all of the enthalpy increase from the journal-bushing pair has already been discussed. Bearings in which the warm lubricant stays within the bearing housing will now be addressed. These bearings are called *self-contained* bearings because the lubricant sump is within the bearing housing and the lubricant is cooled within the housing. These bearings are described as *pillow-block* or *pedestal* bearings. They find use on fans, blowers, pumps, and motors, for example. Integral to design considerations for these bearings is dissipating heat from the bearing housing to the surroundings at the same rate that enthalpy is being generated within the fluid film.

In a self-contained bearing the sump can be positioned as a keywaylike cavity in the bushing, the ends of the cavity not penetrating the end planes of the bushing. Film oil exits the annulus at about one-half of the relative peripheral speeds of the journal and bushing and slowly tumbles the sump lubricant, mixing with the sump contents. Since the film in the top "half" of the cap has cavitated, it contributes essentially nothing to the support of the load, but it does contribute friction. Bearing caps are in use in which the "keyway" sump is expanded peripherally to encompass the top half of the bearing. This reduces friction for the same load, but the included angle β of the bearing has been reduced to 180° . Charts for this case were included in the Raimondi and Boyd paper.

The heat given up by the bearing housing may be estimated from the equation

$$H_{\text{loss}} = \bar{h}_{\text{CR}} A (T_b - T_\infty) \quad (12-17)$$

where H_{loss} = heat dissipated, Btu/h

\bar{h}_{CR} = combined overall coefficient of radiation and convection heat transfer, Btu/(h · ft² · °F)

A = surface area of bearing housing, ft²

T_b = surface temperature of the housing, °F

T_∞ = ambient temperature, °F

The overall coefficient \bar{h}_{CR} depends on the material, surface coating, geometry, even the roughness, the temperature difference between the housing and surrounding objects, and air velocity. After Karelitz,¹⁰ and others, in ordinary industrial environments, the overall coefficient \bar{h}_{CR} can be treated as a constant. Some representative values are

$$\bar{h}_{\text{CR}} = \begin{cases} 2 \text{ Btu}/(\text{h} \cdot \text{ft}^2 \cdot ^\circ\text{F}) & \text{for still air} \\ 2.7 \text{ Btu}/(\text{h} \cdot \text{ft}^2 \cdot ^\circ\text{F}) & \text{for shaft-stirred air} \\ 5.9 \text{ Btu}/(\text{h} \cdot \text{ft}^2 \cdot ^\circ\text{F}) & \text{for air moving at 500 ft/min} \end{cases} \quad (12-18)$$

An expression similar to Eq. (12-17) can be written for the temperature difference $T_f - T_b$ between the lubricant film and the housing surface. This is possible because the bushing and housing are metal and very nearly isothermal. If one defines \bar{T}_f as the *average* film temperature (halfway between the lubricant inlet temperature T_s and

¹⁰G. B. Karelitz, "Heat Dissipation in Self-Contained Bearings," *Trans. ASME*, Vol. 64, 1942, p. 463; D. C. Lemmon and E. R. Booser, "Bearing Oil-Ring Performance," *Trans. ASME*, J. Bas. Engin., Vol. 88, 1960, p. 327.

| Table 12-2

Lubrication System	Conditions	Range of α
Oil ring	Moving air	1–2
	Still air	$\frac{1}{2}$ –1
Oil bath	Moving air	$\frac{1}{2}$ –1
	Still air	$\frac{1}{5}$ – $\frac{2}{5}$

the outlet temperature $T_s + \Delta T$), then the following proportionality has been observed between $\bar{T}_f - T_b$ and the difference between the housing surface temperature and the ambient temperature, $T_b - T_\infty$:

$$\bar{T}_f - T_b = \alpha(T_b - T_\infty) \quad (a)$$

where \bar{T}_f is the average film temperature and α is a constant depending on the lubrication scheme and the bearing housing geometry. Equation (a) may be used to estimate the bearing housing temperature. Table 12-2 provides some guidance concerning suitable values of α . The work of Karelitz allows the broadening of the application of the charts of Raimondi and Boyd, to be applied to a variety of bearings beyond the natural circulation pillow-block bearing.

Solving Eq. (a) for T_b and substituting into Eq. (12-17) gives the bearing heat loss rate to the surroundings as

$$H_{\text{loss}} = \frac{\dot{h}_{\text{CR}} A}{1 + \alpha} (\bar{T}_f - T_\infty) \quad (12-19a)$$

and rewriting Eq. (a) gives

$$T_b = \frac{\bar{T}_f + \alpha T_\infty}{1 + \alpha} \quad (12-19b)$$

In beginning a steady-state analysis the average film temperature is unknown, hence the viscosity of the lubricant in a self-contained bearing is unknown. Finding the equilibrium temperatures is an iterative process wherein a trial average film temperature (and the corresponding viscosity) is used to compare the heat generation rate and the heat loss rate. An adjustment is made to bring these two heat rates into agreement. This can be done on paper with a tabular array to help adjust \bar{T}_f to achieve equality between heat generation and loss rates. A root-finding algorithm can be used. Even a simple one can be programmed for a digital computer.

Because of the shearing action there is a uniformly distributed energy release in the lubricant that heats the lubricant as it works its way around the bearing. The temperature is uniform in the radial direction but increases from the sump temperature T_s by an amount ΔT during the lubricant pass. The exiting lubricant mixes with the sump contents, being cooled to sump temperature. The lubricant in the sump is cooled because the bushing and housing metal are at a nearly uniform lower temperature because of heat losses by convection and radiation to the surroundings at ambient temperature T_∞ . In the usual configurations of such bearings, the bushing and housing metal temperature is approximately midway between the average film temperature $\bar{T}_f = T_s + \Delta T/2$ and the ambient temperature T_∞ . The heat generation rate H_{gen} , at steady state, is equal to the work rate from the frictional torque T . Expressing this in Btu/h requires the conversion constants 2545 Btu/(hp · h) and 1050 (lbf · in)(rev/s)/hp results in $H_{\text{gen}} = 2545 TN/1050$. Then from Eq. (b), Sec. 12-3, the torque is

$T = 4\pi^2 r^3 l \mu / c$, resulting in

$$H_{\text{gen}} = \frac{2545}{1050} \frac{4\pi^2 r^3 l \mu N}{c} N = \frac{95.69 \mu N^2 l r^3}{c} \quad (b)$$

Equating this to Eq. (12-19a) and solving for \bar{T}_f gives

$$\bar{T}_f = T_\infty + 95.69(1 + \alpha) \frac{\mu N^2 l r^3}{\hbar_{\text{CR}} A c} \quad (12-20)$$

EXAMPLE 12-5

Consider a pillow-block bearing with a keyway sump, whose journal rotates at 900 rev/min in shaft-stirred air at 70°F with $\alpha = 1$. The lateral area of the bearing is 40 in². The lubricant is SAE grade 20 oil. The gravity radial load is 100 lbf and the l/d ratio is unity. The bearing has a journal diameter of 2.000 + 0.000/-0.002 in, a bushing bore of 2.002 + 0.004/-0.000 in. For a minimum clearance assembly estimate the steady-state temperatures as well as the minimum film thickness and coefficient of friction.

Solution

The minimum radial clearance, c_{\min} , is

$$c_{\min} = \frac{2.002 - 2.000}{2} = 0.001 \text{ in}$$

$$P = \frac{W}{ld} = \frac{100}{(2)2} = 25 \text{ psi}$$

$$S = \left(\frac{r}{c}\right)^2 \frac{\mu N}{P} = \left(\frac{1}{0.001}\right)^2 \frac{\mu'(15)}{10^6(25)} = 0.6 \mu'$$

where μ' is viscosity in μreyn . The friction horsepower loss, $(\text{hp})_f$, is found as follows:

$$(\text{hp})_f = \frac{f Wr N}{1050} = \frac{W N c}{1050} \frac{fr}{c} = \frac{100(900/60)0.001}{1050} \frac{fr}{c} = 0.001429 \frac{fr}{c} \text{ hp}$$

The heat generation rate H_{gen} , in Btu/h, is

$$H_{\text{gen}} = 2545(\text{hp})_f = 2545(0.001429)fr/c = 3.637 fr/c \text{ Btu/h}$$

From Eq. (12-19a) with $\hbar_{\text{CR}} = 2.7 \text{ Btu}/(\text{h} \cdot \text{ft}^2 \cdot {}^\circ\text{F})$, the rate of heat loss to the environment H_{loss} is

$$H_{\text{loss}} = \frac{\hbar_{\text{CR}} A}{\alpha + 1} (\bar{T}_f - 70) = \frac{2.7(40/144)}{(1+1)} (\bar{T}_f - 70) = 0.375(\bar{T}_f - 70) \text{ Btu/h}$$

Build a table as follows for trial values of \bar{T}_f of 190 and 195°F:

Trial \bar{T}_f	μ'	S	fr/c	H_{gen}	H_{loss}
190	1.15	0.69	13.6	49.5	45.0
195	1.03	0.62	12.2	44.4	46.9

The temperature at which $H_{\text{gen}} = H_{\text{loss}} = 46.3 \text{ Btu/h}$ is 193.4°F . Rounding \bar{T}_f to 193°F we find $\mu' = 1.08 \text{ } \mu\text{reyn}$ and $S = 0.6(1.08) = 0.65$. From Fig. 12-24, $9.70\Delta T_F/P = 4.25^\circ\text{F}/\text{psi}$ and thus

$$\Delta T_F = 4.25P/9.70 = 4.25(25)/9.70 = 11.0^\circ\text{F}$$

$$T_1 = T_s = \bar{T}_f - \Delta T/2 = 193 - 11/2 = 187.5^\circ\text{F}$$

$$T_{\max} = T_1 + \Delta T_F = 187.5 + 11 = 198.5^\circ\text{F}$$

From Eq. (12-19b)

$$T_b = \frac{T_f + \alpha T_\infty}{1 + \alpha} = \frac{193 + (1)70}{1 + 1} = 131.5^\circ\text{F}$$

with $S = 0.65$, the minimum film thickness from Fig. 12-16 is

$$h_0 = \frac{h_0}{c} c = 0.79(0.001) = 0.00079 \text{ in}$$

The coefficient of friction from Fig. 12-18 is

$$f = \frac{fr}{c} \frac{c}{r} = 12.8 \frac{0.001}{1} = 0.0128$$

The parasitic friction torque T is

$$T = fWr = 0.0128(100)(1) = 1.28 \text{ lbf} \cdot \text{in}$$

12-10 Clearance

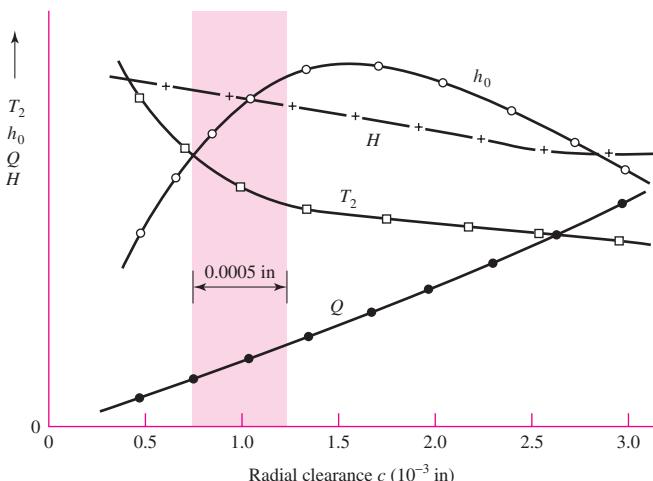
In designing a journal bearing for thick-film lubrication, the engineer must select the grade of oil to be used, together with suitable values for P , N , r , c , and l . A poor selection of these or inadequate control of them during manufacture or in use may result in a film that is too thin, so that the oil flow is insufficient, causing the bearing to overheat and, eventually, fail. Furthermore, the radial clearance c is difficult to hold accurate during manufacture, and it may increase because of wear. What is the effect of an entire range of radial clearances, expected in manufacture, and what will happen to the bearing performance if c increases because of wear? Most of these questions can be answered and the design optimized by plotting curves of the performance as functions of the quantities over which the designer has control.

Figure 12-25 shows the results obtained when the performance of a particular bearing is calculated for a whole range of radial clearances and is plotted with clearance as the independent variable. The bearing used for this graph is the one of Examples 12-1 to 12-4 with SAE 20 oil at an inlet temperature of 100°F . The graph shows that if the clearance is too tight, the temperature will be too high and the minimum film thickness too low. High temperatures may cause the bearing to fail by fatigue. If the oil film is too thin, dirt particles may be unable to pass without scoring or may embed themselves in the bearing. In either event, there will be excessive wear and friction, resulting in high temperatures and possible seizing.

To investigate the problem in more detail, Table 12-3 was prepared using the two types of preferred running fits that seem to be most useful for journal-bearing design

Figure 12-25

A plot of some performance characteristics of the bearing of Exs. 12-1 to 12-4 for radial clearances of 0.0005 to 0.003 in. The bearing outlet temperature is designated T_2 . New bearings should be designed for the shaded zone, because wear will move the operating point to the right.

**Table 12-3**

Maximum, Minimum, and Average Clearances for 1.5-in-Diameter Journal Bearings Based on Type of Fit

Type of Fit	Symbol	Clearance c , in		
		Maximum	Average	Minimum
Close-running	H8/f7	0.00175	0.001125	0.0005
Free-running	H9/d9	0.00395	0.00275	0.00155

Table 12-4

Performance of 1.5-in-Diameter Journal Bearing with Various Clearances. (SAE 20 Lubricant, $T_1 = 100^\circ\text{F}$, $N = 30 \text{ r/s}$, $W = 500 \text{ lbf}$, $L = 1.5 \text{ in}$)

c , in	T_2 , °F	h_0 , in	f	Q , in^3/s	H , Btu/s
0.0005	226	0.00038	0.0113	0.061	0.086
0.001125	142	0.00065	0.0090	0.153	0.068
0.00155	133	0.00077	0.0087	0.218	0.066
0.00175	128	0.00076	0.0084	0.252	0.064
0.00275	118	0.00073	0.0079	0.419	0.060
0.00395	113	0.00069	0.0077	0.617	0.059

(see Table 7-9), p. 397. The results shown in Table 12-3 were obtained by using Eqs. (7-36) and (7-37) of Sec. 7-8. Notice that there is a slight overlap, but the range of clearances for the free-running fit is about twice that of the close-running fit.

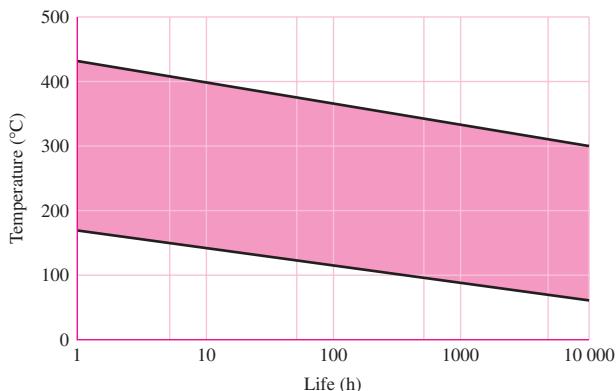
The six clearances of Table 12-3 were used in a computer program to obtain the numerical results shown in Table 12-4. These conform to the results of Fig. 12-25, too. Both the table and the figure show that a tight clearance results in a high temperature. Figure 12-26 can be used to estimate an upper temperature limit when the characteristics of the application are known.

It would seem that a large clearance will permit the dirt particles to pass through and also will permit a large flow of oil, as indicated in Table 12-4. This lowers the temperature and increases the life of the bearing. However, if the clearance becomes too

Figure 12-26

Temperature limits for mineral oils. The lower limit is for oils containing antioxidants and applies when oxygen supply is unlimited. The upper limit applies when insignificant oxygen is present. The life in the shaded zone depends on the amount of oxygen and catalysts present.

(Source: M. J. Neale (ed.), *Tribology Handbook, Section B1*, Newnes-Butterworth, London, 1975.)



large, the bearing becomes noisy and the minimum film thickness begins to decrease again.

In between these two limitations there exists a rather large range of clearances that will result in satisfactory bearing performance.

When both the production tolerance and the future wear on the bearing are considered, it is seen, from Fig. 12-25, that the best compromise is a clearance range slightly to the left of the top of the minimum-film-thickness curve. In this way, future wear will move the operating point to the right and increase the film thickness and decrease the operating temperature.

12-11

Pressure-Fed Bearings

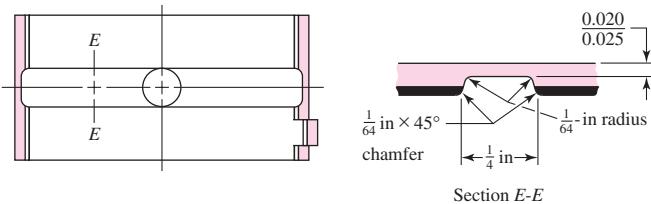
The load-carrying capacity of self-contained natural-circulating journal bearings is quite restricted. The factor limiting better performance is the heat-dissipation capability of the bearing. A first thought of a way to increase heat dissipation is to cool the sump with an external fluid such as water. The high-temperature problem is in the film where the heat is generated but cooling is not possible in the film until later. This does not protect against exceeding the maximum allowable temperature of the lubricant. A second alternative is to reduce the *temperature rise* in the film by dramatically increasing the rate of lubricant flow. The lubricant itself is reducing the temperature rise. A water-cooled sump may still be in the picture. To increase lubricant flow, an external pump must be used with lubricant supplied at pressures of tens of pounds per square inch gage. Because the lubricant is supplied to the bearing under pressure, such bearings are called *pressure-fed bearings*.

To force a greater flow through the bearing and thus obtain an increased cooling effect, a common practice is to use a circumferential groove at the center of the bearing, with an oil-supply hole located opposite the load-bearing zone. Such a bearing is shown in Fig. 12-27. The effect of the groove is to create two half-bearings, each having a smaller l/d ratio than the original. The groove divides the pressure-distribution curve into two lobes and reduces the minimum film thickness, but it has wide acceptance among lubrication engineers because such bearings carry more load without overheating.

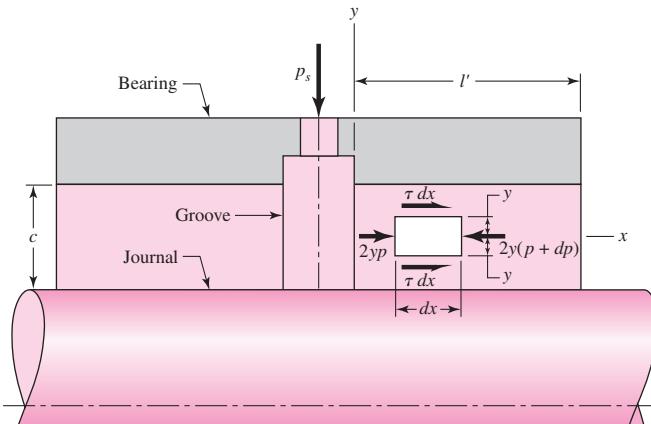
To set up a method of solution for oil flow, we shall assume a groove ample enough that the pressure drop in the groove itself is small. Initially we will neglect eccentricity and then apply a correction factor for this condition. The oil flow, then, is the amount that flows out of the two halves of the bearing in the direction of the concentric shaft. If we neglect the rotation of the shaft, the flow of the lubricant is caused by the supply

Figure 12-27

Centrally located full annular groove. (Courtesy of the Cleveland Graphite Bronze Company, Division of Clevite Corporation.)

**Figure 12-28**

Flow of lubricant from a pressure-fed bearing having a central annular groove.



pressure p_s , shown in Fig. 12-28. Laminar flow is assumed, with the pressure varying linearly from $p = p_s$ at $x = 0$, to $p = 0$ at $x = l'$. Consider the static equilibrium of an element of thickness dx , height $2y$, and unit depth. Note particularly that the origin of the reference system has been chosen at the midpoint of the clearance space and symmetry about the x axis is implied with the shear stresses τ being equal on the top and bottom surfaces. The equilibrium equation in the x direction is

$$-2y(p + dp) + 2yp + 2\tau dx = 0 \quad (a)$$

Expanding and canceling terms, we find that

$$\tau = y \frac{dp}{dx} \quad (b)$$

Newton's equation for viscous flow [Eq. (12-1)] is

$$\tau = \mu \frac{du}{dy} \quad (c)$$

Now eliminating τ from Eqs. (b) and (c) gives

$$\frac{du}{dy} = \frac{1}{\mu} \frac{dp}{dx} y \quad (d)$$

Treating dp/dx as a constant and integrating with respect to y gives

$$u = \frac{1}{2\mu} \frac{dp}{dx} y^2 + C_1 \quad (e)$$

At the boundaries, where $y = \pm c/2$, the velocity u is zero. Using one of these conditions in Eq. (e) gives

$$0 = \frac{1}{2\mu} \frac{dp}{dx} \left(\frac{c}{2}\right)^2 + C_1$$

or

$$C_1 = -\frac{c^2}{8\mu} \frac{dp}{dx}$$

Substituting this constant in Eq. (e) yields

$$u = \frac{1}{8\mu} \frac{dp}{dx} (4y^2 - c^2) \quad (f)$$

Assuming the pressure varies linearly from p_s to 0 at $x = 0$ to l' , respectively, the pressure can be written as

$$p = p_s - \frac{p_s}{l'} x \quad (g)$$

and therefore the pressure gradient is given by

$$\frac{dp}{dx} = -\frac{p_s}{l'} \quad (h)$$

We can now substitute Eq. (h) in Eq. (f) to get the relationship between the oil velocity and the coordinate y :

$$u = \frac{p_s}{8\mu l'} (c^2 - 4y^2) \quad (12-21)$$

Figure 12–29 shows a graph of this relation fitted into the clearance space c so that you can see how the velocity of the lubricant varies from the journal surface to the bearing surface. The distribution is parabolic, as shown, with the maximum velocity occurring at the center, where $y = 0$. The magnitude is, from Eq. (12–21),

$$u_{\max} = \frac{p_s c^2}{8\mu l'} \quad (i)$$

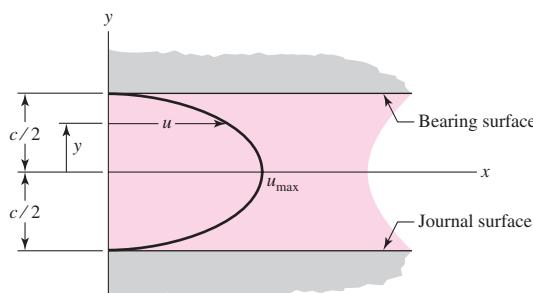
To consider eccentricity, as shown in Fig. 12–30, the film thickness is $h = c - e \cos \theta$. Substituting h for c in Eq. (i), with the average ordinate of a parabola being two-thirds the maximum, the average velocity at any angular position θ is

$$u_{av} = \frac{2}{3} \frac{p_s h^2}{8\mu l'} = \frac{p_s}{12\mu l'} (c - e \cos \theta)^2 \quad (j)$$

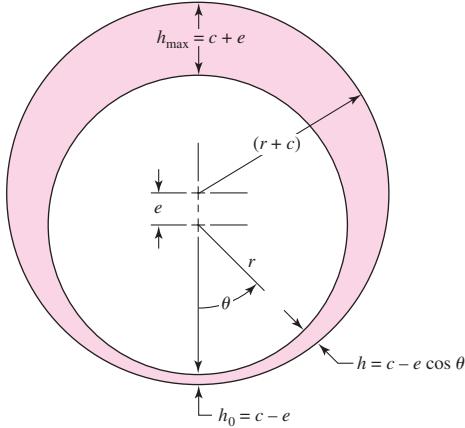
We still have a little further to go in this analysis; so please be patient. Now that we have an expression for the lubricant velocity, we can compute the amount of lubricant

Figure 12–29

Parabolic distribution of the lubricant velocity.



| Figure 12-30



that flows out both ends; the elemental side flow at any position θ (Fig. 12-30) is

$$dQ_s = 2u_{av} dA = 2u_{av}(rh d\theta) \quad (k)$$

where dA is the elemental area. Substituting u_{av} from Eq. (j) and (h) from Fig. 12-30 gives

$$dQ_s = \frac{p_s r}{6\mu l'} (c - e \cos \theta)^3 d\theta \quad (l)$$

Integrating around the bearing gives the total side flow as

$$Q_s = \int dQ_s = \frac{p_s r}{6\mu l'} \int_0^{2\pi} (c - e \cos \theta)^3 d\theta = \frac{p_s r}{6\mu l'} (2\pi c^3 + 3\pi ce^2)$$

Rearranging, with $\epsilon = e/c$, gives

$$Q_s = \frac{\pi p_s r c^3}{3\mu l'} (1 + 1.5\epsilon^2) \quad (12-22)$$

In analyzing the performance of pressure-fed bearings, the bearing length should be taken as l' , as defined in Fig. 12-28. The characteristic pressure in each of the two bearings that constitute the pressure-fed bearing assembly P is given by

$$P = \frac{W/2}{2rl'} = \frac{W}{4rl'} \quad (12-23)$$

The charts for flow variable and flow ratio (Figs. 12-19 and 12-20) do not apply to pressure-fed bearings. Also, the maximum film pressure given by Fig. 12-21 must be increased by the oil supply pressure p_s to obtain the total film pressure.

Since the oil flow has been increased by forced feed, Eq. (12-14) will give a temperature rise that is too high because the side flow carries away all the heat generated. The plumbing in a pressure-fed bearing is depicted schematically in Fig. 12-31. The oil leaves the sump at the externally maintained temperature T_s at the volumetric rate Q_s . The heat gain of the fluid passing through the bearing is

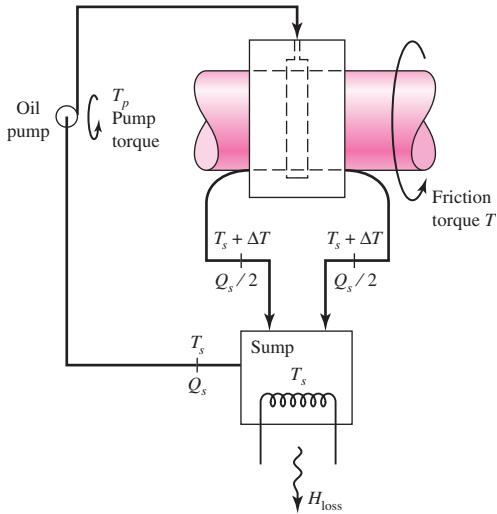
$$H_{\text{gain}} = 2 \rho C_p (Q_s/2) \Delta T = \rho C_p Q_s \Delta T \quad (m)$$

At steady state, the rate at which the journal does frictional work on the fluid film is

$$H_f = \frac{2\pi TN}{J} = \frac{2\pi f WrN}{J} = \frac{2\pi WNc}{J} \frac{fr}{c} \quad (n)$$

Figure 12-31

Pressure-fed centrally located full annular-groove journal bearing with external, coiled lubricant sump.



Equating the heat gain to the frictional work and solving for ΔT gives

$$\Delta T = \frac{2\pi W N c}{J \rho C_p Q_s} \frac{fr}{c} \quad (12-22)$$

Substituting Eq. (12-22) for Q_s in the equation for ΔT gives

$$\Delta T = \frac{2\pi}{J \rho C_p} W N c \frac{fr}{c} \frac{3\mu l'}{(1 + 1.5\epsilon^2)\pi p_s r c^3}$$

The Sommerfeld number may be expressed as

$$S = \left(\frac{r}{c}\right)^2 \frac{\mu N}{P} = \left(\frac{r}{c}\right)^2 \frac{4rl'\mu N}{W}$$

Solving for $\mu N l'$ in the Sommerfeld expression; substituting in the ΔT expression; and using $J = 9336 \text{ lbf} \cdot \text{in/Btu}$, $\rho = 0.0311 \text{ lbm/in}^3$, and $C_p = 0.42 \text{ Btu/(lbm} \cdot {^\circ}\text{F)}$, we find

$$\Delta T_F = \frac{3(fr/c)SW^2}{2J\rho C_p p_s r^4} \frac{1}{(1 + 1.5\epsilon^2)} = \frac{0.0123(fr/c)SW^2}{(1 + 1.5\epsilon^2)p_s r^4} \quad (12-24)$$

where ΔT_F is ΔT in ${}^\circ\text{F}$. The corresponding equation in SI units uses the bearing load W in kN, lubricant supply pressure p_s in kPa, and the journal radius r in mm:

$$\Delta T_C = \frac{978(10^6)}{1 + 1.5\epsilon^2} \frac{(fr/c)SW^2}{p_s r^4} \quad (12-25)$$

An analysis example of a pressure-fed bearing will be useful.

EXAMPLE 12-6

A circumferential-groove pressure-fed bearing is lubricated with SAE grade 20 oil supplied at a gauge pressure of 30 psi. The journal diameter d_j is 1.750 in, with a unilateral tolerance of -0.002 in. The central circumferential bushing has a diameter d_b of 1.753 in, with a unilateral tolerance of $+0.004$ in. The l'/d ratio of the two “half-bearings” that constitute the complete pressure-fed bearing is 1/2. The journal angular speed

is 3000 rev/min, or 50 rev/s, and the radial steady load is 900 lbf. The external sump is maintained at 120°F as long as the necessary heat transfer does not exceed 800 Btu/h.

(a) Find the steady-state average film temperature.

(b) Compare h_0 , T_{\max} , and P_{st} with the Trumpler criteria.

(c) Estimate the volumetric side flow Q_s , the heat loss rate H_{loss} , and the parasitic friction torque.

Solution (a)

$$r = \frac{d_j}{2} = \frac{1.750}{2} = 0.875 \text{ in}$$

$$c_{\min} = \frac{(d_b)_{\min} - (d_j)_{\max}}{2} = \frac{1.753 - 1.750}{2} = 0.0015 \text{ in}$$

Since $l'/d = 1/2$, $l' = d/2 = r = 0.875$ in. Then the pressure due to the load is

$$P = \frac{W}{4rl'} = \frac{900}{4(0.875)0.875} = 294 \text{ psi}$$

The Sommerfeld number S can be expressed as

$$S = \left(\frac{r}{c}\right)^2 \frac{\mu N}{P} = \left(\frac{0.875}{0.0015}\right)^2 \frac{\mu'}{(10^6)} \frac{50}{294} = 0.0579\mu' \quad (1)$$

We will use a tabulation method to find the average film temperature. The first trial average film temperature \bar{T}_f will be 170°F. Using the Seireg curve fit of Table 12–1, we obtain

$$\mu' = 0.0136 \exp[1271.6/(170 + 95)] = 1.650 \text{ } \mu\text{reyn}$$

From Eq. (1)

$$S = 0.0579\mu' = 0.0579(1.650) = 0.0955$$

From Fig. (12–18), $fr/c = 3.3$, and from Fig. (12–16), $\epsilon = 0.80$. From Eq. (12–24),

$$\Delta T_F = \frac{0.0123(3.3)0.0955(900^2)}{[1 + 1.5(0.80)^2]30(0.875^4)} = 91.1^\circ\text{F}$$

$$T_{\text{av}} = T_s + \frac{\Delta T}{2} = 120 + \frac{91.1}{2} = 165.6^\circ\text{F}$$

We form a table, adding a second line with $\bar{T}_f = 168.5^\circ\text{F}$:

Trial \bar{T}_f	μ'	S	fr/c	ϵ	ΔT_F	T_{av}
170	1.65	0.0955	3.3	0.800	91.1	165.6
168.5	1.693	0.0980	3.39	0.792	97.1	168.5

If the iteration had not closed, one could plot trial \bar{T}_f against resulting T_{av} and draw a straight line between them, the intersection with a $\bar{T}_f = T_{\text{av}}$ line defining the new trial \bar{T}_f .

Answer The result of this tabulation is $\bar{T}_f = 168.5$, $\Delta T_F = 97.1^\circ\text{F}$, and $T_{\max} = 120 + 97.1 = 217.1^\circ\text{F}$

(b) Since $h_0 = (1 - \epsilon)c$,

$$h_0 = (1 - 0.792)0.0015 = 0.000312 \text{ in}$$

The required four Trumpler criteria, from “Significant Angular Speed” in Sec. 12–7 are

$$h_0 \geq 0.0002 + 0.00004(1.750) = 0.000270 \text{ in} \quad (\text{OK})$$

Answer $T_{\max} = T_s + \Delta T = 120 + 97.1 = 217.1^\circ\text{F}$ (OK)

$$P_{st} = \frac{W_{st}}{4rl'} = \frac{900}{4(0.875)0.875} = 294 \text{ psi} \quad (\text{OK})$$

The factor of safety on the load is approximately unity. (Not OK.)

(c) From Eq. (12–22),

Answer $Q_s = \frac{\pi(30)0.875(0.0015)^3}{3(1.693)10^{-6}(0.875)} [1 + 1.5(0.80)^2] = 0.123 \text{ in}^3/\text{s}$

$$H_{\text{loss}} = \rho C_p Q_s \Delta T = 0.0311(0.42)0.123(97.1) = 0.156 \text{ Btu/s}$$

or 562 Btu/h or 0.221 hp. The parasitic friction torque T is

Answer $T = fWr = \frac{fr}{c} Wc = 3.39(900)0.0015 = 4.58 \text{ lbf} \cdot \text{in}$

12–12 Loads and Materials

Some help in choosing unit loads and bearing materials is afforded by Tables 12–5 and 12–6. Since the diameter and length of a bearing depend upon the unit load, these tables will help the designer to establish a starting point in the design.

Table 12–5

Range of Unit Loads in Current Use for Sleeve Bearings

Application	Unit Load	
	psi	MPa
Diesel engines:		
Main bearings	900–1700	6–12
Crankpin	1150–2300	8–15
Wristpin	2000–2300	14–15
Electric motors	120–250	0.8–1.5
Steam turbines	120–250	0.8–1.5
Gear reducers	120–250	0.8–1.5
Automotive engines:		
Main bearings	600–750	4–5
Crankpin	1700–2300	10–15
Air compressors:		
Main bearings	140–280	1–2
Crankpin	280–500	2–4
Centrifugal pumps	100–180	0.6–1.2

The length-diameter ratio l/d of a bearing depends upon whether it is expected to run under thin-film-lubrication conditions. A long bearing (large l/d ratio) reduces the coefficient of friction and the side flow of oil and therefore is desirable where thin-film or boundary-value lubrication is present. On the other hand, where forced-feed or positive lubrication is present, the l/d ratio should be relatively small. The short bearing length results in a greater flow of oil out of the ends, thus keeping the bearing cooler. Current practice is to use an l/d ratio of about unity, in general, and then to increase this ratio if thin-film lubrication is likely to occur and to decrease it for thick-film lubrication or high temperatures. If shaft deflection is likely to be severe, a short bearing should be used to prevent metal-to-metal contact at the ends of the bearings.

You should always consider the use of a partial bearing if high temperatures are a problem, because relieving the non-load-bearing area of a bearing can very substantially reduce the heat generated.

The two conflicting requirements of a good bearing material are that it must have a satisfactory compressive and fatigue strength to resist the externally applied loads and that it must be soft and have a low melting point and a low modulus of elasticity. The second set of requirements is necessary to permit the material to wear or break in, since the material can then conform to slight irregularities and absorb and release foreign particles. The resistance to wear and the coefficient of friction are also important because all bearings must operate, at least for part of the time, with thin-film or boundary lubrication.

Additional considerations in the selection of a good bearing material are its ability to resist corrosion and, of course, the cost of producing the bearing. Some of the commonly used materials are listed in Table 12–6, together with their composition and characteristics.

Bearing life can be increased very substantially by depositing a layer of babbitt, or other white metal, in thicknesses from 0.001 to 0.014 in over steel backup material. In fact, a copper-lead layer on steel to provide strength, combined with a babbitt overlay to enhance surface conformability and corrosion resistance, makes an excellent bearing.

Small bushings and thrust collars are often expected to run with thin-film or boundary lubrication. When this is the case, improvements over a solid bearing material can

Table 12–6

Some Characteristics
of Bearing Alloys

Alloy Name	Thickness, in	SAE Number	Clearance Ratio r/c	Load Capacity	Corrosion Resistance
Tin-base babbitt	0.022	12	600–1000	1.0	Excellent
Lead-base babbitt	0.022	15	600–1000	1.2	Very good
Tin-base babbitt	0.004	12	600–1000	1.5	Excellent
Lead-base babbitt	0.004	15	600–1000	1.5	Very good
Leaded bronze	Solid	792	500–1000	3.3	Very good
Copper-lead	0.022	480	500–1000	1.9	Good
Aluminum alloy	Solid		400–500	3.0	Excellent
Silver plus overlay	0.013	17P	600–1000	4.1	Excellent
Cadmium (1.5% Ni)	0.022	18	400–500	1.3	Good
Trimetal 88*				4.1	Excellent
Trimetal 77†				4.1	Very good

*This is a 0.008-in layer of copper-lead on a steel back plus 0.001 in of tin-base babbitt.

†This is a 0.013-in layer of copper-lead on a steel back plus 0.001 in of lead-base babbitt.

be made to add significantly to the life. A powder-metallurgy bushing is porous and permits the oil to penetrate into the bushing material. Sometimes such a bushing may be enclosed by oil-soaked material to provide additional storage space. Bearings are frequently ball-indented to provide small basins for the storage of lubricant while the journal is at rest. This supplies some lubrication during starting. Another method of reducing friction is to indent the bearing wall and to fill the indentations with graphite.

With all these tentative decisions made, a lubricant can be selected and the hydrodynamic analysis made as already presented. The values of the various performance parameters, if plotted as in Fig. 12-25, for example, will then indicate whether a satisfactory design has been achieved or additional iterations are necessary.

12-13 Bearing Types

A bearing may be as simple as a hole machined into a cast-iron machine member. It may still be simple yet require detailed design procedures, as, for example, the two-piece grooved pressure-fed connecting-rod bearing in an automotive engine. Or it may be as elaborate as the large water-cooled, ring-oiled bearings with built-in reservoirs used on heavy machinery.

Figure 12-32 shows two types of bushings. The solid bushing is made by casting, by drawing and machining, or by using a powder-metallurgy process. The lined bushing is usually a split type. In one method of manufacture the molten lining material is cast continuously on thin strip steel. The babbitted strip is then processed through presses, shavers, and broaches, resulting in a lined bushing. Any type of grooving may be cut into the bushings. Bushings are assembled as a press fit and finished by boring, reaming, or burnishing.

Flanged and straight two-piece bearings are shown in Fig. 12-33. These are available in many sizes in both thick- and thin-wall types, with or without lining material. A locking lug positions the bearing and effectively prevents axial or rotational movement of the bearing in the housing.

Some typical groove patterns are shown in Fig. 12-34. In general, the lubricant may be brought in from the end of the bushing, through the shaft, or through the bushing. The flow may be intermittent or continuous. The preferred practice is to bring the

Figure 12-32

Sleeve bushings.

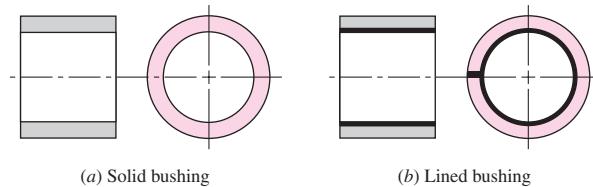


Figure 12-33

Two-piece bushings.

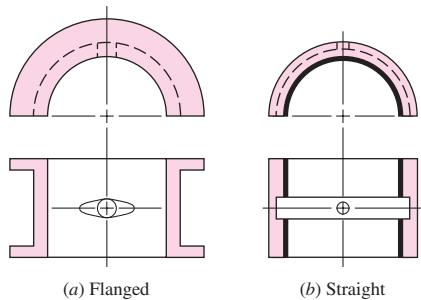
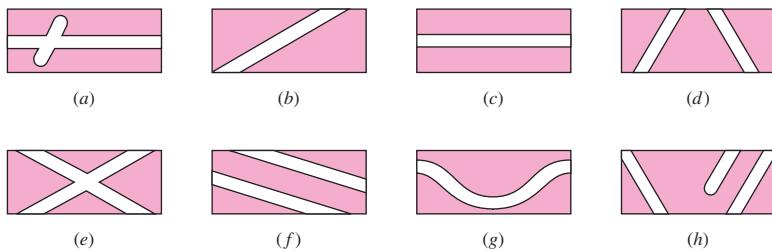


Figure 12-34

Developed views of typical groove patterns. (Courtesy of the Cleveland Graphite Bronze Company, Division of Clevite Corporation.)



oil in at the center of the bushing so that it will flow out both ends, thus increasing the flow and cooling action.

12-14 Thrust Bearings

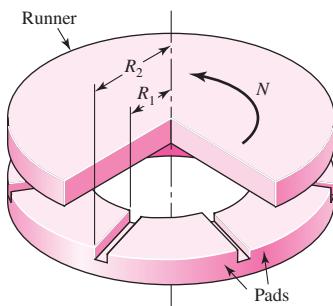
This chapter is devoted to the study of the mechanics of lubrication and its application to the design and analysis of journal bearings. The design and analysis of thrust bearings is an important application of lubrication theory, too. A detailed study of thrust bearings is not included here, because it would not contribute anything significantly different and because of space limitations. Having studied this chapter, you should experience no difficulty in reading the literature on thrust bearings and applying that knowledge to actual design situations.¹¹

Figure 12-35 shows a fixed-pad thrust bearing consisting essentially of a runner sliding over a fixed pad. The lubricant is brought into the radial grooves and pumped into the wedge-shaped space by the motion of the runner. Full-film, or hydrodynamic, lubrication is obtained if the speed of the runner is continuous and sufficiently high, if the lubricant has the correct viscosity, and if it is supplied in sufficient quantity. Figure 12-36 provides a picture of the pressure distribution under conditions of full-film lubrication.

We should note that bearings are frequently made with a flange, as shown in Fig. 12-37. The flange positions the bearing in the housing and also takes a thrust load. Even when it is grooved, however, and has adequate lubrication, such an arrangement is not theoretically a hydrodynamically lubricated thrust bearing. The reason for this is that the clearance space is not wedge-shaped but has a uniform thickness. Similar reasoning would apply to various designs of thrust washers.

Figure 12-35

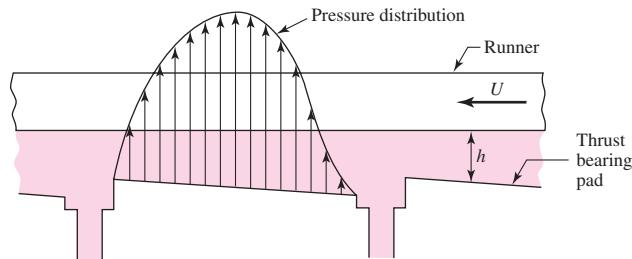
Fixed-pad thrust bearing. (Courtesy of Westinghouse Electric Corporation.)



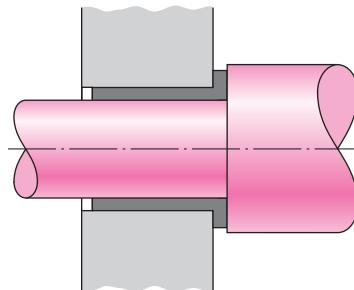
¹¹Harry C. Rippel, *Cast Bronze Thrust Bearing Design Manual*, International Copper Research Association, Inc., 825 Third Ave., New York, NY 10022, 1967. CBBI, 14600 Detroit Ave., Cleveland, OH, 44107, 1967.

Figure 12-36

Pressure distribution of lubricant in a thrust bearing.
(Courtesy of Copper Research Corporation.)

**Figure 12-37**

Flanged sleeve bearing takes both radial and thrust loads.



12-15

Boundary-Lubricated Bearings

When two surfaces slide relative to each other with only a partial lubricant film between them, *boundary lubrication* is said to exist. Boundary- or thin-film lubrication occurs in hydrodynamically lubricated bearings when they are starting or stopping, when the load increases, when the supply of lubricant decreases, or whenever other operating changes happen to occur. There are, of course, a very large number of cases in design in which boundary-lubricated bearings must be used because of the type of application or the competitive situation.

The coefficient of friction for boundary-lubricated surfaces may be greatly decreased by the use of animal or vegetable oils mixed with the mineral oil or grease. Fatty acids, such as stearic acid, palmitic acid, or oleic acid, or several of these, which occur in animal and vegetable fats, are called *oiliness agents*. These acids appear to reduce friction, either because of their strong affinity for certain metallic surfaces or because they form a soap film that binds itself to the metallic surfaces by a chemical reaction. Thus the fatty-acid molecules bind themselves to the journal and bearing surfaces with such great strength that the metallic asperities of the rubbing metals do not weld or shear.

Fatty acids will break down at temperatures of 250°F or more, causing increased friction and wear in thin-film-lubricated bearings. In such cases the *extreme-pressure*, or EP, lubricants may be mixed with the fatty-acid lubricant. These are composed of chemicals such as chlorinated esters or tricresyl phosphate, which form an organic film between the rubbing surfaces. Though the EP lubricants make it possible to operate at higher temperatures, there is the added possibility of excessive chemical corrosion of the sliding surfaces.

When a bearing operates partly under hydrodynamic conditions and partly under dry or thin-film conditions, a *mixed-film lubrication* exists. If the lubricant is supplied by hand oiling, by drop or mechanical feed, or by wick feed, for example, the bearing is

operating under mixed-film conditions. In addition to occurring with a scarcity of lubricant, mixed-film conditions may be present when

- The viscosity is too low.
- The bearing speed is too low.
- The bearing is overloaded.
- The clearance is too tight.
- Journal and bearing are not properly aligned.

Relative motion between surfaces in contact in the presence of a lubricant is called *boundary lubrication*. This condition is present in hydrodynamic film bearings during starting, stopping, overloading, or lubricant deficiency. Some bearings are boundary lubricated (or dry) at all times. To signal this an adjective is placed before the word “bearing.” Commonly applied adjectives (to name a few) are thin-film, boundary friction, Oilite, Oiles, and bushed-pin. The applications include situations in which thick film will not develop and there are low journal speed, oscillating journal, padded slides, light loads, and lifetime lubrication. The characteristics include considerable friction, ability to tolerate expected wear without losing function, and light loading. Such bearings are limited by lubricant temperature, speed, pressure, galling, and cumulative wear. Table 12–7 gives some properties of a range of bushing materials.

Linear Sliding Wear

Consider the sliding block depicted in Fig. 12–38, moving along a plate with contact pressure P' acting over area A , in the presence of a coefficient of sliding friction f_s . The linear measure of wear w is expressed in inches or millimeters. The work done by force $f_s P A$ during displacement S is $f_s P A S$ or $f_s P A V t$, where V is the sliding velocity and t is time. The material volume removed due to wear is wA and is proportional to the work done, that is, $wA \propto f_s P A V t$, or

$$wA = K P A V t$$

Table 12–7

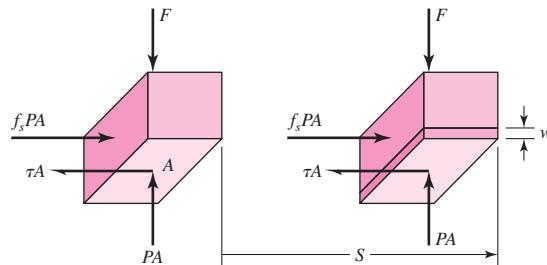
Some Materials for Boundary-Lubricated Bearings and Their Operating Limits

Material	Maximum Load, psi	Maximum Temperature, °F	Maximum Speed, fpm	Maximum PV Value*
Cast bronze	4 500	325	1 500	50 000
Porous bronze	4 500	150	1 500	50 000
Porous iron	8 000	150	800	50 000
Phenolics	6 000	200	2 500	15 000
Nylon	1 000	200	1 000	3 000
Teflon	500	500	100	1 000
Reinforced Teflon	2 500	500	1 000	10 000
Teflon fabric	60 000	500	50	25 000
Delrin	1 000	180	1 000	3 000
Carbon-graphite	600	750	2 500	15 000
Rubber	50	150	4 000	
Wood	2 000	150	2 000	15 000

* P = load, psi; V = speed, fpm.

Figure 12-38

Sliding block subjected to wear.

**Table 12-8**

Wear Factors in U.S. Customary Units*

Source: Oiles America Corp., Plymouth, MI 48170.

Bushing Material	Wear Factor K	Limiting PV
Oiles 800	$3(10^{-10})$	18 000
Oiles 500	$0.6(10^{-10})$	46 700
Polyacetal copolymer	$50(10^{-10})$	5 000
Polyacetal homopolymer	$60(10^{-10})$	3 000
66 nylon	$200(10^{-10})$	2 000
66 nylon + 15% PTFE	$13(10^{-10})$	7 000
+ 15% PTFE + 30% glass	$16(10^{-10})$	10 000
+ 2.5% MoS ₂	$200(10^{-10})$	2 000
6 nylon	$200(10^{-10})$	2 000
Polycarbonate + 15% PTFE	$75(10^{-10})$	7 000
Sintered bronze	$102(10^{-10})$	8 500
Phenol + 25% glass fiber	$8(10^{-10})$	11 500

*dim[K] = in³ · min/(lbf · ft · h), dim [PV] = psi · ft/min.

Table 12-9

Coefficients of Friction

Source: Oiles America Corp., Plymouth, MI 48170.

Type	Bearing	f _s
Plastic	Oiles 80	0.05
Composite	Drymet ST Toughmet	0.03 0.05
Met	Cermet M Oiles 2000 Oiles 300 Oiles 500SP	0.05 0.03 0.03 0.03

where K is the proportionality factor, which includes f_s , and is determined from laboratory testing. The linear wear is then expressed as

$$w = K P V t \quad (12-26)$$

In US customary units, P is expressed in psi, V in fpm (i.e., ft/min), and t in hours. This makes the units of K in in³ · min/(lbf · ft · h). SI units commonly used for K are cm³ · min/(kgf · m · h), where 1 kgf = 9.806 N. Tables 12-8 and 12-9 give some wear factors and coefficients of friction from one manufacturer.

Table 12-10Motion-Related Factor f_1

Mode of Motion	Characteristic Pressure P , psi		Velocity V , ft/min	f_1^*
Rotary	720 or less	720 or less	3.3 or less	1.0
		3.3–33	3.3–33	1.0–1.3
		33–100	33–100	1.3–1.8
	720–3600	720–3600	3.3 or less	1.5
		3.3–33	3.3–33	1.5–2.0
		33–100	33–100	2.0–2.7
Oscillatory	720 or less	>30°	3.3 or less	1.3
		3.3–100	3.3–100	1.3–2.4
		<30°	3.3 or less	2.0
	720–3600	720–3600	3.3–100	2.0
		>30°	3.3 or less	2.0
		<30°	3.3 or less	3.0
Reciprocating	720 or less	33–100	3.3–100	3.0–4.8
		33 or less	33 or less	1.5
	720–3600	33–100	33–100	1.5–3.8
		33 or less	33 or less	2.0
		33–100	33–100	2.0–7.5

*Values of f_1 based on results over an extended period of time on automotive manufacturing machinery.**Table 12-11**Environmental Factor f_2 Source: Oiles America Corp.,
Plymouth, MI 48170.

Ambient Temperature, °F	Foreign Matter	f_2
140 or lower	No	1.0
140 or lower	Yes	3.0–6.0
140–210	No	3.0–6.0
140–210	Yes	6.0–12.0

It is useful to include a modifying factor f_1 depending on motion type, load, and speed and an environment factor f_2 to account for temperature and cleanliness conditions (see Tables 12-10 and 12-11). These factors account for departures from the laboratory conditions under which K was measured. Equation (12-26) can now be written as

$$w = f_1 f_2 K P V t \quad (12-27)$$

Wear, then, is proportional to PV , material property K , operating conditions f_1 and f_2 , and time t .

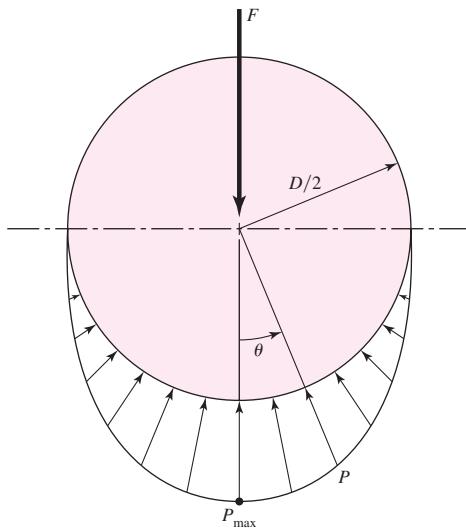
Bushing Wear

Consider a pin of diameter D , rotating at speed N , in a bushing of length L , and supporting a stationary radial load F . The nominal pressure P is given by

$$P = \frac{F}{DL} \quad (12-28)$$

Figure 12-39

Pressure distribution on a boundary-lubricated bushing.



and if N is in rev/min and D is in inches, velocity in ft/min is given by

$$V = \frac{\pi DN}{12} \quad (12-29)$$

Thus PV , in $\text{psi} \cdot \text{ft}/\text{min}$, is

$$PV = \frac{F}{DL} \frac{\pi DN}{12} = \frac{\pi}{12} \frac{FN}{L} \quad (12-30)$$

Note the independence of PV from the journal diameter D .

A time-wear equation similar to Eq. (12-27) can be written. However, before doing so, it is important to note that Eq. (12-28) provides the nominal value of P . Figure 12-39 provides a more accurate representation of the pressure distribution, which can be written as

$$p = P_{\max} \cos \theta \quad -\frac{\pi}{2} \leq \theta \leq \frac{\pi}{2}$$

The vertical component of $p dA$ is $p dA \cos \theta = [pL(D/2) d\theta] \cos \theta = P_{\max}(DL/2) \cos^2 \theta d\theta$. Integrating this from $\theta = -\pi/2$ to $\pi/2$ yields F . Thus,

$$\int_{-\pi/2}^{\pi/2} P_{\max} \left(\frac{DL}{2} \right) \cos^2 \theta d\theta = \frac{\pi}{4} P_{\max} DL = F$$

or

$$P_{\max} = \frac{4}{\pi} \frac{F}{DL} \quad (12-31)$$

Substituting V from Eq. (12-29) and P_{\max} for P from Eq. (12-31) into Eq. (12-27) gives

$$w = f_1 f_2 K \frac{4}{\pi} \frac{F}{DL} \frac{\pi DN t}{12} = \frac{f_1 f_2 K F N t}{3L} \quad (12-32)$$

In designing a bushing, because of various trade-offs it is recommended that the length/diameter ratio be in the range

$$0.5 \leq L/D \leq 2 \quad (12-33)$$

EXAMPLE 12-7

An Oiles SP 500 alloy brass bushing is 1 in long with a 1-in bore and operates in a clean environment at 70°F. The allowable wear without loss of function is 0.005 in. The radial load is 700 lbf. The peripheral velocity is 33 ft/min. Estimate the number of revolutions for radial wear to be 0.005 in. See Fig. 12-40 and Table 12-12 from the manufacturer.

Solution

From Table 12-8, $K = 0.6(10^{-10}) \text{ in}^3 \cdot \text{min}/(\text{lbf} \cdot \text{ft} \cdot \text{h})$; Tables 12-10 and 12-11, $f_1 = 1.3$, $f_2 = 1$; and Table 12-12, $PV = 46\ 700 \text{ psi} \cdot \text{ft}/\text{min}$, $P_{\max} = 3560 \text{ psi}$, $V_{\max} = 100 \text{ ft}/\text{min}$. From Eqs. (12-31), (12-29), and (12-30),

$$P_{\max} = \frac{4}{\pi} \frac{F}{DL} = \frac{4}{\pi} \frac{700}{(1)(1)} = 891 \text{ psi} < 3560 \text{ psi} \quad (\text{OK})$$

$$P = \frac{F}{DL} = \frac{700}{(1)(1)} = 700 \text{ psi}$$

$$V = 33 \text{ ft}/\text{min} < 100 \text{ ft}/\text{min} \quad (\text{OK})$$

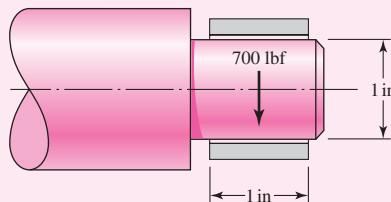
$$PV = 700(33) = 23\ 100 \text{ psi} \cdot \text{ft}/\text{min} < 46\ 700 \text{ psi} \cdot \text{ft}/\text{min} \quad (\text{OK})$$

Equation (12-32) with Eq. (12-29) is

$$w = f_1 f_2 K \frac{4}{\pi} \frac{F}{DL} \frac{\pi D N t}{12} = f_1 f_2 K \frac{4}{\pi} \frac{F}{DL} V t$$

Figure 12-40

Journal/bushing for Ex. 12-7.

**Table 12-12**

Oiles 500 SP (SPBN · SPWN) Service Range and Properties

Source: Oiles America Corp., Plymouth, MI 48170.

Service Range	Units	Allowable
Characteristic pressure P_{\max}	psi	<3560
Velocity V_{\max}	ft/min	<100
PV product	(psi)/(ft/min)	<46 700
Temperature T	°F	<300
Properties	Test Method, Units	Value
Tensile strength	(ASTM E8) psi	>110 000
Elongation	(ASTM E8) %	>12
Compressive strength	(ASTM E9) psi	49 770
Brinell hardness	(ASTM E10) HB	>210
Coefficient of thermal expansion	(10^{-5}) °C	>1.6
Specific gravity		8.2

Solving for t gives

$$t = \frac{\pi DLw}{4f_1 f_2 KVF} = \frac{\pi(1)(1)0.005}{4(1.3)(1)0.6(10^{-10})33(700)} = 2180 \text{ h} = 130\,770 \text{ min}$$

The rotational speed is

$$N = \frac{12V}{\pi D} = \frac{12(33)}{\pi(1)} = 126 \text{ r/min}$$

Answer

$$\text{Cycles} = Nt = 126(130\,770) = 16.5(10^6) \text{ rev}$$

Temperature Rise

At steady state, the rate at which work is done against bearing friction equals the rate at which heat is transferred from the bearing housing to the surroundings by convection and radiation. The rate of heat generation in Btu/h is given by $f_s FV/J$, or

$$H_{\text{gen}} = \frac{f_s F(\pi D)(60N)}{12J} = \frac{5\pi f_s FDN}{J} \quad (12-34)$$

where N is journal speed in rev/min and $J = 778 \text{ ft} \cdot \text{lbf/Btu}$. The rate at which heat is transferred to the surroundings, in Btu/h, is

$$H_{\text{loss}} = \dot{h}_{\text{CR}} A \Delta T = \dot{h}_{\text{CR}} A (T_b - T_\infty) = \frac{\dot{h}_{\text{CR}} A}{2} (T_f - T_\infty) \quad (12-35)$$

where A = housing surface area, ft^2

\dot{h}_{CR} = overall combined coefficient of heat transfer, $\text{Btu}/(\text{h} \cdot \text{ft}^2 \cdot {}^\circ\text{F})$

T_b = housing metal temperature, ${}^\circ\text{F}$

T_f = lubricant temperature, ${}^\circ\text{F}$

The empirical observation that T_b is about midway between T_f and T_∞ has been incorporated in Eq. (12-35). Equating Eqs. (12-34) and (12-35) gives

$$T_f = T_\infty + \frac{10\pi f_s FDN}{J\dot{h}_{\text{CR}}A} \quad (12-36)$$

Although this equation seems to indicate the temperature rise $T_f - T_\infty$ is independent of length L , the housing surface area generally is a function of L . The housing surface area can be initially estimated, and as tuning of the design proceeds, improved results will converge. If the bushing is to be housed in a pillow block, the surface area can be roughly estimated from

$$A \doteq \frac{2\pi DL}{144} \quad (12-37)$$

Substituting Eq. (12-37) into Eq. (12-36) gives

$$T_f \doteq T_\infty + \frac{10\pi f_s FDN}{J\dot{h}_{\text{CR}}(2\pi DL/144)} = T_\infty + \frac{720f_s FN}{J\dot{h}_{\text{CR}}L} \quad (12-38)$$

EXAMPLE 12-8

Choose an Oiles 500 bushing to give a maximum wear of 0.001 in for 800 h of use with a 300 rev/min journal and 50 lbf radial load. Use $\bar{h}_{CR} = 2.7 \text{ Btu}/(\text{h} \cdot \text{ft}^2 \cdot {}^\circ\text{F})$, $T_{max} = 300^\circ\text{F}$, $f_s = 0.03$, and a design factor $n_d = 2$. Table 12-13 lists the available bushing sizes from the manufacturer.

Solution

With a design factor n_d , substitute $n_d F$ for F . First, estimate the bushing length using Eq. (12-32) with $f_1 = f_2 = 1$, and $K = 0.6(10^{-10})$ from Table 12-8:

$$L = \frac{f_1 f_2 K n_d F N t}{3w} = \frac{1(1)0.6(10^{-10})2(50)300(800)}{3(0.001)} = 0.48 \text{ in} \quad (1)$$

From Eq. (12-38) with $f_s = 0.03$ from Table 12-9, $\bar{h}_{CR} = 2.7 \text{ Btu}/(\text{h} \cdot \text{ft}^2 \cdot {}^\circ\text{F})$, and $n_d F$ for F ,

$$L \doteq \frac{720 f_s n_d F N}{J \bar{h}_{CR} (T_f - T_\infty)} = \frac{720(0.03)2(50)300}{778(2.7)(300 - 70)} = 1.34 \text{ in}$$

The two results bracket L such that $0.48 \leq L \leq 1.34$ in. As a start let $L = 1$ in. From Table 12-13, we select $D = 1$ in from the midrange of available bushings.

Table 12-13

Available Bushing Sizes
(in inches) of One
Manufacturer*

ID	OD	$\frac{1}{2}$	$\frac{5}{8}$	$\frac{3}{4}$	$\frac{7}{8}$	1	$1\frac{1}{4}$	$1\frac{1}{2}$	$1\frac{3}{4}$	2	$2\frac{1}{2}$	3	$3\frac{1}{2}$	4	5	<i>L</i>
$\frac{1}{2}$	$\frac{3}{4}$	•	•	•	•	•										
$\frac{5}{8}$	$\frac{7}{8}$		•	•		•			•							
$\frac{3}{4}$	$1\frac{1}{8}$		•	•		•			•							
$\frac{7}{8}$	$1\frac{1}{4}$			•		•	•	•	•							
1	$1\frac{3}{8}$		•		•	•	•	•	•	•	•	•				
1	$1\frac{1}{2}$		•		•		•		•		•					
$1\frac{1}{4}$	$1\frac{5}{8}$			•	•	•	•	•	•	•	•					
$1\frac{1}{2}$	2			•	•	•	•	•	•	•	•					
$1\frac{3}{4}$	$2\frac{1}{4}$				•	•	•	•	•	•	•	•	•	•	•	
2	$2\frac{1}{2}$					•			•	•	•	•				
$2\frac{1}{4}$	$2\frac{3}{4}$						•		•	•	•	•				
$2\frac{1}{2}$	3						•		•		•					
$2\frac{3}{4}$	$3\frac{3}{8}$							•		•	•	•				
3	$3\frac{5}{8}$								•	•	•	•	•			
$3\frac{1}{2}$	$4\frac{1}{8}$								•		•					
4	$4\frac{3}{4}$									•	•					
$4\frac{1}{2}$	$5\frac{3}{8}$										•	•	•			
5	6										•	•	•			

*In a display such as this a manufacturer is likely to show catalog numbers where the • appears.

Trial 1: $D = L = 1$ in.

$$\text{Eq. (12-31): } P_{\max} = \frac{4}{\pi} \frac{n_d F}{DL} = \frac{4}{\pi} \frac{2(50)}{1(1)} = 127 \text{ psi} < 3560 \text{ psi} \quad (\text{OK})$$

$$P = \frac{n_d F}{DL} = \frac{2(50)}{1(1)} = 100 \text{ psi}$$

$$\text{Eq. (12-29): } V = \frac{\pi DN}{12} = \frac{\pi(1)300}{12} = 78.5 \text{ ft/min} < 100 \text{ ft/min} \quad (\text{OK})$$

$$PV = 100(78.5) = 7850 \text{ psi} \cdot \text{ft/min} < 46700 \text{ psi} \cdot \text{ft/min} \quad (\text{OK})$$

From Table 12-9,

V	f ₁
33	1.3
78.5	$f_1 \Rightarrow f_1 = 1.64$
100	1.8

Our second estimate is $L \geq 0.48(1.64) = 0.787$ in. From Table 12-13, there is not much available for $L = \frac{7}{8}$ in. So staying with $L = 1$ in, try $D = \frac{1}{2}$ in.

Trial 2: $D = 0.5$ in, $L = 1$ in.

$$P_{\max} = \frac{4}{\pi} \frac{n_d F}{DL} = \frac{4}{\pi} \frac{2(50)}{0.5(1)} = 255 \text{ psi} < 3560 \text{ psi} \quad (\text{OK})$$

$$P = \frac{n_d F}{DL} = \frac{2(50)}{0.5(1)} = 200 \text{ psi}$$

$$V = \frac{\pi DN}{12} = \frac{\pi(0.5)300}{12} = 39.3 \text{ ft/min} < 100 \text{ ft/min} \quad (\text{OK})$$

Note that PV is not a function of D , and since we did not change L , PV will remain the same:

$$PV = 200(39.3) = 7860 \text{ psi} \cdot \text{ft/min} < 46700 \text{ psi} \cdot \text{ft/min} \quad (\text{OK})$$

From Table 12-9, $f_1 = 1.34$, $L \geq 1.34(0.48) = 0.643$ in. There are many $\frac{3}{4}$ -in bushings to select from. The smallest diameter in Table 12-13 is $D = \frac{1}{2}$ in. This gives an L/D ratio of 1.5, which is acceptable according to Eq. (12-33).

Trial 3: $D = 0.5$ in, $L = 0.75$ in. From trial 2, $V = 39.3$ ft/min does not change.

$$P_{\max} = \frac{4}{\pi} \frac{n_d F}{DL} = \frac{4}{\pi} \frac{2(50)}{0.5(0.75)} = 340 \text{ psi} < 3560 \text{ psi} \quad (\text{OK})$$

$$P = \frac{n_d F}{DL} = \frac{2(50)}{0.5(0.75)} = 267 \text{ psi}$$

$$PV = 267(39.3) = 10490 \text{ psi} \cdot \text{ft/min} < 46700 \text{ psi} \cdot \text{ft/min} \quad (\text{OK})$$

Answer

Select any of the bushings from the trials, where the optimum, from trial 3, is $D = \frac{1}{2}$ in and $L = \frac{3}{4}$ in. Other factors may enter in the overall design that make the other bushings more appropriate.

PROBLEMS

- 12-1** A full journal bearing has a journal diameter of 25 mm, with a unilateral tolerance of -0.03 mm. The bushing bore has a diameter of 25.03 mm and a unilateral tolerance of 0.04 mm. The l/d ratio is $1/2$. The load is 1.2 kN and the journal runs at 1100 rev/min. If the average viscosity is 55 mPa · s, find the minimum film thickness, the power loss, and the side flow for the minimum clearance assembly.
- 12-2** A full journal bearing has a journal diameter of 32 mm, with a unilateral tolerance of -0.012 mm. The bushing bore has a diameter of 32.05 mm and a unilateral tolerance of 0.032 mm. The bearing is 64 mm long. The journal load is 1.75 kN and it runs at a speed of 900 rev/min. Using an average viscosity of 55 mPa · s find the minimum film thickness, the maximum film pressure, and the total oil-flow rate for the minimum clearance assembly.
- 12-3** A journal bearing has a journal diameter of 3.000 in, with a unilateral tolerance of -0.001 in. The bushing bore has a diameter of 3.005 in and a unilateral tolerance of 0.004 in. The bushing is 1.5 in long. The journal speed is 600 rev/min and the load is 800 lbf. For both SAE 10 and SAE 40, lubricants, find the minimum film thickness and the maximum film pressure for an operating temperature of 150°F for the minimum clearance assembly.
- 12-4** A journal bearing has a journal diameter of 3.250 in with a unilateral tolerance of -0.003 in. The bushing bore has a diameter of 3.256 in and a unilateral tolerance of 0.004 in. The bushing is 3 in long and supports a 800-lbf load. The journal speed is 1000 rev/min. Find the minimum oil film thickness and the maximum film pressure for both SAE 20 and SAE 20W-40 lubricants, for the tightest assembly if the operating film temperature is 150°F .
- 12-5** A full journal bearing has a journal with a diameter of 2.000 in and a unilateral tolerance of -0.0012 in. The bushing has a bore with a diameter of 2.0024 and a unilateral tolerance of 0.002 in. The bushing is 1 in long and supports a load of 600 lbf at a speed of 800 rev/min. Find the minimum film thickness, the power loss, and the total lubricant flow if the average film temperature is 130°F and SAE 20 lubricant is used. The tightest assembly is to be analyzed.
- 12-6** A full journal bearing has a shaft journal diameter of 25 mm with a unilateral tolerance of -0.01 mm. The bushing bore has a diameter of 25.04 mm with a unilateral tolerance of 0.03 mm. The l/d ratio is unity. The bushing load is 1.25 kN, and the journal rotates at 1200 rev/min. Analyze the minimum clearance assembly if the average viscosity is 50 mPa · s to find the minimum oil film thickness, the power loss, and the percentage of side flow.
- 12-7** A full journal bearing has a shaft journal with a diameter of 1.25 in and a unilateral tolerance of -0.0006 in. The bushing bore has a diameter of 1.252 in with a unilateral tolerance of 0.0014 in. The bushing bore is 2 in in length. The bearing load is 620 lbf and the journal rotates at 1120 rev/min. Analyze the minimum clearance assembly and find the minimum film thickness, the coefficient of friction, and the total oil flow if the average viscosity is $8.5 \mu\text{reyn}$.
- 12-8** A journal bearing has a shaft diameter of 75.00 mm with a unilateral tolerance of -0.02 mm. The bushing bore has a diameter of 75.10 mm with a unilateral tolerance of 0.06 mm. The bushing is 36 mm long and supports a load of 2 kN. The journal speed is 720 rev/min. For the minimum clearance assembly find the minimum film thickness, the heat loss rate, and the maximum lubricant pressure for SAE 20 and SAE 40 lubricants operating at an average film temperature of 60°C .
- 12-9** A full journal bearing is 28 mm long. The shaft journal has a diameter of 56 mm with a unilateral tolerance of -0.012 mm. The bushing bore has a diameter of 56.05 mm with a unilateral tolerance of 0.012 mm. The load is 2.4 kN and the journal speed is 900 rev/min. For the minimum clearance assembly find the minimum oil-film thickness, the power loss, and the side flow if the operating temperature is 65°C and SAE 40 lubricating oil is used.

- 12-10** A $1\frac{1}{4}$ -in sleeve bearing supports a load of 700 lbf and has a journal speed of 3600 rev/min. An SAE 10 oil is used having an average temperature of 160°F . Using Fig. 12-16, estimate the radial clearance for minimum coefficient of friction f and for maximum load-carrying capacity W . The difference between these two clearances is called the clearance range. Is the resulting range attainable in manufacture?
- 12-11** A full journal bearing has a shaft diameter of 3.000 in with a unilateral tolerance of -0.0004 in. The l/d ratio is unity. The bushing has a bore diameter of 3.003 in with a unilateral tolerance of 0.0012 in. The SAE 40 oil supply is in an axial-groove sump with a steady-state temperature of 140°F . The radial load is 675 lbf. Estimate the average film temperature, the minimum film thickness, the heat loss rate, and the lubricant side-flow rate for the minimum clearance assembly, if the journal speed is 10 rev/s.
- 12-12** A $2\frac{1}{2} \times 2\frac{1}{2}$ -in sleeve bearing uses grade 20 lubricant. The axial-groove sump has a steady-state temperature of 110°F . The shaft journal has a diameter of 2.500 in with a unilateral tolerance of -0.001 in. The bushing bore has a diameter of 2.504 in with a unilateral tolerance of 0.001 in. The journal speed is 1120 rev/min and the radial load is 1200 lbf. Estimate
- (a) The magnitude and location of the minimum oil-film thickness.
 - (b) The eccentricity.
 - (c) The coefficient of friction.
 - (d) The power loss rate.
 - (e) Both the total and side oil-flow rates.
 - (f) The maximum oil-film pressure and its angular location.
 - (g) The terminating position of the oil film.
 - (h) The average temperature of the side flow.
 - (i) The oil temperature at the terminating position of the oil film.
- 12-13** A set of sleeve bearings has a specification of shaft journal diameter of 1.250 in with a unilateral tolerance of -0.001 in. The bushing bore has a diameter of 1.252 in with a unilateral tolerance of 0.003 in. The bushing is $1\frac{1}{4}$ in long. The radial load is 250 lbf and the shaft rotational speed is 1750 rev/min. The lubricant is SAE 10 oil and the axial-groove sump temperature at steady state T_s is 120°F . For the c_{\min} , c_{median} , and c_{\max} assemblies analyze the bearings and observe the changes in S , ϵ , f , Q , Q_s , ΔT , T_{\max} , \bar{T}_f , and hp .
- 12-14** An interpolation equation was given by Raimondi and Boyd, and it is displayed as Eq. (12-16). This equation is a good candidate for a computer program. Write such a program for interactive use. Once ready for service it can save time and reduce errors. Another version of this program can be used with a subprogram that contains curve fits to Raimondi and Boyd charts for computer use.
- 12-15** A natural-circulation pillow-block bearing has a journal diameter D of 2.500 in with a unilateral tolerance of -0.001 in. The bushing bore diameter B is 2.504 in with a unilateral tolerance of 0.004 in. The shaft runs at an angular speed of 1120 rev/min; the bearing uses SAE grade 20 oil and carries a steady load of 300 lbf in shaft-stirred air at 70°F . The lateral area of the pillow-block housing is 60 in^2 . Perform a design assessment using minimum radial clearance for a load of 600 lbf and 300 lbf. Use Trumpler's criteria.
- 12-16** An eight-cylinder diesel engine has a front main bearing with a journal diameter of 3.500 in and a unilateral tolerance of -0.003 in. The bushing bore diameter is 3.505 in with a unilateral tolerance of $+0.005$ in. The bushing length is 2 in. The pressure-fed bearing has a central annular groove 0.250 in wide. The SAE 30 oil comes from a sump at 120°F using a supply pressure of 50 psig. The sump's heat-dissipation capacity is 5000 Btu/h per bearing. For a minimum radial clearance, a speed of 2000 rev/min, and a radial load of 4600 lbf, find the average film temperature and apply Trumpler's criteria in your design assessment.

- 12-17** A pressure-fed bearing has a journal diameter of 50.00 mm with a unilateral tolerance of -0.05 mm. The bushing bore diameter is 50.084 mm with a unilateral tolerance of 0.10 mm. The length of the bushing is 55 mm. Its central annular groove is 5 mm wide and is fed by SAE 30 oil at 55°C at 200 kPa supply gauge pressure. The journal speed is 2880 rev/min carrying a load of 10 kN. The sump can dissipate 300 watts per bearing if necessary. For minimum radial clearances, perform a design assessment using Trumpler's criteria.
- 12-18** Design a central annular-groove pressure-fed bearing with an l/d ratio of 0.5, using SAE grade 20 oil, the lubricant supplied at 30 psig. The exterior oil cooler can maintain the sump temperature at 120°F for heat dissipation rates up to 1500 Btu/h. The load to be carried is 900 lbf at 3000 rev/min. The groove width is $\frac{1}{4}$ in. Use nominal journal diameter d as one design variable and c as the other. Use Trumpler's criteria for your adequacy assessment.
- 12-19** Repeat design problem Prob. 12-18 using the nominal bushing bore B as one decision variable and the radial clearance c as the other. Again, Trumpler's criteria to be used.
- 12-20** Table 12-1 gives the Seireg and Dandage curve fit approximation for the absolute viscosity in customary U.S. engineering units. Show that in SI units of $\text{mPa} \cdot \text{s}$ and a temperature of C degrees Celsius, the viscosity can be expressed as
- $$\mu = 6.89(10^6)\mu_0 \exp[(b/(1.8C + 127))]$$
- where μ_0 and b are from Table 12-1. If the viscosity μ'_0 is expressed in μreyn , then
- $$\mu = 6.89\mu'_0 \exp[(b/(1.8C + 127))]$$
- What is the viscosity of a grade 50 oil at 70°C ? Compare your results with Fig. 12-13.
- 12-21** For Prob. 12-18 a satisfactory design is
- $$d = 2.000_{-0.001}^{+0} \text{ in} \quad b = 2.005_{-0}^{+0.003} \text{ in}$$
- Double the size of the bearing dimensions and quadruple the load to 3600 lbf.
- (a) Analyze the scaled-up bearing for median assembly.
 - (b) Compare the results of a similar analysis for the 2-in bearing, median assembly.
- 12-22** An Oiles SP 500 alloy brass bushing is 0.75 in long with a 0.75-in dia bore and operates in a clean environment at 70°F . The allowable wear without loss of function is 0.004 in. The radial load is 400 lbf. The shaft speed is 250 rev/min. Estimate the number of revolutions for radial wear to be 0.004 in.
- 12-23** Choose an Oiles SP 500 alloy brass bushing to give a maximum wear of 0.002 in for 1000 h of use with a 400 rev/min journal and 100 lbf radial load. Use $\dot{h}_{\text{CR}} = 2.7 \text{ Btu}/(\text{h} \cdot \text{ft}^2 \cdot {}^{\circ}\text{F})$, $T_{\text{max}} = 300^{\circ}\text{F}$, $f_s = 0.03$, and a design factor $n_d = 2$. Table 12-13 lists the bushing sizes available from the manufacturer.

This page intentionally left blank

13

Gears—General

Chapter Outline

13-1	Types of Gears	674
13-2	Nomenclature	675
13-3	Conjugate Action	677
13-4	Involute Properties	678
13-5	Fundamentals	678
13-6	Contact Ratio	684
13-7	Interference	685
13-8	The Forming of Gear Teeth	687
13-9	Straight Bevel Gears	690
13-10	Parallel Helical Gears	691
13-11	Worm Gears	695
13-12	Tooth Systems	696
13-13	Gear Trains	698
13-14	Force Analysis—Spur Gearing	705
13-15	Force Analysis—Bevel Gearing	709
13-16	Force Analysis—Helical Gearing	712
13-17	Force Analysis—Worm Gearing	714

This chapter addresses gear geometry, the kinematic relations, and the forces transmitted by the four principal types of gears: spur, helical, bevel, and worm gears. The forces transmitted between meshing gears supply torsional moments to shafts for motion and power transmission and create forces and moments that affect the shaft and its bearings. The next two chapters will address stress, strength, safety, and reliability of the four types of gears.

13–1 Types of Gears

Spur gears, illustrated in Fig. 13–1, have teeth parallel to the axis of rotation and are used to transmit motion from one shaft to another, parallel, shaft. Of all types, the spur gear is the simplest and, for this reason, will be used to develop the primary kinematic relationships of the tooth form.

Helical gears, shown in Fig. 13–2, have teeth inclined to the axis of rotation. Helical gears can be used for the same applications as spur gears and, when so used, are not as noisy, because of the more gradual engagement of the teeth during meshing. The inclined tooth also develops thrust loads and bending couples, which are not present with spur gearing. Sometimes helical gears are used to transmit motion between nonparallel shafts.

Bevel gears, shown in Fig. 13–3, have teeth formed on conical surfaces and are used mostly for transmitting motion between intersecting shafts. The figure actually illustrates *straight-tooth bevel gears*. *Spiral bevel gears* are cut so the tooth is no longer straight, but forms a circular arc. *Hypoid gears* are quite similar to spiral bevel gears except that the shafts are offset and nonintersecting.

Figure 13–1

Spur gears are used to transmit rotary motion between parallel shafts.

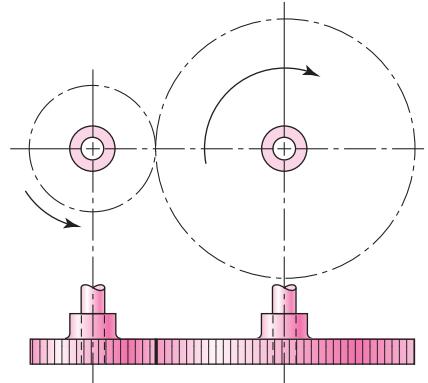


Figure 13–2

Helical gears are used to transmit motion between parallel or nonparallel shafts.

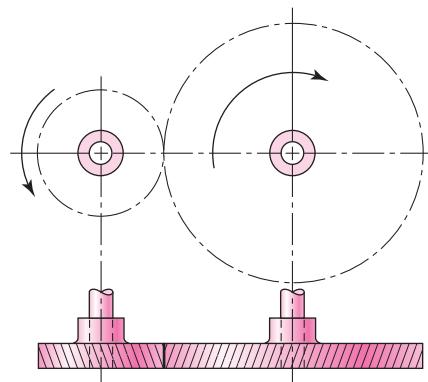
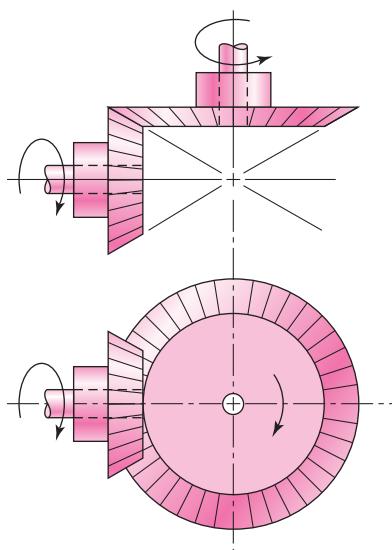
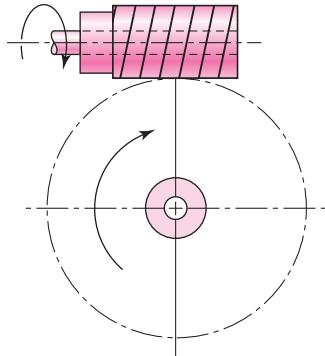


Figure 13–3

Bevel gears are used to transmit rotary motion between intersecting shafts.

**Figure 13–4**

Worm gearsets are used to transmit rotary motion between nonparallel and nonintersecting shafts.



Worms and worm gears, shown in Fig. 13–4, represent the fourth basic gear type. As shown, the worm resembles a screw. The direction of rotation of the worm gear, also called the worm wheel, depends upon the direction of rotation of the worm and upon whether the worm teeth are cut right-hand or left-hand. Worm gearsets are also made so that the teeth of one or both wrap partly around the other. Such sets are called *single-enveloping* and *double-enveloping* worm gearsets. Worm gearsets are mostly used when the speed ratios of the two shafts are quite high, say, 3 or more.

13–2

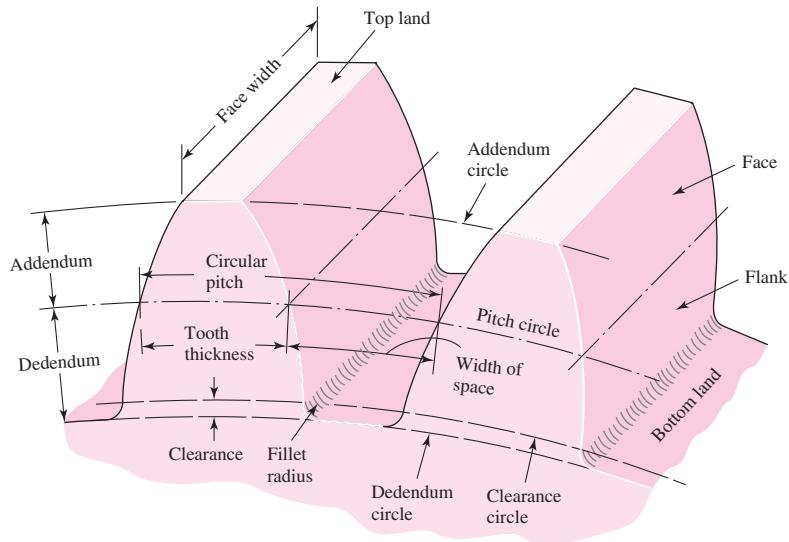
Nomenclature

The terminology of spur-gear teeth is illustrated in Fig. 13–5. The *pitch circle* is a theoretical circle upon which all calculations are usually based; its diameter is the *pitch diameter*. The pitch circles of a pair of mating gears are tangent to each other. A *pinion* is the smaller of two mating gears. The larger is often called the *gear*.

The *circular pitch p* is the distance, measured on the pitch circle, from a point on one tooth to a corresponding point on an adjacent tooth. Thus the circular pitch is equal to the sum of the *tooth thickness* and the *width of space*.

Figure 13-5

Nomenclature of spur-gear teeth.



The *module m* is the ratio of the pitch diameter to the number of teeth. The customary unit of length used is the millimeter. The module is the index of tooth size in SI.

The *diametral pitch P* is the ratio of the number of teeth on the gear to the pitch diameter. Thus, it is the reciprocal of the module. Since diametral pitch is used only with U.S. units, it is expressed as teeth per inch.

The *addendum a* is the radial distance between the *top land* and the *pitch circle*. The *dedendum b* is the radial distance from the *bottom land* to the *pitch circle*. The *whole depth h_t* is the sum of the addendum and the dedendum.

The *clearance circle* is a circle that is tangent to the addendum circle of the mating gear. The *clearance c* is the amount by which the dedendum in a given gear exceeds the addendum of its mating gear. The *backlash* is the amount by which the width of a tooth space exceeds the thickness of the engaging tooth measured on the pitch circles.

You should prove for yourself the validity of the following useful relations:

$$P = \frac{N}{d} \quad (13-1)$$

$$m = \frac{d}{N} \quad (13-2)$$

$$p = \frac{\pi d}{N} = \pi m \quad (13-3)$$

$$pP = \pi \quad (13-4)$$

where P = diametral pitch, teeth per inch

N = number of teeth

d = pitch diameter, in

m = module, mm

d = pitch diameter, mm

p = circular pitch

13–3 Conjugate Action

The following discussion assumes the teeth to be perfectly formed, perfectly smooth, and absolutely rigid. Such an assumption is, of course, unrealistic, because the application of forces will cause deflections.

Mating gear teeth acting against each other to produce rotary motion are similar to cams. When the tooth profiles, or cams, are designed so as to produce a constant angular-velocity ratio during meshing, these are said to have *conjugate action*. In theory, at least, it is possible arbitrarily to select any profile for one tooth and then to find a profile for the meshing tooth that will give conjugate action. One of these solutions is the *involute profile*, which, with few exceptions, is in universal use for gear teeth and is the only one with which we should be concerned.

When one curved surface pushes against another (Fig. 13–6), the point of contact occurs where the two surfaces are tangent to each other (point *c*), and the forces at any instant are directed along the common normal *ab* to the two curves. The line *ab*, representing the direction of action of the forces, is called the *line of action*. The line of action will intersect the line of centers *O–O* at some point *P*. The angular-velocity ratio between the two arms is inversely proportional to their radii to the point *P*. Circles drawn through point *P* from each center are called *pitch circles*, and the radius of each circle is called the *pitch radius*. Point *P* is called the *pitch point*.

Figure 13–6 is useful in making another observation. A pair of gears is really pairs of cams that act through a small arc and, before running off the involute contour, are replaced by another identical pair of cams. The cams can run in either direction and are configured to transmit a constant angular-velocity ratio. If involute curves are used, the gears tolerate changes in center-to-center distance with *no* variation in constant angular-velocity ratio. Furthermore, the rack profiles are straight-flanked, making primary tooling simpler.

To transmit motion at a constant angular-velocity ratio, the pitch point must remain fixed; that is, all the lines of action for every instantaneous point of contact must pass through the same point *P*. In the case of the involute profile, it will be shown that all points of contact occur on the same straight line *ab*, that all normals to the tooth profiles at the point of contact coincide with the line *ab*, and, thus, that these profiles transmit uniform rotary motion.

Figure 13–6

Cam *A* and follower *B* in contact. When the contacting surfaces are involute profiles, the ensuing conjugate action produces a constant angular-velocity ratio.

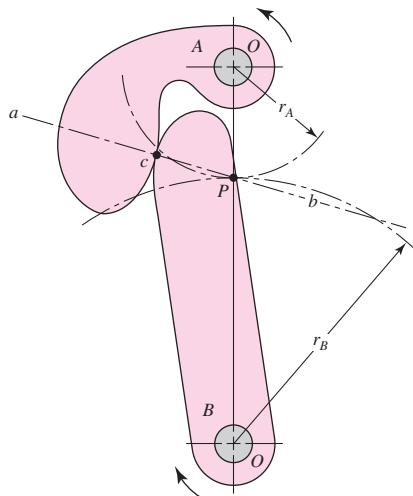
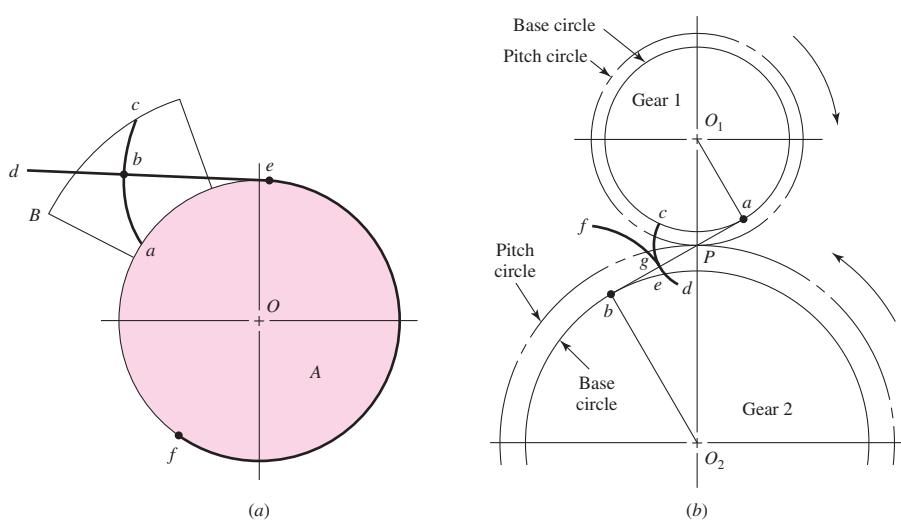


Figure 13-7

- (a) Generation of an involute;
(b) involute action.



13-4 Involute Properties

An involute curve may be generated as shown in Fig. 13-7a. A partial flange *B* is attached to the cylinder *A*, around which is wrapped a cord *def*, which is held tight. Point *b* on the cord represents the tracing point, and as the cord is wrapped and unwrapped about the cylinder, point *b* will trace out the involute curve *ac*. The radius of the curvature of the involute varies continuously, being zero at point *a* and a maximum at point *c*. At point *b* the radius is equal to the distance *be*, since point *b* is instantaneously rotating about point *e*. Thus the generating line *de* is normal to the involute at all points of intersection and, at the same time, is always tangent to the cylinder *A*. The circle on which the involute is generated is called the *base circle*.

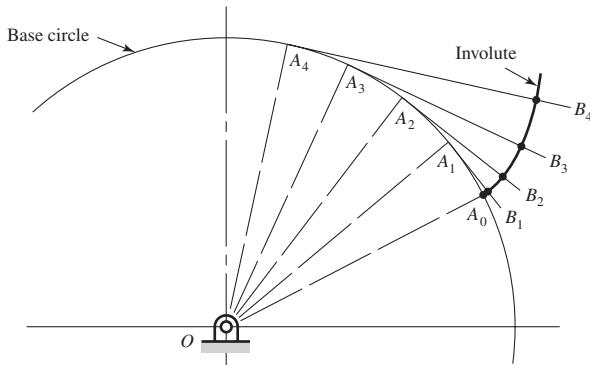
Let us now examine the involute profile to see how it satisfies the requirement for the transmission of uniform motion. In Fig. 13-7b, two gear blanks with fixed centers at *O*₁ and *O*₂ are shown having base circles whose respective radii are *O*₁*a* and *O*₂*b*. We now imagine that a cord is wound clockwise around the base circle of gear 1, pulled tight between points *a* and *b*, and wound counterclockwise around the base circle of gear 2. If, now, the base circles are rotated in different directions so as to keep the cord tight, a point *g* on the cord will trace out the involutes *cd* on gear 1 and *ef* on gear 2. The involutes are thus generated simultaneously by the tracing point. The tracing point, therefore, represents the point of contact, while the portion of the cord *ab* is the generating line. The point of contact moves along the generating line; the generating line does not change position, because it is always tangent to the base circles; and since the generating line is always normal to the involutes at the point of contact, the requirement for uniform motion is satisfied.

13-5 Fundamentals

Among other things, it is necessary that you actually be able to draw the teeth on a pair of meshing gears. You should understand, however, that you are not doing this for manufacturing or shop purposes. Rather, we make drawings of gear teeth to obtain an understanding of the problems involved in the meshing of the mating teeth.

Figure 13-8

Construction of an involute curve.



First, it is necessary to learn how to construct an involute curve. As shown in Fig. 13-8, divide the base circle into a number of equal parts, and construct radial lines OA_0 , OA_1 , OA_2 , etc. Beginning at A_1 , construct perpendiculars A_1B_1 , A_2B_2 , A_3B_3 , etc. Then along A_1B_1 lay off the distance A_1A_0 , along A_2B_2 lay off twice the distance A_1A_0 , etc., producing points through which the involute curve can be constructed.

To investigate the fundamentals of tooth action, let us proceed step by step through the process of constructing the teeth on a pair of gears.

When two gears are in mesh, their pitch circles roll on one another without slipping. Designate the pitch radii as r_1 and r_2 and the angular velocities as ω_1 and ω_2 , respectively. Then the pitch-line velocity is

$$V = |r_1\omega_1| = |r_2\omega_2|$$

Thus the relation between the radii on the angular velocities is

$$\left| \frac{\omega_1}{\omega_2} \right| = \frac{r_2}{r_1} \quad (13-5)$$

Suppose now we wish to design a speed reducer such that the input speed is 1800 rev/min and the output speed is 1200 rev/min. This is a ratio of 3:2; the gear pitch diameters would be in the same ratio, for example, a 4-in pinion driving a 6-in gear. The various dimensions found in gearing are always based on the pitch circles.

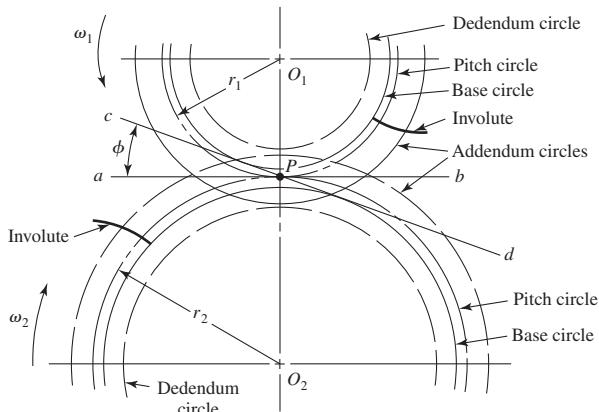
Suppose we specify that an 18-tooth pinion is to mesh with a 30-tooth gear and that the diametral pitch of the gearset is to be 2 teeth per inch. Then, from Eq. (13-1), the pitch diameters of the pinion and gear are, respectively,

$$d_1 = \frac{N_1}{P} = \frac{18}{2} = 9 \text{ in} \quad d_2 = \frac{N_2}{P} = \frac{30}{2} = 15 \text{ in}$$

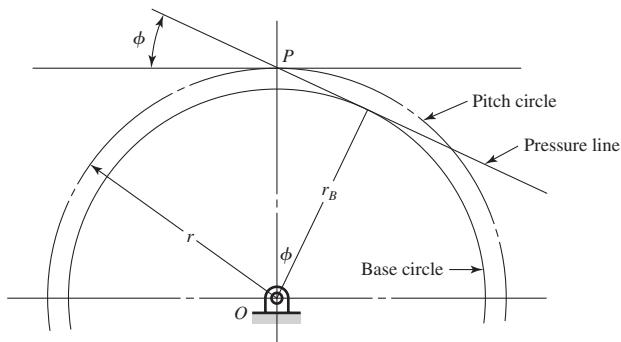
The first step in drawing teeth on a pair of mating gears is shown in Fig. 13-9. The center distance is the sum of the pitch radii, in this case 12 in. So locate the pinion and gear centers O_1 and O_2 , 12 in apart. Then construct the pitch circles of radii r_1 and r_2 . These are tangent at P , the *pitch point*. Next draw line ab , the common tangent, through the pitch point. We now designate gear 1 as the driver, and since it is rotating counter-clockwise, we draw a line cd through point P at an angle ϕ to the common tangent ab . The line cd has three names, all of which are in general use. It is called the *pressure line*, the *generating line*, and the *line of action*. It represents the direction in which the resultant force acts between the gears. The angle ϕ is called the *pressure angle*, and it usually has values of 20 or 25°, though $14\frac{1}{2}^\circ$ was once used.

Figure 13-9

Circles of a gear layout.

**Figure 13-10**

Base circle radius can be related to the pressure angle ϕ and the pitch circle radius by
 $r_b = r \cos \phi$.



Next, on each gear draw a circle tangent to the pressure line. These circles are the *base circles*. Since they are tangent to the pressure line, the pressure angle determines their size. As shown in Fig. 13-10, the radius of the base circle is

$$r_b = r \cos \phi \quad (13-6)$$

where r is the pitch radius.

Now generate an involute on each base circle as previously described and as shown in Fig. 13-9. This involute is to be used for one side of a gear tooth. It is not necessary to draw another curve in the reverse direction for the other side of the tooth, because we are going to use a template which can be turned over to obtain the other side.

The addendum and dedendum distances for standard interchangeable teeth are, as we shall learn later, $1/P$ and $1.25/P$, respectively. Therefore, for the pair of gears we are constructing,

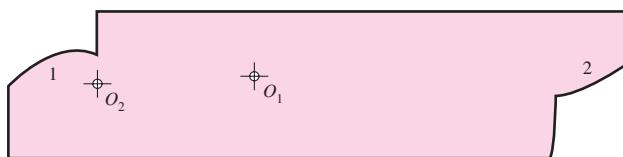
$$a = \frac{1}{P} = \frac{1}{2} = 0.500 \text{ in} \quad b = \frac{1.25}{P} = \frac{1.25}{2} = 0.625 \text{ in}$$

Using these distances, draw the addendum and dedendum circles on the pinion and on the gear as shown in Fig. 13-9.

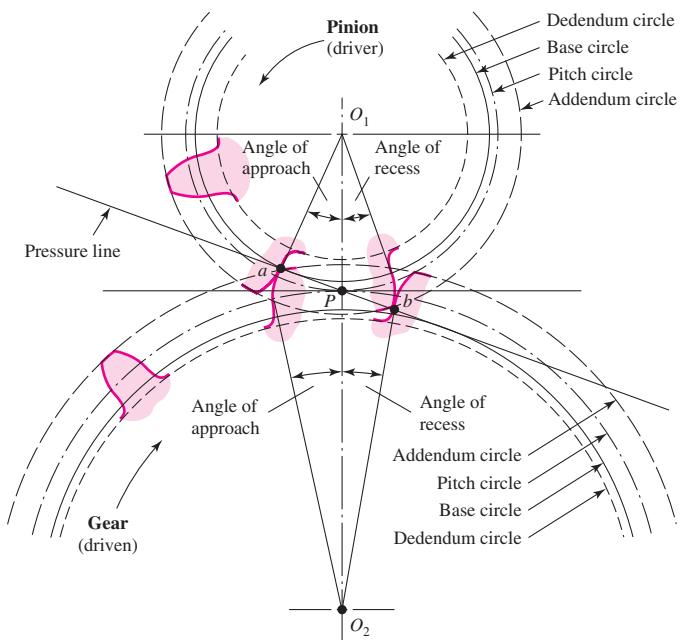
Next, using heavy drawing paper, or preferably, a sheet of 0.015- to 0.020-in clear plastic, cut a template for each involute, being careful to locate the gear centers properly with respect to each involute. Figure 13-11 is a reproduction of the template used to create some of the illustrations for this book. Note that only one side of the tooth profile is formed on the template. To get the other side, turn the template over. For some problems you might wish to construct a template for the entire tooth.

Figure 13-11

A template for drawing gear teeth.

**Figure 13-12**

Tooth action.



To draw a tooth, we must know the tooth thickness. From Eq. (13-4), the circular pitch is

$$p = \frac{\pi}{P} = \frac{\pi}{2} = 1.57 \text{ in}$$

Therefore, the tooth thickness is

$$t = \frac{p}{2} = \frac{1.57}{2} = 0.785 \text{ in}$$

measured on the pitch circle. Using this distance for the tooth thickness as well as the tooth space, draw as many teeth as desired, using the template, after the points have been marked on the pitch circle. In Fig. 13-12 only one tooth has been drawn on each gear. You may run into trouble in drawing these teeth if one of the base circles happens to be larger than the dedendum circle. The reason for this is that the involute begins at the base circle and is undefined below this circle. So, in drawing gear teeth, we usually draw a radial line for the profile below the base circle. The actual shape, however, will depend upon the kind of machine tool used to form the teeth in manufacture, that is, how the profile is generated.

The portion of the tooth between the clearance circle and the dedendum circle includes the fillet. In this instance the clearance is

$$c = b - a = 0.625 - 0.500 = 0.125 \text{ in}$$

The construction is finished when these fillets have been drawn.

Referring again to Fig. 13–12, the pinion with center at O_1 is the driver and turns counterclockwise. The pressure, or generating, line is the same as the cord used in Fig. 13–7a to generate the involute, and contact occurs along this line. The initial contact will take place when the flank of the driver comes into contact with the tip of the driven tooth. This occurs at point a in Fig. 13–12, where the addendum circle of the driven gear crosses the pressure line. If we now construct tooth profiles through point a and draw radial lines from the intersections of these profiles with the pitch circles to the gear centers, we obtain the *angle of approach* for each gear.

As the teeth go into mesh, the point of contact will slide up the side of the driving tooth so that the tip of the driver will be in contact just before contact ends. The final point of contact will therefore be where the addendum circle of the driver crosses the pressure line. This is point b in Fig. 13–12. By drawing another set of tooth profiles through b , we obtain the *angle of recess* for each gear in a manner similar to that of finding the angles of approach. The sum of the angle of approach and the angle of recess for either gear is called the *angle of action*. The line ab is called the *line of action*.

We may imagine a *rack* as a spur gear having an infinitely large pitch diameter. Therefore, the rack has an infinite number of teeth and a base circle which is an infinite distance from the pitch point. The sides of involute teeth on a rack are straight lines making an angle to the line of centers equal to the pressure angle. Figure 13–13 shows an involute rack in mesh with a pinion. Corresponding sides on involute teeth are parallel curves; the *base pitch* is the constant and fundamental distance between them along a common normal as shown in Fig. 13–13. The base pitch is related to the circular pitch by the equation

$$p_b = p_c \cos \phi \quad (13-7)$$

where p_b is the base pitch.

Figure 13–14 shows a pinion in mesh with an *internal*, or *ring*, gear. Note that both of the gears now have their centers of rotation on the same side of the pitch point. Thus the positions of the addendum and dedendum circles with respect to the pitch circle are reversed; the addendum circle of the internal gear lies *inside* the pitch circle. Note, too, from Fig. 13–14, that the base circle of the internal gear lies inside the pitch circle near the addendum circle.

Another interesting observation concerns the fact that the operating diameters of the pitch circles of a pair of meshing gears need not be the same as the respective design pitch diameters of the gears, though this is the way they have been constructed in Fig. 13–12. If we increase the center distance, we create two new operating pitch circles having larger diameters because they must be tangent to each other at the pitch point.

Figure 13–13

Involute-toothed pinion and rack.

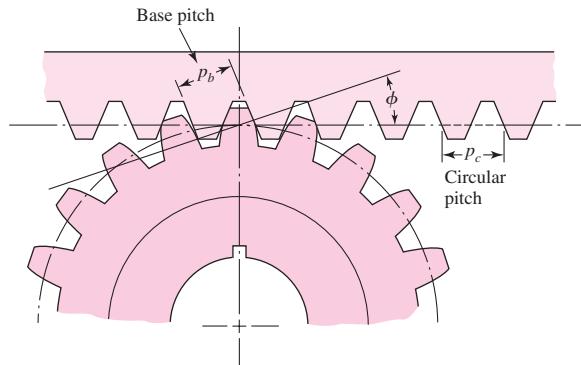
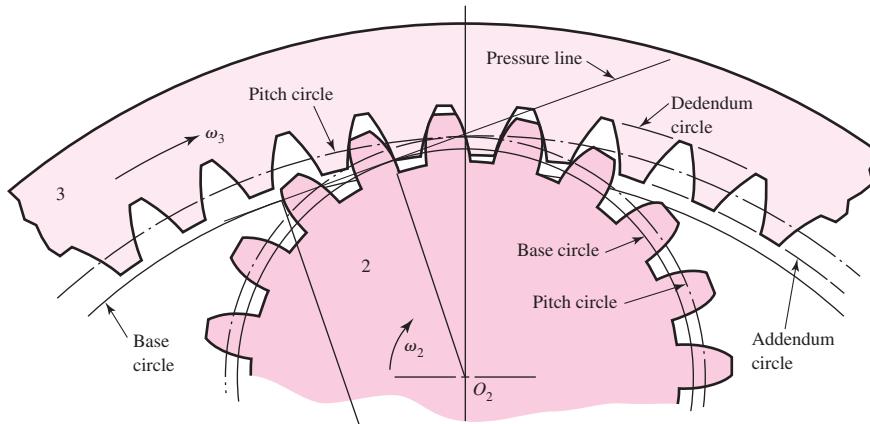


Figure 13–14

Internal gear and pinion.



Thus the pitch circles of gears really do not come into existence until a pair of gears are brought into mesh.

Changing the center distance has no effect on the base circles, because these were used to generate the tooth profiles. Thus the base circle is basic to a gear. Increasing the center distance increases the pressure angle and decreases the length of the line of action, but the teeth are still conjugate, the requirement for uniform motion transmission is still satisfied, and the angular-velocity ratio has not changed.

EXAMPLE 13–1

A gearset consists of a 16-tooth pinion driving a 40-tooth gear. The diametral pitch is 2, and the addendum and dedendum are $1/P$ and $1.25/P$, respectively. The gears are cut using a pressure angle of 20° .

- Compute the circular pitch, the center distance, and the radii of the base circles.
- In mounting these gears, the center distance was incorrectly made $\frac{1}{4}$ in larger. Compute the new values of the pressure angle and the pitch-circle diameters.

Solution

Answer

$$(a) \quad p = \frac{\pi}{P} = \frac{\pi}{2} = 1.57 \text{ in}$$

The pitch diameters of the pinion and gear are, respectively,

$$d_P = \frac{16}{2} = 8 \text{ in} \quad d_G = \frac{40}{2} = 20 \text{ in}$$

Therefore the center distance is

Answer

$$\frac{d_P + d_G}{2} = \frac{8 + 20}{2} = 14 \text{ in}$$

Since the teeth were cut on the 20° pressure angle, the base-circle radii are found to be, using $r_b = r \cos \phi$,

Answer

$$r_b \text{ (pinion)} = \frac{8}{2} \cos 20^\circ = 3.76 \text{ in}$$

Answer

$$r_b \text{ (gear)} = \frac{20}{2} \cos 20^\circ = 9.40 \text{ in}$$

(b) Designating d'_P and d'_G as the new pitch-circle diameters, the $\frac{1}{4}$ -in increase in the center distance requires that

$$\frac{d'_P + d'_G}{2} = 14.250 \quad (1)$$

Also, the velocity ratio does not change, and hence

$$\frac{d'_P}{d'_G} = \frac{16}{40} \quad (2)$$

Solving Eqs. (1) and (2) simultaneously yields

Answer

$$d'_P = 8.143 \text{ in} \quad d'_G = 20.357 \text{ in}$$

Since $r_b = r \cos \phi$, the new pressure angle is

Answer

$$\phi' = \cos^{-1} \frac{r_b \text{ (pinion)}}{d'_P/2} = \cos^{-1} \frac{3.76}{8.143/2} = 22.56^\circ$$

13–6 Contact Ratio

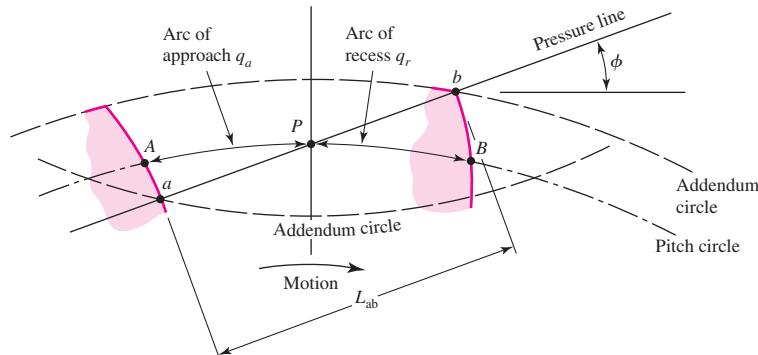
The zone of action of meshing gear teeth is shown in Fig. 13–15. We recall that tooth contact begins and ends at the intersections of the two addendum circles with the pressure line. In Fig. 13–15 initial contact occurs at a and final contact at b . Tooth profiles drawn through these points intersect the pitch circle at A and B , respectively. As shown, the distance AP is called the *arc of approach* q_a , and the distance PB , the *arc of recess* q_r . The sum of these is the *arc of action* q_t .

Now, consider a situation in which the arc of action is exactly equal to the circular pitch, that is, $q_t = p$. This means that one tooth and its space will occupy the entire arc AB . In other words, when a tooth is just beginning contact at a , the previous tooth is simultaneously ending its contact at b . Therefore, during the tooth action from a to b , there will be exactly one pair of teeth in contact.

Next, consider a situation in which the arc of action is greater than the circular pitch, but not very much greater, say, $q_t \doteq 1.2p$. This means that when one pair of teeth is just entering contact at a , another pair, already in contact, will not yet have reached b .

Figure 13–15

Definition of contact ratio.



Thus, for a short period of time, there will be two teeth in contact, one in the vicinity of *A* and another near *B*. As the meshing proceeds, the pair near *B* must cease contact, leaving only a single pair of contacting teeth, until the procedure repeats itself.

Because of the nature of this tooth action, either one or two pairs of teeth in contact, it is convenient to define the term *contact ratio* m_c as

$$m_c = \frac{q_t}{p} \quad (13-8)$$

a number that indicates the average number of pairs of teeth in contact. Note that this ratio is also equal to the length of the path of contact divided by the base pitch. Gears should not generally be designed having contact ratios less than about 1.20, because inaccuracies in mounting might reduce the contact ratio even more, increasing the possibility of impact between the teeth as well as an increase in the noise level.

An easier way to obtain the contact ratio is to measure the line of action *ab* instead of the arc distance *AB*. Since *ab* in Fig. 13–15 is tangent to the base circle when extended, the base pitch p_b must be used to calculate m_c instead of the circular pitch as in Eq. (13–8). If the length of the line of action is L_{ab} , the contact ratio is

$$m_c = \frac{L_{ab}}{p \cos \phi} \quad (13-9)$$

in which Eq. (13–7) was used for the base pitch.

13–7 Interference

The contact of portions of tooth profiles that are not conjugate is called *interference*. Consider Fig. 13–16. Illustrated are two 16-tooth gears that have been cut to the now obsolete $14\frac{1}{2}^\circ$ pressure angle. The driver, gear 2, turns clockwise. The initial and final points of contact are designated *A* and *B*, respectively, and are located on the pressure line. Now notice that the points of tangency of the pressure line with the base circles *C* and *D* are located *inside* of points *A* and *B*. Interference is present.

The interference is explained as follows. Contact begins when the tip of the driven tooth contacts the flank of the driving tooth. In this case the flank of the driving tooth first makes contact with the driven tooth at point *A*, and this occurs *before* the involute portion of the driving tooth comes within range. In other words, contact is occurring below the base circle of gear 2 on the *noninvolute* portion of the flank. The actual effect is that the involute tip or face of the driven gear tends to dig out the noninvolute flank of the driver.

In this example the same effect occurs again as the teeth leave contact. Contact should end at point *D* or before. Since it does not end until point *B*, the effect is for the tip of the driving tooth to dig out, or interfere with, the flank of the driven tooth.

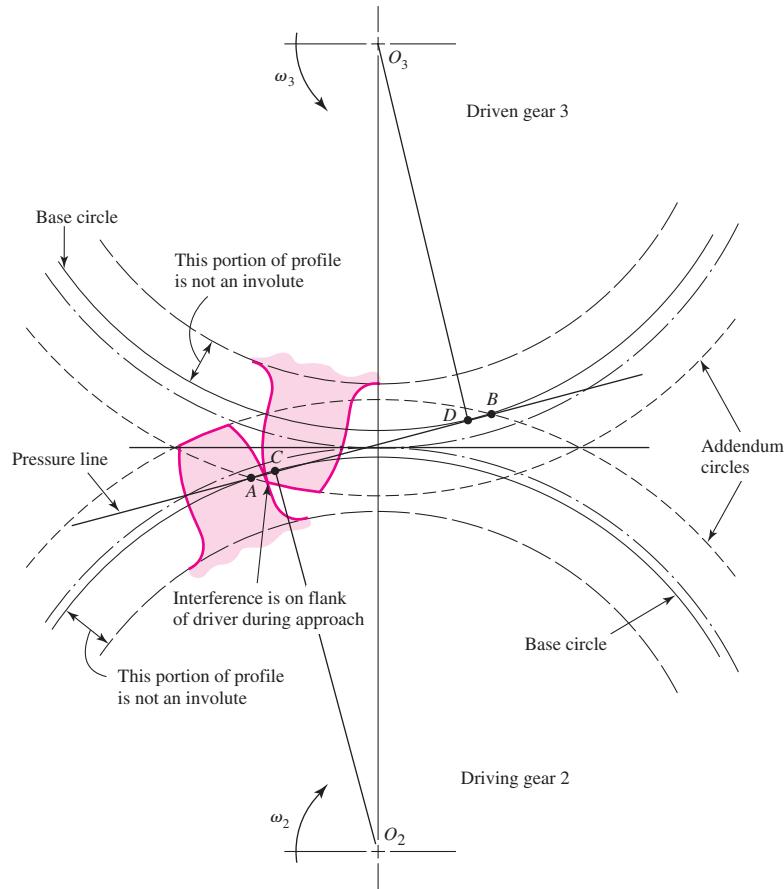
When gear teeth are produced by a generation process, interference is automatically eliminated because the cutting tool removes the interfering portion of the flank. This effect is called *undercutting*; if undercutting is at all pronounced, the undercut tooth is considerably weakened. Thus the effect of eliminating interference by a generation process is merely to substitute another problem for the original one.

The smallest number of teeth on a spur pinion and gear,¹ one-to-one gear ratio, which can exist without interference is N_P . This number of teeth for spur gears is

¹Robert Lipp, "Avoiding Tooth Interference in Gears," *Machine Design*, Vol. 54, No. 1, 1982, pp. 122–124.

Figure 13-16

Interference in the action of gear teeth.



given by

$$N_P = \frac{2k}{3 \sin^2 \phi} \left(1 + \sqrt{1 + 3 \sin^2 \phi} \right) \quad (13-10)$$

where $k = 1$ for full-depth teeth, 0.8 for stub teeth and ϕ = pressure angle.

For a 20° pressure angle, with $k = 1$,

$$N_P = \frac{2(1)}{3 \sin^2 20^\circ} \left(1 + \sqrt{1 + 3 \sin^2 20^\circ} \right) = 12.3 = 13 \text{ teeth}$$

Thus 13 teeth on pinion and gear are interference-free. Realize that 12.3 teeth is possible in meshing arcs, but for fully rotating gears, 13 teeth represents the least number. For a $14\frac{1}{2}^\circ$ pressure angle, $N_P = 23$ teeth, so one can appreciate why few $14\frac{1}{2}^\circ$ -tooth systems are used, as the higher pressure angles can produce a smaller pinion with accompanying smaller center-to-center distances.

If the mating gear has more teeth than the pinion, that is, $m_G = N_G/N_P = m$ is more than one, then the smallest number of teeth on the pinion without interference is given by

$$N_P = \frac{2k}{(1 + 2m) \sin^2 \phi} \left(m + \sqrt{m^2 + (1 + 2m) \sin^2 \phi} \right) \quad (13-11)$$

For example, if $m = 4$, $\phi = 20^\circ$,

$$N_P = \frac{2(1)}{[1 + 2(4)] \sin^2 20^\circ} \left[4 + \sqrt{4^2 + [1 + 2(4)] \sin^2 20^\circ} \right] = 15.4 = 16 \text{ teeth}$$

Thus a 16-tooth pinion will mesh with a 64-tooth gear without interference.

The largest gear with a specified pinion that is interference-free is

$$N_G = \frac{N_P^2 \sin^2 \phi - 4k^2}{4k - 2N_P \sin^2 \phi} \quad (13-12)$$

For example, for a 13-tooth pinion with a pressure angle ϕ of 20° ,

$$N_G = \frac{13^2 \sin^2 20^\circ - 4(1)^2}{4(1) - 2(13) \sin^2 20^\circ} = 16.45 = 16 \text{ teeth}$$

For a 13-tooth spur pinion, the maximum number of gear teeth possible without interference is 16.

The smallest spur pinion that will operate with a rack without interference is

$$N_P = \frac{2(k)}{\sin^2 \phi} \quad (13-13)$$

For a 20° pressure angle full-depth tooth the smallest number of pinion teeth to mesh with a rack is

$$N_P = \frac{2(1)}{\sin^2 20^\circ} = 17.1 = 18 \text{ teeth}$$

Since gear-shaping tools amount to contact with a rack, and the gear-hobbing process is similar, the minimum number of teeth to prevent interference to prevent undercutting by the hobbing process is equal to the value of N_P when N_G is infinite.

The importance of the problem of teeth that have been weakened by undercutting cannot be overemphasized. Of course, interference can be eliminated by using more teeth on the pinion. However, if the pinion is to transmit a given amount of power, more teeth can be used only by increasing the pitch diameter.

Interference can also be reduced by using a larger pressure angle. This results in a smaller base circle, so that more of the tooth profile becomes involute. The demand for smaller pinions with fewer teeth thus favors the use of a 25° pressure angle even though the frictional forces and bearing loads are increased and the contact ratio decreased.

13-8 The Forming of Gear Teeth

There are a large number of ways of forming the teeth of gears, such as *sand casting*, *shell molding*, *investment casting*, *permanent-mold casting*, *die casting*, and *centrifugal casting*. Teeth can also be formed by using the *powder-metallurgy process*; or, by using *extrusion*, a single bar of aluminum may be formed and then sliced into gears. Gears that carry large loads in comparison with their size are usually made of steel and are cut with either *form cutters* or *generating cutters*. In form cutting, the tooth space takes the exact form of the cutter. In generating, a tool having a shape different from the tooth profile is moved relative to the gear blank so as to obtain the proper tooth shape. One of the newest and most promising of the methods of forming teeth is called *cold forming*, or *cold rolling*, in which dies are rolled against steel blanks to form the teeth. The mechanical properties of the metal are greatly improved by the rolling process, and a high-quality generated profile is obtained at the same time.

Gear teeth may be machined by milling, shaping, or hobbing. They may be finished by shaving, burnishing, grinding, or lapping.

Gears made of thermoplastics such as nylon, polycarbonate, acetal are quite popular and are easily manufactured by *injection molding*. These gears are of low to moderate precision, low in cost for high production quantities, and capable of light loads, and can run without lubrication.

Milling

Gear teeth may be cut with a form milling cutter shaped to conform to the tooth space. With this method it is theoretically necessary to use a different cutter for each gear, because a gear having 25 teeth, for example, will have a different-shaped tooth space from one having, say, 24 teeth. Actually, the change in space is not too great, and it has been found that eight cutters may be used to cut with reasonable accuracy any gear in the range of 12 teeth to a rack. A separate set of cutters is, of course, required for each pitch.

Shaping

Teeth may be generated with either a pinion cutter or a rack cutter. The pinion cutter (Fig. 13-17) reciprocates along the vertical axis and is slowly fed into the gear blank to the required depth. When the pitch circles are tangent, both the cutter and the blank rotate slightly after each cutting stroke. Since each tooth of the cutter is a cutting tool, the teeth are all cut after the blank has completed one rotation. The sides of an involute rack tooth are straight. For this reason, a rack-generating tool provides an accurate method of cutting gear teeth. This is also a shaping operation and is illustrated by the drawing of Fig. 13-18. In operation, the cutter reciprocates and is first fed into the gear blank until the pitch circles are tangent. Then, after each cutting stroke, the gear blank

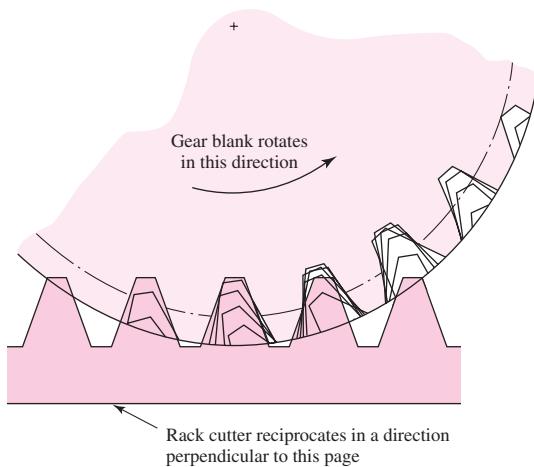
Figure 13-17

Generating a spur gear with a pinion cutter. (Courtesy of Boston Gear Works, Inc.)

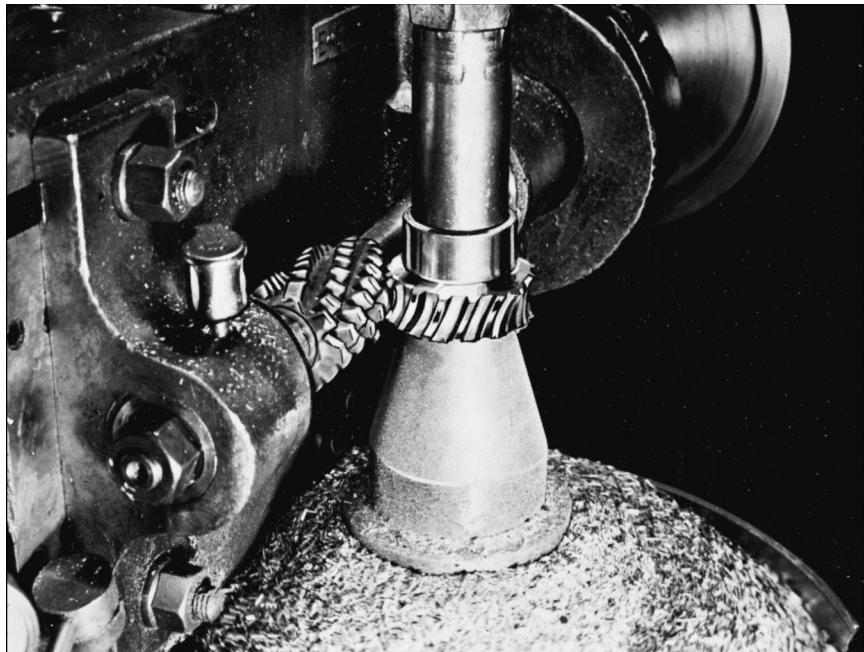


Figure 13-18

Shaping teeth with a rack.
(This is a drawing-board figure that J. E. Shigley executed over 35 years ago in response to a question from a student at the University of Michigan.)

**Figure 13-19**

Hobbing a worm gear.
(Courtesy of Boston Gear Works, Inc.)



and cutter roll slightly on their pitch circles. When the blank and cutter have rolled a distance equal to the circular pitch, the cutter is returned to the starting point, and the process is continued until all the teeth have been cut.

Hobbing

The hobbing process is illustrated in Fig. 13–19. The hob is simply a cutting tool that is shaped like a worm. The teeth have straight sides, as in a rack, but the hob axis must be turned through the lead angle in order to cut spur-gear teeth. For this reason, the teeth generated by a hob have a slightly different shape from those generated by a rack cutter. Both the hob and the blank must be rotated at the proper angular-velocity ratio. The hob is then fed slowly across the face of the blank until all the teeth have been cut.

Finishing

Gears that run at high speeds and transmit large forces may be subjected to additional dynamic forces if there are errors in tooth profiles. Errors may be diminished somewhat by finishing the tooth profiles. The teeth may be finished, after cutting, by either shaving or burnishing. Several shaving machines are available that cut off a minute amount of metal, bringing the accuracy of the tooth profile within the limits of $250 \mu\text{in}$.

Burnishing, like shaving, is used with gears that have been cut but not heat-treated. In burnishing, hardened gears with slightly oversize teeth are run in mesh with the gear until the surfaces become smooth.

Grinding and lapping are used for hardened gear teeth after heat treatment. The grinding operation employs the generating principle and produces very accurate teeth. In lapping, the teeth of the gear and lap slide axially so that the whole surface of the teeth is abraded equally.

13-9 Straight Bevel Gears

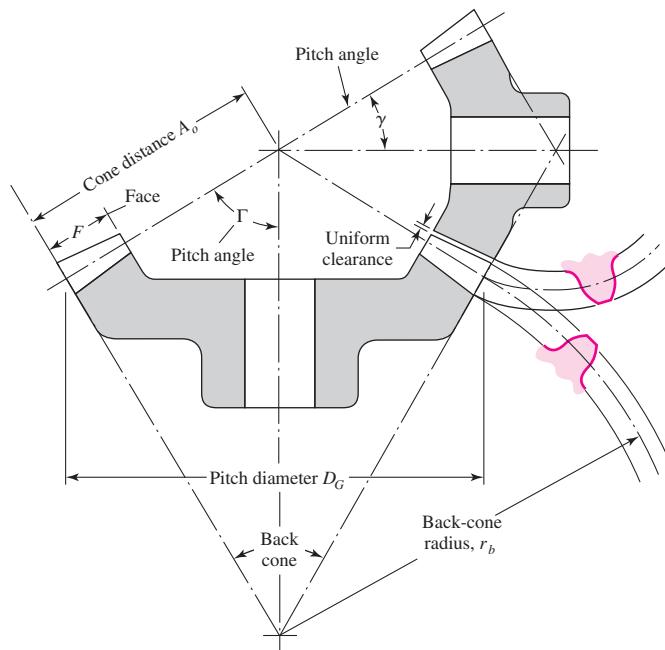
When gears are used to transmit motion between intersecting shafts, some form of bevel gear is required. A bevel gearset is shown in Fig. 13-20. Although bevel gears are usually made for a shaft angle of 90° , they may be produced for almost any angle. The teeth may be cast, milled, or generated. Only the generated teeth may be classed as accurate.

The terminology of bevel gears is illustrated in Fig. 13-20. The pitch of bevel gears is measured at the large end of the tooth, and both the circular pitch and the pitch diameter are calculated in the same manner as for spur gears. It should be noted that the clearance is uniform. The pitch angles are defined by the pitch cones meeting at the apex, as shown in the figure. They are related to the tooth numbers as follows:

$$\tan \gamma = \frac{N_P}{N_G} \quad \tan \Gamma = \frac{N_G}{N_P} \quad (13-14)$$

Figure 13-20

Terminology of bevel gears.



where the subscripts P and G refer to the pinion and gear, respectively, and where γ and Γ are, respectively, the pitch angles of the pinion and gear.

Figure 13–20 shows that the shape of the teeth, when projected on the back cone, is the same as in a spur gear having a radius equal to the back-cone distance r_b . This is called Tredgold's approximation. The number of teeth in this imaginary gear is

$$N' = \frac{2\pi r_b}{p} \quad (13-15)$$

where N' is the *virtual number of teeth* and p is the circular pitch measured at the large end of the teeth. Standard straight-tooth bevel gears are cut by using a 20° pressure angle, unequal addenda and dedenda, and full-depth teeth. This increases the contact ratio, avoids undercut, and increases the strength of the pinion.

13-10

Parallel Helical Gears

Helical gears, used to transmit motion between parallel shafts, are shown in Fig. 13–2. The helix angle is the same on each gear, but one gear must have a right-hand helix and the other a left-hand helix. The shape of the tooth is an involute helicoid and is illustrated in Fig. 13–21. If a piece of paper cut in the shape of a parallelogram is wrapped around a cylinder, the angular edge of the paper becomes a helix. If we unwind this paper, each point on the angular edge generates an involute curve. This surface obtained when every point on the edge generates an involute is called an *involute helicoid*.

The initial contact of spur-gear teeth is a line extending all the way across the face of the tooth. The initial contact of helical-gear teeth is a point that extends into a line as the teeth come into more engagement. In spur gears the line of contact is parallel to the axis of rotation; in helical gears the line is diagonal across the face of the tooth. It is this gradual engagement of the teeth and the smooth transfer of load from one tooth to another that gives helical gears the ability to transmit heavy loads at high speeds. Because of the nature of contact between helical gears, the contact ratio is of only minor importance, and it is the contact area, which is proportional to the face width of the gear, that becomes significant.

Helical gears subject the shaft bearings to both radial and thrust loads. When the thrust loads become high or are objectionable for other reasons, it may be desirable to use double helical gears. A double helical gear (herringbone) is equivalent to two helical gears of opposite hand, mounted side by side on the same shaft. They develop opposite thrust reactions and thus cancel out the thrust load.

When two or more single helical gears are mounted on the same shaft, the hand of the gears should be selected so as to produce the minimum thrust load.

Figure 13-21

An involute helicoid.

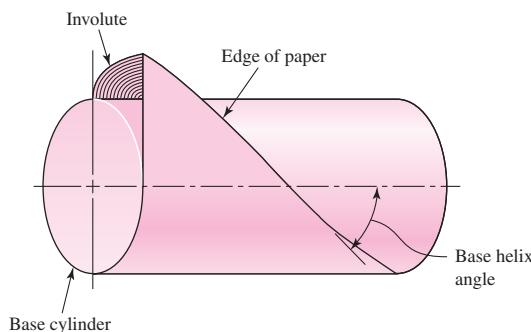


Figure 13-22

Nomenclature of helical gears.

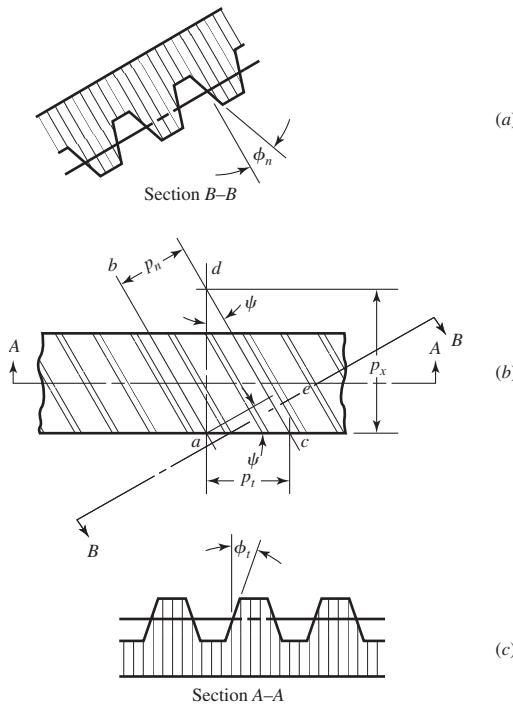


Figure 13-22 represents a portion of the top view of a helical rack. Lines ab and cd are the centerlines of two adjacent helical teeth taken on the same pitch plane. The angle ψ is the *helix angle*. The distance ac is the *transverse circular pitch* p_t in the plane of rotation (usually called the *circular pitch*). The distance ae is the *normal circular pitch* p_n and is related to the transverse circular pitch as follows:

$$p_n = p_t \cos \psi \quad (13-16)$$

The distance ad is called the *axial pitch* p_x and is related by the expression

$$p_x = \frac{p_t}{\tan \psi} \quad (13-17)$$

Since $p_n P_n = \pi$, the *normal diametral pitch* is

$$P_n = \frac{P_t}{\cos \psi} \quad (13-18)$$

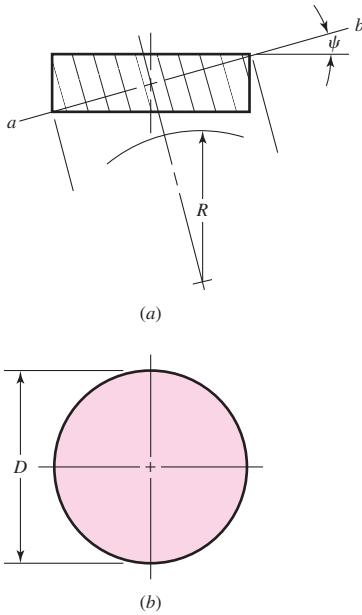
The pressure angle ϕ_n in the normal direction is different from the pressure angle ϕ_t in the direction of rotation, because of the angularity of the teeth. These angles are related by the equation

$$\cos \psi = \frac{\tan \phi_n}{\tan \phi_t} \quad (13-19)$$

Figure 13-23 illustrates a cylinder cut by an oblique plane ab at an angle ψ to a right section. The oblique plane cuts out an arc having a radius of curvature of R . For the condition that $\psi = 0$, the radius of curvature is $R = D/2$. If we imagine the angle ψ to be slowly increased from zero to 90° , we see that R begins at a value of $D/2$ and

Figure 13-23

A cylinder cut by an oblique plane.



increases until, when $\psi = 90^\circ$, $R = \infty$. The radius R is the apparent pitch radius of a helical-gear tooth when viewed in the direction of the tooth elements. A gear of the same pitch and with the radius R will have a greater number of teeth, because of the increased radius. In helical-gear terminology this is called the *virtual number of teeth*. It can be shown by analytical geometry that the virtual number of teeth is related to the actual number by the equation

$$N' = \frac{N}{\cos^3 \psi} \quad (13-20)$$

where N' is the virtual number of teeth and N is the actual number of teeth. It is necessary to know the virtual number of teeth in design for strength and also, sometimes, in cutting helical teeth. This apparently larger radius of curvature means that few teeth may be used on helical gears, because there will be less undercutting.

EXAMPLE 13-2

A stock helical gear has a normal pressure angle of 20° , a helix angle of 25° , and a transverse diametral pitch of 6 teeth/in, and has 18 teeth. Find:

- (a) The pitch diameter
- (b) The transverse, the normal, and the axial pitches
- (c) The normal diametral pitch
- (d) The transverse pressure angle

Solution

Answer (a) $d = \frac{N}{P_t} = \frac{18}{6} = 3 \text{ in}$

Answer (b) $p_t = \frac{\pi}{P_t} = \frac{\pi}{6} = 0.5236 \text{ in}$

Answer

$$p_n = p_t \cos \psi = 0.5236 \cos 25^\circ = 0.4745 \text{ in}$$

Answer

$$p_x = \frac{p_t}{\tan \psi} = \frac{0.5236}{\tan 45^\circ} = 1.123 \text{ in}$$

Answer

(c)

$$P_n = \frac{P_t}{\cos \psi} = \frac{6}{\cos 25^\circ} = 6.620 \text{ teeth/in}$$

Answer

(d)

$$\phi_t = \tan^{-1} \left(\frac{\tan \phi_n}{\cos \psi} \right) = \tan^{-1} \left(\frac{\tan 20^\circ}{\cos 25^\circ} \right) = 21.88^\circ$$

Just like teeth on spur gears, helical-gear teeth can interfere. Equation (13–19) can be solved for the pressure angle ϕ_t in the tangential (rotation) direction to give

$$\phi_t = \tan^{-1} \left(\frac{\tan \phi_n}{\cos \psi} \right)$$

The smallest tooth number N_P of a helical-spur pinion that will run without interference² with a gear with the same number of teeth is

$$N_P = \frac{2k \cos \psi}{3 \sin^2 \phi_t} \left(1 + \sqrt{1 + 3 \sin^2 \phi_t} \right) \quad (13-21)$$

For example, if the normal pressure angle ϕ_n is 20° , the helix angle ψ is 30° , then ϕ_t is

$$\phi_t = \tan^{-1} \left(\frac{\tan 20^\circ}{\cos 30^\circ} \right) = 22.80^\circ$$

$$N_P = \frac{2(1) \cos 30^\circ}{3 \sin^2 22.80^\circ} \left(1 + \sqrt{1 + 3 \sin^2 22.80^\circ} \right) = 8.48 = 9 \text{ teeth}$$

For a given gear ratio $m_G = N_G/N_P = m$, the smallest pinion tooth count is

$$N_P = \frac{2k \cos \psi}{(1 + 2m) \sin^2 \phi_t} \left[m + \sqrt{m^2 + (1 + 2m) \sin^2 \phi_t} \right] \quad (13-22)$$

The largest gear with a specified pinion is given by

$$N_G = \frac{N_P^2 \sin^2 \phi_t - 4k^2 \cos^2 \psi}{4k \cos \psi - 2N_P \sin^2 \phi_t} \quad (13-23)$$

For example, for a nine-tooth pinion with a pressure angle ϕ_n of 20° , a helix angle ψ of 30° , and recalling that the tangential pressure angle ϕ_t is 22.80° ,

$$N_G = \frac{9^2 \sin^2 22.80^\circ - 4(1)^2 \cos^2 30^\circ}{4(1) \cos 30^\circ - 2(9) \sin^2 22.80^\circ} = 12.02 = 12$$

The smallest pinion that can be run with a rack is

$$N_P = \frac{2k \cos \psi}{\sin^2 \phi_t} \quad (13-24)$$

²Op. cit., Robert Lipp, *Machine Design*, pp. 122–124.

For a normal pressure angle ϕ_n of 20° and a helix angle ψ of 30° , and $\phi_t = 22.80^\circ$,

$$N_P = \frac{2(1) \cos 30^\circ}{\sin^2 22.80^\circ} = 11.5 = 12 \text{ teeth}$$

For helical-gear teeth the number of teeth in mesh across the width of the gear will be greater than unity and a term called *face-contact ratio* is used to describe it. This increase of contact ratio, and the gradual sliding engagement of each tooth, results in quieter gears.

13-11 Worm Gears

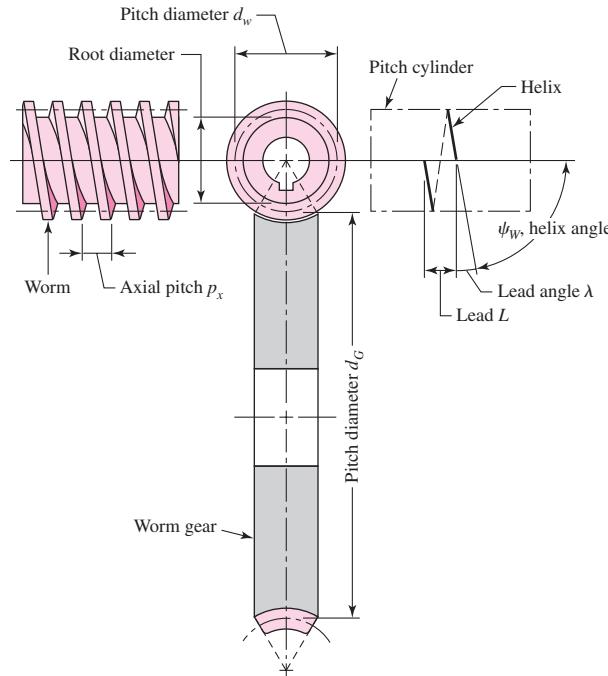
The nomenclature of a worm gearset is shown in Fig. 13-24. The worm and worm gear of a set have the same hand of helix as for crossed helical gears, but the helix angles are usually quite different. The helix angle on the worm is generally quite large, and that on the gear very small. Because of this, it is usual to specify the lead angle λ on the worm and helix angle ψ_G on the gear; the two angles are equal for a 90° shaft angle. The worm lead angle is the complement of the worm helix angle, as shown in Fig. 13-24.

In specifying the pitch of worm gearsets, it is customary to state the *axial pitch* p_x of the worm and the *transverse circular pitch* p_t , often simply called the circular pitch, of the mating gear. These are equal if the shaft angle is 90° . The pitch diameter of the gear is the diameter measured on a plane containing the worm axis, as shown in Fig. 13-24; it is the same as for spur gears and is

$$d_G = \frac{N_G p_t}{\pi} \quad (13-25)$$

Figure 13-24

Nomenclature of a single-enveloping worm gearset.



Since it is not related to the number of teeth, the worm may have any pitch diameter; this diameter should, however, be the same as the pitch diameter of the hob used to cut the worm-gear teeth. Generally, the pitch diameter of the worm should be selected so as to fall into the range

$$\frac{C^{0.875}}{3.0} \leq d_w \leq \frac{C^{0.875}}{1.7} \quad (13-26)$$

where C is the center distance. These proportions appear to result in optimum horsepower capacity of the gearset.

The *lead* L and the *lead angle* λ of the worm have the following relations:

$$L = p_x N_w \quad (13-27)$$

$$\tan \lambda = \frac{L}{\pi d_w} \quad (13-28)$$

13-12 Tooth Systems³

A *tooth system* is a standard that specifies the relationships involving addendum, dedendum, working depth, tooth thickness, and pressure angle. The standards were originally planned to attain interchangeability of gears of all tooth numbers, but of the same pressure angle and pitch.

Table 13-1 contains the standards most used for spur gears. A $14\frac{1}{2}^\circ$ pressure angle was once used for these but is now obsolete; the resulting gears had to be comparatively larger to avoid interference problems.

Table 13-2 is particularly useful in selecting the pitch or module of a gear. Cutters are generally available for the sizes shown in this table.

Table 13-3 lists the standard tooth proportions for straight bevel gears. These sizes apply to the large end of the teeth. The nomenclature is defined in Fig. 13-20.

Standard tooth proportions for helical gears are listed in Table 13-4. Tooth proportions are based on the normal pressure angle; these angles are standardized the same

Table 13-1

Standard and
Commonly Used Tooth
Systems for Spur Gears

Tooth System	Pressure Angle ϕ , deg	Addendum a	Dedendum b
Full depth	20	$1/P_d$ or $1m$	$1.25/P_d$ or $1.25m$
	$22\frac{1}{2}$	$1/P_d$ or $1m$	$1.35/P_d$ or $1.35m$
	25	$1/P_d$ or $1m$	$1.25/P_d$ or $1.25m$
			$1.35/P_d$ or $1.35m$
Stub	20	$0.8/P_d$ or $0.8m$	$1/P_d$ or $1m$

³Standardized by the American Gear Manufacturers Association (AGMA). Write AGMA for a complete list of standards, because changes are made from time to time. The address is: 1500 King Street, Suite 201, Alexandria, VA 22314; or, www.agma.org.

Table 13-2

Tooth Sizes in General
Uses

Diametral Pitch	
Coarse	2, $2\frac{1}{4}$, $2\frac{1}{2}$, 3, 4, 6, 8, 10, 12, 16
Fine	20, 24, 32, 40, 48, 64, 80, 96, 120, 150, 200
Modules	
Preferred	1, 1.25, 1.5, 2, 2.5, 3, 4, 5, 6, 8, 10, 12, 16, 20, 25, 32, 40, 50
Next Choice	1.125, 1.375, 1.75, 2.25, 2.75, 3.5, 4.5, 5.5, 7, 9, 11, 14, 18, 22, 28, 36, 45

Table 13-3

Tooth Proportions for
 20° Straight Bevel-Gear
Teeth

Item	Formula										
Working depth	$h_k = 2.0/P$										
Clearance	$c = (0.188/P) + 0.002 \text{ in}$										
Addendum of gear	$a_G = \frac{0.54}{P} + \frac{0.460}{P(m_{90})^2}$										
Gear ratio	$m_G = N_G/N_P$										
Equivalent 90° ratio	$m_{90} = m_G \text{ when } \Gamma = 90^\circ$ $m_{90} = \sqrt{m_G \frac{\cos \gamma}{\cos \Gamma}}$ when $\Gamma \neq 90^\circ$										
Face width	$F = 0.3A_0 \text{ or } F = \frac{10}{P}, \text{ whichever is smaller}$										
Minimum number of teeth	<table border="1" style="margin-left: auto; margin-right: auto;"> <tr> <td>Pinion</td> <td>16</td> <td>15</td> <td>14</td> <td>13</td> </tr> <tr> <td>Gear</td> <td>16</td> <td>17</td> <td>20</td> <td>30</td> </tr> </table>	Pinion	16	15	14	13	Gear	16	17	20	30
Pinion	16	15	14	13							
Gear	16	17	20	30							

Table 13-4

Standard Tooth
Proportions for Helical
Gears

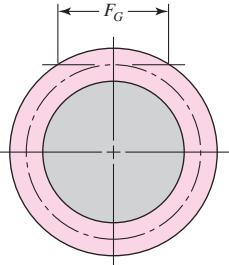
Quantity*	Formula	Quantity*	Formula
Addendum	$\frac{1.00}{P_n}$	External gears:	
Dedendum	$\frac{1.25}{P_n}$	Standard center distance	
Pinion pitch diameter	$\frac{N_p}{P_n \cos \psi}$	$D + d$	
Gear pitch diameter	$\frac{N_G}{P_n \cos \psi}$	Gear outside diameter	
Normal arc tooth thickness [†]	$\frac{\pi}{P_n} - \frac{B_n}{2}$	$D + 2a$	
Pinion base diameter	$d \cos \phi_t$	Pinion outside diameter	
Internal gears:			
Gear base diameter	$D \cos \phi_t$	Center distance	
Base helix angle	$\tan^{-1}(\tan \psi \cos \phi_t)$	$\frac{D - d}{2}$	
		Inside diameter	
		$D - 2a$	
		Root diameter	
		$D + 2b$	

*All dimensions are in inches, and angles are in degrees.

[†] B_n is the normal backlash.

Table 13-5

Recommended Pressure Angles and Tooth Depths for Worm Gearing	Lead Angle λ , deg	Pressure Angle ϕ_n , deg	Addendum a	Dedendum b_G
Angles and Tooth Depths for Worm Gearing	0–15	14 $\frac{1}{2}$	0.3683 p_x	0.3683 p_x
	15–30	20	0.3683 p_x	0.3683 p_x
	30–35	25	0.2865 p_x	0.3314 p_x
	35–40	25	0.2546 p_x	0.2947 p_x
	40–45	30	0.2228 p_x	0.2578 p_x

**Figure 13-25**

A graphical depiction of the face width of the worm of a worm gearset.

as for spur gears. Though there will be exceptions, the face width of helical gears should be at least 2 times the axial pitch to obtain good helical-gear action.

Tooth forms for worm gearing have not been highly standardized, perhaps because there has been less need for it. The pressure angles used depend upon the lead angles and must be large enough to avoid undercutting of the worm-gear tooth on the side at which contact ends. A satisfactory tooth depth, which remains in about the right proportion to the lead angle, may be obtained by making the depth a proportion of the axial circular pitch. Table 13-5 summarizes what may be regarded as good practice for pressure angle and tooth depth.

The *face width* F_G of the worm gear should be made equal to the length of a tangent to the worm pitch circle between its points of intersection with the addendum circle, as shown in Fig. 13-25.

13-13 Gear Trains

Consider a pinion 2 driving a gear 3. The speed of the driven gear is

$$n_3 = \left| \frac{N_2}{N_3} n_2 \right| = \left| \frac{d_2}{d_3} n_2 \right| \quad (13-29)$$

where n = revolutions or rev/min

N = number of teeth

d = pitch diameter

Equation (13-29) applies to any gearset no matter whether the gears are spur, helical, bevel, or worm. The absolute-value signs are used to permit complete freedom in choosing positive and negative directions. In the case of spur and parallel helical gears, the directions ordinarily correspond to the right-hand rule and are positive for counter-clockwise rotation.

Rotational directions are somewhat more difficult to deduce for worm and crossed helical gearsets. Figure 13-26 will be of help in these situations.

The gear train shown in Fig. 13-27 is made up of five gears. The speed of gear 6 is

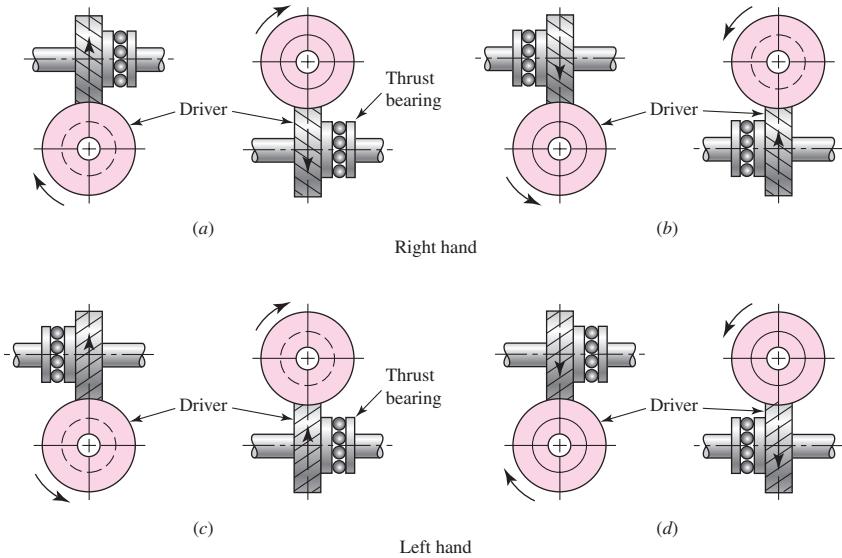
$$n_6 = -\frac{N_2}{N_3} \frac{N_3}{N_4} \frac{N_5}{N_6} n_2 \quad (a)$$

Hence we notice that gear 3 is an idler, that its tooth numbers cancel in Eq. (a), and hence that it affects only the direction of rotation of gear 6. We notice, furthermore, that

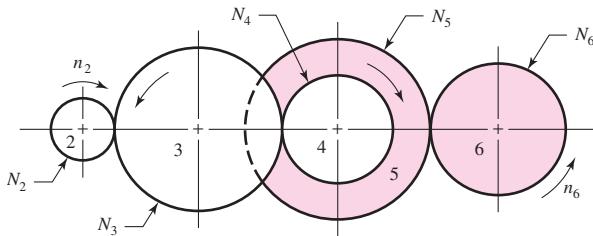
Figure 13-26

Thrust, rotation, and hand relations for crossed helical gears. Note that each pair of drawings refers to a single gearset. These relations also apply to worm gearsets.

(Reproduced by permission, Boston Gear Division, Colfax Corp.)

**Figure 13-27**

A gear train.



gears 2, 3, and 5 are drivers, while 3, 4, and 6 are driven members. We define the *train value* e as

$$e = \frac{\text{product of driving tooth numbers}}{\text{product of driven tooth numbers}} \quad (13-30)$$

Note that pitch diameters can be used in Eq. (13-30) as well. When Eq. (13-30) is used for spur gears, e is positive if the last gear rotates in the same sense as the first, and negative if the last rotates in the opposite sense.

Now we can write

$$n_L = en_F \quad (13-31)$$

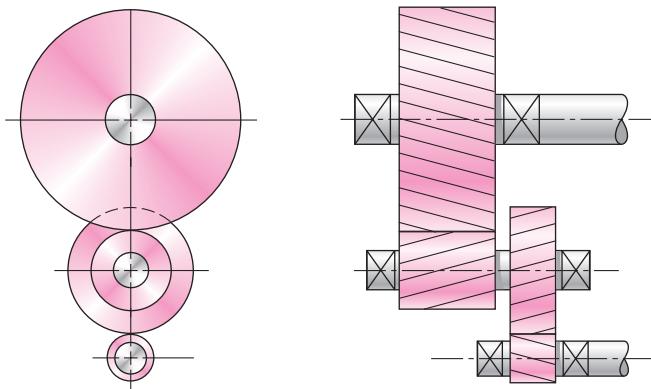
where n_L is the speed of the last gear in the train and n_F is the speed of the first.

As a rough guideline, a train value of up to 10 to 1 can be obtained with one pair of gears. Greater ratios can be obtained in less space and with fewer dynamic problems by compounding additional pairs of gears. A two-stage compound gear train, such as shown in Fig. 13-28, can obtain a train value of up to 100 to 1.

The design of gear trains to accomplish a specific train value is straightforward. Since numbers of teeth on gears must be integers, it is better to determine them first, and then obtain pitch diameters second. Determine the number of stages necessary to obtain the overall ratio, then divide the overall ratio into portions to be accomplished in each

Figure 13-28

A two-stage compound gear train.



stage. To minimize package size, keep the portions as evenly divided between the stages as possible. In cases where the overall train value need only be approximated, each stage can be identical. For example, in a two-stage compound gear train, assign the square root of the overall train value to each stage. If an exact train value is needed, attempt to factor the overall train value into integer components for each stage. Then assign the smallest gear(s) to the minimum number of teeth allowed for the specific ratio of each stage, in order to avoid interference (see Sec. 13-7). Finally, applying the ratio for each stage, determine the necessary number of teeth for the mating gears. Round to the nearest integer and check that the resulting overall ratio is within acceptable tolerance.

EXAMPLE 13-3

A gearbox is needed to provide a 30:1 (± 1 percent) increase in speed, while minimizing the overall gearbox size. Specify appropriate teeth numbers.

Solution

Since the ratio is greater than 10:1, but less than 100:1, a two-stage compound gear train, such as in Figure 13-28, is needed. The portion to be accomplished in each stage is $\sqrt{30} = 5.4772$. For this ratio, assuming a typical 20° pressure angle, the minimum number of teeth to avoid interference is 16, according to Eq. (13-11). The number of teeth necessary for the mating gears is

Answer

$$16\sqrt{30} = 87.64 \approx 88$$

From Eq. (13-30), the overall train value is

$$e = (88/16)(88/16) = 30.25$$

This is within the 1 percent tolerance. If a closer tolerance is desired, then increase the pinion size to the next integer and try again.

EXAMPLE 13-4

A gearbox is needed to provide an *exact* 30:1 increase in speed, while minimizing the overall gearbox size. Specify appropriate teeth numbers.

Solution

The previous example demonstrated the difficulty with finding integer numbers of teeth to provide an exact ratio. In order to obtain integers, factor the overall ratio into two integer stages.

$$e = 30 = (6)(5)$$

$$N_2/N_3 = 6 \quad \text{and} \quad N_4/N_5 = 5$$

With two equations and four unknown numbers of teeth, two free choices are available. Choose N_3 and N_5 to be as small as possible without interference. Assuming a 20° pressure angle, Eq. (13–11) gives the minimum as 16.

Then

$$N_2 = 6 N_3 = 6(16) = 96$$

$$N_4 = 5 N_5 = 5(16) = 80$$

The overall train value is then exact.

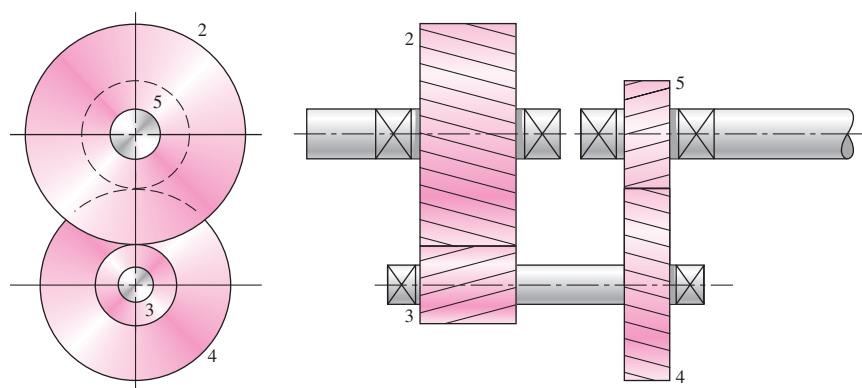
$$e = (96/16)(80/16) = (6)(5) = 30$$

It is sometimes desirable for the input shaft and the output shaft of a two-stage compound gear train to be in-line, as shown in Fig. 13–29. This configuration is called a *compound reverted gear train*. This requires the distances between the shafts to be the same for both stages of the train, which adds to the complexity of the design task. The distance constraint is

$$d_2/2 + d_3/2 = d_4/2 + d_5/2$$

Figure 13–29

A compound reverted gear train.



The diametral pitch relates the diameters and the numbers of teeth, $P = N/d$. Replacing all the diameters gives

$$N_2/(2P) + N_3/(2P) = N_4/(2P) + N_5/(2P)$$

Assuming a constant diametral pitch in both stages, we have the geometry condition stated in terms of numbers of teeth:

$$N_2 + N_3 = N_4 + N_5$$

This condition must be exactly satisfied, in addition to the previous ratio equations, to provide for the in-line condition on the input and output shafts.

EXAMPLE 13-5

A gearbox is needed to provide an exact 30:1 increase in speed, while minimizing the overall gearbox size. The input and output shafts should be in-line. Specify appropriate teeth numbers.

Solution

The governing equations are

$$N_2/N_3 = 6$$

$$N_4/N_5 = 5$$

$$N_2 + N_3 = N_4 + N_5$$

With three equations and four unknown numbers of teeth, only one free choice is available. Of the two smaller gears, N_3 and N_5 , the free choice should be used to minimize N_3 since a greater gear ratio is to be achieved in this stage. To avoid interference, the minimum for N_3 is 16.

Applying the governing equations yields

$$N_2 = 6N_3 = 6(16) = 96$$

$$N_2 + N_3 = 96 + 16 = 112 = N_4 + N_5$$

Substituting $N_4 = 5N_5$ gives

$$112 = 5N_5 + N_5 = 6N_5$$

$$N_5 = 112/6 = 18.67$$

If the train value need only be approximated, then this can be rounded to the nearest integer. But for an exact solution, it is necessary to choose the initial free choice for N_3 such that solution of the rest of the teeth numbers results exactly in integers. This can be done by trial and error, letting $N_3 = 17$, then 18, etc., until it works. Or, the problem can be normalized to quickly determine the minimum free choice. Beginning again, let the free choice be $N_3 = 1$. Applying the governing equations gives

$$N_2 = 6N_3 = 6(1) = 6$$

$$N_2 + N_3 = 6 + 1 = 7 = N_4 + N_5$$

Substituting $N_4 = 5N_5$, we find

$$7 = 5N_5 + N_5 = 6N_5$$

$$N_5 = 7/6$$

This fraction could be eliminated if it were multiplied by a multiple of 6. The free choice for the smallest gear N_3 should be selected as a multiple of 6 that is greater than the minimum allowed to avoid interference. This would indicate that $N_3 = 18$. Repeating the application of the governing equations for the final time yields

$$N_2 = 6N_3 = 6(18) = 108$$

$$N_2 + N_3 = 108 + 18 = 126 = N_4 + N_5$$

$$126 = 5N_5 + N_5 = 6N_5$$

$$N_5 = 126/6 = 21$$

$$N_4 = 5N_5 = 5(21) = 105$$

Thus,

Answer

$$N_2 = 108$$

$$N_3 = 18$$

$$N_4 = 105$$

$$N_5 = 21$$

Checking, we calculate $e = (108/18)(105/21) = (6)(5) = 30$.

And checking the geometry constraint for the in-line requirement, we calculate

$$N_2 + N_3 = N_4 + N_5$$

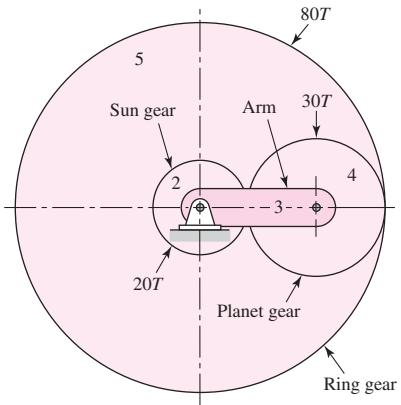
$$108 + 18 = 105 + 21$$

$$126 = 126$$

Unusual effects can be obtained in a gear train by permitting some of the gear axes to rotate about others. Such trains are called *planetary*, or *epicyclic*, *gear trains*. Planetary trains always include a *sun gear*, a *planet carrier* or *arm*, and one or more *planet gears*, as shown in Fig. 13–30. Planetary gear trains are unusual mechanisms because they have two degrees of freedom; that is, for constrained motion, a planetary train must have two inputs. For example, in Fig. 13–30 these two inputs could be the motion of any two of the elements of the train. We might, say, specify that the sun gear rotates at 100 rev/min clockwise and that the ring gear rotates at 50 rev/min counter-clockwise; these are the inputs. The output would be the motion of the arm. In most planetary trains one of the elements is attached to the frame and has no motion.

Figure 13-30

A planetary gear train.

**Figure 13-31**

A gear train on the arm of a planetary gear train.

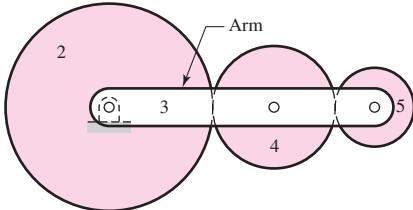


Figure 13-31 shows a planetary train composed of a sun gear 2, an arm or carrier 3, and planet gears 4 and 5. The angular velocity of gear 2 relative to the arm in rev/min is

$$n_{23} = n_2 - n_3 \quad (b)$$

Also, the velocity of gear 5 relative to the arm is

$$n_{53} = n_5 - n_3 \quad (c)$$

Dividing Eq. (c) by Eq. (b) gives

$$\frac{n_{53}}{n_{23}} = \frac{n_5 - n_3}{n_2 - n_3} \quad (d)$$

Equation (d) expresses the ratio of gear 5 to that of gear 2, and both velocities are taken relative to the arm. Now this ratio is the same and is proportional to the tooth numbers, whether the arm is rotating or not. It is the train value. Therefore, we may write

$$e = \frac{n_5 - n_3}{n_2 - n_3} \quad (e)$$

This equation can be used to solve for the output motion of any planetary train. It is more conveniently written in the form

$$e = \frac{n_L - n_A}{n_F - n_A} \quad (13-32)$$

where n_F = rev/min of first gear in planetary train
 n_L = rev/min of last gear in planetary train
 n_A = rev/min of arm

EXAMPLE 13–6

In Fig. 13–30 the sun gear is the input, and it is driven clockwise at 100 rev/min. The ring gear is held stationary by being fastened to the frame. Find the rev/min and direction of rotation of the arm and gear 4.

Solution

Designate $n_F = n_2 = -100$ rev/min, and $n_L = n_5 = 0$. Unlocking gear 5 and holding the arm stationary, in our imagination, we find

$$e = -\left(\frac{20}{30}\right)\left(\frac{30}{80}\right) = -0.25$$

Substituting this value in Eq. (13–32) gives

$$-0.25 = \frac{0 - n_A}{(-100) - n_A}$$

or

Answer

$$n_A = -20 \text{ rev/min}$$

To obtain the speed of gear 4, we follow the procedure outlined by Eqs. (b), (c), and (d). Thus

$$n_{43} = n_4 - n_3 \quad n_{23} = n_2 - n_3$$

and so

$$\frac{n_{43}}{n_{23}} = \frac{n_4 - n_3}{n_2 - n_3} \quad (1)$$

But

$$\frac{n_{43}}{n_{23}} = -\frac{20}{30} = -\frac{2}{3} \quad (2)$$

Substituting the known values in Eq. (1) gives

$$-\frac{2}{3} = \frac{n_4 - (-20)}{(-100) - (-20)}$$

Solving gives

Answer

$$n_4 = 33\frac{1}{3} \text{ rev/min}$$

13–14

Force Analysis—Spur Gearing

Before beginning the force analysis of gear trains, let us agree on the notation to be used. Beginning with the numeral 1 for the frame of the machine, we shall designate the input gear as gear 2, and then number the gears successively 3, 4, etc., until we

arrive at the last gear in the train. Next, there may be several shafts involved, and usually one or two gears are mounted on each shaft as well as other elements. We shall designate the shafts, using lowercase letters of the alphabet, a, b, c , etc.

With this notation we can now speak of the force exerted by gear 2 against gear 3 as F_{23} . The force of gear 2 against a shaft a is F_{a2} . We can also write F_{a2} to mean the force of a shaft a against gear 2. Unfortunately, it is also necessary to use superscripts to indicate directions. The coordinate directions will usually be indicated by the x, y , and z coordinates, and the radial and tangential directions by superscripts r and t . With this notation, F_{43}^t is the tangential component of the force of gear 4 acting against gear 3.

Figure 13–32a shows a pinion mounted on shaft a rotating clockwise at n_2 rev/min and driving a gear on shaft b at n_3 rev/min. The reactions between the mating teeth occur along the pressure line. In Fig. 13–32b the pinion has been separated from the gear and the shaft, and their effects have been replaced by forces. F_{a2} and T_{a2} are the force and torque, respectively, exerted by shaft a against pinion 2. F_{32} is the force exerted by gear 3 against the pinion. Using a similar approach, we obtain the free-body diagram of the gear shown in Fig. 13–32c.

In Fig. 13–33, the free-body diagram of the pinion has been redrawn and the forces have been resolved into tangential and radial components. We now define

$$W_t = F_{32}^t \quad (a)$$

as the *transmitted load*. This tangential load is really the useful component, because the radial component F_{32}^r serves no useful purpose. It does not transmit power. The applied torque and the transmitted load are seen to be related by the equation

$$T = \frac{d}{2} W_t \quad (b)$$

where we have used $T = T_{a2}$ and $d = d_2$ to obtain a general relation.

The power H transmitted through a rotating gear can be obtained from the standard relationship of the product of torque T and angular velocity ω .

$$H = T\omega = (W_t d/2) \omega \quad (13-33)$$

Figure 13–32

Free-body diagrams of the forces and moments acting upon two gears of a simple gear train.

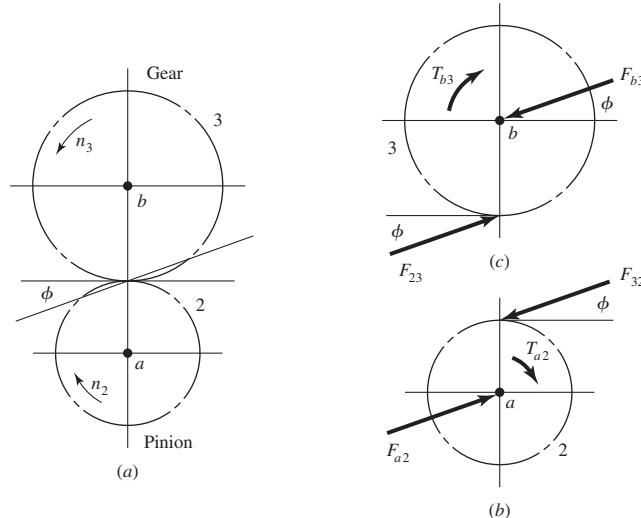
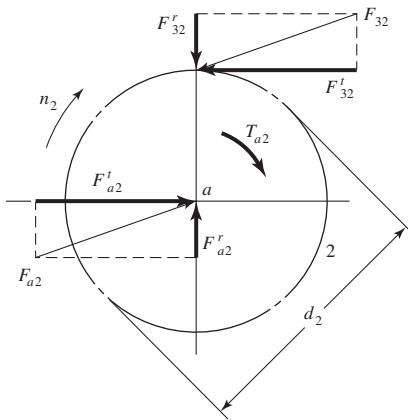


Figure 13-33

Resolution of gear forces.



While any units can be used in this equation, the units of the resulting power will obviously be dependent on the units of the other parameters. It will often be desirable to work with the power in either horsepower or kilowatts, and appropriate conversion factors should be used.

Since meshed gears are reasonably efficient, with losses of less than 2 percent, the power is generally treated as constant through the mesh. Consequently, with a pair of meshed gears, Eq. (13-33) will give the same power regardless of which gear is used for d and ω .

Gear data is often tabulated using *pitch-line velocity*, which is the linear velocity of a point on the gear at the radius of the pitch circle; thus $V = (d/2)\omega$. Converting this to customary units gives

$$V = \pi dn/12 \quad (13-34)$$

where V = pitch-line velocity, ft/min

d = gear diameter, in

n = gear speed, rev/min

Many gear design problems will specify the power and speed, so it is convenient to solve Eq. (13-33) for W_t . With the pitch-line velocity and appropriate conversion factors incorporated, Eq. (13-33) can be rearranged and expressed in customary units as

$$W_t = 33\,000 \frac{H}{V} \quad (13-35)$$

where W_t = transmitted load, lbf

H = power, hp

V = pitch-line velocity, ft/min

The corresponding equation in SI is

$$W_t = \frac{60\,000H}{\pi dn} \quad (13-36)$$

where W_t = transmitted load, kN

H = power, kW

d = gear diameter, mm

n = speed, rev/min

EXAMPLE 13-7

Pinion 2 in Fig. 13–34a runs at 1750 rev/min and transmits 2.5 kW to idler gear 3. The teeth are cut on the 20° full-depth system and have a module of $m = 2.5 \text{ mm}$. Draw a free-body diagram of gear 3 and show all the forces that act upon it.

Solution

The pitch diameters of gears 2 and 3 are

$$d_2 = N_2 m = 20(2.5) = 50 \text{ mm}$$

$$d_3 = N_3 m = 50(2.5) = 125 \text{ mm}$$

From Eq. (13–36) we find the transmitted load to be

$$W_t = \frac{60000H}{\pi d_2 n} = \frac{60000(2.5)}{\pi(50)(1750)} = 0.546 \text{ kN}$$

Thus, the tangential force of gear 2 on gear 3 is $F_{23}^t = 0.546 \text{ kN}$, as shown in Fig. 13–34b. Therefore

$$F_{23}^r = F_{23}^t \tan 20^\circ = (0.546) \tan 20^\circ = 0.199 \text{ kN}$$

and so

$$F_{23} = \frac{F_{23}^t}{\cos 20^\circ} = \frac{0.546}{\cos 20^\circ} = 0.581 \text{ kN}$$

Since gear 3 is an idler, it transmits no power (torque) to its shaft, and so the tangential reaction of gear 4 on gear 3 is also equal to W_t . Therefore

$$F_{43}^t = 0.546 \text{ kN} \quad F_{43}^r = 0.199 \text{ kN} \quad F_{43} = 0.581 \text{ kN}$$

and the directions are shown in Fig. 13–34b.

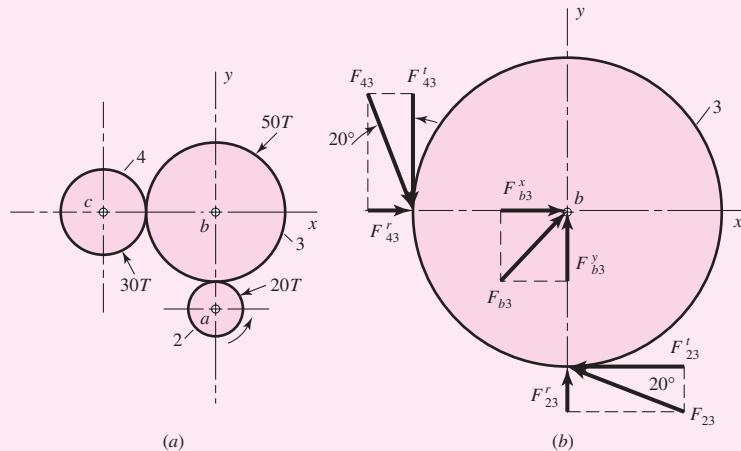
The shaft reactions in the x and y directions are

$$F_{b3}^x = -(F_{23}^t + F_{43}^r) = -(-0.546 + 0.199) = 0.347 \text{ kN}$$

$$F_{b3}^y = -(F_{23}^r + F_{43}^t) = -(0.199 - 0.546) = 0.347 \text{ kN}$$

Figure 13–34

A gear train containing an idler gear. (a) The gear train.
(b) Free-body of the idler gear.



The resultant shaft reaction is

$$F_{b3} = \sqrt{(0.347)^2 + (0.347)^2} = 0.491 \text{ kN}$$

These are shown on the figure.

13-15 Force Analysis—Bevel Gearing

In determining shaft and bearing loads for bevel-gear applications, the usual practice is to use the tangential or transmitted load that would occur if all the forces were concentrated at the midpoint of the tooth. While the actual resultant occurs somewhere between the midpoint and the large end of the tooth, there is only a small error in making this assumption. For the transmitted load, this gives

$$W_t = \frac{T}{r_{av}} \quad (13-37)$$

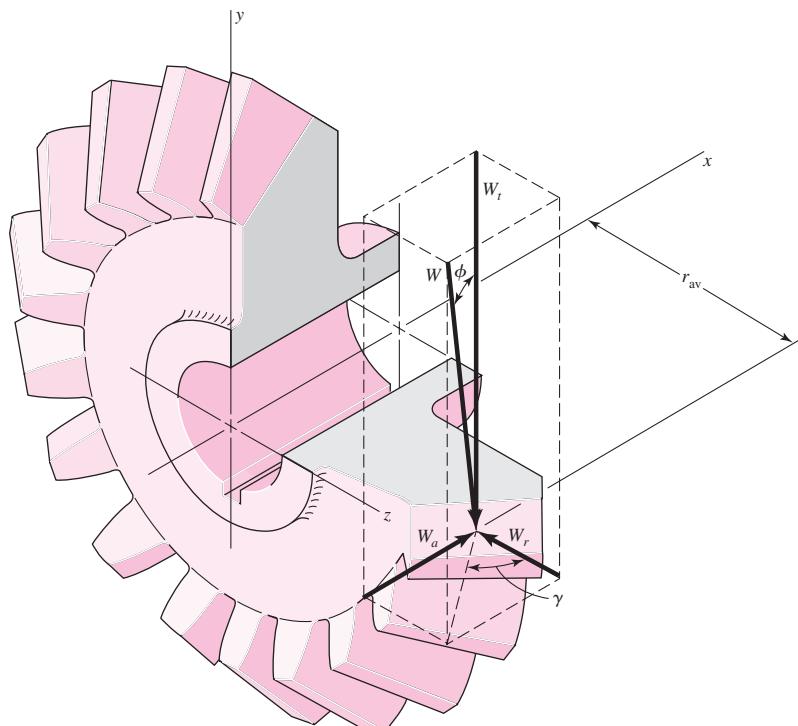
where T is the torque and r_{av} is the pitch radius at the midpoint of the tooth for the gear under consideration.

The forces acting at the center of the tooth are shown in Fig. 13-35. The resultant force W has three components: a tangential force W_t , a radial force W_r , and an axial force W_a . From the trigonometry of the figure,

$$\begin{aligned} W_r &= W_t \tan \phi \cos \gamma \\ W_a &= W_t \tan \phi \sin \gamma \end{aligned} \quad (13-38)$$

Figure 13-35

Bevel-gear tooth forces.



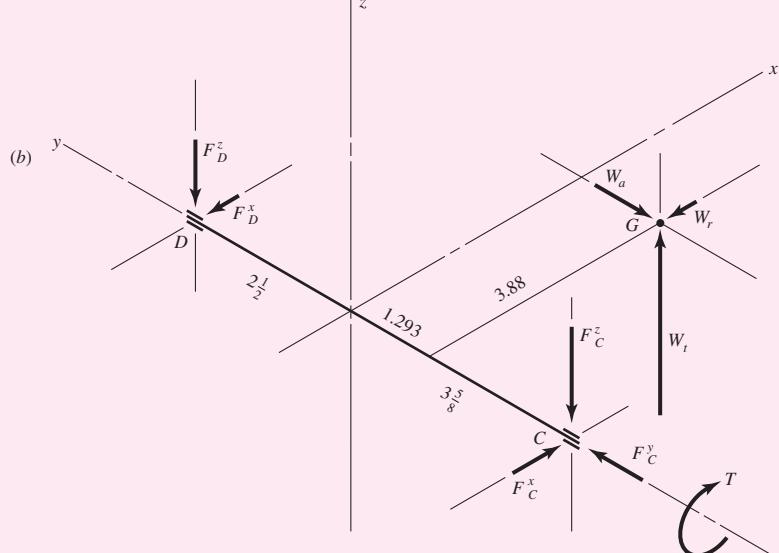
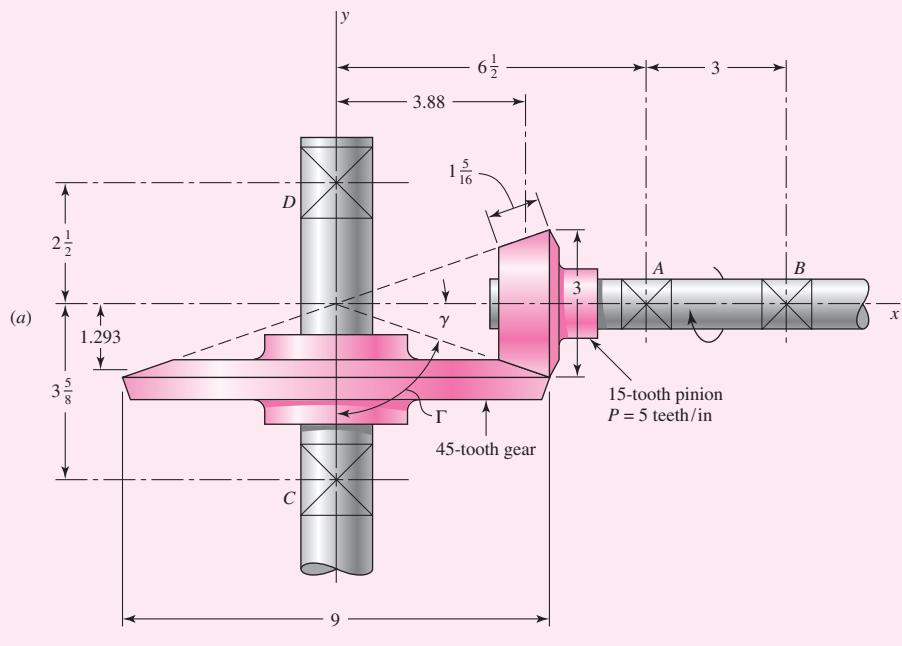
The three forces W_t , W_r , and W_a are at right angles to each other and can be used to determine the bearing loads by using the methods of statics.

EXAMPLE 13-8

The bevel pinion in Fig. 13-36a rotates at 600 rev/min in the direction shown and transmits 5 hp to the gear. The mounting distances, the location of all bearings, and the average pitch radii of the pinion and gear are shown in the figure. For simplicity, the teeth have been replaced by pitch cones. Bearings A and C should take the thrust loads. Find the bearing forces on the gearshaft.

Figure 13-36

- (a) Bevel gearset of Ex. 13-8.
- (b) Free-body diagram of shaft CD. Dimensions in inches.



Solution The pitch angles are

$$\gamma = \tan^{-1} \left(\frac{3}{9} \right) = 18.4^\circ \quad \Gamma = \tan^{-1} \left(\frac{9}{3} \right) = 71.6^\circ$$

The pitch-line velocity corresponding to the average pitch radius is

$$V = \frac{2\pi r_P n}{12} = \frac{2\pi(1.293)(600)}{12} = 406 \text{ ft/min}$$

Therefore the transmitted load is

$$W_t = \frac{33000H}{V} = \frac{(33000)(5)}{406} = 406 \text{ lbf}$$

which acts in the positive z direction, as shown in Fig. 13–36b. We next have

$$W_r = W_t \tan \phi \cos \Gamma = 406 \tan 20^\circ \cos 71.6^\circ = 46.6 \text{ lbf}$$

$$W_a = W_t \tan \phi \sin \Gamma = 406 \tan 20^\circ \sin 71.6^\circ = 140 \text{ lbf}$$

where W_r is in the $-x$ direction and W_a is in the $-y$ direction, as illustrated in the isometric sketch of Fig. 13–36b.

In preparing to take a sum of the moments about bearing D , define the position vector from D to G as

$$\mathbf{R}_G = 3.88\mathbf{i} - (2.5 + 1.293)\mathbf{j} = 3.88\mathbf{i} - 3.793\mathbf{j}$$

We shall also require a vector from D to C :

$$\mathbf{R}_C = -(2.5 + 3.625)\mathbf{j} = -6.125\mathbf{j}$$

Then, summing moments about D gives

$$\mathbf{R}_G \times \mathbf{W} + \mathbf{R}_C \times \mathbf{F}_C + \mathbf{T} = \mathbf{0} \quad (1)$$

When we place the details in Eq. (1), we get

$$(3.88\mathbf{i} - 3.793\mathbf{j}) \times (-46.6\mathbf{i} - 140\mathbf{j} + 406\mathbf{k}) \\ + (-6.125\mathbf{j}) \times (F_C^x\mathbf{i} + F_C^y\mathbf{j} + F_C^z\mathbf{k}) + T\mathbf{j} = \mathbf{0} \quad (2)$$

After the two cross products are taken, the equation becomes

$$(-1540\mathbf{i} - 1575\mathbf{j} - 720\mathbf{k}) + (-6.125F_C^z\mathbf{i} + 6.125F_C^x\mathbf{k}) + T\mathbf{j} = \mathbf{0}$$

from which

$$\mathbf{T} = 1575\mathbf{j} \text{ lbf} \cdot \text{in} \quad F_C^x = 118 \text{ lbf} \quad F_C^z = -251 \text{ lbf} \quad (3)$$

Now sum the forces to zero. Thus

$$\mathbf{F}_D + \mathbf{F}_C + \mathbf{W} = \mathbf{0} \quad (4)$$

When the details are inserted, Eq. (4) becomes

$$(F_D^x\mathbf{i} + F_D^z\mathbf{k}) + (118\mathbf{i} + F_C^y\mathbf{j} - 251\mathbf{k}) + (-46.6\mathbf{i} - 140\mathbf{j} + 406\mathbf{k}) = \mathbf{0} \quad (5)$$

First we see that $F_C^y = 140 \text{ lbf}$, and so

Answer

$$\mathbf{F}_C = 118\mathbf{i} + 140\mathbf{j} - 251\mathbf{k} \text{ lbf}$$

Then, from Eq. (5),

Answer

$$\mathbf{F}_D = -71.4\mathbf{i} - 155\mathbf{k} \text{ lbf}$$

These are all shown in Fig. 13-36b in the proper directions. The analysis for the pinion shaft is quite similar.

13-16

Force Analysis—Helical Gearing

Figure 13-37 is a three-dimensional view of the forces acting against a helical-gear tooth. The point of application of the forces is in the pitch plane and in the center of the gear face. From the geometry of the figure, the three components of the total (normal) tooth force W are

$$W_r = W \sin \phi_n$$

$$W_t = W \cos \phi_n \cos \psi \quad (13-39)$$

$$W_a = W \cos \phi_n \sin \psi$$

where W = total force

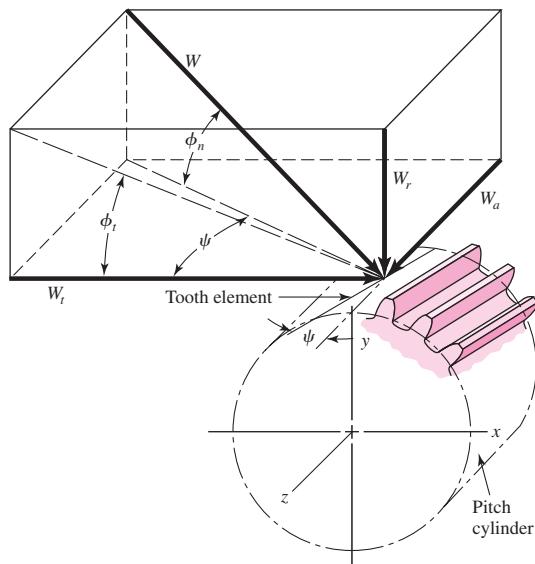
W_r = radial component

W_t = tangential component, also called transmitted load

W_a = axial component, also called thrust load

Figure 13-37

Tooth forces acting on a right-hand helical gear.



Usually W_t is given and the other forces are desired. In this case, it is not difficult to discover that

$$\begin{aligned} W_r &= W_t \tan \phi_t \\ W_a &= W_t \tan \psi \\ W &= \frac{W_t}{\cos \phi_n \cos \psi} \end{aligned} \quad (13-40)$$

EXAMPLE 13-9

In Fig. 13-38 a 1-hp electric motor runs at 1800 rev/min in the clockwise direction, as viewed from the positive x axis. Keyed to the motor shaft is an 18-tooth helical pinion having a normal pressure angle of 20° , a helix angle of 30° , and a normal diametral pitch of 12 teeth/in. The hand of the helix is shown in the figure. Make a three-dimensional sketch of the motor shaft and pinion, and show the forces acting on the pinion and the bearing reactions at A and B . The thrust should be taken out at A .

Solution

From Eq. (13-19) we find

$$\phi_t = \tan^{-1} \frac{\tan \phi_n}{\cos \psi} = \tan^{-1} \frac{\tan 20^\circ}{\cos 30^\circ} = 22.8^\circ$$

Also, $P_t = P_n \cos \psi = 12 \cos 30^\circ = 10.39$ teeth/in. Therefore the pitch diameter of the pinion is $d_p = 18/10.39 = 1.732$ in. The pitch-line velocity is

$$V = \frac{\pi d n}{12} = \frac{\pi (1.732)(1800)}{12} = 816 \text{ ft/min}$$

The transmitted load is

$$W_t = \frac{33000H}{V} = \frac{(33000)(1)}{816} = 40.4 \text{ lbf}$$

From Eq. (13-40) we find

$$W_r = W_t \tan \phi_t = (40.4) \tan 22.8^\circ = 17.0 \text{ lbf}$$

$$W_a = W_t \tan \psi = (40.4) \tan 30^\circ = 23.3 \text{ lbf}$$

$$W = \frac{W_t}{\cos \phi_n \cos \psi} = \frac{40.4}{\cos 20^\circ \cos 30^\circ} = 49.6 \text{ lbf}$$

Figure 13-38

The motor and gear train of Ex. 13-9.

